Metallosupramolecular Helicates and Tetrahedra: transition metal-directed assembly of polypyridyl ligands

Thesis submitted by

Christopher R. K. Glasson B.Sc. (Hons)

March 2009

For the Degree of Doctor of Philosophy

School of Pharmacy and Molecular Sciences

James Cook University

Townsville, Queensland, Australia

Statement of Access

I, the undersigned, author of this work, understand that James Cook University will make this thesis available for use within the University Library and, via the Australian Digital Theses network, for use elsewhere.

I understand that, as an unpublished work, a thesis has significant protection under the Copyright Act and;

> "In consulting this thesis I agree not to copy or closely paraphrase it in whole or in part without the written consent of the author, and to make proper pulbic acknowledgement for any assistance which I have obtained from it."

Beyond this, I do not wish to place any further restriction on access to this work.

_____

Christopher R. K. Glasson

March 2009

Statement of Sources

I declare that this thesis is my own work and has not been submitted in any form for another degree or diploma at any university or other institution of tertiary education. Information derived from the published or unpublished work of others has been acknowledged in the text and a list of references is given.

_____

Christopher R. K. Glasson

March 2009

Statement of Contribution of Others

The work reported in this thesis was conducted under the supervision of Prof. George Meehan (School of Pharmacy and Molecular Sciences at James Cook University) and Prof. Leonard Lindoy (School of Chemistry at the University of Sydney).

X-ray crystallography was in the most part conducted by Dr Jack Clegg (School of Chemistry at the University of Sydney). Other contributors to X-ray crystallography include Dr Murray Davies (School of Pharmacy and Molecular Sciences at James Cook University), Dr Peter Turner (School of Chemistry at the University of Sydney) and Dr John McMurtrie (School of Physical and Chemical Sciences at Queensland University of Technology).

Dr Cherie Motti (at the Australian Institute of Marine Sciences) collected high resolution electrospray mass spectra for many samples reported in this thesis, as well provided training to the candidate on the use of the mass spectral instrument and its software.

DNA binding affinity chromatography experiments were conducted under the guidance of Dr Jayden Smith and Prof. Richard Keene (School of Pharmacy and Molecular Sciences at James Cook University).

Prof. Keith Murray and coworkers (School of Chemistry at Monash University) collected and interpreted the magnetic susceptibility data. A/Prof. John Cashion (Monash University) collected and interpreted the Mössbauer spectra.

This work was funded by an Australian Research Council (ARC-DP) grant to Prof. Len Lindoy and Prof. George Meehan, and JCU Graduate Research Scheme grants to the candidate. Financial support to the candidate was obtained from an Australian

Postgraduate Award and funding during the compilation and writing of the thesis was obtained from a School of Pharmacy and Molecular Sciences Grant.

Christopher R. K. Glasson

March 2009

Acknowledgements

I would like to express my sincere appreciation to my supervisors Prof. George Meehan (James Cook University - JCU) and Prof. Len Lindoy (University of Sydney - USYD) for their patience and perseverance. Whilst our interactions were not always smooth (as might be expected for three strong headed individuals), they never resulted in any long term ill effects. On a serious note, the chemical knowledge and unsurpassed enthusiasm for everything chemical my supervisors demonstrated during the course of my candidature is a true inspiration.

As many of you know the ability to do synthetic chemistry is dependent on being able to characterize the products that are generated. Thus, in no particular order, I would like to acknowledge the specialists who have contributed to the success of this project.

High resolution mass spectrometry has allowed the elucidation of composition for many of the products reported in this thesis. In this regard, I would like to extend a very special thank you to Dr Cherie Motti (Australian Institute of Marine Sciences - AIMS) for her enthusiastic contribution to the mass spectrometry presented in this thesis. I would also like to acknowledge AIMS for the use of the mass spectrometer.

X-ray crystallography has proved to be a most valuable tool for the characterisation of the products described in this thesis. In this regard, I extend a warm thank you to Dr Jack Clegg (USYD) for his almost exhaustive contribution to the crystallography presented in this thesis. Other contributors to the X-ray crystallography include Dr Murray Davies (JCU), Dr Peter Turner (USYD) and Dr John McMurtrie (Queensland University of Technology).

Within Pharmacy and Molecular Sciences at James Cook University many people have kindly contributed to the research that this thesis reports. I would like to extend my gratitude to Professor Richard Keene and members of his research group – in particular Dr Jayden Smith for his contribution and assistance with the DNA binding affinity chromatography, spectrophotometric titration experiments and equilibrium dialysis experiments. I would like to thank Prof. Bruce Bowden for his enthusiastic assistance with the many NMR glitches. Special thanks to Peter Kemppinnen for all his help in the

laboratory. I would also like to thank general members of the School of Pharmacy and Molecular Sciences at James Cook University for the entertaining BBQs, Christmas parties and other celebrations. Special thanks to Curtis Elcoate (brewer extraordinaire - drinking and golfing partner) and Dr Jayden Smith (Tour of Duty legend) for introducing me to the gravity hammer (my preferred mono on mono Halo weapon).

Last of all, but not least, I would like to express a very special thank you to my extended family for their love and support. In particular, I would like to thank my partner Marie, who has constantly supported me, putting up with my moodiness, laziness and innumerable other faults, and my parents for their love and persistence.

Abstract

This thesis reports the synthesis of a range of polypyridyl ligands and their subsequent incorporation into transition metal-directed assembly experiments. These latter experiments were designed to assess the viability of subsequent metal-template reductive amination procedures for the preparation of pseudocryptands, mono- and dinuclear cryptates and larger polycyclic compounds.

The synthesis of polypyridyl derivatives for use in the current project employed a range of modern coupling procedures, including Stille and Suzuki cross-couplings. The former was used to synthesise a range of bipyridines, notably the regioselective cross-coupling between 2,5-dibromopyridine and 2-trimethylstannyl-5-methylpyridine to afford 5-bromo-5′-methylbipyridine (**I**) in high yield. As well, the reaction of 2-trimethylstannyl-5-methylpyridine and 6,6′-dichloro-3,3′-bipyridine in a *bis*-Stille cross-coupling allowed the synthesis of 5,5′-dimethyl-2,2′;5′,5″;2″,2‴-quaterpyridine (**II**), often in yields in excess of 90 %. Alternatively, quaterpyridine **II** could be synthesised by two other methods: a Ni(0)-homocoupling reaction or a modified Suzuki coupling, both using bromobipyridine **I** as the starting material.

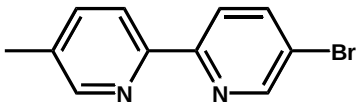

I

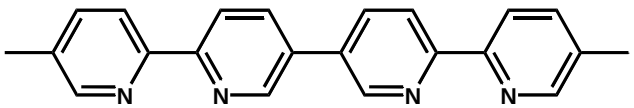

II

The interaction of quaterpyridine **II** with a range of transition metals, including Fe(II), Co(II), Ni(II) and Ru(II) was investigated. The resulting metal-complexes were characterised using a combination of NMR techniques, ESI-HRMS, X-ray crystallography and elemental analysis. The more labile first row transition metals yielded M_4L_6 host-guest complexes of type $[M_4(\mathbf{II})_6 \supset \text{anion}]^{7+}$ (where M = Fe(II), Co(II) and Ni(II) and anion = $[FeCl_4]^-$, BF_4^- and PF_6^-). There is also evidence that the $[Fe_4(\mathbf{II})_6]^{8+}$ host encapsulates $[FeCl_4]^{2-}$, a rare example of the inclusion of a doubly charged species. Interestingly, a series of ^{19}F NMR experiments revealed that the $[Fe_4(\mathbf{II})_6]^{8+}$ host selectively binds PF_6^- over BF_4^-; an observation that most probably reflects a size based

recognition process. Furthermore, a successful synthetic procedure for isolation of the empty cage (free of an encapsulated anion) was developed, indicating that anion templation is not essential for the formation of $[Fe_4(\mathbf{II})_6]^{8+}$.

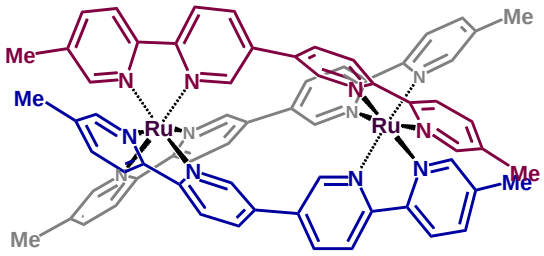

$[Ru_2(\mathbf{II})_3]^{4+}$

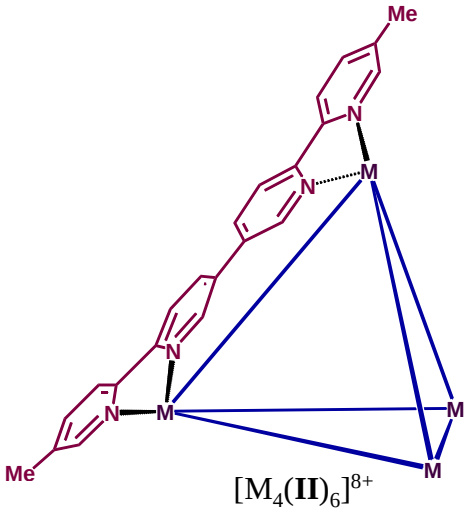

$[M_4(\mathbf{II})_6]^{8+}$

M = Fe, Co and Ni

The interaction of quaterpyridine **II** with $RuCl_3$ in ethylene glycol using microwave heating was found to yield a rare dinuclear helicate, $[Ru_2(\mathbf{II})_3]^{4+}$, in 36% yield. The racemate of this product was resolved by cation exchange chromatography on C-25 Sephadex with 0.1 M (-)-O,O′-dibenzoyl-L-tartaric acid as eluent. Circular dichroism measurements were made to assess the success of the separation of the two enantiomers and the crystallisation of enantiopure material has allowed the assignment of the *M*-$[Ru_2(\mathbf{II})_3]^{4+}$ and *P*-$[Ru_2(\mathbf{II})_3]^{4+}$ forms using X-ray crystallography. In turn, an equilibrium dialysis experiment with calf thymus DNA indicated that *M*-$[Ru_2(\mathbf{II})_3]^{4+}$ binds preferentially over the *P*-$[Ru_2(\mathbf{II})_3]^{4+}$. Furthermore, the use of a Sepharose-immobilized AT dodecanucleotide column resulted in the successful separation of the *M*- and *P*-enantiomers; *M*-$[Ru_2(\mathbf{II})_3]^{4+}$ was strongly retained whilst *P*-$[Ru_2(\mathbf{II})_3]^{4+}$ essentially eluted with the solvent front. Less efficient (but still satisfactory) separations were observed with other DNA motifs; for example, on employing a GC 12-mer and bulge and hairpin sequences. In each case *M*-$[Ru_2(\mathbf{II})_3]^{4+}$ bound to the column more strongly than the *P*-enantiomer.

To investigate the effect that rigidly bridged quaterpyridines might have on analogous octahedral metal-directed assembly outcomes, quaterpyridines **III** and **IV** were synthesised. These ligands were prepared in high yield by *bis*-Suzuki coupling reactions between bromobipyridine **I** and appropriate *bis*-pinacol-diboronic esters using microwave heating.

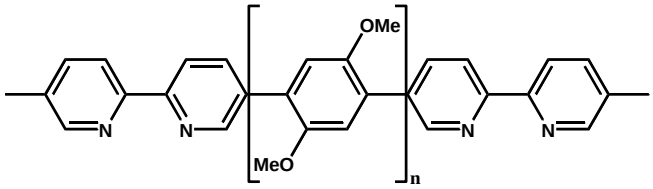

III n = 1
IV n = 2

The interaction of quaterpyridines **III** and **IV** with octahedral metal ions resulted in mixtures of $[M_2L_3]^{4+}$ and $[M_4L_6]^{8+}$ complexes (M = Fe(II) or Ni(II) and L = **III** or **IV**). $[Fe_2L_3]^{4+}$ and $[Fe_4L_6]^{8+}$ were adequately inert to allow their chromatographic separatation and subsequent characterization. A level of control over the relative ratio of these products was demonstrated using a combination of reaction times and the degree of dilution employed for their synthesis; short reaction times and high dilution favoured the formation of $[M_2L_3]^{4+}$ (e.g. $[Ni_2(\mathbf{III})_3]^{4+}$), while long reaction times and normal dilution favoured the formation of $[M_4L_6]^{8+}$ (e.g. $[Fe_4(\mathbf{III})_6 \supset PF_6]^{7+}$). Interestingly, M_2L_3 and M_4L_6 complexes incorporating quaterpyridines **III** and **IV** are fluorescent. With respect to the latter, on interaction with BPh_4^- the larger tetrahedron, $[Fe_4(\mathbf{IV})_6]^{8+}$, yields a change in fluorescence (a fluorescent signal). These observations suggest that complexes incorporating ligands **III** and **IV** might find application as fluorescent sensors.

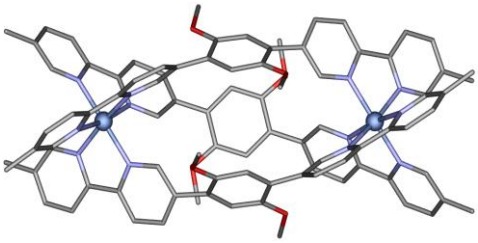

$[Ni_2(\mathbf{III})_3]^{4+}$

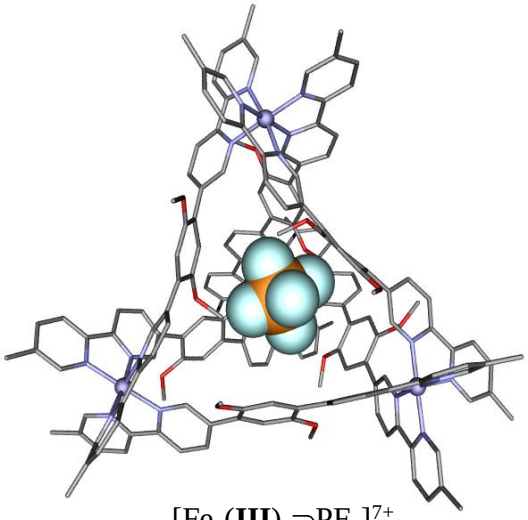

$[Fe_4(\mathbf{III})_6 \supset PF_6]^{7+}$

The isolation of a number of interesting M_2L_3 and M_4L_6 complexes led to the possibility that analogous metal-directed assembly procedures employing appropriately substituted quaterpyridines, related to **III** and **IV**, might allow for the metal-template synthesis of dinuclear cryptates and larger tetranuclear polycyclic species. With this in mind a number of bipyridyl and quaterpyridyl derivatives were synthesized with salicyloxy functionality to allow for subsequent reductive amination procedures. In this regard, dialdehydes **V** – **VII** were synthesised and reacted with Fe(II) in a 2:3 ratio. The resulting products were characterised by NMR and ESI-HRMS, revealing a series of M_2L_3 and M_4L_6 precursor complexes, including $[Fe_4(\mathbf{V})_6](BF_4)_8$, $[Fe_2(\mathbf{VI})_3](PF_6)_8$, $[Fe_4(\mathbf{VI})_6](PF_6)_8$, $[Fe_4(\mathbf{VII})_6](PF_6)_8$ and $[Fe_4(\mathbf{VII})_6](PF_6)_8$. As was the case for the interaction of quaterpyridines **III** and **IV** with Fe(II), the interaction of **VI** and **VII** with Fe(II) yielded mixtures of M_2L_3 and M_4L_6 complexes; the product ratio of which could also be controlled.

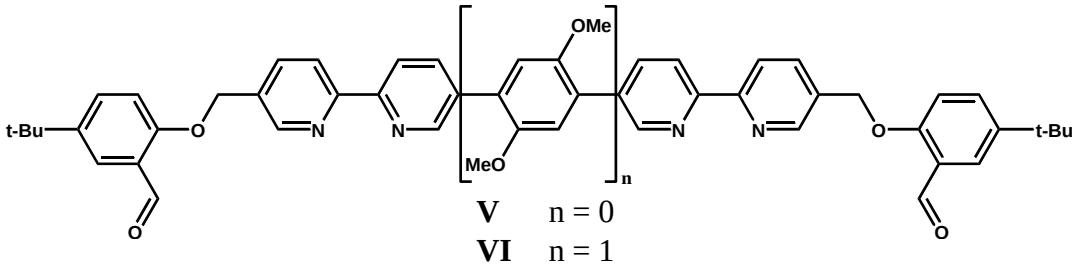

V n = 0
VI n = 1
VII n = 2

Preliminary experiments revealed that reductive amination of $[Fe_2(\mathbf{VI})_3](PF_6)_8$ using NH_4OAc and $NaCNBH_3$ in acetonitrile yields the dinuclear cryptate $[Fe_2(\mathbf{L}^1)](PF_6)_8$ ($\mathbf{L}^1$ = the corresponding cryptand). Reductive amination of the precursor complexes $[Fe_4(\mathbf{V})_6](BF_4)_8$ and $[Fe_4(\mathbf{VII})_6](PF_6)_8$ under these same conditions revealed the production of the unique tetranuclear polycyclic species $[Fe_4(\mathbf{L}^2)](BF_4)_8$ and $[Fe_4(\mathbf{L}^3)](PF_6)_8$ ($\mathbf{L}^2$ and $\mathbf{L}^3$ = the corresponding metal-free polycyclic ligands). The successful syntheses of the latter species required a total of twelve successive *in situ* imine condensation/reduction reactions from a total of fourteen components.

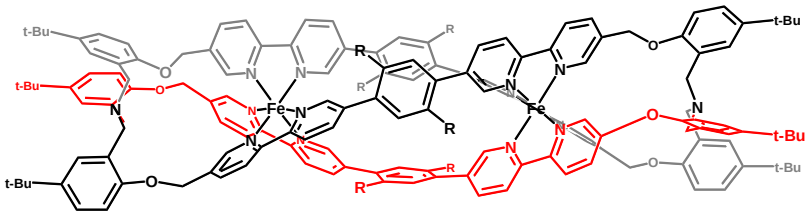

$[Fe_2\mathbf{L}^1]^{4+}$

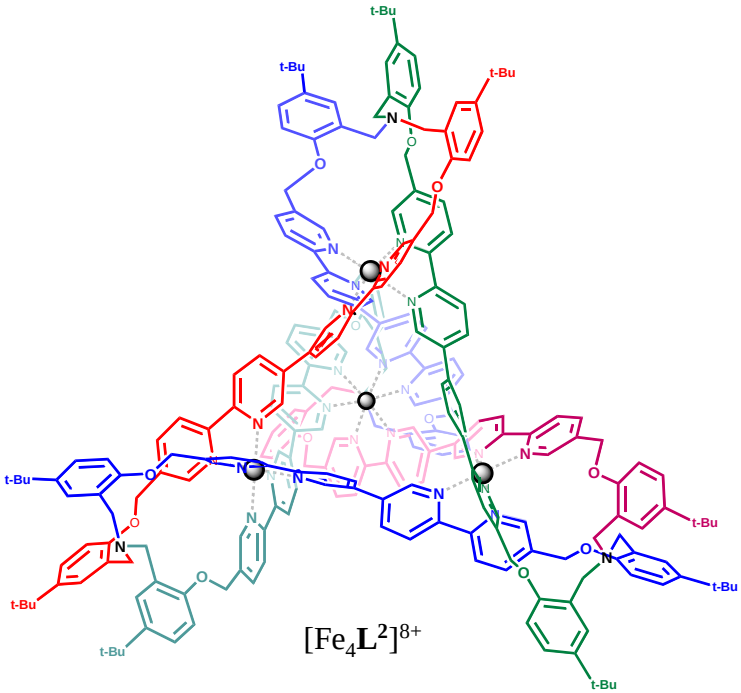

$[Fe_4\mathbf{L}^2]^{8+}$

Table of Contents

Chapter 1

Introduction

1.1 UBIQUITOUS SUPRAMOLECULAR CHEMISTRY

Broadly speaking, the field of supramolecular chemistry embodies molecular structures that are defined by relatively weak and reversible non-covalent bond formations.[1,2] These may include hydrogen bonding, hydrophobic forces, van der Waals forces, π-π interactions, electrostatic effects and metal coordination. In natural biological systems there are many examples of supramolecular aggregates, from the relatively simple lipid bilayers through to the more complex photosystems and electron transfer systems. In fact research in the field of supramolecular chemistry was and is still inspired by nature's ability to synthesize such non-covalent functional aggregates.

Relatively weak non-covalent interactions allow natural systems to employ a synthetic strategy that characteristically results in the thermodynamically most favourable outcome, thus tending towards defect free self-healing behaviour. This strategy is of course known as *"molecular self-assembly"*. Adapted to artificial systems, molecular self-assembly may be viewed as a synthetic strategy that involves designing molecules so that their shape and respective functional complementarities cause system component(s) to spontaneously aggregate into desired supramolecular assemblies. Indeed, as the sensible limits of traditional synthetic methodologies are reached in terms of structural dimension and functionality, molecular self-assembly offers an avenue to develop increasingly large and well organised aggregates with defined function. This realisation provides a strategic basis validating research into the field of nanotechnology in all of its guises.

Molecular recognition is one of the key features influencing molecular self-assembly. This is elegantly demonstrated in many natural supramolecular structures, including enzyme substrate complexes, proteins, sugars, DNA and RNA. An excellent example of complementary molecular recognition is that of double stranded DNA. In this case matched base pairs (complementary base pairing) on adjacent strands lead to complementary hydrogen bonding, and as a consequence, to double stranded DNA with high thermodynamic stability. Other interactions also work to stabilize the double helical arrangement of DNA, such as hydrophobic effects and π-π stacking.

Cooperativity is a phenomenon sometimes observed in supramolecular systems, and an important consideration when rationalizing and predicting supramolecular outcomes in

terms of kinetics and thermodynamics. Cooperativity is often evident in systems that exhibit multiple binding sites that show differential substrate affinity for successive binding events. Positive cooperativity exists when each binding event is favoured by the previous binding event. The classic biological example of positive cooperativity is the binding of oxygen to haemoglobin. Opposing positive cooperativity is negative cooperativity, e.g. successive binding events are disfavoured by the previous binding event. As might be expected, non-cooperative behaviour may also occur where separate binding events occur independently of each other.

The supramolecular chemistry concepts briefly outlined above based on natural examples, are directly transferable to artificial systems and, as such are of key importance to our ability to both understand and control systems of the latter type.

1.2 METALLOSUPRAMOLECULAR CHEMISTRY

Metallosupramolecular chemistry is the branch of supramolecular chemistry that utilizes metal to ligand coordination interactions as structural components.[3-14] The long history of coordination chemistry provides an extensive source of structural and physical data and has enabled the rational design of numerous metallosupramolecular assemblies possessing interesting structural, chemical and physical properties.[1,3-16] These include both well defined discrete and polymeric assemblies. Some well known categories of discrete assemblies include metallocycles,[17-20] helicates,[14,21-23] cages (tetrahedra,[24-28] cylinders,[29] and an extended range of other polyhedral structures),[18,19,24,25,27,29-31] grids,[14-16] rotaxanes[32-35] and catenanes.[32-35] Among the polymeric materials, metal organic frameworks (MOFs) have attracted a great amount of interest over recent years.[36,37] Indeed both discrete and polymeric metallosupramolecular assemblies have been shown to exhibit interesting optical, magnetic,[16] photoactivity,[32,38] electrochemical,[32] catalytic[39-41] and host-guest behavior.[39-42]

One of the most attractive features of incorporating metal coordination into self-assembly systems, over other weaker interactions, is the relative predictability of such interaction.[43] Furthermore, while purely carbon based molecular frameworks are limited to linear, trigonal and tetrahedral geometries, metal ions may allow access to a larger set of predictable geometries. These include linear, trigonal, tetrahedral, square planar, square

pyramidal, octahedral and more. Thus, for example d^{10} metal ions such as Cu^{+} and Zn^{2+} tend to give rise to tetrahedral complexes when 4-coordinate, while first row d^6, d^7 and d^8 in their high spin states most often yield octahedral complexes. However, as is often the case, these general rules can be broken.

Ligand design is of fundamental importance in metallosupramolecular chemisty.[4, 44-47] The discovery and rationalisation of the so-called chelate, macrocyclic, and cryptate effects have continued to inspire the use and development of ligands that exhibit such characteristics. In general, ligand systems resulting in these effects often lead to more predictable complexation behaviour and exhibit greater stability compared to their monodentate ligand counterparts. The discussion below will focus mainly on polypyridyl derivatives incorporating 2,2'-bipyridine to illustrate some important considerations for the rational design and synthesis of metallosupramolecular assemblies.

1.3 POLYPYRIDYL LIGANDS† – GENERAL CONSIDERATIONS

Polypyridyls and related ligand systems have been employed in metallo-supramolecular chemistry since the latter's emergence as a widely studied area of chemistry about 35 years ago. The continued popularity of pyridyl-containing building blocks is perhaps not surprising when one considers that the simpler systems bipyridine and terpyridine, along with their parent pyridine, are all excellent metal coordinating agents and have been intensively studied from the early days of coordination chemistry. As a consequence, there is a very large amount of 'simple' metal ion coordination chemistry involving these ligands available in the literature. This has acted as a foundation upon which both the design and synthesis of new extended metallo systems incorporating di-, tri- and polypyridyl components has taken place.

The aim of the discussion presented below is to provide an overview of representative studies in the metallosupramolecular area involving mostly linear (that is, non-branched) pyridyl-containing ligand derivatives. However, the discussion will start by considering some general features of the 2,2'-bipyridyl ligand and its coordination chemistry. As well, some

† Parts of this section, in particular ***1.2.2 Helicates***, are taken from a review article14. C. R. K. Glasson, L. F. Lindoy and G. V. Meehan, *Coord. Chem. Rev.*, 2008, **252**, 940. published by the candidate and the candidate's supervisors Prof. L. F. Lindoy and Prof. G. V. Meehan.

contemporary work is included in order to illustrate that the chemistry of 2,2'-bipyridyl derivatives continues to evolve. A short discussion on helicates with some fundamental background on self-assembly processes and selected innovations that have driven progress in this field will be presented. Lastly, a brief coverage of dynamic metallosupramolecular systems is included.

1.3.1 2,2'-Bipyridine as a ligand

2,2'-Bipyridine has proven to be one of the most versatile ligands in coordination chemistry owing to its ability to coordinate to most metals in the periodic table.[47-49] Of particular importance to its incorporation into multitopic ligand designs is the predictable way in which 2,2'-bipyridine and its substituted derivatives form chelates, thus allowing freedom to concentrate on other ligand design aspects. Furthermore, transition metal complexes of 2,2'-bipyridine derivatives often exhibit interesting redox and photochemical properties,[38,50,51] allowing for such properties to be incorporated into corresponding metallosupramolecular assemblies.[32]

The symmetry of bidentate ligands is a potentially important consideration as it may have a bearing on the number of stereoisomers that may be obtained for homoleptic octahedral metal complexes. For example, the reaction of an octahedral metal ion with a symmetrical ligand, such as 2,2'-bipyridine, in a 1:3 ratio, respectively, will normally result in a racemic mixture of optical (Δ and Λ) isomers (***Figure 1.1*** a)). However, the reaction of an octahedral metal ion with an unsymmetrical ligand, such as 5-methyl-2,2'-bipyridine, will give mixtures of geometric (*mer* and *fac*) (***Figure 1.1*** b)) and optical isomers, thus leading to a mixture consisting of four isomeric products. In fact if statistics alone were to govern the outcome of the latter reaction, a 3:1 ratio of the *mer* to *fac* isomers would be expected, with each of these geometric isomers consisting of a racemic mixture. The implications of this possibility are unfortunate if, for example the desired product is the Δ-*fac* isomer (e.g. with a statistically based theoretical yield of 12.5 %). In relation to this, steric[52] and electronic effects[53-55] usually alter the statistically expected ratio of stereoisomeric products.

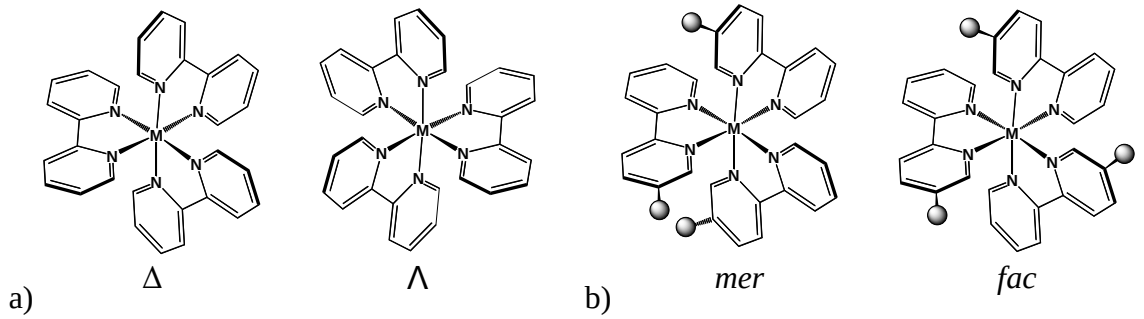

Figure 1.1 Stereoisomers of tris-bipyridyl octahedral metal complexes from, a) symmetrical 2,2'-bipyridine (Δ and Λ optical isomers), and b) unsymmetrical 5-methyl-2,2'-bipyridine (*mer* and *fac* geometrical isomers).

Steric effects may allow a certain level of control over stereochemistry in both bis-chelate tetrahedral and tris-chelate octahedral complexes, thus having important implications for metallosupramolecular design. For example, the *mer*/*fac* isomeric ratio of tris-chelate octahedral metal complexes may be altered by the use of ligands with bulky substituents which leads to an increased expression of the *mer* isomer. In this regard, Fletcher *et al.* reported[52] the exclusive production of the *mer* isomer in the resulting tris-chelate complex from a reaction of $RuCl_3$ and 5-(2,2-dimethylpropyl)-2,2'-bipyridine in a 1:3 ratio. Furthermore, such substituent steric effects will be position dependent. For example, in 2,2'-bipyridines substituent steric interactions are maximised in the 6- and 6'- positions and minimised in the 4- and 4'- positions. In fact 6,6'-disubstituted 2,2'-bipyridines generally do not form stable tris-chelate octahedral complexes.

An elegant application of steric interactions is that of chiral induction which may be achieved by appending chiral functional groups to a ligand chelate.[56,57] For example, the synthesis of tris-chelate complexes using bis-pinene **1** with Fe(II) led to a diastereomeric excess (*de*) in favour of the Δ-$[Fe(\mathbf{1})_3]^{2+}$ (**2**).[58] Interestingly, reaction of **1** with $Ru(DMSO)_4Cl_2$ led to a reversed *de* in favour of Λ-$[Ru(\mathbf{1})_3]^{2+}$. However, if the two Cl^- groups are substituted by another equivalent of **1** using the enantiomerically pure Δ or Λ-$[Ru(\mathbf{1})_2Cl_2]$ under mild conditions, approximatedly 100% Δ or Λ-$[Ru(\mathbf{1})_3]^{2+}$ is isolated, respectively. It should be noted that while tris-chelate octahedral complexes are inherently chiral, bis-chelate tetrahedral complexes are achiral using symmetrical bidentate chelating ligands. However, the use of an unsymmetrical bidentate chelating ligand leads to mixtures of Δ and Λ

enantiomers. Furthermore, by using unsymmetrically substituted bipyridines incorporating chiral substitutents the chirality at the metal centre may sometimes be controlled.

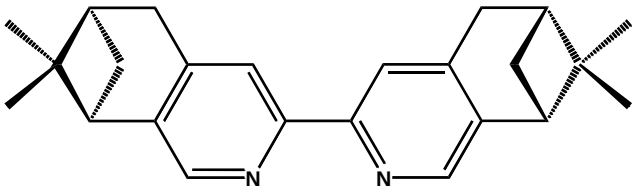

1

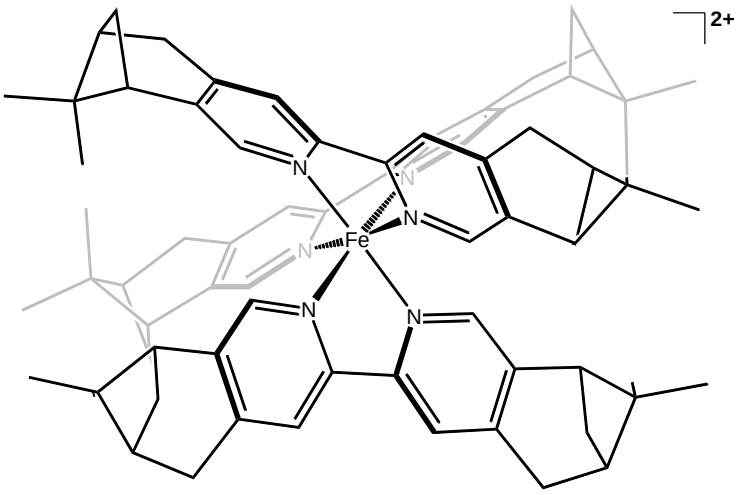

2

Other interactions that may influence chiral induction in the formation of enantiomerically pure tris-bipyridyl complexes include hydrogen bonding, electrostatic and van der Waals interactions as well as solvation effects. In this regard, Williams *et al.* reported[59] the thermodynamically controlled diastereospecific formation of Δ-[Fe(**3**)$_3$]$^{2+}$ (**4**) from bis-(L-valine)-bipyridyine **3**. The crystal structure of this material revealed a unique type of trinuclear triple helicate where two Cl^- anions and the Fe(II) metal centre represent a pseudo-*C3* axis. The structure is held together by coordinate bonds between the iron and the bipyridine chelates as well as by hydrogen bonds and electrostatic interactions between the chlorides and the protonated amino residues on the ligand. Using the N-methyl-L-valine methyl ester analogue of **3** it has subsequently been demonstrated that the observed

stereoselectivity is pH dependent.[60] Thus, acidic pH led to complete diastereoselectivity whereas basic pH led to incomplete diastereoselectivity. In related systems *de* has been measured as a function of the solvent employed.[61] Equilibration in acetone led to a higher *de* than in methanol which competes with the formation of hydrogen bonds between the Cl^- anion and the protonated amino residues.

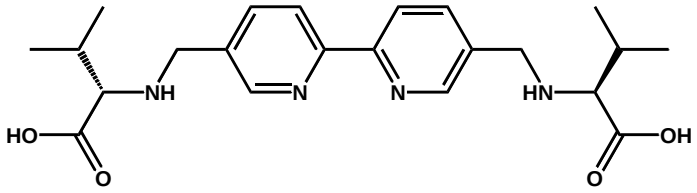

3

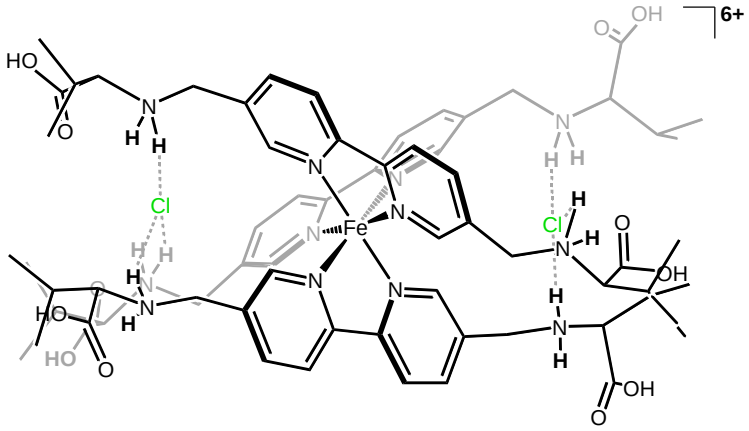

4

1.3.2 Helicates

Transition metal helicates, many incorporating polypyridyl and related ligands[62-72] have been investigated for many years and have played a central role in the development of metallosupramolecular chemistry. Clearly, the importance of self-assembled helical structures in biology has provided both a motivation and inspiration for the study of synthetic systems of this type and aspects of the chemistry and properties of helicates have been reviewed over recent years.[14,21-23,73-78]

Helical metallo-structures ranging from simple single-stranded[79-87] structures through to four-stranded systems[88] are known. Typically, the single-stranded systems are mono- or dinuclear complex species incorporating a variety of ligand types. While the vast majority of helical structures so far reported are linear in nature, less-common examples of circular helicates, in which the metal ions are arranged in a cyclic array (for example, to form a polygonal 'core' of the helix) are also known.[89-95]

Over the years, particular emphasis has been given to the synthesis and properties of double and triple helicates. Clearly a number of design aspects need to be considered in order to successfully generate such arrangements.[14,21-23,45,56,57,96] For example, the number of ligand strands able to coordinate to a given metal centre is determined by the latter's potential coordination number and the 'dentate' nature of the individual metal binding domains along each strand. Four coordinate (tetrahedral) metal centres will be required to combine with bidentate domains to yield two-stranded helices (assuming that all sites are solely occupied by donors from the ligand domains), whereas six-coordinate metals will potentially yield three stranded systems with such a ligand type. If solely tridentate domains are present, then the use of an octahedral metal will generate a two-stranded system. For the above to occur, the ligand strands will normally need to be sufficiently flexible to allow strong metal-domain binding along each ligand's backbone but rigid enough to restrict conformations that may favour non-helicate arrangements.

For helicate formation each metal centre will adopt a similar screw sense; for symmetrical metal helicates incorporating non-chiral ligand strands, a racemic mixture will normally result (the right-handed form designated *P* and the left-handed one *M*). The alternative situation where the optical activity of the metal centres is opposed corresponds to a meso (Δ,Λ) structure and, as implied above, this does not represent a true helicate.

1.3.2.1 Double and triple helicates – design principles

As an extension of earlier studies on the mechanism of helicate formation, Lehn *et al*.[96,97] investigated the kinetic behaviour of double stranded helicate formation involving oligobipyridine ligands of type **5** and showed that products of type $[Cu_3(\mathbf{5})_2]^{2+}$ form, with the kinetics of formation being strongly influenced by the nature of the substituents present. It

was postulated that positive cooperativity occurs for metal binding in such cases leading ultimately to favourable near-tetrahedral coordination around each metal centre. However, subsequently it was shown that positive cooperativity does not occur for such helicate formation and that negative cooperativity in fact appears commonly to occur.[74,76,98-106] Thus, in 2003, Ercolari[99] observed that the previous methods employed to assess cooperativity in such helicate (and also ladder) self-assembly, namely the use of classical Scatchard and Hill plots, were inappropriate because they are only valid when intermolecular binding of a monovalent ligand occurs to a multivalent receptor - this condition is not met in the earlier analysis of helicate formation. Ercolari developed a procedure for the analysis of self-assembly of the above type which included both intermolecular and intramolecular aspects of the assembly process; no evidence for positive cooperativity was then obtained. The original criticism was further theoretically justified by Borkovec *et al.*[98] using statistical mechanics. In more recent work a non-linear (non-statistical) Scatchard-like procedure has been developed for describing metal-binding in the formation of double-stranded helicates.[102] Application of this new procedure to several polymetallic helicates revealed the presence of negative cooperative processes that were attributed mainly to arise from intermetallic repulsions. A procedure for the semi-quantitative estimation (and prediction) of the contribution of intermetallic repulsion to the total free energy of a discrete polymetallic assembly in solution has also been the subject of a recent report.[107]

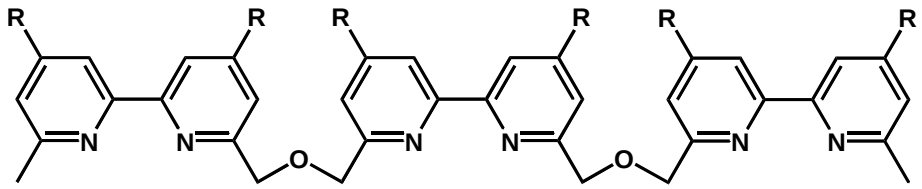

5; L^1, R = $CONEt_2$ and L^2, R = CO_2Et

Thermodynamic and kinetic aspects of the self-assembly of an Fe(II) triple-stranded helicate incorporating a bis(2,2'-bipyridine)diamide propyl-linked derivative have also been investigated in methanol using a combination of electrospray mass spectrometry, potentiometry, spectrophotometry and dissociation kinetics.[63] Three iron(II) complexes, one mononuclear $(FeL_2)^{2+}$ and two dinuclear $(Fe_2L_2)^{4+}$ and $(Fe_2L_3)^{4+}$, species were observed to

occur in solution. Their respective structures were inferred from the (low) spin state of the iron(II) centres as well as from ^{1}H NMR measurements and molecular modelling. In the presence of excess ligand the mechanism for helicate formation was proposed to involve a stepwise wrapping of three bipyridine domains from different ligand strands around a single iron(II) followed by coordination of the second iron(II) to the three resulting pendant bipyridyl entities.

An early investigation by Lehn *et al.*[108] demonstrated the occurrence of self-recognition in the assembly of helicates. This study showed that mixtures of oligo-2,2'-bipyridyl ligands of different strand length failed to form heteroleptic double- and triple-stranded helicates with copper(I). Instead, homoleptic assemblies were generated. Subsequently there have been a considerable number of other studies also aimed at investigating self-recognition processes in the self-assembly of double- and triple-stranded helicates.[14,21,22,75,109-113]

As expected, 'simple' homoleptic double stranded species were obtained when each of **6** – **9** were reacted with Cu(I); namely, **6** and **7** each yielded $[Cu_3L_2]^{3+}$ complexes while **8**

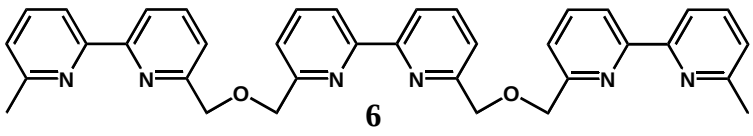

6

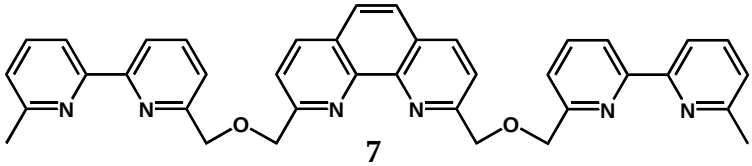

7

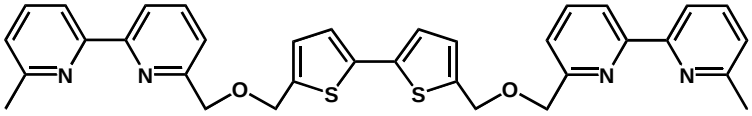

8

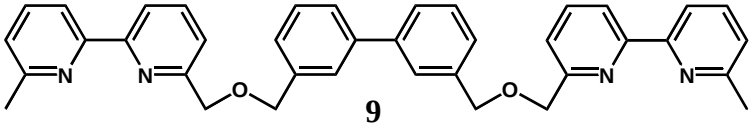

9

gave two complexes of this stoichiometry and **9** gave at least two complexes of type $[Cu_2L_2]^{2+}$.[114] As might be predicted, the differences in the potential shifts obtained in electrochemical studies on a selection of these complexes were found to be in accord with the

central copper(I) ions being bound more strongly than the terminal ions. NMR studies were employed to investigate the speciation that resulted when copper(I) was interacted with mixtures of the above ligands of different strand length. Interestingly, when a mixture of **8** with **6** or **7** was used for helicate synthesis, only homoleptic double-stranded species were formed in solution; when **6** was present with **7**, then the corresponding helicate distribution seemed to follow simple statistics. The reasons for the different behaviour in this latter case are not clear but likely have their origins in the presence of different inter-strand interactions occurring between the respective ligand systems.

Combinations of tridentate (terpyridine, T) and bidentate (bipyridine, B) subunits have been incorporated in strands to give a set of tritopic ligands suitable for double helicate formation with appropriate metal ions. Four ligand strands BBB (**6**), BBT (**10**), TBT (**11**) and TTT (**12**), were synthesised.[23] These were used to form both homo- and hetero-stranded

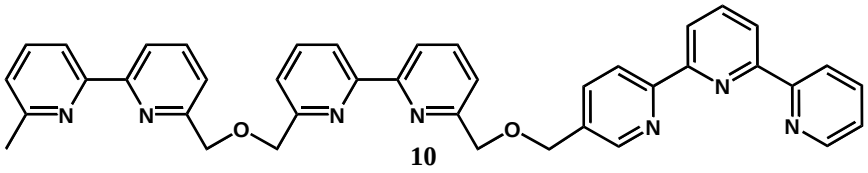

10

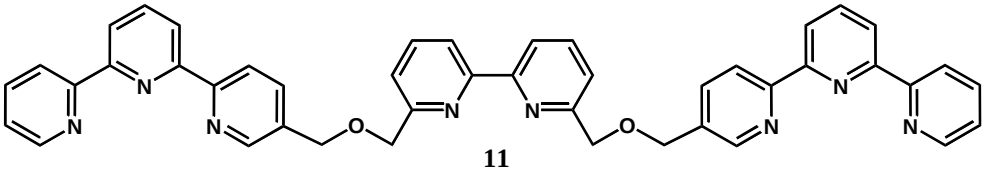

11

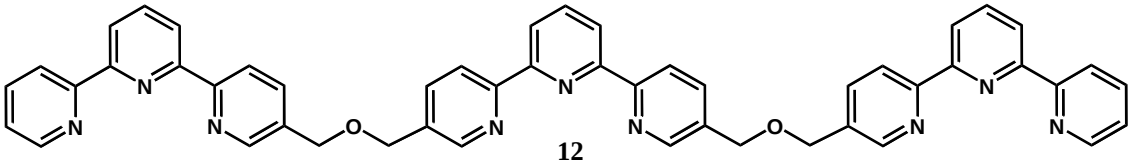

12

helicates incorporating both single- and mixed-domain metal binding sites, depending on the coordination properties of the metal employed. In general, these helicates were found to correspond to systems in which donor-site domain pairing occurred that corresponded to BB, BT, and TT pairs for tetra-, penta-, and hexacoordinate copper(I), copper(II) and zinc(II) cations, respectively. The study demonstrates how ligand and metal ion properties may be collectively employed to influence the nature of individual heterometallic helicates generated.

^{1}H NMR diffusion spectroscopy (diffusion ordered spectroscopy, DOSY)

experiments have been employed to probe the translational diffusion coefficients of homologous series of copper(I) and silver(I) double stranded helicates of type $[M_nL_2]^{n+}$ in acetonitrile solution (where n = 1-5 and L is a range of oxy-bridged polypyridyl ligands that include **5, 6** and **10** together with related derivatives of different strand lengths).[115] An aim of these studies was to correlate the length and bulkiness (in some cases reflecting the presence of substituent's on the periphery of the respective ligands) with the solution diffusion behaviour. The experiments were successful in yielding information concerning the dimensions of the respective helicates when present in solution both individually and as mixtures. With respect to the latter, it was confirmed that a mixture of helicates from the same series, but of different length and nuclearity, gave signals corresponding to homo-stranded helicates corresponding to each component. There was no evidence of 'cross-binding' of ligands of different length under the conditions employed. Apart from the above, helicate formation by other linear ligands incorporating 2,9-disubstituted-1,10-phenanthroline moieties have also been reported.[116-118]

X-ray diffraction studies show that both the thiazole-containing ligands **13** and **14** readily form double helicates of type $[Cu_2(L)_2]^{4+}$ in which both ligands only use their two terminal bidentate (N,N-binding) domains for coordination to copper(II).[119] In the case of **13** this results in two four-coordinate copper(II) centres, with two non-coordinated pyridyl residues present in the centre of each structure; these pendant pyridyl residues are directed towards each other to give a potentially two-coordinate cavity between the metal ions in the centre of the helicate (***Figure 1.2***). Similarly, in the corresponding structure derived from **14** the copper(II) ions are four-coordinate, with each ligand having its central bipyridyl unit uncoordinated. This in turn results in a potentially four-coordinate cavity between the two metal centres. While, in principle, the use of **14** could result in the formation of three potentially bidentate compartments and hence lead to a trinuclear double helicate with all three bidentate sites occupied, no such complex was able to be isolated. It was suggested by the authors that, in part, the trinuclear structure may be disfavoured due to the electrostatic barrier resulting from three dipositive metal ions being located close together. The Cu-Cu separation in the dinuclear helicate is 4.746 Å and insertion of an additional copper ion would result in very close metal–metal contacts.

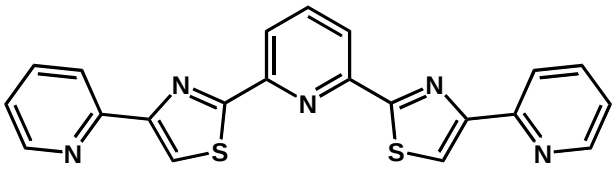

13

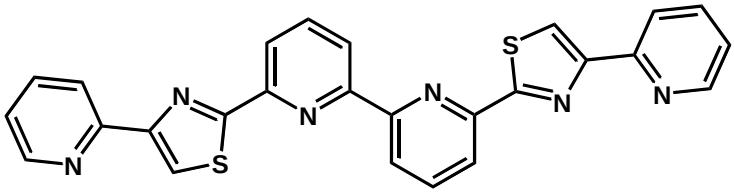

14

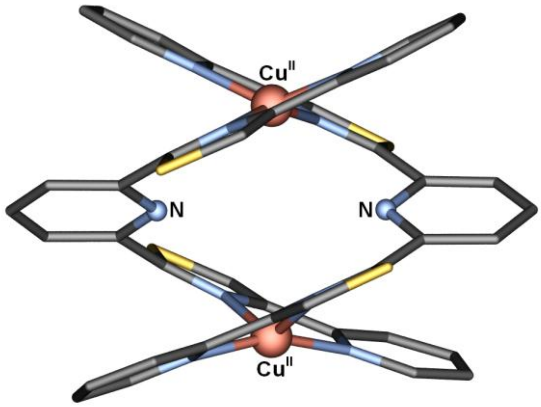

Figure 1.2 View of the $[Cu_2(\mathbf{13})_2]^{4+}$ cation showing the potentially two-coordinate cavity.[119]

1.3.2.2 Chiral induction in helicates

As mentioned earlier (page 9), the use of achiral ligands for helicate formation normally leads to a racemic mixture of products. To generate enantiomeric (*P* or *M*) helicates, a chiral element (chiral auxiliary) usually needs to be present.[56]

Provided the systems are sufficiently kinetically inert, it is sometimes possible to separate enantiomers by conventional resolution procedures such as chromatography on a chiral column (or fractional crystallisation in the case of charged helicates after addition of a homochiral counterion). For example, the racemic dinuclear triple helicate $[Fe_2(\mathbf{15})_3]^{4+}$ is readily resolved using the chiral tris(tetrachlorobenzenediolato)-phosphate(V) TRISPHAT anion.[120] For charged helicates, the configuration adopted may in some cases be controlled

through ion pair formation through the addition of a chiral counter-ion to the reaction solution. Thus, the TRISPHAT anion behaves as an efficient asymmetric directing unit that efficiently controls the configuration of a cationic dicobalt(II) triple helicate, $[Co_2(\mathbf{15})_3]^{4+}$ yielding a *de* of up to 82%.[121] In a prior study[120] it was demonstrated that the enantiomeric purity of the analogous racemic helical $[Fe_2(\mathbf{15})_3]^{4+}$ cation[122] can be efficiently measured using ^{1}H NMR by employing the TRISPHAT anion as a chiral shift reagent.

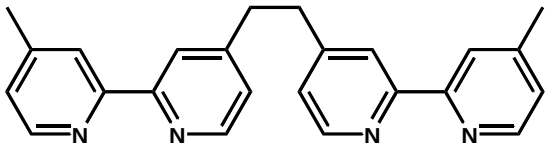

15

The most common strategy for obtaining single-handed helicates has been to incorporate stereogenic elements in the backbones of the ligand strands employed for their synthesis. That is, the presence of one or more chiral centres in the ligand gives the prospect that selective, complementary aggregation of like-handed ligands will occur during helicate assembly. Using such a strategy, the enantioselective syntheses of a considerable range of chiral helicates have now been performed.[123-125] In particular, a large number of pyridine and bipyridine derivative ligands that are chiral through incorporation of structural fragments derived from enantiopure terpenes have been reported by von Zelewsky *et al.* and the use of such systems in metal ion studies was reviewed[56] in 2003. Members of the above ligand family[126,127](and ref therein) have been named CHIRAGENs and have been employed for the synthesis of both linear and circular helicates with predetermined configurations. Examples of this ligand type are given by **16** (5,6-CHIRAGEN[*p*-xylyl]) and **17** (4,5-CHIRAGEN[*m*-xylyl]). Series of related chiral species incorporating, for example, a central pyrazine ring connected to peripheral pyridine or bipyridine moieties, providing bipyridine- and terpyridine-like binding sites, have also been reported.[128] In early work the chiragen **17** was shown to undergo an enantioselective self-assembly process with tetrahedral Cu(I) or Ag(I) to yield circular hexanuclear (double stranded) helicates, each exhibiting C_6-symmetry axes.[92] circular dichroism (CD) spectroscopy confirmed that the configuration of the resulting helix was predetermined by the chiral pinene groups present in the ligands. Chiragen **17** was also shown to interact with labile octahedral metal ions to yield dinuclear helicates of M_2L_3

stoichiometry.[129]

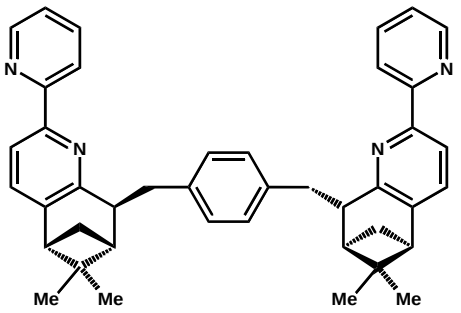

16

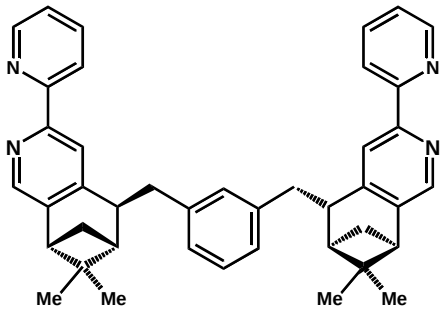

17

Recently, von Zelewsky *et al.*[130] employed the optically pure (-)-L form of **16** for helicate formation. Reaction of a 1:1 mixture of this isomer with copper(I) led to the formation of corresponding hexanuclear circular *P* helicate, $[Cu_6(-)\text{-}\mathbf{16})_6]^{6+}$. An attempted scrambling experiment using a mixture of (+)-**16** and (-)-**16** with copper(I) yielded hexanuclear circular helicates which exhibited complete chiral recognition. The ^{1}H NMR spectrum showed resonances similar to those for $[Cu_6(-)\text{-}\mathbf{16})_6]^{6+}$ and CD spectroscopy revealed that the resulting product was a racemic mixture. Clearly, no mixing of the (+) and (-) ligands occurs upon complexation in this case. The corresponding *meso* ligand, which is composed of one (*RR*) and one (*SS*)-pinene- substituent, was also reacted with both Cu(I) and Ag(I). In contrast to the above, the self-assembly products from these reactions are polymeric. This result exemplifies the dominating role that chiral centres may have on the nature of self-assembly processes of the present type.

Fletcher *et al.*[131] have also synthesised enantiomerically pure ligands of type *R,R*-L and *S,S*-L (where L = N,N'-bis(-2,2'-bipyridyl-5-ylcarbonyl)-(1*S/R*,2*S/R*)-(+/-)-1,2-diaminocyclohexane)) via linking two 2,2'-bipyridine units with a resolved (*R,R*)- or (*S,S*)-1,2-diaminocyclohexane unit (see, for example, **18**). The reaction of these ligands with Fe(II), Zn(II) and Cd(II) gave dinuclear triple helicates of types $[M_2(R,R\text{-L})_3](PF_6)_4$ and $[M_2(S,S\text{-L})_3](PF_6)_4$, respectively; a Co(III) complex of type $[Co_2(R,R\text{-L})_3](PF_6)_6$ was also isolated and it was shown by ^{1}H NMR to consist of two diasterioisomers in an approximately 4 to 1 ratio. CD spectroscopy indicated that the *R,R*-L ligand yielded a *P* helicate, while the *S,S*-L ligand gave the corresponding *M* helicate; however, with the labile transition metal ions

it appears that at least two diastereoisomeric forms exist in solution at room temperature. Modelling studies indicate that the energy difference between the *M* and *P* forms is extremely small.

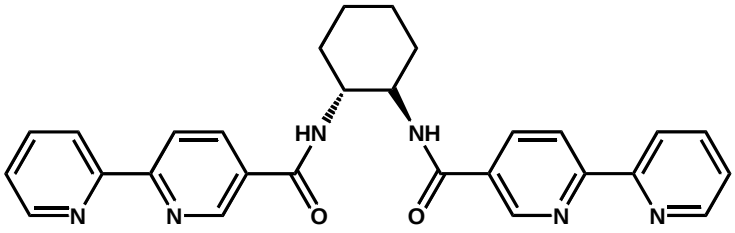

18

The Fletcher group has also reported a new helicate structure that was not accessible by traditional self-assembly procedures. It was obtained in a stepwise procedure by utilising the kinetically inert tripodal metal complex building block, *fac*-tris(5-hydroxymethyl-2,2'-bipyridine)-Ru(II) **19**, as a precursor for the incorporation of additional 2,2'-bipyridine chelating groups in tripodal ligand **20**, followed by coordination to an additional Fe(II) centre in the heterometallic helicate **21**.[132] The introduction of Fe(II), in the final step, led to the formation of heterometallic *meso* and *rac* forms. Thus, it was noted that the ligand was not sufficiently rigid to allow for the Ru(II) centre to direct the helicity at the second metal centre. The isomeric mixture of products was subsequently resolved by cation exchange chromatography allowing characterisation of the *P* (ΔΔ) and *M* (ΛΛ) helicates.

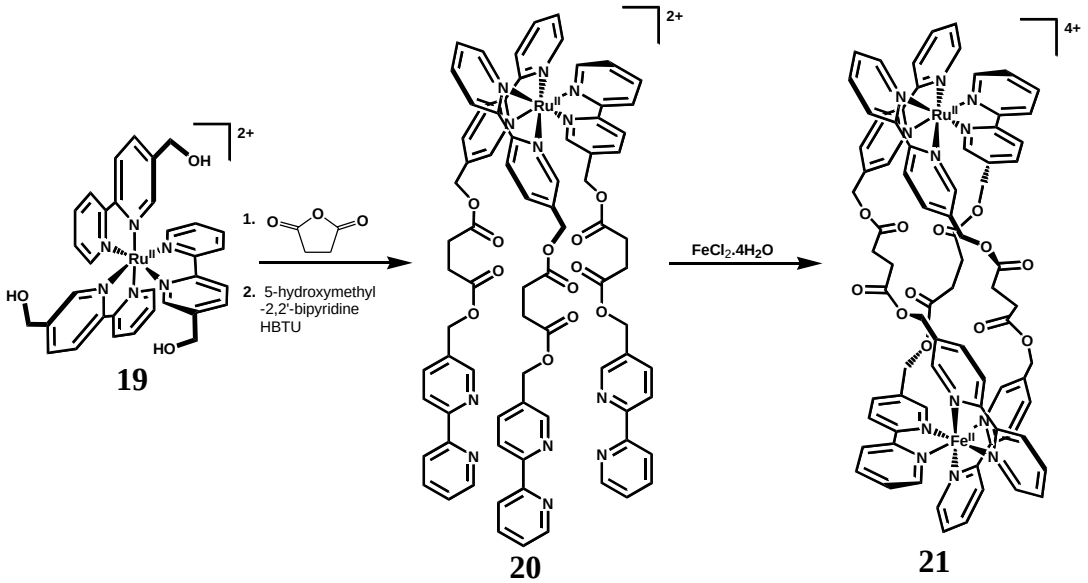

19 **20** **21**

Scheme 1.1[132]

In other studies, the individual ligand strands have been covalently linked by a chiral bridge so that the selective formation of either a *P* or *M* configured helicate is induced.[133] For example, complexation of **22** with $Zn(BF_4)_2$ yields a dinuclear triple stranded helicate whose X-ray structure is shown in ***Figure 1.3***.[134] The latter corresponds to a D_3-symmetric, *P*-configured helicate of type (Δ,Δ)-$[Zn_2(\mathbf{22})_3]^{4+}$.

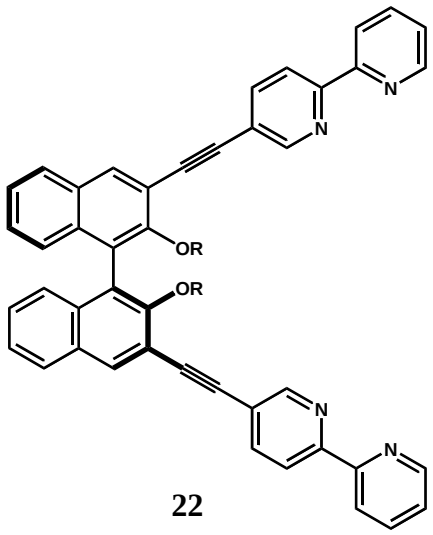

22

(R = methoxymethyl)

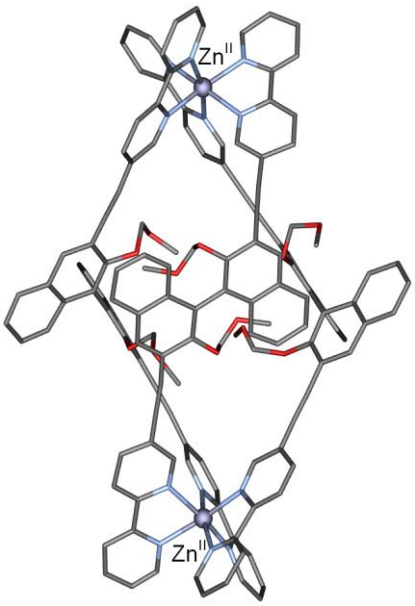

Figure 1.3 X-ray structure of $[Zn_2(\mathbf{22})_3]^{4+}$.[134]

1.4 Linear and Circular Helicates and Polyhedra

The fine interplay between enthalpic and entropic demands in self-assembly processes is often illustrated by the formation of higher order species of the same metal to ligand ratio as for linear helicates. It is noted that, on the one hand enthalpic considerations take into account bonding interactions which may be governed by strain and host-guest interactions, while entropy will tend to favour a larger number of smaller molecular units that fit the specific supramolecular system of interest. Often there is a fine balance between higher and lower nuclearity products leading to highly dynamic systems.

1.4.1 Early reports from Lehn and coworkers

Lehn *et al.*[135] generated an equilibrating mixture of circular inorganic Cu(I) architectures by the interaction of 6,6'''-diphenyl-2,2';5'5";2",2'''-quaterpyridine (**23**) and Cu(I) in a 1:1 ratio (***Figure 1.4*** a)). The major components in this mixture were identified by ESI-MS to fit the general formula $[Cu_n(\mathbf{23})_n]^{n+}$ where n = 2, 3, and 4, consistent with the formation of a dinuclear helicate (**24**), a triangle (**25**) and a square (**26**), respectively. The ^{1}H-NMR spectrum of this material in CD_2Cl_2 gave sharp resonances that indicated the presence of three components. Interestingly, a similar ^{1}H-NMR study in CD_3NO_2 gave a broad averaged set of resonances consistent with equilibration on the NMR timescale. This latter result is a good illustration of the role that solvent choice may play in influencing dynamic processes. X-ray diffraction of crystallised material from this equilibrating mixture resulted in the isolation of the dinuclear copper helicate (***Figure 1.4*** b)). Interestingly π-stacking

a)

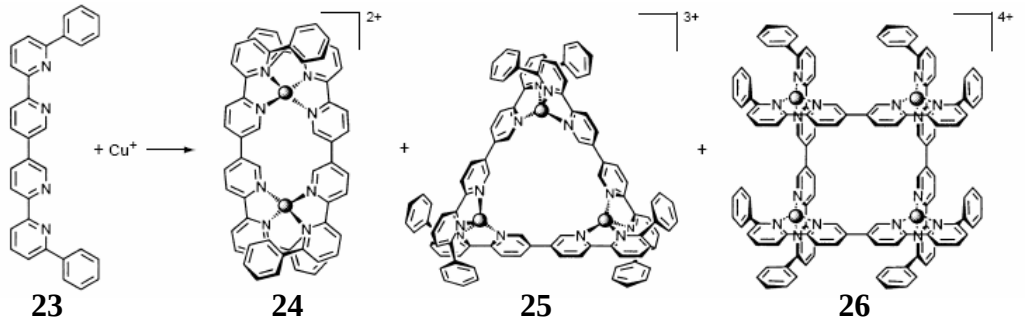

b)

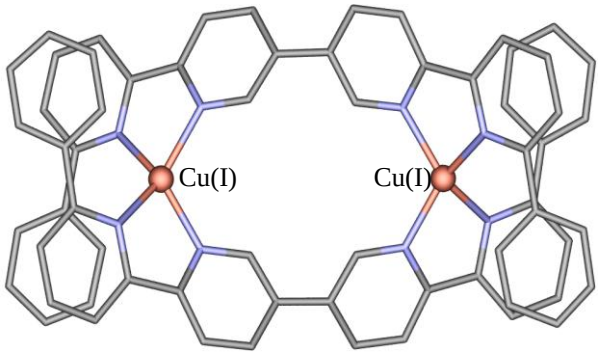

Figure 1.4 a) Schematic representation of the equilibrating mixture of the double-helicate **24**, triangular **25** and square [2 + 2] grid **26** complexes formed from quaterpyridine **23** and CuI; b) X-ray crystal structure of $[Cu_2(\mathbf{23})_2]^{2+}$ (**24**).[135]

interactions contribute to stabilisation of this strained structure, where the quaterpyridyl ligands are curved and the coordination polyhedron of the Cu(I) is distorted such that it lies midway between a tetrahedral and square planar geometry.

A now classical example of thermodynamic control, again reported by Lehn *et al.*,[136] involved the interaction of tris-bidentate hexapyridine **27** and Ni(II) or Fe(II), allowing the isolation of a trinuclear helicate of formula $[Fe_3(\mathbf{27})_3]^{6+}$ (**28**) or the pentanuclear circular helicate $[Fe_5(\mathbf{27})_5\supset Cl]^{9+}$ (**29**) incorporating a guest Cl^- ion. It was reported that shorter reaction times allowed the isolation of $[M_3(\mathbf{27})_3]^{6+}$, indicating that it was a kinetic product, while longer reaction times allowed the isolation of $[M_5(\mathbf{27})_5\supset Cl]^{9+}$ in accord with it being the thermodynamic product. Proposed explanations for the higher thermodynamic stability of $[M_5(\mathbf{27})_5\supset Cl]^{9+}$ over $[M_3(\mathbf{27})_3]^{6+}$ included strain of the bound ligand and/or at the coordination centres in the helicate. Electrostatic interactions with the included Cl^- guest were also implicated. It was noted that $[M_3(\mathbf{27})_3]^{6+}$ does not necessarily lie on the mechanistic pathway to $[M_5(\mathbf{27})_5\supset Cl]^{9+}$ and that preliminary kinetic data indicated that more than one such pathway is present.

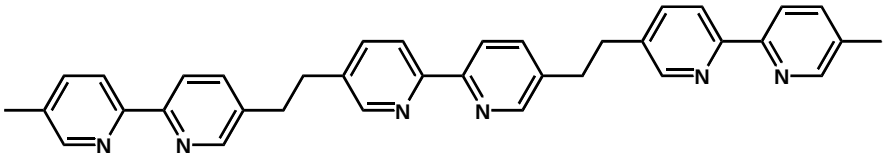

27

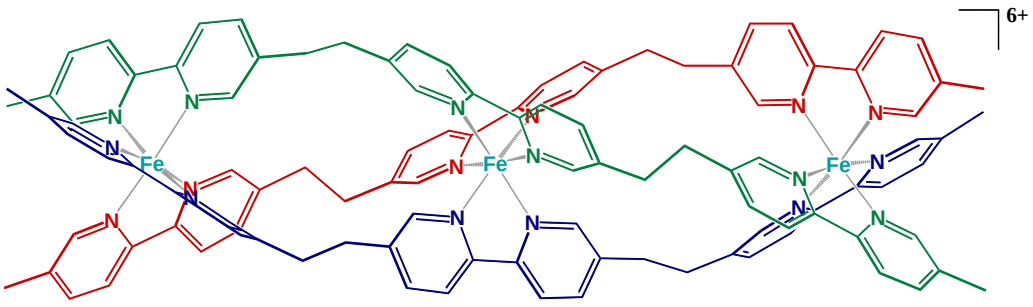

28

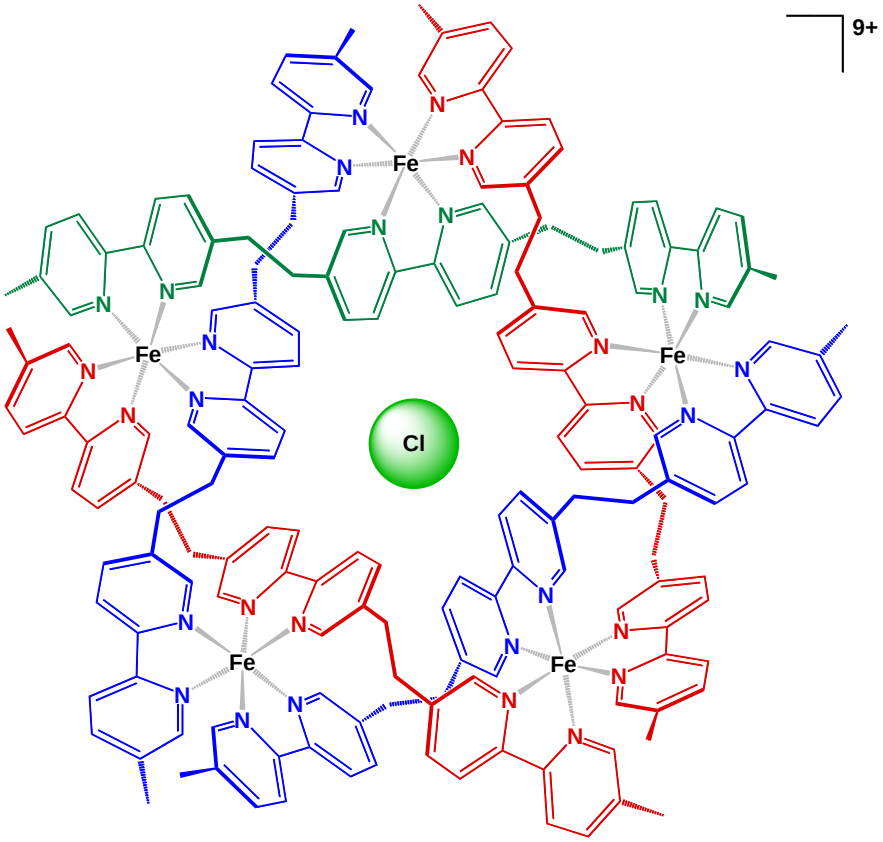

29

In an earlier report,[91] Lehn and coworkers were able to illustrate that the nuclearity of the circular helicates formed with **27** was dependent on the size of the counterion employed. With the smaller Cl^- ion $[Fe_5(\mathbf{27})_5 \supset Cl]^{9+}$ was formed, while with larger counterions, such as SO_4^{2-}, BF_4^- and SiF_6^-, a hexanuclear circular helicate of formula $[Fe_6(\mathbf{27})_6]^{12+}$ resulted. Interestingly the use of Br^-, an anion of intermediate size, gave a 1:1 mixture of $[Fe_5(\mathbf{27})_5 \supset Cl]^{9+}$ and $[Fe_6(\mathbf{27})_6]^{12+}$. The system represents a self-assembled receptor driven by an anion template effect. The 1:1 mixture of Fe(II) and **27** was thus described as a virtual combinatorial library (VCL) of possible receptors (or intermediates) awaiting selection based on the available substrate. To illustrate this, the interchange from one circular helicate to the other was able to be achieved by carrying out an anion exchange from SO_4^{2-} to Cl^-, promoting complete interconversion from $[Fe_6(\mathbf{27})_6]^{12+}$ to $[Fe_5(\mathbf{27})_5 \supset Cl]^{9+}$. Further, in this investigation the bridge between the bidentate chelation domains was lengthened by one sp^3 centre (bridge = CH_2OCH_2; ligand **30**) resulting in the sole isolation of $[Fe_4(\mathbf{30})_4]^{8+}$ circular helicate

regardless of the counterions available. This result was rationalised in terms of the greater flexibility of ligand **30** over **27**, thus promoting less strain in the more entropically favourable tetranuclear complex.

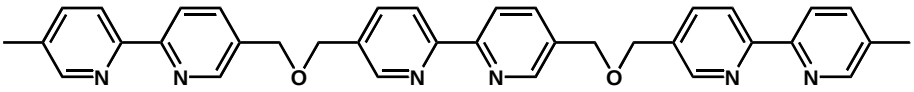

30

1.4.2 Products from the interaction of bis-bidentate ligands with octahedral metal ions

The interaction of octahedral metal ions with linear bis-bidentate ligands has recently been the focus of a number of research groups and has provided excellent insight into the design aspects of higher order metal cluster formation.[4,24-27,137-139] In relation to this, the interaction of two equivalents of an octahedral metal ion with three equivalents of a "linear" bis-bidentate ligand may lead to the formation of complexes that fit the general formula $[M_{2n}L_{3n}]$ {n = 1, 2, 3,…}. Structures of this type include M_2L_3 species (which are often helical), M_4L_6 tetrahedra (often exhibiting interesting host-guest chemistry) and even M_8L_{12} complexes (***Figure 1.5***). Ligand design and the metal ion employed are the major

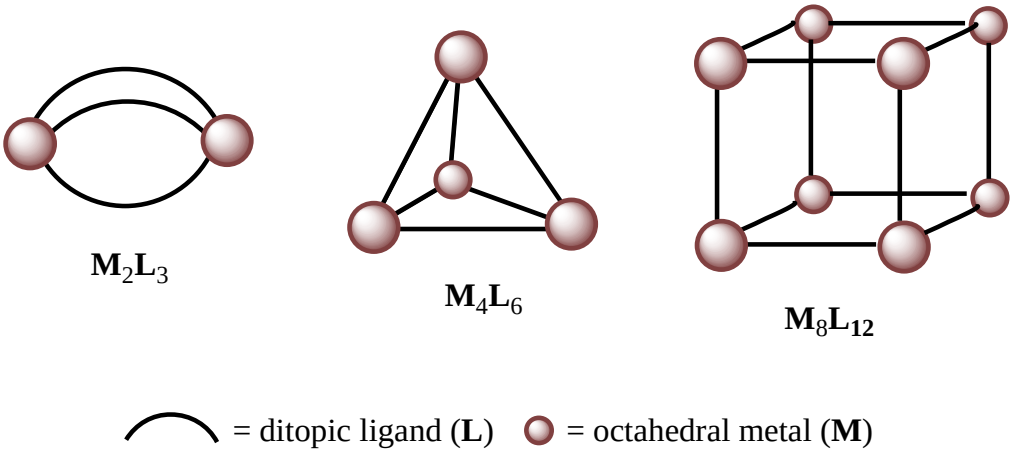

Figure 1.5 Schematic representations of possible structures resulting from the interaction of an octahedral metal ion and a "linear" bis-bidentate bridging ligand in a 2:3 ratio.

contributors to the observed outcome of such metal-directed assembly reactions. However, clearly there are a number of other more subtle influences including guest template effects, secondary interactions (e.g. π-stacking) and solvent effects that may be involved in particular cases.

Raymond and coworkers have designed and synthesized a series of M_4L_6 tetrahedra exhibiting interesting host-guest chemistry.[25,39-42,44,45,86,140-145] For example, they reported[145] the synthesis of the bis(catecholamide) ligand **31**, bridged by a 2,6-diaminoanthracene spacer, and its interaction with Ti(IV) and Ga(III). The reactions were conducted under basic conditions using two different bases, KOH and Me_4NOH. In the reaction using KOH the interaction of two equivalents of a Ti(IV) or Ga(III) salt and three equivalents of bis(catecholamide) **31** led to the formation of M_2L_3 triple helicates (***Figure 1.6***). When this

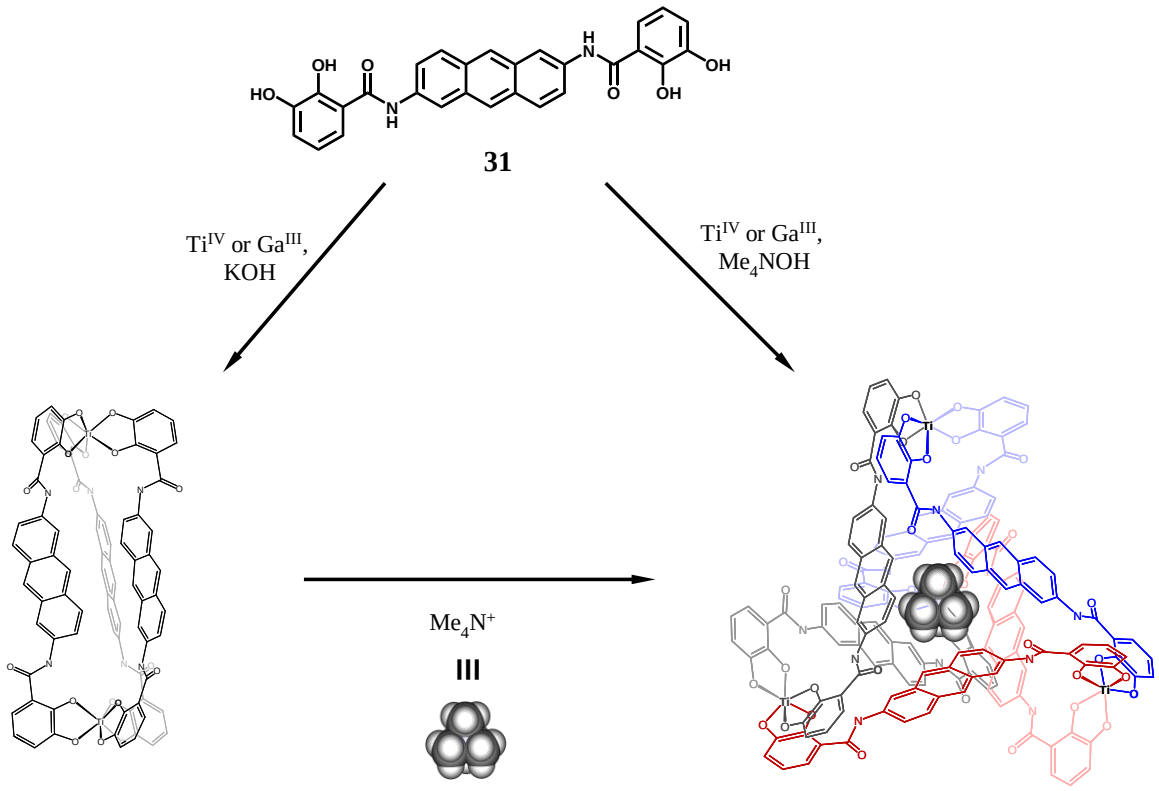

Figure 1.6 A schematic representation of the interconversion of the $[Ti_2(\mathbf{31})_3]^{4-}$ helicate to the $[Ti_4(\mathbf{31})_6 \supset Me_4N^+]^{7-}$ tetrahedral host-guest complex on addition of the guest Me_4N^+.[145]

reaction was repeated using Me_4NOH in place of KOH, M_4L_6 complexes were isolated, each of which encapsulated a Me_4N^+ counterion. It was hypothesized that the formation of the

M_4L_6 host-guest complexes was due to a counterion template effect. This was tested by exposing the M_2L_3 helicate to a Me_4N^+ source and heating the reaction mixture. This promoted the clean conversion of the M_2L_3 species to the M_4L_6 host-guest complex.

In an earlier report Raymond *et al.*[144] also investigated the thermodynamic parameters for host-guest interactions using a similar M_4L_6 host system for which the ligand had previously been designed[142] to favour the above system formation over the corresponding M_2L_3 triple helicate. By calculating association equilibrium constants (K_{eq}) and using van't Hoff plots, the encapsulation process was concluded to be endothermic, with the overall process being entropy driven. Using the Born equation to calculate the free energy of hydration it was argued that the enthalpy of solvation of both the host (bearing a -12 charge) and the guest (bearing a +1 charge) would override the enthalpy gained from the partial charge neutralisation on encapsulation of the guest species. Furthermore, that the positive entropy change on encapsulation of a guest species would be dominated by the desolvation of the host which, based on its approximate 260 Å volume, could hold up to ten water molecules. Attempts to encapsulate a doubly charged guest species were unsuccessful, with it being concluded that the enthalpy of desolvation of the guest was too large in this case, essentially overshadowing the favourable positive entropy term associated with desolvation of the host. The encapsulation was however shown to be dependent on the guest species being charged as isostructural neutral species were not encapsulated, even though they were predicted to be capable of similar van der Waals interactions. However, a subsequent report has indicated that under other conditions non-polar neutral species will occupy the hydrophobic cavity of these M_4L_6 host complexes.[141] As expected, guest encapsulation is limited by the size of the guest cation regardless of the fact that larger ions exhibit lower desolvation enthalpies. In this regard, the M_4L_6 host preferentially binds Et_4N^+ over Pr_4N^+ and shows no affinity for Bu_4N^+.

In a related study, Ward *et al.*[146] investigated the 2:3 interaction of Ni(II) or Co(II) with bis(pyrazolyl-pyridine) **32** (bridged by an *ortho*-xylyl spacer). The FAB mass spectrum of the Ni(II)-containing assembly indicated that an M_2L_3 complex had formed. Interestingly, the X-ray structure of this material did not show the formation of the expected helical structure. Instead, it revealed a complex of type $[Ni_2(\mathbf{32})_3]^{4+}$ (**33**), where two ligands act as tetradentate donors to each of the Ni(II) centres and the third ligand acts as a bridge between

them. The formation of this complex is, at least to some extent, a reflection of the conformational flexibility of **32**. However, illustrating that such metal-directed assembly processes are not necessarily straight forward, the interaction of Co(II) and **32**, in an analogous reaction, led to the isolation of an M_4L_6 complex as its BF_4^- salt. The central cavity of the M_4L_6 host was shown to be occupied by a BF_4^- anion in both the solid state and in solution, thus the product was formulated as $[Co_4(\mathbf{32})_6 \supset BF_4](BF_4)_7$ (**34**). Furthermore, in the absence of the BF_4^- guest the M_4L_6 species was not detected. Consequently it was suggested that the presence of BF_4^- was a crucial element in the formation of the M_4L_6 structure and that it may act as a template for its formation. The formation of the M_2L_3 complex with Ni(II) was rationalised in terms of its smaller ionic radius which would result in the compression of the tetrahedron that may be reflected by sterically unfavourable interaction for guest/template inclusion into the host cavity.[147]

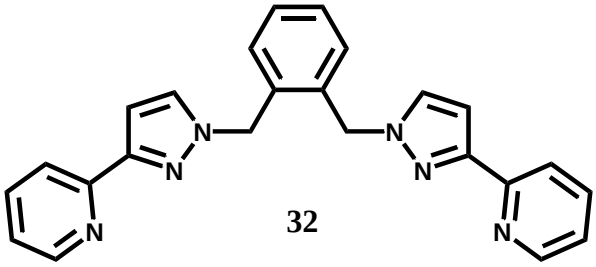

32

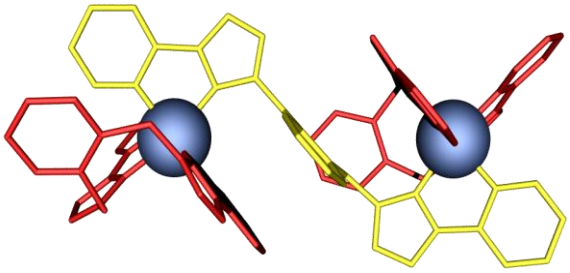

33

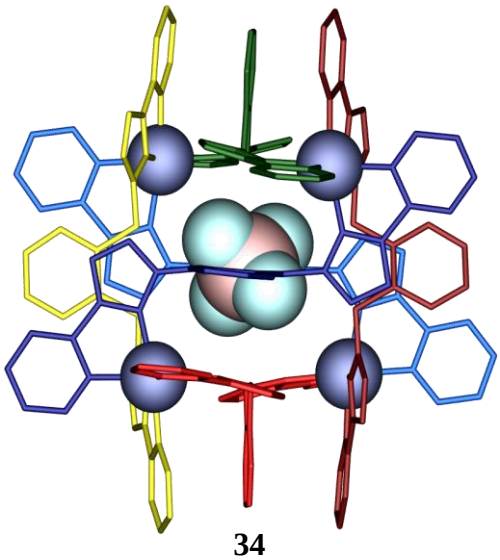

34

Higher order complexes that fit the general formula $M_{2n}L_{3n}$, incorporating "linear" bis-bidentate ligands and octahedral metal ions are rare. In part, this may reflect entropic considerations. One example of an M_8L_{12} complex results from the interaction of Zn(II) with bis(pyrazolyl-pyridine) ligand **35**, containing a 2,6-dimethylenepyridine spacer (***Figure 1.7*** a)).[148] Interestingly, in this case the asymmetric unit consists of four metal centres in a 1:3 *fac*:*mer* isomeric ratio, the perfectly statistical outcome, which is perhaps coincidental.[148] However, no effort was made by the authors to rationalise the formation of this structure over smaller more entropically favourable products similar to those observed in previous studies using closely related ligands. What is noteworthy in this structure is the multiple π-stacking interactions present which most probably go some way to stabilising the octanuclear structure in the solid state. It should be noted that an M_4L_6 cage that employed Co(II) and a bis(pyrazolyl-pyridine) ligand incorporating a 3,3'-dimethylenebiphenyl spacer led to a similar 1:3 mixture of *fac*:*mer* geometrical isomers in the solid state.[149] Again extensive π-π stacking interactions are present. In this regard, all other literature reports of M_4L_6 tetrahedra have metal centres exhibiting *fac* geometry. These latter examples provide a convincing illustration of the effect that ligand conformational flexibility and secondary interactions can play in determining observed self-assembly outcomes.

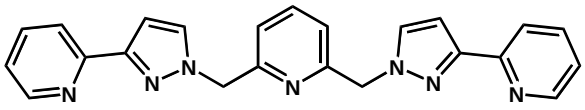

35

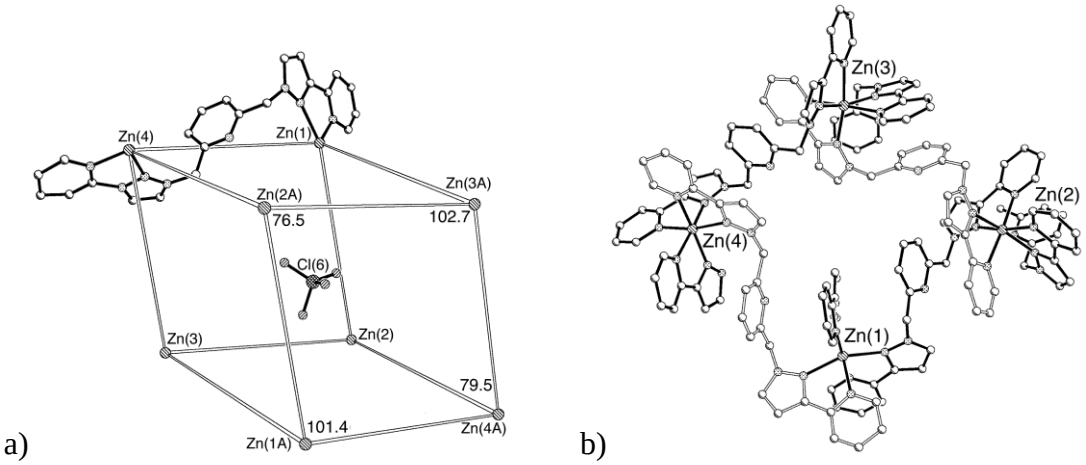

Figure 1.7 a) Schematic representation of $[Zn_8(\mathbf{35})_{12}\supset ClO_4]^{15+}$ and b) the asymmetric unit consisting of half the cube with a 3:1 *mer* : *fac* geometrical isomer distribution.[148]

Another structural motif corresponding to the M_8L_{12} formula resulting from the interaction of octahedral metal with the bis-bidentate ligand **36** has been reported.[150] This structure is essentially an octanuclear molecular ring with alternating singly and doubly bridged metal centres (***Figure 1.8***). The metal centres within each discrete unit are homochiral, resulting in a chiral structure. Interestingly, a perchlorate anion is bound within the torus in the solid state.

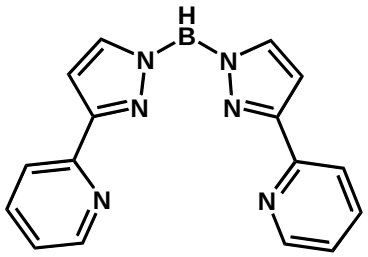

36

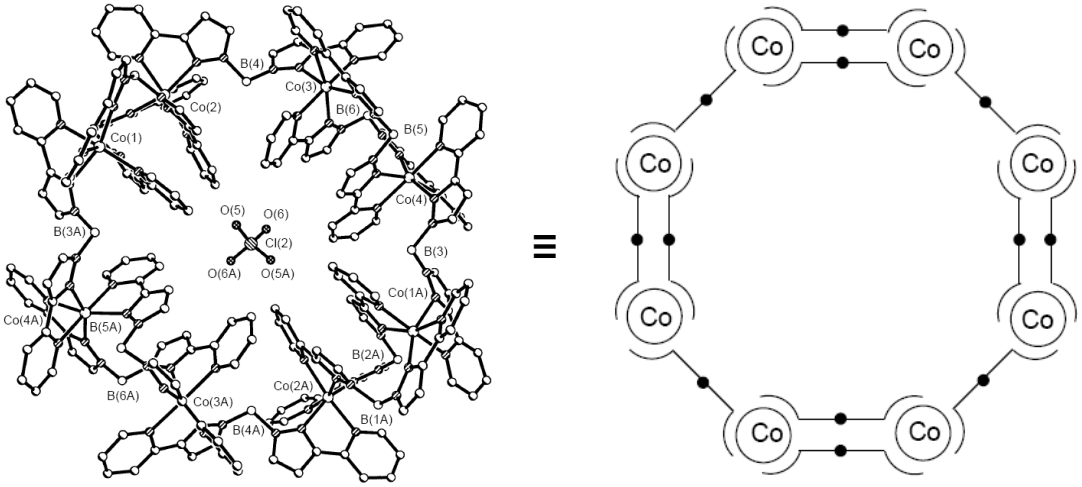

Figure 1.8 The crystal structure of $[Co_8(\mathbf{36})_{12}\supset ClO_4]^{3+}$ (left) and a schematic representation of its novel topological structure (right).[150]

1.5 POTENTIAL APPLICATIONS OF HELICATES AND POLYHEDRA

1.5.1 DNA Binding

The polyanionic and chiral nature of DNA means that cationic metal complexes are potentially well suited for DNA binding applications.[151-159] In and early study Lehn *et al.*[160] investigated the DNA binding ability of cationic homoleptic helicates (H_2 – H_5 in ***Figure 1.9***) formed from the interaction of Cu(I) and polypyridyl ligands (**37**) of varying lengths. DNA melting point analysis indicated that, as the helicates increased in length and nuclearity (charge), there was an increase in binding affinity. The interaction of the metallohelicates with DNA was also shown to inhibit DNA cleavage by restriction enzymes known to bind in the major groove. As a result, it was suggested that given their advantageous dimensions, these helicates were indeed major groove binders. Interestingly, the helicates were shown to bind more strongly to poly-GC duplex DNA, which exhibits a *smaller* major groove and *larger* minor groove, over poly-AT duplex DNA.

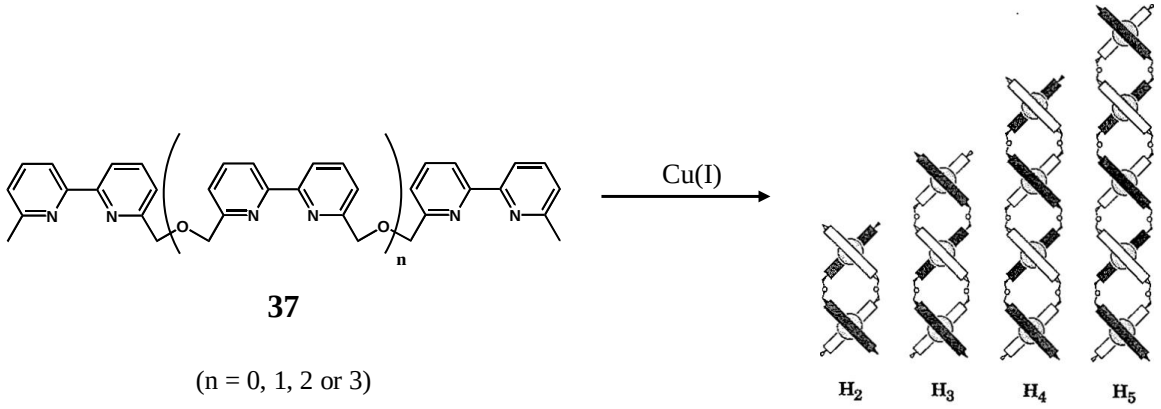

37

(n = 0, 1, 2 or 3)

Figure 1.9 Schematic representation of the products from the interaction of polypyridyl ligands (**37**) with Cu(I).[160]

While increased nuclearity has also been implicated in other studies to lead to increased DNA binding affinity, shape is also an important factor dictating selective binding interactions and showing marked effects on DNA binding affinity. In this regard, numerous studies have been conducted investigating the effects of complex stereochemistry on DNA binding selectivity.[151,154,155,158,159] Perhaps some of the most innovative studies applying helicates in DNA binding studies in recent times have been carried out by the Hannon research group.[64,161-171] They designed dinuclear triple helicates (**39**) based on the interaction of Fe(II)[172] or Ru(II)[168] with the 4,4'-methylenebiphenylene bridged bis(pyridylimine) **38** in a 2:3 ratio. These helicates have the approximate dimensions of major groove binding α-helices known to be DNA recognition components of zinc-finger regulatory proteins. The dinuclear Fe(II) helicate was shown to bind to the major groove by employing 1D and 2D NMR techniques.[161] Furthermore, the interaction of the dinulear helicate with DNA was shown to cause major intramolecular DNA coiling. Not surprisingly, a similar level of DNA coiling was caused by the interaction of the Ru(II) helicate with DNA.[168] The Ru(II) helicate was also shown to exhibit a similar level of cytotoxicity towards various cancer cell lines to that of cisplatin. The overall size and shape of the Fe(II) helicate was subsequently shown to be important by synthesizing larger examples which led to a reduction in DNA coiling.[161,163,171] With respect to stereochemistry, the *M* – helicate was shown to cause increased DNA coiling relative to the *P* – helicate, indicating some subtle variations in binding mode.[166]

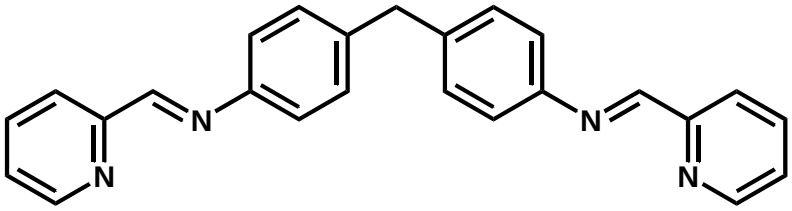

38

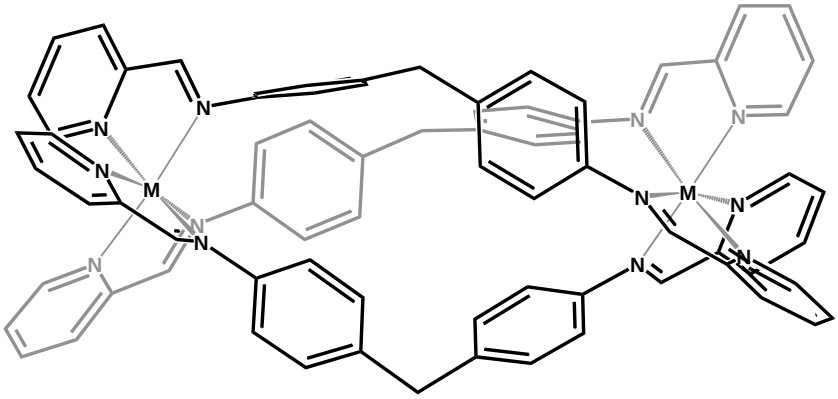

39

Existing synthetic agents that bind to DNA do so essentially in one of five distinct modes.[158] These include, rigid covalent bonds (including coordination bonds) to the DNA bases (e.g. cisplatin), intercalation between the bases, major and minor groove binding and predominantly electrostatic binding to the sugar–phosphate backbone. However, achieving sequence specific binding is normally difficult with simple synthetic agents and as a result most DNA binding agents show some non-specific cytotoxic side effects. In this regard, the Fe(II) version of helicate **39** (described above) was shown to recognise and bind to a three-way junction (3WJ) of a palindromic hexanucleotide (***Figure 1.10***).[167‡] This result exemplified a new mode of DNA binding and apart from providing valuable insight into important DNA structures appears to represent a novel approach towards achieving selective binding.

‡ Palindromic sequences can satisfy their hydrogen bonding requirements by forming duplex structures, 3WJ, 4WJ and higher order junctions.

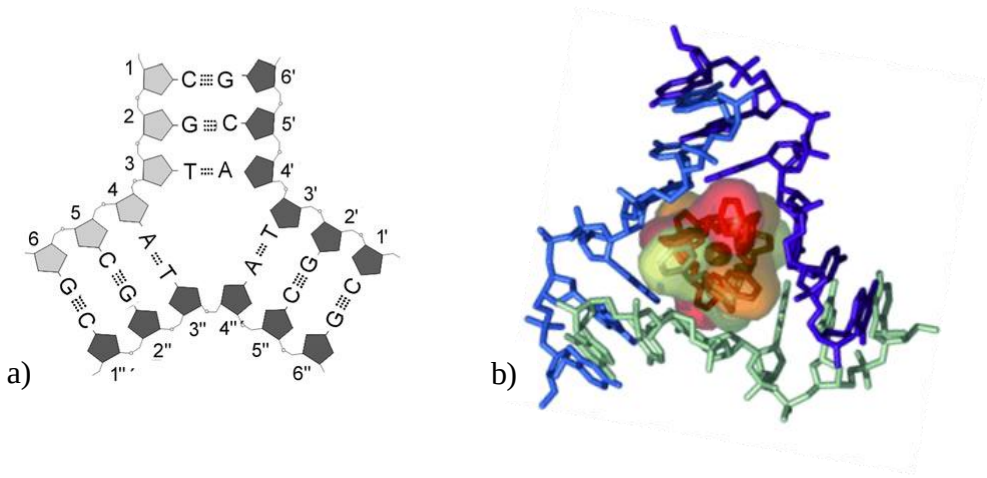

Figure 1.10 a) A schematic representation of the three-way junction formed from the palindromic hexanucleotide, CGTACG, and b) a partial crystal structure representation of **39** bound within the three-way junction.[167]

1.5.2 Nanoreactors

Structures that bear an internal cavity exhibiting a very different chemical environment from that of the surrounding external environment may provide interesting host-guest chemistry. Such systems have been likened to nanoscale reaction vessels or "nanoreactors".[40,173,174] In fact a variety of transformations have been observed within supramolecular nanoscale reaction vessels including Diels-Alder,[175,176] stereospecific photodimerisation,[177] size and shape selective C—H activation of aldehydes by an encapsulated Iridium catalyst,[40,143] as well as aza-Cope rearrangements.[39,41] With respect to the latter, Raymond and coworkers had previously developed an M_4L_6 tetrahedral cage, bearing an overall -12 charge, that exhibited size selectivity for various cationic quaternary ammonium ions.[144] Furthermore, it was noted that while neutral species could be encapsulated they were only bound very weakly.[141] Therefore, a substrate bearing a positive charge which underwent an interconversion to a neutral species may allow catalytic turnover. The aza-Cope rearrangement was selected as it fitted these criteria.[39,41] The substrates in this reaction are quaternary ammonium cations (**A**) that undergo a [3,3]-sigmatropic rearrangement to an iminium cation (**B**) which is subsequently hydrolyzed yielding neutral γ,δ-unsaturated aldehyde products (**C**) (see ***Figure 1.11*** a)). This reaction was found to be

accelerated by up to three orders of magnitude with the effective release of the product facilitating catalytic behaviour. A proposed catalytic pathway is outlined in ***Figure 1.11*** b).

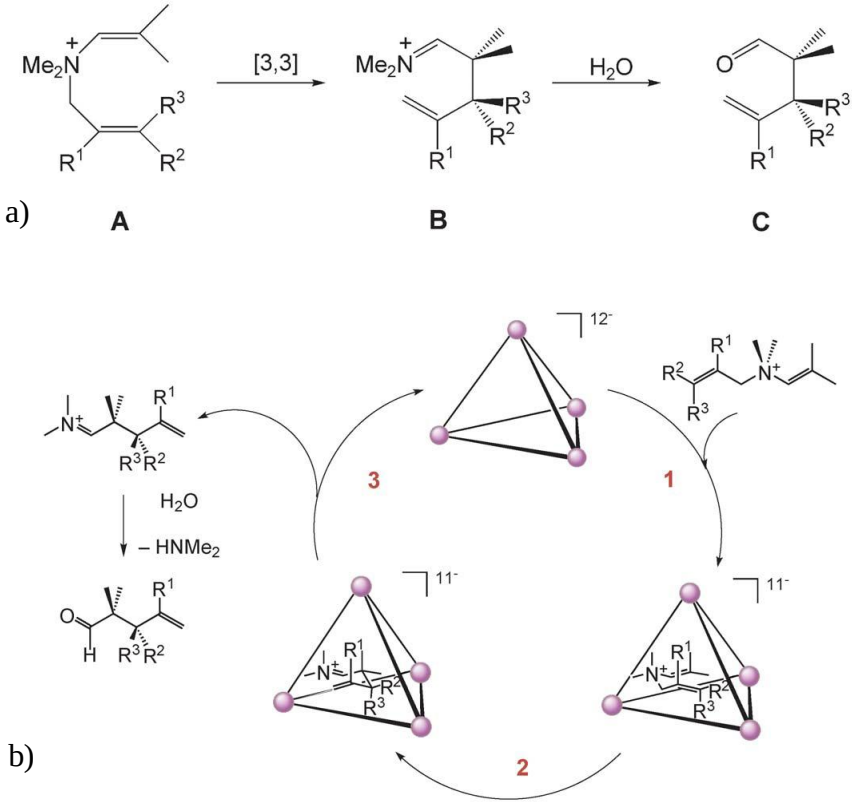

Figure 1.11 a) A generalised aza-Cope rearrangement with, b) the proposed catalytic pathway for the aza-Cope rearrangement in the presence of the M_4L_6 nanoreactor.[39,41]

To further enhance guest selectivity of a M_4L_6 tetrahedral host, Ward and coworkers investigated the possibility of the use of chiral induction to facilitate diastereoselective host-formation.[24] The X-ray structure of crystalline material obtained from the interaction Zn(II) with the bis(pyrazolyl-pyridylpinene) ligand **40** revealed the formation of the *ΛΛΛΛ* tetrahrahedron **41**. Furthermore, the ^{1}H NMR spectrum indicated that in solution a single diastereoisomer of *T*-symmetry was present. These observations go some way to illustrating that chiral induction may be used to facilitate stereoselective host-guest interactions.

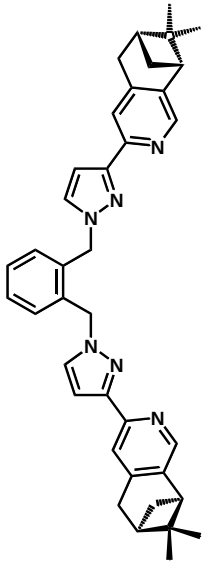

40

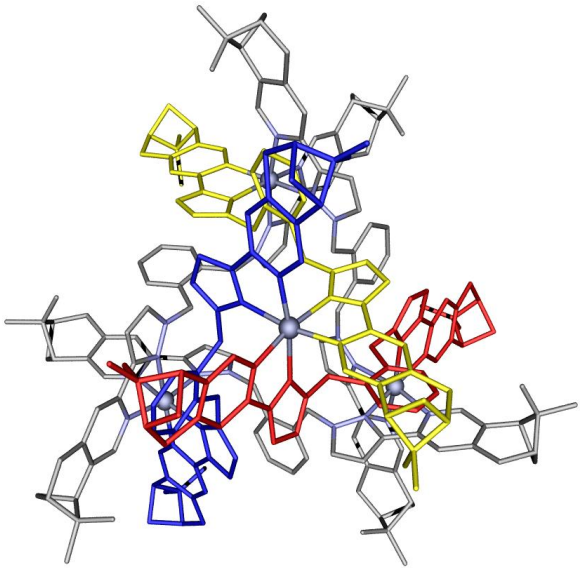

41

1.5.3 Metallosupramolecular templates in synthesis

In order to take advantage of the template effect, metal coordination compounds have also been exploited as templates enabling controlled organic modification in synthetic strategies to yield macrocycles, cryptands,[178,179] catenanes,[1,32,38,180] knots,[32,180-189] Borromean rings[35,190-193] and rotaxanes.[1,32,38] For example, Sauvage and coworkers developed a high yielding synthesis for catenanes which involved the formation of a tetrahedral Cu(I) complex with 2,9-divinyl derivatives of 1,10-phenanthroline and subsequent Grubbs ruthenium ring closing metathesis reaction.[194] The same group has also developed synthetic strategies for the synthesis of the more elaborate interlocking ring systems. In particular, the use of a dinuclear Cu(I) helicate template precursor, generated by the interaction of **42** with Cu(I) in a 1:1 ratio, allowed a Grubbs ruthenium ring-closing metathesis reaction followed by reduction to yield a trefoil knot **43** in 74 % yield (***Scheme 1.2***).[182] This synthetic strategy was a vast improvement on previous approaches which only gave 3 – 30 % yields for the synthesis of related trefoil knots.[181,183-185]

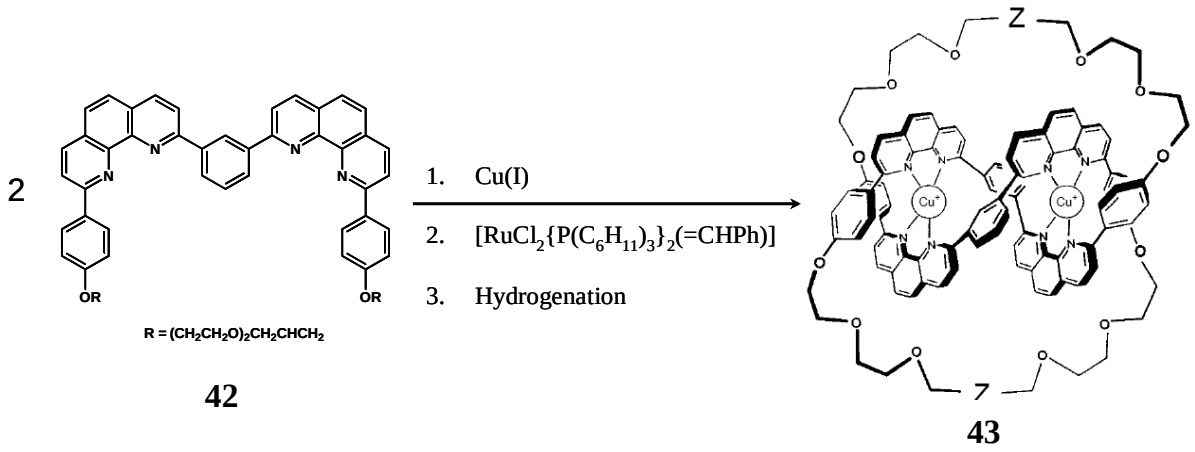

Scheme 1.2[182]

Perhaps one of the most impressive achievements from the use of metal-templates in synthetic chemistry is the formation of Borromean rings.[35,190-193] In this regard, Stoddard and coworkers[190] employed molecular modelling to optimise cooperativity between π-π stacking interactions and coordination geometries as an aid in the design of Borromean rings. As such, the successful self-assembly of a Borromean ring was achieved from 24 components in a near quantitative yield (***Figure 1.12***) by the template-directed formation of 12 imine and 30 dative

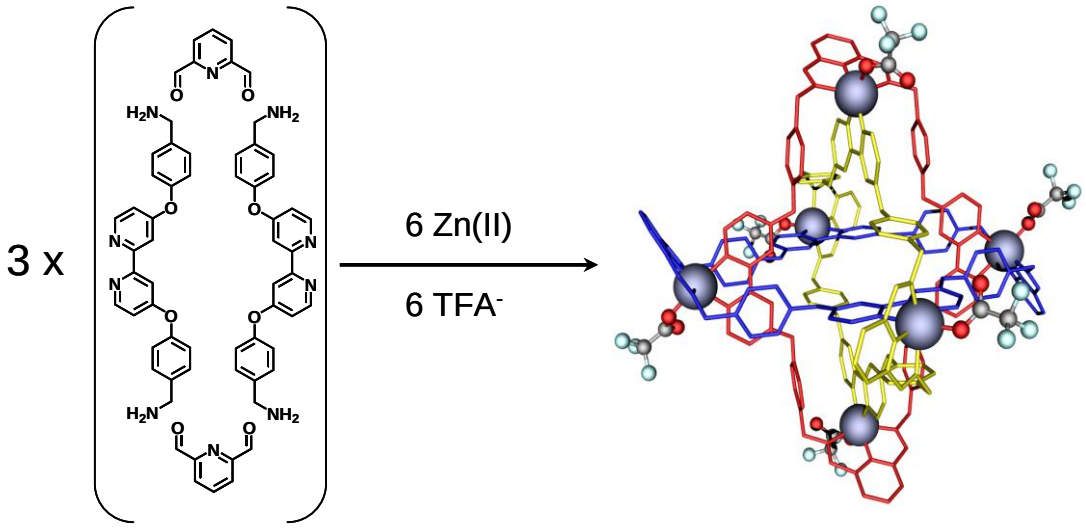

Figure 1.12 Synthetic scheme and crystal structure representation of a Borromean ring.[190]

bonds, associated with the coordination of three interlocked macrocycles to a total of six Zn(II) ions. The X-ray structure of this product reveals six pseudo-octahedral coordinated Zn(II) ions with multiple π-π stacking interactions in accord with the computer aided design predictions. Subsequent reduction of the 12 imine bonds and demetallation yielded the neutral interlocked Borromean rings topology.[193]

1.6 PROJECT ORIGIN AND PROPOSED WORK

In a historical sense, the unusual host-guest selectivity and stability possessed by macrocyclic and macrobicyclic (cryptand) hosts has inspired a great deal of interest in other systems that exhibit such behaviour. Indeed since the early investigations by Cram, Pederson and Lehn on macrocycles and cryptands, [195-200] host systems have become increasingly elaborate allowing the encapsulation of a much more diverse array of guest species.[19,36,40,42, 201-207] In this regard, the present investigation falls within the metallosupramolecular area and is concerned with the design, synthesis and investigation of a range of new metal-containing structures displaying unusual cage architectures. To a large degree, the proposed research depends on synthetic strategies developed within an ongoing collaboration between the candidate's supervisors. This collaboration has seen the development of a range of molecular structures including, macrocycles,[208-210] capsules,[211,212] cryptands,[178,179,213-215] M_3L_3 triangles,[26,216,217] M_2L_3 triple helicates[217,218] and M_4L_6 tetrahedra.[26]

Recently within the candidate's research group several approaches for the synthesis of tris-bipyridyl cryptands **46** (R = H or t-Bu) were investigated (***Figure 1.13*** c)). Among these, a metal-template reductive amination procedure, using the bis-salicyloxy derivative **44** (variable at **R**), provided the most successful synthetic route for the production of the tris-bipyridyl cryptates **45** and, upon demetallation, the free cryptand **46** (***Figure 1.13*** a)).[178,179] As expected, cryptand **46** is an excellent transition metal host, with complexes of Mn(II), Fe(II), Co(II), Ni(II) and Cu(II) being isolated and characterised. Interestingly, the crystal structure of the Ni(II) cryptate (R_1 and R_2 = H) revealed an extended triple helical arrangement (***Figure 1.13*** b)). As an extension of this study, one aim of the current research programme was to extend this bipyridyl system to the quaterpyridyl analogue **47** (***Figure***

1.13 d)), a molecule designed to incorporate two adjacent octahedral metal ions in an extended (chiral) cavity.

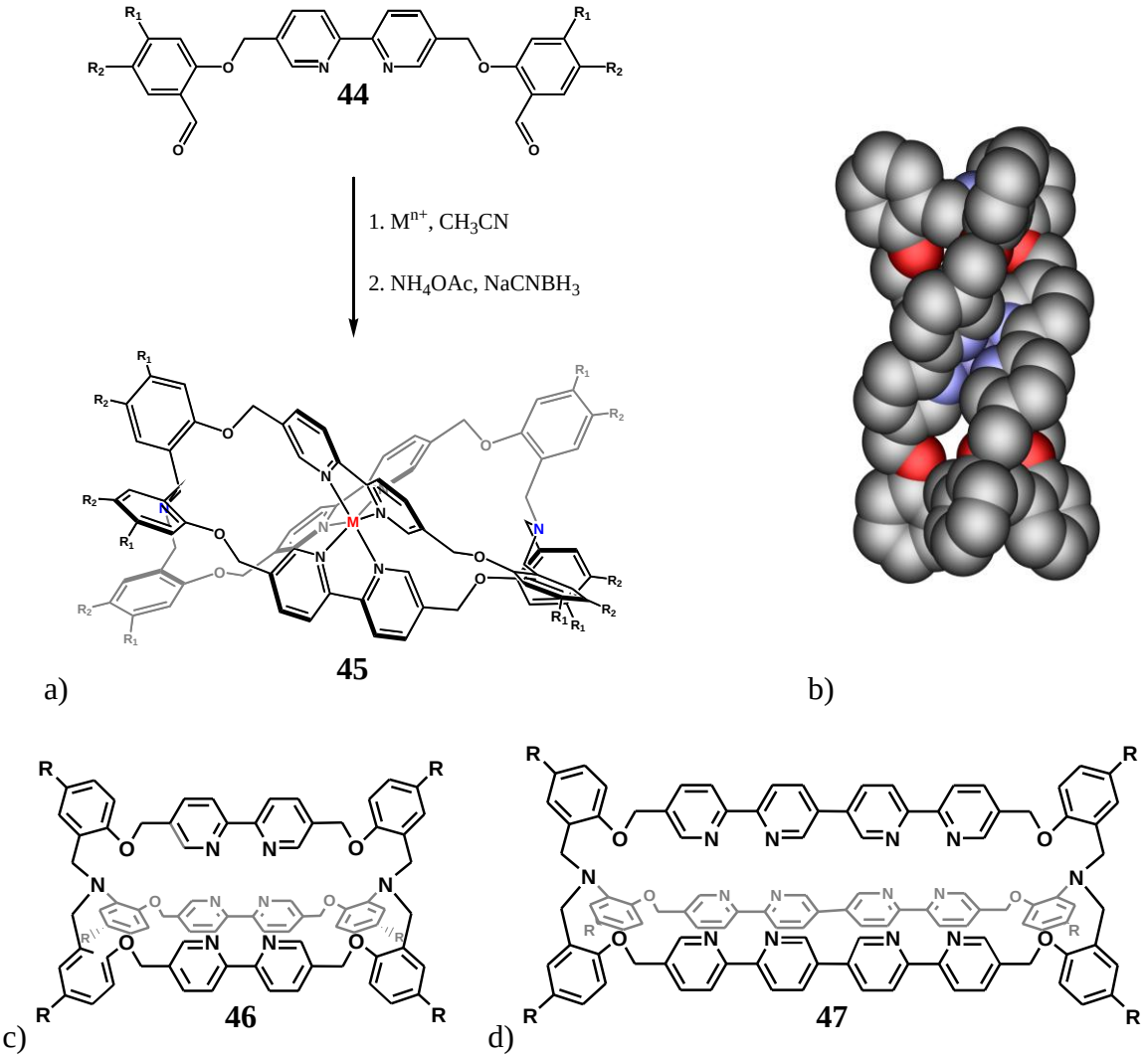

Figure 1.13 a) The metal-template reductive amination procedure for the synthesis of cryptates developed by Perkins *et al.*,[178,179] b) the crystal structure of the Ni(II) cryptate **45**, c) free cyptand **46** and d) the tris-quaterpyridyl cryptand **47** targeted in the present study.

The success of this ambitious proposal relied on the ability to synthesise appropriate quaterpyridyl intermediates, such as dialdehydes of type **48** (variable at **R**) (see Chapter 2 for this work). Perhaps the most challenging aspect of this proposal would be finding appropriate conditions under which the synthesis of cryptand **47** from dialdehyde precursors **48** could be achieved. It was predicted that neither the previously reported stepwise procedure[213-215] nor

the one-pot reductive amination technique[179] used for the synthesis (in very low yield) of cryptand **45**, would provide a viable approach to **47**. Therefore, it was proposed to assess the metal-template reductive amination procedure shown schematically below (***Scheme 1.3***) for this purpose.

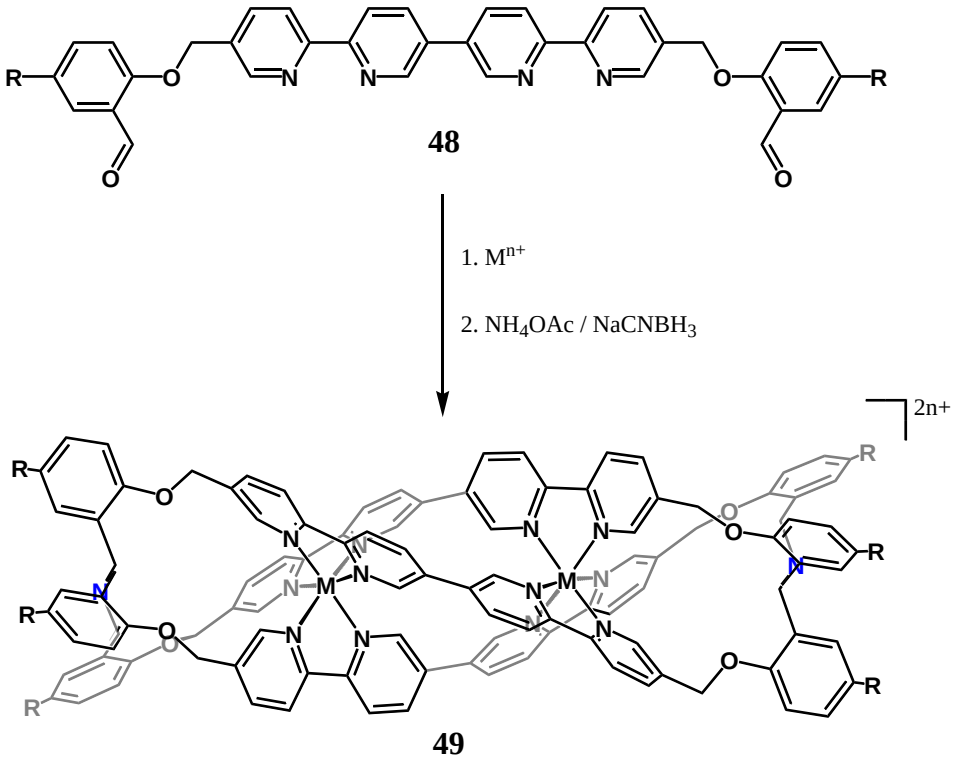

Scheme 1.3

Because dialdehyde **48** is a ditopic ligand, the self-assembly process involved would hold more possibilities (see ***Figure 1.5***, page 22) than for the simpler 2,2′-bipyridyl dialdehyde **44**. Accordingly, for the metal-template reductive amination approach (outlined in ***Scheme 1.3***) to be successful, the interaction of octahedral metal ions and quaterpyridyl dialdehyde **48**, in a 2:3 ratio, would need to yield an M_2L_3 precursor complex. In relation to this, during the candidate's Honours research, 5,5'-dimethyl-2,2';5',5";2",2"'-quaterpyridine (**50**) was employed as a model compound for dialdehyde **48**, in metal-directed assembly experiments. This study found that the interaction of $FeCl_2$ and the quaterpyridine **50** led to the formation of the M_4L_6 complex, $[Fe_4(\mathbf{50})_6 \supset FeCl_4]^{(8-n)+}$, encapsulating a $[FeCl_4]^{n-}$ (n = 1 or

2) guest (***Figure 1.15***). Thus, this result indicated that the proposed metal-template approach for the synthesis of cryptate **49** employing Fe(II) might be problematic.

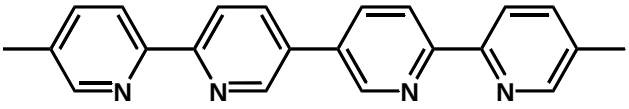

50

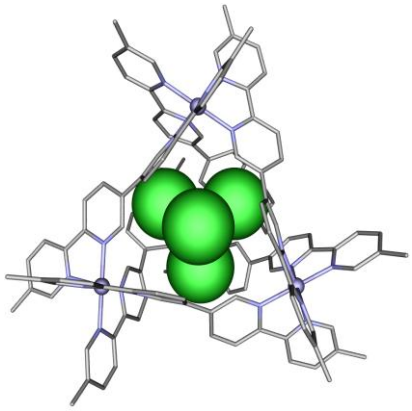

$[Fe_4(\mathbf{50})_6 \supset FeCl_4]^{(8-n)+}$

Figure 1.15 Crystal structure of $[Fe_4(\mathbf{50})_6 \supset FeCl_4]^{(8-n)+}$ (n = 1 or 2) with external countions and hydrogens removed for clarity.

The isolation of $[Fe_4(\mathbf{50})_6 \supset FeCl_4]^{(8-n)+}$ (n = 1 or 2), combined with the interesting host-guest chemistry reported for related systems,[25,42] prompted further investigation of $[Fe_4(\mathbf{50})_6]^{8+}$. This research aimed to elucidate whether or not the formation of the M_4L_6 host complex was guided by a guest-template effect, as is the case for some related systems,[145,219] or whether the complex is predisposed to form due to optimal steric information installed in both its Fe(II) and ligand components. Furthermore, an investigation into the effect that alternative octahedral metal ions, namely Co(II), Ni(II) and Ru(II), might have on analogous metal-directed assembly processes with quaterpyridine **50** was proposed. See Chapter 3 for the results of this research.

The X-ray structure of the M_4L_6 host-guest system, $[Fe_4(\mathbf{50})_6 \supset FeCl_4]^{(8-n)+}$ (n = 1 or 2), and metallosupramolecular assemblies incorporating related 2,2';5',5";2",2'-quaterpyridyl derivatives[135] demonstrated that this rigid "linear" quaterpyridyl motif could undergo significant distortion from its expected linear geometry in strained systems (see for example,

Figure 1.4, page 19). This prompted an investigation into the effects that rigid phenylene- and biphenylene-bridged quaterpyridyl derivatives of type **51** and **52** (see Chapter 2 for synthetic details) might have on metal-directed assembly outcomes. The expectation of this study was that these extended rigidly bridged quaterpyridyl derivatives may alleviate strain, at least to some extent, allowing for the formation of the entropically more favourable M_2L_3 assemblies under thermodynamic control (see Chapter 4). As a result, the isolation of M_2L_3 complexes might allow for the successful metal-template synthesis of dinuclear cryptates using appropriately substituted quaterpyridyl derivatives (see Chapter 5). Alternatively, larger M_4L_6 hosts might be obtained allowing the possibility of interesting host-guest interactions with *larger* guest species (see Chapter 4).

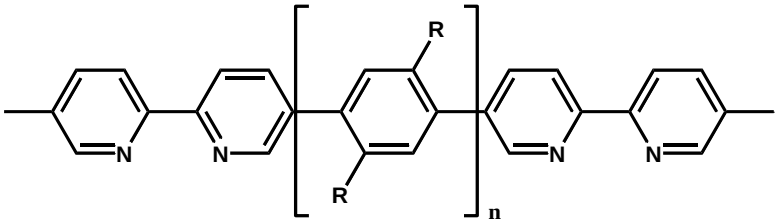

51; n = 1
52; n = 2

Metal-ion complexes of cryptands incorporating bipyridyl and phenanthroline binding domains have the attractive feature of combining the cation inclusion nature of cryptates with the photoactivity of bipyridine and phenanthroline groups. Thus, they may be expected to posses a variety of interesting physical and chemical properties.[220-226] In this regard, the Ru(II) analogue of cryptate **45** was targeted with the expectation that this species might exhibit interesting photophysical properties (see Chapter 5).

The project also aimed to investigate the synthesis of tripodal ligands, such as tris-bipyridyl derivative **53** (variable at $\mathbf{R_1}$ and $\mathbf{R_2}$), and their subsequent interaction with octahedral metal ions. The metal complexes of these tripodal ligands were expected to have a pseudocryptand-like structure with a nitrogen atom for one bridgehead atom and a octahedrally coordinated metal ion for the other.[227-232] It was proposed to synthesize tris-bipyridyl ligands **53** from intermediate monoaldehydes **54** (variable at $\mathbf{R_1}$ and $\mathbf{R_2}$) via the reported one pot reductive amination procedure.[179] See Chapter 5 for the results of this study.

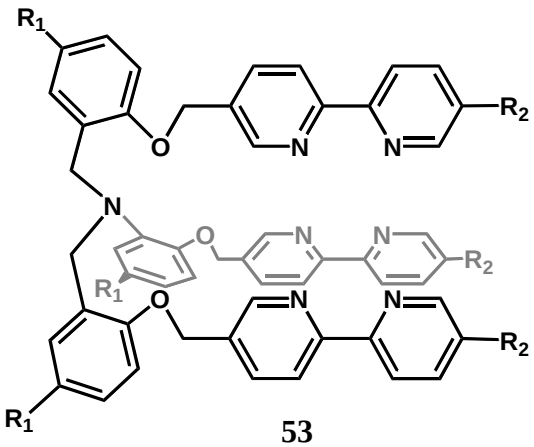

53

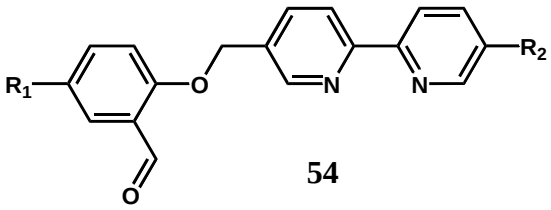

54

Finally, the isolation of $[Fe_4(\mathbf{50})_6]^{8+}$ indicated that it may be possible to employ the metal-template strategy outlined in ***Figure 1.13*** (page 36), incorporating dialdehyde **48**, to synthesize tetranuclear complexes of type **55** – essentially the tetrahedron equivalent(s) of triple helicate(s) **49**. Progress towards this challenging aim is included in Chapter 5.

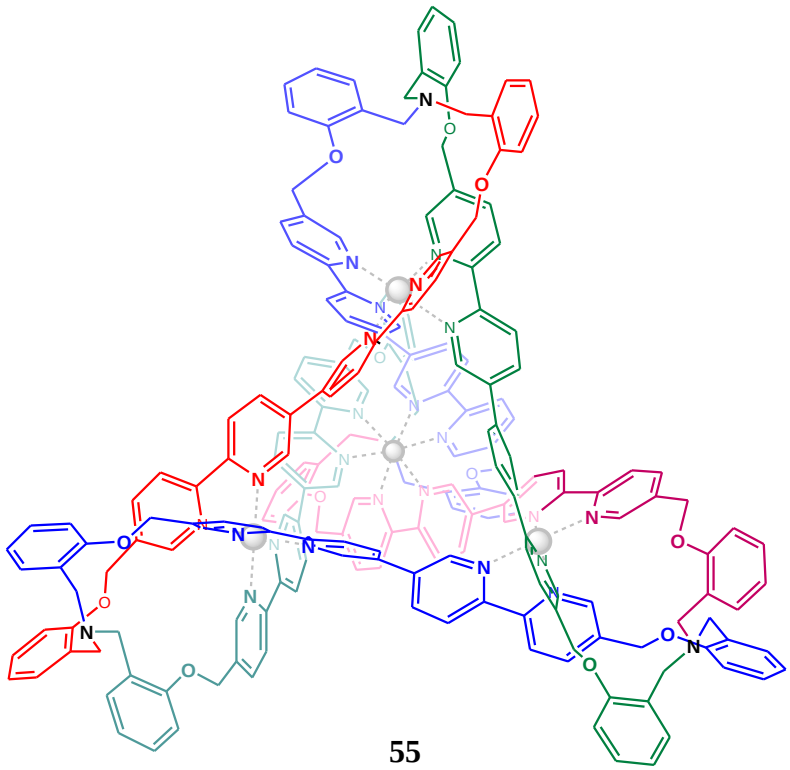

55

1.7 REFERENCES

1. L. F. Lindoy and I. M. Atkinson, *Self-assembly in Supramolecular Chemistry*, Royal Society of Chemistry, Cambridge, UK., 2000.
2. J.-M. Lehn, *Supramolecular Chemistry*, VCH Verlagsgesellschaft, Weinheim, 1995.
3. P. J. Steel and C. M. Fitchett, *Coord. Chem. Rev.*, 2008, **252**, 990.
4. M. Albrecht, M. Fiege and O. Osetska, *Coord. Chem. Rev.*, 2008, **252**, 812.
5. G. Aromí, P. Gamez and J. Reedijk, *Coord. Chem. Rev.*, 2008, **252**, 964.
6. E. C. Constable, *Chem. Soc. Rev.*, 2008, **252**, 842.
7. M. W. Cooke, D. Chartrand and G. S. Hanan, *Coord. Chem. Rev.*, 2008, **252**, 903.
8. S. J. Dalgarno, N. P. Power and J. L. Atwood, *Coord. Chem. Rev.*, 2008, **252**, 825.
9. K. M. Fromm, *Coord. Chem. Rev.*, 2008, **252**, 856.
10. R. Ganguly, B. Sreenivasulu and J. J. Vittal, *Coord. Chem. Rev.*, 2008, **252**, 1027.
11. G. W. Gokel and M. M. Daschbach, *Coord. Chem. Rev.*, 2008, **252**, 886.
12. A. Kumar, S.-S. Sun and A. J. Lees, *Coord. Chem. Rev.*, 2008, **252**, 922.
13. M. P. Suh, Y. E. Cheon and E. Y. Lee, *Coord. Chem. Rev.*, 2008, **252**, 1007.
14. C. R. K. Glasson, L. F. Lindoy and G. V. Meehan, *Coord. Chem. Rev.*, 2008, **252**, 940.
15. M. Ruben, J.-M. Lehn and P. Muller, *Chem. Soc. Rev.*, 2006, **35**, 1056.
16. M. Ruben, J. Rojo, F. J. Romero-Salguero, L. H. Uppadine and J.-M. Lehn, *Angew. Chem. Int. Ed.*, 2004, **43**, 3644.
17. S. J. Lee and W. Lin, *Acc. Chem. Res.*, 2008, **41**, 521.
18. M. Fujita, *Chem. Soc. Rev.*, 1998, **27**, 417.
19. S. Leininger, B. Olenyuk and P. J. Stang, *Chem. Rev.*, 2000, **100**, 853.
20. L. Zhao, B. H. Northrop, Y.-R. Zheng, H.-B. Yang, H. J. Lee, Y. M. Lee, J. Y. Park, K.-W. Chi and P. J. Stang, *J. Org. Chem.*, 2008, **73**, 6580.
21. M. Albrecht, *Chem. Rev.*, 2001, **101**, 3457.
22. M. J. Hannon and L. J. Childs, *Supramol. Chem.*, 2004, **16**, 7.
23. A. Marquis-Rigault, V. Smith, J. Harrowfield, J.-M. Lehn, H. Herschback, R. Sanvito, E. Leize-Wagner and A. Van Dorsselaer, *Chem. Eur. J.*, 2006, **12**, 5632.

24. S. P. Argent, T. Riis-Johannessen, J. C. Jeffery, L. P. Harding and M. D. Ward, *Chem. Commun.*, 2005, 4647.
25. S. M. Biros, R. M. Yeh and K. N. Raymond, *Angew. Chem. Int. Ed.*, 2008, **47**, 6062.
26. J. K. Clegg, L. F. Lindoy, B. Moubaraki, K. S. Murray and J. C. McMurtrie, *Dalton Trans.*, 2004, 2417.
27. R. W. Saalfrank, B. Demleitner, H. Glaser, H. Maid, D. Bathelt, F. Hampel, W. Bauer and M. Teichert, *Chem. Eur. J.*, 2002, **8**, 2679.
28. M. Albrecht, I. Janser and R. Frohlich, *Chem. Commun.*, 2005, 157.
29. P. N. W. Baxter, J.-M. Lehn, G. Baum and D. Fenske, *Chem. Eur. J.*, 1999, **5**, 102.
30. V. Maurizot, M. Yoshizawa, M. Kawano and M. Fujita, *Dalton Trans.*, 2006, 2750.
31. M. Tominaga and M. Fujita, *Bull. Chem. Soc. Jpn.*, 2007, **80**, 1473.
32. B. Champin, P. Mobian and J.-P. Sauvage, *Chem. Soc. Rev.*, 2007, **36**, 358.
33. J.-P. Sauvage, *Chem. Commun.*, 2005, 1507.
34. J.-C. Chambron, J.-P. Collin, V. Heitz, D. Jouvenot, J.-M. Kern, P. Mobian, D. Pomeranc and J.-P. Sauvage, *Eur. J. Org. Chem.*, 2004, **2004**, 1627.
35. C. D. Meyer, C. S. Joiner and J. F. Stoddart, *Chem. Soc. Rev.*, 2007, **36**, 1705.
36. M. Kawano and M. Fujita, *Coord. Chem. Rev.*, 2007, **251**, 2592.
37. C. J. Kepert, *Chem. Commun.*, 2006, 695.
38. S. Saha and J. F. Stoddart, *Chem. Soc. Rev.*, 2007, **36**, 77.
39. D. Fiedler, R. G. Bergman and K. N. Raymond, *Angew. Chem. Int. Ed.*, 2004, **43**, 6565.
40. D. Fiedler, D. H. Leung, R. G. Bergman and K. N. Raymond, *Acc. Chem. Res.*, 2005, **38**, 349.
41. D. Fiedler, H. van Halbeek, R. G. Bergman and K. N. Raymond, *J. Am. Chem. Soc.*, 2006, **128**, 10240.
42. M. D. Pluth and K. N. Raymond, *Chem. Soc. Rev.*, 2007, **36**, 161.
43. C. J. Jones, *Chem. Soc. Rev.*, 1998, **27**, 289.
44. D. L. Caulder and K. N. Raymond, *Dalton Trans.*, 1999, 1185.
45. D. L. Caulder and K. N. Raymond, *Acc. Chem. Res.*, 1999, **32**, 975.
46. E. C. Constable and P. J. Steel, *Coord. Chem. Rev.*, 1989, **93**, 205.
47. P. J. Steel, *Acc. Chem. Res.*, 2005, **38**, 243.

48. C. Kaes, A. Katz and M. W. Hosseini, *Chem. Rev.*, 2000, **100**, 3553.
49. G. R. Newkome, A. K. Patri, E. Holder and U. S. Schubert, *Eur. J. Org. Chem.*, 2004, 235.
50. V. Balzani, G. Bergamini, F. Marchioni and P. Ceroni, *Coord. Chem. Rev.*, 2006, **250**, 1254.
51. M. K. De Armond and M. L. Myrick, *Acc. Chem. Res.*, 1989, **22**, 364.
52. N. C. Fletcher, M. Niewenhuyzen and S. Rainey, *Dalton Trans.*, 2001, 2641.
53. E. A. P. Armstrong, R. T. Brown, M. S. Sekwale, N. C. Fletcher, X.-Q. Gong and P. Hu, *Inorg. Chem.*, 2004, **43**, 1714.
54. A. Grabulosa, M. Beley and P. C. Gros, *Eur. J. Inorg. Chem.*, 2008, 1747.
55. A. A. Tamayo, B. D. Alleyne, B. D. Djurovich, S. Lamansky, I. Tsyba, N. N. Ho, R. Bau and M. E. Tompson, *J. Am. Chem. Soc.*, 2003, **125**, 7377.
56. O. Mamula and A. von Zelewsky, *Coord. Chem. Rev.*, 2003, **242**, 87.
57. N. C. Fletcher, *J. Chem. Soc., Perkins Trans. 1*, 2002, 1831.
58. D. Drahonovsky, U. Knof, L. Jungo, T. Belser, A. Neels, G. C. Labat, H. Stoeckli-Evans and A. v. Zelewsky, *Dalton Trans.*, 2006, 1444.
59. S. G. Telfer, A. F. Williams and G. Bernardinelli, *Chem. Commun.*, 2001, 1498-1499.
60. S. G. Telfer, X.-J. Yang and A. F. Williams, *Dalton Trans.*, 2004, 699.
61. D. R. Ahn, T. W. Kim and J. I. Hong, *J. Org. Chem.*, 2001, **66**, 5008.
62. E. C. Constable, S. M. Elder, M. J. Hannon, A. Martin, P. R. Raithby and D. A. Tocher, *Dalton Trans.*, 1996, 2423.
63. N. Fatin-Rouge, S. Blanc, E. Leize, A. Van Dorsselaer, P. Baret, J. L. Pierre and A. M. Albrecht-Gary, *Inorg. Chem.*, 2000, **39**, 5771.
64. M. J. Hannon, S. Bunce, A. J. Clarke and N. W. Alcock, *Angew. Chem. Int. Ed.*, 1999, **38**, 1277.
65. P. K.-K. Ho, K.-K. Cheung and C.-M. Che, *Chem. Commun.*, 1996, 1197.
66. O. Mamula and A. Von Zelewsky, *Dalton Trans.*, 2000, 219.
67. O. Mamula, A. von Zelewsky, T. Bark and G. Bernardinelli, *Angew. Chem. Int. Ed.*, 1999, **38**, 2945.
68. K. T. Potts, M. P. Wentland, D. Ganguly, G. D. Storrier, S. K. Cha, J. Cha and H. D. Abruna, *Inorg. Chem. Acta*, 1999, **288**, 189.

69. M.-H. Shu, W.-Y. Sun, C.-Y. Duan, W.-X. Tang and W.-J. Zhang, *Trans. Met. Chem.*, 1999, **24**, 628.
70. N. K. Solanki, A. E. H. Wheatley, S. Radojevic, M. McPartlin and M. A. Halcrow, *Dalton Trans.*, 1999, 521.
71. A. F. Williams, *Chem. Eur. J.*, 1997, **3**, 15.
72. R. Ziessel, A. Harriman, A. El-Ghayoury, L. Dounce, E. Leize, H. Nierengarten and A. Van Dorsselaer, *New. J. Chem.*, 2000, **24**, 729.
73. A. Costisor and W. Linert, *Inorg. Chem.*, 2003, **23**, 289.
74. H. Miyake and H. Tsukube, *Supramol. Chem.*, 2005, **17**, 53.
75. C. Piguet, G. Bernardinelli and G. Hopfgartner, *Chem. Rev.*, 1997, **97**, 2005.
76. C. Piguet, M. Borkovec, J. Hamacek and K. Zeckert, *Coord. Chem. Rev.*, 2005, **249**, 705.
77. M. Pons and O. Millit, *Prog. Nucl. Nucl. Magn. Res. Spectro.*, 2001, **38**, 267.
78. R. Ziessel, *Coord. Chem. Rev.*, 2001, **216 - 217**, 195.
79. M.-H. Al-Sayah and N. R. Branda, *Angew. Chem. Int. Ed.*, 2000, **39**, 945.
80. P. K. Bowyer, K. A. Porter, A. D. Rae, A. C. Willis and S. B. Wild, *Chem. Commun.*, 1998, 1153.
81. P. L. Caradoc-Davies and L. R. Hanton, *Chem. Commun.*, 2001, 1098.
82. C. J. Cathey, E. C. Constable, M. J. Hannon, D. A. Tocher and M. D. Ward, *Chem. Commun.*, 1990, 621.
83. O. J. Gelling, F. van Bolhuis and B. L. Feringa, *Chem. Commun.*, 1991, 917.
84. L. F. Lindoy and D. H. Busch, *Inorg. Chem.*, 1974, **13**, 2494.
85. R. W. Mathews, M. McPartlin and I. Scowen, *Dalton Trans.*, 1997, 2861 (and references therein).
86. G. Seeber, B. E. F. Tiedemann and K. E. Raymond, *Top. Curr. Chem.*, 2006, **265**, 147.
87. M. Vazquez, M. R. Bermejo, J. Sanmartin, A. M. Garcia-Deibe, C. Lodeiro and J. Mahia, *Dalton Trans.*, 2002, 870.
88. See, for, example:, D. A. McMorran and P. J. Steel, *Angew. Chem. Int. Ed.*, 1998, **37**, 3297.

89. B. Hasenknopf, J.-M. Lehn, B. Kneisel, G. Baum and D. Fenske, *Angew. Chem. Int. Ed.*, 1996, **35**, 1838.

90. C. Provent, S. Hewage, G. Brand, G. Bernardinelli, L. J. Charbonniere and A. F. Williams, *Angew. Chem. Int. Ed.*, 1997, **36**, 1287.

91. B. Hasenknopf, J.-M. Lehn, N. Boumediene, A. Dupont-Gervais, A. V. Dorsselaer, B. Kneisel and D. Fenske, *J. Am. Chem. Soc.*, 1997, **119**, 10956.

92. O. Mamula, A. Von Zelewsky and G. Bernardinelli, *Angew. Chem. Int. Ed.*, 1998, **37**, 290.

93. C. R. Rice, C. J. Baylies, L. P. Harding, J. C. Jeffery, R. L. Paul and M. D. Ward, *Dalton Trans.*, 2001, 3039.

94. T. Bark, M. Duggeli, H. Stoeckli-Evans and A. Von Zelewsky, *Angew. Chem. Int. Ed.*, 2001, **40**, 2848.

95. S. P. Argent, H. Adams, T. Riis-Johannessen, J. C. Jeffery, L. P. Harding, O. Mamula and M. D. Ward, *Inorg. Chem.*, 2006, **45**, 3905.

96. N. Fatin-Rouge, S. Blanc, A. Pfeil, A. Rigault, A.-M. Albrecht-Gary and J.-M. Lehn, *Helv. Chim. Acta*, 2001, **84**, 1694.

97. A. Pfeil and J.-M. Lehn, *Chem. Commun.*, 1992, 838.

98. M. Borkovec, J. Hamacek and C. Piguet, *Dalton Trans.*, 2004, 4096.

99. G. Ercolani, *J. Am. Chem. Soc.*, 2003, **125**, 16097.

100. J. Hamacek, M. Borkovec and C. Piguet, *Chem. Eur. J.*, 2005, **11**, 5217.

101. J. Hamacek, M. Borkovec and C. Piguet, *Chem. Eur. J.*, 2005, **11**, 5227.

102. J. Hamacek and C. Piguet, *J. Phys. Chem. B.*, 2006, **110**, 7783.

103. A. Harriman, R. Ziessel, J.-C. Moutet and E. Saint-Aman, *Phys. Chem. Chem. Phys.*, 2003, **5**, 1593.

104. S. G. Telfer, B. Bocquet and A. F. Williams, *Inorg. Chem.*, 2001, **40**, 4818.

105. K. Zeckert, J. Hamacek, J.-P. Rivera, S. Floquet, A. Pinto, M. Borkovec and C. Piguet, *J. Am. Chem. Soc.*, 2004, **126**, 11589.

106. R. Ziessel, A. Harriman, J. Suffert, M.-T. Youinou, A. de Cian and J. Fischer, *Angew. Chem. Int. Ed.*, 1997, **36**, 2509.

107. G. Canard and C. Piguet, *Inorg. Chem.*, 2007, **46**, 3511.

108. R. Kramer, J.-M. Lehn and A. Marquis- Rigault, *Proc. Natl. Acad. Sci. U. S. A.*, 1993, **90**, 5394.

109. R. Stiller and J.-M. Lehn, *Eur. J. Inorg. Chem.*, 1998, **1998**, 977.

110. V. C. M. Smith and J. M. Lehn, *Chem. Commun.*, 1996, 2733.

111. D. P. Funeriu, K. Rissanen and J.-M. Lehn, *Proc. Natl. Acad. Sci. USA*, 2001, **98**, 10546.

112. B. Hasenknopf, J. M. Lehn, G. Baum and D. Fenske, *Proc. Nat. Acad. Sci. U.S.A.*, 1996, **93**, 1397.

113. M. Albrecht and M. Schneider, *Eur. J. Inorg. Chem.*, 2002, **2002**, 1301.

114. M. Greenwald, D. Wessely, E. Katz, I. Willner and Y. Cohen, *J. Org. Chem.*, 2000, **65**, 1050.

115. L. Allouche, A. Marquis and J.-M. Lehn, *Chem. Eur. J.*, 2006, **12**, 7520.

116. R. Annuziata, M. Benaglia and A. Bologna, *Magn. Reson. Chem.*, 2002, **40**.

117. F. Cardianali, H. Mamlouk, Y. Rio, N. Armaroli and J.-F. Nierenjgarten, *Chem. Commun.*, 2004, 1582.

118. M. Hutin, R. Frantz and J. R. Nitschke, *Chem. Eur. J.*, 2006, **12**, 4077.

119. C. R. Rice, S. Worl, J. C. Jeffery, R. L. Paul and M. D. Ward, *Dalton Trans.*, 2001, 550.

120. J. J. Jodry and J. Lacour, *Chem. Eur. J.*, 2000, **6**, 4297.

121. J. Lacour, J. J. Jodry and D. Monchaud, *Chem. Commun.*, 2001, 2302.

122. B. R. Serr, K. A. Anderson, C. M. Elliott and O. P. Anderson, *Inorg. Chem.*, 1988, **27**, 4499.

123. C. Provent and A. F. Williams, *Transition Metals in Supramolecular Chemistry*, 1999, Chichester, 1999.

124. A. Von Zelewsky, *Coord. Chem. Rev.*, 1999, **190**, 811.

125. T. Bark and A. Von Zelewsky, *Chimia*, 2000, **54**, 589.

126. M. Dueggeli, C. Goujon-Ginglinger, S. R. Ducotterd, D. Mauron, C. Bonte, A. Von Zelewsky, H. Stoeckli-Evans and A. Neels, *Org. Biomolec. Chem.*, 2003, **1**, 1894.

127. X. Sala, A. M. Rodriguez, M. Rodrigues, I. Romero, T. Parella and A. Von Zelewsky, *J. Org. Chem.*, 2006, **71**, 9283 (and references therein).

128. T. Bark, H. Stoeckli-Evans and A. Von Zelewsky, *J. Chem. Soc., Perkins Trans. 1*, 2002, 1881.
129. H. Mürmer, A. Von Zelewsky and G. Hopfgartner, *Inorg. Chim. Acta*, 1998, **271**, 36.
130. O. Mamula, A. Von Zelewsky, P. Brodard, C. W. Schaepfer, G. Bernardinelli and H. Stoeckli-Evans, *Chem. Eur. J.*, 2005, **11**, 3049.
131. R. Prabaharan, N. C. Fletcher and M. Nieuwenhuyzen, *Dalton Trans.*, 2002, 602.
132. N. C. Fletcher, R. T. Brown and A. P. Doherty, *Inorg. Chem.*, 2006, **45**, 6132.
133. R. Annunziata, M. Benaglia, M. Cinquini, F. Cozzi, C. R. Woods and J. S. Siegel, *Eur. J. Org. Chem.*, 2001, 173.
134. A. Lutzen, M. Hapke, J. Griep-Raming, D. Haase and W. Saak, *Angew. Chem. Int. Ed.*, 2002, **41**, 2086.
135. P. N. W. Baxter, J.-M. Lehn and K. Rissanen, *Chem. Commun.*, 1997, 1323.
136. B. Hasenknopf, J.-M. Lehn, N. Boumediene, E. Leize and A. V. Dorsselaer, *Angew. Chem. Int. Ed.*, 1998, **37**, 3265.
137. M. Albrecht, O. Blau and R. Fröhlich, *Chem. Eur. J.*, 1999, **5**, 48.
138. C. He, L.-Y. Wang, Z.-M. Wang, Y. Liu, C.-S. Liao and C.-H. Yan, *Dalton Trans.*, 2002, 134.
139. P. Mal, D. Schultz, K. Beyeh, K. Rissanen and J. R. Nitschke, *Angew. Chem. Int. Ed.*, 2008, **47**, 8297.
140. T. Beissel, R. E. Powers and K. N. Raymond, *Angew. Chem. Int. Ed.*, 1996, **35**, 1084.
141. S. M. Biros, R. G. Bergman and K. N. Raymond, *J. Am. Chem. Soc.*, 2007, **129**, 12094.
142. D. L. Caulder, R. E. Powers, T. N. Parac and K. N. Raymond, *Angew. Chem. Int. Ed.*, 1998, **37**, 1840.
143. D. H. Leung, R. G. Bergman and K. N. Raymond, *J. Am. Chem. Soc.*, 2006, **128**, 9781.
144. T. N. Parac, D. L. Caulder and K. E. Raymond, *J. Am. Chem. Soc.*, 1998, **120**, 8003.
145. M. Scherer, D. L. Caulder, D. W. Johnson and K. E. Raymond, *Angew. Chem. Int. Ed.*, 1999, **38**, 1587.
146. J. S. Fleming, K. L. V. Mann, C.-A. Carraz, E. Psillakis, J. C. Jeffery, J. A. McCleverty and M. D. Ward, *Angew. Chem. Int. Ed.*, 1998, **37**, 1279.

147. R. L. Paul, Z. R. Bell, J. S. Fleming, J. C. Jeffery, J. A. McCleverty and M. D. Ward, *Heteroat. Chem.*, 2002, **13**, 567.
148. Z. R. Bell, L. P. Harding and M. D. Ward, *Chem. Commun.*, 2003, 2432.
149. R. L. Paul, S. M. Couchman, J. C. Jeffery, J. A. McCleverty, Z. R. Reeves and M. D. Ward, *Dalton Trans.*, 2000, 845.
150. P. L. Jones, K. J. Byrom, J. C. Jeffery, J. A. McCleverty and M. D. Ward, *Chem. Commun.*, 1997, 1361.
151. B. M. Zeglis, V. C. Pierre and J. K. Barton, *Chem. Commun.*, 2007, 4565.
152. V. Brabec and O. Nováková, *Drug Resistance Updates*, 2006, **9**, 111.
153. F. Pierard and A. Kirsch-De Mesmaeker, *Inorg. Chem. Commun.*, 2006, **9**, 111.
154. C. B. Spillane, M. N. V. Dabo, N. C. Fletcher, J. L. Morgan, F. R. Keene, I. Haq and N. J. Buurma, *J. Biol. Inorg. Chem.*, 2008, **102**, 673.
155. J. L. Morgan, C. B. Spillane, J. A. Smith, D. P. Buck, J. G. Collins and F. R. Keene, *Dalton Trans.*, 2007, 4333.
156. T. Biver, F. Secco and M. Venturini, *Coord. Chem. Rev.*, 2008, **252**, 1163.
157. L. J. K. Boerner and J. M. Zaleski, *Curr. Opin. Chem. Biol.*, 2005, **9**, 135.
158. M. J. Hannon, *Chem. Soc. Rev.*, 2007, **36**, 280.
159. C. Metcalfe and J. A. Thomas, *Chem. Soc. Rev.*, 2003, **32**, 215.
160. B. Schoentjes and J.-M. Lehn, *Helv. Chim. Acta*, 1995, **78**, 1.
161. M. J. Hannon, V. Moreno, M. J. Prieto, E. Moldrheim, E. Sletten, I. Meistermann, C. J. Isaac, K. J. Sanders and A. Rodger, *Angew. Chem. Int. Ed.*, 2001, **40**, 879.
162. J. Malina, M. J. Hannon and V. Brabec, *Chem. Eur. J.*, 2007, **13**, 3871.
163. S. Khalid, M. J. Hannon, A. Rodger and P. M. Rodger, *J. Mol. Graphics Modell.*, 2007, **25**, 794.
164. J. Malina, M. J. Hannon and V. Brabec, *Nucl. Acids Res.*, 2008, **36**, 3630.
165. J. Malina, M. J. Hannon and V. Brabec, *Chem. Eur. J.*, 2008, **14**, 10408.
166. I. Meistermann, V. Moreno, M. J. Prieto, E. Moldrheim, E. Sletten, S. Khalid, P. M. Rodger, J. C. Peberdy, C. J. Isaac, A. Rodger and M. J. Hannon, *Proc. Nat. Acad. Sci. U.S.A.*, 2002, **99**, 5069.
167. A. Oleksi, A. G. Blanco, R. Boer, I. Usón, J. Aymamí, A. Rodger, M. J. Hannon and M. Coll, *Angew. Chem. Int. Ed.*, 2006, **45**, 1227.

168. G. I. Pascu, A. C. G. Hotze, C. Sanchez-Cano, B. M. Kariuki and M. J. Hannon, *Angew. Chem. Int. Ed.*, 2007, **46**, 4374.

169. J. C. Peberdy, J. Malina, S. Khalid, M. J. Hannon and A. Rodger, *J. Inorg. Biochem.*, 2007, **101**, 1937.

170. S. Khalid, M. J. Hannon, A. Rodger and P. M. Rodger, *Chem. Eur. J.*, 2006, **12**, 3493.

171. C. Uerpmann, J. Malina, M. Pascu, G. J. Clarkson, V. Moreno, A. Rodger, A. Grandas and M. J. Hannon, *Chem. Eur. J.*, 2005, **11**, 1750.

172. M. J. Hannon, C. L. Painting, A. Jackson, J. Hamblin and W. Errington, *Chem. Commun.*, 1997, 1807.

173. T. S. Koblenz, J. Wassenaar and J. N. H. Reek, *Chem. Soc. Rev.*, 2008, **37**, 247.

174. J.-P. Bourgeois and M. Fujita, *Aust. J. Chem.*, 2002, **55**, 619.

175. J. Kang and J. Rebek, *Nature*, 1997, **385**, 50.

176. J. Kang, J. Santamaria, G. Hilmersson and J. Rebek, *J. Am. Chem. Soc.*, 1998, **120**, 7389.

177. M. Yoshizawa, Y. Takeyama, T. Kusukawa and M. Fujita, *Angew. Chem. Int. Ed.*, 2002, **41**, 1347.

178. D. F. Perkins, L. F. Lindoy, A. McAuley, G. V. Meehan and P. Turner, *Proc. Nat. Acad. Sci. U.S.A.*, 2006, **103**, 532.

179. D. F. Perkins, L. F. Lindoy, G. V. Meehan and P. Turner, *Chem. Commun.*, 2004, 152.

180. C. Dietrich-Buchecker, G. Rapenne and J.-P. Sauvage, *Coord. Chem. Rev.*, 1999, **185-186**, 167.

181. C. Dietrich-Buchecker, J. Guilhem, C. Pascard and J. P. Sauvage, *Angew. Chem. Int. Ed.*, 1990, **29**, 1154.

182. C. Dietrich-Buchecker, G. Rapenne and J.-P. Sauvage, *Chem. Commun.*, 1997, 2053.

183. C. Dietrich-Buchecker and J. P. Sauvage, *Angew. Chem. Int. Ed.*, 1989, **28**, 189.

184. C. Dietrich-Buchecker, J. P. Sauvage, A. De Cian and J. Fischer, *Chem. Commun.*, 1994, 2231.

185. C. O. Dietrich-Buchecker, J. F. Nierengarten, J. P. Sauvage, N. Armaroli, V. Balzani and L. De Cola, *J. Am. Chem. Soc.*, 1993, **115**, 11237.

186. S. C. J. Meskers, H. P. J. M. Dekkers, G. Rapenne and J.-P. Sauvage, *Chem. Eur. J.*, 2000, **6**, 2129.

187. M. Meyer, A. M. Albrecht-Gary, C. O. Dietrich-Buchecker and J. P. Sauvage, *J. Am. Chem. Soc.*, 1997, **119**, 4599.

188. L.-E. Perret-Aebi, A. v. Zelewsky, C. Dietrich-Buchecker and J. P. Sauvage, *Angew. Chem. Int. Ed.*, 2004, **43**, 4482.

189. G. Rapenne, C. Dietrich-Buchecker and J. P. Sauvage, *J. Am. Chem. Soc.*, 1999, **121**, 994.

190. K. S. Chichak, S. J. Cantrill, A. R. Pease, S.-H. Chiu, G. W. V. Cave, J. L. Atwood and J. F. Stoddart, *Science*, 2004, **304**, 1308.

191. K. S. Chichak, S. J. Cantrill and J. F. Stoddart, *Chem. Commun.*, 2005, 3391.

192. K. S. Chichak, A. J. Peters, S. J. Cantrill and J. F. Stoddart, *J. Org. Chem.*, 2005, **70**, 7956.

193. A. J. Peters, K. S. Chichak, S. J. Cantrill and J. F. Stoddart, *Chem. Commun.*, 2005, 3394.

194. B. Mohr, M. Weck, J. P. Sauvage and R. H. Grubbs, *Angew. Chem. Int. Ed.*, 1997, **36**, 1308.

195. B. Dietrich, J. M. Lehn and J. P. Sauvage, *Tetrahedron Lett.*, 1969, **10**, 2885.

196. B. Dietrich, J. M. Lehn and J. P. Sauvage, *Chem. Commun.*, 1973, 15.

197. B. Dietrich, J. M. Lehn and J. P. Sauvage, *Chem. Commun.*, 1970, 1055.

198. J. M. Lehn, *Acc. Chem. Res.*, 1978, **11**, 49.

199. D. J. Cram and S. P. Ho, *J. Am. Chem. Soc.*, 1986, **108**, 2998.

200. C. J. Pedersen and H. K. Frensdorff, *Angew. Chem. Int. Ed.*, 1972, **11**, 16.

201. M. D. Lankshear and P. D. Beer, *Coord. Chem. Rev.*, 2006, **250**, 3142.

202. C. R. Rice, *Coord. Chem. Rev.*, 2006, **250**, 3190.

203. S. O. Kang, M. A. Hossain and K. Bowman-James, *Coord. Chem. Rev.*, 2006, **250**, 3038.

204. K. Wichmann, B. Antonioli, T. Söhnel, M. Wenzel, K. Gloe, K. Gloe, J. R. Price, L. F. Lindoy, A. J. Blake and M. Schröder, *Coord. Chem. Rev.*, 2006, **250**, 2987.

205. J. T. Lenthall and J. W. Steed, *Coord. Chem. Rev.*, 2007, **251**, 1747.

206. Y. Nishioka, T. Yamaguchi, M. Kawano and M. Fujita, *J. Am. Chem. Soc.*, 2008, **130**, 8160.

207. J. Yang, M. B. Dewal, S. Profeta, M. D. Smith, Y. Li and L. S. Shimizu, *J. Am. Chem. Soc.*, 2008, **130**, 612.

208. I. M. Atkinson, J. D. Chartres, A. M. Groth, L. F. Lindoy, M. P. Lowe and G. V. Meehan, *Chem. Commun.*, 2002, 2428.

209. J. D. Chartres, M. S. Davies, L. F. Lindoy, G. V. Meehan and G. Wei, *Inorg. Chem. Commun.*, 2006, **9**, 751.

210. J. D. Chartres, L. F. Lindoy and G. V. Meehan, *Tetrahedron*, 2006, **62**, 4173.

211. D. J. Bray, B. Antonioli, J. K. Clegg, K. Gloe, K. Gloe, K. A. Jolliffe, L. F. Lindoy, G. Wei and M. Wenzel, *Dalton Trans.*, 2008, 1683.

212. D. J. Bray, L.-L. Liao, B. Antonioli, K. Gloe, L. F. Lindoy, J. C. McMurtrie, G. Wei and X.-Y. Zhang, *Dalton Trans.*, 2005, 2082.

213. K. R. Adam, I. M. Atkinson, J. Kim, L. F. Lindoy, O. A. Matthews, G. V. Meehan, F. Raciti, B. W. Skelton, N. Svenstrup and A. H. White, *Dalton Trans.*, 2001, 2388.

214. I. M. Atkinson, A. R. Carroll, R. J. Janssen, L. F. Lindoy, O. A. Mathews and G. V. Meehan, *J. Chem. Soc., Perkins Trans. 1*, 1997, **3**, 295.

215. R. J. Janssen, L. F. Lindoy, O. A. Mathews, G. V. Meehan, A. N. Sobolev and A. H. White, *Chem. Commun.*, 1995, 7.

216. J. K. Clegg, L. F. Lindoy, J. C. McMurtrie and D. Schilter, *Dalton Trans.*, 2006, 3114.

217. J. K. Clegg, K. A. Jolliffe, L. F. Lindoy and G. V. Meehan, *Polish J. Chem.*, 2008, **82**, 1131.

218. J. K. Clegg, L. F. Lindoy, J. C. McMurtrie and D. Schilter, *Dalton Trans.*, 2005, 857.

219. R. L. Paul, Z. R. Bell, J. C. Jeffery, J. A. McCleverty and M. D. Ward, *Proc. Nat. Acad. Sci. U.S.A.*, 2002, **99**, 4883.

220. A. Bencini, A. Bianchi, C. Giorgi, V. Fusi, A. Masotti and P. Paoletti, *J. Org. Chem.*, 2000, **65**, 7686.

221. J.-C. Rodriguz-Ubis, B. Alpha, D. Plancherel and J.-M. Lehn, *Helv. Chim. Acta*, 1984, **67**, 2264.

222. R. Puchta and R. van Eldik, *Eur. J. Inorg. Chem.*, 2007, **2007**, 1120.

223. L. Burai, E. Toth, H. Bazin, M. Benmelouka, Z. Jaszberenyi, L. Helm and A. E. Merbach, *Dalton Trans.*, 2006, 629.

224. J. P. Cross, A. Dadabhoy and P. G. Sammes, *J. Lumin.*, 2004, **110**, 113.

225. A. M. Klonkowski, S. Lis, M. Pietraszkiewicz, Z. Hnatejko, K. Czarnobaj and M. Elbanowski, *Chem. Mater.*, 2003, **15**, 656.

226. N. Sabbatini, M. Guardigli and J.-M. Lehn, *Coord. Chem. Rev.*, 1993, **123**, 201.

227. T. Nabeshima, Y. Tanaka, T. Saiki, S. Akine, C. Ikeda and S. Sato, *Tetrahedron Lett.*, 2006, **47**, 3541.

228. T. Nabeshima and S. Akine, *The Chemical Record*, 2008, **8**, 240.

229. T. Nabeshima, S. Masubuchi, N. Taguchi, S. Akine, T. Saiki and S. Sato, *Tetrahedron Lett.*, 2007, **48**, 1595.

230. K. Sato, Y. Sadamitsu, S. Arai and T. Yamagishi, *Tetrahedron Lett.*, 2007, **48**, 1493.

231. T. Nabeshima, Y. Yoshihira, T. Saiki, S. Akine and E. Horn, *J. Am. Chem. Soc.*, 2003, **125**, 28.

232. T. Nabeshima, *Coord. Chem. Rev.*, 1996, **148**, 151.

Chapter 2

Polypyridyl Synthetic Strategies

2.1 SYNTHETIC BACKGROUND

The versatility of polypyridines in coordination chemistry combined with vast improvements in synthetic methodologies has led to the development of an abundance of synthetic strategies for their synthesis.[1-7] While the most widely employed synthetic strategies for the synthesis of polypyridines today involve transition metal–catalysed coupling reactions[1,2,4,5,7] there are a number of alternative techiques that may be employed. Among these are cyclisation reactions, such as the Kröhnke method,[3,6] that allow the synthesis of both symmetrically and unsymmetrically substituted polypyridines. There are also some more unusual main group coupling reactions, such as those incorporating organo-phosphorus[8] and organo-sulfur reagents.[9-11] Transition metal coupling procedures were employed extensively in the synthetic strategies used in this project, therefore discussion here will briefly cover several possible coupling mechanisms and the various coupling techniques commonly used to generate polypyridines in the literature as well as procedures specifically relevant to the current project. Firstly, however, a brief introduction to the basic principles of pyridine reactivity and synthetic approaches to 2,5-disubstituted pyridines is presented.

2.1.1 Pyridine and the synthesis of its 2,5-disubstituted derivatives

The presence of the nitrogen heteroatom in pyridine results in an electron deficient aromatic ring. As a result pyridine has an increased susceptibility towards nucleophilic substitution, especially at the 2- and 4-positions. However, electrophilic substitution under harsh conditions may occur if an electron donating group is present, such as amino or alkoxy groups. These general observations allow a certain level of control during the synthesis of 2,5-disubstituted pyridines. For example, starting with 2-aminopyridine one can carry out an electophilic substitution at the 5-position because of the electron donating ability of the amino group, followed by nucleophilic substitution of the amino group via a diazonium salt. Because of the reactivity difference between the 2(6) and 3(5) positions on pyridine it is often possible to selectively carry out nucleophilic substitutions at the 2(6) position, without complication from 3(5) substitution. This latter point is a characteristic of 2,5-

dihalopyridines with important implications in the regioselectivity of many cross-coupling procedures.

2.1.2 Modern coupling procedures

There is a large body of literature on aryl-aryl couplings, as a consequence specific discussion here will largely be limited to those coupling procedures used for the synthesis of pyridyl derivatives (a more indepth discussion of aryl-aryl coupling techniques can be found elsewhere).[1,4,5,12-15] The coupling procedures discussed will include the Ullman reaction, Ni(0) homocoupling reactions, as well as Negishi, Stille and Suzuki cross-coupling reactions. A brief discussion of the major proposed catalytic cycles for Ni(0) homocouplings and Pd(0) cross-coupling procedures are also included in this review.

2.1.2.1 Homocoupling

Transition metal catalysed homocoupling procedures provide a facile way for synthesising symmetrically substituted biaryls. These procedures have a number of advantages over cross-coupling techniques. First and foremost, homocoupling avoids the need to pre-synthesize organometallic nucleophiles, such as the zincates, stannanes and boranes needed for Negishi, Stille and Suzuki cross-couplings, respectively. In this regard the synthesis of such nucleophiles, often involving multiple step procedures employing alkyl lithium reagents, leads to a reduced tolerance towards auxiliary functional groups. Ni(0) and Pd(0) complexes are now common catalysts used in homocoupling procedures. In particular, $NiX_2(PPh_3)_2$ in the presence of Et_4NI and zinc dust has become a popular catalytic system.[16-18] In this system, the zinc dust (which may also be replaced by a cathode) acts as a sacrificial reducing agent to regenerate the Ni(0) catalyst. The Et_4NI acts as an I^- source which is postulated to act as a bridge between Ni and Zn in the electron transfer processes.

Several mechanisms for the above Ni(0) catalysed homocoupling have been proposed.[1,16-20] The simplest of these involves the oxidative addition of the aryl halide to Ni(0) to give $ArNi(II)L_2X$. This is followed by the formation of a diaryl-Ni(II) species via metathesis, and reductive elimination.[1,16] However, in the above-mentioned mechanism the

formation of the diaryl-Ni(II) species by metathesis has not been demonstrated in detail, and thus the mechanism remains controversial. An alternative mechanism, involving Ar-Ni(I) and Ar_2-Ni(III) species has been postulated (***Figure 2.1***).[16,18-20] In this mechanism the Ar-Ni(II) species is reduced with a sacrificial reducing agent to an Ar-Ni(I) intermediate which then undergoes a second oxidative addition to another equivalent of aryl halide to give Ar_2-Ni(III). Following this, reductive elimination of the homocoupled biaryl product results in the release of a Ni(I) complex which is reduced to Ni(0) by the sacrificial reducing agent thus regenerating the catalyst. It should be noted that the above mechanistic discussion is also relevant to the analogous Pd(0) homocoupling reactions.[18]

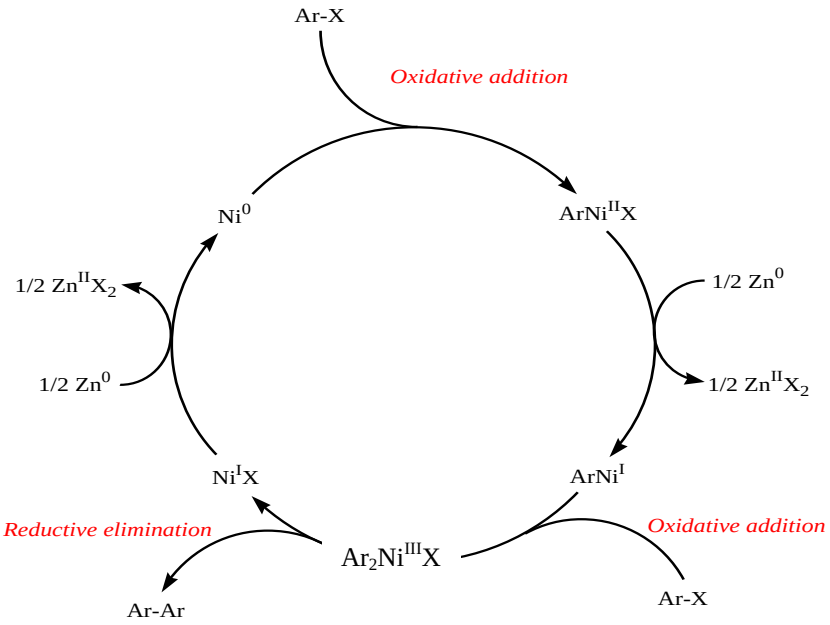

Figure 2.1 A proposed mechanism for the Ni(0) catalysed homocoupling using Zn(0) as the sacrificial reducing agent.[16]

2.1.2.2 Cross – coupling

Over the last three decades Pd(0)-catalysed C – C and C – X (X = heteroatom) cross-coupling reactions have been a major area of interest for the synthesis of unsymmetrical biaryls.[1,4,5,7,12-14,21] These reactions are generally thought to proceed through a mechanism that involves three distinctive steps: i) oxidative addition of the Pd catalyst to the aryl halide,

ii) transmetallation of the nucleophillic organometallic species, and iii) reductive elimination of the product regenerating the Pd catalyst. ***Figure 2.2*** outlines two proposed mechanistic variations on this general theme.

The commonly accepted Pd(0)-catalysed cross-coupling mechanism is outlined in ***Mechanism I (Figure 2.2)*** whereby oxidative addition of the 14-electron activated catalytic complex, $Pd(0)L_2$, to an aryl halide effectively yields the 16-electron *trans*-$ArPd(II)L_2X$ (Ar = aryl; X = halide or triflate) product.[12,22-24] The oxidative addition is proposed to proceed via an associative concerted three-centre transition state leading to *cis*-isomers that rapidly undergo isomerisation to the thermodynamically more stable *trans*-isomers.[23,25,26] Transmetallation via nucleophillic substitution on the *trans*-$ArPd(II)L_2X$ complex then leads to *trans*-$ArPd(II)L_2R$ (R = nucleophile). Following this, isomerisation to give *cis*-$ArPd(II)L_2R$ occurs to allow for the reductive elimination of the biaryl product and subsequent regeneration of the active Pd(0) catalyst. ***Mechanism I*** is well supported by structural evidence for the various intermediates,[23,26-29] however, such evidence does not necessarily preclude alternative catalytic pathways.

Inconsistencies revealed by kinetic studies have indicated that the nucleophilic substitution and reductive elimination steps were actually slower than the entire catalytic cycle outlined in ***Mechanism I***. In this regard, Atmore *et al.*[30] suggested an alternative mechanism in which they tentatively proposed the intermediates outlined in ***Mechanism II*** (***Figure 2.2***) as the minimum kinetic requirement on the basis of kinetic information. This mechanism differs from ***Mechanism I*** in several key ways. Firstly, it is proposed that the active catalyst is the trivalent 16-electron complex, $[Pd(0)L_2\mathbf{A}]^-$ (**A** = Cl, Br, I, AcO and TFA), due to an apparent catalytic requirement of $Pd(0)L_2$ for anionic additives such as **A**.[28,30-35] Further, oxidative addition is indicated to lead to an 18-electron pentacoordinate complex that impedes the formation of the unreactive *trans*-$ArPd(II)L_2R$ isomer.[30,34] Thus, no isomerisation step is required for the final reductive elimination to occur. It was noted that ***Mechanism I*** may still operate as a secondary pathway[34,35] and that employment of $[Pd(0)(PPh_3)_4]$ as the precatalyst without anion additives may proceed via ***Mechanism I***. However, on accumulation of nucleophilic anions ***Mechanism II*** will become operative. Catalysts such as $PdCl_2(PPh_3)_2$, $PdCl_2$dppf and $Pd(OAc)_2(PPh_3)_2$ will each lose an anion and proceed via ***Mechanism II***. Importantly ***Mechanism II*** acknowledges that the ligand

substitution on the Pd catalyst goes via an associative mechanism, whilst ***Mechanism I*** does not. As such, it could be misinterpreted to involve dissociative ligand substitution. Moreover, agostic interactions and solvent coordination have been indicated to have led to a number of such misinterpretations.[23] ***Mechanism II*** also offers an explanation for the anion additive effects that have been observed. However, the precise nature of cross-coupling mechanisms remain controversial and without doubt, reaction specific, especially with respect to the transmetallation steps.

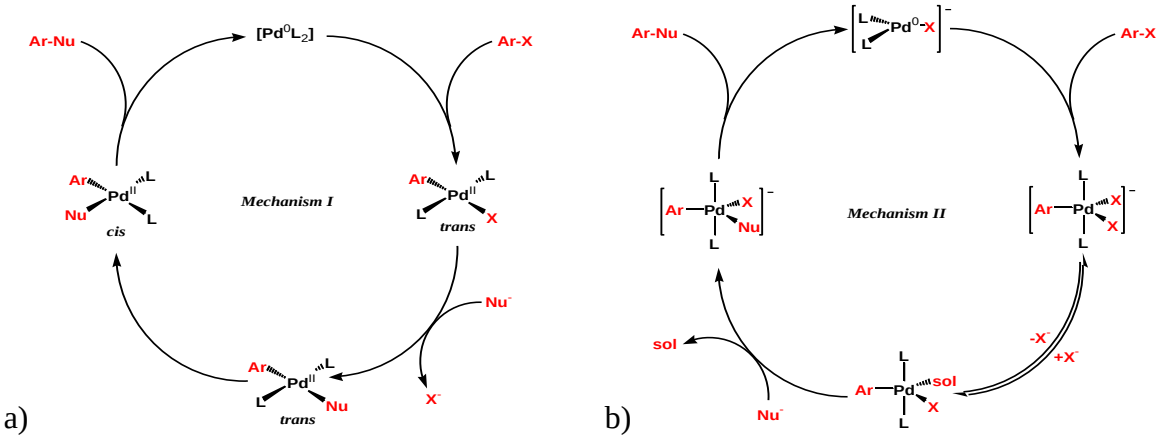

Figure 2.2 Two proposed mechanisms for Pd(0)-catalysed cross-coupling reactions; a) pathway well supported by structural evidence,[12,22-24] and b) pathway described as the minimum kinetic requirement.[30]

Controversy aside, scrutiny of the proposed mechanisms has resulted in a greater understanding of the respective catalytic systems and this in turn has led to a more rational approach to catalyst design.[23,27,32,35-43] For example, the nature of the aryl halide has an important bearing on the rate limiting step in the catalytic cycle. In this regard, the rate of oxidative addition depends on the relative reactivity of the aryl electrophiles, which is generally thought to decrease in the order of I > OTf ≥ Br >> Cl.[12,18,24] Unreactive aryl halides may be activated by the presence of additional electron withdrawing groups, or in the case of chloropyridines, are inherently active enough to allow for oxidative addition.[1,4,42] Relating to this, increased turnover rates observed for palladium catalysts bearing electron rich and bulky ligands (e.g. PCy_3, P(*t*-Bu)$_3$,[36] biarylphosphines,[44-46] N-heterocyclic carbenes, palladocycles and various bidentate[37,39-41,47] ligands)[38,42,48,49] have been attributed to increases

in the rates of oxidative addition (a characteristic with important implications for unreactive aryl chlorides)[38,42] and/or reductive elimination.[38,43] The rationale behind the success of using bulky ligands is that they encourage low-coordinate, low-valent catalytically active complexes by encouraging ligand dissociation. Another way to encourage low coordination is to use a mixture of a phosphine-free ligand $Pd_2(dba)_2$ (dba = dibenzylideneacetone, a weakly coordinating ligand) with a sterically bulky ligand, such as $P(t\text{-}Bu)_3$ or PCy_3, thus leading to a reduction in the Pd:L ratio.[36,38,42] Transmetalation is mostly considered to be the rate limiting step and the mechanisms are dependent on the organometallic employed. Specific discussion of such factors has been given elsewhere.[12,23,25,50,51] Generally, the reductive elimination is thought to be fast for aryl-aryl couplings; however, this aspect of the mechanism may vary considerably and characteristically has shown an inverse relationship with oxidative addition.[12,25,37] As evidence for this bidentate ligands with small bite angles (e.g. 1,2-bis(diisopropylphosphino)propane or dippp) have been observed to favour oxidative addition. However, ligands with a larger bite angle may favour reductive elimination.[23,37]

2.1.2.3 Mechanistic influences on the coupling of pyridines

As indicated above, electron withdrawing groups help to activate aryl chlorides. This is rationalised in terms of the oxidative addition step where Pd(0) has been shown to act as a nucleophile which preferentially attacks the most electron deficient position.[4] This has important implications for aromatic heterocycles, for example pyridines. In theory poly-halogenated pyridyl derivatives should show differential reactivity towards Pd(0) nucleophiles that reflects the ring substitution position. The 2(6)- and 4-carbons should be most electrophilic while the 3(5)-carbons will show less electrophilicity. Typically, cross-coupling where the oxidative addition step is slow will give rise to a marked regeoselectivity, with a bias towards the most electrophilic position. However, cross-couplings where the oxidative addition is fast may also show similar selectivities. For example, oxidative addition may be aided by coordination of heteroatoms leading to nucleophilic substitution in the adjacent position.[4,52]

Thus, Yang et al.[52] reported the regeoselective Suzuki coupling of 2,6-dichloro-nicotinic acid methyl ester **56** under various reaction conditions (***Scheme 2.1***). Reaction of

phenyl boronic acid with **57** using $Pd(PPh_3)_4$ or $Pd(dppf)Cl_2$ as the precatalyst resulted in a preference for coupling at the 6-position to give **58** . However, the same reaction carried out using precatalysts bearing bulky ligands, such as $Pd(PCy_3)_2Cl_2$, resulted in a preference for coupling at the 2-position to give **59**. It was hypothesized that chelation was the cause of this effect and that the process was favoured with the catalytic system that furnished a low-coordinate low-valent Pd catalyst. Evidence in support of this hypothesis was gained from the increased regioselectivity observed for analogous cross-coupling reactions using 2,6-dichloronicotinamide, which will coordinated more strongly than the ester in the above example.

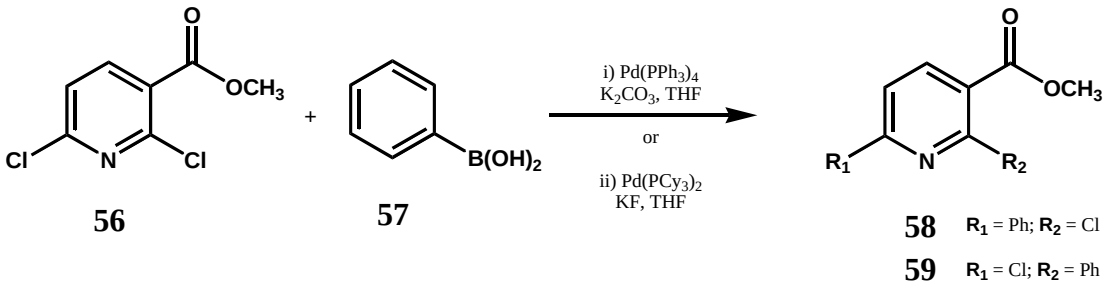

56 **57**

58 R_1 = Ph; R_2 = Cl

59 R_1 = Cl; R_2 = Ph

Scheme 2.1

There are a number of reports describing the regioselective behaviour of 2,4-dihalopyridines in cross-coupling reactions, indicating a preference for coupling at the 2-position due to the greater electrophilicity of this carbon (and the coordinating character of the heteroatom).[4,53-55] This applies to 2,3- and 2,5-dihalopyridines which show a marked difference in the electrophilicity of the halogenated carbons, leading to a bias towards oxidative addition at the 2-position.[4] For example, the Pd(0)-catalysed synthesis of the bipyridine intermediate **62**, used for the synthesis of the natural product nemertelline (3,2′:3′,4′′:2′′:3′′′-quaterpyridine), was conducted by taking advantage of the difference in electrophilicity between the 2- and 3-positions of 2,3-dichloropyridine (**61**) in a Stille cross-coupling reaction to yield stannane **60** (***Scheme 2.2***).[56] A Suzuki cross- coupling reaction was also shown to exhibit similar regioselectivity.[57] Schwab et al.[58] reported an outstanding example of regioselectivity in a Stille cross-coupling of 2-trimethylstannylpyridine (**63**) with 2,5-dibromopyridine (**64**) forming the unsymmetrical 5-bromo-5′-methyl-2,2′-bipyridine (**65**)

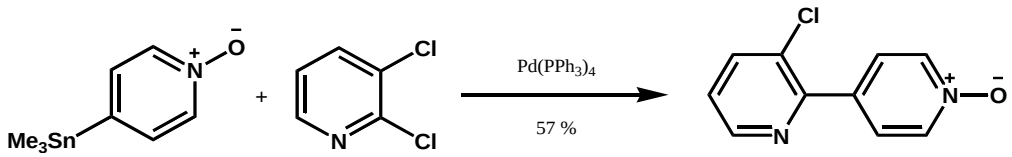

60 **61** **62**

Scheme 2.2

in high yield (***Scheme 2.3***). This latter example of regioselectivity gives rise to the possibility of conducting two successive cross-coupling reactions to access various unsymmetrically substituted 2,2′-bipyridyl derivatives, an important structural arrangement for the current study.

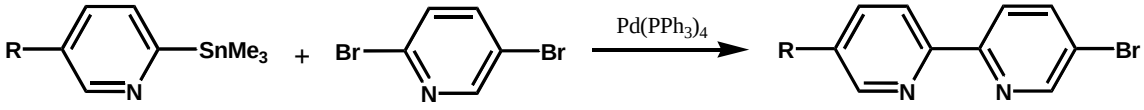

63 **64** **65**

Scheme 2.3

2.1.3 Couplings for the polypyridyl targets of the current project.

For the purpose of designing synthetic strategies for the synthesis of bipyridyl and quaterpyridyl ligands targeted in the current project, a literature search into specifically relevant transition metal catalysed coupling reactions was conducted. This search focused on evaluating possible strategies aimed at reducing the overall number of reaction steps required (by employing convergent procedures where possible). It was also aimed at selecting appropriate functionality on the coupling framents with as little need for protected intermediates as possible. This reviewing process uncovered various promising synthetic methodologies that are summarised below.

2.1.3.1 Ni(0) Homocoupling

Ni(0) catalysis has been extensively used for the homocoupling of aryl halides.[1,6,16,59-63] The Ni(0)-catalysed homocoupling procedure reported by Iyoda *et al.*[16,17] has been employed to synthesize symmetrically substituted 2,2′-, [1,6,16,60,61] 3,3′- [1,16,61,63] and 4,4′-bipyridyl [1,16] derivatives from 2-, 3-, and 4-halopyridines, respectively; notably, the synthesis of 6,6′-dialkoxy-3,3′-bipyridines by Constable *et al.*[63] to generate divergent coordination sites (***Scheme 2.4***). This Ni(II)-catalysed homocoupling has also been used to synthesize terpyridines[62] and quaterpyridines,[62] in particular the synthesis of 2,2′;6′,2″;6″,2‴-quaterpyridine by homocoupling 6-chloro-2,2′-bipyridine.[59] One drawback of the use of $NiCl_2(PPh_3)_2$ as a pre-catalyst for the synthesis of 2,2′-bipyridines is that the product forms stable complexes with Ni(II), necessitating greater catalyst loadings and further steps to remove Ni(II) from the resulting product.[59]

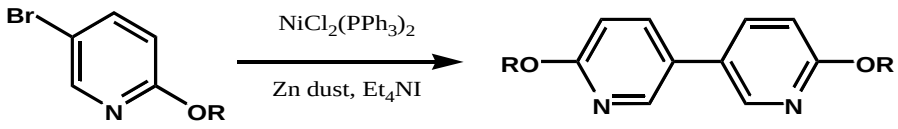

66 **67**

Scheme 2.4

2.1.3.2 Negishi coupling

The Negishi reaction involves the Pd(0) mediated catalytic cross-coupling of aryl or alkenyl halides with organozincate derivatives.[1,2,13,21,64] This is commonly used in the synthesis of polypyridyl systems incorporating unsymmetrically substituted 2,2′-bipyridines because it is often high yielding and is a one pot procedure.[64-68] Baxter[67] employed the Negishi reaction to generate 1,4-bis[5-(2-chloropyridyl)]benzene and 4,4′-bis[5-(2-chloropyridyl)]biphenyl precursors (**71**) for the synthesis of rigidly bridged linear ditopic quaterpyridyl ligands (***Scheme 2.5***). However, the preparation of the arylzinc reagents by metal-exchange of aryllithium reagents limits the range of functional groups that may be

present during the use of this method.[1] As well, the sensitivity of organozinc reagents towards oxygen and water also limits their practicality.

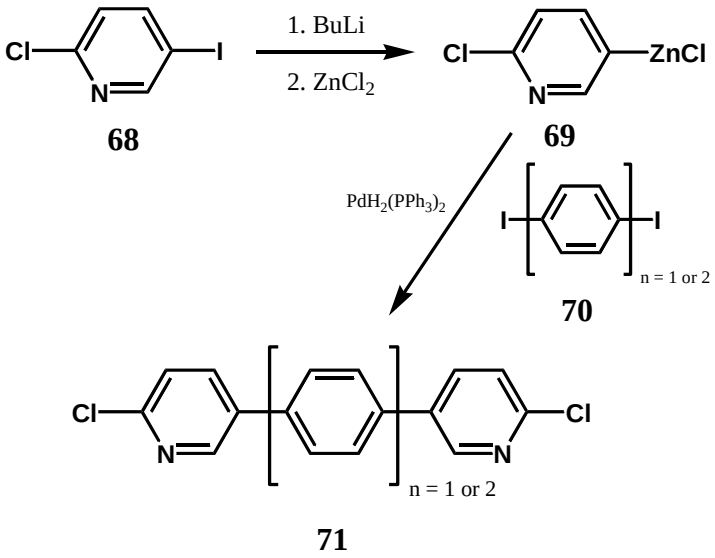

Scheme 2.5

2.1.3.3 Stille coupling

The palladium catalysed coupling of organostannane reagents with electrophiles is known as the Stille reaction.[1,2,13,23] Unlike organozinc halides (discussed above) organostannane reagents are more stable and can be isolated and stored. Furthermore they are compatible with a wide variety of functional groups. The Stille reaction has been widely employed in the synthesis of unsymmetrically substituted 2,2′-bipyridyl, 2,2′;6′2′′-terpyridyl and various quaterpyridyl derivatives.[1,2,58,67,69-73] Of particular interest is the regioselective reaction of 2-trimethylstannylpyridines with 2,5-dibromopyridine to form 5-bromo-2,2′-bipyridine derivatives (***Scheme 2.3***; page 11).[58] These bipyridyl derivatives are interesting intermediates for ligand targets for metallosupramolecular application.[74-77] Also noteworthy, 2,2′;5′5′′;2′′,2′′′-quaterpyridyl derivatives (**74**) have been synthesized using Stille cross-coupling of various 2-trimethylstannylpyridines (**72**) with 6,6′-dibromo-3,3′-bipyridines (***Scheme 2.6***).[69,78]

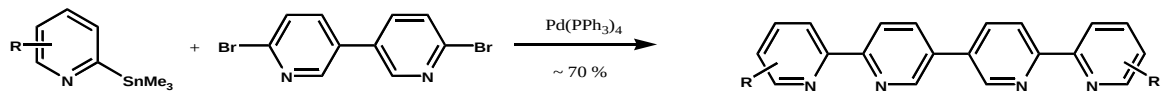

72 **73** **74**

Scheme 2.6

2.1.3.4 Suzuki coupling

The Pd(0)-catalysed cross-coupling of organoboron reagents with electrophiles, known as the Suzuki coupling, is arguably the most widely used transition metal catalysed carbon-carbon bond forming methodology in use today.[1,12,13,79] A combination of factors contribute to this statistic, including the non-toxicity, and air and water stability of many organoboron reagents, as well as the reaction's tolerance towards a wide variety of functional groups. Additional to the latter, Pd(0)-catalysed cross-coupling of alkoxydiboron species with haloarenes provides a convenient, alkyl lithium free, method to synthesise boronic acids and esters.[12,80-83] Suzuki coupling is now widely employed in the synthesis of pyridyl, bipyridyl and larger polypyridyl systems.[76,77,84-91] The employment of Suzuki coupling for the synthesis of 2,2′-bipyridines is however rare, and this is mainly due to the relative instability of the 2-pyridinyl boronic acids or esters.[86,87,92] By contrast, the synthesis and relative stability of 3- and 4-pyridinyl boronic acids and esters has allowed their expanded usage as nucleophiles in coupling procedures.[84-86,89,90] In this context, Suzuki coupling has been used in a high yielding synthesis of 6,6′-dialkoxy-3,3′-bipyridines analogous to that described above in ***Scheme 2.4*** (page 62).[84] However, the most relevant usage of Suzuki couplings for the present project is its use in the convergent synthesis of ditopic and polytopic polypyridyl ligands for use in coordination chemistry.[74-77,91] A particularly relevant example involved a di-coupling of 5-bromo-2,2′-bipyridine (**75**) to 1,4-bis-(4,4,5,5-tetramethyl[1,3,2]dioxaborolan)benzene (**76**) to give the rigidly bridged linear quaterpyridyl ligand **77** (***Scheme 2.7***).[76] Note in this case 5-bromo-2,2′-bipyridine was synthesized using the Stille coupling reaction decribed by Schwab et al.[58]

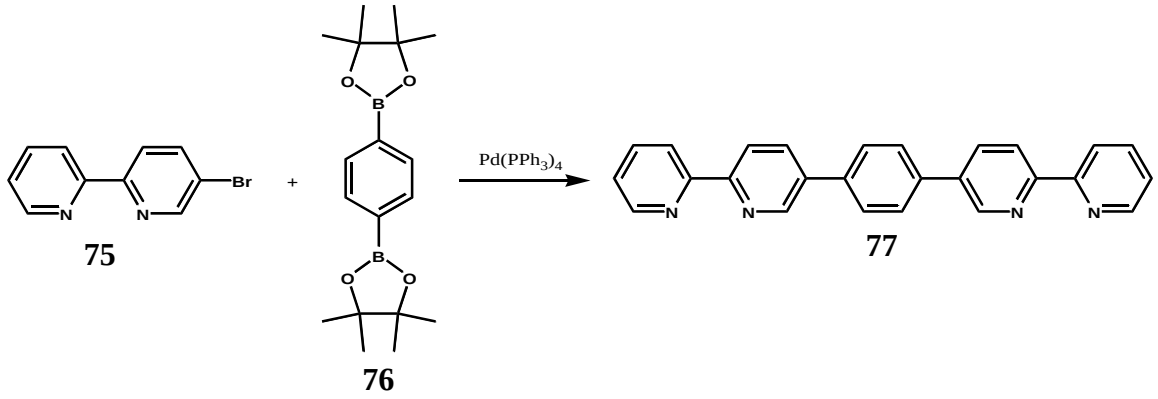

Scheme 2.7

2.1.3.5 Microwave dielectric heating and coupling reactions

One drawback of transition metal catalysed coupling reactions is that they typically require long reaction times using conductive heating. However in recent times it has been found that microwave dielectric heating may result in a dramatic acceleration of these reactions, most often resulting in cleaner reactions with higher yields.[93-97] The source of acceleration of these reactions by microwave heating is still a source of debate.[98,99] However, it may be understood, at least to some extent, in terms of the attainment of higher reaction temperatures and pressures. Because of the high stability of aryl boronic acids and esters towards air and water, many Suzuki couplings are now carried out in water using microwave dielectric heating.[94] Typically, completion of these reactions is on a scale of minutes, while analogous conductively heated reactions may take hours.

2.2 TARGET LIGANDS AND SYNTHETIC APPROACHES

2.2.1 Unsymmetrical salicyloxy- substituted 2,2′-bipyridines.

A proposed investigation into the metal directed self-assembly of tripodal ligands, such as **79** (***Scheme 2.8***), prompted the synthesis of a series of benzaldehyde precursors

related to bipyridine **78** (variable at R_1,R_2 and R_3). It was proposed that a '*one pot*' reductive amination procedure would allow the synthesis of various tripodal ligands related to **79**. This reductive amination procedure will be discussed in more detail in Chapter 5.

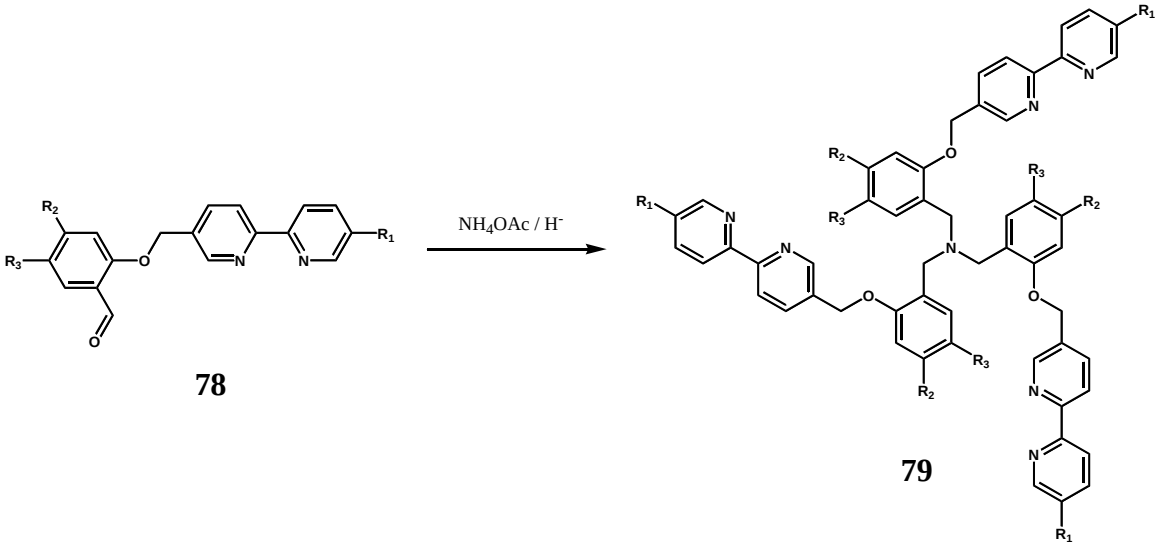

Scheme 2.8

Two general approaches were pursued in order to synthesize unsymmetrical 5,5′-disubstituted-2,2′-bipyridine derivatives analogous to **78**. The first approach involved the *regioselective* functionalisation of the symmetrically substituted 5,5′-dimethyl-2,2′-bipyridine.[65,73,100,101] The second approach involved the functionalisation of the already unsymmetrical 5-bromo-5′-methyl-2,2′-bipyridine with the intention of extending the resulting bipyridines with aryl-aryl coupling procedures.

After careful consideration of several different Pd(0)-catalysed cross-coupling methodologies it was decided that Stille cross-coupling reaction would provide the most convenient approach to the various 2,2′-bipyridine derivatives targeted in the current research. Indeed it has been well documented that the Stille cross-coupling allows for the efficient and regioselective synthesis of 2,2′-bipyridines.[4,58] Another consideration is that only a single stannane (stannane **81**, ***Scheme 2.9***) was required in all the Stille coupling reactions conducted in the project. Consequently stannane **81** was synthesized in gram scale from picoline **80** via a reported halogen/lithiation/transmetallation procedure.[58] The crude product was purified by vacuum distillation to afford the pure product in yields of the order of 65 %. While the crude yield was most probably in excess of 90 %, the relative efficiencies

of subsequent coupling reactions using the crude versus the pure stannane dictated the necessity for its purification. Stille cross-coupling[58,71-73] of stannane **81** and picoline **80** afforded bipyridine **82** in 90 % yield. The ^{1}H NMR spectrum of this symmetrically substituted product revealed only three aromatic ^{1}H signals which were distinguished on the basis of short (^3J) and long (^4J) range couplings,‡ allowing for the straightforward assignment of its ^{1}H NMR spectrum.

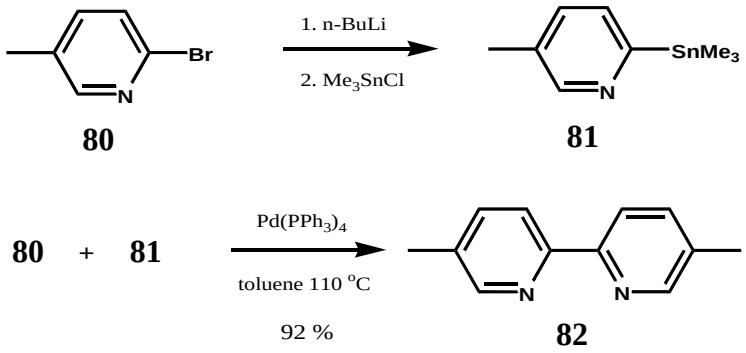

Scheme 2.9

In contrast to the synthesis of bipyridine **82**, Stille cross-coupling of stannane **81** with 2,5-dibromopyridine **83** might be predicted to result in three products, including 2,2′-bipyridine **84** and/or 2,3′-bipyridine **86**, and/or 2,2′;5′2′′-terpyridine **87** (***Scheme 2.10***). However, TLC of the crude reaction material indicated the large predominance of a single product which could be routinely purified by chromatography. The ^{1}H NMR spectrum revealed six aromatic proton signals consistent with the formation of one of the bipyridyl derivatives. Differentiation between the two possible bipyridine products, **84** and **86**, was easily achieved based on a Fe(II) test which gave a positive result (e.g. deep red colour) for **84**. The unsymmetrical substitution pattern of bipyridine **84**, shown by its six aromatic ^{1}H NMR resonances, complicated the assignment of the ^{1}H NMR spectrum. While the relative ring positions of protons were able to be determined based on coupling patterns,‡ complete assignment of the ^{1}H NMR spectrum relied on results from NOESY and COSY experiments.

‡ The 2,5-disubstituted pyridine ring structure has a characteristic ^{1}H NMR shift pattern; the proton in the 6-position has small ^4J couplings (1.5 – 2.8 Hz) to the proton in the 4-position. The proton in the 4-position has a larger ^3J (8 - 9 Hz) to the proton in the 3-position. Occasionally ^5J couplings between the protons in the 3-position and 6-position are observed ($^5J \approx 0.6$ Hz).[102]

NOE's were observed between the methyl protons and aromatic protons in the 4′- and 6′-positions and a ^{1}H COSY experiment confirmed that the couplings were assigned correctly, allowing for the ^{1}H NMR spectrum to be fully assigned (a 1D TOCSY experiment may also be used in the place of the ^{1}H COSY experiment).†

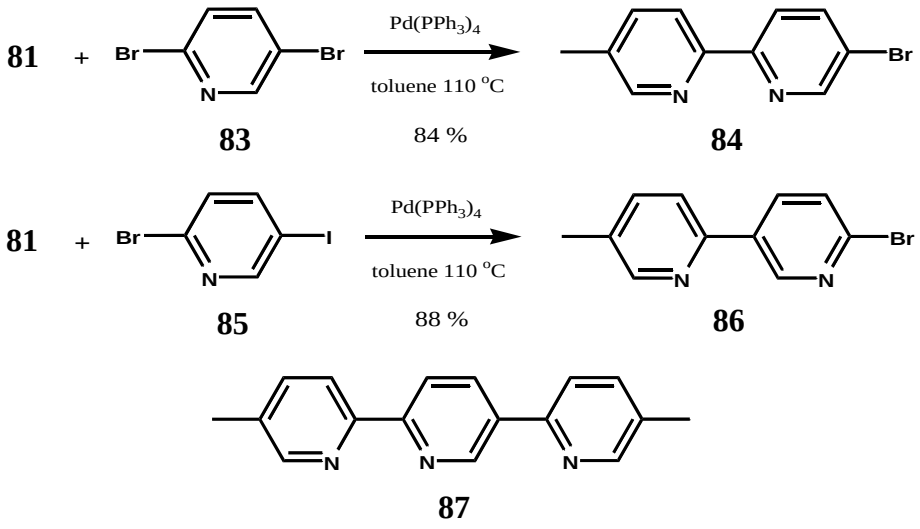

Scheme 2.10

The regioselectivity of the Stille coupling that yielded bipyridine **84** is not an isolated example.[58] However, when an excess of stannane **81** was employed, coupling at the 5-position was *observed*, resulting in the formation of the byproduct terpyridine **87** (***Scheme 2.10***). Interestingly, when a Stille coupling was carried out between stannane **81** and 2-bromo-5-iodopyridine **85** the coupled product was the 2,3′-bipyridine **86** (which was characterised by ^{1}H and ^{13}C NMR in combination with a negative Fe(II) test). Evidently the increased reactivity of the iodo substituent overcomes the reactivity difference between the 2- and 5-positions observed for the coupling of stannane **81** with 2,5-dibromopyridine.

In order to introduce salicyloxy functionality into bipyridines **82** and **84**, their halomethyl derivatives, **93** and **94**, were required for subsequent *O*-alkylation with appropriate salicylaldehydes. Typically halomethylbipyridines, such as **90** (***Scheme 2.11***), are prepared either by radical halogenation[103-105] or from hydroxymethyl precursors.[106,107]

† This general method of assigning the ^{1}H NMR spectra of unsymmetrical 2,2′-bipyridine derivatives was employed throughout the present research programme and discussion in this detail will not be repeated again unless it is specifically warranted (exemplary spectra are presented in Appendix A).

Unfortunately, radical methods usually lead to mixtures of halogenated products that often prove difficult to separate. The alternative synthesis of halomethylbipyridines, via hydroxymethyl precursors, involves multiple moderate yielding steps leading to low overall yields.[104,108-110] A recent development provides an alternative high yielding methodology which involves substitution of trimethylsilylmethyl intermediates, such as **89** (***Scheme 2.11***), with an electrophilic halogen source (e.g. BrF_2CCF_2Br or Cl_3CCCl_3), in the presence of a source of F^- (e.g. TBAF or CsF).[65,73,100,101] The silylmethyl intermediate **89** may be generated in high yield from bipyridyl precursors of type **88** by sequential treatment with LDA and trimethylsilyl chloride. Moreover, it has been reported[73] that the regioselective synthesis

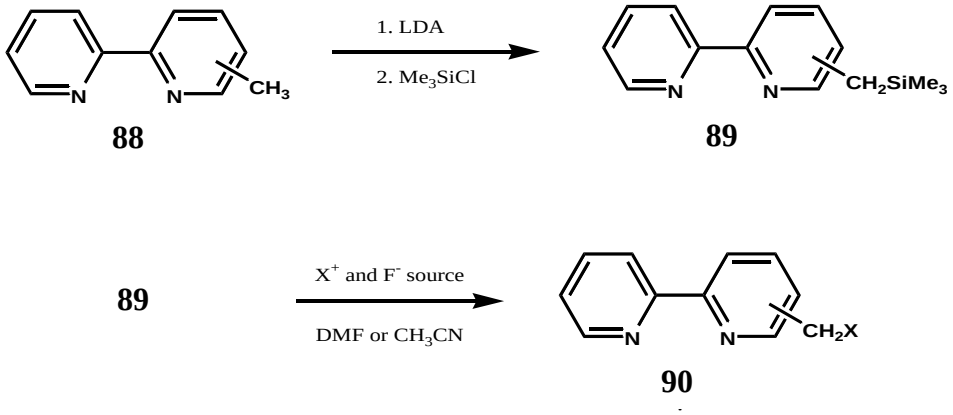

Scheme 2.11 [65,73,100,101]

of 5-methyl-5′-trimethylsilylmethyl-2,2′-bipyridine can be accessed as a result of the insolubility of the *mono*-lithiated intermediate. Thus this procedure provides a useful approach for the synthesis of the target unsymmetrically substituted bipyridyl derivatives from the symmetrically substituted bipyridine **82**.

The procedure outlined in ***Scheme 2.11*** was employed in the present study allowing for the gram scale conversion of bipyridine **82** to the (trimethylsilyl)methyl derivative **91**, in yields of 60 – 80 % (***Scheme 2.10***). The ^{1}H NMR spectrum of **91** revealed a high field methylene resonance (δ = 2.11 ppm), a trimethylsilyl proton resonance (δ = 0.03 ppm) and the apparent loss of the 2,2′-bipyridyl *C2*-symmetry, consistent with this monosilated product having formed. It is noted that significant amounts of bis-(trimethylsilyl)methyl bipy **92** is formed if reactions are extended beyond the reported 1 minute (see *Section 2.2.2* for a brief

description of the targeted synthesis of **92**).[73] Most likely this latter factor was the source of the high variability of recorded yields for this synthesis. Regardless of this complication, the mono- and bis-(trimethylsilyl)methyl products **91** and **92**, could be routinely separated using standard chromatographic techniques, in contrast to the derived mono- and bis-halomethyl bipyridyl derivatives. Silane **91** was then converted to chloromethyl bipyridine **93** using Cl_3CCCl_3 and CsF in 85 % yield (***Scheme 2.12***). The observed downfield shifted methylene peak (δ = 4.62 ppm) in the ^{1}H NMR spectrum of **93** was consistent with the formation of the chloromethyl product. It should be noted that the previous report [65,73,100,101] of halogentation via this methodology employed $C_2Br_2F_4$ as the electrophilic halogen source affording the bromomethyl analogue of chloromethyl bipy **93**. The electrospray high resolution mass spectrum (ESI-HRMS) confirmed the isolation of chloromethyl bipyridine **93** by showing ions corresponding to both protonated (calcd for [**7** + H]$^+$: 219.0683, found 219.0676) and sodiated (calcd for [**7** + Na]$^+$: 241.0503, found 241.0497) species.

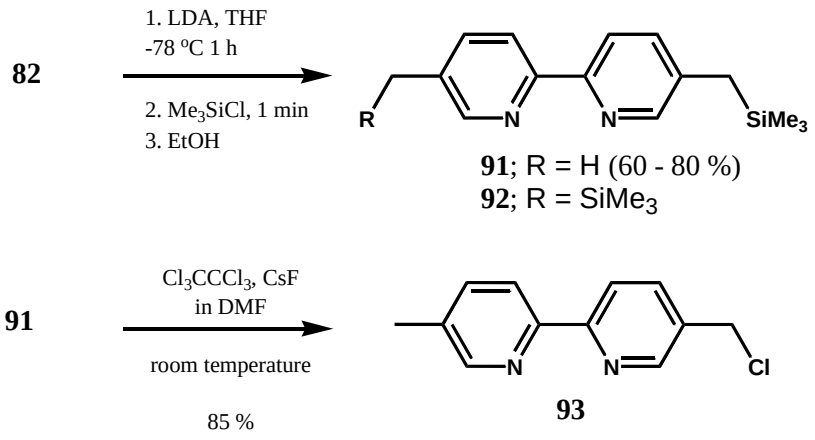

Scheme 2.12

Bromomethylbipyridine **94** (***Scheme 2.13***) is an interesting unsymmetrical bipyridine intermediate that proved invaluable for the success of the current research program. This intermediate was able to be extended by using two high yielding synthetic procedures – base catalysed nucleophilic substitution at the benzylic halide and transition metal-catalysed coupling reactions at the aryl halide. Thus, **94** is a valuable intermediate for the synthesis of both the unsymmetrical bipyridyl target outlined below in this section and for the symmetrically substituted quaterpyridyl derivatives to be discussed in *Section 2.2.3*. The one

step radical halogenation of methylbipyridine **84** using N-bromosuccinimide (NBS) was chosen for the synthesis of bromomethyl-bipyridine **94** as the added complication of the corresponding bis-halomethyl product was absent. This afforded **94** in reasonable yields, varying from 60 – 70%. The methylene proton signal at 4.53 ppm in the ^{1}H NMR spectrum of **94** is consistent with the formation of the mono-bromomethyl product.

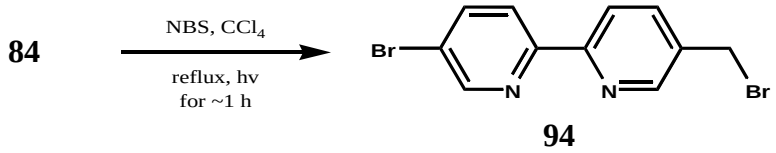

Scheme 2.13

A series of *O*-alkylations using various salicylaldehydes (required for the reductive amination procedure outlined in ***Scheme 2.8***, page 66) were conducted to introduce the salicyloxy functionality into the unsymmetrical 2,2′-bipyridines **93** and **94** (***Scheme 2.14***).

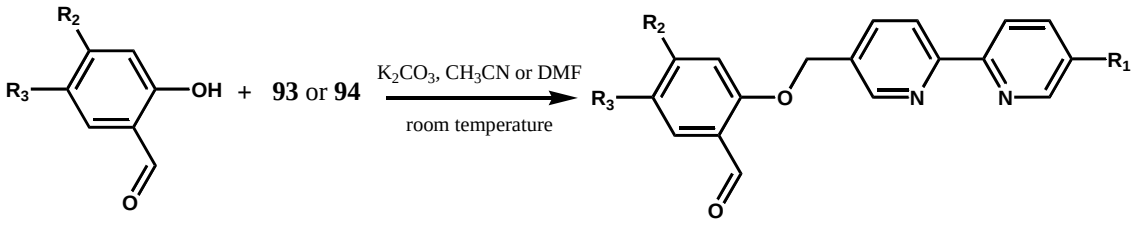

95; R_2 = H; R_3 = H
96; R_2 = H; R_3 = *t-butyl*
97; R_2 = H; R_3 = *t-octyl*
98; R_2 = OTHP; R_3 = H

99; R_1 = Me; R_2 = H; R_3 = H
100; R_1 = Me; R_2 = H; R_3 = *t-butyl*
101; R_1 = Br; R_2 = H; R_3 = H
102; R_1 = Br; R_2 = H; R_3 = *t-butyl*
103; R_1 = Br; R_2 = H R_3 = *t-octyl*
104; R_1 = Me; R_2 = OTHP; R_3 = H
105; R_1 = Br; R_2 = OTHP; R_3 = H

Scheme 2.14

Two general procedures were employed: base catalysed phase transfer alkylations and base catalysed alkylations in polar aprotic solvents. The phase transfer methodology employs an aqueous NaOH solution with an organic solution of phenol to generate the nucleophilic phenoxide ion. An alternative to phase transfer catalysis, is the use of base catalysed nucleophilic substitution involving dry aprotic solvents and using K_2CO_3 as the base. This

latter approach was the preferred method in the current work. However, the phase transfer reaction was initially employed in the project.

Chloromethyl bipyridine **93** was reacted with salicylaldehydes, **95** and **96,** in the presence of K_2CO_3, to afford the mono-aldhehyde derivatives **99** and **100** in 93 % and 95 % yield, respectively. The downfield shifted methylene proton resonances (in the region of 5.2 – 5.3 ppm in $CDCl_3$) of the salicyloxymethyl ether products, **99** and **100**, are diagnostic of the O – C bond formation. Aldehyde **14** was also prepared via the phase transfer method described above, resulting in a yield of 83 %. The recorded yields were consistently inferior using phase transfer catalysis and as a result this methodology was only employed early in the project.

Bromomethyl bipyridine **94** was reacted with salicylaldehydes **95**, **96** and **97** affording **101**, **103** and **104** in yields greater than 90 % (***Scheme 2.12***). These reactions were clean with no observable side products resulting from a possible nucleophilic attack at the 5-bromo functional group, reflecting the poor reactivity of the pyridines 5-bromo-substituent towards nucleophilic substitution. Aldehyde derivatives **101** – **104** were key intermediates for the synthesis of the dialdehydes to be discussed in *Section 2.2.3*. Interestingly, the tri-substituted benzene function in aldehydes **100**, **102** and **103** result in a similar ^{1}H NMR pattern to that of 2,5-disubstituted pyridine rings. Thus, there are three similar sets of tri-substituted aromatic protons observed in their ^{1}H NMR spectra (for a representative spectrum see ***Figure 2.3***). It is noted that the proton signals of the aryl ring are shifted upfield relative

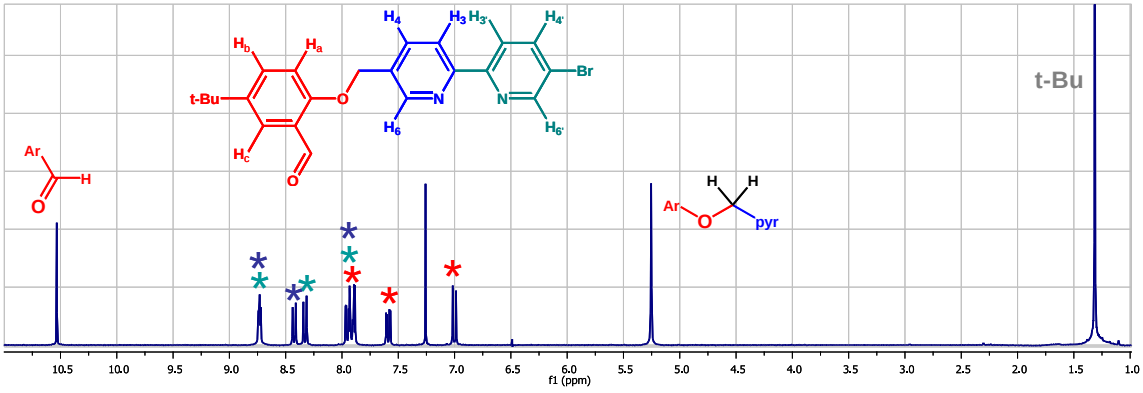

Figure 2.3 The ^{1}H NMR spectrum of aldehyde **102** in $CDCl_3$ (δ = 7.27) is illustrated with colour coded structure and asterisks.

to those of the protons on the pyridyl ring. ***Figure 2.3*** also illustrates other key resonances in the spectrum common to many aldehyde derivatives studied in the project. In particular, the methylene signal at 5.25 ppm is diagnositic of the successful O – C bond formation.

An interest in the possibility of further functionalisation of tripodal tris-bipyridyl adducts (***Scheme 2.8***, page 66) led to an investigation into appropriate intermediates. The utility of the *O*-alkylation procedure, and reports that 2,4-dihydroxybenzaldehyde is able to be regeoselectively protected at the 4-position with a tetrahydropyranyl (THP) group led to its employment here.[111,112] Furthermore, the THP protecting group is stable under the basic conditions used for the *O*-alkylation reaction to make the corresponding salicyloxybipyridyl derivatives. With this in mind, 2,4-dihydroxybenzaldehyde was converted to THP-derivative **98** using a reported procedure.[111,112] THP-derivative **98** was then reacted with halomethyl-bipyridines **93** and **94** to afford **104** and **105** in high yields. The THP protecting group of **105** was easily removed by extraction into 2 M HCl followed by neutralisation to give **106** in quantitative yield (***Scheme 2.15***).

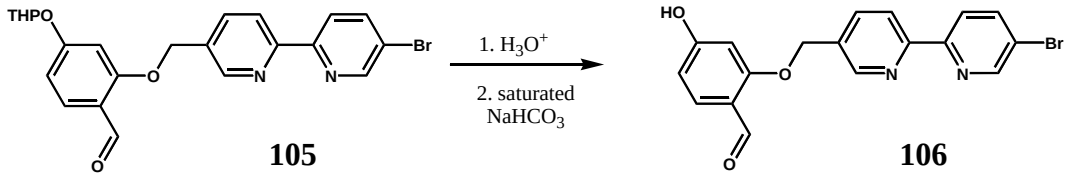

Scheme 2.15

Alkylation of hydroxy-salicyloxybipyridine **106** with 1-iodoheptane gave bipyridine derivative **107** (***Scheme 2.16***). In this case the heptyl group in **107** was introduced as a proof of concept as well as to promote the solubility of intended derivatives.

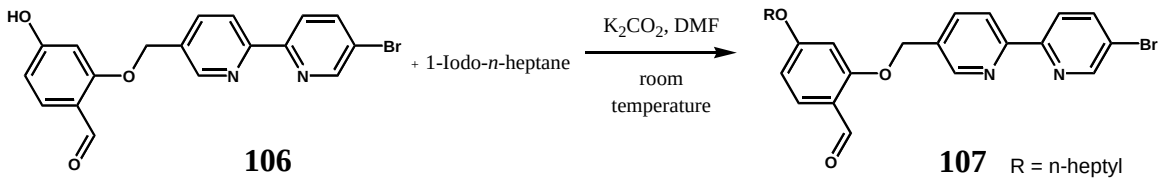

Scheme 2.16

The Suzuki coupling procedure was chosen as the preferred aryl-aryl bond formation procedure for the extension of 5-bromo-2,2′-bipyridines such as **84**, due to its reported tolerance towards a wide range of functional groups (including carbonyl groups) and the relative ease of isolation and stability of boronic acids and esters.[12] Importantly, the latter results in boronic acids/esters being able to be stored for extended periods and reacted with a range of aryl halides. To this end, boronic ester **108** (***Scheme 2.17***) was prepared using a two step synthetic approach from *para*-bromophenol. In the first step the phenol was protected with a THP group followed by conversion to **108** using a previously described method.[113-116] This procedure involves lithiation of the protected bromophenol with butyllithium followed by addition of 2-isopropoxy-4,4′:5,5′-tetramethyl-1,3,2-dioxaboralane. Water was then added to quench the reaction followed by the removal of the THF and subsequent extraction of the alkaline (pH in the range of 11-14) aqueous phase with Et_2O. However, only poor yields (20 – 30 %) of boronic ester **108** were obtained. It was thought that excess OH^- might be forming charged adducts with the boronic ester thus increasing the product's water solubility. Consequently *careful* adjustment of the aqueous quench solutions to within the pH range of 7 – 8 with HCl resulted in improved yields of **108** and other boronic ester products (to be discussed in *Section 2.2.3*).

Suzuki coupling between boronic ester **108** and bromobipyridine **84** was carried out using a variation on a reported method (***Scheme 2.17***).[93,117] In the current synthesis the reaction was heated using microwave energy for a total of 10 minutes in a DMF : H_2O (2 : 1) solvent mixture. This procedure resulted in the isolation of bipyridine **109** in a 75 % yield.

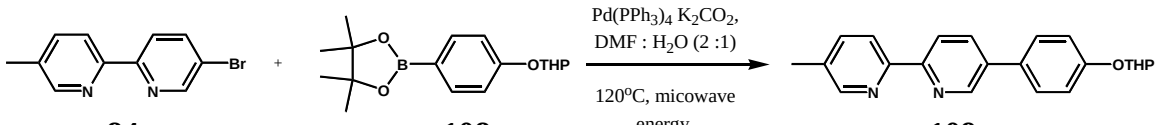

84 **108** **109**

Scheme 2.17

Further Suzuki coupling reactions with boronic ester **108** and bromobipyridines **102** and **107** were then conducted to afford **110** and **111** in 77 % and 74 % yields, respectively (***Scheme 2.18***). These reactions were typically complete within 10 minutes. A convenient feature of the microwave-driven Suzuki coupling procedure employed here is that the

relatively short reaction times reduce the degree of catalyst poisoning that occurs. Thus, the catalyst may be easily separated by the addition of excess water which precipitates the product and allows its isolation by filtration. In combination with this, the hydrophobic nature of both salicyloxybipyridines **110** and **111** fortuitously allowed a simple cold methanol wash of the precipitate to give relatively pure products which could be used in subsequent reactions.

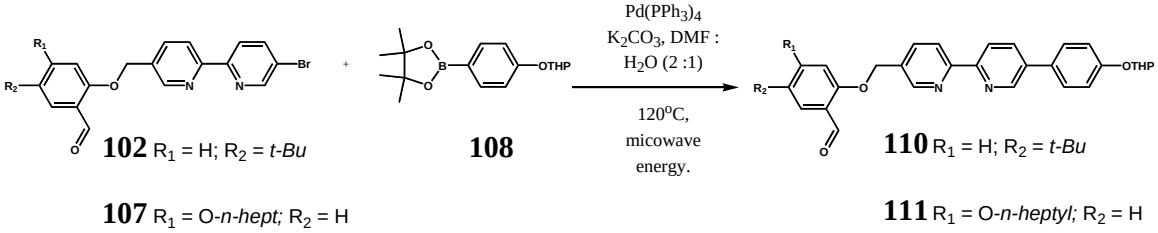

102 R_1 = H; R_2 = *t-Bu*

107 R_1 = O-*n-hept;* R_2 = H

108

110 R_1 = H; R_2 = *t-Bu*

111 R_1 = O-*n-heptyl;* R_2 = H

Scheme 2.18

2.2.2 Symmetrically substituted 2,2′-bipyridines.

A series of symmetrically substituted bipyridyl dialdehydes were targeted for employment in metal-template reductive amination procedures analogous to those developed by Perkins *et al.*[118,119] (***Scheme 2.19***). Dialdehyde **113** (***Scheme 2.21***) was synthesized with

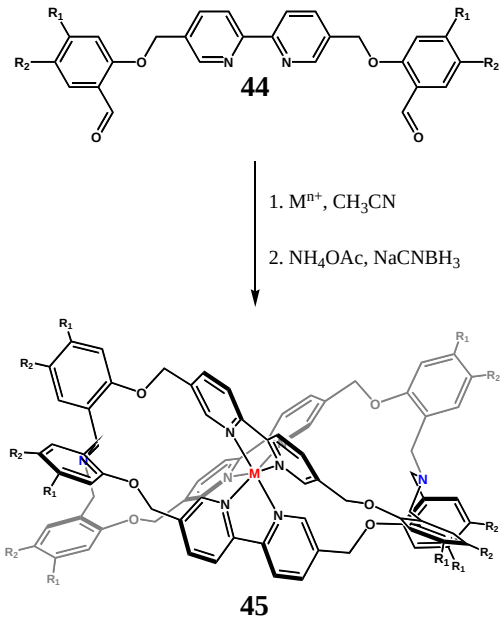

44

45

Scheme 2.19[118,119]

the aim of investigating this reported metal-template reductive amination procedure. As an extension of the previously published work of Perkins *et al.* the synthesis of the analogous Ru(II) cryptates was intended. Further, the possibility of performing additional functionalisation of related pre-formed cryptates using protected dialdehydes, such as **114** and **116** (***Scheme 2.21***), was also planned.

Dimethylbipyridine **82** was the primary starting material for the research outlined above. Initially **82** needed to be converted to its bis-halomethyl derivative. In this regard, bis-halomethyl derivatives of 6,6′- and 4,4′-dimethyl-2,2′-bipyridines have been reported[100,101,120] to have been prepared via the corresponding bis-(timethylsilylmethyl) intermediates as outlined in ***Scheme 2.11*** (page 69) and in the present study this methodology was extended to include the of 5,5′-chloromethyl-2,2′-bipyridine. The procedure employed hexamethylphosphoramide (HMPA) as a co-solvent to overcome the insolubility of the corresponding mono-lithiated bipyridyl intermediate, thus promoting bis-lithiation and allowing the production of the required bis-(trimethylsilylmethyl) intermediate **92**.This silane was then converted to 5,5′-chloromethyl-2,2′-bipyridine using Cl_3CCCl_3 and CsF in high yield. While this procedure represents a controlled approach to the synthesis of 5,5′-chloromethyl-2,2′-bipyridine, it involves a time consuming two-step procedure using expensive reagents. Thus, the advantages of a higher overall yield and ease of purification are somewhat diminished relative to the use of a one step radical halogenation procedure. As a result, radical halogenation with NBS was chosen allowing for the gram scale synthesis of bis-bromomethyl bipyridine **112** (***Scheme 2.20***) in yields of up to 70 %.

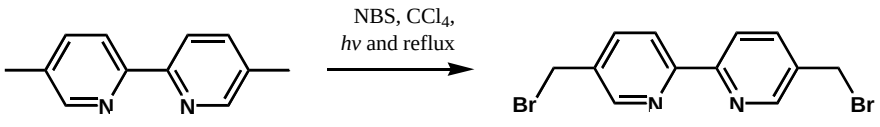

82 **112**

Scheme 2.20

Using the same base catalysed *O*-alkylation procedure outlined above, both dialdehydes **113** and **114** were synthesized in high yields by the reaction of bis-bromomethylbipyridine **112** with the salicylaldehydes **96** and **98**, respectively (***Scheme 2.21***).

The yield of the previously reported dialdehyde **113** was improved from the 84 % achieved under phase transfer base catalysis, to 95 % with the current procedure.

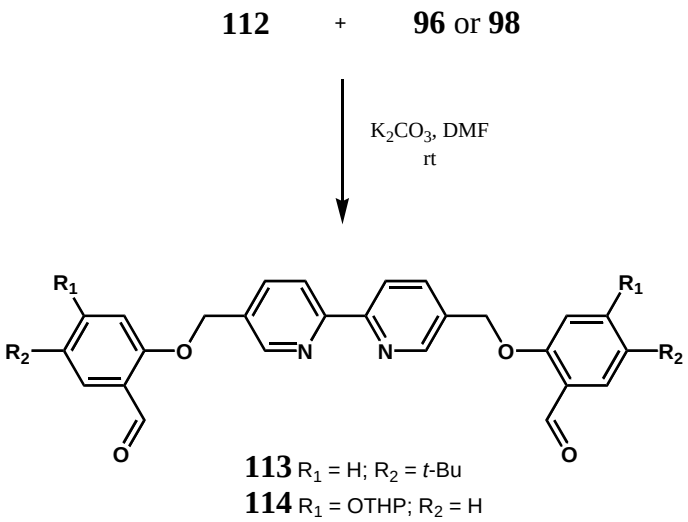

Scheme 2.21

The formation of diastereomers during the synthesis of dialdehyde **114** resulted in the NMR characterisation of its corresponding *tris*-chelate Fe(II) complex being impeded. Thus, the THP group was replaced with the more robust non-chiral *para*-methoxybenzyl (PMB) protecting group. Removal of the THP group was conducted with HCl, allowing the isolation of the sparingly soluble *bis*-phenol **115**. The subsequent *O*-alkylation of **115** with *para*-methoxybenyl chloride gave the PMB protected dialdehyde **116** in high yield (***Scheme 2.22***). It is worth noting that the selective protection of the 4-hydroxy group as a tetrahyropyranyl ether and subsequent *O*-alkylation of the 2-hydroxy group of 2,4-dihydroxybenzaldehyde were still necessary steps in the synthesis of dialdehyde **116**.

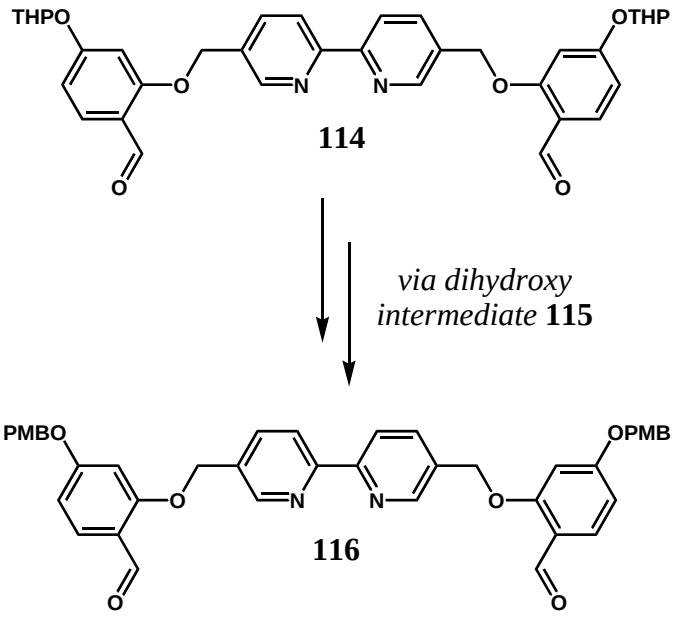

Scheme 2.22

2.2.3 Rigidly bridged ditopic quaterpyridyl ligands.

The aim to extend the previously reported mononuclear tris-bipyridyl cryptate (***Scheme 2.19***, page 76) to a ditopic system prompted the synthesis of a variety of rigid ditopic bis-bidentate quaterpyridyl ligand systems. With such systems there is potentially a range of metallosupramollecular outcomes that may occur as a result of metal-directed assembly procedures employing octahedral metal ions. Possible 'simple' discrete structures of general formula $[M_{2n}L_{3n}]^{n+}$ {n = 1, 2 and 3} that may result are illustrated in ***Figure 2.4***. In this regard, a series of ditopic quaterpyridines were synthesized to investigate the outcome of such interactions with octahedral metal ions. Initially, 5,5′′′-dimethyl-2,2′;5′,5′′;2′′,2′′′-quaterpyridine (**50**) (***Scheme 2.23***), was targeted for these proposed metal directed assembly studies.

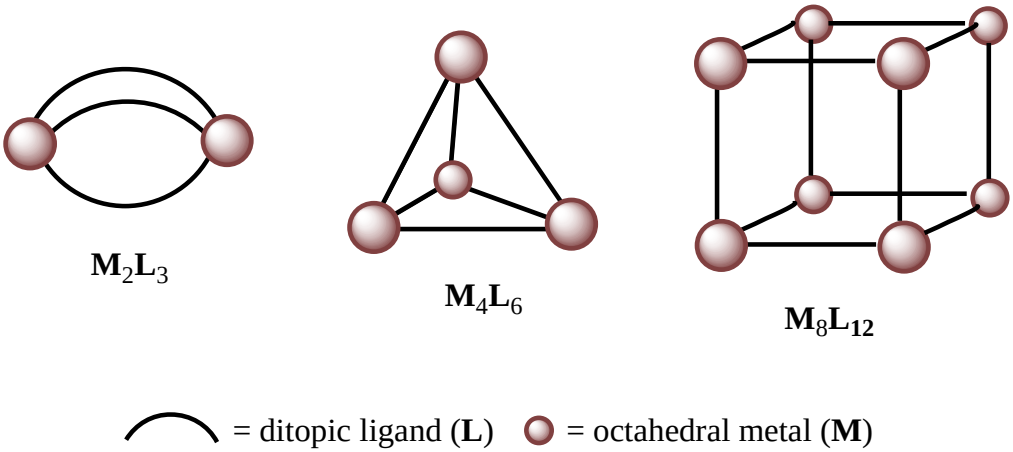

Figure 2.4 Schematic illustrations of some potential metallosupramolecular structures arising from the metal-directed assembly using an octahedral metal ion with rigid di-bidentate bridging ligand of the present type in a 2:3 ratio.

The original synthetic approach for quaterpyridine **50** (modelled on a reported[69] synthesis) involved two key aspects: the synthesis of its divergent 6,6′-dichloro-3,3′-bipyridine **121** bridge and the formation of the two convergent chelating domains of quaterpyridine **50** (***Scheme 2.23***). The synthesis of the former was initiated by the iodination of 2-aminopyridine **117** affording 5-iodo-2-aminopyridine **118**.[121] Aminopyridine **118** was then converted to 2-bromo-5-iodopyridine **85** via nucleophilic substitution of its diazonium salt.[121,122] Regioselective nucleophilic substitution of 2-bromopyridine **85** with sodium methoxide afforded 5-iodo-2-methoxypyridine **119**.[63] The methoxy-group in pyridine **119** acts as a protecting group in its Ni(0)-catalysed homocoupling, thus allowing the synthesis of divergent 3,3′-bipyridine **120** in a yield of 93 %. This is a distinct improvement on the reported yield of 70 %.[63] The successful isolation of bipyridine **120** was confirmed by comparison of its ^{1}H NMR spectrum with that of the reported spectrum. The synthesis of the divergent bridge, dichlorobipyridine **121**, involved deprotection/halogenation under modified Vilsmeier – Hack conditions.[63,123] In this procedure reaction of **120** with $POCl_3$ in DMF afforded **121** in 87 % yield.

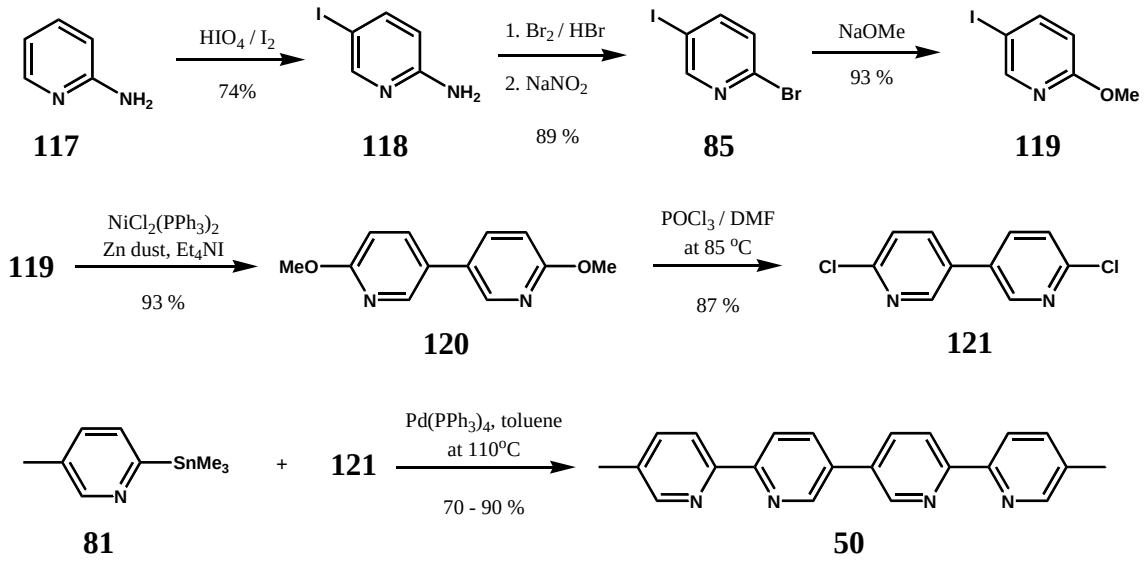

Scheme 2.23

A Stille coupling of two equivalents of stannane **81** with one equivalent of bipyridine **121** yielded the desired quaterpyridine **50** in yields ranging from 70 – 90 %. This sparingly soluble material was purified by recrystallisation from refluxing DMF. The ^{1}H NMR spectrum of **50** bears some resemblance to that of bromobipyridine **84**, revealing a single methyl signal and six aromatic signals. NOEs were observed between the methyl group and protons in the 4,4′′′- and 6,6′′′- positions. This combinded with the results from a ^{1}H COSY experiment confirming ^{1}H – ^{1}H couplings permitted full assignment of the ^{1}H NMR spectrum of **50**. Furthermore, the HRMS of quaterpyridine **50** contained ions corresponding to both protonated (calcd for [**50** + H]$^{+}$: 339.1604, found 339.1591) and sodiated (calcd for [**50** + Na]$^{+}$: 361.1424, found 361.1411) species.

A series of bridged quaterpyridines were also synthesised as a result of the interesting metallosupramolecular structures obtained with quaterpyridine **50** (see Chapter 3). In particular, an interest in the steric constraints that sp^{2} hybridisation places on metal-directed assembly outcomes led specifically to the investigation of arylene bridged quaterpyridines (see Chapter 4). The latter retain analogous rigidity to that of quaterpyridine **50** itself. Thus, phenylene and biphenylene bridged quaterpyridines, **126** and **127**, previously synthesized via a predominantly divergent approach,[67] were targeted using a more convergent route involving a *bis*-Suzuki coupling of bromobipyridine **84** employing the *bis*-boronic esters, **122** and **123**

(***Scheme 2.24***). Thus, quaterpyridines **126** and **127** were synthesised in 70 % and 82 % yields, respectively, via microwave-driven Suzuki couplings. As previously reported,[67] quaterpyridines **126** and **127** were confirmed to be highly insoluble and recrystallisation from high boiling point solvents, such as pyridine or DMF, was necessary for their purification. In relation to their low solubility, Baxter reported[67] running ^{1}H NMR spectra of **126** and **127** in deuterated DMF at 100 °C. However, as only ^{1}H NMR evidence was needed for comparison of the spectra of our products to the reported spectra, spectra collected at 298 K using dilute CD_2Cl_2 solutions proved adequate in the present study.

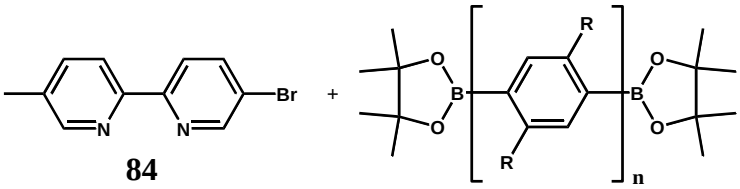

122; R = H; n =1
123; R = H; n = 2
124; R = OMe; n = 1
125; R = OMe; n = 2

$Pd(PPh_3)_4$ / K_2CO_3
in DMF : H_2O (3:1)
microwave 120 ^oC

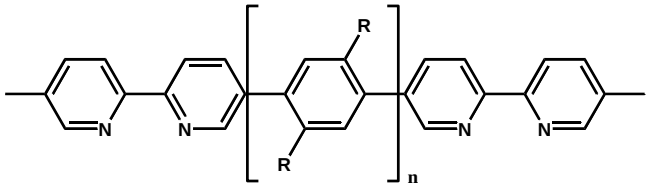

126; R = H; n =1
127; R = H; n = 2
128; R = OMe; n = 1
129; R = OMe; n = 2

Scheme 2.24

Unfortunately the insoluble nature of **126** and **127** inhibited the formation of stable metal complexes with Fe(II) salts, thus prompting an investigation into more soluble analogues. As a consequence, the incorporation of 1,4-dialkoxy-substituted phenylene bridges was considered desirable for two reasons. Firstly, they should be readily cleaved to give the corresponding phenols which would facilitate further functionalisation. Secondly, the

oxidative demethylation of phenolic ethers to give quinones[124] may allow for the adjustment of electron and energy transfer properties of the ligand.

The synthesis of quaterpyridine **128** in 83 % and **129** in 95 % yield was conducted using microwave driven *bis*-Suzuki couplings of bipyridine **84** with boronic esters **124** and **125,** respectively (***Scheme 2.24***). Unlike the poor solubility of **126** and **127**, quaterpyridines **128** and **129** were quite soluble in a range of solvents. Thus, NMR characterisation in chlorinated organic solvents was possible. ^{1}H and ^{13}C NMR spectra of quaterpyridines **128** and **129** were consistent with the expected two fold symmetry for these products. The 2,2′-bipyridyl moities of both **128** and **129** were assigned using NOESY and COSY measurements. A similar ^{1}H NMR resonance pattern was observed for **50** & **126** – **129**. The 'inner' pyridyl protons experience greater deshielding and therefore are situated further downfield relative to those of their equivalent outer pyridyl protons. As expected, the assignment of shifts corresponding to the dimethoxyphenylene bridge of **128** was straightforward, with one aromatic singlet (δ = 7.07 ppm) and one methoxy singlet (δ = 3.86 ppm) being evident. However, the presence of closely spaced peaks for the different aromatic and methoxy protons on the tetramethoxybiphenylene-bridge of **129** unfortunately made full assignment of its ^{1}H NMR spectrum difficult. However, HRMS data of **129** allowed its unambiguous characterisation due to the presence of molecular ions corresponding to both protonated (calcd for [**129** + H]$^{+}$: 611.2653, found 611.2623) and sodiated (calcd for [**129** + Na]$^{+}$: 633.2472, found 633.2467) species.

Boronic esters **122** – **125** were synthesized by a modification of the method employed for synthesising boronic ester **108** (***Scheme 2.17*** page 74).[113-116] The more reactive *t*-BuLi was employed in two-fold excess and reaction times were extended up to 3 hours at -78 °C to ensure that bis-lithiation had occurred. Precipitation and colour changes observed during the addition of *t*-BuLi, for the synthesis of boronic esters **122** – **125**, were presumed to indicate the formation of both the mono- and bis-lithiated intermediates. For example, in the synthesis of boronic ester **125** the first equivalent of *t*-BuLi resulted in a light pink coloured slurry that changed to pale yellow after the addition of the fourth equivalent. In a similar manner, on addition of the first equivalent of 2-isopropoxy-4,4′:5,5′-tetramethyl-[1,3,2]-dioxaboralane to the reaction mixture a purple slurry was observed which faded to a colourless suspension after the addition of the fourth equivalent.

While the aryl halides 1,4-dibromobenzene and 4,4′-dibromo-biphenyl used in the synthesis of boronic esters **122** and **123** could be purchased, 1,4-diiodo-2,5-dimethoxy-benzene **131** and 4,4′-dibromo-2,2′,6,6′-tetramethoxybiphenylene **134** needed to be synthesized. 1,4-Diiodo-2,5-dimethoxybenzene **130** was prepared in a multigram scale synthesis via a reported method (***Scheme 2.25***).[125] This procedure involved the treatment of 1,4-dimethoxybenzene **130** with iodine monochloride to afford **131** in 82 % yield.

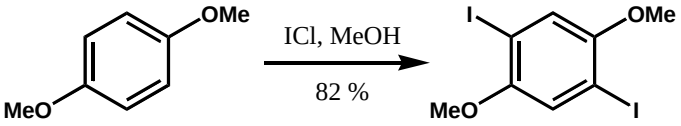

130 **131**

Scheme 2.25

The preparation of dibromobiphenyl **134** was a little more involved (***Scheme 2.26***). Electrophilic substitution of 1,4-dimethoxybenzene **130** with N-bromosuccinimide (NBS) in

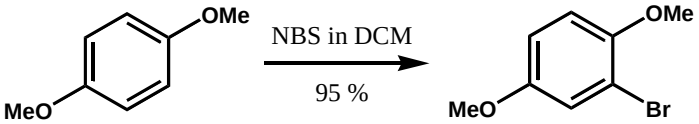

130 **132**

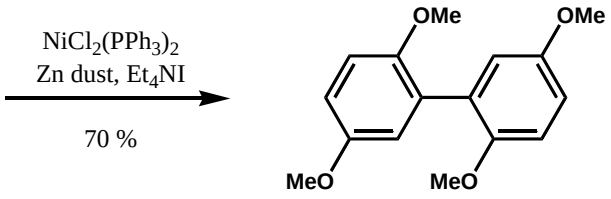

133

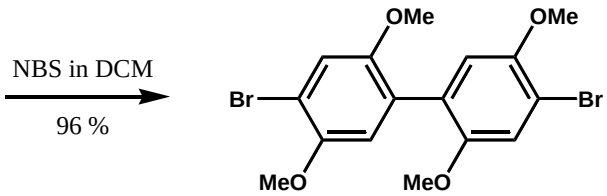

134

Scheme 2.26

refluxing DCM gave the 2-bromo derivative **132** in 95 % yield.[126] Homocoupling of **132** using $[NiCl_2(PPh_3)_2]$/Zn in THF[16] yielded biphenyl **133** in 70 % yield. The latter could then be regioselectively brominated at the 4,4′-positions with NBS in refluxing CH_2Cl_2, affording dibromobiphenyl **134** in 96 % yield. This straightforward three-step synthetic strategy afforded dibromobiphenyl **134** in an overall yield of 63 %.

The identification of M_2L_3 and M_4L_6 metal complexes (where M = Fe(II), Co(II), Ni(II) or Ru(II) and L = quaterpyridines **50**, **128** or **129** – see Chapters 3 and 4) indicated the possibility that a metal-template procedure, analogous to that employed by Perkins *et al.*,[118, 119] might enable the synthesis of the targeted dinuclear cryptates **136** (***Scheme 2.27***) (and perhaps even larger tetranuclear tetracyclic compounds). Hence, an investigation into the synthesis of appropriate dialdehyde intermediates, such as **135**, was conducted.

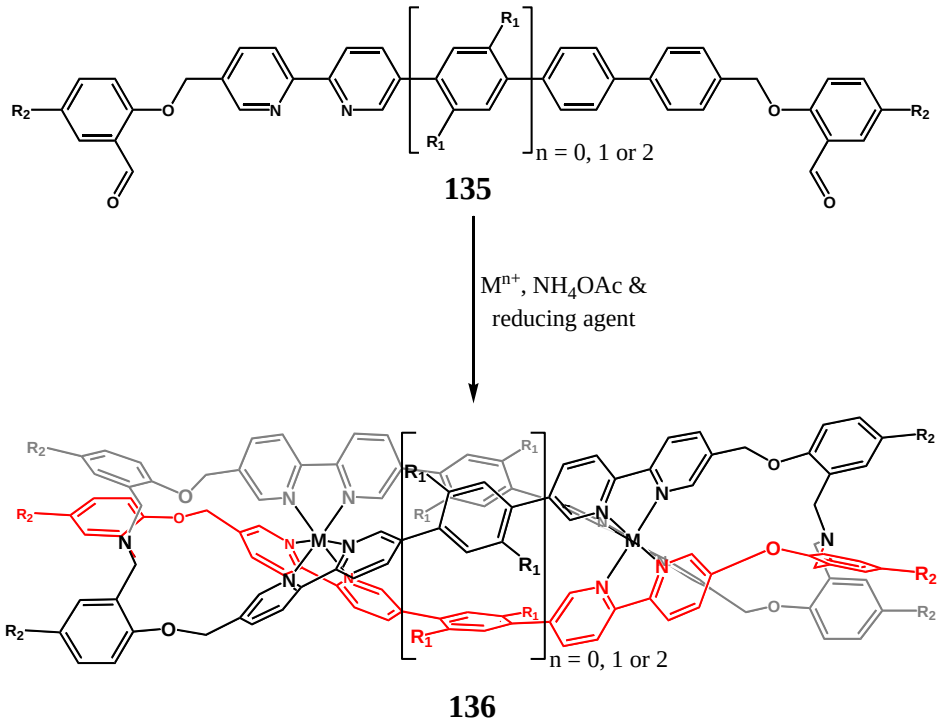

Scheme 2.27

The synthesis of the phenylene and biphenylene bridged dialdehyde derivatives employing bromobypyridines **101** and **102** in *bis*-Suzuki coupling reactions with boronic esters **122** – **125** allowed access to the dialdehydes **137** – **142** (***Scheme 2.28***). The ^1H and ^{13}C

NMR spectra of **137** – **142** were consistent with the formation of products with the expected two-fold symmetry and HRMS confirmed the expected formulation of these products.

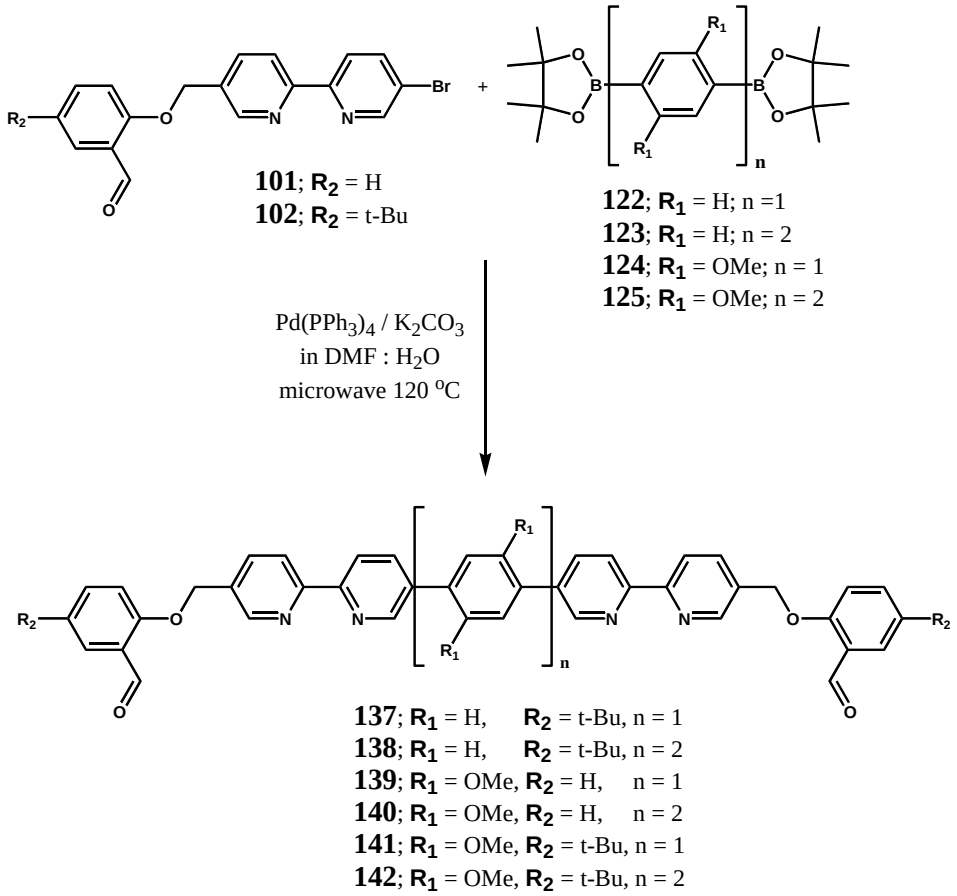

Scheme 2.28

As an example dialdehyde **142** is now used to exemplify the procedure employed to allocate the resonances in the ^{1}H NMR spectra of dialdehydes **137** – **142** (***Figure 2.5***). Resonances for the two equivalent aldehyde protons (δ = 10.55) and *t*-butyl substituents (δ = 1.33) were clearly observed. The two different methoxyl signals partially overlap (δ = 3.83 and 3.84 ppm) and a resonance corresponding to the methylene protons (δ = 5.29) was also present. A ^{1}H COSY experiment for **142** confirmed the expected couplings obtained from direct inspection of the ^{1}H NMR spectrum. To assign the protons on the inner and outer pyridyl rings a 1D NOESY experiment was conducted in which the methylene protons at 5.29 ppm were irradiated. A total of three NOEs were observed. Two of these NOE signals

at 8.79 and 7.96 ppm, correspond to outer pyridyl protons at the 6′′′- and 4′′′-positions, respectively. The third NOE signal corresponds to the proton in the 3-position on the salicyloxy functionality. Unfortunately, due to signal overlap there remained a difficulty in distinguishing between the 3,3′- and 6,6′- aromatic protons and the 2,2′- and 5,5′- methoxyl protons of the tetramethyoxy biphenylene bridge. However, a HRMS confirmed the identity of the product. The spectrum contained molecular ions corresponding to both protonated (calcd for [**142** + H]$^+$: 963.4333, found 963.4277) and sodiated (calcd for [**142** + Na]$^+$: 985.4152, found 985.4089) species.

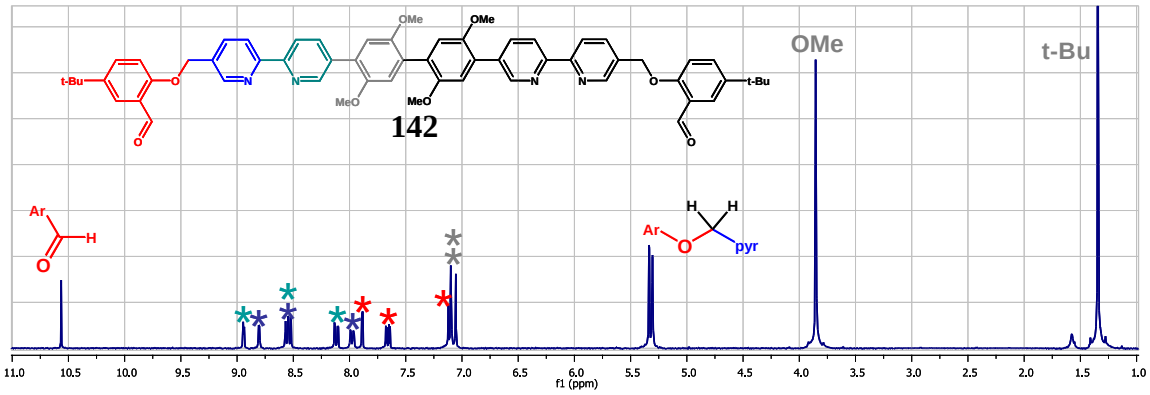

Figure 2.5. The ^{1}H NMR spectrum of dialdehyde **142** in CD_2Cl_2 (δ = 5.33) with colour coded assignments shown.

The synthesis of dialdehyde derivatives from quaterpyridine **50** (namely **144** and **145** in ***Scheme 2.29***) proved to be a little more challenging. In a similar manner to that used for the synthesis of the unsymmetrical and symmetrically substituted bipyridyl derivatives outlined in *Sections 2.2.2* and *2.2.3*, the corresponding halomethyl derivative of **50** was required for a subsequent *O*-alkylation reaction with appropriate salicylaldehydes. The synthesis of halomethyl derivatives of dimethylquaterpyridine **50** via its *bis*-(trimethylsilyl)methyl intermediate was planned, in the hope that this intermediate might exhibit increased solubility that would allow its purification by chromatography. Unfortunately, due to the very low solubility of **50**, lithiation of the methyl substitutents with LDA proved not possible. This latter observation led instead to the employment of radical halogenation. The radical halogenation of dimethylquaterpyridine **50** was conducted with NBS in refluxing carbon tetrachloride and resulted in a mixture of brominated products that

included bis-bromomethyl **143** (***Scheme 2.29***). The presence of a proton signal attributable to a bromomethyl group (δ = 4.57 ppm) in the ^{1}H NMR spectrum of this sparingly soluble material, suggested the successful bromination of **50**. Further, the presence of six aromatic shifts in the spectrum indicated the predominance of a product possessing *C2*-symmetry, consistent with the formation of the bis-bromomethyl derivative **143**. However, there were also signals indicating the presence of other brominated products with these proving difficult to remove. Reflecting this, the *O*-alkylation of the crude bis-bromomethyl **144** product was performed. In this case the reaction was carried out under phase transfer conditions. Thus, reaction of crude bis-bromomethyl **143** with salicylaldehydes **96** and **97** afforded dialdehydes **144** and **145** in 65 % and 67 % yields after purification. These products were fortunately soluble and hence able to be purified by chromatography although the chromatographic procedure using silica gel turned out to be an arduous exercise. In future, if this synthetic procedure is to be repeated, investigation into the possible use of reverse phase chromatography is recommended.

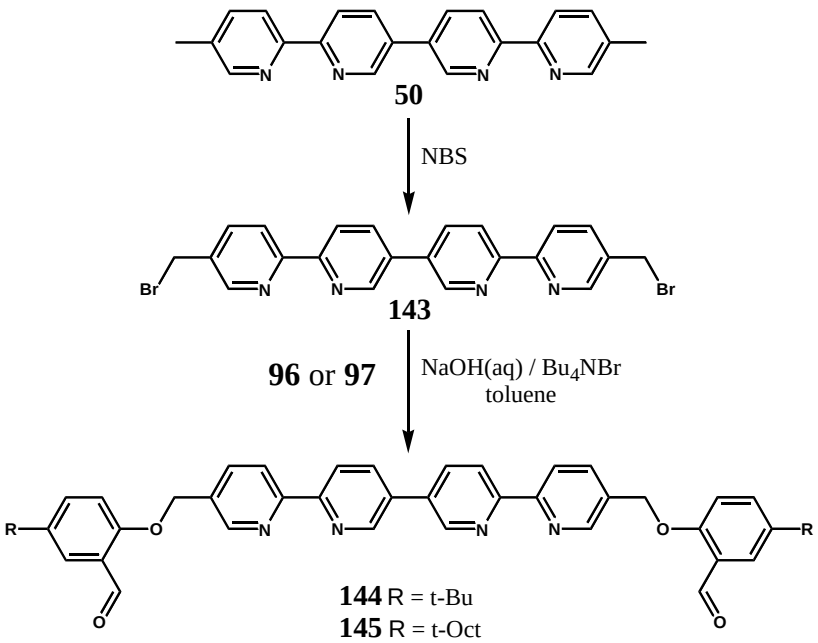

Scheme 2.29

The difficulties (outlined above) experienced during the synthesis of dialdehydes **144** and **145** prompted an investigation of alternative approaches. One alternative involved the

employment of a more convergent synthetic strategy involving the homocoupling of unsymmetrically substituted bromo bipyridines, such as **101** – **103**. The Ni(0)-catalysed homocoupling reaction employed to synthesize 3,3′-bipyridine **120** was considered a possible strategy for this (more) convergent approach, as a procedure of this type had been employed previously to prepare related quaterpyridyl ligands.[59] In this procedure bromobipyridine **84**, used as a model compound, was successfully homocoupled affording quaterpyridine **50** in a yield of 72 % (***Scheme 2.30***). The successful synthesis of **50** by this procedure, combined with the report[16] that carbonyl substituents are unreactive under the reaction conditions employed, represented an alternative for the synthesis of dialdehydes **144** and **145** via the homocoupling of bromo-bipyridines **102** and **103**, respectively. Unfortunately, the attempted synthesis of dialdehyde **144**, by homocoupling of monoaldehyde **102** under the conditions outlined in ***Scheme 2.30*** led to complicated reaction mixtures. It should be noted that the formation of Ni(II) complexes may complicate the workup process using this procedure. This latter point combined with the relatively high catalyst loadings led to the termination of investigations into this coupling procedure.

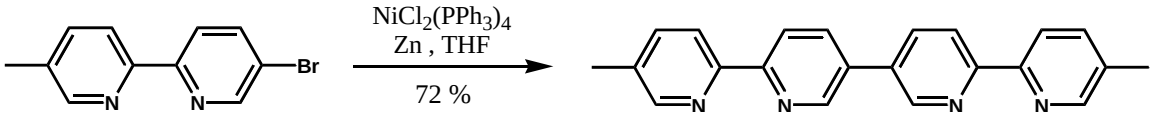

84 **50**

Scheme 2.30

Suzuki coupling was also considered as another attractive alternative for the synthesis of dialdehydes **144** and **145** from bromobipyridines **101** and **102**. Essentially, being a cross-coupling technique, this would involve the synthesis of boronic acids or esters of both bromobipyridines **101** and **102**. However, employment of the standard procedure for making boronic acids or esters involves treatment with BuLi and, as such, the aldehyde groups of the bromobipyridines would need to be protected. Fortunately an alternative procedure for generating boronic esters has been reported.[12,80-83] This involves a Pd(0)-catalysed cross-coupling between an aryl-halide, such as **146**, and an alkoxydiboron species, such as bis-(pinacolato)diboron **147**, to yield the corresponding boronic ester **148** (***Scheme 2.31***).

Futhermore, it was indicated that this procedure is tolerant of the presence of a wide variety of function groups, including aldehydes.[80,81]

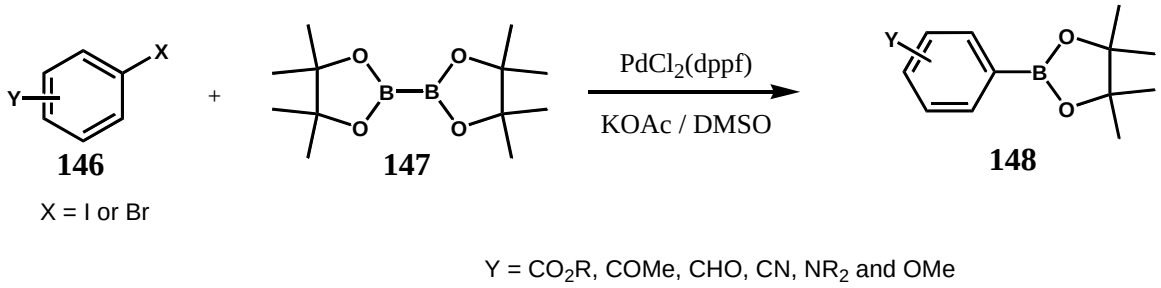

146

X = I or Br

147

148

Y = CO_2R, COMe, CHO, CN, NR_2 and OMe

Scheme 2.31[12,80-83]

Bromobipyridine **84** was employed to investigate the potential of the coupling procedure outlined in ***Scheme 2.31***. Under the conditions shown this reaction resulted in the formation of the apparently 'homocoupled' product, quaterpyridine **50**, in 70 % yield. However, when this reaction was repeated in the absence of diboron **147** no homocoupled product was observed; subsequently addition of **147** led to the rapid formation of quaterpyridine **50**. Interestingly, the 70 % yield of **50** may indicate that the rate of carbon to carbon bond formation is faster than that of the carbon to boron bond formation; or else the yield of the quaterpyridine **50** would be outweighed by that of the intended boronic ester. This otherwise undesirable side reaction does not represent an isolated example, as there are individual reports that describe reaction conditions that favour homocoupled products.[81,127] However, in the current project variation of the reaction conditions appeared to have little effect on the overall yield of quaterpyridine **50**. The use of $Pd(PPh_3)_4$ as catalyst under the conditions outlined in ***Scheme 2.32*** also allowed the successful synthesis of **50** in 70 % yield. Although this yield is essentially the same as that observed under the conditions outlined in ***Scheme 2.31***, $Pd(PPh_3)_4$ provided more consistent results and is a cheaper catalyst than $PdCl_2$(dppf). Furthermore, the low catalyst loadings compared to those needed for the Ni(0) homocoupling reaction (***Scheme 2.30***), simplified the necessary purification procedures greatly.

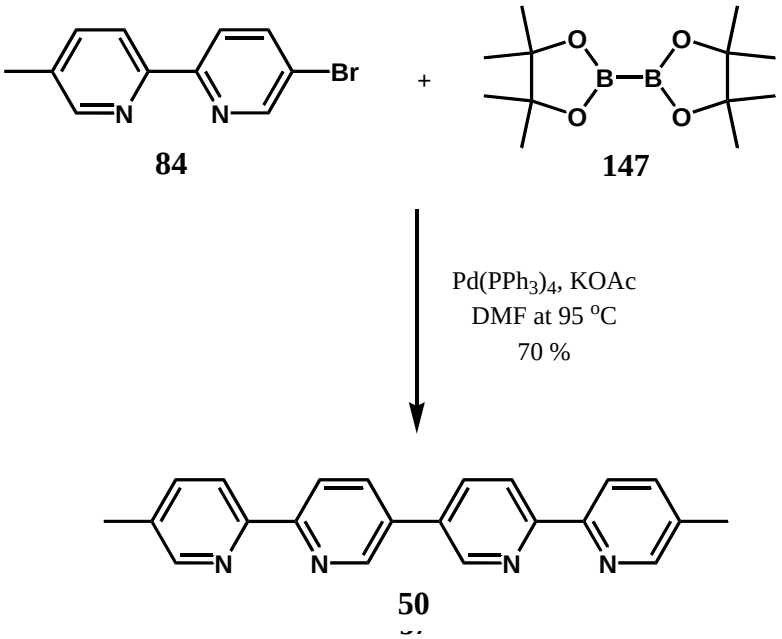

Scheme 2.32

The production of quaterpyridine **50** under the condition described in ***Scheme 2.32*** represents an attractive one pot alternative for the synthesis of dialdehydes **144** and **145** from bromobipyridines **102** and **103**, respectively (***Scheme 2.33***). In this regard, bromobipyridine

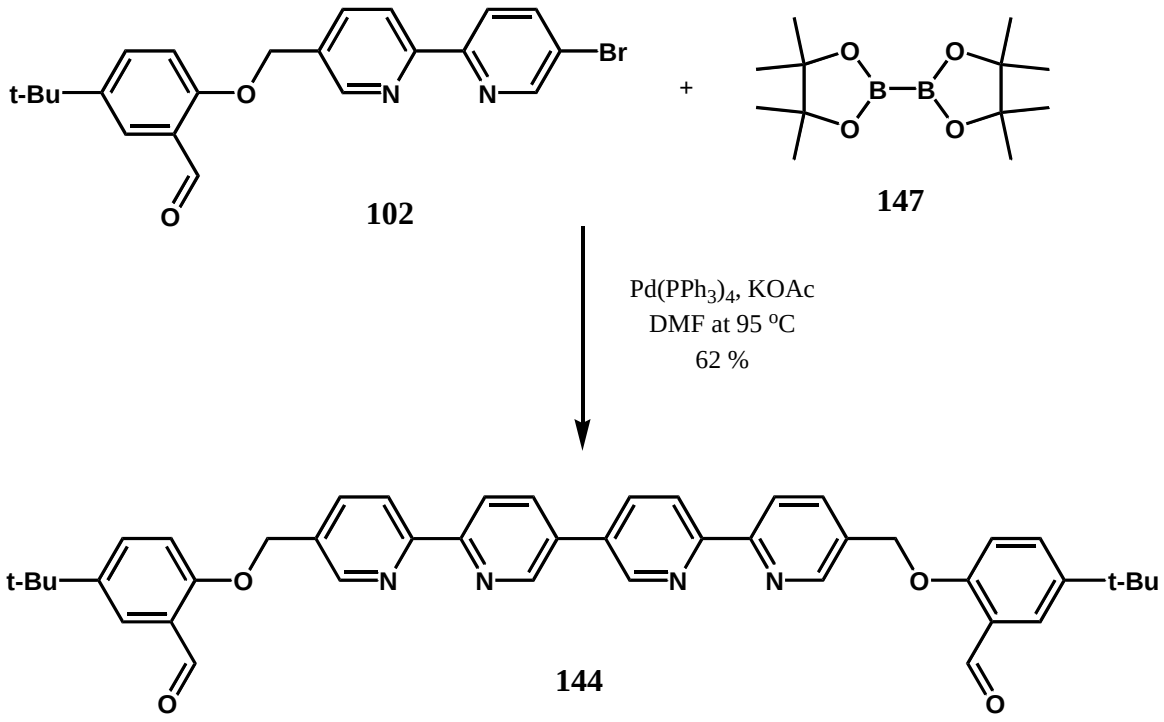

Scheme 2.33

102 was reacted with diboron **147** to afford dialdehyde **144** in a 62 % yield. Although the latter approach resulted in a yield that was no improvement over the 65 % yield observed using the previous synthetic approach (***Scheme 2.29***, page 87), the ease of product isolation in the former case made it the preferred method. Another advantage of this more convergent approach was that the bromobipyridyl starting materials **101** – **103** were also required for the synthesis of the rigidly bridged dialdehydes **137** – **142**, reagents also employed in the present study.

2.2.4 Flexibly bridged substituted ditopic quaterpyridyl ligands.

Prior to the current work, all reported metal-directed assembly experiments that have yielded M_2L_3 helicates have employed bis-bidentate ligands with at least one sp^3 hydbridized atom incorporated in their bridging unit.[128-130] This observation no doubt reflects the greater conformational flexibility required for the formation of many helicates. A brief discussion of the synthesis and characterisation of an isomeric series of flexibly bridged quaterpyridines, employing 1,2- , 1,3- and 1,4-diphenoxy bridged quaterpyridines (***Scheme 2.34***) follows.

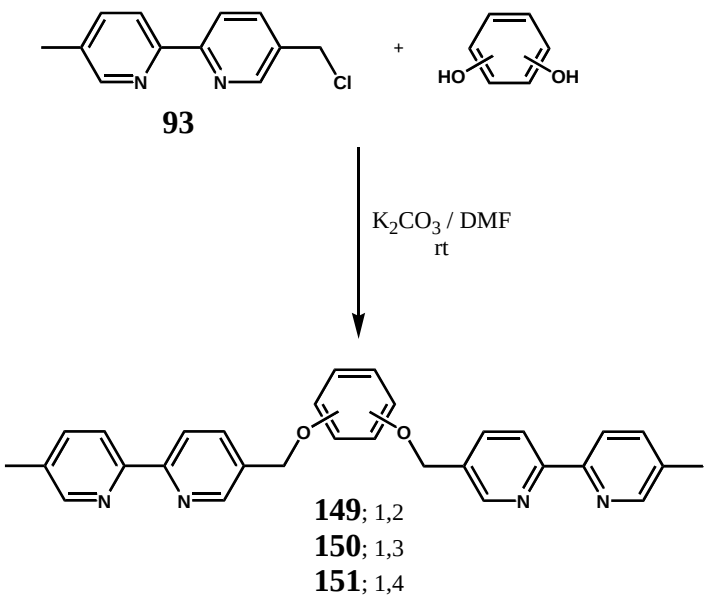

Scheme 2.34

The reaction of bipyridine **93** with catachol, resorcinol and hydroquinone in the presence of K_2CO_3 in DMF afforded quaterpyridines **149**, **150** and **151** in 90, 93 and 58 % yields, respectively (***Scheme 2.34***). This series of compounds vary significantly in terms of their physical characteristics. For example quaterpyridines **149** and **150** are quite soluble in chlorinated solvents, while **151** is only sparingly soluble. The ^{1}H and ^{13}C NMR of these bridged quaterpyridyl products are indicative of their expected *C2*-symmetries. NOEs were observed between methyl protons at ~ 2.4 ppm and protons in the 4′- and 6′-positions allowing the full assignment of the ^{1}H NMR spectra of these compounds.

2.3 EXPERIMENTAL

Solvent and Reagents

All reagents were of analytical grade unless otherwise indicated.

Chromatography grade solvents were distilled through a fractionation column (1 metre) packed with glass helices. Dimethylformamide (DMF) was dried over CaH_2 overnight and distilled under reduced pressure (40 °C / 11 mbar) before use. Dimethylsulfoxide (DMSO) was also dried over CaH_2 and distilled under reduced pressure (70 – 80 °C / 11 mbar). Dichloromethane (DCM) was dried by distillation from CaH_2. MeOH was dried by distillation from magnesium turnings activated with iodine. Toluene was dried by distillation from sodium wire. Dry tetrahydrofuran (THF) was obtained by distillation from a blue coloured mixture of sodium wire and benzophenone (sodium benzophenone ketyl). The saturated NH_3 solution was obtained by bubbling dry NH_3 gas through chilled water until the specific gravity of the solution was approximately 0.88. This solution was stored in a sealed glass container at 4 °C.

2,5-Dibromopyridine (**83**), 2-amino-5-methylpyridine, N-bromosuccinimide (NBS), $Pd(PPh_3)_4$, $PdCl_2$(ddpf), salicylaldehyde (**95**), 1,4-dibromobenzene, 4,4′-dibromo-biphenyl, 1-chloromethyl-4-methoxybenzene, 4-bromophenol, n-BuLi, t-BuLi, trimethylstannylchloride, trimethylsilylchloride and 2-Isopropoxy-4,4,5,5-tetramethyl-[1,3,2]dioxaborolane were purchased from Sigma Aldrich and used without further purification. t-Butylsalicylaldehyde **96** and t-octylsalicylaldehyde **97** were synthesized previously in our laboratory using reported methods.[131, 132] Anhydrous grade Na_2SO_4 was employed for drying organic extracts described in the experimental. $NiCl_2(PPh_3)_2$ was synthesised using a published method.[133,134]

Chromatography

Reactions were monitored by analytical TLC on cut strips of precoated plastic backed sheets (Merck silica gel 60 F254, 0.25 mm thickness). Vacuum assisted column chromatography was performed using Merck Kieselgel 60H.

Nuclear Magnetic Resonance (NMR) Spectroscopy

^{1}H NMR spectra were recorded on a Bruker AM-300 or a Varian Mercury 300 MHz spectrometer (300.133 MHz) at 298 K. Proton and carbon chemical shifts are quoted as δ values relative to the respective deuterated solvents residual proton or carbon chemical shifts. Residual proton resonances of the deuterated solvents were used as reference and were corrected to the values listed by the Cambridge Isotope Laboratory; $CDCl_3$ (δ_H = 7.27(s); δ_C = 77.23(t)), CD_2Cl_2 (δ_H = 5.32; δ_C = 54.00 (5)), $(CD_3)_2O$ (δ_H = 2.05 (quin); δ_C =206.68(13) and 29.92(hept)), CD_3OD (δ_H = 4.87(s) and δ_H = 3.31(quin); δ_C = 49.15(hept)), CD_3CN (δ_H = 1.95(quin); δ_C = 118.69(s) and 1.39(hept)), $(CD_3)_2NCDO$ (δ_H = 8.03(s), 2.93(quin) and 2.75(quin); δ_C = 163.15(t), 34.89(hept) and 29.76 (hept)) and $(CD_3)_2SO$ (δ_H = 2.50(quin); δ_C = 39.51(hept)). Coupling constants (*J*) are reported in Hertz, with signal multiplicity designated as singlet (s), doublet (d), triplet (t), quartet (q), quintet (quin), septet (sept), heptet (hept), multiplet (m) and broad (br).

Mass Spectrometry and Microanalysis

Electrospray (ES) high resolution fourier transform ion cyclotron resonance mass spectrometry (FTICR-MS) measurements were performed by Dr Cherie Motti (Australian Institute of Marine Sciences) or the candidate at the Australian Institute of Marine Sciences, Cape Cleveland, Townsville. The instrument is an unmodified Bruker BioAPEX 47e mass spectrometer equipped with an Analytica of Branford model 103426 (Branford, CT) electrospray ionisation (ESI) source. Direct infusion of the samples (0.2 mg/mL in MeOH) were carried out using a Cole Palmer 74900 syringe pump at a rate of 100 μL/h. N_2 (sourced from a Domnick Hunter UHPLCMS18 nitrogen generator, flow of 3 L/min and maintained at 200 °C) was used as the drying gas to assist in desolvation of the droplets produced by ESI from an on axis grounded needle directed to a metal capped nickel coated glass capillary, approximately 1 cm away. All experiments were controlled and data reduction performed using Bruker Daltonics XMASS ver. 7.0.3.0 software. All measurements were conducted in positive mode.

Microanalysis was conducted by The Campbell Microanalyticall Laboratory, Department of Chemistry, University of Otago, Dunedin, New Zealand.

Numbering system used to report assignments of ^{1}H NMR spectra

For the purpose of identifying ^{1}H NMR assignments, several of the more complex compounds of each class investigated are used to illustrate the numbering system employed. The protons on the salicyloxy and unsymmetrical phenylene groups are identified by letters (e.g. a, b, c, d and e). The pyridyl protons are numbered traditionally with the distinction between pyridyl rings being made by primes. The Chemdraw structures of **99**, **110**, **111** and **142** below serve to illustrate the respective numbering conventions. For clarity only one side of the *C2*-symmetric ligand **142** is given. Appart from some simpler derivatives which are systematically named the majority of the names appearing in the experimental use the Chemdraw convention.

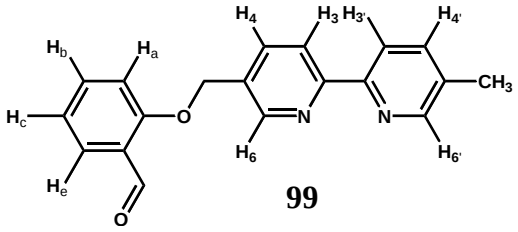

99

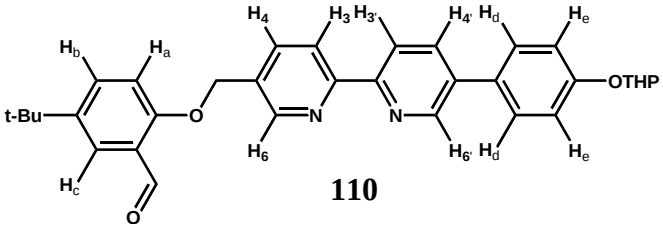

110

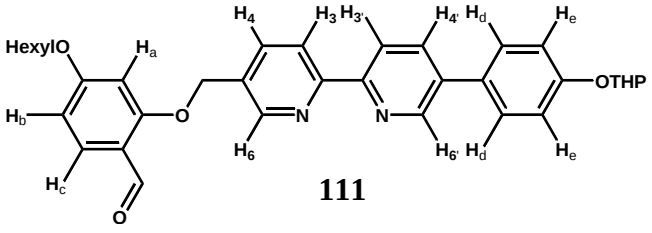

111

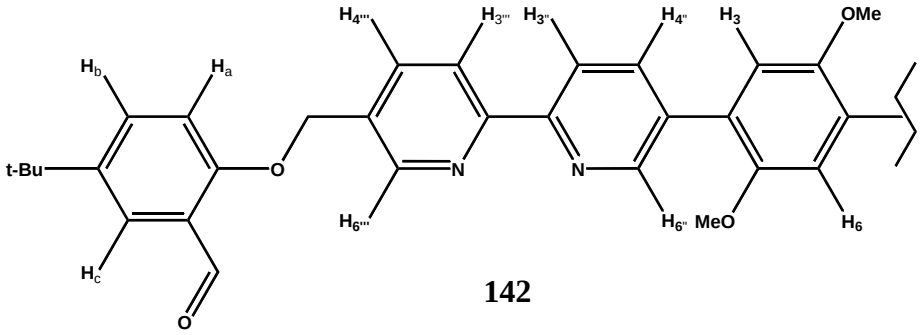

142

The following experimental descriptions generally follow the format outlined for publishing authors by *Eur. J. Org. Chem.*

2.3.1 Unsymmetrical salicyloxy-substituted 2,2′-bipyridines.

2-Bromo-5-methylpyridine (80):[121, 122] Br_2 (40 cm^3) was added dropwise to a stirred solution of 2-amino-5-methylpyridine (30 g, 0.277 mol) in 48 % HBr (300 cm^3) while keeping the temperature below –10 °C. This solution was stirred for a further 2 h at -10 °C. A solution of $NaNO_2$ (51.0 g, 0.739 mol) in water (100 cm^3) was then added dropwise to the stirred reaction mixture keeping the temperature below -5 °C. This solution was then allowed to warm to room temperature over 1 h and was then stirred for a further 1 h. Following this, the reaction mixture was cooled to below 0 °C and carefully neutralized using 5 M NaOH (360 cm^3). The solution was then extracted with diethyl ether (3 x 400 cm^3) and the combined organic fractions were sequentially washed with a dilute solution of $Na_2S_2O_3$ followed by distilled water (400 cm^3). This solution was dried over Na_2SO_4 and the solvent removed on the rotary evaporator affording **80** in >99 % purity as a low melting point crystalline solid (43.44 g, 91.6 %). ^{1}H NMR (300 MHz, $CDCl_3$): δ = 2.29 (s, 3 H, CH_3), 7.36 (d, J = 1.5 Hz, 1 H, H-3), 7.36 (d, J = 1.5 Hz, 1 H, H-4), 8.20 (s, 1 H, H-6).

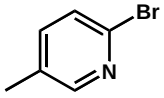

2-Trimethylstannyl-5-methyl pyridine (81):[58] 1.9 M n-BuLi in cyclohexane (28.9 cm^3) was added dropwise to a stirred solution of **80** (8.55 g, 0.05 mol) in dry THF (100 cm^3) at -78 ºC. On completion of the addition the solution was held at -78 ºC for a further 1.5 h. 1 M trimethylstannyl chloride in THF (57.8 cm^3) was added dropwise to this solution. The reaction mixture was held at -78 ºC for a further 3 h and then allowed to warm to room

temperature where it was stirred for a further 1 h. The solvent was removed under vacuum and the product was taken up in n-hexane (100 cm^3) and the solution filtered. The hexane was removed under vacuum to yield a brown oil (96 % yield; 95 % purity). The product was purified by vacuum distillation affording **81** as a viscous colourless oil (8.3 g, 65 %; b.p. 56-61ºC at 1 mm Hg). ^{1}H NMR (300 MHz, $CDCl_3$): δ = 0.32 (s, 9 H, $Sn(CH_3)_3$), 2.29 (s, 3 H, CH_3), 7.34 (d, J = 1.8 Hz, 1H, H-3), 7.34 (d, J = 1.8 Hz, 1 H, H-4), 8.59 (s, 1 H, H-6).

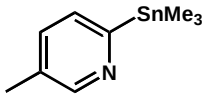

5,5′-Dimethyl-2,2′-bipyridine (82):[58, 71-73] A stirred solution of **81** (2.0 g, 7.8 mmol) and **80** (1.26 g, 7.4 mmol) in dry toluene (20 cm^3) was degassed with N_2 for 0.5 h. To this solution 4 mol % of $Pd(PPh_3)_4$ (342 mg, 0.3 mmol) was added and degassing was continued for a further 0.5 h. This solution was refluxed for 20 h then allowed to cool to room temperature before extraction with 4M HCl (3 x 30 cm^3). The acid layers were neutralized with 2M NaOH and the resulting solid that formed was extracted with DCM (3 x 40 cm^3). The combined organic fractions were dried over anhydrous Na_2SO_4 before the DCM was removed under vacuum. The product was chromatographed on silica gel in 97.5 % DCM : 2 % MeOH : 0.5 % $NH_{3(aq)}$ affording **82** as a white powder (1.17 g, 86 %). ^{1}H NMR (300 MHz, $CDCl_3$): δ = 2.38 (s, 6 H, CH_3), 7.60 (dd, ^3J = 8.4, ^4J = 2.1 Hz, 2 H; H-4,4′), 8.23 (d, ^3J = 8.4 Hz, 2 H, H-3,3′), 8.48 (d, ^4J = 2.1 Hz, 1 H, H-6,6′).

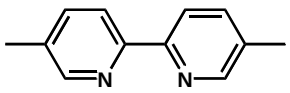

5-Bromo-5′-methyl-2,2′-bipyridine (84): A stirred solution of **81** (2.81 g, 0.011 mol) and 2,5-dibromopyridine **83** (2.37 g, 0.010 mol) in toluene (20 cm^3) was degassed with nitrogen for 0.5 h. To this solution 2 mol % of $Pd(PPh_3)_4$ (231 mg) was added and the solution degassed for a further 10 min. The reaction mixture was then heated at reflux for 20 h. The mixture was filtered and the solvent removed under vacuum. The resulting solid was re-dissolved in DCM (50 cm^3) and the solution extracted with 4 M HCl (3 x 30 cm^3). The aqueous layers were neutralized with 2 M NaOH and the resulting solid was extracted with DCM (3 x 40 cm^3). The combined extracts were dried over Na_2SO_4. The solvent was removed and the product that remained was chromatographed on silica gel in 97 % DCM : 2

% MeOH : 0.5 % $NH_{3(aq)}$ affording **84** (2.49 g, 84 %) as a white powder, mp 122 - 123ºC. ^{1}H NMR (300 MHz, $CDCl_3$): δ = 2.40 (s, 3H; CH_3), 7.63 (dd, ^3J = 8.1, ^4J = 2.1 Hz, 1 H, H-4′), 7.92 (dd, ^3J = 8.7, ^4J = 2.4 Hz, 1 H, H-4), 8.25 (d, ^3J = 8.1 Hz, 1 H, H-3′), 8.28 (d, ^3J = 8.7 Hz, 1 H, H-3), 8.50 (d, ^4J = 2.1 Hz, 1 H, H-6′), 8.70 (d, ^4J = 2.4 Hz, 1 H, H-6); ^{13}C NMR (75 MHz, $CDCl_3$): δ = 18.64, 121.13, 121.28, 122.55, 134.41, 138.59, 139.79, 149.15, 150.45, 152.34, 154.10.

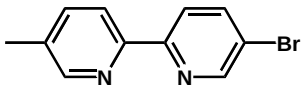

2-Bromo-5-iodopyridine (85):[121, 122] Br_2 (19.6 cm^3, 0.382 mol) was added dropwise to a stirred solution of **118** (30 g, 0.136 mol) in 48% HBr (300 cm^3) while keeping the temperature below –10 °C. The temperature was maintained for a further 2 h at -10˚C. followed by the dropwise addition of $NaNO_2$ (25 g, 0.362 mol) in water (38 cm^3). The reaction mixture was allowed to warm to room temperature over 1 h and was then stirred for a further 1 h. Following this, the reaction mixture was cooled to below 0˚C and carefully neutralized using 5 M NaOH (120 cm^3). The product was extracted from the reaction mixture with diethyl ether (3x150 cm^3) and the combined organic fractions were washed with a dilute solution of $Na_2S_2O_3$ and water. The ether solution was dried over Na_2SO_4 and the solvent removed on the rotary evaporator. The product was recrystallised from a chloroform:petrol mixture to afford **85** (34.3 g, 89 %) as brown needles: mp 120.2-120.6˚C (lit.[121] 122.5˚C). ^{1}H NMR (300 MHz, $CDCl_3$): δ = 7.28 (d, ^3J = 8.1 Hz, 1 H, H-3), 7.82 (dd, ^3J = 8.1, ^4J = 2.4 Hz, 1 H, H-4), 8.58 (d, ^4J = 2.4 Hz, 1H, H-6).

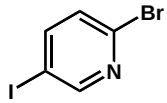

6′-Bromo-5-methyl-[2,3′]bipyridine (86): A stirred solution of **81** (513 mg, 2.0 mmol) and 5-iodo-2-bromopyridine **85** (560 mg, 2.0 mmol) in toluene (10 cm^3) was degassed with nitrogen for 0.5 h. To this solution was added 2 mol % of $Pd(PPh_3)_4$ (46 mg, 0.04 mmol) and the solution degassed for a further 10 min. The reaction mixture was then heated at reflux for 6 h. The mixture was filtered and the solvent removed under vacuum. The resulting solid was re-dissolved in DCM (30 cm^3) and the solution was extracted with 4 M HCl (3 x 10 cm^3). The aqueous layers were neutralized with 2 M NaOH and the solid that formed was extracted with DCM (3 x 20 cm^3). The combined extracts were dried over Na_2SO_4. The solvent was

removed and the solid that remained was chromatographed on silica gel with DCM as eluent, to afford **86** (440 mg, 88 %) as an off white powder. ^{1}H NMR (300 MHz, $CDCl_3$): δ = 2.39 (s, 3H; CH_3), 7.50 (d, ^{3}J = 8.3 Hz, 1 H, H-3), 7.55 (m, 2 H, H-5′,4′), 8.18 (dd, ^{3}J = 8.3, ^{4}J = 2.4 Hz, 1 H, H-4), 8.47 (br s, 1 H, H-2′), 8.86 (d, ^{4}J = 2.4 Hz, 1 H, H-6); ^{13}C NMR (75 MHz, $CDCl_3$): δ = 18.49, 120.11, 128.21, 133.23, 134.35, 136.82, 137.81, 142.27, 148.43, 150.77, 150.90.

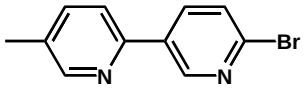

2-{5"-Methyl-[2′,2"]bipyridinyl}-5-methylpyridine (87): This byproduct was formed in a repeat of the procedure for **84** when 1.2 equivalents of stannane **81** were employed instead of only 1 equivalent. It was isolated as the lower Rf material under the chromatographic conditions used to obtain **84**. ^{1}H NMR (300 MHz, $CDCl_3$): δ = 2.39 (s, 3 H, CH_3), 2.40 (s, 3 H, CH_3), 7.60 (dd, ^{3}J = 8.1, ^{4}J = 2.1 Hz, 1 H, H-4), 7.66 (dd, ^{3}J = 8.1, ^{4}J = 2.1 Hz, 1 H, H-4′′), 7.70 (d, ^{3}J = 8.1 Hz, 1 H, H-3), 8.36 (d, ^{3}J = 8.1 Hz, 1 H, H-3′′), 8.43 (dd, ^{3}J = 8.1, ^{4}J = 2.1 Hz, 1 H, H-4′), 8.48 (dd, ^{3}J = 8.1, ^{5}J = 0.9 Hz, 1 H, H-3′), 8.53 (d, ^{4}J = 2.1 Hz, 1 H, H-6), 8.56 (d, ^{4}J = 2.1 Hz, 1 H, H-6′′), 9.23 (dd, ^{4}J = 2.1, ^{5}J = 0.9 Hz, 1 H, H-6′); ^{13}C NMR (75 MHz, $CDCl_3$): δ = 18.50, 18.64, 120.35, 121.07, 121.25, 132.86, 134.00, 134.67, 135.36, 137.79, 138.06, 147.51, 149.63, 150.69, 152.01, 153.10, 155.75; positive ion ESI-HRMS: m/z (M = $C_{17}H_{15}N_3$ in DCM / MeOH): calcd for [M + H]$^{+}$: 262.1339, found 262.1331; calcd for [M + Na]$^{+}$: 284.1158, found 284.1152.

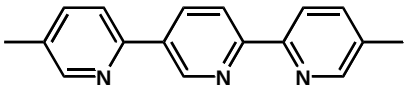

5-Trimethylsilylmethyl-5′-methyl-2,2′-bipyridine (91):[65, 73] LDA was prepared by adding 1.5 M n-BuLi (4.4 cm^3) dropwise to a stirred solution of dry diisopropylamine (0.758 g, 7.5 mmol) in THF (15 cm^3) at -78˚C. This solution was stirred for a further 0.5 h and allowed to warm to 0ºC for 10 min. The resulting LDA solution was cooled to -78ºC and a solution of **82** (552mg, 3 mmol) was added dropwise. The reaction was allowed to continue for 2 h and Me_3SiCl (760mg, 7 mmol) was then added rapidly. The reaction was quenched with 3 cm^3 of MeOH after 3 min. The solvent was then removed under vacuum and the resulting paste was taken up in DCM and the solution filtered. The DCM was then removed under vacuum and the solid that remained was purified by chromatography on deactivated silica gel with 60 %

petrol and 40 % ethyl acetate as eluent to afford **91** as a waxy white solid (614 mg, 80 %). ^{1}H NMR (300 MHz, $CDCl_3$): δ = 0.02 (9H, s, $Si(CH_3)_3$), 2.11 (s, 2 H, CH_2), 2.38 (s, 3 H, CH_3), 7.44 (dd, ^{3}J = 8.3, ^{4}J = 2.1 Hz, 1 H, H-4), 7.61 (ddd, ^{3}J = 8.1, ^{4}J = 2.1, ^{5}J = 0.6 Hz, 1 H, H-4′), 8.22 (d, ^{3}J = 8.3 Hz, 1 H, H-3), 8.24 (d, ^{3}J = 8.1 Hz, 1 H, H-3′), 8.34 (d, ^{4}J = 2.1 Hz, 1 H, H-6), 8.48 (dd, ^{4}J = 2.1, ^{5}J = 0.6 Hz, 1 H, H-6′); ^{13}C NMR (75 MHz, $CDCl_3$): δ = -1.79, 18.55, 24.21, 120.44, 120.64, 133.12, 136.46, 136.65, 137.81, 148.47, 149.57, 152.27, 153.80.

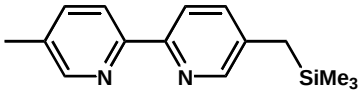

5,5′-Bis(trimethylsilylmethyl)-2,2′-bipyridine (92): LDA was prepared by adding 1.9 M n-BuLi (1.42 cm^3) dropwise to a stirred solution of dry diisopropylamine (0.42ml, 3 mmol) in THF (8 cm^3) at -78ºC. This solution was stirred for a further 0.5 h and then allowed to warm to 0ºC for 10 min. The resulting LDA solution was cooled to -78ºC and a solution of **82** (100 mg, 0.54 mmol) and dry hexamethylphosphoramide (1.13 cm^3, 6.48 mmol) in THF (5 cm^3) was added dropwise resulted in a deep red/brown opaque solution. This solution was stirred for a further 2 h followed by the addition of dry trimethylsilyl chloride (217 mg, 2 mmol). The reaction mixture then stirred at -78ºC for a further 0.5 h. The resulting transparent red solution was then quenched with 2 cm^3 of absolute ethanol. Saturated $NaHCO_3$ (10 cm^3) was then added and the product was extracted into ethyl acetate (3 x 40 cm^3). The combined organic fractions were dried over anhydrous Na_2SO_4. The solvent was then removed under vacuum and the solid that remained was chromatographed on deactivated silica gel with petrol (60 %) and ethyl acetate (40 %) as eluent to afford **92** as a waxy white solid (142 mg, 80 %). ^{1}H NMR (300 MHz, $CDCl_3$): δ = 0.02 (18H, s, $Si(CH_3)_3$), 2.12 (s, 4 H, CH_2), 7.45 (dd, ^{3}J = 7.8, ^{4}J = 1.8 Hz, 2 H, H-4,4′), 8.22 (d, ^{3}J = 7.8 Hz, 2 H, H-3,3′), 8.34 (d, ^{4}J = 1.8 Hz, 2 H, H-6,6′); ^{13}C NMR (75 MHz, $CDCl_3$): δ = 2.06, 23.92, 120.16, 136.11, 136.18, 148.22, 152.21.

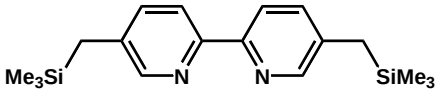

In a repeat of the above experiment the quenched reaction solution was allowed to stand at room temperature overnight. This led to the growth of crystals suitable for X-ray structure analysis. The resulting structure confirmed its formulation as **92**.

5-Chloromethyl-5′-methyl-2,2′-bipyridine (93): A solution of **92** (475 mg, 1.85 mmol), hexachloroethane (876 mg, 3.70 mmol) and anhydrous CsF (562 mg, 3.70 mmol) in acetonitrile (20 cm^3) was heated at 60˚C with stirring for 6 h. The acetonitrile was removed and replaced with DCM (50 cm^3) and the resulting solution was filtered. The organic phase was washed with water (30 cm^3) then brine (30 cm^3) followed by drying over Na_2SO_4. The solvent was removed under vacuum and the solid that remained was chromatographed on silica gel with DCM (97.5 %), MeOH (2 %) and saturated NH_3 (0.5 %) as eluent to afford **92** (344 mg, 85 %) as a pure white crystalline solid. ^{1}H NMR (300 MHz, $CDCl_3$): δ = 2.37 (s, 3 H, CH_3), 4.62 (s, 2 H, CH_2Cl), 7.62 (ddd, ^3J = 8.1, ^4J = 1.8, ^5J = 0.6 Hz, 1 H, H-4′), 7.82 (dd, ^3J = 8.1, ^4J = 2.4 Hz, 1 H, H-4), 8.27 (d, ^3J = 8.1 Hz, 1 H, H-3′), 8.36 (d, ^3J = 8.1 Hz, 1 H, H-3), 8.48 (dd, ^4J = 1.8, ^5J = 0.6 Hz, 1 H, H-6′), 8.63 (d, ^4J = 2.4 Hz, 1 H, H-6); ^{13}C NMR (75 MHz, $CDCl_3$): δ = 18.60, 43.36, 120.98, 121.07, 133.10, 134.05, 137.39, 137.93, 149.15, 149.70, 153.05, 156.27; positive ion ESI-HRMS: m/z (*M* = $C_{12}H_{11}N_2Cl$ in DCM / MeOH): calcd for $[M+H]^+$: 219.0683, found 219.0676; calcd for $[M+Na]^+$: 241.0503, found 241.0497.

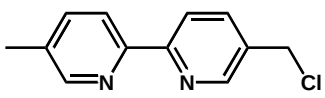

5′-Bromo-5-bromomethyl-2,2′-bipyridine (94): A solution of **84** (2.49 g, 10 mmol) and N-bromosuccinimide (1.78 g, 10 mmol) in CCl_4 (40 cm^3) was irradiated with a broad spectrum tungsten white light whilst under reflux for 30 min. The CCl_4 was removed, H_2O (40 cm^3) added, and the mixture was stirred for 0.5 h. Following filtration of the mixture the solid was washed with a minimum amount of water, chilled methanol then ether. The resulting product was chromatographed on silica gel with petrol (40 %) and DCM (60 %) as eluent to afford **94** (2.1 g, 64 %) as a white solid. ^{1}H NMR (300 MHz, $CDCl_3$): δ = 4.53 (s, 2 H, CH_2Br), 7.85 (dd, ^3J = 8.1, ^4J = 2.4 Hz, 1 H, H-4), 7.94 (dd, ^3J = 8.7, ^4J = 2.4 Hz, 1 H, H-4′), 8.32 (d, ^3J = 8.7 Hz, 1 H, H-3′), 8.37 (d, ^3J = 8.1 Hz, 1 H, H-3), 8.67 (d, ^4J = 2.4 Hz, 1 H, H-6), 8.72 (d, ^4J = 2.4 Hz, 1 H, H-6′); ^{13}C NMR (75 MHz, $CDCl_3$): δ = 29.93, 121.25, 122.76, 122.83, 134.28,

138.09, 139.83, 149.46, 150.52, 154.04, 155.18; positive ion ESI-HRMS: m/z (M = $C_{11}H_8Br_2N_2$ in DCM / MeOH): calcd for $[M+H]^+$: 326.9128, found 326.9137; calcd for $[M+Na]^+$: 348.8947, found 348.8959.

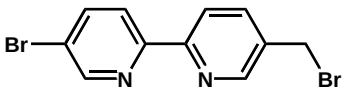

2-Hydroxy-4-(-pyran-2-yloxy)-benzaldehyde (98):[111, 112] A solution of 2,4-dihydroxy-benzaldehyde (825 mg, 6 mmol), dihydropyran (606 mg, 7.2 mmol) and pyridinium *p*-toluenesulfonate (151 mg, 0.6 mmol) in DCM (30 cm^3) was stirred at room temperature for 4 h. The reaction volume was increased to 50 cm^3, the mixture was washed with brine (30 cm^3) and then dried over Na_2SO_4. The solvent was removed under vacuum and the oily product that remained was chromatographed on silica gel with petrol (50 %) and DCM (50 %) as eluent to afforded **98** (1.29 g, 97 %) as a low melting point crystalline solid. ^{1}H NMR (300 MHz, $CDCl_3$): δ = 1.4-2.1 (br m, 6 H, $(CH_2)_3$), 3.6-4.0 (m, 2 H; CH_2O), 5.49 (t, ^3J = 3.0 Hz, 1 H, O-CH-O), 6.61 (d, ^4J = 2.4 Hz, 1 H, H-3), 6.64 (dd, ^3J = 8.4, ^4J = 2.4 Hz, 1 H, H-5), 7.42 (d, ^3J = 8.4 Hz, 1 H, H-6), 9.70 (s, 1 H, CHO), 11.35 (s, 1 H, ArOH); ^{13}C NMR (75 MHz, $CDCl_3$): δ = 19.85, 25.58, 30.84, 63.30, 95.10, 103.23, 109.21, 136.31, 164.64, 164.74, 194.60.

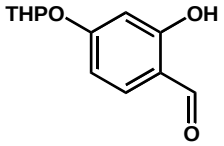

2-(5′-Methyl-[2,2′]bipyridinyl-5-ylmethoxy)-benzaldehyde (99): A DMF (10 cm^3) solution of salicylaldehyde **95** (230 mg, 1.88 mmol) and chloromethylbipyridine **93** (343 mg, 1.57 mmol) in the presence of K_2CO_3 (650 mg, 4.7 mmol) was stirred at room temperature over 10 h. H_2O (20 cm^3) was then added to the reaction mixture, and the resulting precipitate filtered off and washed with water followed by a minimum volume of chilled MeOH. The crude product was purified by chromatography on silica gel with DCM (98.75 %), MeOH (1 %) and saturated NH_3 (0.25 %) as eluent to afford **99** (477 mg, 94 %) as a white solid. ^{1}H NMR (300 MHz, $CDCl_3$): δ = 2.41 (s, 3 H, CH_3), 5.27 (s, 2 H, OCH_2), 7.06 (d, ^3J = 8.4 Hz, 1 H, H-a), 7.13 (dd, ^3J = 7.8, ^3J = 7.2 Hz, 1 H, H-c), 7.56 (ddd, ^3J = 8.4, ^3J = 7.8, ^4J = 1.8 Hz, 1 H, H-b), 7.67 (dd, ^3J = 8.1, ^4J = 1.5 Hz, 1 H, H-4′), 7.88 (dd, ^3J = 7.8, ^4J = 1.8 Hz, 1 H, H-d), 7.93 (dd, ^3J = 8.1, ^4J = 2.1 Hz, 1 H, H-4), 8.31 (d, ^3J = 8.1 Hz, 1 H, H-3′), 8.45 (d, ^3J = 8.1 Hz, 1 H, H-3), 8.53 (d, ^4J = 1.5 Hz, 1 H, H-6′), 8.75 (d, ^4J = 2.1 Hz, 1 H, H-6), 10.55 (s, 1 H,

CHO); ^{13}C NMR (75 MHz, $CDCl_3$): δ = 18.64, 68.19, 113.01, 121.24, 121.27, 121.68, 125.42, 129.02, 131.77, 134.31, 136.18, 136.55, 138.46, 148.39, 149.32, 152.76, 155.88, 160.73, 189.62; positive ion ESI-HRMS: m/z (M = $C_{19}H_{16}N_2O_2$ in DCM / MeOH): calcd for $[M+Na]^+$: 327.1104, found 327.1117.

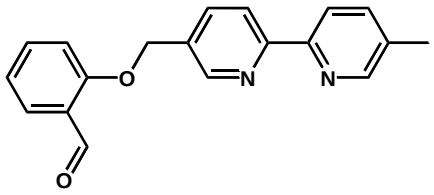

5-*tert*-Butyl-2-(5′-methyl-[2,2′]bipyridinyl-5-ylmethoxy)-benzaldehyde (100): A stirred solution of 5-tert-butylsalycylaldehyde **96** (267 mg, 1.5 mmol) and n-Bu_4NI (55 mg, 0.15 mmol) in toluene (10 cm^3) was refluxed under phase transfer conditions with aqueous 0.2 M NaOH (7 cm^3) for 0.5 h. Asolution of **93** (219 mg, 1 mmol) in toluene (5 cm^3) was added to this mixture and heating at reflux was continued for 24 h. The reaction mixture was cooled and 30 cm^3 of DCM was added. The organic phase was separated from the aqueous phase and washed with 1 M NaOH, then water followed by drying over Na_2SO_4. The solvent was removed under vacuum and the solid that remained chromatographed on silica gel with DCM (98.75 %), MeOH (1 %) and saturated NH_3 (0.25 %) as eluent to afford **100** (278 mg, 77 %) as a waxy white solid. ^{1}H NMR (300 MHz, $CDCl_3$): δ = 1.30 (s, 9 H, C(CH_3)$_3$), 2.38 (s, 3 H, CH_3), 5.22 (s, 2 H, OCH_2Ar), 6.99 (d, ^3J = 8.7 Hz, 1 H, H-a), 7.57 (dd, ^3J = 8.7, ^4J = 2.7 Hz, 1 H, H-b), 7.62 (dd, ^3J = 8.1, ^4J = 2.1 Hz, 1 H, H-4′), 7.87 (dd, ^3J = 8.1, ^4J = 2.4 Hz, 1 H, H-4), 7.88 (d, ^4J = 2.7 Hz, 1 H, H-c), 8.28 (d, ^3J = 8.1 Hz, 1 H, H-3′), 8.40 (d, ^3J = 8.1 Hz,, 1 H, H-3), 8.50 (d, ^4J = 2.4 Hz, 1 H, H-6′), 8.72 (d, ^4J = 2.4 Hz, 1 H, H-6), 10.53 (s, 1H, CHO); ^{13}C NMR (75 MHz, $CDCl_3$): δ = 18.60, 31.49, 34.48, 68.31, 112.01, 120.93, 120.97, 124.47, 125.43, 126.53, 132.84, 133.34, 133.87, 136.38, 137.88, 137.92, 144.06, 148.37, 149.73, 149.82, 189.91; positive ion ESI-HRMS: m/z (M = $C_{23}H_{24}N_2O_2$ in DCM / MeOH): calcd for $[M+H]^+$: 361.1916, found 361.1897; calcd for $[M+Na]^+$: 383.1735, found 383.1710.

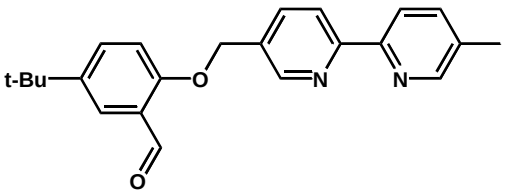

Compound **100** was also prepared via the procedure outlined for **99** from 5-*tert*-butylsalycylaldehyde (1.18 g, 6.6 mmol), **93** (1.21 g, 5.5 mmol) and K_2CO_3 (2.73 g, 20 mmol) in DMF (30 cm^3). Yield 342 mg (95 %).

2-(5′-Bromo-[2,2′]bipyridinyl-5-ylmethoxy)-benzaldehyde (101): Procedure as per the synthesis of **99** from bromomethylbipyridine **94** (200 mg, 0.61 mmol), salicylaldehyde **95** (100 mg, 0.8 mmol) and K_2CO_3 (252 mg, 1.83 mmol) in DMF (10 cm^3). Standard workup afforded bromobipyridine **101** (223 mg, 99 %) as a white powder. ^{1}H NMR (300 MHz, $CDCl_3$): δ = 5.26 (s, 2 H, OCH_2Ar), 7.08 (m, 2 H, H-a,c), 7.56 (ddd, ^3J = 8.4, ^3J = 7.5, ^4J = 2.1 Hz, 1 H, H-b)), 7.87 (dd, ^3J = 8.1, ^4J = 2.0 Hz, 1 H, H-4′), 7.91 (dd, ^3J = 7.5, ^4J = 2.4 Hz, 1 H, H-4), 7.92 (dd, ^3J = 8.4, ^4J = 2.1 Hz, 1 H, H-d), 8.33 (d, ^3J = 8.4 Hz, 1 H, H-3′), 8.43 (d, ^3J = 8.4 Hz, 1 H, H-3), 8.72 (d, ^4J = 2.1 Hz, 1 H, H-6′), 8.74 (d, ^4J = 2.0 Hz, 1 H, H-6), 10.54 (s, 1 H, CHO); ^{13}C NMR (75 MHz, $CDCl_3$): δ = 68.14, 112.98, 121.20, 121.67, 121.73, 122.66, 125.43, 129.09, 132.22, 136.19, 136.53, 139.82, 148.41, 150.51, 154.24, 155.49, 160.68, 189.57; positive ion ESI-HRMS: m/z (*M* = $C_{18}H_{13}BrN_2O_2$ in DCM / MeOH): calcd for $[M+H]^+$: 391.0053, found 391.0067.

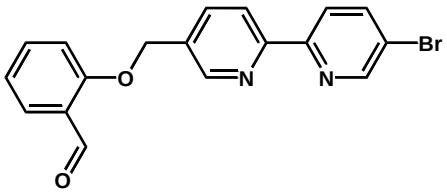

2-(5′-Bromo-[2,2′]bipyridinyl-5-ylmethoxy)-5-tert-butyl-benzaldehyde (102): Procedure as per the synthesis of **99** from bromomethylbipyridine **94** (328 mg, 1 mmol), 5-*tert*-butylsalicylaldehyde (214 mg, 1.2 mmol) and K_2CO_3 (414 mg, 3 mmol) in DMF (15 cm^3). The product was chromatographed on silica gel with DCM as eluent to afford **17** (383 mg, 90 %) as a white solid. ^{1}H NMR (300 MHz, $CDCl_3$): δ = 1.32 (s, 9 H; $C(CH_3)_3$), 5.25 (s, 2 H, OCH_2), 7.01 (d, ^3J = 9.0 Hz, 1 H, H-a), 7.59 (dd, ^3J = 9.0, ^4J = 2.7 Hz, 1 H, H-b), 7.89 (d, ^4J = 2.7 Hz, 1 H, H-c), 7.94 (dd, ^3J = 7.8, ^4J = 2.4 Hz, 1 H, H-4′), 7.96 (dd, ^3J = 8.4, ^4J = 2.7 Hz, 1 H, H-4), 8.36 (d, ^3J = 8.4 Hz, 1 H, H-3), 8.44 (d, ^3J = 7.8 Hz, 1 H, H-3′), 8.75 (d, ^4J = 2.7 Hz, 1 H, H-6), 8.75 (d, ^4J = 2.4 Hz, 1 H, H-6′), 10.54 (s, 1 H, CHO); ^{13}C NMR (75 MHz, $CDCl_3$): δ = 31.49, 34.54, 68.16, 112.79, 121.31, 121.69, 122.74, 124.80, 125.59, 132.55, 133.36, 136.66, 139.85, 144.69, 148.22, 150.54, 153.98, 155.20, 158.69, 189.85; positive ion

ESI-HRMS: m/z (M = $C_{22}H_{21}BrN_2O_2$ in DCM / MeOH): calcd for $[M+H]^+$: 425.0859, found 425.0849; calcd for $[M+Na]^+$: 447.0679, found 447.0663.

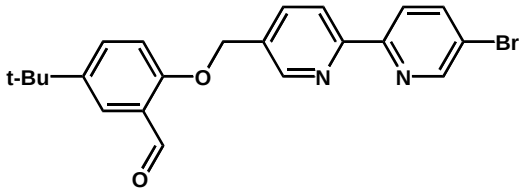

2-(5′-Bromo-[2,2′]bipyridinyl-5-ylmethoxy)-5-(1,1,3,3-tetramethylbutyl)-benzaldehyde (103): Procedure as per the synthesis of **99** from bromomethylbipyridine **94** (328 mg, 1 mmol), 5-*tert*-octylsalicylaldehyde **97** (279 mg, 1.2 mmol) and K_2CO_3 (414 mg, 3 mmol) in DMF (15 cm^3). The product was chromatographed on silica gel with DCM as eluent to afford **103** (445 mg, 93 %) as a white solid. ^{1}H NMR (300 MHz, $CDCl_3$): δ = 0.73 (s, 9 H, $C(CH_3)_3$), 1.38 (s, 6 H, $C(CH_3)_2$), 1.77 (s, 2 H, CH_2), 5.27 (s, 2 H, OCH_2Ar), 7.06 (d, ^3J = 8.8, 1 H, H-a), 7.63 (dd, ^3J = 8.8, ^4J = 2.7 Hz, 1 H, H-b), 7.86 (d, ^3J = 2.7 Hz, 1 H, H-c), 7.95 (dd, ^3J = 8.2, ^4J = 2.3 Hz, 1 H, H-4′), 7.98 (dd, ^3J = 8.7, ^4J = 2.4, 1 H, H-4), 8.38 (dd, ^3J = 8.5, ^5J = 0.6 Hz, 1 H, H-3′), 8.45 (d, ^3J = 8.2 Hz, 1 H, H-3), 8.74 (dd, ^4J = 2.4, ^5J = 0.6 Hz, 1 H, H-6′), 8.76 (d, ^4J = 2.3 Hz, 1 H, H-6), 10.53 (s, 1 H, CHO); ^{13}C NMR (75 MHz, $CDCl_3$): δ = 31.47, 31.76, 32.40, 38.28, 56.76, 68.29, 112.65, 120.79, 121.42, 122.47, 124.66, 125.97, 132.63, 134.10, 136.43, 139.73, 143.58, 148.56, 150.39, 154.48, 155.30, 158.76, 189.56; positive ion ESI-HRMS: m/z (M = $C_{26}H_{29}BrN_2O_2$ in DCM / MeOH): calcd for $[M+H]^+$: 481.1491, found 481.1542; calcd for $[M+Na]^+$: 503.1310, found 503.1367.

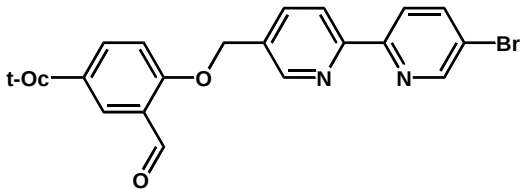

2-(5′-Methyl-[2,2′]bipyridinyl-5-ylmethoxy)-4-(tetrahydropyran-2-yloxy)-benzaldehyde (104): Procedure as per the synthesis of **99** from chloromethylbipyridine **93** (110 mg, 0.5 mmol), THP protected benzalehyde **98** (122 mg, 0.55 mmol) and K_2CO_3 (180 mg, 1.3 mmol) in DMF (8 cm^3). The product was chromatographed on silica gel with DCM as eluent to afford **104** (180 mg, 89 %) as a white solid. ^{1}H NMR (300 MHz, $CDCl_3$): δ = 1.50-2.10 (br m, 6 H, $(CH_2)_3$), 2.38 (s, 3 H, CH_3), 3.58-3.66 (br m, 1 H, O*CH*CH_2), 3.76-3.86 (br m, 1 H, O*CH*CH_2), 5.21 (s, 2 H; OCH_2Ar), 5.49 (t, ^3J = 2.9 Hz, 1 H, O-CH-O), 6.70-6.75 (m, 2 H, H-a,b), 7.63 (dd, ^3J = 8.1, ^4J = 2.1 Hz, 1 H, H-4), 7.80 (d, ^3J = 9.0 Hz, 1 H, H-c), 7.89 (dd, ^3J = 8.4, ^4J = 2.1 Hz, 1 H, H-4′), 8.29 (d, ^3J = 8.1 Hz, 1 H, H-3), 8.42 (d, ^3J = 8.4 Hz, 1 H, H-3′),

8.50 (d, ^4J = 2.1 Hz, 1 H, H-6), 8.72 (d, ^4J = 2.1 Hz, 1 H, H-6′), 10.36 (s, 1 H, CHO); ^{13}C NMR (75 MHz, $CDCl_3$): δ = 18.52, 18.60, 25.19, 30.22, 62.22, 68.12, 96.50, 100.97, 109.51, 119.85, 121.05, 121.07, 130.68, 131.60, 134.08, 136.46, 138.07, 148.40, 149.61, 153.05, 156.21, 162.40, 163.90, 188.24; positive ion ESI-HRMS: m/z (M = $C_{24}H_{24}N_2O_4$ in DCM / MeOH): calcd for $[M+H]^+$: 405.1809, found 405.1788; calcd for $[M+Na]^+$: 427.1628, found 427.1591.

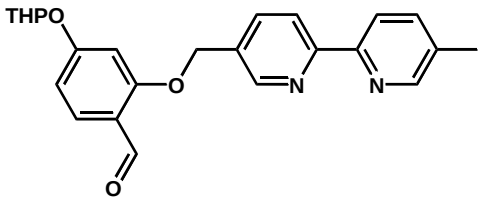

2-(5′-Bromo-[2,2′]bipyridinyl-5-ylmethoxy)-4-(tetrahydropyran-2-yloxy)-benzaldehyde (105): Procedure as per the synthesis of **99** from bromomethylbipyridine **94** (328 mg, 1 mmol), THP protected benzalehyde **98** (267 mg, 1.2 mmol) and K_2CO_3 (414 mg, 3 mmol) in DMF (15 cm^3). The product was chromatographed on silica gel with DCM as eluent to afford **105** (470 mg, 92 %) as a waxy white solid. ^{1}H NMR (300 MHz, $CDCl_3$): δ = 1.50-2.10 (br m, 6 H, $(CH_2)_3$), 3.6-3.7 (m, 1 H, OCH_2CH$_2$), 3.83 (m, 1 H, OCH_2CH$_2$), 5.24 (s, 2 H, O-CH_2Ar), 5.52 (t, ^3J = 3.0 Hz, 1 H, O-CH-O), 6.74 (d, ^4J = 2.1 Hz, 1 H, H-a), 6.75 (dd, ^3J = 9.3, ^4J = 2.1 Hz, 1 H, H-b), 7.83 (d, ^3J = 9.3 Hz, 1 H, H-c), 7.93 (dd, ^3J = 8.1, ^4J = 2.1 Hz, 1 H, H-4′), 7.96 (dd, ^3J = 8.4, ^4J = 2.1 Hz, 1 H, H-4), 8.34 (d, ^3J = 8.4 Hz, 1 H, H-3), 8.43 (d, ^3J = 8.1 Hz, 1 H, H-3′), 8.73 (d, ^4J = 2.1 Hz, 1 H, H-6), 8.74 (d, ^4J = 2.1 Hz, 1 H, H-6′), 10.37 (s, 1 H, CHO); ^{13}C NMR (75 MHz, $CDCl_3$): δ = 18.53, 25.22, 30.24, 62.25, 68.06, 96.52, 100.94, 109.59, 119.87, 121.21, 121.66, 122.68, 130.86, 132.21, 136.61, 139.84, 148.43, 150.54, 155.46, 162.34, 163.92, 188.25.

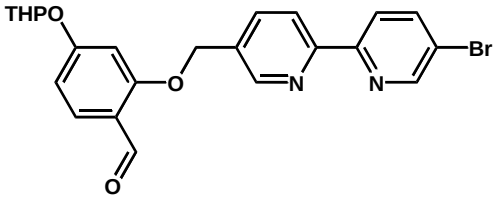

2-(5′-Bromo-[2,2′]bipyridinyl-5-ylmethoxy)-4-hydroxybenzaldehyde (106): THP derivative **105** (400 mg, 0.85 mmol) was stirred in 2 M HCl (20 cm^3) overnight. This solution was neutralised with $NaHCO_3$ and the resulting precipitate isolated by filtration. Successive washes with H_2O, a minimum volume of cold MeOH and Et_2O, afforded **106** (322 mg, 98 %) as a sparingly soluble white powder. ^{1}H NMR (300 MHz, CD_3OD): δ = 5.27 (s, 2 H, OCH_2Ar), 6.37 (d, ^3J = 8.4 Hz, 1 H, H-b), 6.47 (s, 1 H, H-a), 7.52 (d, ^3J = 8.4 Hz, 1 H, H-c),

8.05 (dd, ^3J = 8.4, ^4J = 2.0 Hz, 1 H, H-4′), 8.18 (dd, ^3J = 8.4, ^4J = 2.4 Hz, 1 H, H-4), 8.32 (d, ^3J = 8.4 Hz, 1 H, H-3′), 8.36 (d, ^3J = 8.4 Hz, 1 H, H-3), 8.79 (d, ^4J = 2.0 Hz, 1 H, H-6′), 8.81 (d, ^4J = 2.4 Hz, 1 H, H-6), 10.09 (s, 1 H, CHO).

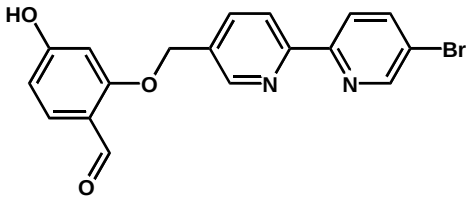

2-(5′-Bromo-[2,2′]bipyridinyl-5-ylmethoxy)-4-heptyloxybenzaldehyde (107): Procedure as per the synthesis of **99** from bromobipyridine **106** (200 mg, 0.52 mmol), iodoheptane (176 mg, 0.78 mmol) and K_2CO_3 (215 mg, 1.56 mmol) was stirred at 60 °C in DMF (8 cm^3) for 1.5 h. Water was added and the resulting solid was washed with H_2O. The crude product was recrystallised from a minimum of methanol to afford **107** (190 mg, 76 %) as white needles. ^{1}H NMR (300 MHz, $CDCl_3$): δ = 0.88 (t, ^3J = 6.9 Hz, 3 H, CH_3), 1.2-1.4 (m, 8 H, $(CH_2)_4$), 1.82 (p, ^3J = 6.9 Hz, 2 H, O-CH_2*CH_2*CH_2), 3.19 (t, ^3J = 6.9 Hz, 2 H, O*CH_2*CH_2), 6.23 (d, ^4J = 2.1 Hz, 1 H, H-a), 6.59 (dd, ^3J = 8.7, ^4J = 2.1 Hz, 1 H, H-b), 7.84 (d, ^3J = 8.7 Hz, 1 H, H-c), 7.94 (dd, ^3J = 8.1, ^4J = 2.1 Hz, 1 H, H-4′), 7.96 (dd, ^3J = 8.4, ^4J = 2.4 Hz, 1 H, H-4), 8.35 (d, ^3J = 8.4 Hz, 1 H, H-3), 8.44 (d, ^3J = 8.1 Hz, 1 H, H-3′), 8.74 (d, ^4J = 2.4 Hz, 1 H, H-6), 8.75 (d, ^4J = 2.1 Hz, 1 H, H-6′), 10.36 (s, 1 H, CHO); ^{13}C NMR (75 MHz, $CDCl_3$): δ = 14.31, 22.82, 26.14, 29.22, 29.27, 31.96, 68.03, 68.82, 99.82, 107.12, 119.33, 121.30, 121.69, 122.72, 131.18, 132.29, 136.69, 139.84, 148.21, 150.54, 154.12, 155.31, 162.37, 165.97, 188.11.

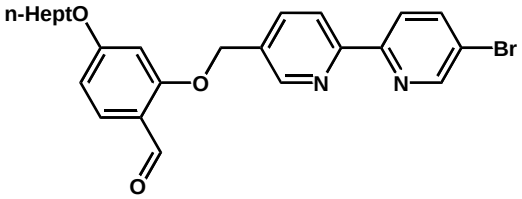

2-[4-(4,4,5,5-Tetramethyl-[1,3,2]dioxaborolan-2-yl)-phenoxy]-tetrahydropyran (108): The phenolic group of 4-bromophenol (5.19 g, 0.03 mol) was protected as per the procedure for **98** from dihydropyran (3.03 g, 0.036 mol) and pyridinium *p*-toluenesulfonate (0.75 g, 0.003 mol) in DCM (50 cm^3). The product was chromatographed on silica gel with DCM (50 %) and petrol (50 %) as eluent to afford the protected phenol (6.70 g, 87 %). *n*-BuLi (1.4 M in cyclohexane, 28 cm^3) was added dropwise to a stirred solution of the protected phenol (6.70 g, 0.026 mol) in THF (50 cm^3) at -78 °C. To the resulting slurry (at -78 °C) 2-isopropoxy-4,4′:5,5′-tetramethyl-1,3,2-dioxaboralane (7.26 g, 0.039 mol) was added and the

reaction mixture was allowed to warm to room temperature. It was then stirred for 12 h. The THF was removed and Et_2O (50 cm^3) and H_2O (50 cm^3) added. The separated aqueous layer was adjusted to pH ~ 7 – 8, extracted with Et_2O and the organic extract dried over Na_2SO_4. The solvent was removed under vacuum and the solid that remained chromatographed on silica gel with DCM (20 %) and petrol (80 %) as eluent to afford **108** (5.69 g, 72 %) as a low melting point solid. ^{1}H NMR (300 MHz, $CDCl_3$): δ = 1.33 (s, 12 H, $OC(CH_3)_2$), 1.50-2.10 (m, 6 H, $(CH_2)_3$), 3.55-3.65 (m, 1 H, O*CH*CH_2), 3.83-3.93 (m, 1 H, O*CH*CH_2), 5.49 (t, ^3J = 3.0 Hz, 1 H, O-CH-O), 7.04 (d, ^3J = 8.7 Hz, 2 H, H-2,6), 7.75 (d, ^3J = 8.7 Hz, 2 H, H-3,5); ^{13}C NMR (75 MHz, $CDCl_3$): δ = 18.85, 25.04, 25.09, 25.40, 30.47, 62.14, 83.80, 96.06, 115.90, 136.63.

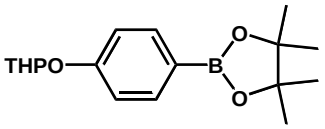

5-Methyl-5′-[4-(tetrahydro-pyran-2-yloxy)-phenyl]-[2,2′]bipyridine (109): A solution of bipyridine **84** (249 mg, 1 mmol), boronic ester **108** (335 mg, 1.1 mmol) and Na_2CO_3 (212 mg, 2 mmol in 5 cm^3 of H_2O) in DMF (10 cm^3) was degassed with N_2. $Pd(PPh_3)_4$ (35 mg, 0.03 mmol) was added to this solution and the reaction mixture was heated with microwave energy in a sealed pressurised microwave vessel with temperature and pressure sensors and a magnetic stirrer bar (Step 1 – the temperature was ramped to 120 °C over 2 min using 100 % of 400 W; Step 2 – the solution was held at 120 °C for 8 - 20 min using 30 % of 400 W). H_2O (20 cm^3) was added and the resulting precipitate was isolated by filtration and washed sequentially with H_2O then cold MeOH to afford **109** (260 mg, 75 %) as a white solid. ^{1}H NMR (300 MHz, $CDCl_3$): δ = 1.6-2.1 (m, 6 H, $(CH_2)_3$), 2.42 (s, 3 H, CH_3), 3.6-3.7 (m, 1 H, O*CH*CH_2), 3.9-4.0 (m, 1 H, O*CH*CH_2), 5.50 (t, ^3J = 3.0 Hz, 1 H, O-CH-O), 7.18 (d, ^3J = 8.7 Hz, 2 H, H-b), 7.58 (d, ^3J = 8.7 Hz, 2 H, H-a), 7.66 (dd, ^3J = 8.1, ^4J = 2.1 Hz, 1 H, H-4), 7.98 (dd, ^3J = 8.4, ^4J = 2.4 Hz, 1 H, H-4′), 8.34 (d, ^3J = 8.1 Hz, 1 H, H-3), 8.43 (d, ^3J = 8.4 Hz, 1 H, H-3′), 8.53 (d, ^3J = 2.1 Hz, 1 H, H-6), 8.88 (d, ^3J = 2.4 Hz, 1 H, H-6′); ^{13}C NMR (75 MHz, $CDCl_3$): δ = 18.60, 18.87, 25.36, 30.46, 62.25, 96.47, 117.30, 121.35, 121.49, 128.30, 130.57, 134.15, 135.47, 136.59, 138.82, 146.98, 148.89, 152.32, 153.03, 157.66, 162.20, 162.47; positive

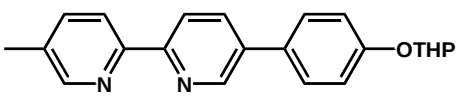

ion ESI-HRMS: m/z (M = $C_{22}H_{22}N_2O_2$ in DCM / MeOH): calcd for $[M + H]^+$: 347.1754, found 347.1749; calcd for $[M + Na]^+$: 369.1574, found 369.1563.

5-*tert*-Butyl-2-{5′-[4-(tetrahydropyran-2-yloxy)-phenyl]-[2,2′]bipyridinyl-5-ylmethoxy}-benzaldehyde (110): Procedure as per the synthesis of **99** from bromobipyridine **102** (213 mg, 0.5 mmol), boronic ester **108** (183 mg, 0.6 mmol), Na_2CO_3 (106 mg, 1 mmol dissolved in 5 cm^3 H_2O) and $Pd(PPh_3)_4$ (17.3 mg, 0.015 mmol) in DMF (10 cm^3). H_2O (30 ml) was added to the reaction mixture and the precipitate that resulted filtered off and washed with excess water and a minimum amount of cold MeOH to give **110** (200 mg, 77 % (>95 % pure)). This product was used for the next step without further purification. ^{1}H NMR (300 MHz, $CDCl_3$): δ = 1.32 (s, 9 H, $C(CH_3)_3$), 1.50-2.10 (m, 6 H, $(CH_2)_3$), 3.6-3.7 (m, 1 H, O$CH_2$$CH_2$), 3.88-3.98 (m, 1 H, O$CH_2$$CH_2$), 5.28 (s, 2 H, O-$CH_2$Ar), 5.51 (t, ^3J = 3.0 Hz, 1 H, O-CH-O), 7.02 (d, ^3J = 9.0 Hz, 1 H, H-a), 7.19 (d, ^3J = 8.7 Hz, 2 H, H-e), 7.59 (d, ^3J = 8.7 Hz, 2 H, H-d), 7.60 (dd, ^3J = 9.0, ^4J = 2.7 Hz, 1 H, H-b), 7.90 (d, ^4J = 2.7 Hz, 1 H, H-c), 7.95 (dd, ^3J = 8.1, ^4J = 2.1 Hz, 1 H, H-4), 8.03 (dd, ^3J = 8.1, ^4J = 2.1 Hz, 1 H, H-4′), 8.48 (d, ^3J = 8.1 Hz, 1 H, H-3), 8.53 (d, ^3J = 8.1 Hz, 1 H, H-3′), 8.78 (d, ^4J = 2.1 Hz, 1 H, H-6), 8.91 (s, ^4J = 2.1 Hz, 1 H, H-6′), 10.55 (s, 1 H; CHO); ^{13}C NMR (75 MHz, $CDCl_3$): δ = 18.82, 25.33, 30.42, 31.47, 34.53, 62.30, 67.89, 76.50, 96.49, 112.78, 117.55, 122.71, 123.24, 124.82, 125.81, 128.43, 128.56, 128.87, 133.37, 133.72, 137.59, 137.88, 138.15, 144.31, 144.55, 144.87, 147.87, 158.43, 189.73; positive ion ESI-HRMS: m/z (M = $C_{33}H_{34}N_2O_4$ in DCM / MeOH): calcd for $[M + H]^+$: 523.2597, found 523.2576; calcd for $[M + Na]^+$: 545.2416, found 545.2392.

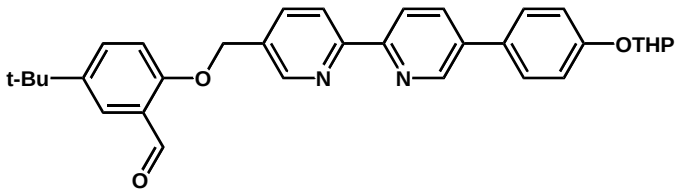

4-Heptyloxy-2-{5′-[4-(tetrahydro-pyran-2-yloxy)-phenyl]-[2,2′]bipyridinyl-5-ylmethoxy}-benzaldehyde (111): Procedure as per the synthesis of **99** from bromobipyridine **107** (180 mg, 0.37 mmol), boronic ester **108** (136 mg, 0.45 mmol), Na_2CO_3 (78.85 mg, 0.74 mmol, dissolved in 5 cm^3 H_2O) and $Pd(PPh_3)_4$ (13 mg, 0.01 mmol) in DMF (10 cm^3). The product was chromatographed on silica gel with DCM as eluent to afford **111** (160 mg, 74 %)

as a white powder. ^{1}H NMR (300 MHz, $CDCl_3$): δ = 0.89 (t, ^{3}J = 6.9 Hz, 3 H, CH_2CH_3), 1.2-1.5 (m, 5 H), 1.6-2.1 (m, 8 H, $(CH_2)_4$), 3.6-3.7 (m, 1 H, OCH_2CH_2), 3.9-4.0 (m, 1 H, OCH_2CH_2), 4.01 (t, ^{3}J = 6.6 Hz, 2 H, OCH_2CH_2), 5.23 (s, 2 H, O-CH_2Ar), 5.49 (t, ^{3}J = 3.0 Hz, 1 H, O-CH-O), 6.53 (d, ^{4}J = 2.1 Hz, 1 H, H-a), 6.57 (dd, ^{3}J = 8.7, ^{4}J = 2.1 Hz, 1 H, H-b), 7.18 (d, ^{3}J = 8.7 Hz, 2 H, H-e), 7.58 (d, ^{3}J = 8.7 Hz, 2 H, H-d), 7.84 (d, ^{3}J = 8.7 Hz, 1 H, H-c), 7.92 (dd, ^{3}J = 8.1, ^{4}J = 2.4 Hz, 1 H, H-4′), 7.98 (dd, ^{3}J = 8.4, ^{4}J = 2.4 Hz, 1 H, H-4), 8.45 (d, ^{3}J = 8.4 Hz, 1 H, H-3), 8.48 (d, ^{3}J = 8.1 Hz, 1 H, H-3′), 8.75 (d, ^{4}J = 2.4 Hz, 1 H, H-6′), 8.89 (d, ^{4}J = 2.4 Hz, 1 H, H-6), 10.36 (s, 1 H, CHO); ^{13}C NMR (75 MHz, $CDCl_3$): δ = 14.28, 18.87, 22.78, 25.35, 26.09, 29.19, 29.23, 30.46, 31.92, 62.25, 68.12, 68.74, 96.47, 99.73, 107.05, 117.26, 119.28, 121.11, 121.27, 128.29, 130.83, 130.98, 131.60, 135.00, 136.33, 136.57, 147.46, 148.36, 153.90, 156.22, 157.55, 162.44, 165.91, 188.12.

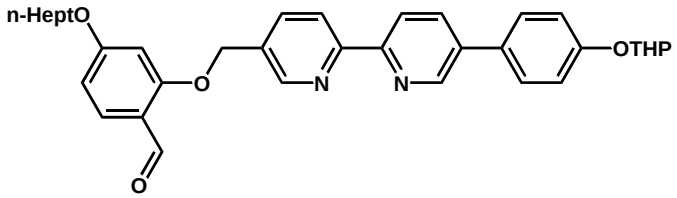

2.3.2 Symmetrically substituted 2,2′-bipyridines

5,5′-Bis-bromomethyl-[2,2′]bipyridine (112):[103-105] Procedure as per the synthesis of **94** from dimethylbipyridine **82** (1.47 g, 8 mmol), N-bromosuccinimide (2.85 g, 16 mmol) in CCl_4 (40 cm^3). The CCl_4 was removed, H_2O (40 cm^3) and MeOH (40 cm^3) added and the mixture was stirred for 0.5 hr. The solid material was isolated by filtration and sequentially washed with H_2O, MeOH then DCM to yield **112** (1.92 g, 70 %) as a semi-pure (>95 %) sparingly soluble white solid. This material was used for subsequent synthetic procedures without further purification. ^{1}H NMR (300 MHz, $CDCl_3$): δ = 4.53 (s, 4 H, CH_2Br), 7.87 (dd, ^{3}J = 8.4, ^{4}J = 2.1 Hz, 2 H, H-4,4′), 8.42 (d, ^{3}J = 8.4 Hz, 2 H, H-3,3′), 8.68 (d, ^{4}J = 2.1 Hz, 2 H, H-6,6′). *"Note that it has been observed elsewhere that prolonged exposure to **112** can cause severe irritation and an allergic response."*

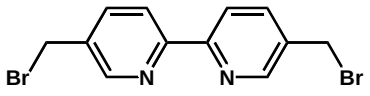

5,5′-Bis(2-formyl-4-*tert*-butylphenoxymethyl)-2,2′-bipyridine (113): Procedure as per the synthesis of **99** from bis-bromomethylbipyridine **112** (1.14 g, 3.33 mmol), salicylaldehyde **96** (1.78 g, 10 mmol) and K_2CO_3 (4.10 g, 30 mmol) in DMF (30 cm^3) with a reaction time of 10 h. The product was chromatographed on silica gel with DCM as eluent to afford **113** (1.59 g, 89 %) as a white powder. ^{1}H NMR (300 MHz, CD_2Cl_2): δ = 1.31 (s, 18 H, $C(CH_3)_3$), 5.27 (s, 4 H, OCH_2Ar), 7.00 (d, ^3J = 8.7 Hz, 2 H, H-a), 7.59 (dd, ^3J = 8.7, ^4J = 2.7 Hz, 2 H, H-b) 7.89 (d, ^4J = 2.7 Hz, 2 H, H-c), 7.95 (dd, ^3J = 8.1, ^4J = 2.1 Hz, 2 H, H-4,4′), 8.50 (d, ^3J = 8.1 Hz, 2 H, H-3,3′), 8.77 (d, ^4J = 2.1 Hz, 2 H, H-6,6′), 10.53 (s, 2 H, CHO); ^{13}C NMR (75 MHz, CD_2Cl_2): δ = 31.49, 34.53, 68.16, 112.82, 121.62, 124.79, 125.58, 132.62, 133.38, 136.76, 144.68, 148.20, 155.25, 158.69, 189.87.

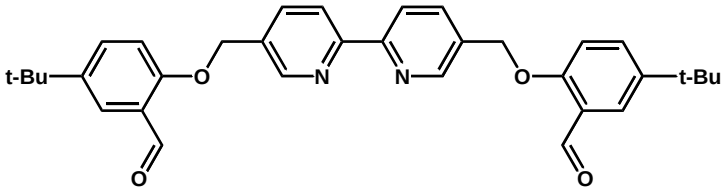

5,5′-Bis[2-formyl-5-(tetrahydropyran-2-yloxy)phenoxymethyl]-2,2′-bipyridine (114): Procedure as per the synthesis of **99** from bis-bromomethylbipyridine **112** (0.68 g, 2 mmol), aldehyde **98** (1.0 g, 4.5 mmol) and K_2CO_3 (1.66 g, 12 mmol) in DMF (20 cm^3). Standard workup afforded **114** (1.11 g, 90 %) as a white powder. ^{1}H NMR (300 MHz, CD_2Cl_2): δ = 1.6-2.1 (m, 6 H, $(CH_2)_3$), 3.6-3.7 (m, 2 H, OCH_2CH_2), 3.8-3.9 (m, 2 H, OCH_2CH_2), 5.27 (s, 4 H, OCH_2Ar), 6.76 (dd, ^3J = 8.4, ^4J = 1.8 Hz, 2 H, H-b), 6.80 (d, ^4J = 1.8 Hz, 2 H, H-a), 7.79 (d, ^3J = 8.4 Hz, 2 H, H-c), 7.96 (dd, ^3J = 8.1, ^4J = 2.1 Hz, 2 H, H-4,4′), 8.51 (d, ^3J = 8.1 Hz, 2 H, H-3,3′), 8.78 (d, ^4J = 2.1 Hz, 2 H, H-6,6′), 10.38 (s, 2 H, CHO); ^{13}C NMR (75 MHz, CD_2Cl_2): δ = 18.68, 25.23, 30.25, 62.33, 68.22, 96.69, 101.20, 109.40, 119.88, 120.97, 130.37, 132.18, 136.43, 148.58, 155.91, 162.46, 163.93, 187.90; positive ion ESI-HRMS: m/z (M = $C_{36}H_{36}N_2O_8$ in DCM / MeOH): calcd for $[M+H]^+$: 625.2544, found 625.2511; calcd for $[M+Na]^+$: 647.2364, found 647.2349.

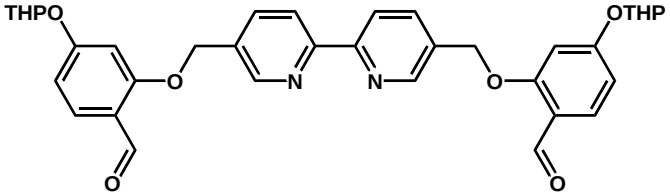

5,5′-Bis[2-formyl-5-hydroxyphenoxymethyl]-2,2′-bipyridine (115): Dialdehyde **114** (200 mg, 0.32 mmol) was taken up in 2 M HCl (30 cm^3) and the solution was stirred overnight then neutralised with saturated $NaHCO_3$ and the precipitate that resulted was isolated by filtration. Sequential washes with minimum volumes of water, cold MeOH and Et_2O, respectively afforded **115** (144 mg, 99 %) as a sparingly soluble white powder. This product was used for subsequent reactions without further purification. ^{1}H NMR (300 MHz, CD_3OD): δ = 5.29 (s, 4 H, OCH_2Ar), 6.42 (d, ^3J = 8.4, 2 H, H-b), 6.53 (br s, 2 H, H-a), 7.55 (d, ^3J = 8.4 Hz, 2 H, H-c), 8.05 (dd, ^3J = 8.1, ^4J = 1.8 Hz, 2 H, H-4,4′), 8.41 (d, ^3J = 8.1 Hz, 2 H, H-3,3′), 8.79 (d, ^4J = 1.8 Hz, 2 H, H-6,6′), 10.14 (s, 2 H, CHO); positive ion ESI-HRMS: m/z (M = $C_{26}H_{20}N_2O_6$ in DCM / MeOH): calcd for $[M+Na]^+$: 479.1219, found 479.1175.

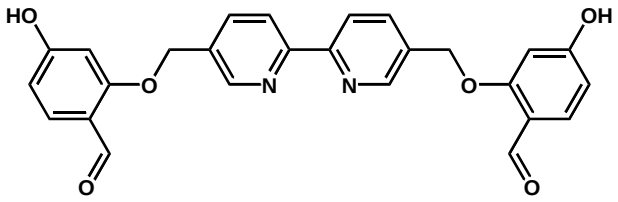

5,5′-Bis[2-formyl-5-(4-Methoxy-benzyloxy)phenoxymethyl]-2,2′-bipyridine (116): Procedure as per the synthesis of **99** from bipyridine **115** (100 mg, 0.219 mmol), 1-chloromethyl-4-methoxybenzene (85 mg, 0.536 mmol) and K_2CO_3 (180 mg, 1.30 mmol) in DMF (10 cm^3). Standard workup afforded **116** (133 mg, 87 %) as a white powder. This product was used in subsequent reactions without further purification. ^{1}H NMR (300 MHz, CD_3OD): δ = 3.82 (s, 6 H, OCH_3), 5.08 (s, 4 H, OCH_2Ar), 5.25 (s, 4 H, OCH_2Ar), 6.67 (d, ^4J = 2.1 Hz, 2 H, H-a), 6.70 (dd, ^3J = 8.7, ^4J = 2.1 Hz, 2 H, H-b), 6.94 (d, ^3J = 8.7 Hz, 4 H, H-d), 7.37 (d, ^3J = 8.7 Hz, 4 H, H-e), 7.83 (d, ^3J = 8.7 Hz, 2 H, H-c), 7.95 (dd, ^3J = 8.1, ^4J = 2.1 Hz, 2 H, H-4,4′), 8.51 (d, ^3J = 8.1 Hz, 2 H, H-3,3′), 8.77 (d, ^4J = 2.1 Hz, 2 H, H-6,6′), 10.37 (s, 2 H, CHO); ^{13}C NMR (75 MHz, $CDCl_3$): δ = 55.47, 68.24, 70.48, 100.16, 107.47, 114.20, 119.60, 121.01, 128.14, 129.65, 130.64, 132.12, 148.51, 155.92, 160.03, 162.50, 165.47, 187.79; positive ion ESI-HRMS: m/z (M = $C_{42}H_{36}N_2O_8$ in DCM / MeOH): calcd for $[M+H]^+$: 697.2544, found 697.2548; calcd for $[M+Na]^+$: 719.2364, found 719.2371.

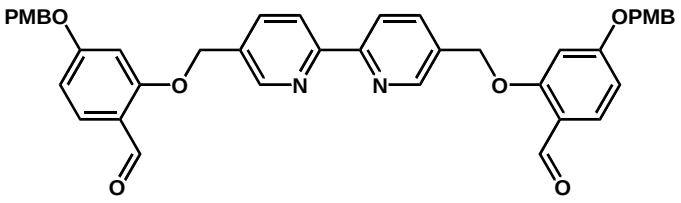

2.3.3 Rigidly-bridged, substituted, ditopic quaterpyridyl ligands.

2-Amino-5-iodopyridine (118):[121] 2-Aminopyridine **117** (49.1 g, 0.52 mol), periodic acid hexahydrate (24.0 g, 0.11 mol) and iodine (53.8 g, 0.21 mol) were dissolved in a mixture of acetic acid (300 cm^3), water (60 cm^3) and sulfuric acid (9 cm^3). The resulting solution was heated at 80 °C with stirring until the colour changed from a dark brown to light brown (4 h). The reaction mixture was allowed to cool to room temperature. It was then treated with a dilute solution of $Na_2S_2O_3$, followed by neutralisation with NaOH. The product was extracted with dichloromethane and the organic layer dried over Na_2SO_4. The solvent was removed and the solid that remained was recrystallised from 50 : 50 chloroform petrol to afford **118** (84.9 g, 74%) as pale yellow/brown crystals: mp 127 - 127.8 °C (lit.[121] 129 °C). ^{1}H NMR (300 MHz, $CDCl_3$): δ = 4.44 (br, 2 H, NH_2), 6.36 (d, ^3J = 8.7 Hz, 1 H, H-3), 7.63 (dd, ^3J = 8.7, ^4J = 2.4 Hz, 1 H, H-4), 8.22 (d, ^4J = 2.4 Hz, 1 H, H-6).

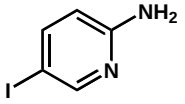

5-Iodo-2-methoxypyridine (119):[63] Sodium metal (4.42 g, 0.192 mol) was added to dry methanol (150 cm^3) and to the resulting methoxide solution was added **85** (18.0 g, 0.064 mol). The resulting solution was refluxed with stirring for ~18 h. The mixture was allowed to cool to room temperature and the methanol was removed under vacuum. The residue that remained was partitioned between DCM and H_2O to remove excess sodium methoxide. The organic layer was then dried over Na_2SO_4. The solvent was removed under vacuum and the oil that remained was chromatographed on silica gel with DCM as eluent to afford **119** (13.98 g, 93 %) as a colourless viscous oil. ^{1}H NMR (300 MHz, $CDCl_3$): δ = 3.89 (s, 3 H, OCH_3), 6.59 (d, ^3J = 8.7 Hz, 1 H, H-3), 7.77 (dd, ^3J = 8.7, ^4J = 2.1 Hz, 1 H, H-4), 8.33 (d, ^4J = 2.1 Hz, 1 H, H-6).

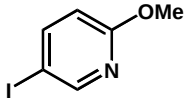

6,6′-Dimethoxy-3,3′-bipyridine (120):[63] A suspension of $[NiCl_2(PPh_3)_2]$ (9.7 g, 0.015 mol), zinc metal (4.84 g, 0.074 mol) and tetraethylammonium iodide (11.42 g, 0.044 mol) in dry THF (80 cm^3) was degassed with N_2 for 0.5 h. This solution was then stirred until a deep maroon colour developed (~0.5 h). To this was added a nitrogen purged solution of **119** (10.3 g, 0.044 mol) and the reaction mixture was heated at 50 °C for 20 h. On cooling to room temperature, 5 M NH_3 (100 cm^3) was added and the resulting reaction mixture stirred

overnight. Ethyl acetate (80 cm^3) was added and the mixture was filtered through celite. The organic phase was isolated and the aqueous layer was extracted with ethyl acetate (80 cm^3). The organic fractions were combined and extracted with 4 M HCl (3 x 60 cm^3). The aqueous layer was neutralised with NaOH pellets, extracted with DCM (3 x 60 cm^3) and the DCM extracts dried over Na_2SO_4. The solvent was removed under vacuum and the solid that remained was chromatographed on silica gel with DCM as eluent to afford **120** (4.55 g, 95 %) as a white powder. The product may be recrystallised from ethanol to afford **120** as fine white needles: mp 104.0 – 105.5ºC (lit.[63] 102-103ºC). ^{1}H NMR (300 MHz, $CDCl_3$): δ = 3.97 (s, 6 H, OCH_3), 6.82 (d, ^3J = 7.8 Hz, 2 H, H-5,5′), 7.71 (dd, ^3J = 7.8, ^4J = 2.7 Hz, 2 H, H-4,4′), 8.32 (d, ^4J = 2.7 Hz, 2 H, H-2,2′).

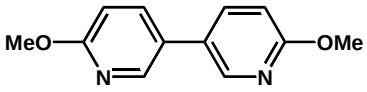

6,6′-Dichloro-3,3′-bipyridine (121):[63] Phosphorus oxychloride (13.2 cm^3, 0.141 mol) was added dropwise to a stirred solution of **120** (3.77 g, 0.0174 mol) in dry DMF (60 cm^3) at 0 ºC. Stirring was continued at 0 ºC for 1 h and then the mixture was heated to 85 ºC for 18 h. Stirring was ceased and the reaction mixture was cooled to room temperature and then – 15 ºC. The resulting microcrystalline product was isolated by filtration and washed with excess water. The crystals were freeze dried to afford **121** (3.43 g, 87 %) as pale yellow crystals: ^{1}H NMR (300 MHz, $CDCl_3$): δ = 7.46 (dd, ^3J = 8.4, ^5J = 0.6 Hz, 2 H, H-5,5′), 7.83 (dd, ^3J = 8.4, ^4J = 2.7 Hz, 2 H, H-4,4′), 8.59 (dd, ^4J = 2.7, ^5J = 0.6 Hz, 2 H, H-2,2′).

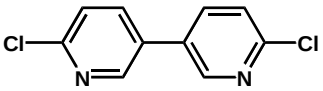

5,5‴-Dimethyl-2,2′:5′,5″:2″,2‴-quaterpyridine (50):[78] Procedure as per the synthesis of **82** using dichlorobipyridine **121** (2.0 g, 9.13 mmol), 2-trimethylstannyl-5-methylpyridine **81** (5.61 g, 21.9 mmol) and $Pd(PPh_3)_4$ (0.99 g, 0.86 mmol) in dry toluene (20 cm^3). The product is sparingly soluble in toluene which allowed for its isolation by filtration. The product was recrystallised from DMF to afford **50** (2.56 g, 83%) as a sparingly soluble powder. ^{1}H NMR (300 MHz, $CDCl_3$): δ = 2.43 (s, 6 H, CH_3), 7.70 (dd, ^3J = 8.1, ^4J = 2.2 Hz, 2 H, H-4,4‴), 8.08 (dd, ^3J = 8.2, ^4J = 2.1 Hz, 2 H, H-4′,4″), 8.39 (d, ^3J = 8.1 Hz, 2 H, H-3,3‴), 8.56 (d, ^3J = 8.2 Hz, 2 H, H-3′,3″), 8.60 (d, ^4J = 2.2 Hz, 2 H, H-6,6‴), 8.98 (d, ^4J = 2.1 Hz, 2 H, H-6′,6″); ^{13}C NMR (75 MHz, $CDCl_3$): δ = 18.44, 121.86, 133.27, 134.87, 135.65, 139.42, 139.69, 137.01,

147.41, 148.00, 151.22; positive ion ESI-HRMS: m/z (M = $C_{22}H_{19}N_4$ in DCM / MeOH): calcd for $[M + H]^+$: 339.1604, found 339.1591; calcd for $[M + Na]^+$: 361.1424, found 361.1411.

Alternative Synthesis a): Procedure as per the synthesis of **120** from bromobipyridine **84** (125 mg, 0.5 mmol), $NiCl_2(PPh_3)_2$ (113 mg, 0.18 mmol), zinc dust (30 mg, 0.45 mmol) and Et_4NI (77 mg, 0.3 mmol). The crude product was taken up in 4 M HCl (10 cm^3). This solution was neutralised with saturated $NaHCO_3$ solution and the product isolated by filtration. The product was recrystallised from DMF, affording **50** (60 mg, 71 %) as a cream coloured powder.

Alternative Synthesis b): A stirred solution of bromo-bipyridine **84** (25 mg, 0.1 mmol), bis-pinacolatodiboron **147** (15 mg, 0.06 mmol), $Pd(PPh_3)_4$ (3.5 mg, 0.003 mmol) and KOAc (29.4 mg, 0.3 mmol) in DMF (2 cm^3) was degassed with N_2 for 15 min. Following this, the reaction mixture was heated to 95 °C for 4 h. After cooling to room temperature, H_2O (~ 4 cm^3) was added and the resulting precipitate isolated by filtration. Successive washes with MeOH and Et_2O afforded **50** (12 mg, 70 %) as a cream coloured powder.

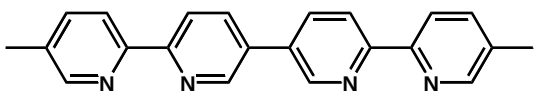

1,4-Bis-(4,4,5,5-tetramethyl[1,3,2]dioxaborolan)benzene (122): *t*-BuLi (9.4 cm^3, 1.7 M in pentane, 16 mmol) was added dropwise to a stirred solution of 1,4-dibromobenzene (944 mg, 4 mmol) in THF (30 cm^3) at -78 °C. The reaction was stirred for a further 1 h at -78 °C and this was followed by the dropwise addition of 2-isopropoxy-4,4,5,5-tetramethyl-[1,3,2]dioxaborolane (2.98 g, 16 mmol). The reaction mixture was allowed to warm to room temperature and stirred overnight. After removal of the THF under vacuum, H_2O (30 cm^3) was added and the pH adjusted to ~ 7 – 8 using 1 M HCl. The product was extracted with Et_2O (2 x 30 cm^3) and the combined organic phases washed with brine and dried over Na_2SO_4. The solvent was removed under vacuum and the crude material purified by recrystallisation from petrol affording **122** (740 mg, 57 %) as white needle shaped crystals.

^{1}H NMR (300 MHz, $CDCl_3$): δ = 1.35 (s, 24 H, CH_3), 7.80 (s, 4 H); ^{13}C NMR (75 MHz, $CDCl_3$): δ = 25.10, 84.07, 134.10.

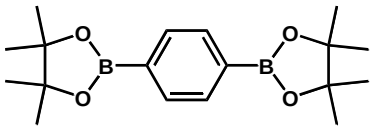

4,4′-(4,4,5,5-tetramethyl[1,3,2]dioxaborolan)biphenyl (123): Procedure as per the synthesis of **122** from 4,4′-dibromobiphenyl (312 mg, 1 mmol), *t*-BuLi (3.6 cm^3, 1.7 M in pentane, 3.6 mmol) and 2-isopropoxy-4,4,5,5-tetramethyl-[1,3,2]dioxaborolane (742 mg, 4 mmol) in THF (20 cm^3) at -78 ^{o}C. The crude material was purified by recrystallisation from petrol to afford **123** (276 mg, 68 %) as small white crystals. ^{1}H NMR (300 MHz, $CDCl_3$): δ = 1.37 (s, 24 H, CH_3), 7.63 (d, ^{3}J = 8.4 Hz, 4 H, H-3,3′,5,5′), 7.88 (d, ^{3}J = 8.4 Hz, 4 H, H-2,2′,6,6′).

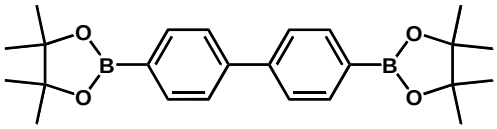

1,4′-Bis-(4,4,5,5-tetramethyl[1,3,2]dioxaborolan)-2,5-dimethoxybenzene (124): Procedure as per the synthesis of **122** from 1,4-diiodo-2,5-dimethoxybenzene **131** (1.56 g, 4 mmol), *t*-BuLi (9.4 cm^3, 1.7 M in pentane, 16 mmol) and 2-isopropoxy-4,4,5,5-tetramethyl-[1,3,2]dioxaborolane (2.98 g, 16 mmol) in THF (30 cm^3). The crude product was recrystallised from petrol to afford **124** (1.17 g, 80 %) as white microcrystals. ^{1}H NMR (300 MHz, $CDCl_3$): δ = 1.36 (s, 24 H, CH_3), 3.75 (s, 6 H, OCH_3), 7.05 (s, 2 H, H-3,6); ^{13}C NMR (75 MHz, $CDCl_3$): δ = 25.05, 57.17, 83.81, 119.03, 158.27.

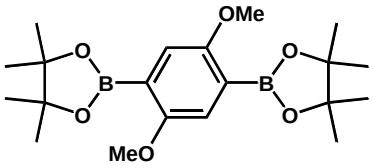

4,4′-Bis-(4,4,5,5-tetramethyl[1,3,2]dioxaborolan)-1,1′-(2,2′,5,5′-tetramethoxy)biphenyl (125): Procedure as per the synthesis of **122** from 4,4′-dibromo-2,5,2′,5′-tetramethoxy-biphenyl **134** (1.3 g, 3 mmol), *t*-BuLi (7 cm^3, 1.7 M in pentane, 12 mmol) and 2-isopropoxy-4,4,5,5-tetramethyl-[1,3,2]dioxaborolane (2.23 g, 12 mmol) in THF (30 cm^3). The THF was removed under vacuum followed by the addition of H_2O. This mixture was neutralised with 2 M HCl and then extracted with DCM (2 x 50 cm^3). The combined organic fractions were

dried over Na_2SO_4. The DCM was removed and the solid that remained recrystallised from petrol to afford **125** (1.1 g, 70 %) as white microcrystals. ^{1}H NMR (300 MHz, $CDCl_3$): δ = 1.36 (s, 24 H, CH_3), 3.75 (s, 6 H, OCH_3), 3.79 (s, 6 H, OCH_3) 6.80 (s, 2 H, H-6,6′), 7.30 (s, 2 H, H-3,3′); ^{13}C NMR (75 MHz, $CDCl_3$): δ = 25.05, 56.87, 57.12, 83.69, 114.88, 119.83, 132.03, 150.95, 158.60.

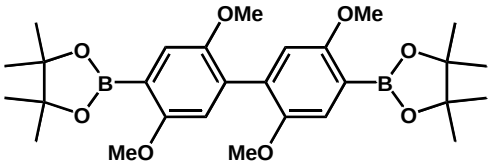

1,4-Bis[5′-(5′′-methyl-2′,2′′-bipyridyl)]benzene (126):[67] Procedure as per the synthesis of **109** from bromobipyridine **84** (143 mg, 0.58 mmol), bis-boronic ester **122** (79 mg, 0.24 mmol), K_2CO_3 (200 mg, 1.4 mmol, dissolved in H_2O (2 cm^3)) and $Pd(PPh_3)_4$ (17 mg, 0.015 mmol) in DMF (6 cm^3). Recrystallisation of the crude product from DMF afforded **126** (70 mg, 70 %) as a pale yellow microcrystalline powder. ^{1}H NMR (300 MHz, CD_2Cl_2): δ = 2.42 (s, 6 H, CH_3), 7.68 (b d, ^3J = 8.4, 2 H, H-4′′), 7.85 (s, 4 H, H-2,3,5,6), 8.11 (dd, ^3J = 8.1, ^4J = 2.1 Hz, 2 H, H-4′), 8.39 (d, ^3J = 8.4 Hz, 2 H, H-3′′), 8.52 (d, ^3J = 8.1 Hz, 2 H, H-3′), 8.53 (br s, 2 H, H-6′′), 8.98 (d, ^4J = 2.1 Hz, 2 H, H-6′).

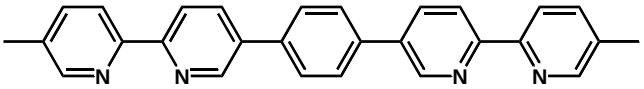

4,4′-Bis[5′′-(5′′′-methyl-2′′,2′′′-bipyridyl)]biphenyl (127):[67] Procedure as per the synthesis of **109** from bromobipyridine **84** (175 mg, 0.704 mmol), bis-boronic ester **123** (130 mg, 0.320 mmol), K_2CO_3 (200 mg, 1.4 mmol, dissolved in H_2O (2 cm^3)) and $Pd(PPh_3)_4$ (24 mg, 0.021 mmol) in DMF (6 cm^3). Recrystallisation of the crude product from DMF afforded **127** (90 mg, 57 %) as a pale yellow powder. ^{1}H NMR (300 MHz, CD_2Cl_2): δ = 2.41 (s, 6 H, CH_3), 7.68 (br d, ^3J = 7.8 Hz, 2 H, H-4′′′), 7.84 (s, 8 H, H-2,2′,3,3′,5,5′,6,6′), 8.11 (dd, ^3J = 8.1, ^4J = 2.7 Hz, 2 H, H-4′′), 8.38 (d, ^3J = 7.8 Hz, 2 H, H-3′′′), 8.51 (d, ^3J = 8.1 Hz, 2 H, H-3′′), 8.54 (br s, 2 H, H-6′′′), 8.98 (d, ^4J = 2.7 Hz, 2 H, H-6′′).

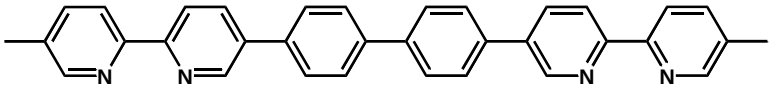

1,4-Bis[5′-(5′′-methyl-2′,2′′-bipyridyl)]-2,5-dimethoxybenzene (128): Procedure as per the synthesis of **109** from bromobipyridine **84** (1.49 g, 6 mmol), bis-boronic ester **124** (1.00 g, 2.7 mmol), K_2CO_3 (2.50 g, 18 mmol, dissolved in H_2O (5 cm^3)) and $Pd(PPh_3)_4$ (208 mg, 0.18 mmol) in DMF (15 cm^3). Recrystallisation of the crude product from MeOH afforded **128** (1.06 g, 83 %) as pale yellow microcrystals. ^{1}H NMR (300 MHz, $CDCl_3$): δ = 2.42 (s, 6 H, CH_3), 3.86 (s, 6 H, OCH_3), 7.07 (s, 2 H, H-3,6), 7.67 (dd, ^3J = 8.1 Hz, ^4J = 1.8 Hz, 2 H, H-4′′), 8.07 (dd, ^3J = 8.1 Hz, ^4J = 2.1 Hz, 2 H, H-4′), 8.36 (d, ^3J = 8.1 Hz, 2 H, H-3′′), 8.46 (d, ^3J = 8.1 Hz, 2 H, H-3′); 8.55 (d, ^4J = 1.8 Hz, 2 H, H-6′′), 8.91 (d, ^4J = 2.1 Hz, 2 H, H-6′); ^{13}C NMR (75 MHz, $CDCl_3$): δ = 18.64, 56.67, 114.47, 120.29, 120.45, 120.93, 127.51, 127.74, 133.77, 137.91, 149.64, 149.77, 151.32, 153.46, 154.74; positive ion ESI-HRMS: m/z (*M* = $C_{30}H_{27}N_4O_2$ in DCM / MeOH): calcd for $[M + H]^+$: 475.2134, found 475.2124; calcd for $[M + Na]^+$: 497.1954, found 497.1940.

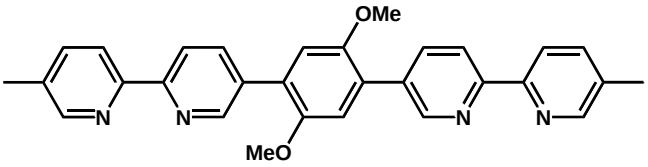

4,4′-Bis[5′′-(5′′′-methyl-2′′,2′′′-bipyridyl)]-(2,2′,5,5′-tetramethoxy)biphenyl (129): Procedure as per the synthesis of **109** from bromobipyridine **84** (277 mg, 1.11 mmol), bis-boronic ester **125** (263 mg, 0.5 mmol), K_2CO_3 (460 mg, 3.33 mmol) and $Pd(PPh_3)_4$ (38 mg, 0.03 mmol) in DMF (7 cm3). After standard workup the crude product was purified by chromatography on silica gel with DCM (97.5 %), MeOH (2 %) and saturated aqueous NH_3 (0.5 %) as eluent to afford **129** (260 mg, 95 %) as an off-white solid. ^{1}H NMR (300 MHz, $CDCl_3$): δ = 2.41 (s, 6H, CH_3), 3.82 (s, 6H, 2,2′ or 5,5′-OCH_3), 3.85 (s, 6H, 2,2′ or 5,5′-OCH_3), 7.03 (s, 2H, H-3,3′ or 6,6′), 7.06 (s, 2H, H-3,3′ or 6,6′), 7.69 (dd, ^3J = 8.1 Hz, ^4J = 1.5 Hz, 2H, H-4′′′), 8.09 (dd, ^3J = 8.3 Hz, ^4J = 2.1 Hz, 2H, H-4′′), 8.38 (d, ^3J = 8.1 Hz, 2H, H-3′′′), 8.48 (d, ^3J = 8.3 Hz, 2H, H-3′′), 8.54 (d, ^4J = 1.5 Hz, 2H, H-6′′′), 8.94 (d, ^4J = 2.1 Hz, 2H, H-6′′); ^{13}C NMR (75 MHz, $CDCl_3$): δ = 18.60, 56.53, 56.85, 114.19, 115.50, 120.62, 121.09, 126.83, 128.16, 133.87, 134.30, 138.20, 149.45, 149.54, 150.71, 151.52, 153.06, 153.96; positive ion ESI-HRMS: m/z (*M* = $C_{38}H_{34}N_4O_4$ in DCM / MeOH): calcd for $[M + H]^+$: 611.2653, found 611.2623; calcd for [*M* +

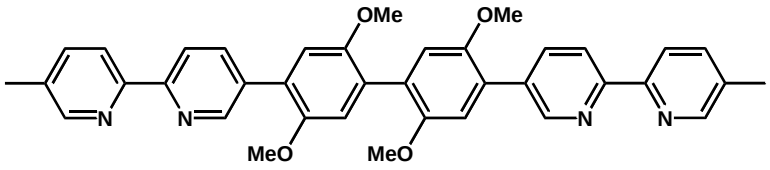

Na]$^+$: 633.2472, found 633.2467.

1,4-Diiodo-2,5-dimethoxybenzene (131):[125] Iodine monochloride (21 g, 0.13 mol) was added dropwise to MeOH (30 cm^3) at 0 °C. To this a solution of 1,4-dimethoxybenzene **130** (4.15 g, 0.030 mol) in MeOH (30 cm^3) was carefully added, keeping the temperature below 10 °C. The resulting solution was refluxed for 5 h. On cooling the solution to room temperature the product crystallised out and was isolated by filtration to afford **131** (9.61 g, 82 %) as small white crystals. ^{1}H NMR (300 MHz, $CDCl_3$): δ = 3.81 (s, 6 H, OCH_3), 7.18 (s, 2 H, H-3,6).

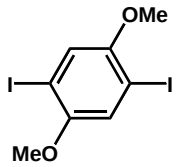

2-Bromo-1,4-dimethoxybenzene (132):[126] A stirred solution of 1,4-dimethoxybenzene **130** (1.38 g, 1 mmol) and N-bromosuccinimide (1.78 g, 1 mmol) in DCM (20 cm^3) was refluxed for 5 h. The reaction mixture was extracted with H_2O (3 x 30 cm^3) and the resulting solution dried over Na_2SO_4. The solvent was removed and the solid that remained chromatographed on silica gel with DCM as eluent to afford **132** (2.04 g, 95 %) as a white crystalline solid. ^{1}H NMR (300 MHz, $CDCl_3$): δ = 3.74 (s, 3 H, OCH_3), 3.84 (s, 3 H, OCH_3), 6.83 (m, 2 H, H-5,6), 7.11 (m, 1 H, H-3).

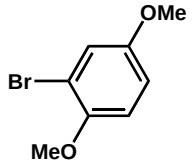

2,5,2′,5′-Tetramethoxybiphenyl (133): Procedure as per the synthesis of **120** from bromobenzene **132** (4.34 g, 20 mmol), $NiCl_2(PPh_3)_2$ (4.38 g, 7 mmol), Zn dust (1.96 g, 30 mmol) and Et_4NI (5.66 g, 22 mmol) in THF (50 cm^3). The crude product was purified by chromatography on silica gel with a 2 : 1 mixture of petrol : DCM as eluent to afford **133** (1.92 g, 70 %) as a white crystalline solid. ^{1}H NMR (300 MHz, $CDCl_3$): δ = 3.74 (s, 6 H, OCH_3), 3.79 (s, 6 H, OCH_3), 6.84-6.95 (m, 6 H, H-3,3′,4,4′,6,6′).

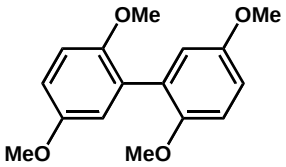

4,4′-Dibromo-2,5,2′,5′-tetramethoxy-biphenyl (134): A stirred solution of tetramethoxybiphenyl **133** (1.70 g, 6.2 mmol) and N-bromosuccinimide (3.31 g, 18.6 mmol) in DCM (30 cm^3) was refluxed for 10 h. The resulting reaction mixture was washed with H_2O

and the organic layer dried over Na_2SO_4. The crude material was purified by chromatography on silica gel with a 1 : 1 mixture of DCM : petrol as eluent to afford **134** (2.57 g, 96 %) as a white crystaline solid. ^{1}H NMR (300 MHz, $CDCl_3$): δ = 3.74 (s, 6 H, OCH_3), 3.86 (s, 6 H, OCH_3), 6.83 (s, 2 H, H-6,6′), 7.18 (s, 2 H, H-3,3′); ^{13}C NMR (75 MHz, $CDCl_3$): δ = 56.79, 57.10, 111.17, 115.42, 117.06, 126.85, 150.06, 151.42.

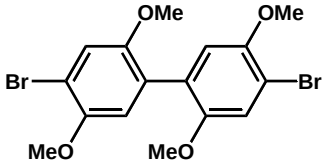

1,4-Bis[5′-(5′′-(2-formyl-4-*tert*-butylphenoxymethyl)-2′,2′′-bipyridinyl)]benzene (137): Procedure as per the synthesis of **109** from bromobipyridine **102** (133 mg, 0.31 mmol), bis-boronic ester **122** (43 mg, 0.13 mmol), K_2CO_3 (110 mg, 0.8 mmol, dissolved in H_2O (1.5 cm^3)) and $Pd(PPh_3)_4$ (9 mg, 0.008 mmol) in DMF (4.5 cm^3). Recrystallisation of the crude product from from DMF afforded **137** (75 mg, 75 %) as sparingly soluble white flake shaped crystals. ^{1}H NMR (300 MHz, $(CD_3)_2NCDO$): δ = 1.49 (s, 18 H, $C(CH_3)_3$), 5.68 (s, 4 H, OCH_2), 7.09 (d, ^3J = 8.7 Hz, 2 H, H-a), 7.97 (dd, ^3J = 8.7 Hz, ^4J = 2.7 Hz, 2 H, H-b), 7.99 (d, ^4J = 2.7 Hz, 2 H, H-c), 8.25 (s, 4 H, H-2,3,5,6), 8.41 (dd, ^3J = 8.4 Hz, ^4J = 2.1 Hz, 2 H, H-4′′), 8.60 (dd, ^3J = 8.1 Hz, ^4J = 2.4 Hz, 2 H, H-4′), 8.76 (d, ^3J = 8.1 Hz, 2 H, H-3′), 8.78 (d, ^3J = 8.4 Hz, 2 H, H-3′′), 9.13 (d, ^4J = 2.1 Hz, 2 H, H-6′′), 9.35 (d, ^4J = 2.4 Hz, 2 H, H-6′), 10.73 (s, 2 H, CHO).

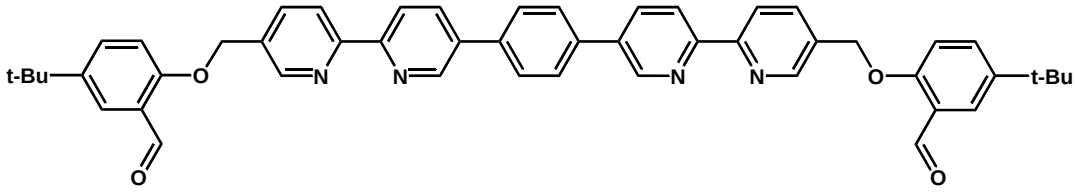

4,4′-Bis[5′′-(5′′′-(2-formyl-4-*tert*-butylphenoxymethyl)-2′′,2′′′-bipyridinyl)]biphenyl (138): A stirred solution of bromobipyridine **102** (65 mg, 15.4 mmol), bis-boronic ester **123** (25 mg, 0.00616 mmol) and Na_2CO_3 (39 mg, 0.37 mmol, dissolved in 0.5 cm^3 of H_2O) in DMF (5 cm^3) was degassed with N_2. $Pd(PPh_3)_4$ (9 mg, 0.00077 mmol) was then added and the reaction mixture heated at 85 ^oC for 12 h. H_2O (10 cm^3) was added to the reaction mixture and the resulting precipitate was isolated by filtration. The crude product

was recrystallised from DMF to yield **138** (41 mg, 80 %) as sparingly soluble microcrystals. ^{1}H NMR (300 MHz, $CDCl_3$ / C_5D_5N): δ = 1.29 (s, 18 H, $C(CH_3)_3$), 5.26 (s, 4 H, OCH_2Ar), 7.01 (d, ^3J = 9.0 Hz, 2 H, H-a), 7.58 (dd, ^3J = 9.0, ^4J = 2.7 Hz, 2 H, H-b), 7.77 (br s, 8 H, H-2,2′,3,3′,5,5′,6,6′), 7.88 (d, ^4J = 2.7 Hz, 2 H, H-c), 7.92 (dd, ^3J = 8.7, ^4J = 2.1 Hz, 2 H, H-4′′′), 8.08 (dd, ^3J = 8.4, ^4J = 2.4 Hz, 2 H, H-4′′), 8.49 (d, ^3J = 8.7 Hz, 2 H, H-3′′ or 3′′′), 8.50 (d, ^3J = 8.4 Hz, 2 H, H-3′′ or 3′′′), 8.76 (d, ^4J = 2.1 Hz, 2 H, H-6′′′), 8.98 (d, ^4J = 2.4 Hz, 2 H, H-6′′), 10.53 (s, 2 H, CHO).

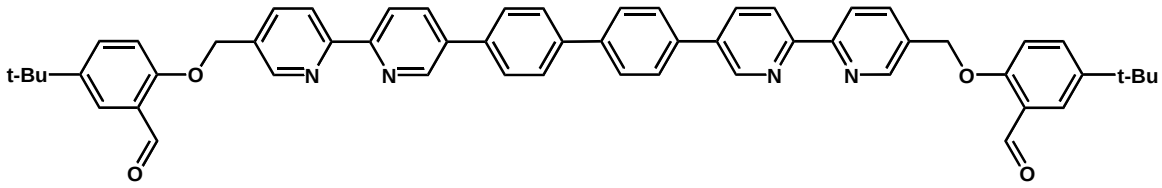

1,4-Bis[5′-(5′′-(2-formylphenoxymethyl)-2′,2′′-bipyridinyl)]-2,5-dimethoxybenzene (139): Procedure as per the synthesis of **109** from bromobipyridine **101** (100 mg, 0.27 mmol), bis-boronic ester **124** (46 mg, 0.12 mmol), K_2CO_3 (112 mg, 0.81 mmol dissolved in 1 cm^3 H_2O) and $Pd(PPh_3)_4$ (9 mg, 0.0073 mmol) in DMF (5 cm^3). The crude product was recrystallised from a 5 : 1 mixture of DMF : H_2O to afford **139** (76 mg, 88 %) as sparingly soluble flake-shaped pale yellow crystals. ^{1}H NMR (300 MHz, CD_2Cl_2): δ = 3.89 (s, 6H, OCH_3), 5.32 (s, 4H, OCH_2Ar), 7.12 (s, 2 H, H-3,6), 7.13 (m, 4 H, H-a,c), 7.63 (dd, ^3J = 8.4, ^3J = 7.5 Hz, 2 H, H-b), 7.85 (dd, ^3J = 8.4, ^4J = 2.1 Hz, 2 H, H-d), 7.97 (br d, ^3J = 8.1 Hz, 2 H, H-4′′), 8.12 (d, ^3J = 7.5 Hz, 2 H, H-4′), 8.53 (d, ^3J = 8.1 Hz, 2 H, H-3′′), 8.56 (d, ^3J = 7.5 Hz, 2 H, H-3′), 8.81 (br s, 2 H, H-6′′), 8.93 (br s, 2 H, H-6′), 10.57 (s, 2 H, CHO).

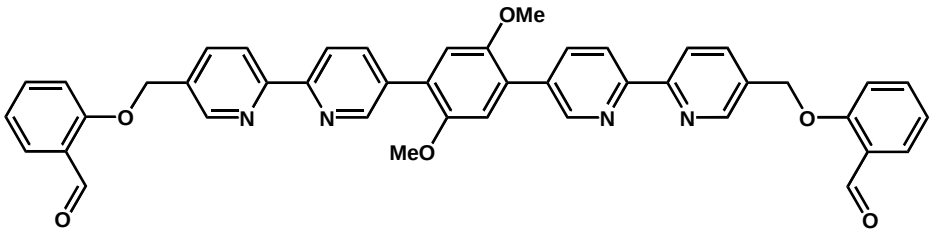

4,4′-Bis[5′′-(5′′′-(2-formylphenoxymethyl)-2′′,2′′′-bipyridinyl)]-1,1′-(2,2′,5,5′-tetramethoxy)biphenyl (140): Procedure as per synthesis of **109** from bromobipyridine **101**

(100 mg, 0.27 mmol), bis-boronic ester **125** (64 mg, 0.12 mmol), K_2CO_3 (112 mg, 0.81 mmol, dissolved in 1 cm^3 H_2O) and $Pd(PPh_3)_4$ (9 mg, 0.0073 mmol) in DMF (5 cm^3). The crude product was recrystallised from a 5:1 mixture of DMF : $H_2O$to afford **140** (94 mg, 81 %) as a yellow powder. ^{1}H NMR (300 MHz, CD_2Cl_2): δ = 3.85 (s, 12 H, OCH_3), 5.32 (s, 4 H, OCH_2Ar), 7.05 (s, 2 H, H-3,3′ or 6,6′), 7.10 (s, 2 H, H-3,3′ or 6,6′), 7.14 (m, 4 H, H-a,c), 7.63 (ddd, ^3J = 8.4, ^3J = 7.5, ^4J = 1.8 Hz, 2 H, H-b), 7.86 (dd, ^3J = 7.5, ^4J = 1.8 Hz, 2 H, H-d), 7.97 (dd, ^3J = 8.1, ^4J = 2.4 Hz, 2 H, H-4′′′), 8.12 (dd, ^3J = 8.4, ^4J = 2.4 Hz, 2 H, H-4′′), 8.53 (d, ^3J = 8.1 Hz, 2 H, H-3′), 8.56 (d, ^3J = 8.4 Hz, 2 H, H-3′′), 8.81 (d, ^4J = 2.4 Hz, 2 H, H-6′′′), 8.93 (d, ^4J = 2.4 Hz, 2 H, H-6′′), 10.57 (s, 2 H, CHO); ^{13}C NMR (75 MHz, CD_2Cl_2): δ = 56.53, 56.67, 68.36, 112.98, 114.00, 115.57, 120.37, 120.86, 124.84, 125.12, 126.85, 128.35, 132.18, 133.311, 134.56, 136.37, 137.81, 144.49, 148.58, 149.88, 150.73, 151.64, 154.21, 156.24, 158.91,189.62.

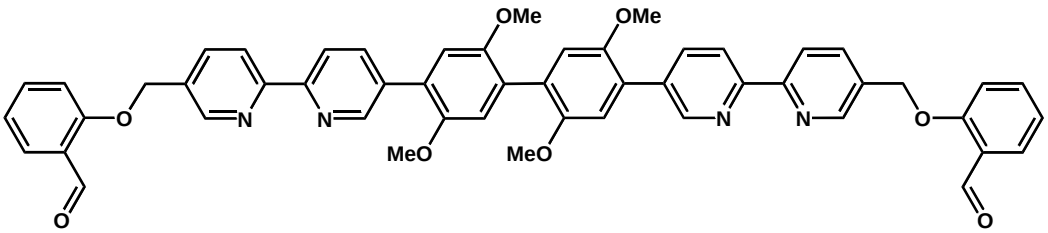

1,4-Bis[5′-(5′′-(2-formyl-4-*tert*-butylphenoxymethyl)-2′,2′′-bipyridinyl)]-2,5-dimethoxybenzene (141): Procedure as per synthesis of **109** using bromobipyridine **102** (950 mg, 2.2 mmol), bis-boronic ester **124** (390 mg, 1.0 mmol), K_2CO_3 (910 mg, 6.6 mmol, dissolved in 7 cm^3 H_2O) and $Pd(PPh_3)_4$ (120 mg, 0.1 mmol) in DMF (14 cm^3). The cooled reaction mixture precipitated flake shaped pale yellow crystals of **141** (766 mg, 93 %) which were isolated by filtration. ^{1}H NMR (300 MHz, CD_2Cl_2): δ = 1.33 (s, 18 H, $C(CH_3)_3$), 3.87 (s, 6 H, OCH_3), 5.29 (s, 4 H, OCH_2), 7.09 (d, ^3J = 8.7 Hz, 2 H, H-a), 7.12 (s, 2 H, H-3,6), 7.64 (dd, ^3J = 8.7 Hz, ^4J = 2.7 Hz, 2 H, H-b), 7.87 (d, ^4J = 2.7 Hz, 2 H, H-c), 7.96 (dd, ^3J = 8.1 Hz, ^4J = 2.1 Hz, 2 H, H-4′′), 8.10 (dd, ^3J = 8.4 Hz, ^4J = 2.4 Hz, 2 H, H-4′), 8.52 (d, ^3J = 8.4 Hz, 2 H, H-3′), 8.54 (d, ^3J = 8.1 Hz, 2 H, H-3′′), 8.79 (d, ^4J = 2.1 Hz, 2 H, H-6′′), 8.92 (d, ^4J = 2.4 Hz, 2 H, H-6′), 10.55 (s, 2 H, CHO); ^{13}C NMR (75 MHz, CD_2Cl_2): δ = 31.21, 34.39, 56.58, 68.39, 112.97, 114.41, 120.39, 120.88, 124.84, 125.13, 127.65, 132.23, 133.32, 134.26,

136.38, 137.78, 144.49, 148.58, 149.83, 151.33, 154.35, 156.17, 158.90, 189.62; positive ion ESI-HRMS: m/z (M = $C_{52}H_{50}N_4O_6$ in DCM / MeOH): calcd for $[M + H]^+$: 827.3803, found 827.3725; calcd for $[M + Na]^+$: 633.2472, found 633.2467.

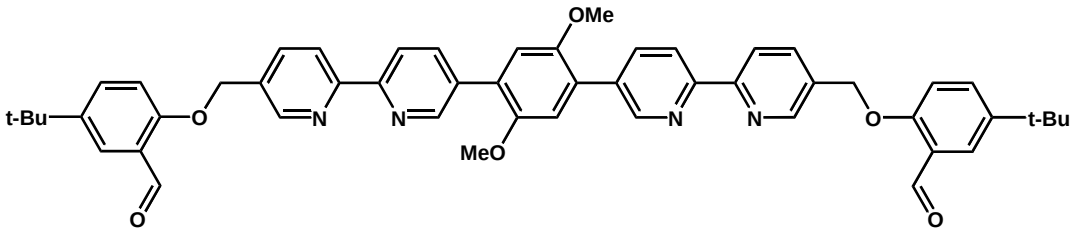

4,4′-Bis[5′′-(5′′′-(2-formyl-4-*tert*-butylphenoxymethyl)-2′′,2′′′-bipyridinyl)]-1,1′-(2,2′,5,5′-tetramethoxy)biphenyl (142): Procedure as per the synthesis of **109** using bromobipyridine **102** (950 mg, 2.2 mmol), bis-boronic ester **125** (390 mg, 1.0 mmol), K_2CO_3 (910 mg, 6.6 mmol, dissolved in 7 cm^3 H_2O) and $Pd(PPh_3)_4$ (120 mg, 0.1 mmol) in DMF (14 cm^3). The crude product was recrystallised from DMF/H_2O to afford **142** (766 mg, 93 %) as a pale yellow crystalline solid. ^{1}H NMR (CD_2Cl_2, 300 MHz): δ = 1.33 (s, 18 H, $C(CH_3)_3$), 3.83 (s, 6 H, OCH_3), 3.84 (s, 6 H, OCH_3), 5.29 (s, 4 H, OCH_2Ar), 7.04 (s, 2 H, H-3,3′ or 6,6′), 7.08 (s, 2 H, H-3,3′ or 6,6′), 7.09 (d, ^3J = 8.7 Hz, 2 H, H-a), 7.64 (dd, ^3J = 8.7 Hz, ^4J = 2.4 Hz, 2 H, H-b), 7.87 (d, ^4J = 2.4 Hz, 2 H, H-c), 7.96 (dd, ^3J = 8.1 Hz, ^4J = 2.4 Hz, 2 H, H-4′′′), 8.11 (dd, ^3J = 8.4 Hz, ^4J = 2.4 Hz, 2 H, H-4′′), 8.52 (dd, ^3J = 8.4, J^5 = 0.6 Hz, 2 H, H-3′′), 8.54 (d, ^3J = 8.1 Hz, 2 H, H-3′′′), 8.79 (d, ^4J = 2.4 Hz, 2 H, H-6′′′), 8.93 (dd, ^4J = 2.4, J^5 = 0.6 Hz, 2 H, H-6′′), 10.55 (s, 2 H, CHO); ^{13}C NMR (75 MHz, CD_2Cl_2): δ = 31.22, 34.39, 56.54, 56.67, 68.41, 112.98, 114, 00, 115.57, 120.37, 120.86, 124.85, 125.12, 126.85, 128.35, 132.18, 133.31, 134.56, 136.37, 137.81, 144.49, 148.58, 149.88, 150.73, 151.64, 154.21, 156.24, 158.91, 189.62; positive ion ESI-HRMS: m/z (M = $C_{60}H_{58}N_4O_8$ in DCM / MeOH): calcd for $[M + H]^+$: 963.4333, found 963.4277; calcd for $[M + Na]^+$: 985.4152, found 985.4089.

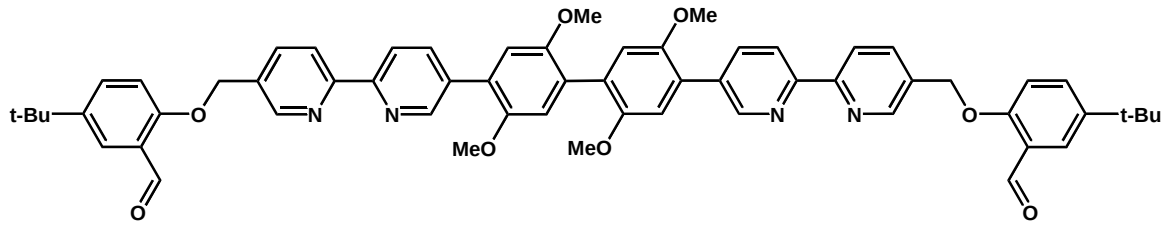

5,5‴-Bis(bromomethyl)-2,2′:5′,5″:2″,2‴-quaterpyridine (143): A stirred suspension of **50** (620 mg, 1.83 mmol), N-bromosuccimide (658 mg, 3.7 mmol), and azobisisobutyronitrile (8 mg, 0.05 mmol) in carbon tetrachloride (40 cm^3) was refluxed while irradiating with a tungsten lamp. After 5 h the irradiation and heating were discontinued and the reaction mixture allowed to cool to room temperature. The resulting solid was filtered off and determined, using ^{1}H NMR spectroscopy, to be a mixture of mainly the mono- and bis-dibromo of products as well as succinimide. Semi-purification was able to be achieved via a hot solvent extraction procedure using DCM to remove the succinimide. This resulted in a mixture of 80% bis-dibromo and 20% monobromo products with the total yield of the two products of 61% (446mg, 49% product). This mixture was used for the next step without further purification (reflecting its insolubility). ^{1}H NMR (300 MHz, $CDCl_3$): δ = 4.57 (s, 4 H, CH_2Br), 7.92 (dd, ^3J = 8.4, ^4J = 1.8 Hz, 2 H, H-4,4‴), 8.59 (dd, ^3J = 8.1, ^4J = 2.4 Hz, 2H, H-4′,4″), 8.51 (d, ^3J = 8.4 Hz, 2 H, H-3,3‴), 8.59 (d, ^3J = 8.1 Hz, 2 H, H-3′,3″), 8.74 (d, ^4J = 1.8 Hz, 2 H, H-6,6‴), 9.01 (d, ^4J = 2.4 Hz, 2 H, H-6′,6″).

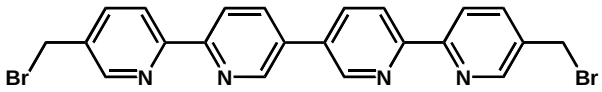

5,5‴-Bis[(2‴′-formyl-4‴′-*tert*-butylphenoxy)methyl]-2,2′:5′,5″:2″,2‴-quaterpyridine (144): A stirred solution of 5-*tert*-butylsalycylaldehyde (535 mg, 3 mmol) and tetrabutylammonium bromide (33 mg, 0.1 mmol) in toluene (10 cm^3) was refluxed under phase transfer conditions with NaOH (112 mg, 2.8 mmol) in H_2O (10 cm^3) for 0.5 h. A suspension of crude **143** (496 mg, 1 mmol) in toluene (15 cm^3) was added to this mixture and the refluxing continued for 24 h. The reaction mixture was cooled and 100 cm^3 of DCM was added. The organic phase was separated from the aqueous phase and washed with 1M NaOH (3 x 40 cm^3) then water (40 cm^3) and the organic layer dried over Na_2SO_4. The solvent was removed under vacuum and the solid that remained was chromatographed on silica gel with DCM (99.5 %), MeOH (0.4 %) and saturated $NH_{3(aq)}$ (0.1 %) as eluent to afford **144** (448 mg, 65 %) as a white solid. ^{1}H NMR (300 MHz, $CDCl_3$): δ = 1.32 (s, 18 H, $C(CH_3)_3$), 5.29 (s, 4 H, CH_2O), 7.03 (d, ^3J = 9.0 Hz, 2 H, H-a), 7.60 (dd, ^3J = 9.0, ^4J = 2.7 Hz, 2 H, H-b), 7.90 (d, ^4J = 2.7 Hz, 2 H, H-c), 7.96 (dd, ^3J = 8.4, ^3J = 2.1 Hz, 2 H, H-4,4‴), 8.12 (dd, ^3J = 8.4, ^4J =

2.1 Hz, 2 H, H-4′,4″), 8.53 (d, ^{3}J = 8.4 Hz, 2 H, H-3,3‴), 8.57 (d, ^{3}J = 8.4 Hz, 2 H, H-3′,3″), 8.80 (d, ^{4}J = 2.1 Hz, 2 H, H-6,6‴), 9.01 (d, ^{4}J = 2.1 Hz, 2 H, H-6′,6″), 10.55 (s, 2H, *CH*O); ^{13}C NMR (75 MHz, $CDCl_3$): δ = 31.22, 34.25, 67.94, 112.55, 121.20, 121.36, 124.54, 125.28, 132.24, 133.09, 133.15, 135.26, 136.30, 144.40, 147.33, 148.10, 155.03, 155.27, 158.47, 189.60; positive ion ESI-HRMS: m/z (*M* = $C_{44}H_{42}N_4O_4$ in DCM / MeOH): calcd for $[M+H]^+$: 691.3284, found 691.3238; calcd for $[M+Na]^+$: 713.3104, found 713.3058.

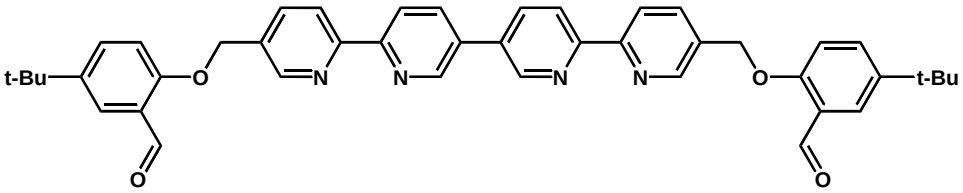

Alternative synthesis a): Procedure as per synthesis of **120.** *Alternative synthesis b).* As per synthesis of **50** from bromobipyridine **102** (43 mg, 0.1 mmol), *bis*-pinacolatodiboron **147** (30 mg, 0.12 mmol), $Pd(PPh_3)_4$ (3.5 mg, 0.003 mmol) and KOAc (30 mg, 0.31 mmol) in DMF (2 cm^3). The product was recrystallised from DMF to affording dialdehyde **144** (21 mg, 62 %) as an off-white powder.

5,5‴-bis[(2‴′-formyl-4‴′-tert-octylphenoxy)methyl]-2,2′:5′,5″:2″,2‴-quaterpyridine (145): Procedure as per synthesis of **144** from 5-*tert*-octylsalycylaldehyde (348 mg, 1.5 mmol), crude **143** (248 mg, 0.5 mmol), tetrabutylammonium bromide (16 mg, 0.5 mmol) in toluene (5 cm^3) and NaOH (52 mg, 1.3 mmol) in H_2O (5 cm^3). The crude product was chromatographed on silica gel with DCM (99.5 %), MeOH (0.4 %) and saturated $NH_{3(aq)}$ (0.1 %) as eluent to afford **145** (268 mg, 67 %) as a white solid. ^{1}H NMR (300 MHz, $CDCl_3$): δ = 0.71 (s, 18 H, $C(CH_3)_3$), 1.37 (s, 12 H, $ArC(CH_3)_2$), 1.73 (s, 4 H, $RCH_2C(CH_3)_3$), 5.27 (s, 4 H, OCH_2Ar), 7.02 (d, ^{3}J = 8.7 Hz, 2 H, H-a), 7.59 (dd, ^{3}J = 8.7, ^{4}J = 2.5 Hz, 2 H, H-b), 8.88 (d, ^{4}J = 2.5 Hz, 2 H, H-c), 7.95 (dd, ^{3}J = 8.4, ^{4}J = 1.8 Hz, 2 H, H-4,4‴), 8.11 (dd, ^{3}J = 8.4, ^{4}J = 2.3 Hz, 2 H, H-4′,4″), 8.52 (d, ^{3}J = 8.4 Hz, 2 H, H-3,3‴), 8.57 (d, ^{3}J = 8.4 Hz, 2 H, H-3′,3″), 8.79 (d, ^{4}J = 1.8 Hz, 2 H, H-6,6‴), 9.00 (d, ^{4}J = 2.3 Hz, 2 H, H-6′,6″), 10.55 (2H, s, CHO); ^{13}C NMR (75 MHz, $CDCl_3$): δ = 31.47, 31.83, 32.35, 38.17, 56.68, 68.04, 112.29, 121.18, 121.26, 124.40, 126.05, 132.06, 133.89, 135.26, 136.28, 143.55, 147.42, 148.28,

155.48, 155.54, 158.49, 189.69; positive ion ESI-HRMS: m/z (M = $C_{52}H_{58}N_4O_4$ in DCM / MeOH): calcd for $[M+H]^+$: 803.4531, found 803.4514; calcd for $[M+Na]^+$: 825.4350, found 825.4299.

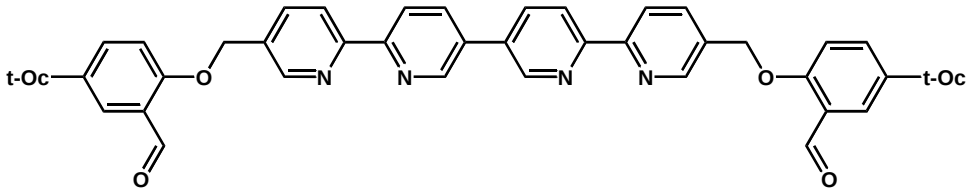

2.3.4 Flexibly-bridged, substituted, ditopic quaterpyridyl ligands.

1,2-Bis-(5′-methyl-[2,2′]bipyridinyl-5-ylmethoxy)benzene (149): Procedure as per the synthesis of **99** from chloromethylbipyridine **93** (241 mg, 1.1 mmol), catechol (55 mg, 0.5 mmol) and K_2CO_3 (415 mg, 3.0 mmol) were reacted in DMF (10 cm^3) for 12 h. Standard workup yielded **149** (215 mg, 90 %) as a white powder. ^{1}H NMR ($CDCl_3$, 300 MHz): δ = 2.40 (s, 6 H, CH_3), 5.22 (s, 4 H, OCH_2Ar), 6.96 (m, 4 H, H-a,b), 7.63 (dd, ^3J = 8.1, ^4J = 1.8 Hz, 2 H, H-4′), 7.90 (dd, ^3J = 8.1, ^4J = 2.1 Hz, 2 H, H-4), 8.29 (d, ^3J = 8.1 Hz, 2 H, H-3′), 8.38 (d, ^3J = 8.1 Hz, 2 H, H-3), 8.50 (d, ^4J = 1.8 Hz, 2 H, H-6′), 8.72 (d, ^4J = 2.1 Hz, 2 H, H-6); ^{13}C NMR (75 MHz, $CDCl_3$): δ = 18.61, 69.17, 115.70, 120.97, 121.07, 122.43, 132.73, 133.86, 136.57, 137.97, 148.45, 148.87, 149.61, 153.26, 155.88; positive ion ESI-HRMS: m/z (M = $C_{30}H_{26}N_4O_2$ in DCM / MeOH): calcd for $[M + Na]^+$: 497.1948, found 497.1948.

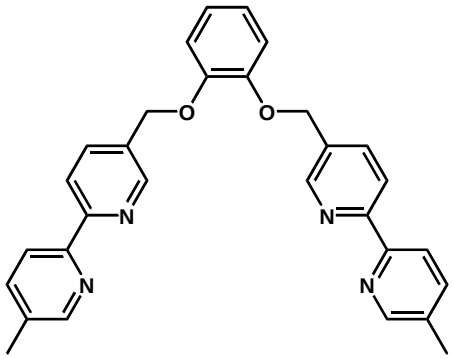

1,3-Bis-(5′-methyl-[2,2′]bipyridinyl-5-ylmethoxy)-benzene (150): Procedure as per the synthesis of **99** from chloromethylbipyridine **93** (241 mg, 1.1 mmol), resorcinol (55 mg, 0.5 mmol) and K_2CO_3 (415 mg, 3.0 mmol) were reacted in DMF (10 cm^3) for 12 h. Standard workup yielded **150** (220 mg, 93 %) as a white powder. ^{1}H NMR ($CDCl_3$, 300 MHz): δ = 2.41 (s, 6 H, CH_3), 5.12 (s, 4 H, OCH_2Ar), 6.64 (dd, ^3J = 8.1, ^4J = 2.3 Hz, 2 H, H-b), 6.65 (d,

^{4}J = 2.3 Hz, 1 H, H-a), 7.23 (t, ^{3}J = 8.1 Hz, 1 H, H-c), 7.65 (dd, ^{3}J = 8.1, ^{4}J = 2.1 Hz, 2 H, H-4′), 7.89 (dd, ^{3}J = 8.1, ^{4}J = 2.1 Hz, 2 H, H-4), 8.30 (d, ^{3}J = 8.1 Hz, 2 H, H-3′), 8.41 (d, ^{3}J = 8.1 Hz, 2 H, H-3), 8.52 (d, ^{4}J = 2.1 Hz, 2 H, H-6′), 8.72 (d, ^{4}J = 2.1 Hz, 2 H, H-6); ^{13}C NMR (75 MHz, $CDCl_3$): δ = 18.61, 67.75, 102.60, 107.89, 120.99, 121.07, 130.41, 132.43, 133.96, 136.61, 138.05, 148.50, 149.60, 153.21, 155.93, 159.88; positive ion ESI-HRMS: m/z (*M* = $C_{30}H_{26}N_4O_2$ in DCM / MeOH): calcd for $[M+H]^+$: 475.2129, found 475.2200; calcd for $[M + Na]^+$: 497.1948, found 497.1945.

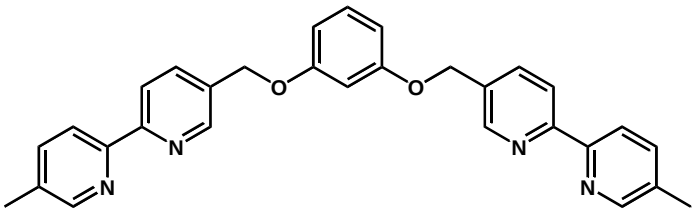

1,4-Bis-(5′-methyl-[2,2′]bipyridinyl-5-ylmethoxy)-benzene (151): Procedure as per the synthesis **99** from chloromethylbipyridine **93** (241 mg, 1.1 mmol), hydroquinone (55 mg, 0.5 mmol) and K_2CO_3 (415 mg, 3.0 mmol) were reacted in DMF (10 cm^3) for 12 h. Standard workup yielded **151** (138 mg, 58 %) as a sparingly soluble white powder. ^{1}H NMR ($CDCl_3$, 300 MHz): δ = 2.41 (s, 6 H, CH_3), 5.09 (s, 4 H, OCH_2Ar), 7.65 (dd, ^{3}J = 8.1, ^{4}J = 1.8 Hz, 2 H, H-4′), 7.89 (dd, ^{3}J = 8.4, ^{4}J = 2.1 Hz, 2 H, H-4), 8.31 (d, ^{3}J = 8.1 Hz, 2 H, H-3′), 8.41 (d, ^{3}J = 8.4 Hz, 2 H, H-3), 8.52 (d, ^{4}J = 1.8 Hz, 2 H, H-6′), 8.71 (d, ^{4}J = 2.1 Hz, 2 H, H-6); positive ion ESI-HRMS: m/z (*M* = $C_{30}H_{26}N_4O_2$ in DCM / MeOH): calcd for $[M + Na]^+$: 497.1948, found 497.1956.

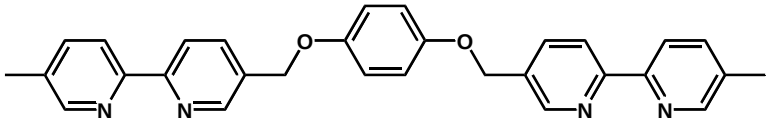

2.4 REFERENCES

1. J. Hassan, M. Sevignon, C. Gozzi, E. Schulz and M. Lemaire, *Chem. Rev.*, 2002, **102**, 1359.
2. G. R. Newkome, A. K. Patri, E. Holder and U. S. Schubert, *Eur. J. Org. Chem.*, 2004, 235.
3. F. Kröhnke, *Synthesis*, 1976, 1.
4. S. Schröter, C. Stock and T. Bach, *Tetrahedron*, 2005, **61**, 2245.
5. C. J. Handy, A. S. Manoso, W. T. McElroy, W. M. Seganish and P. DeShong, *Tetrahedron*, 2005, **61**, 12201.
6. N. C. Fletcher, *Perkin Trans. 1*, 2002, 1831.
7. V. N. Kalinin, *Synthesis*, 1992, 413.
8. Y. Uchida, R. Kajita, Y. Kawasaki and S. Oae, *Tetrahedron Lett.*, 1995, **36**, 4077.
9. J. Uensishi, T. Tanaka, S. Wakabayashi and S. Oae, *Tetrahedron Lett.*, 1990, **31**, 4625.
10. E. C. Constable, S. M. Elder, J. Healy and D. A. Tocher, *Dalton Trans.*, 1990, 1669.
11. C. M. Amb and S. C. Rasmussen, *J. Org. Chem.*, 2006, **71**, 4696.
12. N. Miyaura and A. Suzuki, *Chem. Rev.*, 1995, **95**, 2457.
13. K. C. Nicolaou, P. G. Bulger and D. Sarlah, *Angew. Chem. Int. Ed.*, 2005, **44**, 4442.
14. S. P. Stanforth, *Tetrahedron*, 1998, **54**, 263.
15. I. Beletskaya and A. V. Cheprakov, *Coord. Chem. Rev.*, 2004, **248**, 2337.
16. M. Iyoda, H. Otsuka, K. Sato, N. Nisato and M. Oda, *Bull. Chem. Soc. Jpn.*, 1990, **63**, 80.
17. M. Iyoda, M. Sakaitani, H. Otsuka and M. Oda, *Tetrahedron Letters*, 1985, **26**, 4777.
18. A. Jutand and A. Mosleh, *J. Org. Chem.*, 1997, **62**, 261.
19. C. Amatore and A. Jutand, *Organometallics*, 1988, **7**, 2003.
20. I. Colon and D. R. Kelsey, *J. Org. Chem.*, 1986, **51**, 2627.
21. P. Knochel and R. D. Singer, *Chem. Rev.*, 1993, **93**, 2117.
22. J. K. Stille, *Angew. Chem. Int. Ed.*, 1986, **25**, 508.
23. P. Espinet and A. M. Echavarren, *Angew. Chem. Int. Ed.*, 2004, **43**, 4704.
24. J. K. Stille and K. S. Y. Lau, *Acc. Chem. Res.*, 1977, **10**, 434.

25. A. L. Casado and P. Espinet, *J. Am. Chem. Soc.*, 1998, **120**, 8978.
26. A. L. Casado and P. Espinet, *Organometallics*, 1998, **17**, 954.
27. L. S. Santos, G. B. Rosso, R. A. Pilli and M. N. Eberlin, *J. Org. Chem.*, 2007, **72**, 5809.
28. A. H. Roy and J. F. Hartwig, *Organometallics*, 2004, **23**, 194.
29. G. Espino, A. Kurbangalieva and J. M. Brown, *Chem. Commun.*, 2007, 1742.
30. C. Amatore, A. Jutand and A. Suarez, *J. Am. Chem. Soc.*, 1993, **115**, 9531.
31. S. Kozuch, S. Shaik, A. Jutand and C. Amatore, *Chem. Eur. J.*, 2004, **10**, 3072.
32. S. Kozuch, C. Amatore, A. Jutand and S. Shaik, *Organometallics*, 2005, **24**, 2319.
33. C. Amatore, M. Azzabi and A. Jutand, *J. Am. Chem. Soc.*, 1991, **113**, 8375.
34. C. Amatore and A. Jutand, *Acc. Chem. Res.*, 2000, **33**, 314.
35. K. Fagnou and M. Lautens, *Angew. Chem. Int. Ed.*, 2002, **41**, 26.
36. A. F. Littke, C. Dai and G. C. Fu, *J. Am. Chem. Soc.*, 2000, **122**, 4020.
37. P. W. N. M. van Leeuwen, P. C. J. Kamer, J. N. H. Reek and P. Dierkes, *Chem. Rev.*, 2000, **100**, 2741.
38. U. Christmann and R. Vilar, *Angew. Chem. Int. Ed.*, 2005, **44**, 366.
39. P. Dierkes and P. W. N. M. van Leeuwen, *Dalton Trans.*, 1999, 1519.
40. M. Kranenburg, P. C. J. Kramer and P. W. N. M. Van Leeuwen, *Eur. J. Inorg. Chem.*, 1998, 155.
41. A. Fihri, P. Meuniew and J.-C. Hierso, *Coord. Chem. Rev.*, 2007, **251**, 2017.
42. A. F. Littke and G. C. Fu, *Angew. Chem. Int. Ed.*, 2002, **41**, 4176.
43. E. A. Mitchell and M. C. Baird, *Organometallics*, 2007, **26**, 5230.
44. S. D. Walker, T. E. Barder, J. R. Martinelli and S. L. Buchwald, *Angew. Chem. Int. Ed.*, 2004, **43**, 1871.
45. T. E. Barder, S. D. Walker, J. R. Martinelli and S. L. Buchwald, *J. Am. Chem. Soc.*, 2005, **127**, 4685.
46. R. Martin and S. L. Buchwald, *Acc. Chem. Res.*, 2008, **41**, 1461.
47. Z. Weng, S. Teo and T. S. A. Hor, *Acc. Chem. Res.*, 2007, **40**, 676.
48. M. Miura, *Angew. Chem. Int. Ed.*, 2004, **43**, 2201.
49. V. Farina, *Adv. Synth. Catal.*, 2004, **346**, 1553.

50. A. L. Casado, P. Espinet, A. M. Gallego and J. M. Martinez-Ilarduya, *Chem. Commun.*, 2001, 339.
51. J. A. Casares, P. Espinet, B. Fuentes and G. Salas, *J. Am. Chem. Soc.*, 2007, **129**, 3508.
52. W. Yang, Y. Wang and J. R. Corte, *Org. Lett.*, 2003, **5**, 3131.
53. C. Sicre, J.-L. Alonso-Gomez and M. M. Cid, *Tetrahedron*, 2006, **62**, 11063.
54. C. Sicre, A. A. C. Braga, F. Maeras and M. M. Cid, *Tetrahedron*, 2008, **64**, 7437.
55. C. Sicre and M. M. Cid, *Org. Lett.*, 2005, **7**, 5737.
56. J. A. Zolewicz and J. M. A. Cruskie, *Tetrahedron*, 1995, **51**, 11393.
57. M. P. Cruskie, Jr., J. A. Zoltewicz and K. A. Abboud, *J. Org. Chem.*, 1995, **60**, 7491.
58. P. F. H. Schwab, F. Fleischer and J. Michl, *J. Org. Chem.*, 2002, **67**, 443.
59. E. C. Constable, S. M. Elder, M. J. Hannon, A. Martin, P. R. Raithby and D. A. Tocher, *Dalton Trans.*, 1996, 2423.
60. J. Hassan, V. Penalva, L. Lavenot, C. Gozzi and M. Lemaire, *Tetrahedron*, 1998, **54**, 13793.
61. E. Rajalakshmanan and V. Alexander, *Synth. Commun.*, 2005, **35**, 891.
62. S. Yanagida, T. Ogata, Y. Kuwana, Y. Wada, K. Murakoshi, A. Ishida, S. Takamuku, M. Kusaba and N. Nakashima, *Perkins Trans. 2*, 1996, 1963.
63. E. C. Constable, D. Morris and S. Carr, *New J. Chem*, 1998, 287.
64. A. Lützen, M. Hapke, H. Staats and J. Bunzen, *Eur. J. Org. Chem.*, 2003, 3948.
65. S. A. Savage, A. P. Smith and C. L. Fraser, *J. Org. Chem.*, 1998, **63**, 10048.
66. A. Lützen and M. Hapke, *Eur. J. Org. Chem.*, 2002, 2292.
67. P. N. W. Baxter, *J. Org. Chem.*, 2000, **65**, 1257.
68. Y. Q. Fang, M. I. J. Polson and G. S. Hanan, *Inorg. Chem.*, 2003, **42**, 5.
69. P. Baxter, J.-M. Lehn, A. DeCian and J. Fischer, *Angew. Chem. Int. Ed.*, 1993, **32**, 69.
70. C. Barolo, M. K. Nazeeruddin, S. Fantacci, D. DiCenso, P. Comte, P. Liska, G. Viscardi, P. Quagliotto, F. DeAngelis, S. Ito and M. Gratzel, *Inorg. Chem.*, 2006, **45**, 4642.
71. M. Heller and U. S. Schubert, *J. Org. Chem.*, 2002, **67**, 8269.
72. U. S. Schubert and C. Eschbaumer, *Org. Lett.*, 1999, **1**, 1027.

73. U. S. Schubert, C. Eschbaumer and G. Hochwimmer, *Tetrahedron Lett.*, 1998, **39**, 8643.
74. K. J. Arm and J. A. G. Williams, *Chem. Commun.*, 2005, 230.
75. T. Haino, M. Kobayashi, M. Chikaraishi and Y. Fukazawa, *Chem. Commun.*, 2005, 2321.
76. S. Bin-Salamon, S. H. Brewer, E. C. Depperman, S. Franzen, J. W. Kampf, M. L. Kirk, R. K. Kumar, S. Lappi, K. Peariso, K. E. Preuss and D. A. Shultz, *Inorg. Chem.*, 2006, **45**, 4461.
77. S. Welter, N. Salluce, A. Benetti, N. Rot, P. Belser, P. Sonar, A. C. Grimsdale, K. Mullen, M. Lutz, A. L. Spek and L. De Cola, *Inorg. Chem.*, 2005, **44**, 4706.
78. K. Warnmark, P. Baxter and J.-M. Lehn, *Chem. Commun.*, 1998, 993.
79. A. Suzuki, *Chem. Commun.*, 2005, 4759.
80. T. Ishiyama, K. Ishida and N. Miyaura, *Tetrahedron*, 2001, **57**, 9813.
81. T. Ishiyama, M. Murata and N. Miyaura, *J. Org. Chem.*, 1995, **60**, 7508.
82. Timothy E. B. Stephen L. B. Kelvin L. Billingsley, *Angew. Chem. Int. Ed.*, 2007, **46**, 5359.
83. M. Sumimoto, N. Iwane, T. Takahama and S. Sakaki, *J. Am. Chem. Soc.*, 2004, **126**, 10457.
84. P. R. Parry, C. Wang, A. S. Batsanov, M. R. Bryce and B. Tarbit, *J. Org. Chem.*, 2002, **67**, 7541.
85. A. E. Thompson, G. Hughes, A. S. Batsanov, M. R. Bryce, P. R. Parry and B. Tarbit, *J. Org. Chem.*, 2005, **70**, 388.
86. A. Bouillon, J. C. Lancelot, V. Collot, P. R. Bovy and S. Rault, *Tetrahedron*, 2002, **58**, 2885.
87. A. Bouillon, J. C. Lancelot, J. S. Santos, V. Collot, P. R. Bovy and S. Rault, *Tetrahedron*, 2003, **59**, 10043.
88. A. Bouillon, A. S. Voisin, A. Robic, J. C. Lancelot, V. Collot and S. Rault, *J. Org. Chem.*, 2003, **68**, 10178.
89. C. L. Cioffi, W. T. Spencer, J. J. Richards and R. J. Herr, *J. Org. Chem.*, 2004, **69**, 2210.

90. W. L. Dorian, M. S. Jensen, R. S. Hoerrner, D. Cai, R. D. Larsen and P. J. Reider, *J. Org. Chem.*, 2002, **67**, 5394.
91. M. Querol, B. Bozic, N. Salluce and P. Belser, *Polyhedron*, 2003, **22**, 655.
92. P. Gros, A. Doudouh and Y. Fort, *Tetrahedron Lett.*, 2004, **45**, 6239.
93. P. Appukkuttan and E. Van der Eycken, *Eur. J. Org. Chem.*, 2008, 1133
94. N. E. Leadbeater, *Chem. Commun.*, 2005, 2881.
95. S. A. Galema, *Chem. Soc. Rev.*, 1997, **26**, 233.
96. C. Gabriel, S. Gabriel, E. H. Grant, B. S. J. Halstead and D. M. P. Mingos, *Chem. Soc. Rev.*, 1998, **27**, 213.
97. C. O. Kappe, *Angew. Chem. Int. Ed.*, 2004, **43**, 6250.
98. N. Kuhnert, *Angew. Chem. Int. Ed.*, 2002, **41**, 1863.
99. C. R. Strauss, *Angew. Chem. Int. Ed.*, 2002, **41**, 3589.
100. C. L. Fraser, N. R. Anastasi and J. J. S. Lamba, *J. Org. Chem.*, 1997, **62**, 9314.
101. J. J. S. Lamba and C. L. Fraser, *J. Am. Chem. Soc.*, 1997, **119**, 1801.
102. R. M. Silverstein, F. X. Webster and D. J. Kiemle, *Spectrometric Identification of Organic Compounds*, Seventh edn., Wiley, New York, 2005.
103. F. Ebmeyer and F. Voegtle, *Chem. Ber.*, 1989, **122**, 1725.
104. E. Lindner, R. Veigel, K. Ortner, C. Nachtigal and M. Steimann, *Eur. J. Inorg. Chem.*, 2000, 959.
105. R. Ziessel, M. Hissler and G. Ulrich, *Synthesis*, 1998, **9**, 1339.
106. G. R. Newkome, W. E. Puckett, G. E. Kiefer, V. D. Gupta, Y. Xia, M. Coreil and M. A. Hackney, *J. Org. Chem.*, 1982, **47**, 4116.
107. I. Yildiz, J. Mukherjee, M. Tomasulo and F. M. Raymo, *Adv. Funct. Mater.*, 2007, **17**, 814.
108. G. R. Newkome, J. Gross and A. K. Patri, *J. Org. Chem.*, 1997, **62**, 3013.
109. H. F. M. Nelissen, M. C. Feiters and R. J. M. Nolte, *J. Org. Chem.*, 2002, **67**, 5901.
110. S. G. Telfer, G. Bernardinelli and A. F. Williams, *Dalton Trans.*, 2003, 435.
111. S. F. Nielsen, M. Chen, T. G. Theander, A. Kharazmi and S. Brøgger Christensen, *Bioorg. Med. Chem. Lett.*, 1995, **5**, 449.
112. M. R. Saberi, T. K. Vinh, S. W. Yee, B. J. N. Griffiths, P. J. Evans and C. Simons, *J. Med. Chem.*, 2006, **49**, 1016.

113. H. Usta, A. Facchetti and T. J. Marks, *Org. Lett.*, 2008, **10**, 1385.
114. K. L. Chan, M. J. McKiernan, C. R. Towns and A. B. Holmes, *J. Am. Chem. Soc.*, 2005, **127**, 7662.
115. N. K. Garg, R. Sarpong and B. M. Stoltz, *J. Am. Chem. Soc.*, 2002, **124**, 13179.
116. A. C. Spivey, F. Zhu, M. B. Mitchell, S. G. Davey and R. L. Jarvest, *J. Org. Chem.*, 2003, **68**, 7379.
117. P. Appukkuttan, A. B. Orts, R. P. Chandran, J. L. Goeman, J. Van der Eycken, W. Dehaen and E. Van der Eycken, *Eur. J. Org. Chem.*, 2004, 3277.
118. D. F. Perkins, L. F. Lindoy, A. McAuley, G. V. Meehan and P. Turner, *Proc. Nat. Acad. Sci. U.S.A.*, 2006, **103**, 532.
119. D. F. Perkins, L. F. Lindoy, G. V. Meehan and P. Turner, *Chem. Commun.*, 2004, 152.
120. A. P. Smith, P. S. Corbin and C. L. Fraser, *Tetrahedron Lett.*, 2000, **41**, 2787.
121. Y. Hama, Y. Nobuhara, Y. Aso, T. Otsubo and F. Ogura, *Bull. Chem. Soc. Jpn.*, 1988, **61**, 1683.
122. P. M. Windscheif and F. Vogtle, *Synthesis*, 1994, 87.
123. M.-J. Shiao, L.-M. Shyu and K.-Y. Tarng, *Synth. Commun.*, 1990, **20**, 2971.
124. H. Tohma, H. Morioka, Y. Hrayama, M. Hashizume and Y. Kita, *Tetrahedron Lett.*, 2001, **42**, 6899.
125. K. Wariishi, S. i. Morishima and Y. Inagaki, *Org. Process Res. Dev.*, 2003, **7**, 98.
126. R. H. Mitchell, Y.-H. Lai and R. V. Williams, *J. Org. Chem.*, 1979, **44**, 4733.
127. M. A. Brimble and M. Y. H. Lai, *Org. Biomol. Chem.*, 2003, **1**, 2084.
128. M. Albrecht, *Chem. Rev.*, 2001, **101**, 3457.
129. C. R. K. Glasson, L. F. Lindoy and G. V. Meehan, *Coord. Chem. Rev.*, 2008, 2**52**, 940.
130. M. J. Hannon and L. J. Childs, *Supramolecular Chemistry*, 2004, **16**, 7.
131. L. F. Lindoy, G. V. Meehan and N. Svenstrup, *Synthesis*, 1998, 1029.
132. R. Aldred, R. Johnston, D. Levin and J. Neilan, *J. Chem. Soc. Perkins Trans. 1*, 1994, 1823.
133. L. M. Venanzi, *J. Chem. Soc.*, 1958, 719.
134. F. A. Cotton, O. D. Faut and D. M. L. Goodgame, *J. Am. Chem. Soc.*, 1961, **83**, 344.

Chapter 3

Transition Metal-Directed Assembly experiments with 5,5'''-dimethyl-2,2':5',5'':2'',2'''-quaterpyridine.

3.1 BACKGROUND

The design and synthesis of new molecular assemblies incorporating transition metal ions as structural elements has received very considerable attention over recent years.[1-4] Incorporation of transition metals in such systems yields the potential for generating additional functionality – including (unusual) optical, magnetic, photoactive, electrochemical and/or catalytic behaviour. The successful synthesis of a given system of this type normally depends on an appropriate match of the steric and electronic information inherent in both the chosen ligand system and metal ion; however, other considerations, including interligand stacking, templation and solvent effects, may also play a role.

Recently research within our group has focused on the assembly of cage-like systems that incorporate a central cavity and thus exhibit a potential for host-guest chemistry. A number of such structures have now been developed, including capsules,[5, 6] cryptands[7-11] and tetrahedra.[12] In this context it has now been well documented that bis-bidentate ligand systems may interact with octahedral metal ions to yield triple helical species of type M_2L_3 or larger species having stoichiometries that are a multiple of this ratio (***Figure 3.1***). Numerous helicates fitting the M_2L_3 formula have now been described (see Chapter 1, *Section 1.3.2*). Higher order structures reported that fit this stoichiometric ratio include M_4L_6 tetrahedra [12-39] M_8L_{12} cubes[40, 41] and even $M_{12}L_{18}$ complexes.[41, 42]

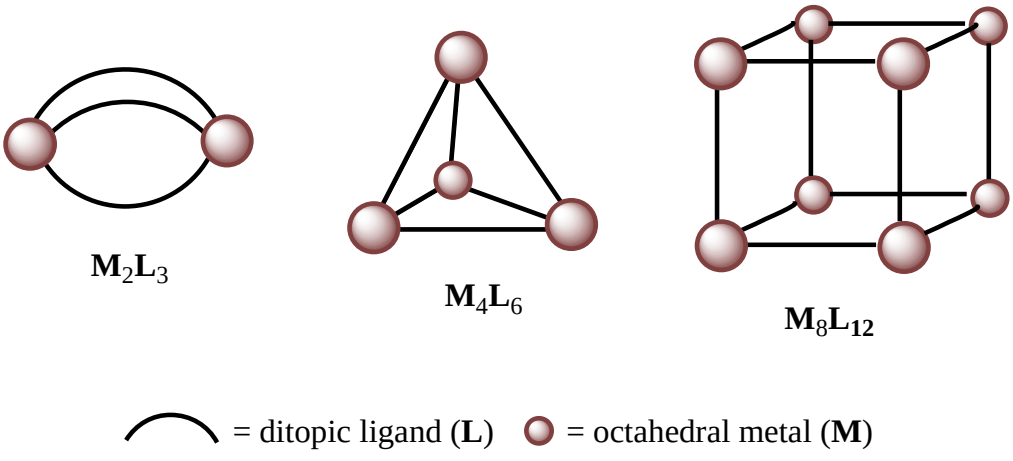

Figure 3.1. Schematic representations of possible structures resulting from the interaction of an octahedral metal ion and a "linear" bis-bidentate bridging ligand in a 2:3 ratio.

Initially the work reported in this chapter was focused on finding conditions under which the metal-template procedure reported by Perkins *et al.*[10, 11] (see ***Figure 1.13***; Chapter 1, page 36) could be used to make dinuclear cryptands. As indicated previously, for this synthetic strategy to be successful the interaction of an octahedral metal ion and dialdehyde **48** would need to yield an M_2L_3 precursor complex **152** (***Scheme 3.1***). To assess this

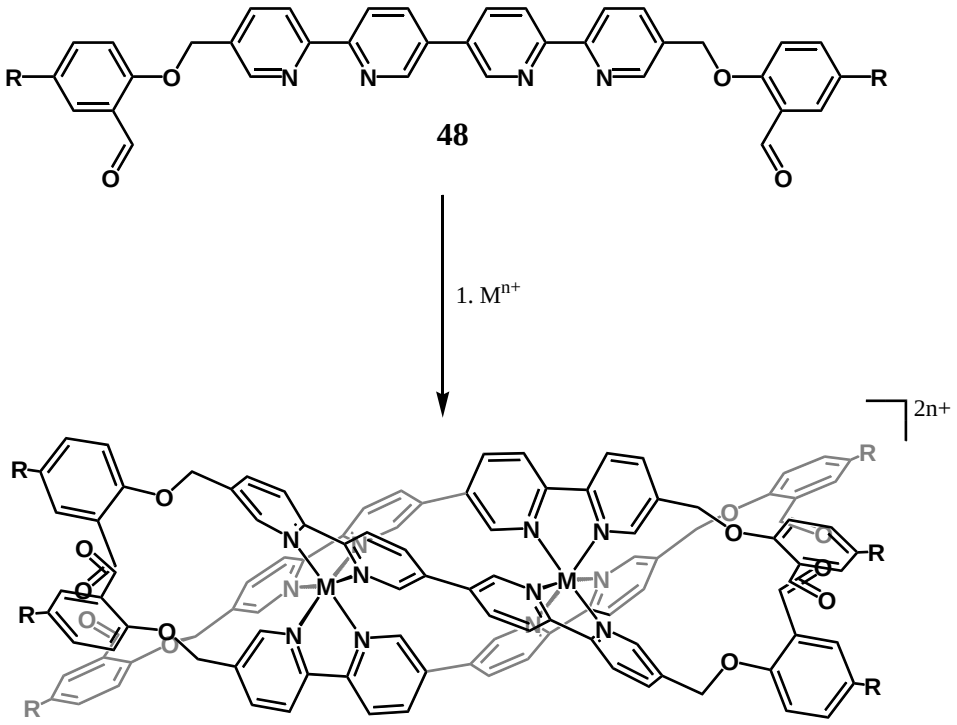

Scheme 3.1

interaction the dimethylquaterpyridine **50** was employed as a simpler quaterpyridine model for the more elaborate dialdehyde **48**. In the first instance d^6 Fe(II) salts were used as the metal ion source, due to the tendency of this ion to form low-spin diamagnetic tris-bipyridyl complexes, allowing the self-assembly processes to be followed using NMR spectroscopy. A variety of other metal ions have subsequently been investigated, including Co(II), Ni(II), Ru(II) and Ru(III). This chapter will report on the metal directed assembly processes that have allowed the isolation of $[M_4(\mathbf{50})_6]^{8+}$ (M = Fe, Co and Ni), complexes that exhibit

interesting host-guest chemistry, as well as of a $[Ru_2(\mathbf{50})_3]^{2+}$ helicate with interesting DNA binding properties.

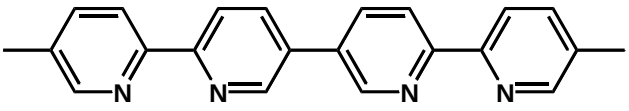

50

3.2 M_4L_6 HOST-GUEST COMPLEXES

3.2.1 Honours research

In the candidate's Honours research the interaction of Fe(II), as its chloro salt, with quaterpyridine **50** in a 2:3 ratio was investigated. The crystal structure of the resulting material, isolated as its PF_6^- salt, showed that the product was a unique tetranuclear M_4L_6 complex of formula $[Fe_4(\mathbf{50})_6 \supset FeCl_4](PF_6)_x$ (x = 6 or 7) (**153** in ***Figure 3.2***) with a tetrahedral $[FeCl_4]^{n-}$ (n = 1 or 2) anion occupying the central cavity (***Figure 3.2*** b)). The

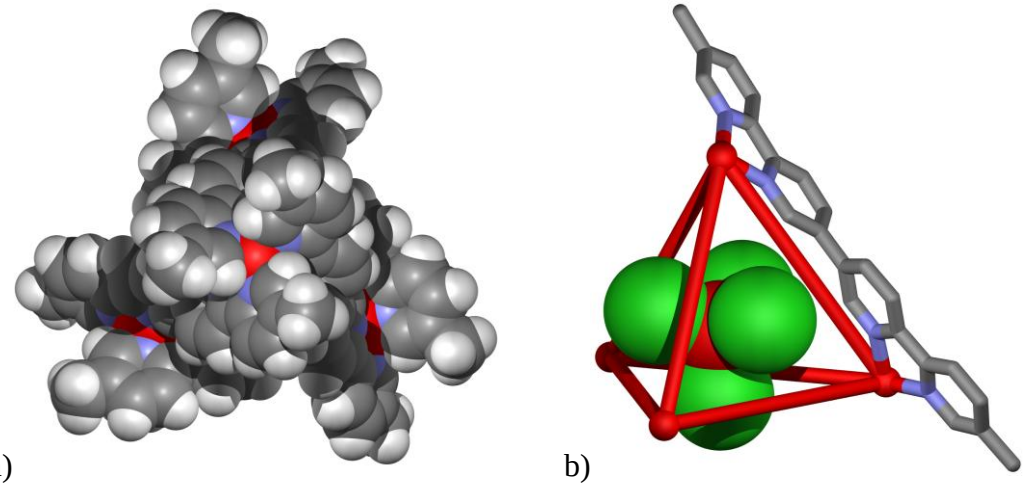

a) b)

Figure 3.2 a) Space filling representation of the crystal structure of $[Fe_4(\mathbf{50})_6 \supset FeCl_4]^{(8-n)+}$ looking down the C_3 axis of the *ΔΔΔΔ* enantiomer and b) Schematic representation of the encapsulated tetrahedral $[FeCl_4]^{n-}$ anion, (n = 1 or 2).

product crystallised in the cubic space group $P\bar{4}3n$ and individual Fe(II) centres lie on 3-fold special positions and the ligands surround a 4-fold axis. The asymmetric unit contains 1/12 of the complex which consists of a racemic mixture in which the four chiral *pseudo*-octahedral Fe(II) metal centres at the apices are either all Λ configuration or all of the Δ configuration. The metal to metal distance between each of the Fe(II) centres at the apices is 9.43 Å, equating to an approximate cavity volume of 100 $Å^3$.

The encapsulated $[FeCl_4]^{n-}$ anion has perfect tetrahedral symmetry with Cl—Fe—Cl bond angles of 109.5º and Fe—Cl bond lengths of 2.20 Å. This latter bond length is more characteristic of the $[Fe^{III}Cl_4]^-$ anion,[43-50,ℑ] although it is possible that the Fe—Cl bond lengths are compressed in the present case due to steric and/or electronic effects arising from their encapsulation. Because of this possibility, and since there could be some ambiguity in modelling the number of PF_6^- counter ions in the refinement of the crystal structure, further experimental evidence for the precise stoichiometry of M_4L_6 host-guest complex **153**, was sought. In turn, this information was expected to confirm the oxidation state of the encapsulated tetrahedral iron chloride species.

3.2.2 Further studies of the encapsulated $[FeCl_4]^{n-}$ (n = 1 or 2) guest species[ℵ]

In an attempt to determine the oxidation state of the iron centre of the tetrachloroferrate anion included in the M_4L_6 host-guest complex described above, microanalysis, bulk electrolysis, high resolution mass spectrometry, and magnetic susceptibility measurements were carried out.

Repeated microanalysis of recrystallised material dried under high vacuum overnight, with measurement of C, H, N and P percentages, could be made to correspond to two possibilities depending on the level of solvent of crystallisation assigned to the structure. In the first instance the formula that fitted best, $[Fe_4(\mathbf{50})_6 \supset FeCl_4](PF_6)_7.CH_3OH$, was in

[ℑ] A manual search of the Cambridge Crystallographic Database indicated that Fe-Cl bond lengths for non-encapsulated $Fe(III)Cl_4^-$ anions averaged around 2.18 Å; those for analogous $Fe(II)Cl_4^{2-}$ anions averaged around 2.32 Å.

[ℵ] This work was commenced during the candidate's Honours year and continued and extended during his PhD research.

agreement with the tetrachloroferrate guest possessing an Fe(III) centre. However, the results were also able to be fitted to the formula $[Fe_4(\mathbf{50})_6](PF_6)_8.8CH_3OH$ consistent with the absence of a tetrachloroferrate guest. To complicated matters further, an earlier C, H and N microanalysis could be fitted to the formula $[Fe_4(\mathbf{50})_6 \supset FeCl_4](PF_6)_6.12H_2O$ in keeping with the presence of a tetrachloroferrate guest with an Fe(II) centre. With respect to the latter result, it should be noted that the P content was not measured and that the microanalysis results were obtained for initially precipitated product and not recrystallised product.

An oxidative bulk electrolysis (BE) conducted on one of the recrystallised samples indicated a $4e^-$ oxidative process supporting the presence of only four Fe(II) centres (see ***Appendix C*** for details of the electrochemistry). Thus, this latter result would indicate that the formula of the complex was indeed $[Fe_4(\mathbf{50})_6 \supset FeCl_4](PF_6)_7$ with an encapsulated $[FeCl_4]^-$ (with an Fe(III) centre). It seemed likely at this stage from the combined results of the crystallographic data, the microanalysis, and BE experiment that the encapsulated tetrachloroferrate ion indeed had an Fe(III) centre.

In agreement with the microanalysis and BE results, ESI-HRMS of this crystalline material gave peaks fitting +3, +4, +5, +6 and +7 charge states, corresponding to successive losses of 3, 4, 5, 6 and 7 PF_6^- ions from the formula $[Fe_4(\mathbf{50})_6 \supset FeCl_4](PF_6)_7$, respectively (see ***Figure 3.3*** b for the isotopic distribution of the +3 ion). However, on closer inspection of the mass spectrum, two other series of peaks were observed which corresponded to the successive losses of PF_6^- ions from the formulae $[Fe_4(\mathbf{50})_6 \supset FeCl_4](PF_6)_6$ and $[Fe_4(\mathbf{50})_6](PF_6)_8$ (Figure ***Figure 3.3*** a)). While the latter series could be explained by the loss of the tetrachloroferrate guest under the mass spectrometry conditions employed, the former series was a source of ambiguity that could not be simply explained. It is worth noting that all mass spectral analyses of repeat preparations of this compound have also resulted in the observation of the above mentioned series of ions. The combination of the crystallographic and microanalytical data, as well as the results from the BE experiment would suggest that the complex starts out as $[Fe_4(\mathbf{50})_6 \supset FeCl_4](PF_6)_7$ (i.e. $[Fe^{III}Cl_4]^-$) but is subsequently reduced to $[Fe_4(\mathbf{50})_6 \supset FeCl_4](PF_6)_6$ (i.e. $[Fe^{II}Cl_4]^{2-}$) in the electrospray process. This possibility may not be that surprising since the electrospray ionisation source is essentially a modified electrochemical cell.[51, 52]

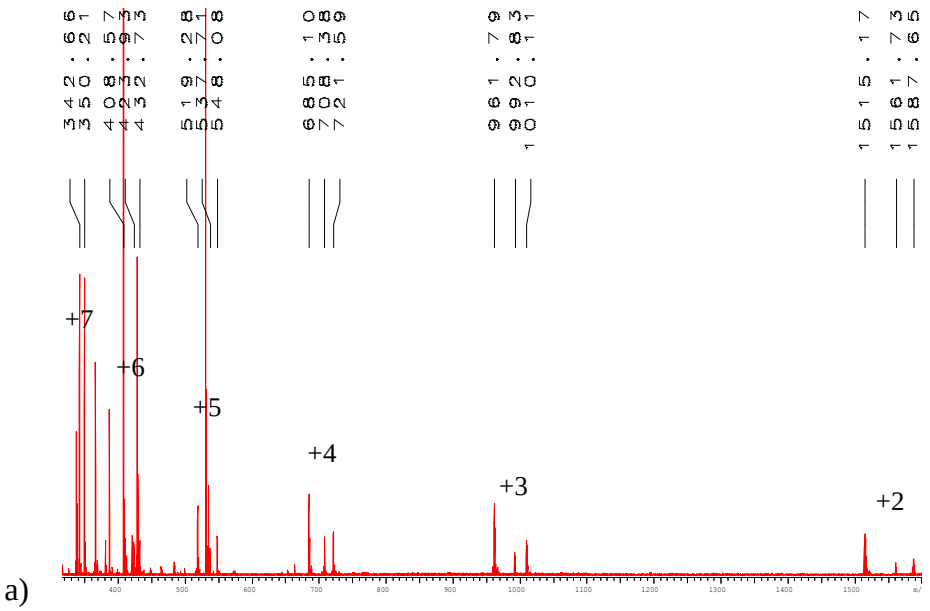

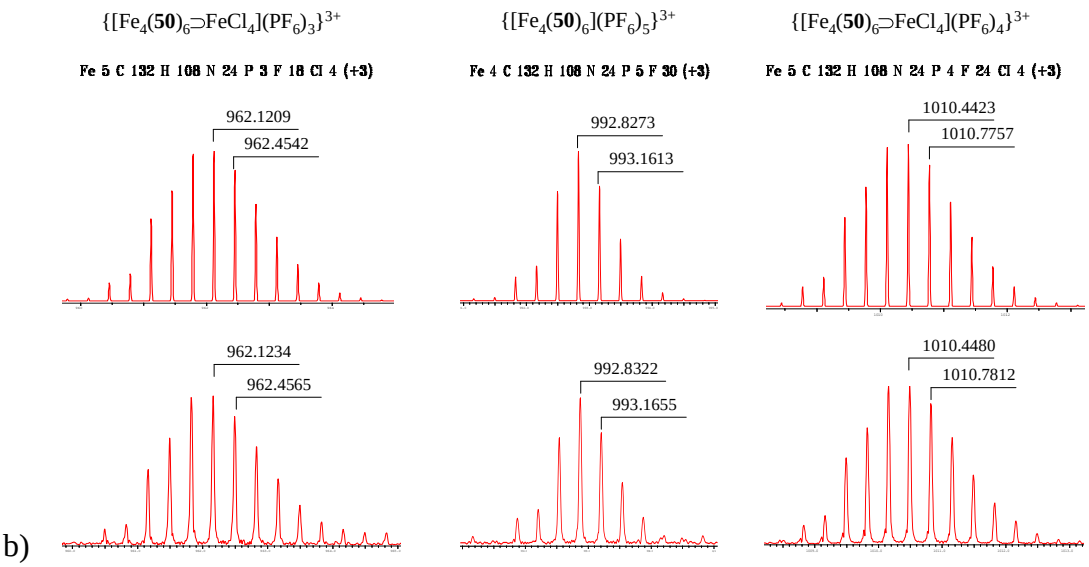

Figure 3.3 a) The mass spectrum of $[Fe_4(\mathbf{50})_6{\supset}FeCl_4](PF_6)_n$ (n = 6 or 7) revealing +2 to +7 ion clusters, and b) the theoretical (top) and observed (bottom) isotopic distributions for the three +3 ions observed (formulae shown above each).

At this stage of the discussion, the conditions used for the synthesis of $[Fe_4(\mathbf{50})_6{\supset}FeCl_4](PF_6)_n$ (n = 6 or 7) are worthy of note; namely the reaction was carried out under nitrogen using dry degassed THF/acetonitrile solutions. The use of weakly coordinating solvents such as THF and acetonitrile are known to promote the formation of

$[FeCl_4]^{n-}$ (n = 1 or 2) species.[53] Furthermore, the use of such solvents under an inert atmosphere was reported[54-56] to reduce the possibility of oxidation of Fe(II) species to Fe(III) species, known to occur in acetonitrile solutions.[57-60] However, in the present preparation exposure to air during purification and recrystallisation occured and this may have led to the oxidation, or partial oxidation, of $[Fe^{II}Cl_4]^{2-}$ to $[Fe^{III}Cl_4]^-$; although, one could argue that the encapsulated tetrachloroferrate ion might be protected from such oxidation. Either way, the oxidation state of the Fe centre in the tetrachloroferrate species remains somewhat ambiguous. However, there is no doubt that the encapsulation of this tetrachlorometallate represents an interesting host-guest system.[37]

In a quite separate experiment, aimed at investigating whether or not the M_4L_6 complex could indeed form in the absence of an appropriate guest species, $Fe(BPh_4)_2$ was employed as the Fe(II) source. The $Fe(BPh_4)_2$ was generated by the addition of an acetonitrile solution of $FeCl_2.5H_2O$ to a solution containing an excess of $NaBPh_4$ in acetonitrile. Subsequently, the resulting NaCl precipitate was removed by filtration allowing the isolation of the acetonitrile solution of $Fe(BPh_4)_2$. To this solution an excess of quaterpyridine **50** was added and the mixture refluxed overnight. The solvent was reduced in volume and the product was purified by filtration through Sephadex LH-20. Although the ^{1}H NMR spectrum of the chromatographed product was significantly paramagnetically broadened, the presence of a single methyl signal was indicative of the presence of a symmetrical species in which quaterpyridine **50** retained its C_2 symmetry.

Crystals suitable for X-ray crystallography were grown by diffusion of ether into an acetonitrile solution of the above product. Unexpectedly, the crystal structure of this material revealed that a tetrachloroferrate[†] ion had again been encapsulated within an M_4L_6 host **154** (***Figure 3.4*** a)), thus, explaining the paramagnetic behaviour observed in the ^{1}H NMR spectrum. Clearly during the preparation of $Fe(BPh_4)_2$ all the Cl^- had not been removed. Interestingly, the Fe—Cl bond lengths in the crystal, with a range of 2.32 - 2.33 Å, were more characteristic of Fe(II).[47-49ℑ] As well, the metal to metal distances for this M_4L_6 complex

[†] Note that either possible guest species, a $^6A_1$ $[Fe^{III}Cl_4]^-$ or a ^5E $[Fe^{II}Cl_4]^{2-}$, may lead to paramagnetic broadening in NMR spectra.

ℑ A manual search of the Cambridge Crystallographic Database indicated that Fe-Cl bond lengths for non-encapsulated $[Fe^{III}Cl_4]^-$ anions averaged around 2.18 Å; those for analogous $[Fe^{II}Cl_4]^{2-}$ anions averaged around 2.32 Å.

were slightly smaller (averaging 9.37 Å) than those recorded for $[Fe_4(\mathbf{50})_6 \supset FeCl_4](PF_6)_n$ (n = 6 or 7) (9.43 Å). This latter observation would lead to a reduction in the effective cavity size of the tetrahedral host. Thus, on steric grounds alone, it could be argued that an increase in possible Fe—Cl bond compression (i.e. shorter bond lengths) of the tetrachloroferrate guest would result. The number of BPh_4^- counterions present in the unit cell also point towards the tetrachloroferrate guest bearing an Fe(II) centre (i.e. there are six BPh_4^- anions per M_4L_6).

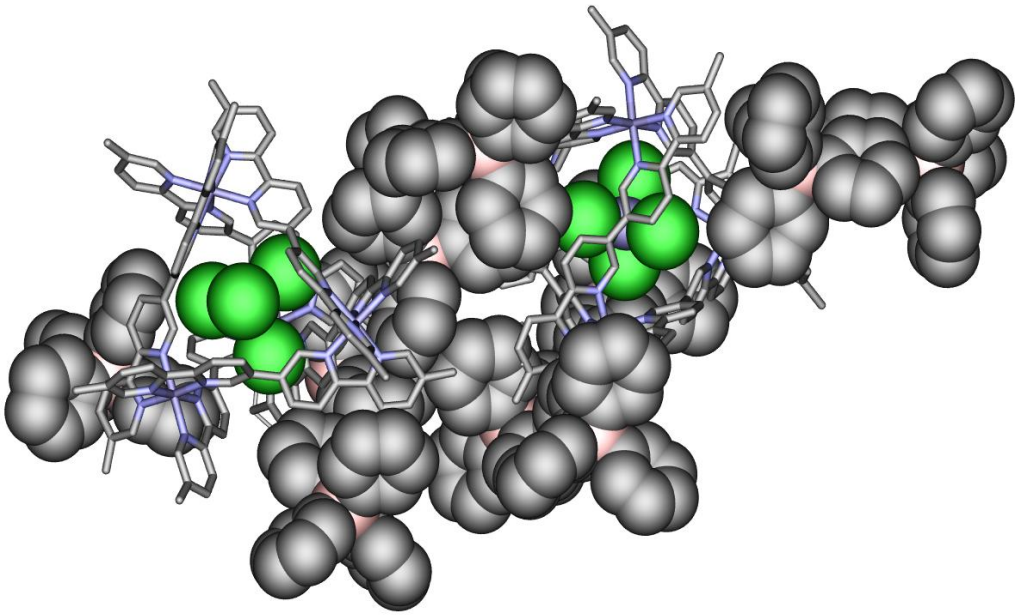

Figure 3.4 Crystal structure representation of two out of the four $[Fe_4(\mathbf{50})_6 \supset FeCl_4](BPh_4)_6$, **154,** units that exist in the unit cell.

In support of the crystallographic data, ESI-HRMS of this material gave +2, +3 and +4 ions corresponding to the loss of 2, 3 and 4 tetraphenylborate ions from the formula $[Fe_4(\mathbf{50})_6 \supset FeCl_4](BPh_4)_6$, respectively. Therefore, this indicated that the tetrachloroferrate guest in this sample possesses an Fe(II) centre. Furthermore, there was no mass spectral evidence of the M_4L_6 host encapsulating a tetrachloroferrate guest with a Fe(III) centre. This result is indeed interesting as the electrospray was run under similar condition to those used for analysis of the $[Fe_4(\mathbf{50})_6 \supset FeCl_4](PF_6)_n$ (n = 6 or 7) species, for which ions corresponding to both possible oxidation states of the Fe in the tetrachloroferrate species were observed.

A magnetochemical investigation of $[Fe_4(\mathbf{50})_6 \supset FeCl_4](PF_6)_n$ (n = 6 or 7) was undertaken in an attempt to help confirm its composition.[‡] This analysis was run on recrystallised material that had been characterised by collecting the mass spectrum, microanalysis and even another X-ray crystallographic data set. Combining these data indicated that the product fitted the formula $[Fe_4(\mathbf{50})_6 \supset FeCl_4](PF_6)_7.CH_3OH$ best (i.e. with the $^6A_1$ Fe(III)Cl_4^- guest). In ***Figure 3.5*** a), it can be seen that the magnetic moment per Fe_5 host guest cluster decreases more or less linearly, from 4.75 μ_B at 300 K to about 4.2 μ_B at

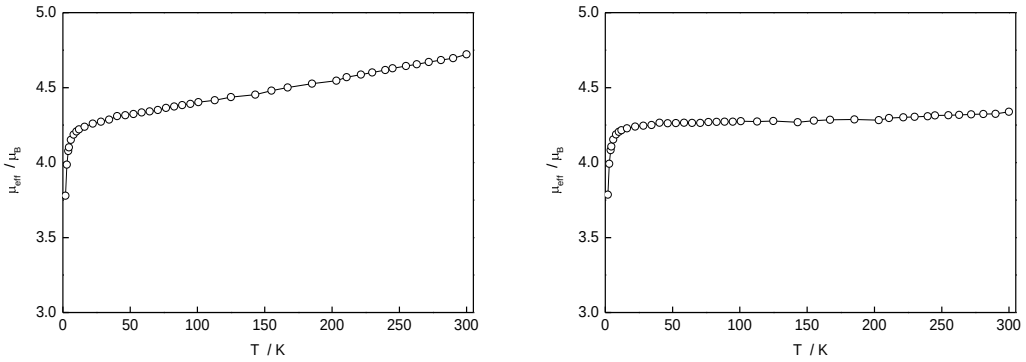

a) b)

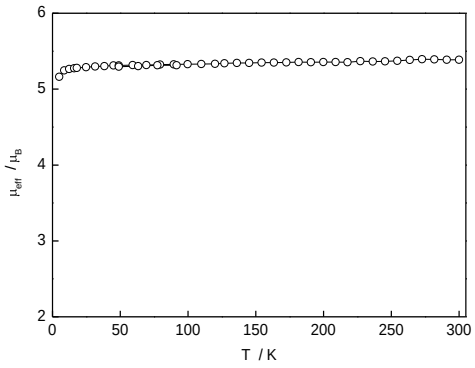

c)

Figure 3.5 Plots of magnetic moment μ_{eff}/μ_B, per Fe_5 Cluster, versus temperature (T / K) for $[Fe_4(\mathbf{50})_6 \supset FeCl_4](PF_6)_n$ (n = 6 or 7) (field of 1 Tesla); a) illustrating a small TIP contribution from the four low-spin d^6 Fe(II) members of the present cage, b) corrected for the TIP contribution from the four low-spin d^6 Fe(II) members, and c) repeated sample showing a magnetic moment more indicative of $^6A_1$ $[Fe^{III}Cl_4]^-$.

[‡] The results were obtained by Professor Keith Murray and coworkers at Monash University, Melbourne; the author acknowledges Professor Murray for his interpretation of the results.

10 K, then more rapidly to reach 3.6 μ_B at 2 K. The corresponding molar susceptibility χ_m versus temperature is Curie-Weiss like. This kind of μ_{eff} versus temperature plot has a shape which is reminiscent of polyoxomolybdate(VI) clusters (POMs), containing a paramagnetic ion, which have a large temperature independent paramagnetic susceptibility (TIP) originating from second order Zeeman effects (on the '*diamagnetic*' Mo(VI) ions).[61, 62] The four apical low-spin d^6 Fe(II) members of the present cage, while nominally diamagnetic, in fact also display such a TIP contribution. Thus, in order to estimate the TIP contribution of $[Fe_4(\mathbf{50})_6 \supset FeCl_4](PF_6)_n$ (n = 6 or 7), the μ_{eff} plot was forced to be linear in the 10 – 300 K region (i.e. Curie dependence in susceptibility) by subtracting a TIP contribution of 1600 x 10^{-6} cm^3 mol^{-1}, that is 400 x 10^{-6} cm^3 mol^{-1} per apical low-spin d^6 Fe(II) member, a typical value.[63] Any TIP for the tetrahedral $[FeCl_4]^{n-}$ (n = 1 or 2) guest was expected to be negligible. As for the POMs, the diamagnetic corrections and the TIP contribution are of a somewhat similar magnitude. The TIP-corrected plot, shown in ***Figure 3.5*** b), levels off at a value of approximately 4.3 μ_B, at the bottom end of the range expected for ^5E $[Fe^{II}Cl_4]^{2-}$ species; well below the value of 5.9 μ_B expected for the $^6A_1$ $[Fe^{III}Cl_4]^-$. Even allowing for small errors in estimating the molar mass, and the corresponding diamagnetic correction, the magnetic moment data suggest that the entrapped anion is the ^5E $[Fe^{II}Cl_4]^{2-}$ and not the expected $^6A_1$ $[Fe^{III}Cl_4]^-$.

The apparently conflicting result from the X-ray crystallography, mass spectrometry, microanalysis and the above magnetic susceptibility data prompted a repeat of the magnetic susceptibility measurements on a new sample. As for the previous sample, the new sample was characterised by ESI-HRMS and microanalysis, confirming the presence of the tetrachloroferrate guest. A plot of the magnetic moment, per Fe_5, versus temperature for the second sample is shown in ***Figure 3.5*** c). Interestingly, in this case the μ_{eff} values remain constant between 300 and 6 K, at 5.3 μ_B, with a small decrease occurring below this (to reach 5.2 μ_B at 2 K). The corresponding χ_m values are Curie-like. In this case the overall temperature independence in μ_{eff} is perhaps more compatible with the presence of a $^6A_1$ $[Fe^{III}Cl_4]^-$ anion than a ^5E $[Fe^{II}Cl_4]^{2-}$ anion. Unfortunately, the actual values of μ_{eff} again cannot unambiguously distinguish the two oxidation state possibilities. The expected μ_{eff} value, per Fe_5, for four low spin Fe(II) t_{2g}^6 centres (TIP approximately 0.0004 cm^3 mol^{-1}; μ_{eff} = 0.98 μ_B at 300 K and 0.56 μ_B at 100 K) plus one Fe(III) (μ_{eff} = 5.9 μ_B at 300 K and 100 K) is

6.0 μ_B at 300 K and 5.94 μ_B at 100 K, is clearly bigger than the observed value. The ^5E ground state for a $[Fe^{II}Cl_4]^{2-}$ anion is expected to lead to Curie-Weiss like susceptibilities, via spin-orbit coupling and second order Zeeman contributions (TIP); μ_{eff} values reported for such salts can be as high as 5.4 μ_B.[64] When the susceptibilities for the four low-spin Fe(II)-bipyridyl centres are included, the μ_{eff} value, per Fe_5, would again be expected to be approximately 6 μ_B at 300 K. Thus, from the magnetism study alone, a dilemma remains concerning the repeat samples and measurements in that they do not allow unambiguous determination of the oxidation state of the iron centre in the tetrachloroferrate guest.

Unfortunately the ambiguity surrounding the absolute stoichiometry of $[Fe_4(\mathbf{50})_6 \supset FeCl_4](PF_6)_n$ (n = 6 or 7) has not yet been resolved. There are several possibilities which could explain the difficulty in fully characterising this compound. For example, if co-crystals formed with a high percentage of $[FeCl_4]^-$ guests and another singly charged guest (e.g. PF_6^-) this may lead to the depressed magnetochemical values observed. However, it does not explain the observation of both $[Fe^{II}Cl_4]^{2-}$ and $[Fe^{III}Cl_4]^-$ entities in the mass spectrum which would suggest that both species are indeed encapsulated. On balance, however, the results presented above would support the view that the complex possesses the formula $[Fe_4(\mathbf{50})_6 \supset FeCl_4](PF_6)_7$ with the encapsulated anion being $[Fe^{III}Cl_4]^-$. Further attempts to confirm the assignment of the tetrachloroferrate species will involve the collection of both Raman and Mössbauer* spectra.

3.2.3 $[Fe_4(50)_6]^{8+}$, a selective host.

As the above saga unravelled, two other anion inclusion complexes of type $[Fe_4(\mathbf{50})_6 \supset anion]^{7+}$ (where anion = BF_4^- or PF_6^-) were isolated. Thus reaction of Fe(II) tetrafluoroborate with quaterpyridine **50** in acetonitrile in a 2:3 ratio generated a deep red colour, characteristic of a $[Fe(2,2'\text{-bipyridine})_3]^{2+}$ (low-spin) chromophore in the reaction solution, and led to the isolation of a dark red product of stoichiometry $[Fe_4(\mathbf{50})_6](BF_4)_8.4H_2O$, **155**. This product yielded a UV-Vis spectrum that exhibited a band at 529 nm (ε/dm^3 mol^{-1} cm^{-1} 21 800), similar to the MLCT band reported for [Fe(2,2′-

* Results from an intial Mössbauer spectrum, collect by Associate Professor John Cashion of Monash University, proved inconclusive.

bipyridine)$_3$]$^{2+}$.[65] The ^{1}H NMR (***Figure 3.6*** a)) and ^{13}C NMR spectra of the product in CD_3CN were both in accord with the presence of a single compound of high symmetry in which all four ligands are in equivalent environments. ^{1}H-^{1}H COSY and NOESY experiments allowed the complete assignment of the ^{1}H NMR spectrum of the product (see ***Figure 3.6*** b) for labelled ^{1}H positions). High resolution ESI-HRMS gave +2, +3, and +4 ions with masses corresponding to those calculated for successive losses of BF_4^- anions from the parent species of formula $[Fe_4(\mathbf{50})_6](BF_4)_8$; this result is thus in keeping with a structure incorporating a +8 charged M_4L_6 assembly.

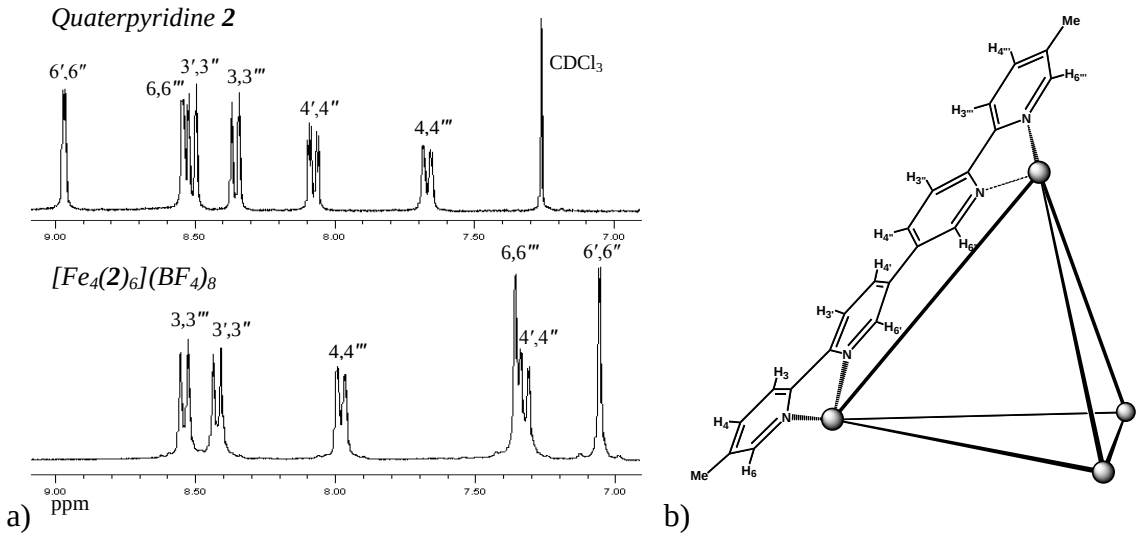

Figure 3.6 a) The assigned ^{1}H NMR spectrum of the free quaterpyridine **50** (in $CDCl_3$ at 300 K) versus that of $[Fe_4(\mathbf{50})_6](BF_4)_8$, **155** (in CD_3CN at 300 K), and b) a schematic representation of the M_4L_6 complex showing the numbering scheme of **50**.

Crystals of the above assembly suitable for X-ray diffraction were grown from THF/CH_3CN and the resulting structure showed a tetrahedral assembly of type $[Fe_4(\mathbf{50})_6 \supset BF_4](BF_4)_7.3CH_3CN.6THF.3.6H_2O$ (***Figure 3.7***) in which four octahedrally coordinated Fe(II) centres occupy the vertices of the tetrahedron and six quaterpyridine **50** ligands define the edges; a BF_4^- anion occupies the central cavity giving the overall cationic assembly a +7 charge. This latter charge is balanced by seven BF_4^- counterions that were arranged in the crystal lattice. The product crystallizes in the cubic space group $P\bar{4}3n$ and individual Fe(II) centres lie on 3-fold special positions and the ligands surround a 4-fold axis. Each of the two bipyridyl units of a given quaterpyridine **50** is twisted by nearly 60° with

respect to the other as the three-fold twist about the metal centres extends throughout the molecule. There is only one third of an Fe(II) and half of one ligand in the asymmetric unit (one twelfth of the entire molecule). Individual tetrahedra contain homochiral metal centres; that is, each tetrahedron is either *ΛΛΛΛ* or *ΔΔΔΔ*. As the space group contains *n*-glides, each crystal represents a racemic mixture. The chiral twist associated with each tetrahedron is evident when viewed down one of the C_3 axes (***Figure 3.7*** (a)). The distance between each of the Fe(II) centres is 9.45 Å, which corresponds to an encapsulated volume of approximately 100 Å^3. It is worthy of note that $[Fe_4(\mathbf{50})_6 \supset BF_4](BF_4)_7$ crystallises in the same space group as the original tetrachloroferrate inclusion complex $[Fe_4(\mathbf{50})_6 \supset FeCl_4](PF_6)_n$ (n = 6 or 7). This may indicate the same number of externally situated counterions in the latter case, in further support of it being formulated as $[Fe_4(\mathbf{50})_6 \supset FeCl_4](PF_6)_7$.

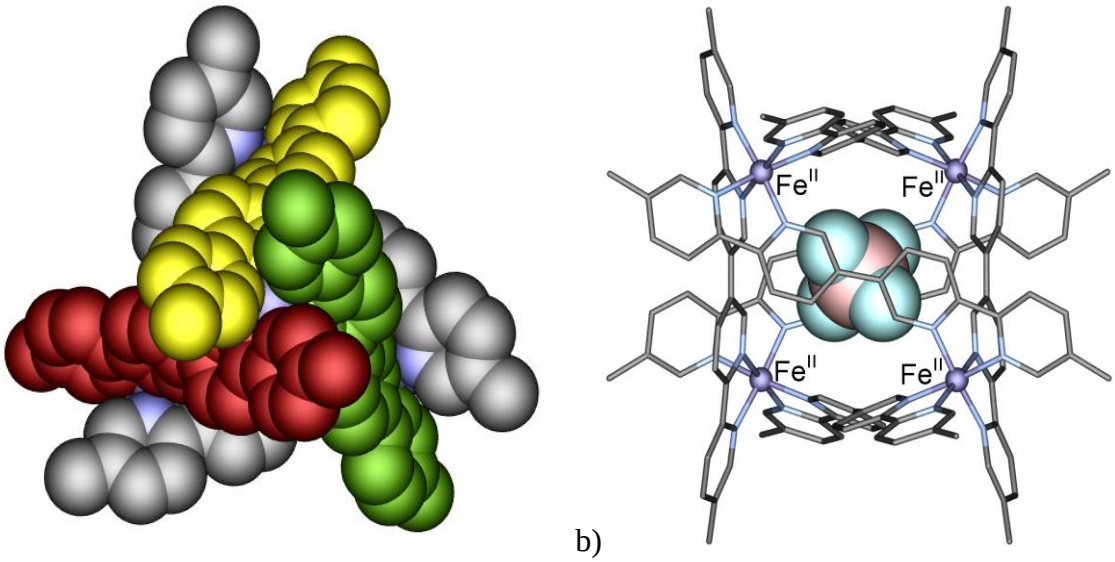

a) b)

Figure 3.7 Crystal structure of the cation in the $[Fe_4(\mathbf{50})_6 \supset BF_4]^{7+}$ assembly (*exo*-anions and solvents not shown), a) Space filling depiction viewed down the C_3 axis of the *ΔΔΔΔ* enantiomer, and b) depiction of the host-guest complex.

Substitution of Fe(II) tetrafluoroborate by Fe(II) bromide in the above synthetic procedure followed by treatment with potassium hexafluorophosphate and subsequent chromatographic purification, again produced a deep red crystalline solid whose ESI-HRMS was related to that just discussed. This showed the presence of +2 to +7 charged ions, consistent with the sequential loss of up to seven PF_6^- anions from a parent species of type

$[Fe_4(\mathbf{50})_6](PF_6)_8$, **156** (***Figure 3.8*** a)). The crystallographic data of this material, collected using synchrotron radiation, once again confirmed the production of a M_4L_6 tetrahedron of the formula $[Fe_4(\mathbf{50})_6 \supset PF_6](PF_6)_7.9CH_3OH.6H_2O$ with an encapsulated PF_6^- anion (***Figure 3.8*** b)). The latter is disordered over two positions, both located on a 12-fold special position.

This product also crystallizes in the cubic space group $P\bar{4}3n$. Interestingly, isolation of the M_4L_6 tetrahedron with the encapsulated PF_6^- guest illustrates that guest ion competition might be a factor in the tetrachloroferrate host-guest complex, $[Fe_4(\mathbf{50})_6 \supset FeCl_4](PF_6)_n$ (n = 6 or 7). The latter point could support the possibility of a mixed crystal consisting of variable proportion of $[Fe_4(\mathbf{50})_6 \supset PF_6](PF_6)_7$ and $[Fe_4(\mathbf{50})_6 \supset FeCl_4](PF_6)_7$, thus explaining the inconsistent magnetic susceptibility results. Indeed the mass spectrum of $[Fe_4(\mathbf{50})_6 \supset FeCl_4](PF_6)_n$ (n = 6 or 7) does not discount this possibility.

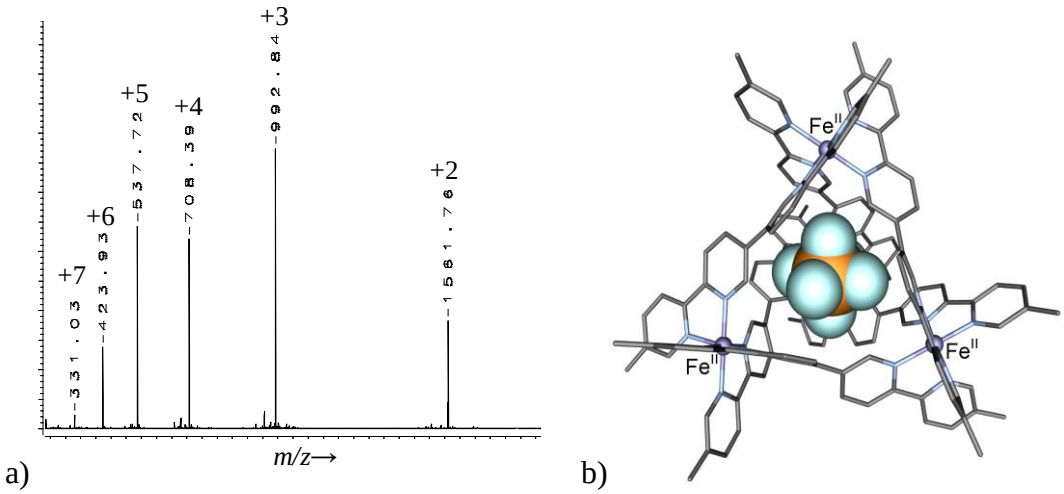

Figure 3.8 a) ESI-HRMS illustrating +2 to +7 ions resulting from successive losses of PF_6^- from the formula $[Fe_4(\mathbf{50})_6](PF_6)_8$, **156**, and b) crystal structure of $[Fe_4(\mathbf{2})_6 \supset PF_6]^{7+}$ with counterions, hydrogens and solvent removed for clarity.

For a comparison with $[Fe_4(\mathbf{50})_6 \supset FeCl_4](PF_6)_n$ (n = 6 or 7), the magnetic susceptibility of both $[Fe_4(\mathbf{50})_6](PF_6)_8$ and $[Fe_4(\mathbf{50})_6](BF_4)_8$ were measured. The molar magnetic moment measurements for $[Fe_4(\mathbf{50})_6 \supset BF_4](BF_4)_7$ were broadly in agreement with four low spin apical d^6 Fe(II) centres, with μ_{eff} values of approximately 1.5 μ_B per Fe(II) at 300 K dropping to 1.1 μ_B at 4 K (***Figure 3.9*** a)). This is a little higher than that expected for a normal temperature independent paramagnetic (TIP) term for low-spin d^6 Fe(II), which is usually about 0.8 μ_B per Fe(II). This might have indicated some paramagnetic impurity or

decomposition in the analysed sample, however the clearly diamagnetic NMR spectrum of this sample would suggest not. There is no sudden change in μ_{eff} which might have indicated spin crossover behaviour. Similarly, $[Fe_4(\mathbf{50})_6\supset PF_6](PF_6)_7$ was broadly in agreement with four low-spin apical d^6 Fe(II) centres, with μ_{eff} values of approximately 1.3 μ_B per Fe(II) at 300 K falling to 0.4 μ_B at 4 K (***Figure 3.9*** b)). Both samples have a second order Zeeman (TIP) contribution giving the small positive moment value.

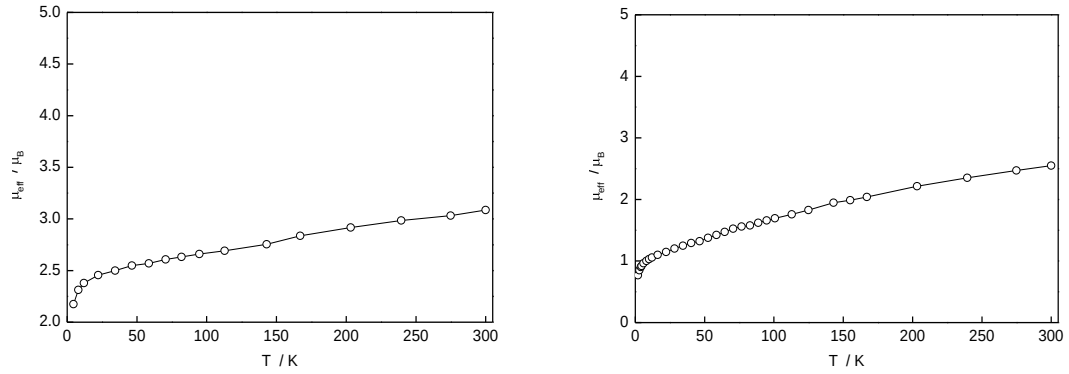

a) b)

Figure 3.9 Plots of magnetic moment versus temperature at a field of 1 Tesla for, a) $[Fe_4(\mathbf{50})_6\supset BF_4](BF_4)_7.7H_2O$ with a diamagnetic correction of –1.682 x 10^{-3} cm^3mol^{-1} from Pascals constants, and b) $[Fe_4(\mathbf{50})_6\supset PF_6](PF_6)_7.9CH_3OH.6H_2O$ with a diamagnetic correction of –1.700 x 10^{-3} cm^3mol^{-1} from Pascals constants.

Despite the solid-state structure of $[Fe_4(\mathbf{50})_6\supset BF_4](BF_4)_7$ showing an encapsulated BF_4^- guest, the ^{19}F NMR spectrum of this product in CD_3CN gave no evidence for the BF_4^- counter-ions existing in two environments over the temperature range 273.5 – 295 K (***Figure 3.10*** a)).[§] This is in accord with rapid *endo-exo* BF_4^- exchange, with respect to the NMR timescale, in the solution of the anion inclusion complex $[Fe_4(\mathbf{50})_6\supset BF_4](BF_4)_7$ that was observed in the solid state. Conversely, the ^{19}F NMR spectrum of $[Fe_4(\mathbf{50})_6\supset PF_6](PF_6)_7$ in CD_3CN clearly showed that the PF_6^- counterions were in two environments in a 7:1 ratio (***Figure 3.10*** b)). This result is in keeping with the product being formulated as $[Fe_4(\mathbf{50})_6\supset PF_6](PF_6)_7$ in solution, with PF_6^- exchange between the *endo* and *exo* environments being slow (or absent) on the NMR timescale; furthermore over a temperature range of 273 –

[§] Note that the two observed signals were in an approximate 1:4 ratio, consistent with the ratio expected for ^{19}F attached to the two different boron isotopes, ^{10}B and ^{11}B, whose natural abundances are ~20 % and ~80 %, respectively.

350 K the ^{19}F NMR spectra revealed no significant change in peak widths. Clearly these results are in accord with the PF_6^- guest species being strongly held within the cage.

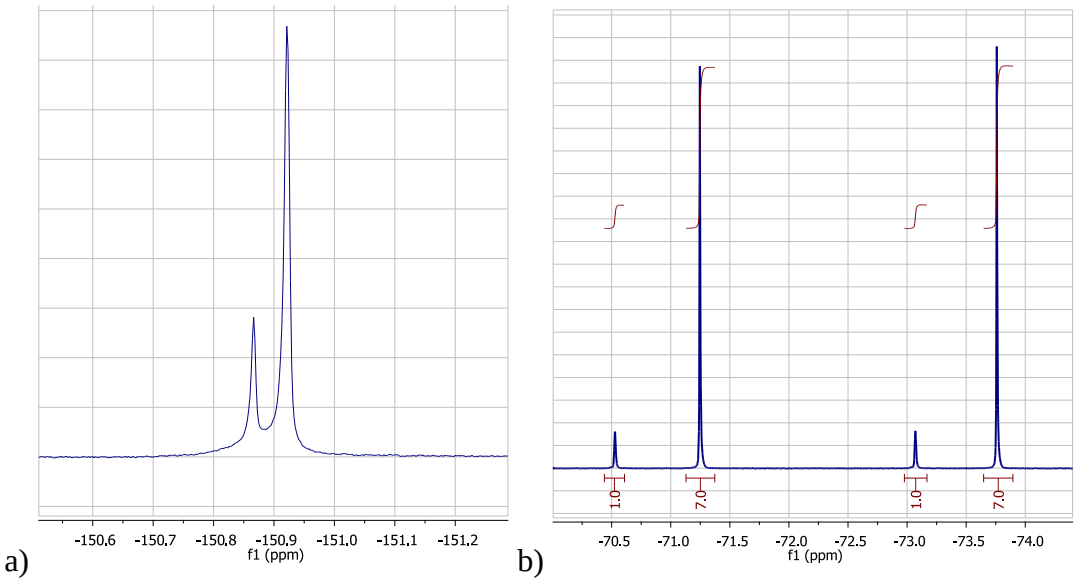

a) b)

Figure 3.10 ^{19}F NMR run in CD_3CN at 300 K of inclusion complexes, a) $[Fe_4(\mathbf{50})_6 \supset BF_4](BF_4)_7$, and b) $[Fe_4(\mathbf{50})_6 \supset PF_6](PF_6)_7$.

The different anion exchange inclusion behaviour for BF_4^- versus PF_6^-, as revealed by the ^{19}F NMR results raises the question of whether the BF_4^- exchange in the case of $[Fe_4(\mathbf{50})_6 \supset BF_4](BF_4)_7$ occurs via this anion passing through a side of the tetrahedron or whether Fe—N bond breaking is involved; both mechanisms have been considered for guest exchange in related tetrahedral species.[66, 67] In this regard, Ward *et al.*[67] described the anion binding behaviour in a related M_4L_6 host-guest complex. Using variable temperature ^{19}F NMR they calculated the free energy of activation for anion exchange to be approximately 50 kJ mol^{-1}, for both BF_4^- and PF_6^- counterions. Furthermore, they suggested that since the cleavage of two Co—N coordinated bonds (for the metal chelate used in their case) was likely to involve activation energies of the order of hundreds of kJ mol^{-1}, thus the activation energy of anion exchange calculated was likely to reflect a through-side exchange mechanism. In the present case, the apparent fast exchange also seems unlikely to involve bond cleavage given that the postulated exchange is fast on the NMR time scale and also that low-spin Fe(II) (d^6 configuration) is a moderately kinetically inert metal ion. In support of this, inspection of a space filling molecular model suggests that BF_4^- anion exchange without

bond-breaking appears feasible provided moderate flexing/twisting of the bound ligands is able to occur (***Figure 3.11***). From size considerations alone, such a mechanism appears less likely for the larger PF_6^- ion (but it cannot be ruled out). At this point it is interesting to compare the relative size of all the guest species so far encapsulated. The large size of the $[FeCl_4]^-$ limits the number of orientations it can have in the host complex, in keeping with its ordered orientation within the host complex (i.e. the Cl atoms are oriented into the four faces of the tetrahedron), compared with the BF_4^- and PF_6^- guests which show disorder in their respective crystal structures.

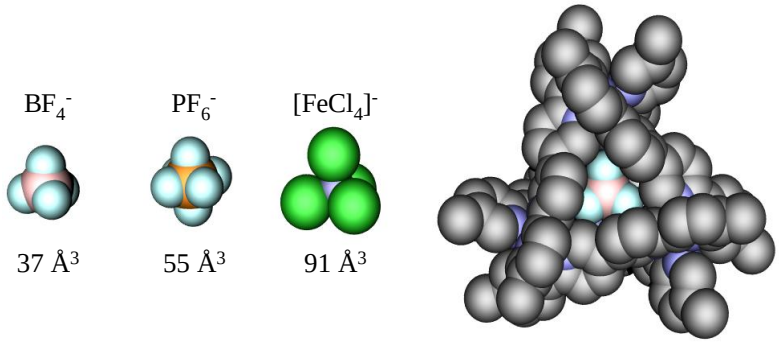

Figure 3.11 Space filling representation of guest anions encapsulated within the $[Fe_4(\mathbf{50})_6]^{8+}$ host (with their respective volumes calculated from van der Waals radii) and space filling representation of the $[Fe_4(\mathbf{50})_6 \supset BF_4]^{7+}$ host-guest complex.

Intriguingly, in a further ^{19}F NMR experiment, slow replacement of encapsulated BF_4^- was observed to occur in the presence of a moderate excess of PF_6^- at 300 K over a period of 80 minutes (with no further change in the spectrum occurring after 24 hours). This result is perhaps best interpreted as involving 'fast' through-side exchange of encapsulated BF_4^- while entry into the 'empty' cage by PF_6^- occurs either via a slow (minutes) bond breaking mechanism or via a size-inhibited, through-side process. In any case both interpretations imply a degree of anion selectivity by the cage, with PF_6^- being bound more strongly than BF_4^- within the cavity. In keeping with this, an attempt to induce the reverse exchange process (taking $[Fe_4(\mathbf{50})_6 \supset PF_6)](PF_6)_7.2H_2O$ in CDCN and adding BF_4^- under similar conditions) yielded no change in the initial spectrum after 24 hours. Interestingly, ^{19}F NMR experiments of $[Fe_4(\mathbf{50})_6 \supset PF_6)](PF_6)_7$ run in DMSO-d_6 resulted in a slow coalescence of PF_6^- signals over several hours. Repeated ^1H NMR spectra of this solution over 24 hours revealed

increased complexity consistent with degradation of the cage. Furthermore, over a period of a week, needle shaped crystals of quaterpyridine **50** had formed in the NMR tube. The DMSO thus appears to successfully compete for coordination sites at the metal apices. This same effect was not observed for either DMF or acetonitrile solutions of $[Fe_4(\mathbf{50})_6 \supset PF_6)](PF_6)_7$ over the same time period. These results fit reported trends for the relative coordinating strengths of these solvents (i.e. CH_3CN < DMF < DMSO).[53]

3.2.4 Microwave driven Fe(II) directed assembly involving quaterpyridine 50

Previous reports[30, 37] have concluded that the formation of related tetrahedral M_4L_6 host-guest species of type $[M_4L_6 \supset guest]$ involve a guest ion template process. At this stage, it seemed that an anion template mechanism might also apply for the present systems. Evidence bearing on this was obtained in a further synthetic study in which Fe(II) chloride was employed as the metal salt and, as before, reacted with quaterpyridine **50** in a 2:3 stoichiometric ratio. In this case the synthesis was performed in a microwave reactor at 393 K with water (rather than acetonitrile) as solvent. It is important to note that a negligible concentration of $[FeCl_4]^{2-}$ will be present in water under the conditions employed. On completion of this reaction, excess Zn(II) chloride was added to the reaction solution in order to precipitate the product as its $[ZnCl_4]^{2-}$ salt; the latter is a well-known "precipitating" anion in metal coordination chemistry. Instant precipitation of a deep red solid occurred on addition of the latter ion. The ^{1}H NMR spectrum of this crude material indicated the presence of a product of high symmetry. Crystals suitable for X-ray diffraction were grown from THF/CH_3CN and the resulting structure confirmed the presence of the usual tetrahedral $[Fe_4(\mathbf{50})_6]^{8+}$ cage structure, but in this case there was *no anion* included in its cavity (***Figure 3.12***). Instead, the latter is occupied by disordered solvent molecules. The cage is again chiral although two-fold symmetric and crystallising in the monoclinic *P*2/n space group. It appears that the absence of a polyatomic anion during the main reaction sequence coupled with the relative insolubility of the $[Fe_4(\mathbf{50})_6][ZnCl_4]_4$, species **157**, may be important contributions to the isolation of the anion-free cage in this case. While this result does not *preclude* a templating role for the anions encapsulated in the structures discussed previously, it does

suggest that such a polyatomic anion is *not essential* for assembly of the present $[Fe_4(\mathbf{50})_6]^{8+}$ cage structure.

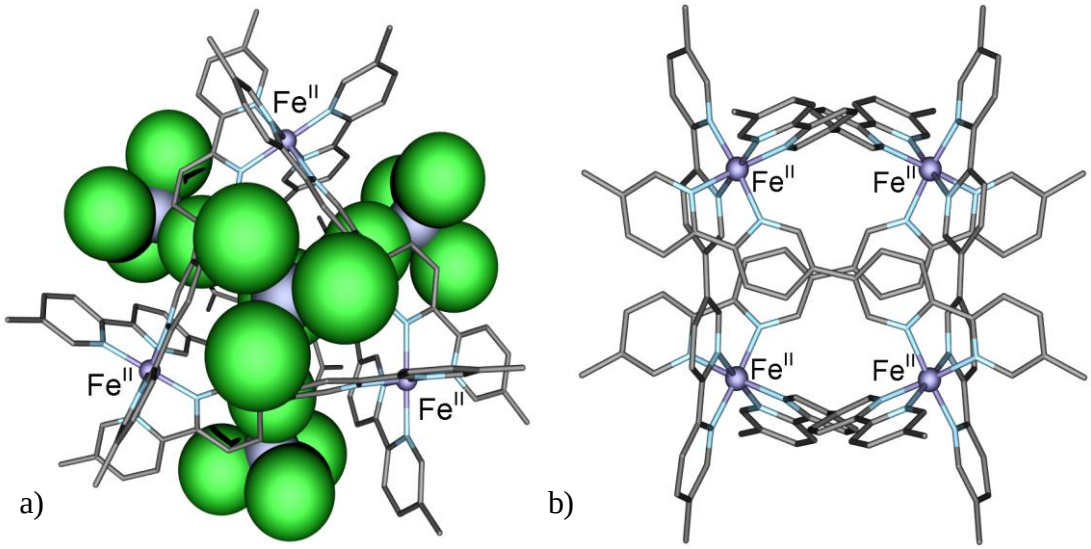

Figure 3.12 a) The '*empty*' cage in $[Fe_4(\mathbf{50})_6]([ZnCl_4])_4.CH_3CN.5{\cdot}5THF.2{\cdot}5H_2O$, **157**, illustrating the locations of the four *exo* $[ZnCl_4]^{2-}$ counter-ions (solvent molecules removed) and b) $[Fe_4(\mathbf{50})_6]^{8+}$ cation with $[ZnCl_4]^{2-}$ counter-ions and solvent molecules removed.

When $[ZnCl_4]^{2-}$ was substituted by either PF_6^- or BF_4^- to precipitate the product from the synthesis performed using microwave heating, described above, the inclusion species $[Fe_4(\mathbf{50})_6(PF_6)](PF_6)_7$ (characterized by NMR and ESI-HRMS) and $[Fe_4(\mathbf{50})_6(BF_4)](BF_4)_7$ (characterized by NMR, ESI-HRMS and a second X-ray structure determination) were isolated. It is interesting to note that $[ZnCl_4]^{2-}$ was not encapsulated (regardless of it having ample opportunity to do so during the characterisation of the complex) while the isostructural $[FeCl_4]^{2-}$, in $[Fe_4(\mathbf{50})_6{\supset}FeCl_4](BPh_4)_6$ (**154**), was observed to undergo encapsulation by the M_4L_6 cage (see page 144). In this regard, repeated attempts to include other multiply charged anions (e.g. SO_4^{2-} and PO_4^{3-}) were unsuccessful. These latter results are in agreement with results published by Raymond *et al.*[28, 68] who argued that highly charged guests were too strongly solvated to allow for encapsulation. Therefore, the isolation of the M_4L_6 complex **154** apparently encapsulating the doubly charged $[FeCl_4]^{2-}$ guest is an isolated example of such an inclusion complex. Perhaps this is an indication of the smaller metal to metal distances of the $[Fe_4(\mathbf{50})_6]^{8+}$ cage compared to that reported by Raymond *et. al.*[21] This would result in a greater effective electrostatic repulsion in the former, in turn leading to a more

favourable enthalpic contribution for anion encapsulation. In combination with this, the larger BPh_4^- counterion would not compete for encapsulation. Interestingly, individual Cl atoms of the tetrachlorozincate anions are directed into the *exo*-faces of the tetrahedral cage which will alleviate some of the expected electrostatic repulsion associated with the +8 charged cage.

3.2.5 Resolution of the racemic $[Fe_4(50)_6]^{8+}$ tetrahedron

Separation of the *ΛΛΛΛ* and *ΔΔΔΔ* enantiomers was achieved by chromatography of the racemic $[Fe_4(\mathbf{50})_6]^{8+}$ on C-25 Sephadex with 0.15 M (-)-O,O′-dibenzoyl-L-tartaric acid as eluent.[69] Circular dichroism (CD) measurements were undertaken to determine the purity of the separated enantiomers of $[Fe_4(\mathbf{50})_6]^{8+}$ (***Figure 3.13***). It should be noted that over the course of several weeks there was very little evidence of a reduction in CD signal intensity in accord with the very slow racemisation of the separated enantiomers. Furthermore, measurement of this solution after approximately one year revealed that the separated enantiomers had not fully racemised. Although this observation was strictly qualitative it is in agreement with previous observations from studies of related M_4L_6 complexes.[70, 71] The M_4L_6 moieties in these latter studies were described as being mechanically coupled, resulting in vastly decreased rates of racemisation compared to simpler mononuclear or even helical analogues.

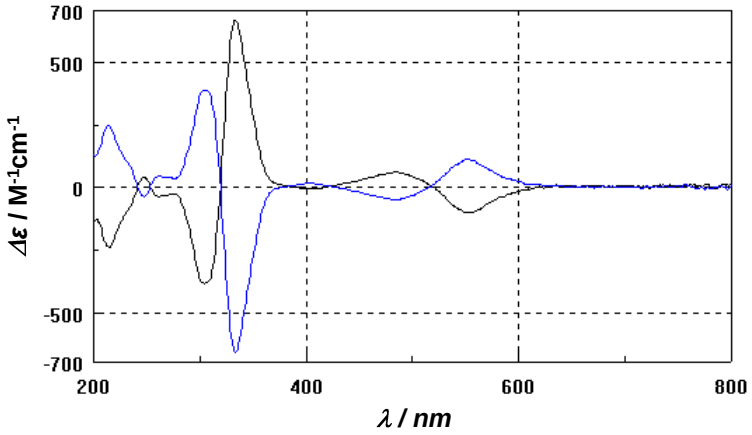

Figure 3.13 The overlaid CD spectra for the band 1 *(blue)* and band 2 *(black)* enantiomers of $[Fe_4(\mathbf{50})_6](PF_6)_8$ in acetonitrile.

3.2.6 Microwave driven Co(II) or Ni(II) directed assembly involving quaterpyridine 50

The interaction of both Co(II) and Ni(II) with quaterpyridine **50** was also investigated. These attempted self-assembly processes were carried out using two equivalents of $MCl_2.6H_2O$ (M = Co or Ni) to three equivalents of quaterpyridine **50** using a microwave reactor, with methanol as the solvent. The resulting Co(II) and Ni(II) complexes were precipitated using an excess of aqueous KPF_6. The crystals of both the Co(II) and Ni(II) products were quite disordered, however using unit cell analysis these products were each concluded to be M_4L_6 tetrahedra. Furthermore, they crystallise in the same space group ($P\bar{4}3n$) as $[Fe_4(\mathbf{50})_6 \supset PF_6](PF_6)_7$. As well, the crystallographic data suggest analogous encapsulation of PF_6^-. The ESI-HRMS of the Co(II) and Ni(II) products revealed ions that were in agreement with the successive losses of PF_6^- from both the formulae $[Co_4(\mathbf{50})_6](PF_6)_8$, **158**, and $[Ni_4(\mathbf{50})_6](PF_6)_8$, **159**, respectively (for example see ***Figure 3.14***).

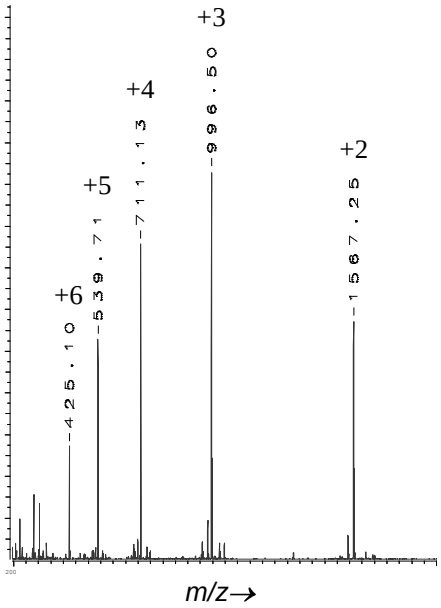

Figure 3.14 ESI-HRMS depicting successive losses of PF_6^- from the formula $[Ni_4(\mathbf{50})_6](PF_6)_8$, **159**.

Evidently the predominant product from the interaction of the labile Co(II) and Ni(II) metal ions or the moderately inert Fe(II) metal ion and quaterpyridine **50**, in a 2:3 ratio, is an M_4L_6 structure. There was, however, mass spectral evidence indicating the presence of

$[Ni_2(\mathbf{50})_3](PF_6)_4$ in the MS solution matrix. ***Figure 3.15*** a) depicts the overlapping experimental peaks corresponding to the mixture of $\{[Ni_2(\mathbf{50})_3](PF_6)_3\}^+$ and $\{[Ni_4(\mathbf{50})_6](PF_6)_6\}^{2+}$. The overlayed theoretical distribution for $\{[Ni_2(\mathbf{50})_3](PF_6)_3\}^+$ and $\{[Ni_4(\mathbf{50})_6](PF_6)_6\}^{2+}$ are also shown. Note that every second isotopic peak in the experimental isotopic distribution is more intense consistent with the overlap of ions with

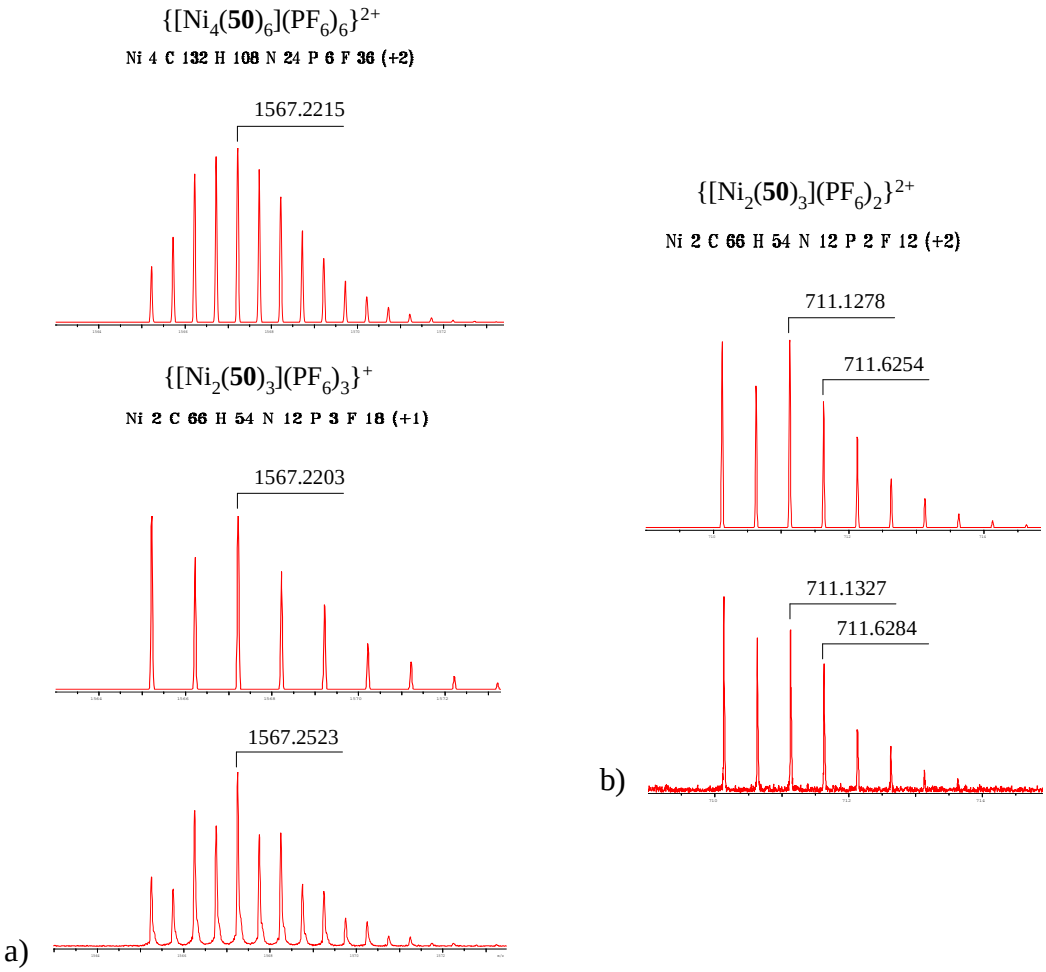

Figure 3.15 a) The observed isotopic distribution corresponding to the overlap of $\{[Ni_2(\mathbf{50})_3](PF_6)_3\}^+$ and $\{[Ni_4(\mathbf{50})_6](PF_6)_6\}^{2+}$ (bottom) versus the theoretical isotopic distribution for both $\{[Ni_2(\mathbf{50})_3](PF_6)_3\}^+$ (top) and $\{[Ni_4(\mathbf{50})_6](PF_6)_6\}^{2+}$ (middle) and b) the observed isotopic distribution corresponding to $\{[Ni_2(\mathbf{50})_3](PF_6)_2\}^{2+}$ (bottom) versus its theoretical isotope distribution (top).

similar m/z ratios but different charge states. To further validate the existence of $[Ni_2(\mathbf{50})_3](PF_6)_4$ in solution, an experimental isotopic distribution consistent with $\{[Ni_2(\mathbf{50})_3](PF_6)_2\}^{2+}$ was observed (***Figure 3.15*** b)). It should be noted that the experimental

and theoretical isotopic distributions for this latter species are not a perfect match, which is most probably due to instrument tuning; however, the expected mass is within 2 ppm. Even though it cannot be ruled out that these peaks are fragment ions, the mass spectra of neither $[Fe_4(\mathbf{50})_6 \supset PF_6](PF_6)_7$ nor $[Co_4(\mathbf{50})_6](PF_6)_8$ showed any evidence for the existence of M_2L_3 complexes under similar conditions. These results combined with the crystallographic data suggest that reaction of Ni(II) with quaterpyrdine **50** leads to a mixture of M_2L_3 and M_4L_6 complexes.

3.3 A RARE $[Ru_2(50)_3]^{4+}$ HELICATE

Polypyridyl Ru(II) complexes display a range of interesting characteristic properties that include inertness, redox properties, excited state reactivity, luminescence emission and excited state lifetimes.[72-74] As a consequence metallosupramolecular systems incorporating polypyridyl Ru(II) moieties have been incorporated into molecular machines,[75, 76] molecular electronic components,[77-80] solar cell dye sensitizers,[79, 81] luminescence sensors,[79] novel drug analogues and DNA binders.[82-84] A range of reports have described the synthesis of Ru(II) structures using self-assembly processes. These reports describe the production of metallocycles,[85] cubes,[86] heterometallic[87, 88] and homometallic[89] helicates.

It is now well established that bis-bidentate ligand systems may interact with octahedral metal ions to yield triple helical species of type $[M_2L_3]^{n+}$.[90-93] However, helicate formation may be hindered when employing inert metal ions by the kinetic formation of polymeric material. In a paper by Pascu *et al.*[89] the interaction of Ru(II) with a bis-diimine ligand led to the formation of the single example of a $[Ru_2L_3]^{4+}$ helicate reported so far. This study reported a 1% yield reflecting the inherent difficulty of working with kinetically inert metal ions. To combat such low yields, a number of elegant synthetic strategies have been successfully employed. Fletcher *et al.*[94] utilized a tethered tris-bipyridyl ligand to kinetically enhance the formation of the required facial geometric isomer in a stepwise synthetic approach to a heterometallic helicate. In further reports Torelli *et al.*[87, 88] outlined the use of a tris(diimine) Ru(II) complex as a novel 'labile' partner to synthesize several Ru(II)-*f*-block heterometallic helicates in high yield.

The previous sections of this chapter outlined the successful synthesis of $[M_4(\mathbf{50})_6]^{8+}$ (M = Fe(II), Co(II) and Ni(II)) tetrahedron complexes based on the interaction of M(II) with quaterpyridine **50** in a 2:3 ratio, respectively. These results prompted an investigation of the use of second row d^6 Ru(II) in analogous metal-directed assembly processes with quaterpyridine **50**. This section deals with the synthesis and characterisation of a new $[Ru_2(\mathbf{50})_3]^{4+}$ helicate based on the interaction of Ru(II) with **50**. The results of DNA binding experiments with $[Ru_2(\mathbf{50})_3]^{4+}$ are also presented.

Initially, a self-assembly reaction was attempted employing $RuCl_3$ and quaterpyridine **50** in a 2 : 3 ratio in ethanol under reflux for 2 weeks. This approach led to the production of a brown intractable polymeric material. The reaction was repeated under microwave irradiation in ethylene glycol at a temperature of 230 $^{\circ}$C for 4.5 hour resulting in an orange solution, characteristic of the $[Ru(bpy)_3]^{2+}$ chromophore. The resulting product, isolated as its PF_6^- salt, was purified by chromatography on silica gel giving a moderate yield of 36 %. The seven observed ^{1}H NMR resonances and eleven ^{13}C NMR resonances are consistent with **50** possessing *C2*-symmetry within the complex. ^{1}H-^{1}H COSY and NOESY experiments allowed the full assignment of the ^{1}H NMR spectrum. Microanalysis for C, H and N was in agreement with a 2:3 Ru:**50** ratio. A ESI-HRMS of this material gave +1 and +2 ions corresponding to two successive losses of PF_6^- ions from the formula $[Ru_2(\mathbf{50})_3](PF_6)_4$, **160** (***Figure 3.16***).

Crystals suitable for X-ray diffraction were grown from Et_2O/CH_3CN and the resulting structure confirmed a helical assembly of type $[Ru_2(\mathbf{50})_3]^{4+}$ (***Figure 3.17***). The structure crystallizes in the chiral space group $P6_3$ with two independent complexes per unit cell; thus each crystal is itself optically active.[ψ] The two octahedral Ru(II) centres are separated by 7.6 Å and bridged by three quaterpyridine ligands such that the stereochemistry of the metal centres of each discrete unit is either $\Delta\Delta$ (*P*) or $\Lambda\Lambda$ (*M*). There is a significant distortion from planarity of each sp^2 hybridized ligand indicating that induced ligand strain is present (***Figure 3.17*** a)). The chiral twist associated with the helix is 59 º and extends for 17.6 Å along the length of each ligand.

[ψ] The crystal used in the present study proved to be a 15 % racemic twin as evidenced by a refined Flack parameter of 0.15.

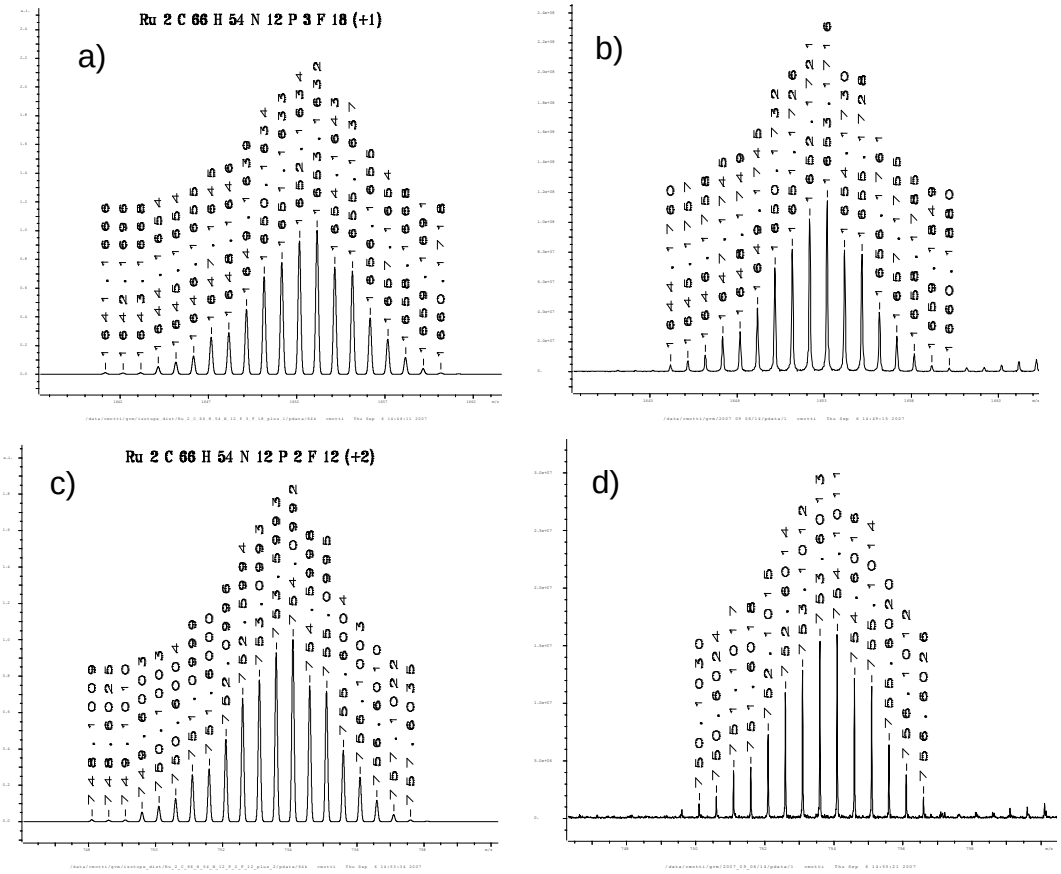

Figure 3.16 Partial ESI-HRMS of $[Ru_2(\mathbf{50})_3](PF_6)_4$, a) and b) are the theoretical and experimental isotopic distributions for $\{[Ru_2(\mathbf{50})_3](PF_6)_3\}^+$, respectively; c) and d) are the theoretical and experimental isotopic distributions for $\{[Ru_2(\mathbf{50})_3](PF_6)_2\}^{2+}$, respectively.

It appears that the following factors may influence the different structure obtained for the present Ru(II) assembly compared with that for the corresponding M_4L_6 (M = Fe, Co and Ni) assemblies of **50** reported earlier. The larger size of the Ru(II) ion relative to M(II) may serve to ameliorate the degree of ligand strain required for the formation of the entropically-favoured $[Ru_2(\mathbf{50})_3]^{4+}$ helicate over its larger $[M_4(\mathbf{50})_6]^{8+}$ analogue. Alternatively, the slower kinetics of formation in the former case could also be important if the smaller unit is essentially a kinetic product. However, with respect to this it is noted that the microwave synthesis of the octahedral Ru(II) complex of an unsymmetrically-substituted bipyridine ligand in ethyleneglycol at 200 °C (similar conditions to those used by us) has recently been reported to result in stereocontrol of ligand binding such that the *fac*-isomer was the sole

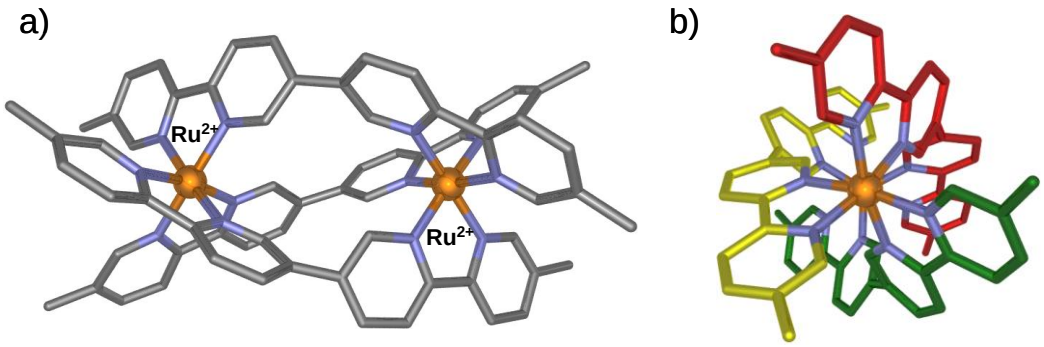

Figure 3.17 Crystal structure of $[Ru_2(\mathbf{50})_3](PF_6)_4 \bullet 1.125H_2O \bullet 2.25MeCN$, **160**. a) perpendicular to the principal C_3-axis and b) viewed down the C_3-axis (hydrogens, counterions and solvent are removed for clarity).

product obtained.[95] This outcome was postulated to reflect the enhanced lability of at least one of the coordinated ligands under the high energy conditions employed.[†] It appears likely that a similar situation may also apply to the present synthesis. Preferential formation of the *fac*-isomers of related octahedral Ru(II) complexes under thermodynamic control has also been reported by Fletcher *et al.*[94] and Torelli *et al.*[87] The latter made comment on an apparent increase in the rate of *mer/fac* isomerization in a related system as a result of increased solvent polarity (i.e. through the use of ethylene glycol).

The red-orange colour of $[Ru_2(\mathbf{50})_3]^{4+}$ is typical of a $[Ru(bpy)_3]^{2+}$ chromophore[74, 96] with the UV/Vis absorption spectrum revealing an MLCT band at 469 nm (ε/dm^3 mol^{-1} cm^{-1} 22700) in acetonitrile (***Figure 3.18***). Excitation at the MLCT wavelength (469 nm) of the complex in acetonitrile resulted in an emission centred at 604 nm. $[Ru_2(\mathbf{50})_3]^{4+}$ (as its Cl^- salt) also emits strongly in water revealing little evidence of solvent mediated nonradiative vibrational quenching. It is noted that, ideally, solvent mediated quenching may be a desired property for some applications, for example, for application as a DNA binding probe. [82-84, 97, 98] If, for instance, strong nonradiative vibrational quenching of emission is observed in aqueous solutions it may be expected that upon DNA binding a degree of desolvation must occur, thus potentially resulting in an increase in emission intensity – a property often referred to as the "light switch" effect.

[†] Rationalisation of this proposed lability was mostly avoided apart from a vague mention of a possible *trans*-effect due to the asymmetry of nitrogen donors of the unsymmetrical bipyridyl derivatives employed in this complexation study.

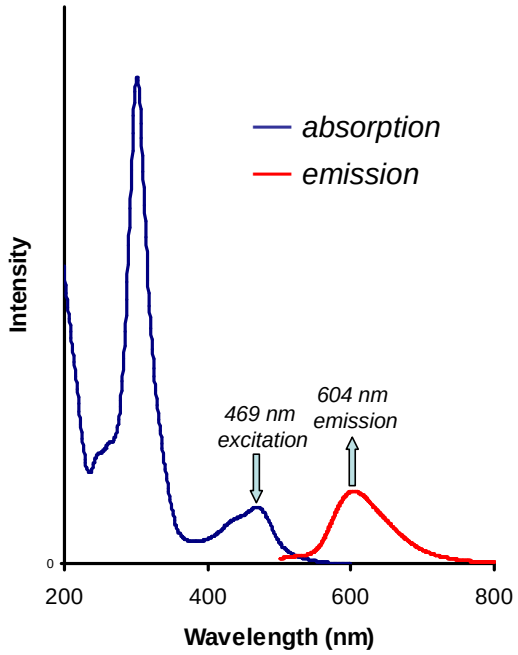

Figure 3.18 The absorption and emission spectra of $[Ru_2(\mathbf{50})_3]^{4+}$ in acetonitrile.

The uninterrupted sp^2 hybridization of the three quaterpyridyl bridging ligands suggests the possibility of electronic communication between the Ru(II) centres. Accordingly, cyclic voltammetry (CV) was conducted on the complex to evaluate whether any separation of the oxidation potentials occurs between the metal centres. The CV results show a single *pseudo*-reversible redox wave ($E_{1/2}$ = 1.43V; ΔEp = 101 mV; 2 e^-) under the conditions employed (***Figure 3.19***). There is no indication of a separation of the two oxidation processes, indicating an absence of significant communication between the metal centres under the conditions employed, perhaps reflecting the observation from the X-ray determination (***Figure 3.18***) that the two 2,2′-bipyridyl chelates of each quaterpyridine are twisted out of plane by 70 - 80°.[80]

Separation of the *P*- and *M*-helicates was achieved by chromatography of the racemic mixture of $[Ru_2(\mathbf{50})_3]^{4+}$ on C-25 Sephadex with 0.1 M (-)-O,O′-dibenzoyl-L-tartaric acid as eluent.[69] Circular dichroism (CD) measurements were undertaken to confirm the purity of the separated *P*- and *M*-enantiomers (***Figure 3.20***). A crystal structure of the complex with an

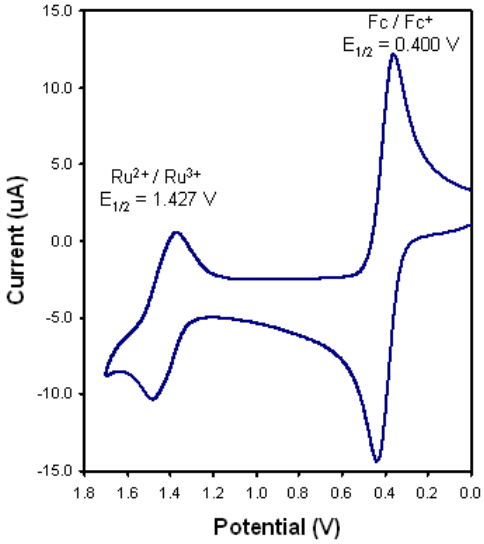

Figure 3.19 Cyclic voltammogram of $[Ru_2(\mathbf{50})_3](PF_6)_4$ with two redox couples belonging to Ru^{2+} / Ru^{3+} (1.427 V) and Fc / Fc^{+} (0.400 V).

observed negative Cotton effect for the π – π* transition at 325 nm allowed its absolute configuration to be unambiguously assigned as the *P*-enantiomer (see ***Appendix B*** for crystallographic details). Thus, the material with an observed positive Cotton effect for the π – π* transition was deduced to be the *M*-enantiomer. Interestingly, the corresponding signs of the Cotton effects for the π – π* transition in the CD spectra of the *P*- and *M*-$[Ru_2(\mathbf{50})_3]^{4+}$ forms are the same as those of the simpler mononuclear analogues, *Δ*- and *Λ*-$[Ru(bipy)_3]^{2+}$, respectively.[99-101] This is in conflict with reports[102-105] of related dinuclear species that have been observed to exhibit "internuclear" exciton coupling leading to an inversion of the sign of the Cotton effect for their respective π – π* transitions relative to those of their mononuclear analogues. Indeed, it has been indicated that such internuclear exciton coupling has distance dependence ($1/R^2$);[104, 106] thus, the close proximity of the bipyridyl chromophores in the current example suggested that internuclear exciton coupling might have been important. It is clear from the current example that caution must be exercised when attempting to relate the sign of the Cotton effect for the lowest energy π – π* transition of a sample of unknown configuration to that of a related model compounds. Interestingly, no reduction in the CD signals of the solutions of the enantiomerically pure helicates was observed over four months, in accord with the expected high inertness of $[Ru_2(\mathbf{50})_3]^{4+}$.

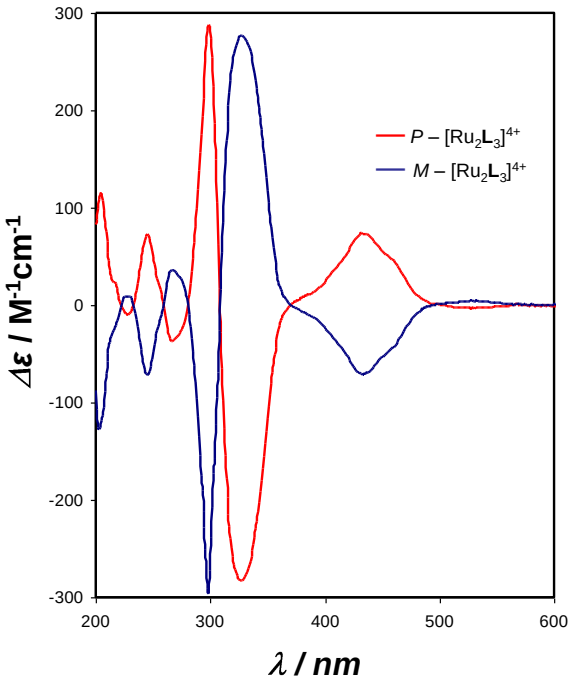

Figure 3.20 The overlaid CD spectra for the *P* and *M* enantiomers of $[Ru_2(\mathbf{50})_3]^{4+}$ in acetonitrile.

3.3.1 $[Ru_2(50)_3]^{4+}$ DNA binding studies.

Reports[82, 89, 102, 107-119] that related metallo-helicates exhibit interesting DNA binding characteristics prompted us to investigate the ability of $[Ru_2(\mathbf{50})_3]^{4+}$ to bind to DNA. An indication that the enantiomers of $[Ru_2(\mathbf{50})_3]^{4+}$ do indeed bind selectively with duplex DNA was obtained from their efficient separation by the DNA affinity chromatography procedure reported by Smith *et al.*[120] (see ***Appendix D.1*** for details). Using a Sepharose-immobilized AT dodecanucleotide column, an impressive separation of the enantiomers was observed; the *M*-helicate was strongly retained whilst the *P*-helicate essentially eluted with the solvent front. Less efficient (but still satisfactory) separations were observed with other DNA motifs, for example a GC 12-mer and bulge and hairpin sequences. In each case the *M*-helicate bound to the column more strongly than the *P*-enantiomer. Control experiments confirmed that the binding was due to the bound DNA sequences and not the biotinolated streptavidin or the sepharose column. Interestingly, an incomplete separation of the *P*- and *M*-helicates was

achieved on a sepharose column. However, the order of elution was reversed leading to the *M*-helicate eluting prior to the *P*-helicate.

A spectrophotometric binding study[121] of the enantiomers of $[Ru_2(\mathbf{50})_3]^{4+}$ with calf thymus DNA (ct-DNA) was also conducted (see ***Appendix D.2***). Binding constants obtained for both the *P*- and *M*-helicates were in the range of 10^5 to 10^6 M^{-1} indicating little evidence of the apparent enantioselectivity observed from the affinity chromatography discussed above. To investigate this point further, an equilibrium dialysis experiment was conducted using the racemic helicate and ct-DNA (see ***Appendix D.3***). This experiment clearly showed preferential dialysis of *M*-$[Ru_2(\mathbf{50})_3]^{4+}$ in agreement with the observed chromatographic affinities (***Figure 3.21***). The observed binding preference of the *M*-$[Ru_2(\mathbf{50})_3]^{4+}$ form to various B-DNA sequences is in agreement with observations made by Hannon *et al.*[102] with a related dinuclear triple helicate.

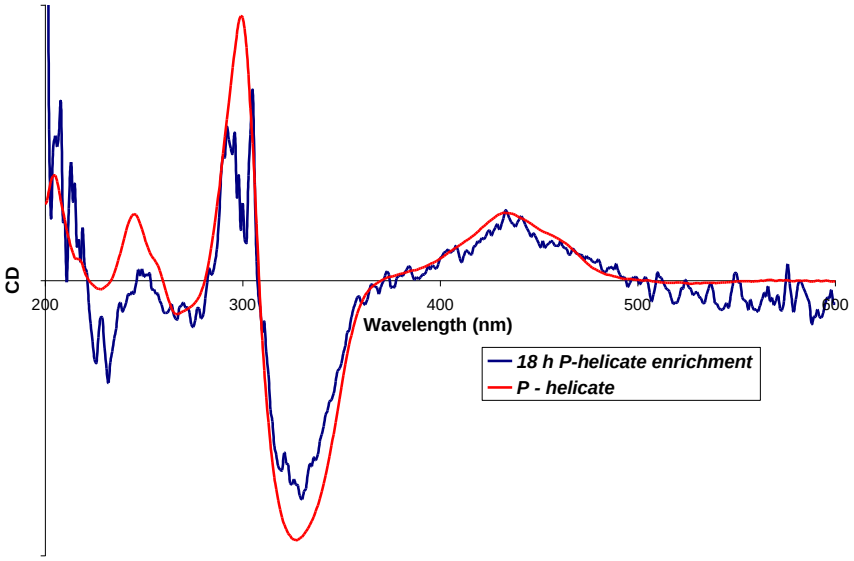

Figure 3.21 CD of the $[Ru_2(\mathbf{50})_3]Cl_4$ solution after 18 hours of dialysis indicating an enrichment in the *P*-helicate.

3.4 CONCLUSIONS

In conclusion, the results presented in the present chapter describe the synthesis and characterisation of a new class of anion binding tetrahedra capable of encapsulating a range of anionic guest species. These include singly charged BF_4^-, PF_6^- and $FeCl_4^-$ as well as the doubly charged $FeCl_4^{2-}$. While examples of BF_4^- and PF_6^- anions being encapsulated within M_4L_6 structures have been reported previously,[34] in the present study it has been possible to clearly demonstrate that $[Fe_4(\mathbf{50})_6]^{8+}$ exhibits unusual anion selectivity for PF_6^- over BF_4^-. Although some ambiguity remains with respect to the assignment of the oxidation state of the encapsulated tetrachoroferrate anion in $[Fe_4(\mathbf{50})_6 \supset FeCl_4](PF_6)_n$ (n = 6 or 7), it appears that both $[FeCl_4]^-$ and $[FeCl_4]^{2-}$ are able to be encapsulated. In this regard, if further data is able to confirm the encapsulation of $[FeCl_4]^{2-}$, $[Fe_4(\mathbf{50})_6 \supset FeCl_4](BPh_4)_6$ would represent the sole example of encapsulation of a doubly charged guest within a M_4L_6 host system. Finally, a successful synthetic procedure for the isolation of the cage free of an encapsulated anionic guest was also reported – a result with implications for the role of anion templation (or otherwise) in the formation of tetrahedral structures of the present type.

We have also demonstrated the synthesis of a quite rare dinuclear helicate, $[Ru_2(\mathbf{50})_3]^{4+}$, in a 36% yield that almost certainly indicates a level of thermodynamic control in the self-assembly process involved in its formation. The helicate product is a racemate which can be separated efficiently into its *P*- and *M*-enantiomers by DNA-based affinity chromatography. Although further work (in particular NMR binding studies) is required to elucidate the precise DNA-binding mode(s) of this complex, current evidence indicates, on balance, selective binding of the *M*-helicate. Finally, the isolation of $[Ru_2(\mathbf{50})_3]^{4+}$ indicated that the production of dinuclear cryptates incorporating dialdehyde **48** (page 136) in a metal-template reductive amination process using ruthenium might be successful.

3.5 EXPERIMENTAL

See Chapter 2, *Section 2.3* for a general descriptions of techniques and materials.

X-ray structure data

X-ray structural data for were collected and refined by Dr Jack Clegg (University of Sydney) on a Bruker-Nonius APEX2-X8-FR591 diffractometer employing graphite-monochromated Mo-Kα radiation generated from a rotating anode (0.71073 Å) with ω and ψ scans. Data were collected at 150 K to approximately 56° 2θ. Alternatively, data was collected by Dr Peter Turner using double diamond monochromated synchrotron radiation (0.48595 Å) with ω and ψ scans at the the ChemMatCARS beamline at the Advanced Photon Source at approximately 100 K. Further details for each structure are outlined in ***Appendix B.***

3.5.1 Experimental for M_4L_6 host – guest complexes

$[Fe_4(50)_6 \supset FeCl_4](PF_6)_7.CH_3OH$ (153): A stirred solution of quaterpyridine **50** (338 mg, 1 mmol) and $FeCl_2.5H_2O$ (217 mg, 1 mmol) in dry CH_3CN (30 cm^3) was degassed with N_2 for 0.5 h. This reaction mixture was then refluxed overnight resulting in a purple suspension. The solvent was removed under vacuum and the solid taken up in H_2O (30 cm^3) and stirred for 1 h (or until the solid was completely dissolved). This solution was filtered though celite and chormatographed on Sephadex C25 eluting with 1 M NaCl. The product was precipited with KPF_6 and isolated by filtration to afford **153** (270 mg, 47 %) as a deep red powder. UV/Vis (CH_3CN, nm): λ_{max}(ε / dm^3 mol^{-1} cm^{-1}) = 251 (60 441), 271 (56 902), 320 (248 843), 532 (18 786); ^{1}H NMR (300 MHz, CD_3CN): δ = 2.19 (s, 36 H, CH_3), 6.75 (br s, 12 H, H-6′,6′′), 7.19 (br d, ^3J = 8.4 Hz, 12 H, H-4′,4′′), 7.50 (br s, 12 H, H-6,6′′′), 7.95 (br d, ^3J = 8.1 Hz, 12 H, H-4,4′′′), 8.37 (br d, ^3J = 8.4 Hz, 12 H, H-3′,3′′), 8.47 (br d, ^3J = 8.1 Hz, 12 H, H-3,3′′′); positive ion ESI-HRMS: (1st series) m/z (M = $C_{132}H_{108}N_{24}P_6F_{36}Fe_5Cl_4$ in CH_3CN / MeOH): calcd for $[M - 2PF_6]^{2+}$: 1515.1637, found 1515.2444; calcd for $[M - 3PF_6]^{3+}$: 961.7875, found 961.8172; calcd for $[M - 4PF_6]^{4+}$: 685.0995, found 685.1147; calcd for $[M - 5PF_6]^{5+}$: 519.0866, found 519.0936; calcd for $[M - 6PF_6]^{6+}$: 408.4114, found 408.4162; (2nd series) m/z (M = $C_{132}H_{108}N_{24}P_8F_{48}Fe_4$ in CH_3CN / MeOH): calcd for $[M - 2PF_6]^{2+}$: 1561.7233,

found 1561.7375; calcd for $[M - 3PF_6]^{3+}$: 992.8273, found 992.8278; calcd for $[M - 4PF_6]^{4+}$: 708.3793, found 708.3912; calcd for $[M - 5PF_6]^{5+}$: 537.7105, found 537.7178; calcd for $[M - 6PF_6]^{6+}$: 423.9313, found 423.9360; calcd for $[M - 7PF_6]^{7+}$: 342.6604, found 342.6648; (3^{rd} series) m/z ($M = C_{132}H_{108}N_{24}P_7F_{42}Fe_5Cl_4$ in CH_3CN / MeOH): calcd for $[M - 2PF_6]^{2+}$: 1587.6458, found 1587.6503; calcd for $[M - 3PF_6]^{3+}$: 1010.1089, found 1010.1158; calcd for $[M - 4PF_6]^{4+}$: 721.3405, found 721.3487; calcd for $[M - 5PF_6]^{5+}$: 548.0795, found 548.0863; calcd for $[M - 6PF_6]^{6+}$: 432.5721, found 432.5766; calcd for $[M - 2PF_6]^{7+}$: 350.0668, found 350.0716; elemental analysis (%) calcd for $C_{132}H_{108}N_{24}P_7F_{42}Fe_5Cl_4.CH_3OH$ (3495.2444 g mol^{-1}): C 45.66, H 3.23, N 9.62, P 6.20; found: C 45.42, H 3.46, N 9.64, P 9.31; X-ray quality crystals were obtained by diffusion of MeOH into a solution of the product in CH_3CN.

$[Fe_4(50)_6 \supset FeCl_4](BPh_4)_6.2CH_3OH.4CH_3CN$ (154): $Fe(BPh_4)_2$ was generated by adding $NaBPh_4$ (137 mg, 0.4 mmol) to a solution of $FeCl_2.5H_2O$ (43 mg, 0.2 mmol) in dry degassed CH_3CN (10 cm^3). The resulting precipitate was removed by filtration and quaterpyridine **50** (100 mg, 0.3 mmol) was added. This reaction mixture was then refluxed overnight under nitrogen. The crude product was purified on Sephadex LH-20 with CH_3CN as eluant to afford **154** (160 mg, 70 %) as a deep red solid. ^1H NMR (300 MHz, CD_3CN): δ = 2.17 (s, 36 H, CH_3), a series of very broad aromatic resonances were also observed; positive ion ESI-HRMS: m/z ($M = C_{274}H_{228}B_8Fe_5N_{24}Cl_4$ in CH_3CN / MeOH): calcd for $[M - 2BPh_4]^{2+}$: 1864.0700, found 1864.0783; calcd for $[M - 3BPh_4]^{3+}$: 1136.3241, found 1136.3288; calcd for $[M - 4BPh_4]^{4+}$: 772.4511, found 772.4528; calcd for $[M - 5BPh_4]^{5+}$: 554.1273, found 554.1276; elemental analysis (%) calcd for $C_{274}H_{228}B_8Fe_5N_{24}Cl_4.2CH_3OH.4CH_3CN$ (4591.62 g mol^-): C, 74.74; H, 5.44; N, 8.53; Found: C 74.75, H 5.33, N 8.52; X-ray quality crystals were obtained by diffusion of MeOH into an CH_3CN solution of the above product.

$[Fe_4(50)_6 \supset BF_4)](BF_4)_7 \cdot 4H_2O$ (155): A solution of $Fe(BF_4)_2.6H_2O$ (47 mg, 0.14 mmol) and **50** (78 mg, 0.23 mmol) in dry degassed CH_3CN (10 cm^3) was heated at reflux (under nitrogen) for 5 h resulting in a characteristic deep red solution. The solvent was evaporated and the crude material was purified by chromatography on Sephadex LH-20 with CH_3CN as eluent to afford **155** (87 mg, 84 %) as a deep red solid. UV/Vis (CH_3CN, nm): λ_{max}(ε / dm^3 mol^{-1} cm^{-1}) = 271 (82 049), 318 (288 680), 529 (21 768); ^1H NMR (300 MHz, CD_3CN): δ =

2.20 (s, 36 H, CH_3), 7.05 (d, ^4J = 1.8 Hz, 12 H, H-6′,6″), 7.31 (dd, ^3J = 8.4, ^4J = 1.8 Hz, 12 H, H-4′,4″), 7.37 (d, ^4J = 1.2 Hz, 12 H, H-6,6‴), 7.97 (dd, ^3J = 8.4, ^4J = 1.2 Hz, 12 H, H-4,4‴), 8.41 (d, ^3J = 8.4 Hz, 12 H, H-3′,3″), 8.53 (d, ^3J = 8.4 Hz, 12 H, H-3,3‴); ^{13}C NMR (75 MHz, CD_3CN): δ = 18.79, 123.58, 125.27, 136.51, 139.95, 140.19, 140.58, 152.29, 155.60, 156.34, 160.38; ^{19}F NMR (282.4 MHz, CD_3CN): δ = -151.00 (s; B^{11}-F), -150.94 (s; B^{10}-F); positive ion ESI-HRMS: m/z (M = $C_{132}H_{108}B_8F_{32}Fe_4N_{24}$ in CH_3CN / MeOH): calcd for $[M - 2BF_4]^{2+}$: 1387.3416, found 1387.3591; calcd for $[M - 3BF_4]^{3+}$: 895.8930, found 895.8923; calcd for $[M - 4BF_4]^{4+}$: 650.1693, found 650.1742; elemental analysis (%) calcd for $C_{132}H_{108}B_8F_{32}Fe_4N_{24}.4H_2O$ (3020.22 g mol^{-1}): C 52.44, H 3.87, N 11.13; found: C 52.26, H 3.78, N 11.08; X-ray quality crystals were obtained by diffusion of THF into an CH_3CN solution of the product.

$[Fe_4(50)_6\supset PF_6](PF_6)_7\cdot 2H_2O$ (156): A solution of $FeBr_2$ (21 mg, 0.14 mmol) and **50** (78 mg, 0.23 mmol) in dry degassed CH_3CN (10 cm^3) was heated under reflux for 24 h (under nitrogen) resulting in a dark red solution. The solvent was evaporated and the deep red solid was taken up in water and excess KPF_6 (110 mg, 0.6 mmol) was added. The crude product was purified by chromatography on Sephadex LH-20 with CH_3CN as eluant to afford **156** (84 mg, 96 %) as a deep red solid. UV/Vis (CH_3CN, nm): λ_{max}(ε / dm^3 mol^{-1} cm^{-1}) = 271 (80,948), 320 (340,147), 534 (25,756); ^{1}H NMR (300 MHz, CD_3CN): δ = 2.23 (s, 36 H, CH_3), 6.77 (s, 12 H, H-6′,6″), 7.23 (d, ^3J = 7.2 Hz, 12 H, H-4′,4″), 7.55 (s, 12 H, H-6,6‴), 7.97 (d, ^3J = 8.1 Hz, 12 H, H-4,4‴), 8.42 (d, ^3J = 7.2 Hz, 12 H, H-3′,3″), 8.49 (d, ^3J = 8.1 Hz, 12 H, H-3,3‴); ^{13}C NMR (75 MHz, CD_3CN): δ = 18.78, 123.21, 125.06, 135.96, 138.73, 139.84, 140.54, 153.48, 155.80, 156.28, 159.78; ^{19}F NMR (282.4 MHz, CD_3CN): δ = -73.09 (d, ^1J = 707.1 Hz, 42 F, $7PF_6$), -72.45 (d, ^1J = 717.3 Hz, 6 F, $1PF_6$); positive ion ESI-HRMS: m/z (M = $C_{132}H_{108}P_8F_{48}Fe_4N_{24}$ in CH_3CN / MeOH): calcd for $[M - 2PF_6]^{2+}$: 1561.7233, found 1561.7274; calcd for $[M - 3PF_6]^{3+}$: 992.8273, found 992.8323; calcd for $[M - 4PF_6]^{4+}$: 708.3793, found 708.3785; calcd for $[M - 5PF_6]^{5+}$: 537.7105, found 537.7178; calcd for $[M - 6PF_6]^{6+}$: 423.9313, found 423.9360; calcd for $[M - 7PF_6]^{7+}$: 342.6604, found 342.6648; elemental analysis (%) calcd for $C_{132}H_{108}F_{48}Fe_4N_{24}P_8.2H_2O$ (3449.47 g mol^{-}): C 45.93, H 3.27, N 9.75; found: C 45.75, H 3.23, N 9.81; X-ray quality crystals were obtained by diffusion of MeOH into an CH_3CN solution of the product.

$[Fe_4(50)_6][ZnCl_4]_4.CH_3CN.5\cdot5THF.2\cdot5H_2O$ (157): A mixture of quaterpyridine **50** (50 mg, 0.148 mmol) and $FeCl_2.5H_2O$ (21.5 mg, 0.099 mmol) in H_2O (10 cm^3) was degassed with N_2 for 0.5 h. The reaction mixture was then heated with microwave energy in a sealed pressurised microwave vessel with temperature and pressure sensors and a magnetic stirrer bar (Step 1 - ramped to 150 °C over 2 min using 100 % of 400 W; step 2 – held at 150 °C for 10 min using 30 % of 400 W). The reaction mixture was allowed to cool to room temperature and was filtered through celite. To this solution was added $ZnCl_2$ (68 mg, 0.5 mmol) in 1 M HCl (1 cm^3), and the resulting precipitate was filtered off and washed with a minimum of cold H_2O. Thin layer chromatography on silica gel, with a mobile phase of CH_3CN, KNO_3 (aq) and water (7:0.5:1) indicated the presence of one major product. ^{1}H NMR (300 MHz, CD_3CN): δ = 2.16 (s, 36 H, CH_3), 7.18 (s, 12 H, H-6′,6″), 7.32 (s, 12 H, H-6,6‴), 7.55 (d, ^3J = 7.8 Hz, 12 H, H-4′,4″), 7.92 (d, ^3J = 7.5 Hz, 12 H, H-4,4‴), 8.54 (d, ^3J = 8.1 Hz, 12 H, H-3′,3″), 8.72 (d, ^3J = 8.4 Hz, 12 H, H-3,3‴); X-ray quality crystals were obtained by diffusion of THF into an CH_3CN solution of the above product.

$[Co_4(50)_6\supset PF_6](PF_6)_7.2H_2O$ (158): A solution of $CoCl_2.6H_2O$ (23.4 mg, 0.1 mmol) and quaterpyridine **50** (50 mg, 0.148 mmol) in MeOH (10 cm^3) was heated with microwave energy in a sealed pressurised microwave vessel with temperature and pressure sensors and a magnetic stirrer bar (Step 1 - ramped to 130 °C over 2 min using 100 % of 400 W; Step 2 – held at 130 °C for 20 min using 25 % of 400 W). Excess NH_4PF_6 in H_2O (20 cm^3) was then added and the resulting solid isolated by filtration. This material was recrystallised by diffusion of MeOH into an acetonitrile solution affording **158** (30 mg, 35 %) as yellow / brown cubic shaped crystals. Positive ion ESI-HRMS: m/z (M = $C_{132}H_{108}N_{24}P_8F_{48}Co_4$ in CH_3CN / MeOH): calcd for $[M - 2PF_6]^{2+}$: 1567.7193, found 1567.7495; calcd for $[M - 3PF_6]^{3+}$: 996.8247, found 996.8374; elemental analysis (%) calcd for $C_{132}H_{108}F_{48}Co_4N_{24}P_8.4H_2O$ (3496.41 g mol^{-}): C 45.30, H 3.34, N 9.61; found: C 45.23, H 3.22, N 9.50.

$[Ni_4(50)_6\supset PF_6](PF_6)_7.2H_2O$ (159): $NiCl_2.6H_2O$ (52 mg, 0.2 mmol) and quaterpyridine **50** (110 mg, 0.33 mmol) in MeOH (10 cm^3) was heated with microwave energy in a sealed

pressurised microwave vessel with temperature and pressure sensors and a magnetic stirrer bar (Step 1 – ramped to 130 °C over 2 min using 100 % of 400 W; Step 2 – held at 130 °C for 20 min using 25 % of 400 W). Excess NH_3PF_6 in H_2O (20 cm^3) was then added and the resulting solid isolated by filtration. This material was recrystallised by diffusion of MeOH into an acetonitrile solution affording **159** (80 mg, 47 %) as yellow cubic shaped crystals. Positive ion ESI-HRMS: m/z (M = $C_{132}H_{108}P_8F_{48}Ni_4N_{24}$ in CH_3CN / MeOH): calcd for $[M - 2PF_6]^{2+}$: 1567.2214, found 1567.2513; calcd for $[M - 3PF_6]^{3+}$: 996.4927, found 996.5054; calcd for $[M - 4PF_6]^{4+}$: 711.1283, found 711.1344; calcd for $[M - 5PF_6]^{5+}$: 539.7104, found 539.7143; calcd for $[M - 6PF_6]^{6+}$: 425.0976, found 425.1003; elemental analysis (%) calcd for $C_{132}H_{108}F_{48}Ni_4N_{24}P_8.4H_2O$ (3492.42 g mol^-): C 45.36, H 3.35, N 9.62; found: C 45.20, H 3.15, N 9.47.

3.5.2 Ru(II) M_2L_3 experimental

$[Ru_2(50)_3](PF_6)_4.3MeOH$ (160): A solution of $RuCl_3$ (80.77 mg, 0.39 mmol) and a suspension of quaterpyridine **50** (200 mg, 0.59 mmol) in dry degassed ethylene glycol (20 cm^3) was reacted using microwave energy (65% of 400 watts in a pressure vessel), while maintaining the temperature at 225^{o}C, for 4.5 h. Water was added to the orange solution and an excess of NH_4PF_6 (200 mg, 1.23 mmol) was added. The resulting orange solid that formed was filtered off and washed with water. This crude material was purified by chromatography on silica gel with a mixture of acetonitrile, saturated aqueous KNO_3 and H_2O (14:1:2 respectively) as the eluent to afford **160** (125 mg, 36 %) as an orange crystalline solid. UV/Vis (CH_3CN, nm): $\lambda_{max}(\varepsilon$ / dm^3 mol^{-1} $cm^{-1}) = 469$ (22700); ^{1}H NMR (300 MHz, CD_3CN): δ = 2.28 (s, 18 H, CH_3), 7.31 (dd, J^4 = 1.2, J^5 = 0.6, 6 H, H-6,6′′′), 7.95 (ddd, J^3 = 8.4, J^4 = 1.8, J^5 = 0.6, 6 H, H-4,4′′′), 8.06 (d, J^4 = 1.8, 6 H, H-6′,6′′), 8.17 (dd, J^3 = 8.4, J^4 = 1.8, 6 H, H-4′,4′′), 8.42 (d, J^3 = 8.4, 6 H, H-3,3′′′), 8.43 (d, J^3 = 8.4, 6 H, H-3′,3′′); ^{13}C NMR (75 MHz, CD_3CN): δ = 19.58, 125.09, 125.95, 137.88, 138.89, 140.31, 141.07, 151.15, 153.84, 155.29, 159.96; positive ion ESI-HRMS: m/z (M = $Ru_2C_{66}H_{54}N_{12}P_4F_{24}$ in CH_3CN / MeOH): calcd for $[M - 1PF_6]^{1+}$: 1653.1632, found 1653.1716; calcd for $[M - 2PF_6]^{2+}$: 754.0992, found 754.1011; elemental analysis (%) calcd for $C_{66}H_{54}N_{12}F_{24}P_4Ru_2.3CH_3OH$ (1894.20 g mol^-): C

43.71, H 3.51, N 8.87; found: C 43.86, H 3.51, N 8.97; X-ray quality crystals were obtained by diffusion of MeOH into an CH_3CN solution of the product.

3.6 REFERENCES

1. J.-M. Lehn, *Supramolecular Chemistry*, VCH Verlagsgesellschaft, Weinheim, 1995.
2. L. F. Lindoy and I. M. Atkinson, *Self-assembly in Supramolecular Chemistry*, Royal Society of Chemistry, Cambridge, UK., 2000.
3. S. Leininger, B. Olenyuk and P. J. Stang, *Chem. Rev.*, 2000, **100**, 853-908.
4. R. M. Yeh, A. V. Davis and K. N. Raymond, in *Comprehensive Coordination Chemistry II*, eds. J. A. McClevety and T. J. Meyer, Elsevier, Oxford, Editon edn., 2004, vol. 7, p. 327.
5. D. J. Bray, B. Antonioli, J. K. Clegg, K. Gloe, K. Gloe, K. A. Jolliffe, L. F. Lindoy, G. Wei and M. Wenzel, *Dalton Trans.*, 2008, 1683-1685.
6. D. J. Bray, L.-L. Liao, B. Antonioli, K. Gloe, L. F. Lindoy, J. C. McMurtrie, G. Wei and X.-Y. Zhang, *Dalton Trans.*, 2005, 2082-2083.
7. K. R. Adam, I. M. Atkinson, J. Kim, L. F. Lindoy, O. A. Matthews, G. V. Meehan, F. Raciti, B. W. Skelton, N. Svenstrup and A. H. White, *Dalton Trans.*, 2001, 2388-2397.
8. I. M. Atkinson, A. R. Carroll, R. J. Janssen, L. F. Lindoy, O. A. Mathews and G. V. Meehan, *J. Chem. Soc., Perkins Trans. 1*, 1997, **3**, 295 - 301.
9. R. J. Janssen, L. F. Lindoy, O. A. Mathews, G. V. Meehan, A. N. Sobolev and A. H. White, *Chem. Commun.*, 1995, **7**.
10. D. F. Perkins, L. F. Lindoy, A. McAuley, G. V. Meehan and P. Turner, *Proc. Nat. Acad. Sci. U.S.A.*, 2006, **103**, 532-537.
11. D. F. Perkins, L. F. Lindoy, G. V. Meehan and P. Turner, *Chem. Commun.*, 2004, 152-153.
12. J. K. Clegg, L. F. Lindoy, B. Moubaraki, K. S. Murray and J. C. McMurtrie, *Dalton Trans.*, 2004, 2417-2423.

13. R. W. Saalfrank, R. Burack, A. Breit, D. Stalke, R. Herbst-Irmer, J. Daub, M. Porsch, E. Bill, M. Muther and A. X. Trautwein, *Angew. Chem. Int. Ed.*, 1994, **33**, 1621 - 1623.
14. R. W. Saalfrank, B. Demleitner, H. Glaser, H. Maid, D. Bathelt, F. Hampel, W. Bauer and M. Teichert, *Chem. Eur. J.*, 2002, **8**, 2679-2683.
15. R. W. Saalfrank, N. Low, B. Demleitner, D. Stalke and M. Teichert, *Chem. Eur. J.*, 1998, **4**, 1305 - 1311.
16. R. W. Saalfrank, A. Stark, M. Bremer and H.-U. Hummel, *Angew. Chem. Int. Ed.*, 1990, **29**, 311 - 314.
17. R. W. Saalfrank, A. Stark, K. Peters and H. G. von Schnering, *Angew. Chem. Int. Ed.*, 1988, **27**, 851 - 853.
18. T. Beissel, R. E. Powers and K. N. Raymond, *Angew. Chem. Int. Ed.*, 1996, **35**, 1084 - 1086.
19. S. M. Biros, R. G. Bergman and K. N. Raymond, *J. Am. Chem. Soc.*, 2007, **129**, 12094-12095.
20. S. M. Biros, R. M. Yeh and K. N. Raymond, *Angew. Chem. Int. Ed.*, 2008, **47**, 6062-6064.
21. D. L. Caulder, R. E. Powers, T. N. Parac and K. N. Raymond, *Angew. Chem. Int. Ed.*, 1998, **37**, 1840 - 1843.
22. D. L. Caulder and K. E. Raymond, *Dalton Trans.*, 1999, 1185 - 1200.
23. D. L. Caulder and K. N. Raymond, *Acc. Chem. Res.*, 1999, **32**, 975-982.
24. D. Fiedler, R. G. Bergman and K. N. Raymond, *Angew. Chem. Int. Ed.*, 2004, **43**, 6565.
25. D. Fiedler, D. H. Leung, R. G. Bergman and K. N. Raymond, *Acc. Chem. Res.*, 2005, **38**, 349-358.
26. D. Fiedler, H. vanHalbeek, R. G. Bergman and K. N. Raymond, *J. Am. Chem. Soc.*, 2006, **128**, 10240-10252.
27. D. H. Leung, R. G. Bergman and K. N. Raymond, *J. Am. Chem. Soc.*, 2006, **128**, 9781-9797.
28. T. N. Parac, D. L. Caulder and K. E. Raymond, *J. Am. Chem. Soc.*, 1998, **120**, 8003 - 8004.

29. M. D. Pluth and K. N. Raymond, *Chem. Soc. Rev.*, 2007, **36**, 161-171.
30. M. Scherer, D. L. Caulder, D. W. Johnson and K. E. Raymond, *Angew. Chem. Int. Ed.*, 1999, **38**, 1587 - 1592.
31. G. Seeber, B. E. F. Tiedemann and K. E. Raymond, *Top. Curr. Chem.*, 2006, **265**, 147.
32. S. P. Argent, T. Riis-Johannessen, J. C. Jeffery, L. P. Harding and M. D. Ward, *Chem. Commun.*, 2005, 4647-4649.
33. J. S. Fleming, K. L. V. Mann, C.-A. Carraz, E. Psillakis, J. C. Jeffery, J. A. McCleverty and M. D. Ward, *Angew. Chem. Int. Ed.*, 1998, **37**, 1279 - 1281.
34. R. Frantz, S. Grange, N. K. Al-Rasbi, M. D. Ward and J. Lacour, *Chem. Commun.*, 2007, 1459 - 1461.
35. R. L. Paul, Z. R. Bell, J. S. Fleming, J. C. Jeffery, J. A. McCleverty and M. D. Ward, *Heteroat. Chem.*, 2002, **13**, 567 - 573.
36. R. L. Paul, Z. R. Bell, J. C. Jeffery, L. P. Harding, J. A. McCleverty and M. D. Ward, *Polyhedron*, 2003, **22**, 781 - 787.
37. R. L. Paul, Z. R. Bell, J. C. Jeffery, J. A. McCleverty and M. D. Ward, *Proc. Nat. Acad. Sci. U.S.A.*, 2002, **99**, 4883 - 4888.
38. R. L. Paul, S. M. Couchman, J. C. Jeffery, J. A. McCleverty, Z. R. Reeves and M. D. Ward, *Dalton Trans.*, 2000, 845 - 851.
39. M. Albrecht, I. Janser, S. Burk and P. Weis, *Dalton Trans.*, 2006, 2875-2880.
40. Z. R. Bell, L. P. Harding and M. D. Ward, *Chem. Commun.*, 2003, 2432 - 2433.
41. I. S. Tidmarsh, T. B. Faust, H. Adams, L. P. Harding, L. Russo, W. Clegg and M. D. Ward, *J. Am. Chem. Soc.*, 2008.
42. S. P. Argent, H. Adams, T. Riis-Johannessen, J. C. Jeffery, L. P. Harding, O. Mamula and M. D. Ward, *Inorg. Chem.*, 2006, **45**, 3905.
43. J. W. Lauher and J. A. Ibers, *Inorg. Chem.*, 1975, **14**, 348.
44. D. Wyrzykowski, T. Maniecki, A. Patteck-Janczyk, J. Stanek and Z. Warnke, *Thermochimica Acta*, 2005, **435**, 92.
45. L. Mihiri, D. Ariyananda and R. E. Norman, *Acta Cryst.*, 2002, **E58**, m775.
46. M. P. Batten, A. J. Canty, K. J. Cavell, T. S. Ruther, B. W. and A. H. White, *Acta Cryst.*, 2004, **C60**, m311.

47. J. A. Ayllon, I. C. Santos, R. T. Henriques, M. Almeida, E. B. Lopes, J. Morgado, L. Alcacer, L. F. Veiros and M. T. Duarte, *Dalton Trans.*, 1995, 3543-3549.
48. B. D. James, S. M. Juraya, J. Liesegang, W. M. Reiff, B. W. Skelton and A. H. White, *Inorg. Chem. Acta*, 2001, **312**, 88.
49. P. Kulkarni, S. Pahye and E. Sinn, *Inorg. Chem. Commun.*, 2003, **6**, 1129.
50. T.-Toan and L. F. Dahl, *J. Am. Chem. Soc.*, 1971, **93**, 2654.
51. G. J. Van Berkel, *J. Mass Spectrom.*, 2000, **35**, 773-783.
52. G. J. Van Berkel, *J. Anal. At. Spectrom.*, 1998, **13**, 603 - 607.
53. V. Gutmann, *Coord. Chem. Rev.*, 1967, **2**, 239-256.
54. B. J. Hathaway and D. G. Holah, *J. Chem. Soc.*, 1964, 2408 - 2416.
55. C. J. Barbour, J. H. Cameron and J. M. Winfield, *Dalton Trans.*, 1980, 2001.
56. A. P. Zuur and W. L. Groeneveld, *Rec. Trav. Chim.*, 1967, **86**, 1089.
57. J. Reedijk and W. L. Groeneveld, *Rec. Trav. Chim.*, 1968, **87**, 513.
58. J. Reedijk, *Rec. Trav. Chim.*, 1969, **88**, 86.
59. J. Reedijk, A. P. Zuur and W. L. Groeneveld, *Rec. Trav. Chim.*, 1967, **86**, 1127.
60. J. Reedijk and W. L. Groeneveld, *Rec. Trav. Chim.*, 1967, **86**, 1103.
61. T. Vu, A. M. Bond, D. C. R. Hockless, B. Moubaraki, K. S. Murray, G. Lazarev and A. G. Wedd, *Inorg. Chem.*, 2001, **40**, 65-72.
62. S. Juraja, T. Vu, P. J. S. Richardt, A. M. Bond, T. J. Cardwell, J. D. Cashion, G. D. Fallon, G. Lazarev, B. Moubaraki, K. S. Murray and A. G. Wedd, *Inorg. Chem.*, 2002, **41**, 1072-1078.
63. B. N. Figgis, *Introduction to ligand fields*, Interscience Publishers, New York, 1966.
64. F. E. Mabbs and D. J. Machin, *Magnetism and transition metal complexes*, Chapman and Hall, London, 1973.
65. F. W. Cagle and G. F. Smith, *J. Am. Chem. Soc.*, 1947, **69**, 1860-1862.
66. A. V. Davis and K. N. Raymond, *J. Am. Chem. Soc.*, 2005, **127**, 7912-7919.
67. R. L. Paul, S. P. Argent, J. C. Jeffery, L. P. Harding, J. M. Lynam and M. D. Ward, *Dalton Trans.*, 2004, 3453-3458.
68. D. H. Leung, R. G. Bergman and K. N. Raymond, *J. Am. Chem. Soc.*, 2008, **130**, 2798-2805.

69. G. Rapenne, J. P. Sauvage, B. T. Patterson and F. R. Keene, *Chem. Commun.*, 1999, 1853 - 1854.
70. A. V. Davis, D. Fiedler, M. Ziegler, A. Terpin and K. N. Raymond, *J. Am. Chem. Soc.*, 2007, **129**, 15354.
71. A. J. Terpin, M. Ziegler, D. W. Johnson and K. N. Raymond, *Angew. Chem. Int. Ed.*, 2001, **40**, 157.
72. S. Campagna, F. Puntoriero, F. Nastasi, G. Bergamini and V. Balzani, *Photochemistry and photophysics of coordination compounds: ruthenium.*, Springer Berlin / Heidelberg, 2007.
73. J. F. Endicott, H. B. Schlegel, M. J. Uddin and D. S. Seniveratne, *Coord. Chem. Rev.*, 2002, **229**, 95-106.
74. A. Juris, V. Balzani, F. Barigelletti, S. Campagna, P. Belser and A. von Zelewsky, *Coord. Chem. Rev.*, 1988, **84**, 85-277.
75. V. Balzani, G. Bergamini, F. Marchioni and P. Ceroni, *Coord. Chem. Rev.*, 2006, **250**, 1254-1266.
76. S. Bonnet, J. P. Collin, M. Koizumi, P. Mobian and J. P. Sauvage, *Adv. Mater.*, 2006, **18**, 1239-1250.
77. D. M. Bassani, J.-M. Lehn, S. Serroni, F. Puntoriero and S. Campagna, *Chem. Eur. J.*, 2003, **9**, 5936-5946.
78. N. Robertson and C. A. McGowan, *Chem. Soc. Rev.*, 2003, **32**, 96-103.
79. J. G. Vos and J. M. Kelly, *Dalton Trans.*, 2006, 4869-4883.
80. R. Ziessel, M. Hissler, A. El-ghayoury and A. Harriman, *Coord. Chem. Rev.*, 1998, **178-180**, 1251-1298.
81. A. S. Polo, M. K. Itokazu and N. Y. Murakami Iha, *Coord. Chem. Rev.*, 2004, **248**, 1343-1361.
82. M. J. Hannon, *Chem. Soc. Rev.*, 2007, **36**, 280-295.
83. C. Metcalfe and J. A. Thomas, *Chem. Soc. Rev.*, 2003, **32**, 215-224.
84. B. M. Zeglis, V. C. Pierre and J. K. Barton, *Chem. Commun.*, 2007, 4565-4579.
85. H. S. Chow, E. C. Constable, C. E. Housecroft, M. Neuburger and S. Schaffner, *Polyhedron*, 2006, **25**, 1831-1843.

86. S. Roche, C. Haslam, S. L. Heath and J. A. Thomas, *Chem. Commun.*, 1998, 1681 - 1682.
87. S. Torelli, S. Delahaye, A. Hauser, G. Bernardinelli and C. Piguet, *Chem. Eur. J.*, 2004, **10**, 3503-3516.
88. S. Torelli, D. Imbert, M. Cantuel, G. Bernardinelli, S. Delahaye, A. Hauser, J.-C. G. Bünzli and C. Piguet, *Chem. Eur. J.*, 2005, **11**, 3228-3242.
89. G. I. Pascu, A. C. G. Hotze, C. Sanchez-Cano, B. M. Kariuki and M. J. Hannon, *Angew. Chem. Int. Ed.*, 2007, **46**, 4374-4378.
90. M. Albrecht, *Chem. Rev.*, 2001, **101**, 3457-3498.
91. C. R. K. Glasson, L. F. Lindoy and G. V. Meehan, *Coord. Chem. Rev.*, 2008, **252**, 940-963.
92. M. J. Hannon and L. J. Childs, *Supramol. Chem.*, 2004, **16**, 7 - 22.
93. C. Piguet, G. Bernardinelli and G. Hopfgartner, *Chem. Rev.*, 1997, **97**, 2005-2062.
94. N. C. Fletcher, R. T. Brown and A. P. Doherty, *Inorg. Chem.*, 2006, **45**, 6132-6134.
95. A. Grabulosa, M. Beley and P. C. Gros, *Eur. J. Inorg. Chem.*, 2008, **2008**, 1747-1751.
96. E. A. P. Armstrong, R. T. Brown, M. S. Sekwale, N. C. Fletcher, X.-Q. Gong and P. Hu, *Inorg. Chem.*, 2004, **43**, 1714.
97. L.-N. Ji, X.-H. Zou and J.-G. Liu, *Cood. Chem. Rev.*, 2001, **216-217**, 513.
98. F. Gao, H. Chao and L.-N. Ji, *Chem. Biodivers.*, 2008, **5**, 1962.
99. B. Bosnich, *Acc. Chem. Res.*, 1969, **2**, 266-273.
100. S. F. Mason, *Inorg. Chim. Acta Rev.*, 1968, **2**, 89-109.
101. M. Ziegler and A. von Zelewsky, *Coord. Chem. Rev.*, 1998, **177**, 257-300.
102. I. Meistermann, V. Moreno, M. J. Prieto, E. Moldrheim, E. Sletten, S. Khalid, P. M. Rodger, J. C. Peberdy, C. J. Isaac, A. Rodger and M. J. Hannon, *Proc. Nat. Acad. Sci. U.S.A.*, 2002, **99**, 5069 - 5074.
103. S. G. Telfer, R. Kuroda and T. Sato, *Chem. Commun.*, 2003, 1064.
104. S. G. Telfer, N. Tajima and R. Kuroda, *J. Am. Chem. Soc.*, 2004, **126**, 1408.
105. S. G. Telfer, N. Tajima, R. Kuroda, M. Cantuel and C. Piguet, *Inorg. Chem.*, 2004, **43**, 5302.
106. N. Harada, S.-M. L. Chen and K. Nakanishi, *J. Am. Chem. Soc.*, 1975, **97**, 5345-5352.
107. B. Schoentjes and J.-M. Lehn, *Helv. Chim. Acta*, 1995, **78**, 1-12.

108. L. J. Childs, J. Malina, B. E. Rolfsnes, M. Pascu, M. J. Prieto, M. J. Broome, P. M. Rodger, E. Sletten, V. Moreno, A. Rodger and M. J. Hannon, *Chem. Eur. J.*, 2006, **12**, 4919-4927.

109. M. J. Hannon, S. Bunce, A. J. Clarke and N. W. Alcock, *Angew. Chem. Int. Ed.*, 1999, **38**, 1277.

110. M. J. Hannon, V. Moreno, M. J. Prieto, E. Moldrheim, E. Sletten, I. Meistermann, C. J. Isaac, K. J. Sanders and A. Rodger, *Angew. Chem. Int. Ed.*, 2001, **40**, 879-884.

111. S. Khalid, M. J. Hannon, A. Rodger and P. M. Rodger, *Chem. Eur. J.*, 2006, **12**, 3493-3506.

112. S. Khalid, M. J. Hannon, A. Rodger and P. M. Rodger, *J. Mol. Graphics Modell.*, 2007, **25**, 794-800.

113. J. Malina, M. J. Hannon and V. Brabec, *Chem. Eur. J.*, 2007, **13**, 3871-3877.

114. J. Malina, M. J. Hannon and V. Brabec, *Nucl. Acids Res.*, 2008, **36**, 3630-3638.

115. J. Malina, M. J. Hannon and V. Brabec, *Chem. Eur. J.*, 2008, **9999**, NA.

116. A. Oleksi, A. G. Blanco, R. Boer, I. Usón, J. Aymamí, A. Rodger, M. J. Hannon and M. Coll, *Angew. Chem. Int. Ed.*, 2006, **45**, 1227-1231.

117. J. C. Peberdy, J. Malina, S. Khalid, M. J. Hannon and A. Rodger, *J. Inorg. Biochem.*, 2007, **101**, 1937-1945.

118. F. Tuna, M. R. Lees, G. J. Clarkson and M. J. Hannon, *Chem. Eur. J.*, 2004, **10**, 5737-5750.

119. C. Uerpmann, J. Malina, M. Pascu, G. J. Clarkson, V. Moreno, A. Rodger, A. Grandas and M. J. Hannon, *Chem. Eur. J.*, 2005, **11**, 1750-1756.

120. J. A. Smith and F. R. Keene, *Chem. Commun.*, 2006, 2583-2585.

121. A. M. Pyle, J. P. Rehmann, R. Meshoyrer, C. V. Kumar, N. J. Turro and J. K. Barton, *J. Am. Chem. Soc.*, 1989, **111**, 3051-3058.

Chapter 4

Octahedral Metal-directed Assembly of Bridged Quaterpyridines

4.1 BACKGROUND

The balance between flexibility and rigidity of di- and polytopic ligands employed in self-assembly processes is an important consideration for the design of supramolecular architectures.[1-6] For example, in the present study quaterpyridine **50**, a rigid linear ditopic ligand, yields M_4L_6 tetrahedra when interacted with labile and moderately inert octahedral metal ions (see ***Figure 4.1***). On the other hand, the interaction of octahedral metal ions with

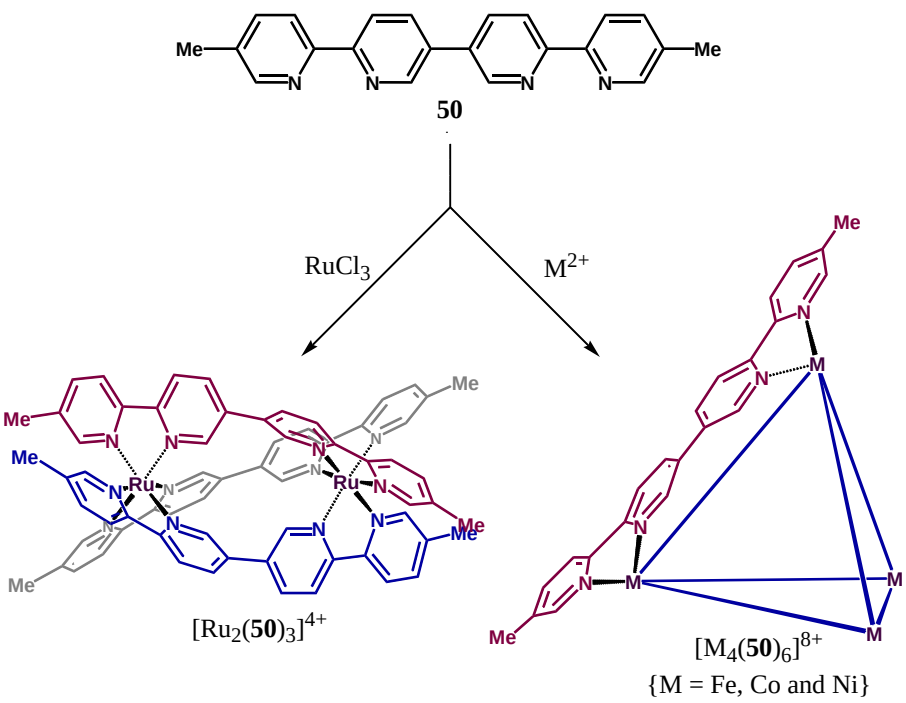

Figure 4.1 Different metallosupramolecular assemblies resulting from the use of different metal ions.

bis-bidentate ligands incorporating some flexibility in the form of sp^3 hybridised linking groups and thus with increased conformational freedom, allows the formation of M_2L_3 triple helicates in some instances.[7-10] However, there are exceptions to the above generalisation. Albrecht *et al.* reported[6,11] the formation of triple-helicates from the interaction of octahedral metal ions and bis(catechol) ligands linked by rigid phenylene and biphenylene spacer units. With respect to this, the comment was made that there is some flexibility at the C(aryl)—C(aryl) single bonds.[6] These observations by Albrecht, combined with the observation that the highly strained $[Ru_2(\mathbf{50})_3]^{4+}$ helicate was able to form (see ***Figure 4.1***), prompted an

investigation into the effects that extended quaterpyridines (see below) might have on metal directed assembly outcomes. For this purpose the rigidly bridged quaterpyridines **126** – **129** were synthesised (see Chapter 2 *Section 2.2.3* for details). It was envisaged that the increased separation between the two chelating moieties might reduce strain in M_2L_3 helicates analogous to $[Ru_2(\mathbf{50})_3]^{4+}$, thus allowing the formation of stable helicates with more labile metal ions, such as Fe(II) and Ni(II). The alternative outcome of this investigation would be the production of M_4L_6 tetrahedra with increased cavity volume. The synthesis of a range of M_2L_3 helicates and M_4L_6 tetrahedra derived from the interaction of **126** – **129** with octahedral metal ions is reported in *Section 4.2.1* and *Section 4.2.2*.

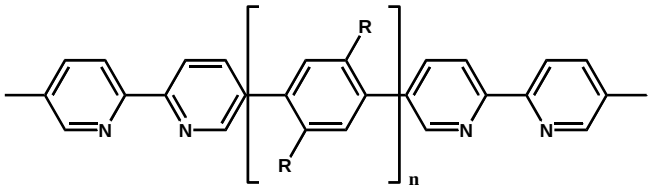

126; R = H; n =1
127; R = H; n = 2
128; R = OMe; n = 1
129; R = OMe; n = 2

Prior to the current work, most reported metal-directed assembly experiments that yielded M_2L_3 helicates have employed bis-bidentate ligands with sp^3 hydbridized atoms incorporated in the spacer between the chelating moieties.[3,7-10] This latter observation is no doubt a reflection of the greater conformational flexibility required for the formation of many helicates. However, greater conformational flexibility does not necessarily guarantee the formation of helical species. Indeed, the number of carbon sp^3 centres has been shown to be important in determining whether or not a helicate forms or whether the corresponding *meso*-isomer forms.[3] In this regard, even numbers of sp^3 carbons has been shown to favour helicate formation, while odd numbers favour the formation of *meso*-isomers. With respect to this, the outcomes from the metal-directed assembly processes of flexibly-bridged quaterpyridines **149** – **151** with both Fe(II) and Ni(II) will be discussed in *Section 4.2.4*. It should be noted that while this latter series of ligands has two sp^3 carbons in their respective spacer units, there are also two heteroatoms which were excluded from the general rules outlined by

Albrecht.[3] As well, the observations in this previous report were made for ligands that had linear spacers, such as the hydroquinone-bridged quaterpyridine **151**.

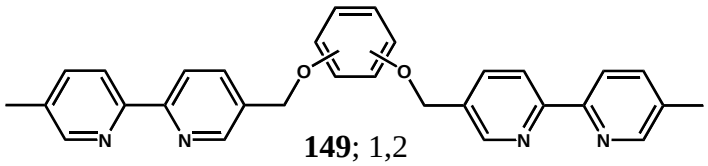

149; 1,2
150; 1,3
151; 1,4

4.2 $[M_2L_3]^{4+}$ HELICATES AND $[M_4L_6]^{8+}$ TETRAHEDRA

Initially quaterpyridines **126** and **127** were reacted with $FeCl_2.5H_2O$ using microwave heating with methanol as solvent. Metal complexes were indicated to have formed due to the observed deep red colouration of the corresponding reaction solutions. However, on cooling these reaction mixtures the deep red colouration faded and ligands **126** and **127** were observed to precipitate. In this regard, the ^1H NMR spectra of the soluble fractions from the above reactions, isolated as their PF_6^- salts, indicated that these products were paramagnetic. This latter observation was thought to be the result of the presence of coordinatively unsaturated Fe(II) metal centres (i.e. mono- and/or bis-chelate Fe(II) complexes) and as such investigation of these samples was discontinued.

Preliminary mass spectral evidence suggests that the reaction of Ru(II) with **126** and **127** using microwave heating and ethylene glycol as solvent led to the formation of M_2L_3 complexes. It is envisaged that these M_2L_3 complexes, together with $[Ru_2(\mathbf{50})_3]^{4+}$, will enable an instructive comparative DNA binding study of helicates of varying lengths with the same charge state.[12,13] However, at this time no further work has been conducted by the author on these samples and consequently they will not be mentioned further.

Due to their above-mentioned solubility problems, ligands **126** and **127** have not been used for any further metal directed assembly experiments so far and will not be discussed further. The follow discussion will focus on outcomes from the interaction of quaterpyridines **128**, **129** and **149** – **151** with Fe(II) and Ni(II).

4.2.1 $[M_2(128)_3]^{4+}$ helicates and $[M_4(128)_6]^{8+}$ tetrahedra

TLC of the reaction solution from the metal directed assembly of quaterpyridine **128** with Fe(II) indicated that a mixture of two deep red products had formed. A ^{1}H NMR spectrum of the crude material indicated the presence of two products in which the two fold symmetry of quaterpyridine **128** was retained. These two products were separated chromatographically using two methods. First, a successful separation was achieved using cation exchange chromatography on Sephadex C25 eluting with 1 M NaCl. TLC of the separated products indicated that the higher R_f material on TLC elutes first from the cation exchange column. Subsequently, chromatography on silica gel using reported conditions[14] allowed an efficient (cost-effective) alternative means of separation.

The ^{1}H NMR and ^{13}C NMR spectra of the two isolated products were quite different. However, in both cases it was evident that quaterpyridine **128** showed C_2 symmetry within the complexes (i.e. there were eight ^{1}H and fifteen ^{13}C resonances). This combined with the diamagnetic nature of the products, as indicated by their sharp NMR spectra, led to the assumption that the d^6 Fe(II) centres were coordinatively saturated (e.g. $[Fe(bpy)_3]^{2+}$). As a result, possible products were expected to be of the general formula $[Fe_{2n}(\mathbf{128})_{3n}]^{4n+}$ (n = 1, 2, 3,…). In this regard, the ESI-HRMS of the high R_f material gave +2, +3, and +4 ions corresponding to successive losses of PF_6^- from the formula $[Fe_2(\mathbf{128})_3](PF_6)_4$, **161**. The mass spectrum of the lower R_f material gave +3, +4, and +5 ions corresponding to successive losses of PF_6^- from the formula $[Fe_4(\mathbf{128})_6](PF_6)_8$, **162**. Thus, the ^{1}H NMR spectrum of the crude material could now be interpreted to indicate a 1:2 ratio of $[Fe_2(\mathbf{128})_3](PF_6)_4$ to $[Fe_4(\mathbf{128})_6](PF_6)_8$.

Now that the formula of each complex had been elucidated, a comparison of their corresponding ^{1}H NMR spectra was considered likely to be more instructive. The ^{1}H NMR spectrum of $[Fe_2(\mathbf{128})_3](PF_6)_4$ showed upfield shifted resonances (***Figure 4.2*** b)) for protons in both the 6′- and 6′′-positions, compared to those of the free ligand (***Figure 4.2*** a)), due to the former falling within the shielding cone of the adjacent bipyridine units (i.e. those around the same metal centre). Similarly, the ^{1}H NMR spectrum of $[Fe_4(\mathbf{128})_6](PF_6)_8$ (***Figure 4.2*** c)) revealed that the 6′- and 6′′-proton resonances were also shifted upfield compared to those of the free ligand. However, in this latter case, the 6′-proton resonance is 0.9 ppm downfield of

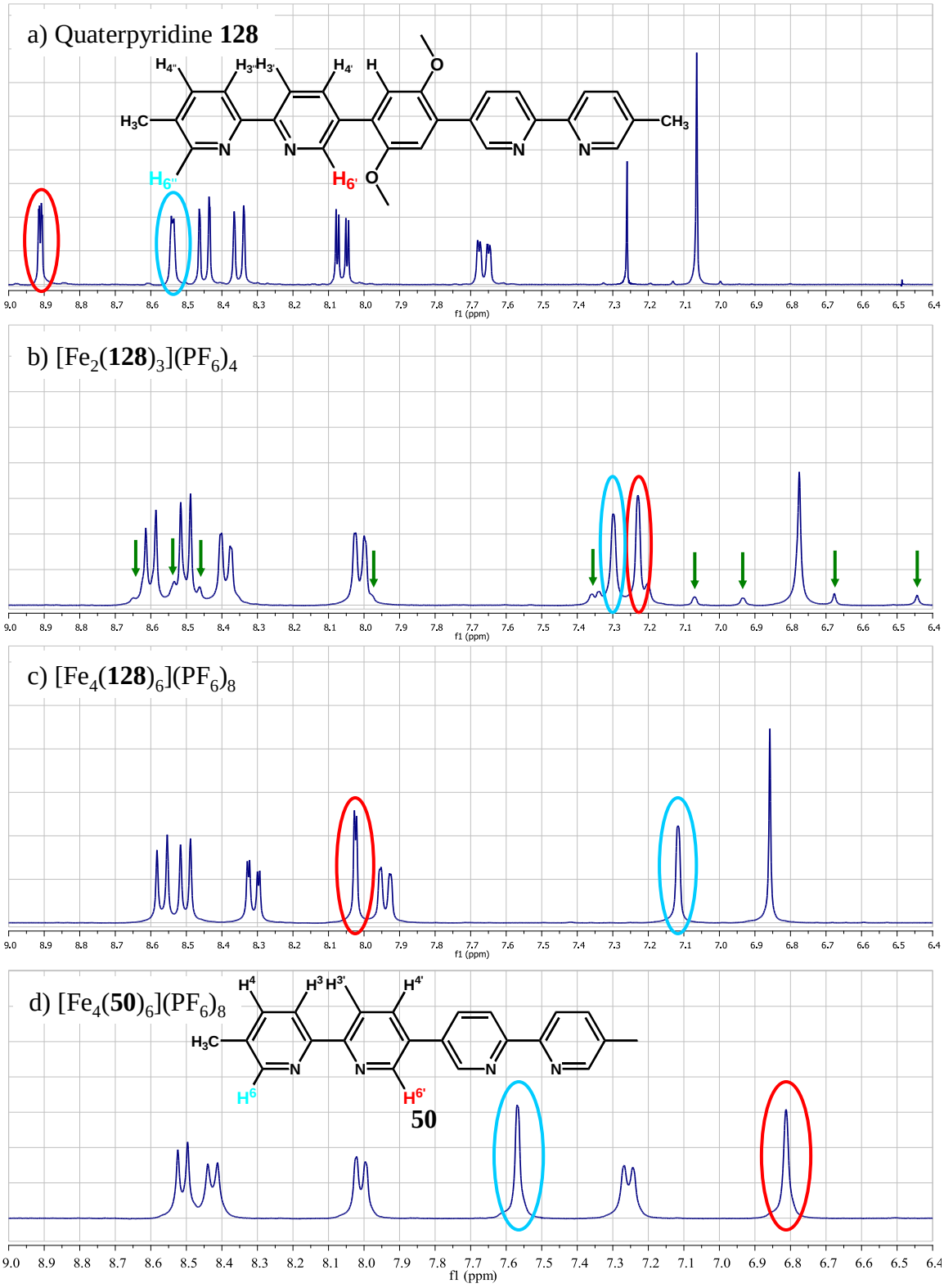

Figure 4.2 From top to bottom - ^{1}H NMR of the aromatic region of a) quaterpyridine **128** (in $CDCl_3$), and b) [Fe$_2$(**128**)$_3$](PF$_6$)$_4$, c) [Fe$_4$(**128**)$_6$](PF$_6$)$_8$ and d) [Fe$_4$(**50**)$_6$](PF$_6$)$_8$ (all in CD_3CN).

the H-6′ resonance in $[Fe_2(\mathbf{128})_3](PF_6)_4$. Another interesting observation was made on inspection of the ^{1}H NMR spectrum of the related M_4L_6 host-guest complex, $[Fe_4(\mathbf{50})_6 \supset PF_6](PF_6)_7$ (***Figure 4.2*** d)) (described in Chapter 3). In this latter complex the 6′-6′′-protons are shifted furthest upfield, in contrast to the 6′-protons of $[Fe_4(\mathbf{128})_6](PF_6)_8$. So why do the 6′-protons in $[Fe_4(\mathbf{128})_6](PF_6)_8$ experience less shielding? One explanation could be that the larger cavity size results in less electron density experienced from a closely situated PF_6^- guest and/or adjacent Fe(II) tris-bipyridyl moieties within the M_4L_6 complex. With respect to the former possibility, a ^{19}F NMR spectrum of $[Fe_4(\mathbf{128})_6](PF_6)_8$ indicated that the PF_6^- counterions existed in a single environment, thus indicating fast exchange on the NMR time scale. This latter observation is consistent with the expected larger size of both the cavity and the faces of the $[Fe_4(\mathbf{128})_6]^{8+}$ complex cation.

Interestingly, the ^{1}H NMR spectrum of $[Fe_2(\mathbf{128})_3](PF_6)_4$ indicated the presence of dynamic behaviour which was moderately slow on the NMR timescale (***Figure 4.2*** b)) see green arrows). Perhaps related to this observation is the fact that over extended periods of time (months) there was evidence that $[Fe_2(\mathbf{128})_3](PF_6)_4$ in solution slowly interconverted to $[Fe_4(\mathbf{128})_6](PF_6)_8$. In fact for extended reaction times using microwave heating $[Fe_4(\mathbf{128})_6](PF_6)_8$ was observed to be the sole product formed. This latter observation strongly suggests that the M_4L_6 complex is the thermodynamic product while the M_2L_3 complex is a kinetic product.

Crystals of $[Fe_4(\mathbf{128})_6](PF_6)_8$ suitable for X-ray diffraction were grown from THF/CH_3CN and the resulting structure confirmed a tetrahedral assembly (***Figure 4.3***). Interestingly, a PF_6^- anion is encapsulated within the cage such that the solid state formula is $[Fe_4(\mathbf{128})_6 \supset PF_6](PF_6)_7$ (***Figure 4.3*** a)). The product crystallizes in the centrosymmetric triclinic space group *P-1* and individual Fe(II) centres in each tetrahedron contain homochiral metal centres; that is, each tetrahedron is either *ΛΛΛΛ* or *ΔΔΔΔ*. The chiral twist associated with each M_4L_6 tetrahedron is evident when viewed down one of the C_3-axes (***Figure 4.3*** b)). The average distance between each of the Fe(II) centres is 13.43 Å, which corresponds to an encapsulated volume of approximately 285 Å^3.

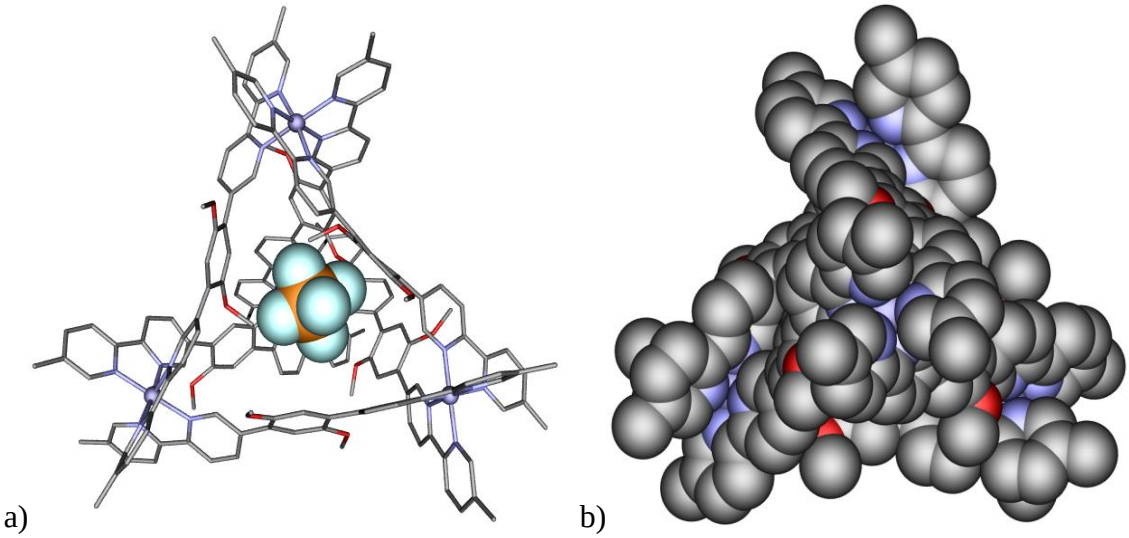

Figure 4.3 Representations of the crystal structure of $[Fe_4(\mathbf{128})_6 \supset PF_6](PF_6)_7$, **162**, a) illustrates the encapsulated PF_6^- guest, and b) a space filling diagram view down a C_3-axis (hydrogens, counterions and solvent are removed for clarity).

Unfortunately, attempts to grow crystals of $[Fe_2(\mathbf{128})_3](PF_6)_4$ suitable for X-ray crystallography were unsuccessful. However, a product from an analogous metal-directed assembly experiment with quaterpyridine **128**, using Ni(II) as the octahedral metal ion, gave crystal growth from THF/CH_3CN. The crystal structure of this material revealed a M_2L_3 triple helicate of formula $[Ni_2(\mathbf{128})_3](PF_6)_4$, **163** (***Figure 4.4***). The helicate crystallizes in the non-centrosymmetric hexagonal chiral space group $P6_322$ with two independent complexes per unit cell; thus each crystal is itself optically active. The two octahedral Ni(II) centres are separated by 11.8 Å and bridged by three quaterpyridine ligands such that the stereochemistry

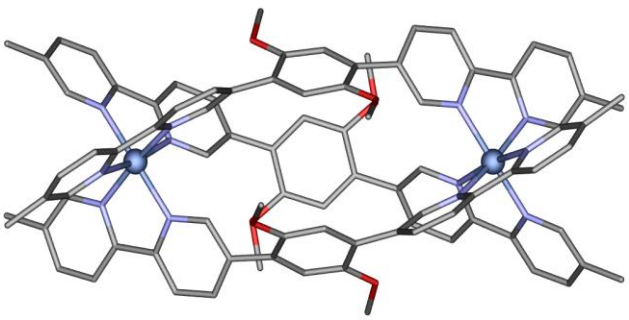

Figure 4.4 Crystal structure of $[Ni_2(\mathbf{128})_3](PF_6)_4$ **163** viewed perpendicular to its C_3-axis.

of the metal centres of each discrete unit are either $\Delta\Delta$ (*P*) or $\Lambda\Lambda$ (*M*). Interestingly, while the elemental analysis of the Ni(II) helicate fits the formula $[Ni_2(\mathbf{128})_3](PF_6)_4.2H_2O$, the ESI-HRMS indicated that, in solution at least, a mixture of M_2L_3 and M_4L_6 complexes was present. This observation either represented a fortuitous selection of a homogeneous crystal in the crystallographic study or a fractional driven crystallization process. In any case, due to the sterically demanding nature of quaterpyridine **128**, $[Ni_2(\mathbf{128})_3](PF_6)_4$ is almost certainly similar in structure to $[Fe_2(\mathbf{128})_3](PF_6)_4$.

The red colouration of both $[Fe_2(\mathbf{128})_3](PF_6)_4$ and $[Fe_4(\mathbf{128})_6](PF_6)_8$ is characteristic of the $[Fe(bpy)_3]^{2+}$ chromophore.[15] There is a slight red shift, essentially within experimental error, for the MLCT band of $[Fe_2(\mathbf{128})_3](PF_6)_4$ (537 nm) compared to that of $[Fe_4(\mathbf{128})_6](PF_6)_8$ (535 nm) (***Figure 4.5*** a)). The most noticeable difference in the UV-vis

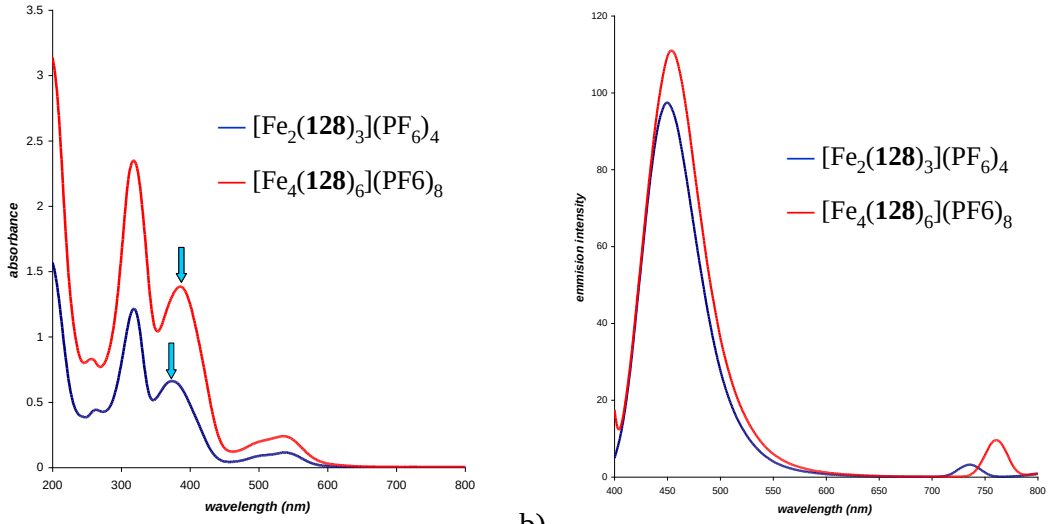

a) b)

Figure 4.5 a) Overlaid UV-vis spectra and b) fluorescence spectra for $[Fe_{2n}(\mathbf{128})_{3n}](PF_6)_{4n}$ (n = 1 and 2).

spectra are the CT bands associated with the presence of the dimethoxyphenylene-bridge. Here, a 12 nm blue shift is observed for $[Fe_2(\mathbf{128})_3](PF_6)_4$ (374 nm) compared to that of $[Fe_4(\mathbf{128})_6](PF_6)_8$ (386 nm). As might be expected, the molar extinction coefficients of the absorptions for the M_2L_3 complex are approximately one half those for the M_4L_6 complex. Fluorescence spectroscopy revealed a strong emission at 450 nm (blue) and a weaker emission at 736 nm resulting from excitation of $[Fe_2(\mathbf{128})_3](PF_6)_4$ at 374 nm (***Figure 4.5*** b)).

Similarly, a strong emission at 455 nm and a weaker emission at 761 nm was observed when $[Fe_4(\mathbf{128})_6](PF_6)_8$ was irradiated at 386 nm. Interestingly, the higher energy emissions of both complexes are strongly concentration dependent indicating the occurrence of intermolecular quenching and thus the possibility of aggregation behaviour. The higher energy emission is also quenched when HCl (g) is bubbled through acetonitrile solutions of these complexes.

The above photophysical characteristics suggest potential applications for these complexes. Selective anion signalling is a topic of much current interest,[16-21], thus one possibility for the present system is its use for fluorescent signalling of a host-guest interaction in an application as a guest-specific sensor.[22-27] In particular, complexes such as $[Fe_4(\mathbf{128})_6](PF_6)_8$ could represent a novel class of size-selective anion sensing devices. Certainly there is a need to explore such possible applications in the future.

4.2.2 $[M_2(129)_3]^{4+}$ helicates and $[M_4(129)_6]^{8+}$ tetrahedra

The metal-directed assembly of tetramethoxybiphenylene quaterpyridine **129** with Fe(II) resulted in the production of both $[Fe_2(\mathbf{129})_3](PF_6)_4$, **164**, and $[Fe_4(\mathbf{129})_6](PF_6)_8$, **165**, in an approximate 1:9 ratio. The mass spectrum of $[Fe_2(\mathbf{129})_3](PF_6)_4$ gave +3 and +4 ions consistent with the successive losses of PF_6^- from its formula. At 300 K the ^{1}H NMR spectrum of $[Fe_2(\mathbf{129})_3](PF_6)_4$ showed five relatively sharp aromatic signals corresponding to pyridyl protons in the 3- and 4-positions together with the phenylene protons in the 6,6′-positions. There were also three broad aromatic peaks corresponding to pyridyl protons in the 6′′-positions and biphenylene protons in the 3,3′-positions. This is indicative of the presence of a dynamic process taking place on the NMR timescale. In this regard, variable temperature NMR measurements resulted in a clear change in the ^{1}H NMR spectrum (see ***Figure 4.6***). At 290 K the broad peaks are broadened further, whilst at 310 K the peaks begin to sharpen; some minor signal shifts were also observed. Interestingly, while the M_2L_3 and M_4L_6 complexes can be easily separated chromatographically, signs that the M_2L_3 complex in acetonitrile interconverted to the M_4L_6 complex was evident after two to three days. Similar to the metal-directed assembly of dimethoxyphenylene-bridged quaterpyridine **128** with Fe(II), the M_4L_6 complex appears to be the thermodynamically favoured product in the present case as well.

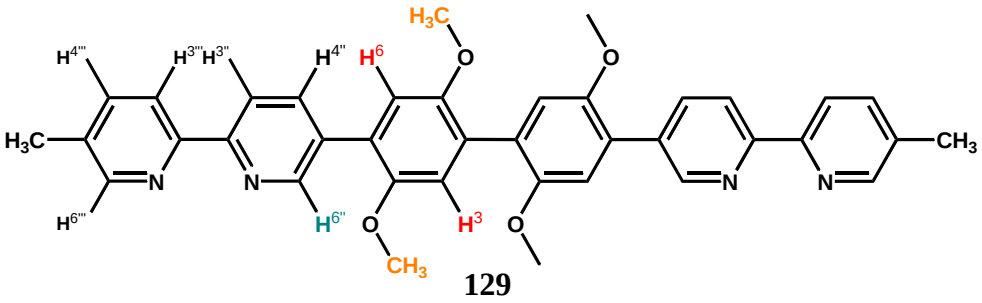

129

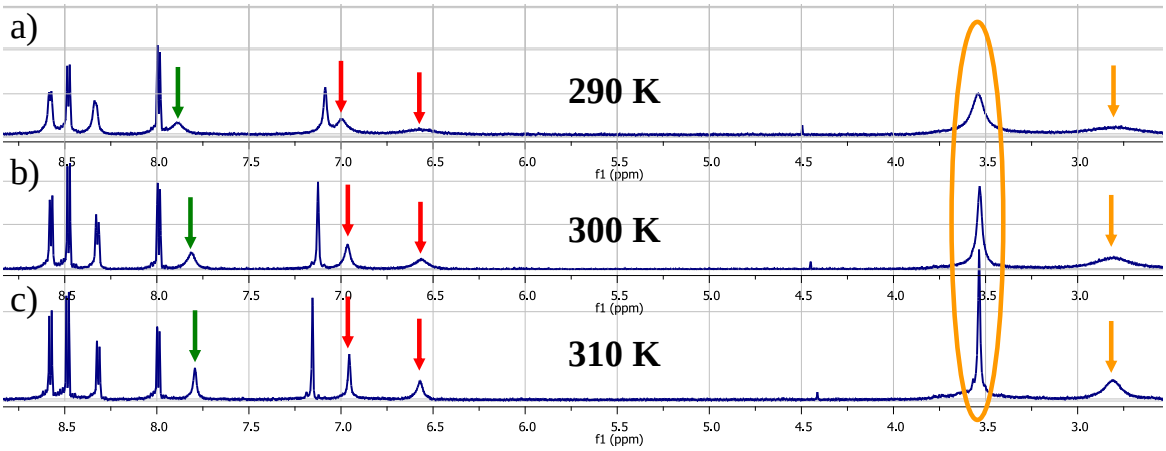

Figure 4.6 Variable temperature ^{1}H NMR spectra of [Fe_2(**129**)$_3$](PF_6)$_4$ in CD_3CN run at a) 290 K, b) 300 K, and c) 310 K.

In contrast to the ^{1}H NMR spectrum of [Fe_2(**129**)$_3$](PF_6)$_4$, [Fe_4(**129**)$_6$](PF_6)$_8$ gave a sharp spectrum with the expected eleven ^{1}H and nineteen ^{13}C resonances, indicating that quaterpyridine **129** exhibits C_2-symmetry within the complex. Again protons in the 6′′- and 6′′′-positions give resonances shifted upfield relative to those of the free ligand (***Figure 4.7***). [Fe_4(**129**)$_6$](PF_6)$_8$ is also stable in solution for months, consistent with it being the thermodynamically favoured product. The mass spectrum of this material gave +3 to +7 ions corresponding to successive losses of PF_6^- from the formula [Fe_4(**129**)$_6$](PF_6)$_8$.

The red colour of [Fe_2(**129**)$_3$](PF_6)$_4$ and [Fe_4(**129**)$_6$](PF_6)$_8$ is once again characteristic of the $[Fe(bpy)_3]^{2+}$ chromophore.[15] There is an apparent slight red shift, which may be within experimental error, for the MLCT band of [Fe_2(**129**)$_3$](PF_6)$_4$ (532 nm) compared to that of [Fe_4(**129**)$_6$](PF_6)$_8$ (529 nm). The most noticeable difference in the UV-vis spectra are the CT bands associated with the presence of the tetramethoxybiphenylene-bridge. Here an 11 nm

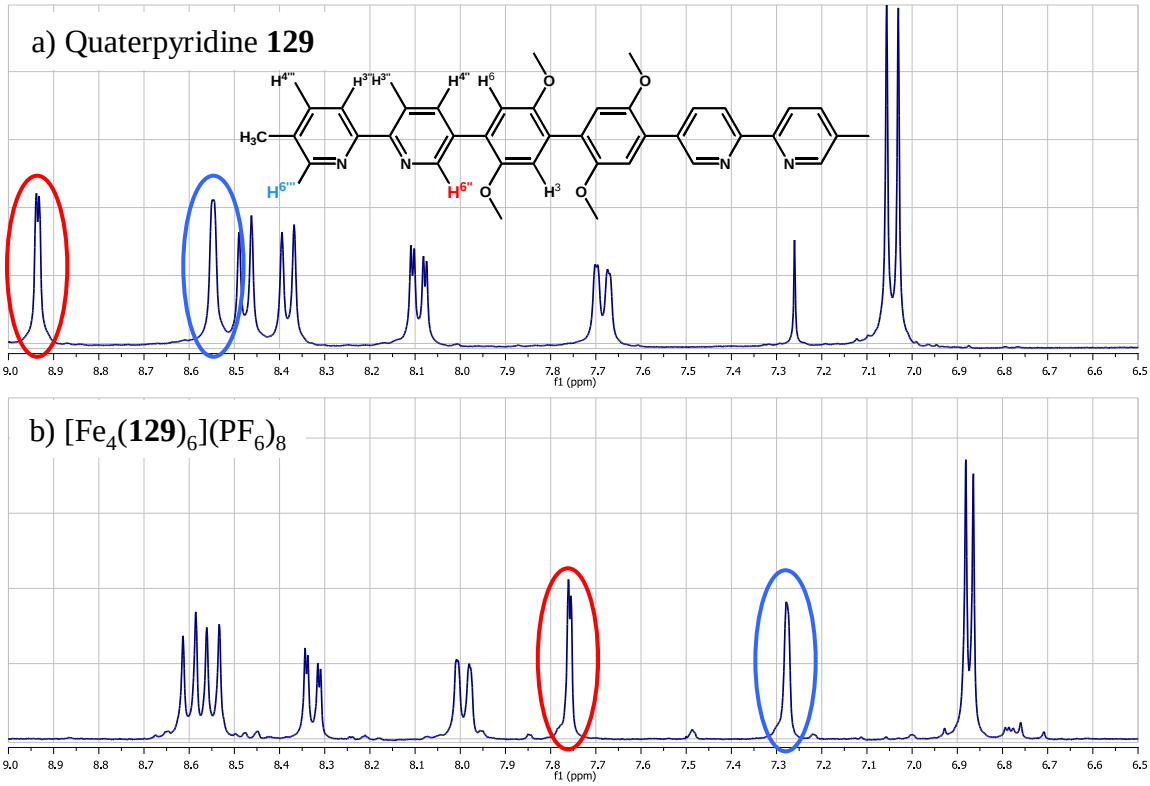

Figure 4.7 Comparison of the ^{1}H NMR spectra of the free quaterpyridine **129** in $CDCl_3$ and its M_4L_6 complex $[Fe_4(\mathbf{129})_6](PF_6)_8$ in CD_3CN.

blue shift is observed for $[Fe_2(\mathbf{129})_3](PF_6)_4$ (365 nm) relative to that for $[Fe_4(\mathbf{129})_6](PF_6)_8$ (376 nm) (***Figure 4.8*** a)). There is a strong emission at 451 nm (blue) and a weaker emission at 719 nm resulting from excitation of $[Fe_2(\mathbf{129})_3](PF_6)_4$ at 365 nm. Similarly a strong emission at 453 nm and a weaker emission at 743 nm was observed when $[Fe_4(\mathbf{129})_6](PF_6)_8$ was irradiated at 376 nm. Similar to $[Fe_{2n}(\mathbf{128})_{3n}](PF_6)_{4n}$ [28], the higher energy emissions for both complexes are strongly concentration dependent indicating the occurrence of intermolecular quenching and thus the possibility of aggregation behaviour occurring.

Crystals of $[Fe_4(\mathbf{129})_6](PF_6)_8$ suitable for X-ray diffraction were grown from THF/CH_3CN and the resulting structure confirmed the presence of a tetrahedral assembly (***Figure 4.9*** a)). The product crystallizes in the centric tetragonal space group $I\,4_1/a$. The structure is achiral due to each tetrahedron possessing a mixture of two Λ and two Δ metal centres. The average Fe—Fe distance is 16.9 Å, which corresponds to an impressive cavity volume of approximately 570 Å^3. Note that although the ^{1}H NMR of this material indicated that quaterpyridine **129** existed on a C_2-axis of symmetry within the complex, it is evident

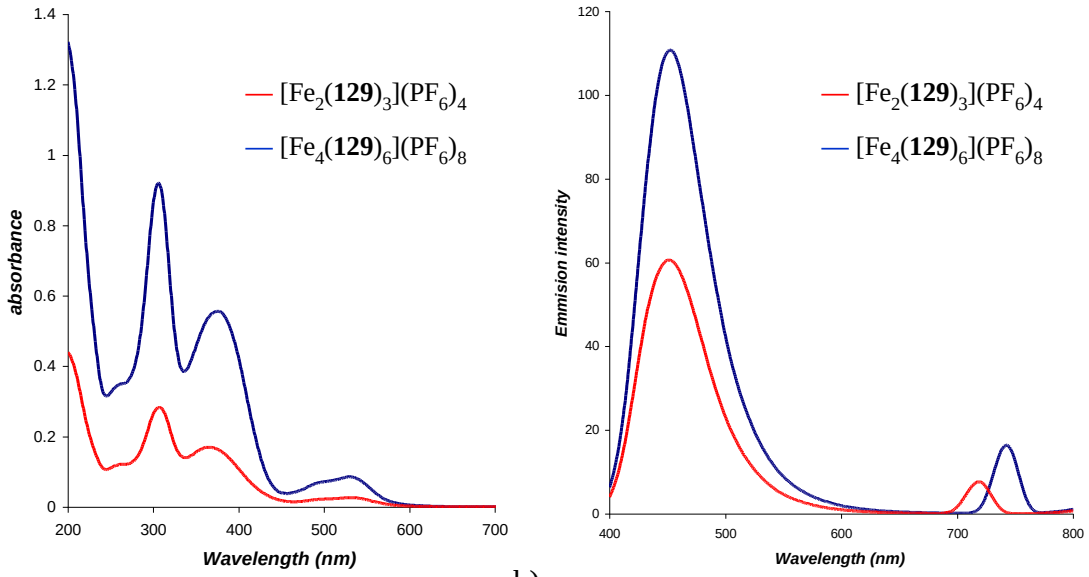

a) b)

Figure 4.8 a) UV-visible and b) fluorescence emission spectra of $[Fe_2(\mathbf{129})_3](PF_6)_4$ and $[Fe_4(\mathbf{129})_6](PF_6)_8$.

that this is not the case in the solid state. Perhaps this indicates the presence of a level of fast equilibration in solution with respect to the NMR timescale. However, reported rates [29-31] for the racemisation reaction of $[Fe_2(bpy)_3)]^{2+}$ (using a range of experimental conditions) are slow in comparison to the NMR timescale. The fast racemisation of metal centres hypothesis thus seems unlikely, particularly since M_4L_6 systems related to the current system are reported to result in much slower rates of racemisation than their mononuclear counterparts.[32] Alternatively, the preferential crystallisation of the *ΛΛΔΔ* stereoisomer following a slow isomerisation from either *ΛΛΛΛ* or *ΔΔΔΔ*- steroisomers may occur. Interestingly, an analogous metal-directed assembly of quaterpyridine **129** using $NiCl_2.6H_2O$ in place of $Fe(BF_4).6H_2O$, yielded homochiral tetrahedra such that each tetrahedron was either *ΛΛΛΛ* or *ΔΔΔΔ*-$[Ni_4(\mathbf{47})_6](PF_6)_8$, **166** (***Figure 4.9*** b)). This product crystallized in the triclinic space group *P-1*. The Ni—Ni distances averaged 17.4 Å, which corresponds to an encapsulated volume of approximately 620 $Å^3$. It should be noted that the ESI-HRMS of this latter material revealed the presence of both the M_2L_3 and M_4L_6 assemblies. It is evident from the two structures illustrated in ***Figure 4.9*** that the increased length of the biphenylene-bridged quaterpyridine **129** is less sterically restrictive in M_4L_6 complexes compared to its shorter quaterpyridyl analogues, **50** and **128**.

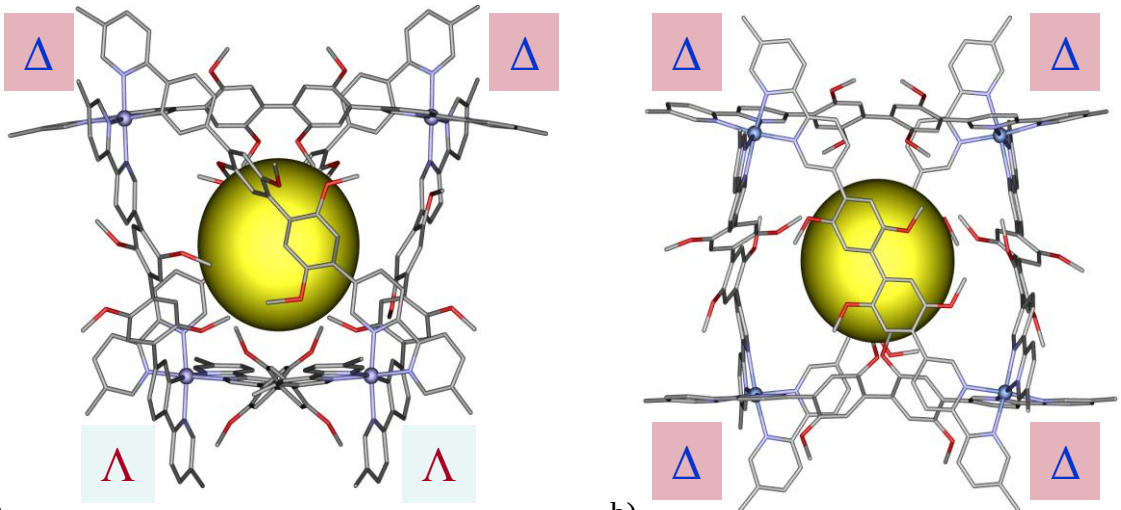

a) b)

Figure 4.9 Crystal structure of a) $[Fe_4(\mathbf{129})_6](PF_6)_8$ and b) $[Ni_4(\mathbf{129})_6](PF_6)_4$ (hydrogens, counterions and solvent are removed for clarity).

Analogous to results reported by Lehn *et al.*,[33] control of the outcomes of the above mentioned metal-directed assembly experiments incorporating either of the bridged quaterpyridines **128** or **129** with Fe(II) may be achieved. Extended reaction times were observed to lead to the sole production of M_4L_6 tetrahedra suggesting that this is the preferred thermodynamic outcome for Fe(II) assembly formation in both cases. On using shorter reaction times under high dilution conditions, the production of M_2L_3 complexes over M_4L_6 complexes was observed to be favoured. In fact in the case of the interaction of Fe(II) and **128** the helicate to tetrahedron product ratio could be altered from a 0:1 ratio all the way to a 7:1 ratio, as evidence by ^{1}H NMR.

4.2.3 Host-guest chemistry

The previous observation that $[Fe_4(\mathbf{50})_6](PF_6)_8$ shows a strong affinity for PF_6^- over BF_4^- led to an analogous selectivity study being conducted for the larger Fe(II) tetrahedra incorporating quaterpyridines **128** and **129**. As might be expected, inspection of the crystal structures of these larger M_4L_6 assemblies revealed much larger facial openings (see ***Figure 4.10***) in keeping with the relatively small PF_6^- ion being able to travel freely in and out of these larger systems. Consistent with this hypothesis, ^{19}F NMR spectra of both

$[Fe_4(\mathbf{128})_6](PF_6)_8$ and $[Fe_4(\mathbf{129})_6](PF_6)_8$ indicated that the PF_6^- ions underwent fast exchange to yield only a single ^{19}F resonance in each case.

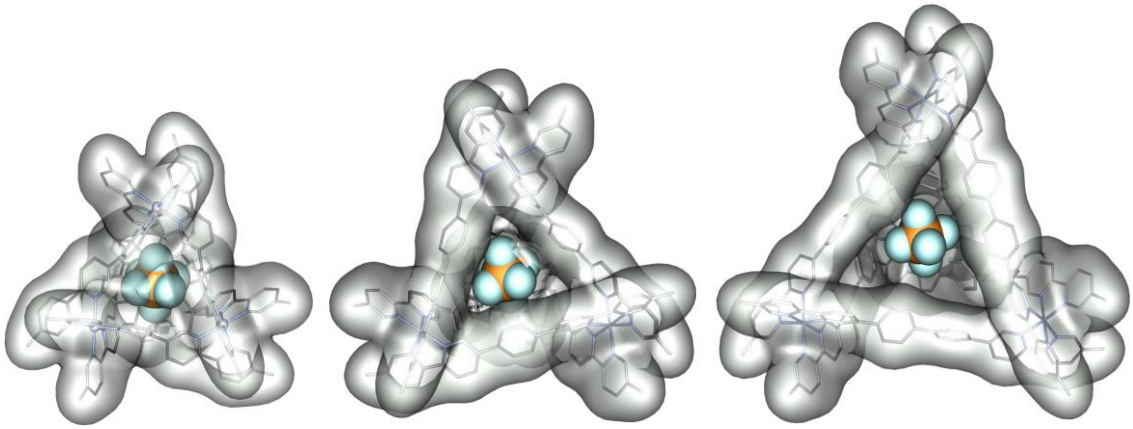

a = 9.45 Å V = ~99 Å^3 | a = 13.43 Å V = ~285 Å^3 | a = 17.23 Å V = ~620 Å^3

Figure 4.10 Space filling models based on the corresponding crystallographic structures for comparing the respective M_4L_6 (M = Fe(II) or Ni(II)) tetrahedra derived from **50**, **128** and **129** (hydrogens, anions, solvent and methoxy groups removed for clarity).

The larger size of $[Fe_4(\mathbf{129})_6]^{8+}$ prompted an investigation into the possibility it may be able to encapsulate BPh_4^-. ^1H NMR experiments designed to investigate this possibility were conducted. Starting with the BF_4^- salt of $[Fe_4(\mathbf{129})_6]^{8+}$ one equivalent of BPh_4^- was added. Comparison of the ^1H NMR spectra of this product (***Figure 4.11*** c)) with that of the starting product, $[Fe_4(\mathbf{129})_6](BF_4)_8$ (***Figure 4.11*** a)), indicated significant broadening of the 6,6′-proton and the 2,2′-methoxy-proton signals. The dynamic nature of the process involved was investigated using variable temperature NMR (***Figure 4.11*** b) to d)). At lower temperatures further broadening occurs until at 280 K the before-mentioned peaks are almost

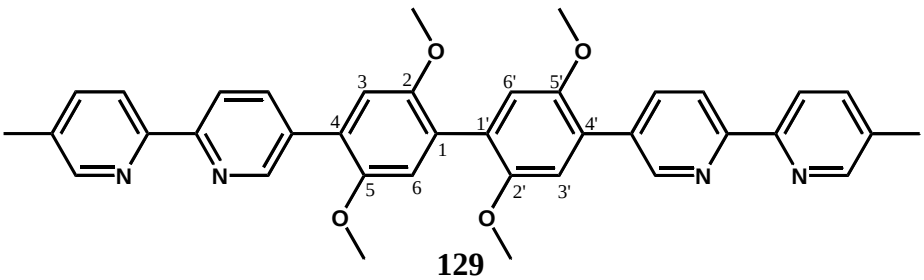

129

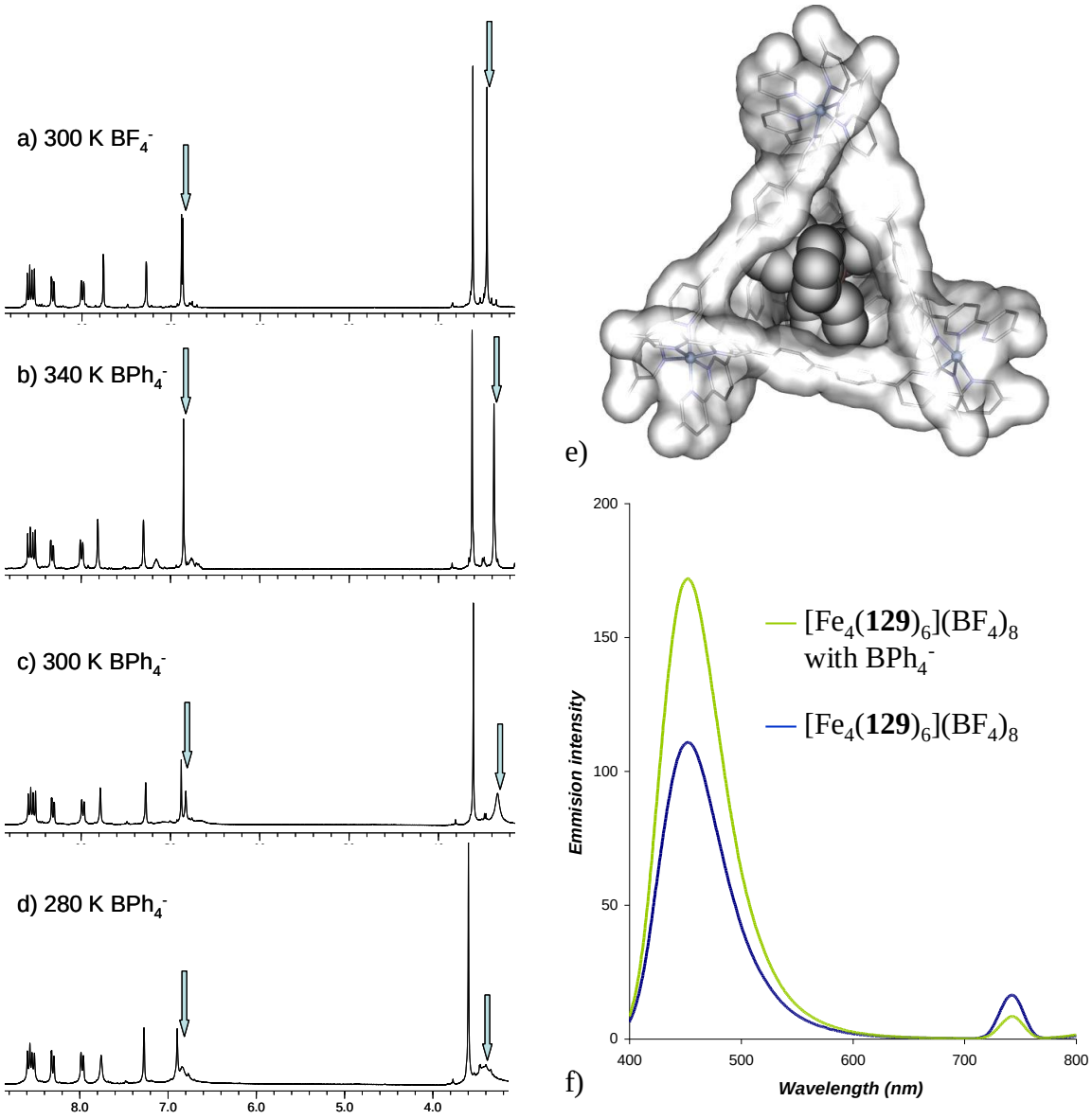

Figure 4.11 ^{1}H NMR spectrum of a) $[Fe_4(\mathbf{129})_6](BF_4)_8$, b) to d) variable temperature ^{1}H NMR spectra after addition of one equivalent of BPh_4^-, e) model of $[Fe_4(\mathbf{129})_6 \supset BPh_4]^{7+}$ with proposed encapsulation of BPh_4^- guest, and f) fluorescence spectra before and after addition of BPh_4^- to a solution of $[Fe_4(\mathbf{129})_6](BF_4)_8$ in acetonitrile.

completely obscured. On increasing the temperature to 340 K the rate of the dynamic process involved increased leading to a sharpening of these peaks. This behaviour is consistent with an anion exchange process occurring on the NMR timescale. From close inspection of the crystal structure of $[Fe_4(\mathbf{129})_6]^{8+}$, paying particular attention to the size of the faces, it seems

likely that a BPh_4^- anion would be able to undergo a 'through side' exchange process (***Figure 4.11*** e)).

Another indication that the BPh_4^- was encapsulated within this large M_4L_6 cage came from a fluorescence study. Again starting with a acetonitrile solution of the BF_4^- salt of $[Fe_4(\mathbf{129})_6]^{8+}$, one equivalent of BPh_4^- was added. Comparison of the fluorescence emission spectra of this solution with that of the starting complex, $[Fe_4(\mathbf{129})_6](BF_4)_8$, on irradiation at 376 nm, revealed a large increase in emission intensity at 453 nm for the former and an equally large decrease at 742 nm (***Figure 4.11*** f)). This enhancement of the higher energy emission may be related to partial desolvation of the M_4L_6 cavity and a subsequent reduction in solvent mediated quenching.[19]

The observations outlined above for M_4L_6 complexes incorporating quaterpyridines **128** and **129** have stemmed from preliminary work only and clearly further more detailed investigation is required to fully elucidate the behaviour described.

4.2.4 M_2L_3 complexes incorporating flexibly bridged quaterpyridines 149 – 151.

The final section of this chapter outlines the outcomes from metal-directed assembly reactions involving the interaction of either Fe(II) or Ni(II) with each of the flexibly bridged quaterpyridines **149** – **151**. In the first instance Fe(II) was reacted with each of quaterpyridines **149** – **151** in a 2:3 ratio. As previously stated, Fe(II) was used in the hope that these metal-directed assembly procedures could be followed by ^{1}H NMR.

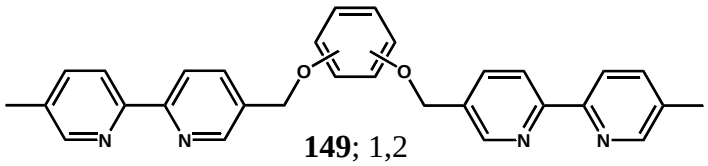

149; 1,2
150; 1,3
151; 1,4

TLC of the crude material from the interaction of $FeCl_2.5H_2O$ with catechol-bridged quaterpyridine **149**, using microwave heating with MeOH as solvent, indicated the predominance of a single product. This was purified by chromatography on silica gel and isolated as its PF_6^- salt. The ^{1}H NMR spectrum of this material indicated that the ligand

retained its two-fold symmetry within the complex; there were eight aromatic resonances (***Figure 4.12*** a)). However, there was evidence for the presence of another product of high symmetry (see red arrows in ***Figure 4.12*** a)).

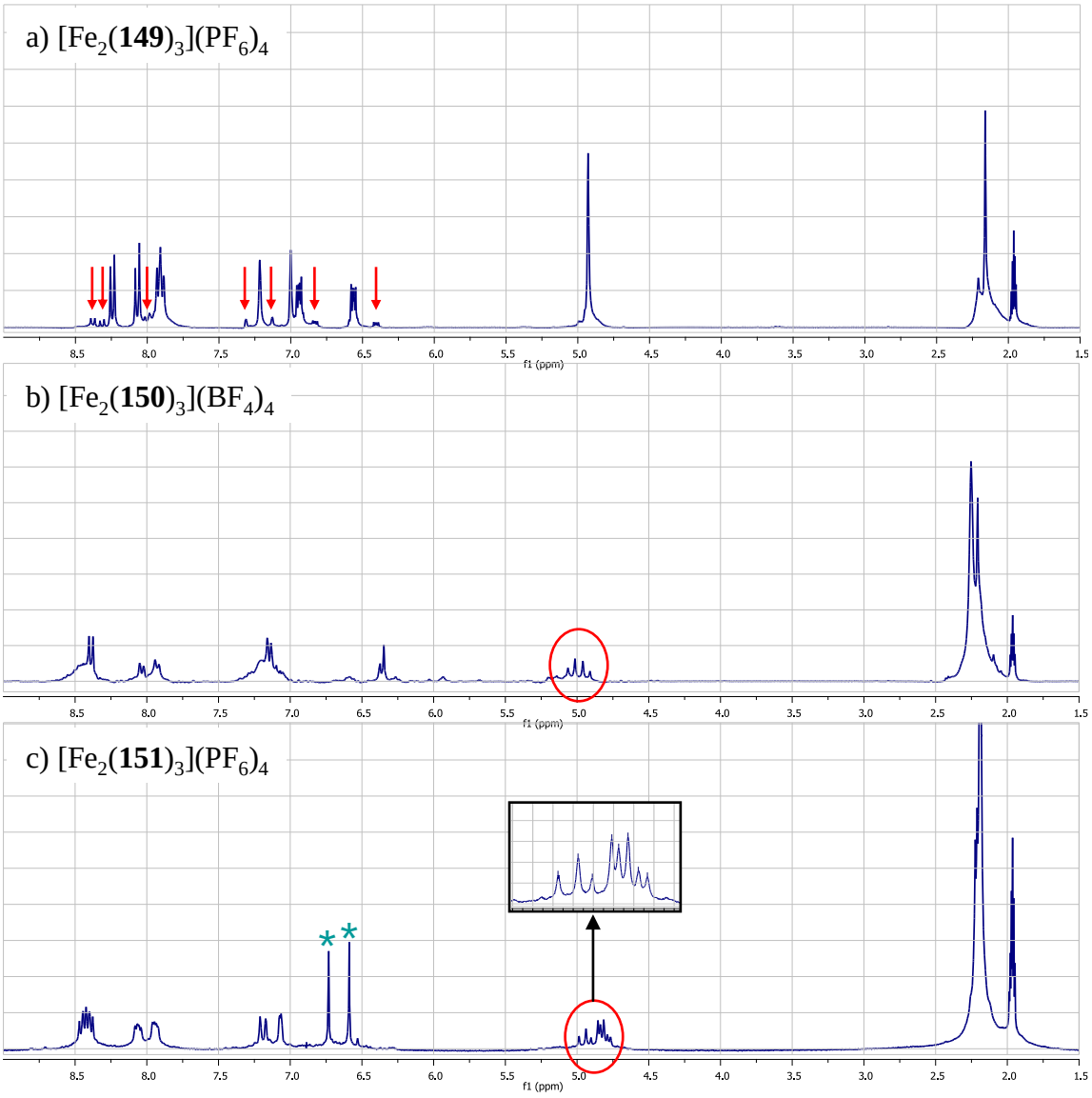

Figure 4.12 ^{1}H NMR spectra in CD_3CN of a) $[Fe_2(\mathbf{149})_3](PF_6)_4$, b) $[Fe_2(\mathbf{150})_3](BF_4)_4$ and c) $[Fe_2(\mathbf{151})_3](PF_6)_4$.

The ESI-HRMS of the above product revealed +2 to +4 ions corresponding to successive losses of PF_6^- from the formula $[Fe_2(\mathbf{149})_3](PF_6)_4$, **167** (***Figure 4.13*** a)). There was also evidence of a second series of ions corresponding to the successive losses of PF_6^- anions

from the formula $[Fe_4(\mathbf{149})_6](PF_6)_8$. The presence of this latter series is exemplified by the theoretical and observed isotopic distributions for the +5 ion, $\{[Fe_4(\mathbf{149})_6](PF_6)_3\}^{5+}$ (***Figure 4.13*** b)). The difference between this latter isotopic distribution and that for the +2 ion observed for the M_2L_3 series is worthy of note (see expanded peak in ***Figure 4.13*** a)). The relative intensities of peaks belonging to the M_2L_3 complex compared to those for the M_4L_6 complex is consistent with the former being the major product (it is noted that this interpretation of peak intensities may be misleading). Thus, the M_4L_6 complex may account for the symmetrical by-product observed in the ^{1}H NMR spectrum of this material. Based on the ^{1}H NMR spectrum and mass spectrum of the M_2L_3 complex, it can be assumed that the structure is either helical (i.e. ΔΔ or ΛΛ) or a *meso*-complex (ΔΛ). Note that if this M_2L_3 complex had two ligands acting as tetradentate donors to each metal ion, and the third as a bridge between the two metal ions, the ^{1}H NMR spectrum would be more complex than that observed, thus ruling this possibility out.

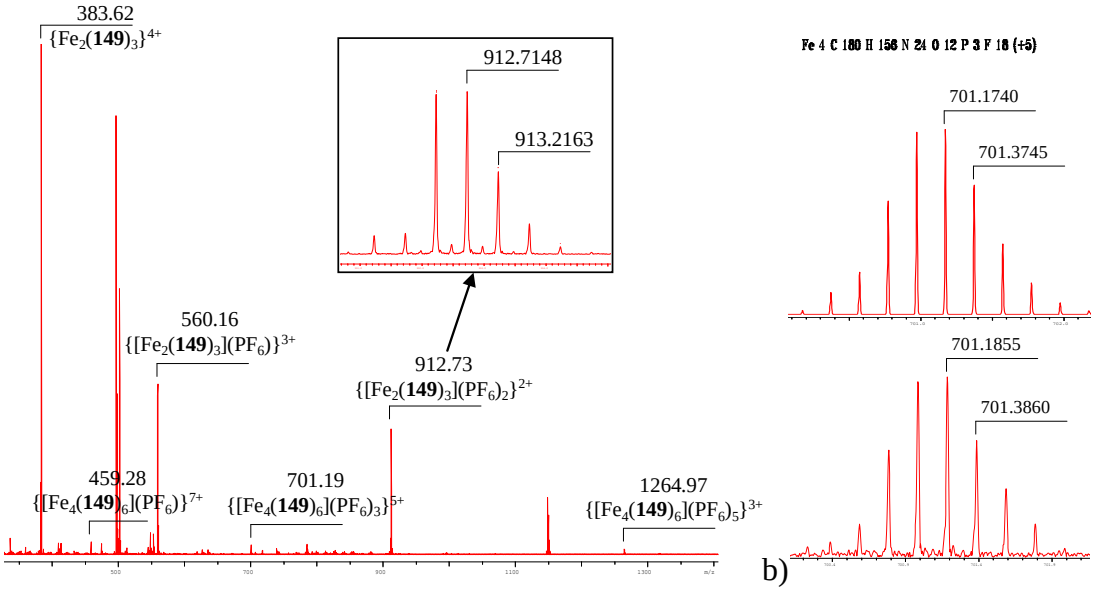

Figure 4.13 a) ESI-HRMS spectrum of $[Fe_2(\mathbf{149})_3](PF_6)_4$ showing evidence for the presence of $[Fe_4(\mathbf{149})_6](PF_6)_8$, and b) the theoretical and observed isotopic distributions for the +5 ion $\{[Fe_4(\mathbf{149})_6](PF_6)_3\}^{5+}$.

The TLC of the product from an analogous metal-directed assembly experiment employing $Fe(BF_4)_2.6H_2O$ and the resorcinol-bridged quaterpyridine **150** indicated the formation of a complex mixture of products. In this case, purification by chromatography on

silica gel resulted in the decomposition of the product. As a result, size exclusion chromatography was then employed and resulted in a semi-purified product (i.e. that was an improvement on the crude reaction mixture). The ^{1}H NMR spectrum of this material indicated that a product was present in which the ligand had retained its two-fold symmetry within the complex (***Figure 4.12*** b)). Non-equivalence of the phenoxymethylene protons is indicated by their splitting into an AB system. There is an underlying broadness to the spectrum indicative of some paramagnetic impurity or perhaps a dynamic process occurring on the NMR timescale. ESI-HRMS allowed the identification of +2 and +3 ions corresponding to the successive losses of BF_4^- from the formula $[Fe_2(\mathbf{150})_3](BF_4)_4$, **168**; ions corresponding to a M_4L_6 complex were not observed. As was the case for $[Fe_2(\mathbf{149})_3](BF_4)_4$, a crystal structure is required to determine which of the possible structural isomeric forms this species takes, but unfortunately suitable crystals were not forthcoming.

Finally, the interaction of the hydroquinone-bridged quaterpyridine **151** with $FeCl_2.5H_2O$ gave a predominance of a single product (as evidenced by TLC analysis). This material was purified by chromatography on silica gel and isolated as its PF_6^- salt. Interestingly, unlike for the previous two complexes, **167** and **168**, the ^{1}H NMR spectrum of this material indicated that the ligand existed in two different environments within the complex, or that the two ends of the originally two-fold symmetrical ligand were now non-equivalent. The most obvious proton resonances that reflect this are those that correspond to the hydroquinone-bridge protons, which in the free ligand are equivalent, but are now two singlets (see peaks marked with asterisks in ***Figure 4.12*** c)). As well, there are two overlapping AB systems for the phenoxymethylene protons (see expanded peaks marked with red circle in ***Figure 4.12*** c)). The ESI-HRMS of this material revealed +2 and +3 ion species corresponding to successive losses of PF_6^- from the formula $[Fe_2(\mathbf{151})_3](PF_6)_4$, **169**. Thus, based on the ^{1}H NMR spectrum and mass spectrum of this product, one might predict that two of the three ligands act as tetradentate donors to each metal ion within the complex, while the last acts as a bridge between them. Indeed, such an arrangement was observed for a similar metal-directed assembly product reported by Ward *et al.*[34] Furthermore, examination of a CPK model suggested that this structural motif is structurally plausible for $[Fe_2(\mathbf{151})_3](PF_6)_4$. Nevertheless, further structural evidence is required to confirm this

possibility. It should be noted that the ESI-HRMS of **169** also revealed much less intense ions corresponding to the successive losses of PF_6^- from the formula $[Fe_4(\mathbf{151})_6](PF_6)_8$.

In a subsequent set of experiments, a similar series of metal-directed assembly products were obtained by employing $NiCl_2.6H_2O$ in place of $FeCl_2.5H_2O$, when reacted with quaterpyridines **149** – **151**. The ESI-HRMS of the resulting products indicated that the major species were the M_2L_3 complexes, $[Ni_2(\mathbf{149})_3](PF_6)_4$, **170**, $[Ni_2(\mathbf{150})_3](PF_6)_4$, **171** and $[Ni_2(\mathbf{151})_3](PF_6)_4$, **172** (for a representative spectrum see ***Figure 4.14*** a)). Analogous to the equivalent Fe(II) M_2L_3 complexes incorporating quaterpyridines **149** and **151**, there was also some evidence of the formation of M_4L_6 complexes for the metal-directed assemblies incorporating these ligands and Ni(II) (see ***Figure 4.14*** c)). In these two cases, +3 ion species corresponding to the loss of three PF_6^- anions from the formulae $[Ni_4(\mathbf{149})_6](PF_6)_8$ and $[Ni_4(\mathbf{151})_6](PF_6)_8$ were observed. Note that the accuracy of the masses of these latter isotopic distributions were poor (approximately 30 ppm) and that the addition of the internal standard, STFA, resulted in these peaks no longer being observed. However, the good agreement between the theoretical and observed isotopic distributions leaves little doubt to the identity of these species. Interestingly, $[Ni_2(\mathbf{150})_3](PF_6)_4$ only gave ions corresponding to the loss of PF_6^- anions from this formula.

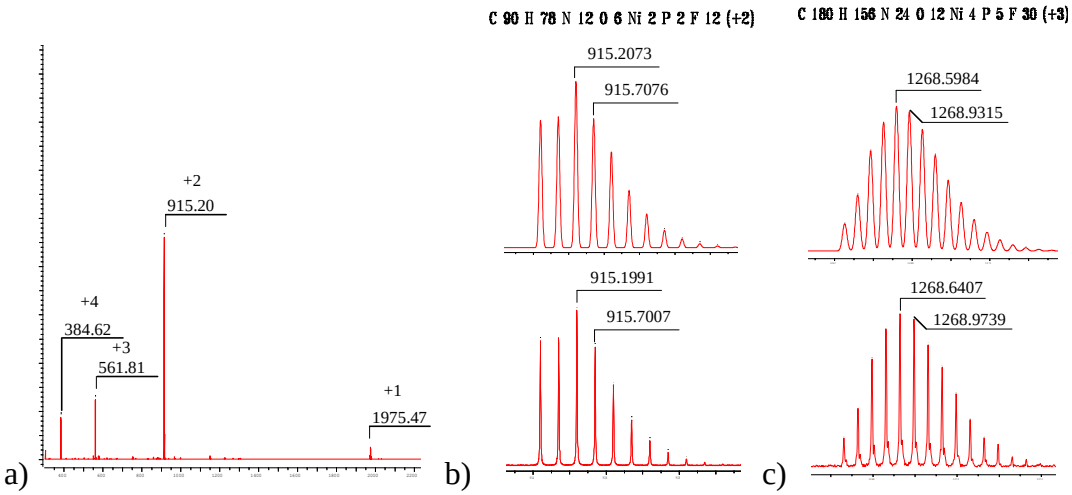

Figure 4.14 a) The mass spectrum of $[Ni_2(\mathbf{149})_3](PF_6)_4$ and the theoretical and observed isotopic distributions for, b) the +2 ion $\{[Ni_2(\mathbf{149})_3](PF_6)_2\}^{2+}$ and c) the +3 ion $\{[Ni_4(\mathbf{149})_6](PF_6)_5\}^{3+}$.

Fortunately, X-ray quality crystals of the above Ni(II) M_2L_3 complexes were able to be grown, allowing a comparison of their respective structures. Crystals of $[Ni_2(\mathbf{149})_3](PF_6)_4$ suitable for X-ray diffraction were grown from THF/CH_3CN. The structure confirmed the formulation of the product as being the M_2L_3 complex (***Figure 4.15*** a)). The product crystallised in the centrosymmetric monoclinic space group C 2/c. The two octahedral Ni(II) centres are separated by 10.8 Å and bridged by three quaterpyridine ligands such that the stereochemistry of the metal centres of each discrete unit are either $\Delta\Delta$ (*P*) or $\Lambda\Lambda$ (*M*). In this regard the space filling representation of the crystal structure shown in ***Figure 4.15*** b) best illustrates the helical twist of this complex. Thus, $[Ni_2(\mathbf{149})_3](PF_6)_4$ represents a true helicate in the solid state and may bear a similar structure to that of the Fe(II) complex $[Fe_2(\mathbf{149})_3](PF_6)_4$. It seems certain at least that the latter species is either a helicate or possibly even a *meso*-helicate. In this regard, the successful chiral resolution of $[Fe_2(\mathbf{149})_3](PF_6)_4$ by chromatography on chiral media[35,36] or alternatively, by fractional crystallisation using a chiral anion, may aid in the elucidation of the stereochemistry of this species.

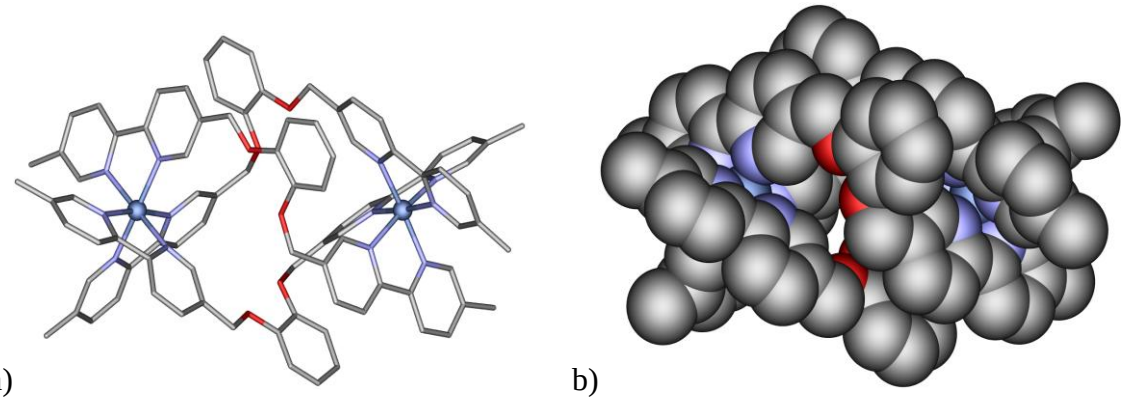

a) b)

Figure 4.15 a) Stick representation of the crystal structure of $[Ni_2(\mathbf{149})_3](PF_6)_4$ and b) space filling representation illustrating the helicity of this complex (hyrdogens, counterions and solvents removed for clarity).

Crystals of $[Ni_2(\mathbf{150})_3](PF_6)_4$ suitable for X-ray diffraction were grown from THF/CH_3CN. This complex crystallised in the centrosymmetric monoclinic space group P 21/c. The two octahedral Ni(II) centres are separated by 12.8 Å and bridged by three quaterpyridine ligands such that the stereochemistry of the metal centres of each discrete unit are either $\Delta\Delta$ (*P*) or $\Lambda\Lambda$ (*M*). The crystal structure reveals that a PF_6^- anion is encapsulated

such that in the solid state the structure is formulated as $[Ni_2(\mathbf{150})_3 \supset PF_6](PF_6)_3$ (***Figure 4.16*** a)). It was realised that a comparison of this latter structure with that of the Fe(II) equivalent, $[Fe_2(\mathbf{150})_3](BF_4)_4$, might be able to be made if a ^{19}F NMR spectrum were to reveal that the BF_4^- counterions existed in more that one environment. However, ideally, to obtain a true comparison, this latter complex would need to be isolated as its PF_6^- salt. In any case, inspection of the space filling representation of $[Ni_2(\mathbf{150})_3 \supset PF_6](PF_6)_3$ (***Figure 4.16*** b)) would suggest that an anion exchange process may well be quite fast under ambient conditions; low temperature ^{19}F NMR measurements on $[Fe_2(\mathbf{150})_3 \supset BF_4](BF_4)_3$ might provide experimental evidence for this.

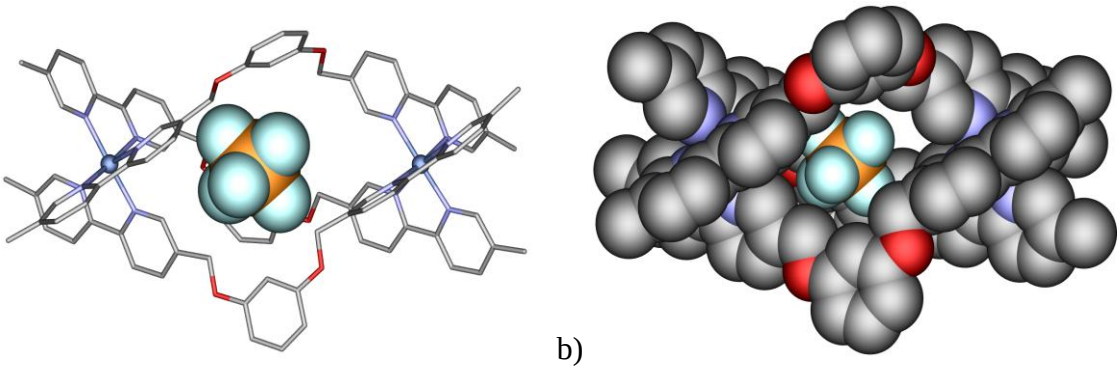

a) b)

Figure 4.16 a) Stick representation of the crystal structure of $[Ni_2(\mathbf{150})_3](PF_6)_4$ and b) space filling representation illustrating the helicity of this complex with the encapsulated PF_6^- anion (hyrdogens, counterions and solvents removed for clarity).

Crystals of $[Ni_2(\mathbf{151})_3](PF_6)_4$ suitable for X-ray diffraction were grown from THF/CH_3CN. The crystal structure of this material confirmed its formulation as $[Ni_2(\mathbf{151})_3](PF_6)_4$ (***Figure 4.17*** a)). This product crystallised in the centrosymmetric triclinic space group *P-1*. The two octahedral Ni(II) centres are separated by 14.1 Å and bridged by three quaterpyridine ligands such that the stereochemistry of the metal centres of each discrete unit are either *ΔΔ* (*P*) or *ΛΛ* (*M*) (i.e. a true helicate ***Figure 4.17*** b)). Interestingly, in this example the three ligands exist in two completely different conformations within the complex. For two ligands one of the bipyridyl groups is at approximately 80° to the plane of the hydroquinone bridge which is coplanar to the other bipyridyl group (***Figure 4.17*** c)). The other ligand is in a linear conformation within the complex with each coordination domain 180° to the other (***Figure 4.17*** d)). The latter is related to the S-shaped conformation that

Albrecht described[3] as being beneficial for helicate formation. Interestingly, the two observed ligand conformations in the crystal structure of $[Ni_2(\mathbf{151})_3](PF_6)_4$ may also help to explain the asymmetry observed in the ^{1}H NMR spectrum of $[Fe_2(\mathbf{151})_3](PF_6)_4$.

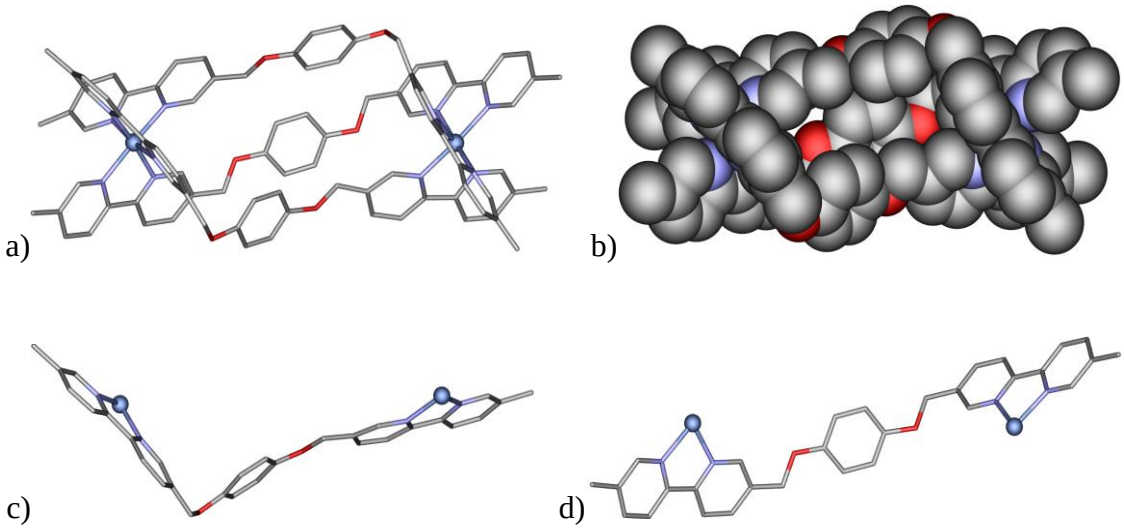

Figure 4.17 a) Stick representation of the crystal structure of $[Ni_2(\mathbf{151})_3](PF_6)_4$ and b) space filling representation illustrating the helicity of this complex, c) and d) represent the two conformations the ligand have in the complex (hyrdogens, counterions and solvents removed for clarity).

4.3 CONCLUSIONS

The interaction of quaterpyridines **128** and **129** with octahedral metal ions resulted in mixtures of M_2L_3 and M_4L_6 complexes. A level of control over the relative ratio of these products was demonstrated using a combination of reaction times and the degree of dilution employed for the synthesis. The successful synthesis of M_2L_3 helicates suggests that it may be possible to gain access to the proposed dinuclear cryptates through the use of appropriately substituted dialdehyde derivatives (see Chapter 5 *Section 5.2.4*). The extended quaterpyridines **128** and **129** have also allowed the formation of larger M_4L_6 tetrahedra with the potential to encapsulate guest species of larger size. In this regard, the larger tetrahedron, $[Fe_4(\mathbf{129})_6]^{8+}$, on interaction with BPh_4^- yields a fluorescent signal. It will be of interest in future studies to investigate the interaction of the M_4L_6 complexes incorporating both

quaterpyridines **128** and **129** with other potential guest species. It should be noted that there is potential for the substitution pattern of the phenylene and biphenylene bridges of these two ligands to be altered appropriately in order to optimise host-guest interactions.

The interaction Fe(II) and Ni(II) with quaterpyridines **149** and **151** predominantly resulted in the formation of M_2L_3 complexes. However, there was also evidence for the formation of the M_4L_6 complexes as well. The interaction of both Fe(II) and Ni(II) with quaterpyridine **150** yielded M_2L_3 complexes. In the Ni(II) complex, crystallographic data confirmed the formation of a host-guest species between the M_2L_3 helicate and the guest PF_6^- counterion. In this latter case there was no indication of the formation of an M_4L_6 complex, perhaps indicating the optimal geometry of this ligand for helicate formation compared to that of ligands **149** and **151** or, more speculatively, the operation of a favoured anion-template effect.

4.4 EXPERIMENTAL

See Chapter 2, section 2.3 Experimental, for general descriptions of techniques and materials and Chapter 3, section 3.5 Experimental, for X-ray structural data collection.

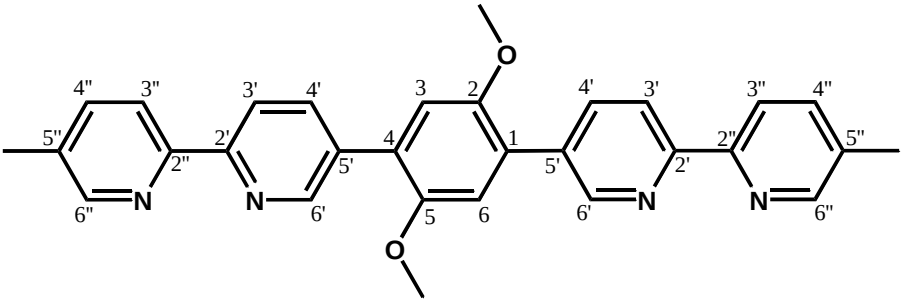

128

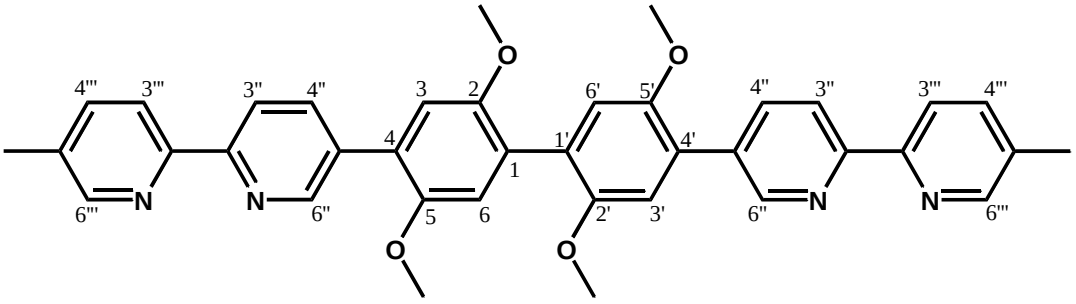

129

$[Fe_2(128)_3](PF_6)_4$ (161): A mixture of $Fe(BF_4)_2.6H_2O$ (24 mg, 0.07 mmol) and quaterpyridine **128** (50 mg, 0.105 mmol) in CH_3CN (50 cm^3) was heated with microwave energy in a sealed pressurised microwave vessel with temperature and pressure sensors and a magnetic stirrer bar (Step 1 – ramped to 130 °C over 2 min using 100 % of 400 W; Step 2 – held at 130 °C for 10 min using 25 % of 400 W). The crude product was purified by chromatography on silica gel with CH_3CN, H_2O and saturated KNO_3 (7:1:0.5) as eluent. The purified product was isolated by precipitation with excess aqueous NH_4PF_6 in H_2O (20 cm^3) followed by filtration, to afford **161** (49 mg, 70 %) as a red solid. UV/Vis (CH_3CN, nm): $\lambda_{max}(\varepsilon$ / dm^3 mol^{-1} cm^{-1}) = 263 (50 358), 318 (138 001), 374 (75 366), 537 (13 186); ^{1}H NMR (300 MHz, CD_3CN): δ = 2.28 (s, 18 H, CH_3), 3.49 (s, 18 H, OCH_3), 6.78 (s, 6 H, H-3,6), 7.23 (d, ^4J = 1.2 Hz, 6 H, H-6'), 7.30 (d, ^4J = 1.2 Hz, 6 H, H-6''), 8.01(dd, ^3J = 8.1 Hz, ^4J = 1.2 Hz, 6 H, H-4'), 8.39 (dd, ^3J = 8.4 Hz, ^4J = 1.2 Hz, 6 H, H-4''); 8.50 (d, ^3J = 8.1 Hz, 6 H, H-3'), 8.91 (d, ^3J = 8.4 Hz, 6 H, H-3''); ^{13}C NMR (75 MHz, CD_3CN): δ = 19.09, 58.22, 116.80, 124.60, 124.89, 126.13, 137.22, 137.37, 139.88, 140.52, 151.21, 154.53, 156.02, 157.02, 159.58; positive ion ESI-HRMS: m/z (M = $C_{90}H_{78}P_4F_{24}Fe_2N_{12}$ in CH_3CN / MeOH): calcd for $[M - 2PF_6]^{2+}$: 912.7086, found 912.7042; calcd for $[M - 3PF_6]^{3+}$: 560.1508, found 560.1490; calcd for $[M - 4PF_6]^{4+}$: 383.8719, found 383.8708.

$[Fe_4(128)_6](PF_6)_8$ (162): A mixture of $Fe(BF_4)_2.6H_2O$ (24 mg, 0.07 mmol) and quaterpyridine **128** (50 mg, 0.105 mmol) in CH_3CN (10 cm^3) was heated with microwave energy in a sealed pressurised microwave vessel with temperature and pressure sensors and a magnetic stirrer bar (Step 1 – ramped to 130 °C over 2 min using 100 % of 400 W; Step 2 – held at 130 °C for 30 min using 25 % of 400 W). The crude product was purified by chromatography on silica gel with CH_3CN, H_2O and saturated KNO_3 (7:1:0.5) as eluent. The purified product was isolated by precipitation with excess aqueous NH_3PF_6 in H_2O (20 cm^3) followed by filtration **162** (68 mg, 96 %) as a red solid. UV/Vis (CH_3CN, nm): $\lambda_{max}(\varepsilon$ / dm^3 mol^{-1} cm^{-1}) = 256 (94 411), 318 (266 837), 386 (157 445), 535 (27 418); ^{1}H NMR (300 MHz, CD_3CN): δ = 2.19 (s, 36 H, CH_3), 3.35 (s, 36 H, OCH_3), 6.86 (s, 12 H, H-3,6), 7.12 (d, ^4J = 1.2 Hz, 12 H, H-6'), 7.94 (dd, ^3J = 8.4 Hz, ^4J = 1.2 Hz, 12 H, H-4'), 8.02 (d, ^4J = 1.8 Hz, 12 H, H-6''), 8.31 (dd, ^3J = 8.7 Hz, ^4J = 1.8 Hz, 12 H, H-4''); 8.50 (d, ^3J = 8.4 Hz, 12 H, H-3'), 8.57 (d, ^3J = 8.7 Hz, 12 H, H-3''); ^{13}C NMR (75 MHz, CD_3CN): δ = 18.91, 57.45, 114.87,

124.28, 124.50, 125.91, 136.27, 139.09, 139.62, 140.45, 151.99, 155.25, 155.38, 157.16, 158.89; ^{19}F NMR (282.4 MHz, CD_3CN): δ = -73.28 (d, ^1J = 706.8 Hz, 48 F, $8PF_6$); positive ion ESI-HRMS: m/z (M = $C_{180}H_{156}P_8F_{48}Fe_4N_{24}$ in CH_3CN / MeOH): calcd for $[M - 3PF_6]^{3+}$: 1264.9324, found 1264.9310; calcd for $[M - 4PF_6]^{4+}$: 912.4581, found 912.4574; calcd for $[M - 5PF_6]^{5+}$: 700.9736, found 700.9731; elemental analysis (%) calcd for $C_{180}H_{156}P_8F_{48}Fe_4N_{24}O_{12}.6H_2O$ (4336.75 g mol^{-1}): C 49.80, H 3.90, N 7.75; found: C 49.85, H 3.94, N 7.35; X-ray quality crystals were obtained by diffusion of MeOH into an CH_3CN solution of the product.

$[Ni_2(128)_3](PF_6)_4$ (163): A mixture of $NiCl_2.6H_2O$ (13.3 mg, 0.056 mmol) and quaterpyridine **128** (40 mg, 0.084 mmol) in MeOH (10 cm^3) was heated with microwave energy in a sealed pressurised microwave vessel with temperature and pressure sensors and a magnetic stirrer bar (Step 1 – ramped to 130 °C over 2 min using 100 % of 400 W; Step 2 – held at 130 °C for 20 min using 25 % of 400 W). Excess NH_4PF_6 in H_2O (20 cm^3) was then added and the resulting solid isolated by filtration. The isolated product was obtained in near to quantitative yield. This material was recrystallised by diffusion of THF into a CH_3CN solution to afford **163** (48 mg, 39 %) as yellow cubic shaped crystals. Positive ion ESI-HRMS: m/z (M = $C_{90}H_{78}P_4F_{24}Ni_2N_{24}$ in CH_3CN / MeOH): calcd for $[M - 2PF_6]^{2+}$: 915.2073, found 915,2093; elemental analysis (%) calcd for $C_{90}H_{78}P_4F_{24}Ni_2N_{12}O_6.2H_2O$ (2154.37 g mol^{-1}): C 50.13, H 3.84, N 7.80; found: C 50.14, H 3.95, N 7.89; X-ray quality crystals were obtained by diffusion of THF into an CH_3CN solution of the product.

The crude product before recrystallisation also showed evidence for the presence of the corresponding M_4L_6 complex, $[Ni_4(\mathbf{128})_6](PF_6)_8$. Positive ion ESI-HRMS: m/z (M = $C_{180}H_{156}P_8F_{48}Ni_4N_{24}$ in CH_3CN / MeOH): calcd for $[M - 3PF_6]^{3+}$: 1268.5984, found 1268.5931.

$[Fe_2(129)_3](PF_6)_4$ (164): A mixture of $Fe(BF_4)_2.6H_2O$ (7.4 mg, 0.022 mmol) and quaterpyridine **129** (20 mg, 0.033 mmol) in CH_3CN (50 cm^3) was heated with microwave energy in a sealed pressurised microwave vessel with temperature and pressure sensors and a magnetic stirrer bar (Step 1 – ramped to 130 °C over 2 min using 100 % of 400 W; Step 2 –

held at 130 °C for 10 min using 25 % of 400 W). The crude product was purified by chromatography on silica gel with CH_3CN, H_2O and saturated KNO_3 (7:1:0.5) as eluent. The purified product was isolated by precipitation with excess aqueous NH_4PF_6 in H_2O (20 cm^3) followed by filtration, to afford **164** (17 mg, 62 %) as a red solid. UV/Vis (CH_3CN, nm): $\lambda_{max}(\varepsilon$ / dm^3 mol^{-1} $cm^{-1}) =$ 267 (40 156), 307 (100 390), 365 (60 387), 532 (9555); ^{1}H NMR (300 MHz, CD_3CN): δ = 2.29 (s, 18 H, CH_3), 2.82 (br s, 18 H, OCH_3), 3.56 (s, 18 H, OCH_3), 6.59 (br s, 6 H), 7.00 (br s, 6 H), 7.15 (s, 6 H), 7.84 (br s, 6 H), 8.02 (dd, ^3J = 8.1 Hz, ^4J = 1.2 Hz, 6 H), 8.36 (dd, ^3J = 8.4 Hz, ^4J = 1.8 Hz, 6 H), 8.51 (d, ^3J = 8.1 Hz), 8.61 (d, ^3J = 8.4 Hz, 6 H); positive ion ESI-HRMS: m/z (M = $C_{114}H_{102}P_4F_{24}Fe_2N_{12}$ in CH_3CN / MeOH): calcd for $[M - 3PF_6]^{3+}$: 696.2033, found 696.2033; calcd for $[M - 4PF_6]^{4+}$: 485.9113, found 485.9084.

$[Fe_4(129)_6](PF_6)_8$ (165): A mixture of $FeCl_2.5H_2O$ (12 mg, 0.055 mmol) and quaterpyridine **129** (50 mg, 0.082 mmol) in MeOH (10 cm^3) was heated with microwave energy in a sealed pressurised microwave vessel with temperature and pressure sensors and a magnetic stirrer bar (Step 1 – ramped to 130 °C over 2 min using 100 % of 400 W; Step 2 – held at 130 °C for 20 min using 25 % of 400 W). The crude product was purified by chromatography on silica gel with CH_3CN, H_2O and saturated KNO_3 (7:1:0.5) as eluent. The purified product was isolated by precipitation with excess aqueous NH_4PF_6 in H_2O (20 cm^3) followed by filtration, to afford **165** (62 mg, 90 %) as a red solid. UV/Vis (CH_3CN, nm): $\lambda_{max}(\varepsilon$ / dm^3 mol^{-1} $cm^{-1}) =$ 271 (114 304), 306 (310 254), 376 (187 839), 529 (29 000); ^{1}H NMR (300 MHz, CD_3CN): δ = 2.24 (s, 36 H, CH_3), 3.43 (s, 36 H, 2,2'-OCH_3), 3.57 (s, 36 H, 5,5'-OCH_3), 6.86 (s, 12 H, H-6,6'), 6.88 (s, 12 H, H-3,3'), 7.28 (s, 12 H, H-6'''), 7.76 (d, ^4J = 1.8 Hz, 12 H, H-6''), 8.01 (d, ^3J = 8.1 Hz, 12 H, H-4'''), 8.33 (dd, ^3J = 8.4 Hz, ^4J = 1.8 Hz, 12 H, H-4''); 8.55 (d, ^3J = 8.1 Hz, 12 H, H-3'''), 8.60 (d, ^3J = 8.4 Hz, 12 H, H-3''); ^{13}C NMR (75 MHz, CD_3CN): δ = 18.94, 56.97, 57.09, 114.47, 116.72, 123.81, 124.51, 124.72, 129.52, 137.42, 139.45, 139.83, 140.35, 150.79, 152.35, 155.13, 155.44, 157.40, 158.50; ^{19}F NMR (282.4 MHz, CD_3CN): δ = -73.49 (d, ^1J = 706.1 Hz, 48 F, $8PF_6$); positive ion ESI-HRMS: m/z (M = $C_{228}H_{204}P_8F_{48}Fe_4N_{24}$ in CH_3CN / MeOH): calcd for $[M - 3PF_6]^{3+}$: 1537.3716, found 1537.3467; calcd for $[M - 4PF_6]^{4+}$: 1116.7875, found 1116.7867; calcd for $[M - 5PF_6]^{5+}$: 864.4370, found 864.4375; calcd for $[M - 6PF_6]^{6+}$: 696.2034, found 696.1976; calcd for $[M - 7PF_6]^{7+}$: 576.0365, found 576.0365; elemental analysis (%) calcd for

$C_{228}H_{204}P_8F_{48}Fe_4N_{24}O_{24}.7H_2O$ (5171.08 g mol^{-1}): C 52.91, H 4.25, N 6.50; found: C 52.99, H 3.96, N 6.46; X-ray quality crystals were obtained by diffusion of THF into an CH_3CN solution of the product.

$[Ni_4(129)_6](PF_6)_8$ (166): A mixture of $NiCl_2.6H_2O$ (5.2 mg, 0.022 mmol) and quaterpyridine **129** (20 mg, 0.033 mmol) in MeOH (10 cm^3) was heated with microwave energy in a sealed pressurised microwave vessel with temperature and pressure sensors and a magnetic stirrer bar (Step 1 – ramped to 130 °C over 2 min using 100 % of 400 W; Step 2 – held at 130 °C for 20 min using 25 % of 400 W). Excess NH_4PF_6 in H_2O (20 cm^3) was then added and the resulting solid isolated by filtration. The isolated product was obtained in near quantitative yields. This material was recrystallised by diffusion of THF into a acetonitrile solution to afford **166** (15 mg, 58 %) as yellow cubic shaped crystals. Positive ion ESI-HRMS: m/z (*M* = $C_{228}H_{204}P_8F_{48}Ni_4N_{24}$ in CH_3CN / MeOH): calcd for $[M - 3PF_6]^{3+}$: 1541.0371, found 1541.0573; X-ray quality crystals were obtained by diffusion of THF into a CH_3CN solution of the product.

The crude product before recrystallisation also showed evidence for the presence of the corresponding M_2L_3 complex, $[Ni_2(\mathbf{129})_3](PF_6)_4$. Positive ion ESI-HRMS: m/z (*M* = $C_{114}H_{102}P_4F_{24}Ni_2N_{12}$ in CH_3CN / MeOH): calcd for $[M - 2PF_6]^{2+}$: 1119.2866, found 1119.2896.

$[Fe_2(149)_3](PF_6)_4$ (167): A mixture of $FeCl_2.5H_2O$ (30 mg, 0.14 mmol) and quaterpyridine **149** (110 mg, 0.232 mmol) in MeOH (10 cm^3) was heated with microwave energy in a sealed pressurised microwave vessel with temperature and pressure sensors (Step 1 – ramped to 130 °C over 2 min using 100 % of 400 W; Step 2 – held at 130 °C for 20 min using 25 % of 400 W). The crude product was purified by chromatography on silica gel with CH_3CN, H_2O and saturated KNO_3 (7:1:0.5) as eluent. The purified product was isolated by precipitation with excess aqueous NH_4PF_6 in H_2O (20 cm^3) followed by filtration, to afford **167** (132 mg, 90 %) as a semi-pure red solid. ^{1}H NMR (300 MHz, CD_3CN): δ = 2.16 (s, 18 H, CH_3), 4.93 (s, 12 H, OCH_2Ar), 6.56 (dd, J^3 = 6.0 Hz, J^4 = 3.6 Hz, 6 H, Ar-H), 6.94 (dd, J^3 = 6.0 Hz, J^4 = 3.6 Hz, 6 H, Ar-H), 7.00 (br s, 6 H), 7.22 (br s, 6 H), 7.91 (br m, 12 H), 8.07 (d, J^3 = 8.4 Hz, 6 H), 8.24

(d, J^3 = 8.3 Hz, 6 H), see ***Figure 4.12 a)***; positive ion ESI-HRMS: m/z (M = $C_{90}H_{78}P_4F_{24}Fe_2N_{12}O_6$ in CH_3CN / MeOH): calcd for $[M - 2PF_6]^{2+}$: 912.2073, found 912.2130; calcd for $[M - 3PF_6]^{3+}$: 559.8166, found 559.8168; calcd for $[M - 4PF_6]^{4+}$: 383.6213, found 383.6210.

$[Fe_2(150)_3](BF_4)_4$ (168): A mixture of $Fe(BF_4)_2.6H_2O$ (47 mg, 0.14 mmol) and quaterpyridine **150** (110 mg, 0.232 mmol) in CH_3CN (10 cm^3) was heated with microwave energy in a sealed pressurised microwave vessel with temperature and pressure sensors (Step 1 – ramped to 130 °C over 2 min using 100 % of 400 W; Step 2 – held at 130 °C for 20 min using 25 % of 400 W). The solvent was evaporated and the crude material was purified by chromatography on Sephadex LH-20 with CH_3CN as eluent. This allowed the isolation of **168** (109 mg, 83 %) as a deep red solid. ^{1}H NMR (300 MHz, CD_3CN): δ = 2.21 (s, 18 H, CH_3), 4.94 (d, J^2 = 14.8 Hz, 6 H, OCH_2Ar), 5.04 (d, J^2 = 14.8 Hz, 6 H, OCH_2Ar), 6.35, 6.38, 7.15, 7.93, 8.04, 8.39, see ***Figure 4.12 b)***; positive ion ESI-HRMS: m/z (M = $C_{90}H_{78}B_4F_{16}Fe_2N_{12}O_6$ in CH_3CN / MeOH): calcd for $[M - 2BF_4]^{2+}$: 854.2472, found 854.2486; calcd for $[M - 3BF_4]^{3+}$: 540.4966, found 540.4973.

$[Fe_2(151)_3](PF_6)_4$ (169): A mixture of $FeCl_2.5H_2O$ (30 mg, 0.14 mmol) and quaterpyridine **151** (110 mg, 0.232 mmol) in MeOH (10 cm^3) was heated with microwave energy in a sealed pressurised microwave vessel with temperature and pressure sensors (Step 1 – ramped to 130 °C over 2 min using 100 % of 400 W; Step 2 – held at 130 °C for 20 min using 25 % of 400 W).). The crude product was purified by chromatography on silica gel with CH_3CN, H_2O and saturated KNO_3 (7:1:0.5) as eluent. The purified product was isolated by precipitation with excess aqueous NH_4PF_6 in H_2O (20 cm^3) followed by filtration, to afford **169** (125 mg, 85 %) as a red solid. ^{1}H NMR (300 MHz, CD_3CN): δ = 2.21 (s, CH_3), 2.22 (s, CH_3), 4.79 (d, J^2 = 14.5 Hz, OCH_2Ar), 4.81 (d, J^2 = 14.9 Hz, OCH_2Ar), 4.88 (d, J^2 = 14.5 Hz, OCH_2Ar), 4.96 (d, J^2 = 14.9 Hz, OCH_2Ar), 6.59 (s, 6 H, Ar-H), 6.73 (s, 6 H, Ar-H), 7.06 (s, 3 H), 7.07 (s, 3 H), 7.17 (s, 3 H), 7.21 (s, 3 H), 7.94 (m, 6 H), 8.06 (m, 6 H), 8.42 (m, 12 H), see ***Figure 4.12 c)***; positive ion ESI-HRMS: m/z (M = $C_{90}H_{78}P_4F_{24}Fe_2N_{12}O_6$ in CH_3CN / MeOH): calcd for $[M - 2PF_6]^{2+}$: 912.2073, found 912.2130; calcd for $[M - 3PF_6]^{3+}$: 559.8166, found 559.8179.

$[Ni_2(149)_3](PF_6)_4$ (170): A stirred solution of $NiCl_2.6H_2O$ (17 mg, 0.07 mmol) and quaterpyridine **149** (50 mg, 0.105 mmol) in MeOH (10 cm^3) was heated with microwave energy in a sealed pressurised microwave vessel with temperature and pressure sensors (Step 1 – ramped to 130 °C over 2 min using 100 % of 400 W; Step 2 – held at 130 °C for 20 min using 25 % of 400 W). The product was isolated by precipitation with excess aqueous NH_4PF_6 in H_2O (20 cm^3) followed by filtration affording **170** quantitatively as a yellow solid. Positive ion ESI-HRMS: m/z (M = $C_{90}H_{78}P_4F_{24}Ni_2N_{12}O_6$ in CH_3CN / MeOH): calcd for $[M - 2PF_6]^{2+}$: 915.2073, found 915.1991; calcd for $[M - 3PF_6]^{3+}$: 561.8166, found 561.8224; calcd for $[M - 4PF_6]^{4+}$: 385.1213, found 385.1229; elemental analysis (%) calcd for $C_{90}H_{78}P_4F_{24}Ni_2N_{12}O_6.4H_2O$ (2190.39 g mol^{-1}): C 49.31, H 3.96, N 7.67; found: C 49.15, H 3.75, N 7.55; X-ray quality crystals were obtained by diffusion of THF into an CH_3CN solution of the product.

The crude product before recrystallisation also showed evidence for the presence of the corresponding M_4L_6 complex, $[Ni_4(\mathbf{149})_6](PF_6)_8$. Positive ion ESI-HRMS: m/z (M = $C_{180}H_{156}P_8F_{48}Ni_4N_{24}O_{12}$ in CH_3CN / MeOH): calcd for $[M - 3PF_6]^{3+}$: 1268.5984, found 1268.6407.

$[Ni_2(150)_3](PF_6)_4$ (171): A stirred solution of $NiCl_2.6H_2O$ (17 mg, 0.07 mmol) and quaterpyridine **150** (50 mg, 0.105 mmol) in MeOH (10 cm^3) was heated with microwave energy in a sealed pressurised microwave vessel with temperature and pressure sensors (Step 1 – ramped to 130 °C over 2 min using 100 % of 400 W; Step 2 – held at 130 °C for 20 min using 25 % of 400 W). The product was isolated by precipitation with excess aqueous NH_4PF_6 in H_2O (20 cm^3) followed by filtration affording **171** quantitatively as a yellow solid. Positive ion ESI-HRMS: m/z (M = $C_{90}H_{78}P_4F_{24}Ni_2N_{12}O_6$ in CH_3CN / MeOH): calcd for $[M - 2PF_6]^{2+}$: 915.2073, found 915.1989; calcd for $[M - 3PF_6]^{3+}$: 561.8130, found 561.8224; calcd for $[M - 4PF_6]^{4+}$: 385.1213, found 385.1192; elemental analysis (%) calcd for $C_{90}H_{78}P_4F_{24}Ni_2N_{12}O_6.4H_2O$ (2190.39 g mol^{-1}): C 49.31, H 3.96, N 7.67; found: C 49.31, H 3.72, N 7.66; X-ray quality crystals were obtained by diffusion of THF into an CH_3CN solution of the product.

$[Ni_2(151)_3](PF_6)_4$ (172): A stirred solution of $NiCl_2.6H_2O$ (17 mg, 0.07 mmol) and quaterpyridine **150** (50 mg, 0.105 mmol) in MeOH (10 cm^3) was heated with microwave energy in a sealed pressurised microwave vessel with temperature and pressure sensors (Step 1 – ramped to 130 °C over 2 min using 100 % of 400 W; Step 2 – held at 130 °C for 20 min using 25 % of 400 W). The product was isolated by precipitation with excess aqueous NH_4PF_6 in H_2O (20 cm^3) followed by filtration affording **172** quantitatively as a yellow solid. Positive ion ESI-HRMS: m/z (M = $C_{90}H_{78}P_4F_{24}Ni_2N_{12}O_6$ in CH_3CN / MeOH): calcd for $[M - 2PF_6]^{2+}$: 915.2073, found 915.1974; calcd for $[M - 3PF_6]^{3+}$: 561.8130, found 561.8131; calcd for $[M - 4PF_6]^{4+}$: 385.1213, found 385.1235; elemental analysis (%) calcd for $C_{90}H_{78}P_4F_{24}Ni_2N_{12}O_6.4H_2O$ (2190.39 g mol^{-1}): C 49.31, H 3.96, N 7.67; found: C 49.43, H 3.80, N 7.75; X-ray quality crystals were obtained by diffusion of THF into an CH_3CN solution of the product.

The crude product before recrystallisation also showed evidence for the presence of the corresponding M_4L_6 complex, $[Ni_4(\mathbf{151})_6](PF_6)_8$. Positive ion ESI-HRMS: m/z (M = $C_{180}H_{156}P_8F_{48}Ni_4N_{24}O_{12}$ in CH_3CN / MeOH): calcd for $[M - 3PF_6]^{3+}$: 1268.5984, found 1268.6423.

4.7 REFERENCES

1. P. J. Steel, *Acc. Chem. Res.*, 2005, **38**, 243.
2. M. Albrecht and R. Frohlich, *Bull. Chem. Soc. Jpn*, 2007, **80**, 797.
3. M. Albrecht, *Chem. Eur. J.*, 2000, **6**, 3485.
4. M. Albrecht, *Chem. Soc. Rev.*, 1998, **27**, 281.
5. D. L. Caulder and K. N. Raymond, *Angew. Chem. Int. Ed.*, 1997, **36**, 1440.
6. M. Albrecht and M. Schneider, *Eur. J. Inorg. Chem.*, 2002, **2002**, 1301.
7. M. Albrecht, *Chem. Rev.*, 2001, **101**, 3457.
8. C. R. K. Glasson, L. F. Lindoy and G. V. Meehan, *Coord. Chem. Rev.*, 2008, **252**, 940.
9. M. J. Hannon and L. J. Childs, *Supramol. Chem.*, 2004, **16**, 7.
10. C. Piguet, G. Bernardinelli and G. Hopfgartner, *Chem. Rev.*, 1997, **97**, 2005.
11. M. Albrecht, M. Schneider and R. Frohlich, *New. J. Chem.*, 1998, 753.
12. B. Schoentjes and J.-M. Lehn, *Helv. Chim. Acta*, 1995, **78**, 1.
13. C. Uerpmann, J. Malina, M. Pascu, G. J. Clarkson, V. Moreno, A. Rodger, A. Grandas and M. J. Hannon, *Chem. Eur. J.*, 2005, **11**, 1750.
14. E. C. Constable, P. Harverson, C. E. Housecroft, E. Nordlander and J. Olsson, *Polyhedron*, 2006, **25**, 437.
15. F. W. Cagle and G. F. Smith, *J. Am. Chem. Soc.*, 1947, **69**, 1860.
16. S. K. Kim, H. N. Kim, Z. Xiaoru, H. N. Lee, H. N. Lee, J. H. Soh, K. M. K. Swamy and J. Yoon, *Supramolecular Chemistry*, 2007, **19**, 221.
17. J. Yoon, S. K. Kim, N. J. Singh and K. S. Kim, *Chem. Soc. Rev.*, 2006, **35**, 355.
18. T. Gunnlaugsson, H. D. P. Ali, M. Glynn, P. E. Kruger, G. M. Hussey, F. M. Pfeffer, C. M. G. dos Santos and J. Tierney, *J. Fluoresc.*, 2005, **15**, 287.
19. T. Gunnlaugsson, M. Glynn, G. M. Tocci, P. E. Kruger and F. M. Pfeffer, *Coord. Chem. Rev.*, 2006, **250**, 3094.
20. S. J. Dickson, M. J. Paterson, C. E. Willans, K. M. Anderson and J. W. Steed, *Chem. Eur. J.*, 2008, **14**, 7296.
21. L. Rodriguez, J. C. Lima, A. J. Parola, F. Pina, R. Meitz, R. Aucejo, E. Garcia-Espana, J. M. Llinares, C. Soriano and J. Alarcon, *Inorg. Chem.*, 2008, **47**, 6173.

22. F. Pina, M. A. Bernardo and E. García-España, *Eur. J. Inorg. Chem.*, 2000, **2000**, 2143.
23. L. Prodi, *New J. Chem.*, 2005, **29**, 20.
24. R. A. Bissel, A. P. de Silva, H. Q. N. Gunaratne, P. L. M. Lynch, G. E. M. Maguire and K. R. A. S. Sandanayake, *Chem. Soc. Rev.*, 1992, **21**, 187.
25. C. M. G. dos Santos, A. J. Harte, S. J. Quinn and T. Gunnlaugsson, *Coord. Chem. Rev.*, 2008, **252**, 2512.
26. D. M. Bailey, A. Hennig, V. D. Uzunova and W. M. Nau, *Chem. Eur. J.*, 2008, **14**, 6069.
27. L. Fabbrizzi, M. Licchelli, L. Parodi, A. Poggi and A. Taglietti, *J. Fluoresc.*, 1998, **8**, 263.
28. D. R. Ahn, T. W. Kim and J. I. Hong, *J. Org. Chem.*, 2001, **66**, 5008.
29. F. Basolo, J. C. Hayes and H. M. Neumann, *J. Am. Chem. Soc.*, 1953, **75**, 5102.
30. F. Basolo, J. C. Hayes and H. M. Neumann, *J. Am. Chem. Soc.*, 1954, **76**, 3807.
31. S. Tachiyashiki and H. Yamatera, *Bull. Chem. Soc. Jpn*, 1981, **54**, 3340.
32. T. Beissel, R. E. Powers, T. N. Parac and K. N. Raymond, *J. Am. Chem. Soc.*, 1999, **121**, 4200.
33. B. Hasenknopf, J.-M. Lehn, N. Boumediene, E. Leize and A. V. Dorsselaer, *Angew. Chem. Int. Ed.*, 1998, **37**, 3265.
34. R. L. Paul, Z. R. Bell, J. S. Fleming, J. C. Jeffery, J. A. McCleverty and M. D. Ward, *Heteroat. Chem.*, 2002, **13**, 567.
35. J. A. Smith and F. R. Keene, *Chem. Commun.*, 2006, 2583.
36. G. Rapenne, J. P. Sauvage, B. T. Patterson and F. R. Keene, *Chem. Commun.*, 1999, 1853.

Chapter 5

Metal-template Reductive Amination; Pseudocryptands, Cryptates and Tetranuclear Polycycles

5.1 SYNTHETIC BACKGROUND

Metal ions have been extensively exploited as templates enabling controlled synthesis of increasingly elaborate molecular architectures.[1] These include macrocycles,[2] cryptands,[3,4] catenanes,[5-8] knots,[6,7,9-17] Borromean rings[18-21] and rotaxanes.[5,6,8] The background of the present study originates from previous work conducted within the Lindoy and Meehan research groups that focused on the synthesis of a range of macrocycles[2] and macrobicycles (cryptands).[3,4,22-24] With respect to the latter, this research resulted in the development of a metal-template reductive amination procedure for the synthesis of tris-bipyridyl cryptates of type **45** (R_1 = H and R_2 = H or *t*-Bu) and, upon demetallation, cryptands (***Scheme 5.1***).[3,4] The success of this synthetic strategy depended on several factors: favourable orientation of the

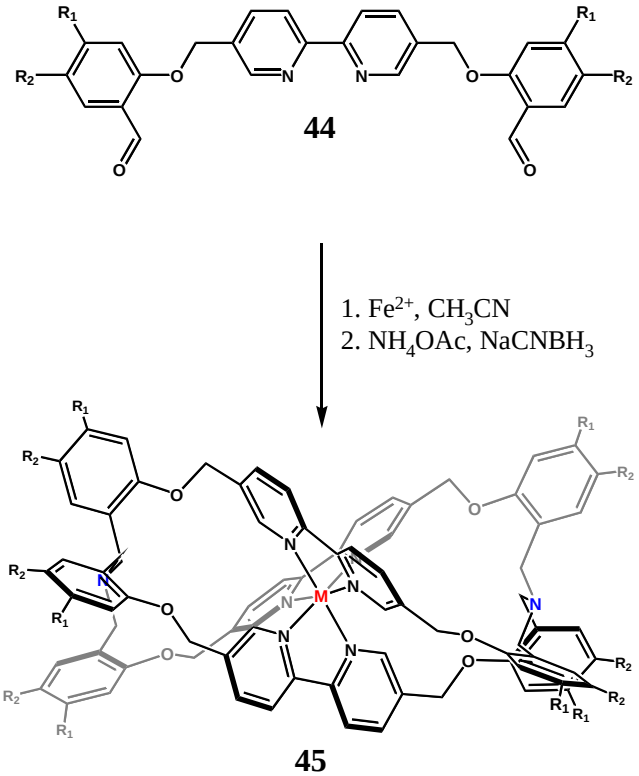

Scheme 5.1

aldehyde functionality in the tris-bipyridyl metal-template intermediates, and appropriate conditions to allow three successive reductive amination events to occur to generate each tripodal nitrogen bridgehead. The former of these requirements will depend on the geometry

around the metal ion and the conformational flexibility of the aldehyde bearing groups. The latter requirement will be influenced by the rates of unfavourable competing reactions (such as reduction of the aldehyde to an alcohol) relative to the intended successive reductive amination reactions. This chapter outlines the optimisation of the above methodology for the preparation of pseudocryptates, mono- and dinuclear cryptates and more elaborate systems.

5.2 TARGET MOLECULES AND SYNTHETIC APPROACH

5.2.1 Tripodal ligand synthesis

Compared to the cryptate synthesis outlined in ***Scheme 5.1***, the synthesis of tripodal systems from a one-pot reductive amination procedure was considered to be attractive, due to the possibility of reducing the likelihood of forming polymeric material. Two general approaches were investigated. In the first case, the synthesis of tertiary amines from benzyl (Bn) and *para*-methoxybenzyl (PMB) protected salicylaldehyde derivatives **172** and **173** (***Scheme 5.2***), followed by deprotection and subsequent *O*-alkylation with 5-halomethyl-5′-substituted-2,2′-bipyridyl derivatives, was examined. The second method used a more direct one-pot reductive amination procedure involving 5-salicyloxy derivatives, of type **99** and **100** (***Scheme 5.3***).

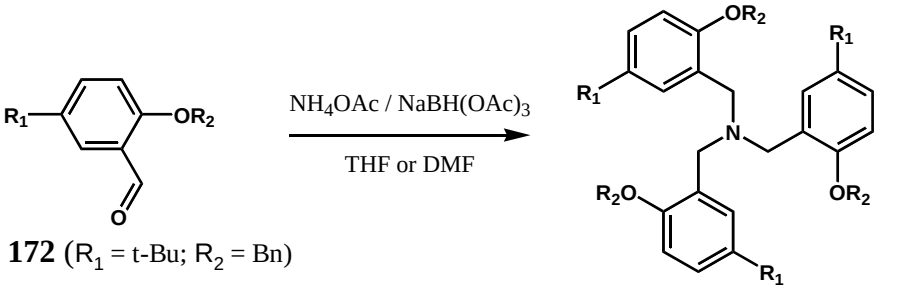

172 (R_1 = t-Bu; R_2 = Bn)

173 (R_1 = H; R_2 = PMB)

174 (R_1 = t-Bu; R_2 = Bn)

175 (R_1 = H; R_2 = PMB)

Scheme 5.2

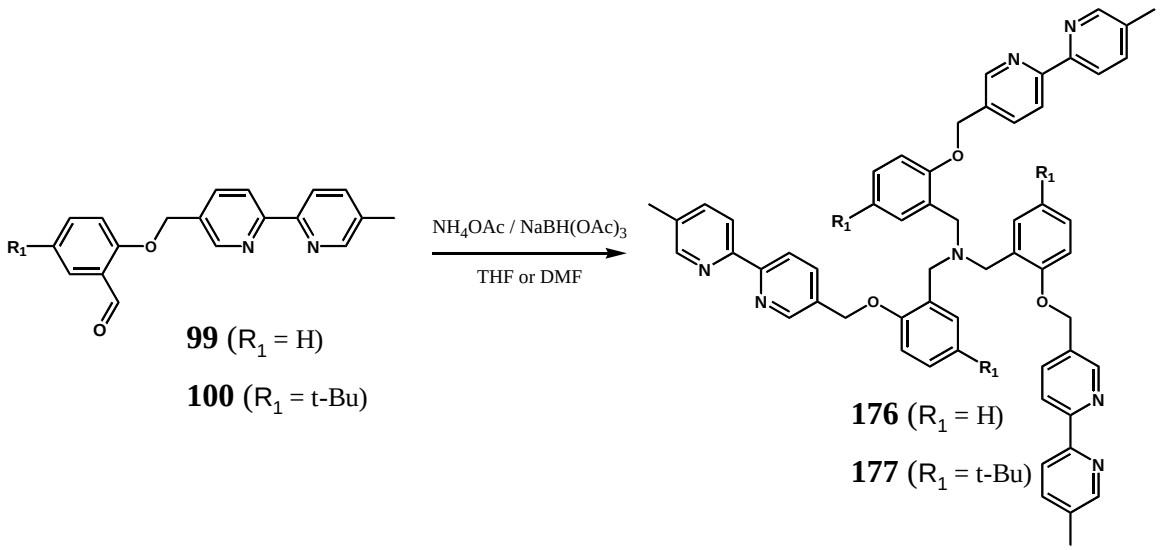

Scheme 5.3

The synthesis of tertiary amines **174** and **175** was unsuccessful using the reductive amination conditions employed for the one-pot synthesis of cryptand **46**.[4] Although the synthesis of tertiary triphenolamine derivatives may be performed either by Mannich reactions[25] or by alkylation of appropriate primary amines,[26] reductive amination was preferred in the present study in order to further explore appropriate conditions for the more elaborate one-pot metal-template synthesis of cryptates. In this regard, Licini *et al.*[27] have recently reported conditions used to successfully synthesize tripodal species related to **174** and **175**, starting from various protected salicylaldehydes. In this latter report one equivalent of both NH_4OAc and $NaBH(OAc)_3$ in THF afforded tertiary amines in yields of 50 – 75 %. Unfortunately, when applied to aldehyde **172**, these conditions resulted in mixtures of primary, secondary and tertiary amines, as well as unchanged **172** and its alcohol reduction product. The use of a five times excess of both NH_4OAc and $NaBH(OAc)_3$ resulted in the production of a similar mixture of amines and alcohol, but with no starting aldehyde. When the mixture of amines was isolated and reacted with a further equivalent of aldehyde **172** and $NaBH(OAc)_3$, in an attempt to drive the reaction to the tertiary amine, an increase in the reduction of **172** to the corresponding alcohol was observed to occur. This may be explained by the slow formation of the required quaternary iminium ion intermediate due to a sterically hindered secondary amine and/or slow reduction due to the sterically hindered nature of this same intermediate. Either way, alternative conditions were investigated in order to minimise

the reduction of aldehyde. Primarily, this work focused on alternative solvent and temperature regimes. Solvents that have been successfully employed for reductive aminations using $NaBH(OAc)_3$, such as toluene,[28] DCM,[28,29] 1,2-dichoroethane (DCE),[28,30,31] THF,[27,28,31,32] DMF,[29] CH_3CN[28,33,34] and DMSO,[35] were all trialled. In hindsight, a more structured study, incorporating HPLC analysis of reaction product ratios, would probably have provided more useful data. However, simple TLC experiments were used to assess the degree of the undesired reduction of aldehyde to alcohol. The most successful outcome was obtained via a variation of those conditions reported by Licini *et al.*,[27] with the replacement of THF by DMF. The procedure resulted in no observable reduction of aldehyde. Thus, the synthesis of tertiary amines **174** and **175** was successfully achieved in yields comparable with those reported by Licini.[27]

Fortuitously, crystals of tertiary amine **174** suitable for X-ray diffraction were grown by slow evaporation of a DCM/petrol solution of this product (***Figure 5.1***). The product crystallizes in the centric trigonal space group *R-3*. In this structure the nitrogen lone pair is

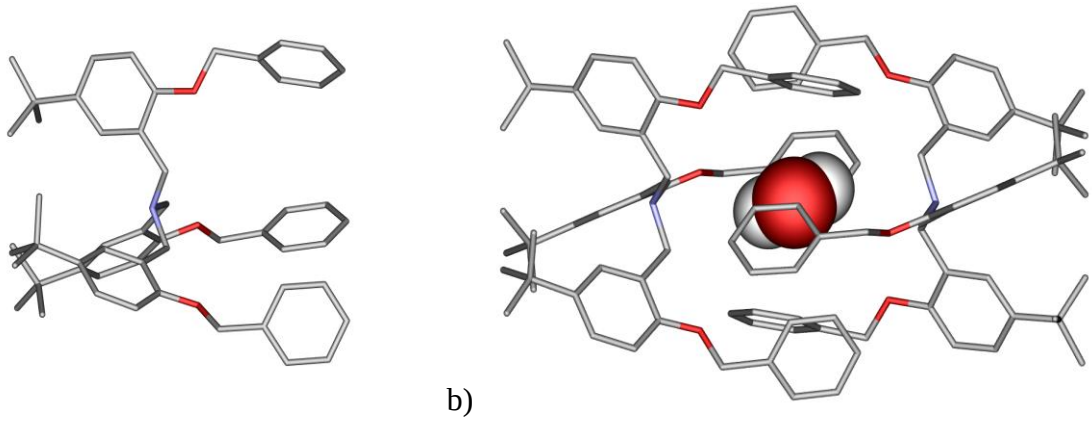

a) b)

Figure 5.1 X-ray structure of a) tris-salicyloxyamine **174** and b) illustration of the solid state inclusion of a water molecule.

oriented *exo*. Interestingly, in the crystal structure two of the tripodal amine molecules interlock forming a cavity which is occupied, by what is thought to be a water molecule (***Figure 5.1*** b)). While this latter observation was quite unexpected, it does pose the possibility that appropriately substituted tertiary amines of this type may allow such cavity-containing assemblies to form in solution. This latter system might be envisaged as being

related to previous capsules reported by Bray *et al.* [36,37] from the interaction of Cu(II) or Ag(I) with tripodal ligands in a 3:2 ratio.

Following the successful synthesis of amines **174** and **175**, the synthesis of tripodal ligands **176** and **177** directly from their precursor aldehydes **99** and **100** was attempted. Both of these experiments resulted in mixtures of primary, secondary and tertiary amines. Unfortunately, attempts to push the reaction (as described above) to the tertiary amine by the addition of excess aldehyde were unsuccessful. At best, mixtures of secondary and tertiary amines were observed in addition to substantial amounts of reduced aldehyde. Furthermore, while chromatographic separation of the alcohol from the amines was straightforward, separation of the mixture of amines proved to be very difficult. As a result, the lack of pure tripodal ligands **176** and **177** inhibited meaningful metal complexation studies. Perhaps the difficulty in forming tertiary amines in these bipyridyl appended species is due to slow formation of the corresponding quaternary iminium ion intermediates and/or the subsequent reduction of these species, again reflecting steric influences. Either way, the rate of reduction of aldehyde becomes competitive with the reductive amination process leading to significant losses of the valuable starting aldehydes, **99** and **100**.

In view of the above findings, amine **175** was deprotected with methanolic HCl. The resulting triphenol material was then reacted with chloromethylbipyridine **93** in the presence of K_2CO_3 to afford tripodal ligand **177** in 70 % yield. While the latter yield is quite acceptable, the overall yield of this tripodal ligand from 5-*tert*-butylsalicylaldehyde **96** is a disappointing 33 % (and required a four step synthesis). Some preliminary complexation studies of tripodal ligand **175** with Fe(II) indicated that it forms 1:1 metal to ligand complexes (as evidenced by ESI-HRMS). However, this stepwise synthetic approach seemed somewhat inefficient and complicated, compared to what was initially thought to be a straightforward synthesis via a one-pot reductive amination procedure. Thus, the possible use of a metal-template procedure as an alternative synthetic methodology was investigated.

5.2.2 Metal-template synthesis of pseudocryptands

Initially, a metal-template synthetic approach for the synthesis of pseudocryptands (***Scheme 5.4***) was not considered due to the probability that the tris-chelate octahedral

complexes of monoaldehydes **99** and **100** would generate mixtures of *mer*/*fac* geometric isomers (Chapter 1 *Figure 1.1*, page 6). In this regard, it is noted that the success of a metal-template procedure would depend on the formation of *fac* geometric isomers or require a relatively fast rate of *mer*/*fac* isomerisation compared to that for the reductive amination. With respect to the latter point, the use of more labile octahedral metals in the formation of the tris-chelate octahedral intermediate complex should facilitate an increased rate of *mer*/*fac* isomerisation.

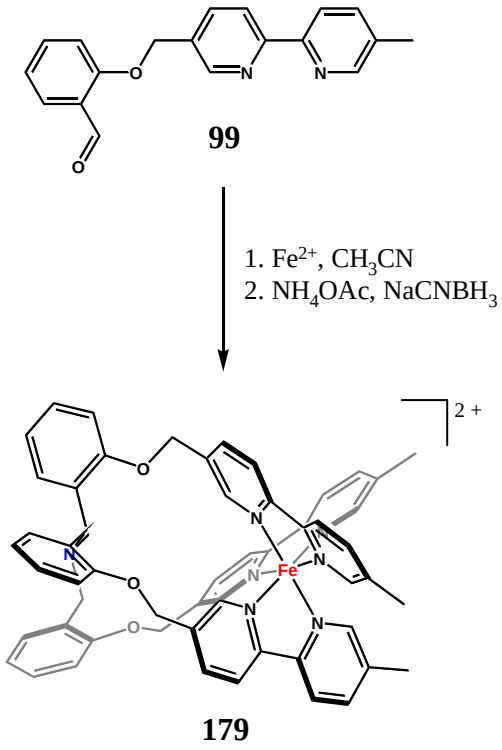

Scheme 5.4

Even though low-spin Fe(II) tends to form moderately inert tris-bipyridyl type complexes it was employed to assess the ratio of *mer* to *fac* geometric isomers formed in its tris-chelate complexes of aldehyde **99**. Hence, $Fe(BF_4)_2$ and monoaldehyde **99** (see ***Figure 5.2*** a) for the ^1H NMR spectrum of **99**) were reacted in refluxing acetonitrile in a 1:3 ratio. The ^1H NMR spectrum of a small amount of the reaction product, isolated as its PF_6^- salt, revealed a complex mixture of signals consistent with the presence of a mixture of *mer* and *fac* geometric isomers (***Figure 5.1*** b)). The aldehyde protons of the complexed ligand gave

the four signals expected for a *mer*/*fac* mixture of geometric isomers. It should be noted that no free ligand was detectable in this sample and that coodinatively unsaturated Fe(II) bipyridyl metal complexes (e.g. $[Fe(\mathbf{99})X_4]^{2+}$ or $[Fe(\mathbf{99})_2X_2]^{2+}$; X = solvent) are generally paramagnetic. Therefore, since the ^{1}H NMR spectrum is sharp and consistent with a diamagnetic low spin d^6 Fe(II) product, the formula of this product was

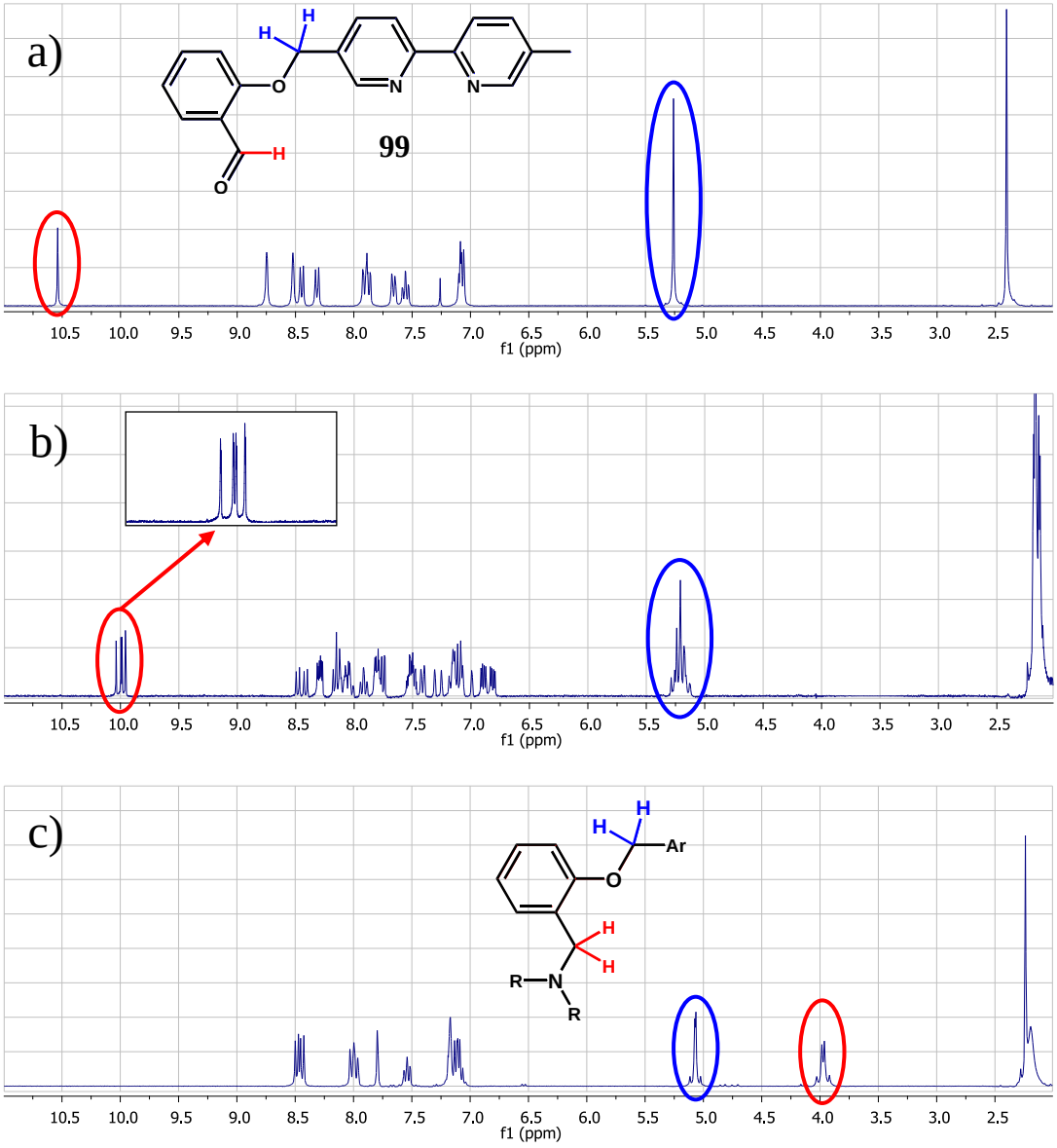

Figure 5.2 ^{1}H NMR spectra for a) free aldehyde **99** in $CDCl_3$, b) the crude reaction mixture consisting of *mer* and *fac* isomers of $[Fe(\mathbf{99})_3](PF_6)_2$ and c) the reductive amination mononuclear product $[Fe(\mathbf{176})](PF_6)_2$, both in CD_3CN.

expected to be $[Fe(\mathbf{99})_3](PF_6)_2$. Indeed, the ESI-HRMS data supported this expectation with the observation of +1 and +2 ions consistent with the successive losses of PF_6^- from the formula $[Fe(\mathbf{99})_3](PF_6)_2$, **178**. In light of the above results, if one considers that three of the aldehyde peaks belong to *mer*-$[Fe(\mathbf{99})_3](PF_6)_2$ and the remaining one to *fac*-$[Fe(\mathbf{99})_3](PF_6)_2$, these isomers are present in an approximate 3:1 ratio, respectively (***Figure 5.2*** b) expanded inset). The ^{1}H NMR spectrum also revealed that the methylene protons (Ar-CH_2-O) were non-equivalent, giving rise to an AB system (partially obscured), consistent with the presence of restricted rotation about the Ar-CH_2-O- bonds of the salicyloxy functionality for at least one of the geometric isomers.

Under high dilution conditions, reductive amination of crude $[Fe(\mathbf{99})_3](BF_4)_2$ was carried out by the addition of an excess of both NH_4OAc and $NaCNBH_3$. It is important to note that this reaction was conducted at 0 °C for 2 hr and then allowed to warm to room temperature overnight. Surprisingly, compared to the tris-chelate intermediate, the crude product of this reductive amination procedure revealed a markedly simplified ^{1}H NMR spectrum (***Figure 5.2*** c)), consistent with the formation of a *fac* isomer or the targeted pseudocryptand. This product was able to be purified by chromatography to afford $[Fe(\mathbf{176})](PF_6)_2$, **179**, in a yield of 62 %. This yield suggests that the rate of mer/fac isomerisation, although slow on the NMR timescale, is relatively fast with respect to the reductive amination over the course of the reaction. Of note, the ^{1}H NMR spectrum revealed that protons on the methylene group adjacent to the nitrogen bridgehead atom gave non-equivalent resonances at 3.94 and 4.01 ppm. Furthermore, non-equivalence of the salicyloxymethylene protons, were in keeping with the expected rigidity of this tris-salicylylamine capping unit. Confirmation of the product's composition was obtained by means of its mass spectrum, which revealed +1 and +2 species corresponding to successive losses of PF_6^- from the formula $[Fe(\mathbf{176})](PF_6)_2$, **179**.

Crystals of the above assembly suitable for X-ray diffraction were grown from CH_3OH/CH_3CN and the resulting structure revealed the expected pseudocryptate structure of type $[Fe(\mathbf{176})](PF_6)_2$ (***Figure 5.3***). The product crystallizes in the centric trigonal space group *R-3*. The lone pair of electrons is oriented *endo* in the solid state in a similar manner to the Fe(II) complex of cryptand **46** previously reported.[3] As expected, the crystal structure of

[Fe(**176**)]$(PF_6)_2$ revealed a small cavity between the nitrogen bridgehead atom and the Fe(II) metal centre.

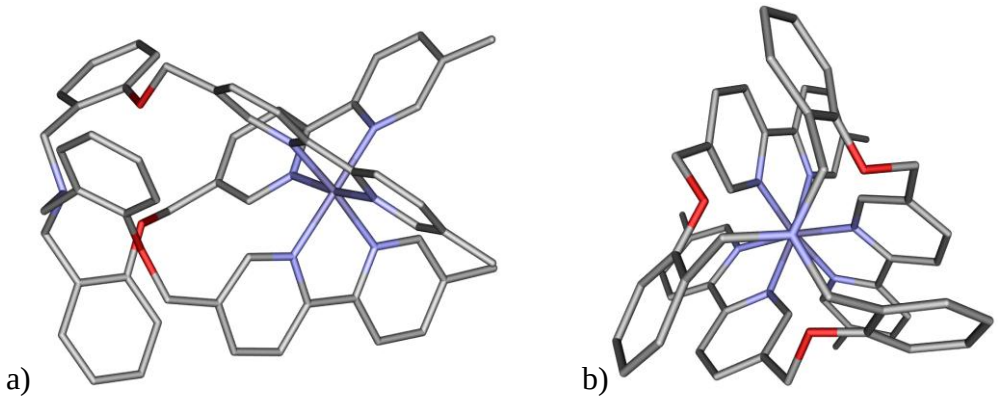

Figure 5.3 X-ray crystal structure representations, a) perpendicular to the C_3-axis and b) viewed down the C_3-axis of [Fe(**176**)]$^{2+}$ (hydrogens, solvent and counterions removed for clarity).

The successful synthesis of pseudocryptand **179** indicated that the metal-template approach may be useful for the synthesis of other more elaborate pseudocryptands. With this in mind aldehyde **110**, with added functionality in the form of a protected phenol, was synthesized (Chapter 2 *Section 2.2.1* for synthetic details). In this case, the metal-template synthesis using Fe(II) resulted in the isolation of pseudocryptand **180** (***Scheme 5.5***) in a yield of 77 %. Even though the chiral THP protecting group leads to mixtures of diastereomers, the ^{1}H NMR spectrum of this product was indicative of the three pendant bipyridyl chelates being in the same environment (e.g. with a total of eleven aromatic resonances). As observed for [Fe(**176**)]$(PF_6)_2$, an AB system centered at 3.99 ppm, corresponding to non-equivalent protons of the methylene groups adjacent to the nitrogen bridgehead atom, was observed. Combined with this latter observation, the disappearance of the aldehyde resonances at approximately 10 ppm was in agreement with the successful reductive amination of these groups. Confirmation of the product's composition was obtained by means of its mass spectrum, which gave a +2 ion corresponding to the loss of two PF_6^- ions from the formula [Fe(**110**)]$(PF_6)_2$, **180**.

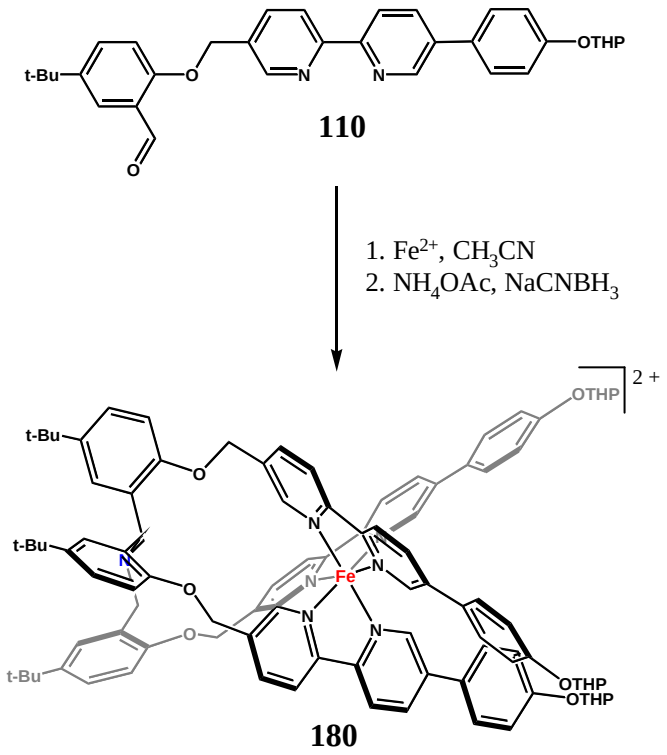

Scheme 5.5

At this point, no further studies of these pseudocryptands have been conducted. However, it is predicted that optimization of the metal-template reductive amination procedure will lead to further improvements in the yields of the pseudocryptands and, upon demetallation, the corresponding tripodal ligands. In this regard, it is thought that the employment of a more labile octahedral metal, such as Ni(II), allowing faster *mer*/*fac* isomerisation rates, might lead to higher yields. The deprotection of pseudocryptand **180** is expected to lead to very different solubility characteristics, as well as the possibility of further derivatisation of this complex.

5.2.3 Metal-template synthesis of mononuclear cryptates

Dialdehydes **113** and **116** were synthesized for the purpose of using them in metal-template cryptate syntheses. In the first instance, dialdehyde **113** was intended to be used to further investigate the previously reported metal-template methodology employed to synthesize cryptate **45** (R_1 = H and R_2 = *t*-Bu, ***Scheme 5.6***). In the current work, the synthesis

of cryptate **45** was achieved in comparable yields with a few minor changes to the reported procedure. It had been reported[4] that the reductive amination procedure was conducted at 50 °C. This temperature regime resulted in the significant reduction of aldehyde **113** as well as the intended reductive amination. Since the successful synthesis of cryptate **45** requires a total of six reductive amination events per molecule, the loss of aldehyde **113** through its reduction would lead to inseparable product mixtures and therefore complete failure of this approach. Due to this initial result, a circuitous series of experiments ensued, finally resulting in a simple reduction in reaction temperature to 0 °C prior to the addition of the $NaCNBH_3$, which allowed the synthesis of **45** in a yield of 80%.

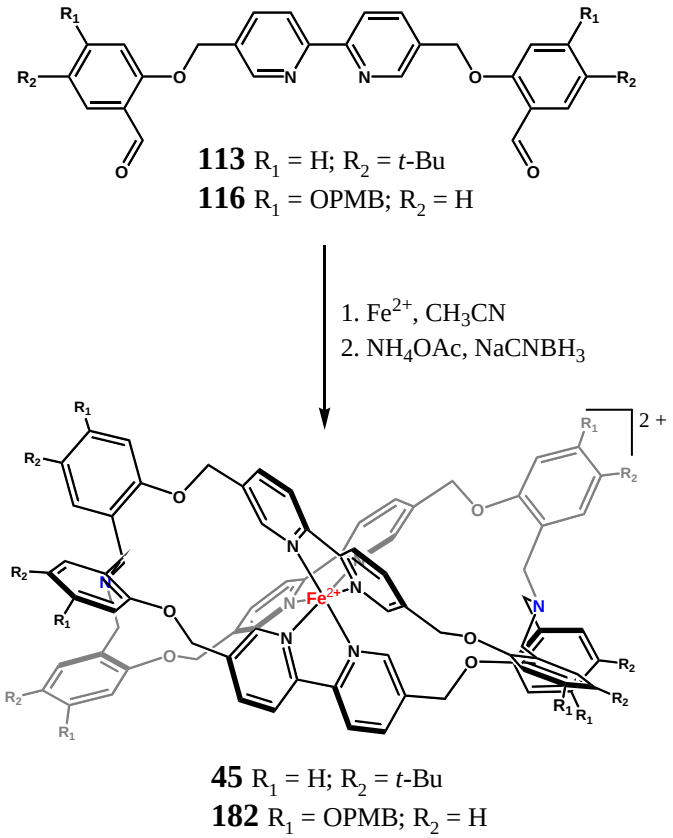

Scheme 5.6

With the intention of being able to derivatise the preformed cryptate, dialdehyde **116** was incorporated into the metal-template synthesis outlined in ***Scheme 5.6***. Its corresponding tris-chelate complex with Fe(II), $[Fe(\mathbf{116})_3](PF_6)_2$, **181**, gave a diamagnetic ^{1}H NMR spectrum in CD_3CN that showed all the ligands in equivalent environments (***Figure 5.4*** a)).

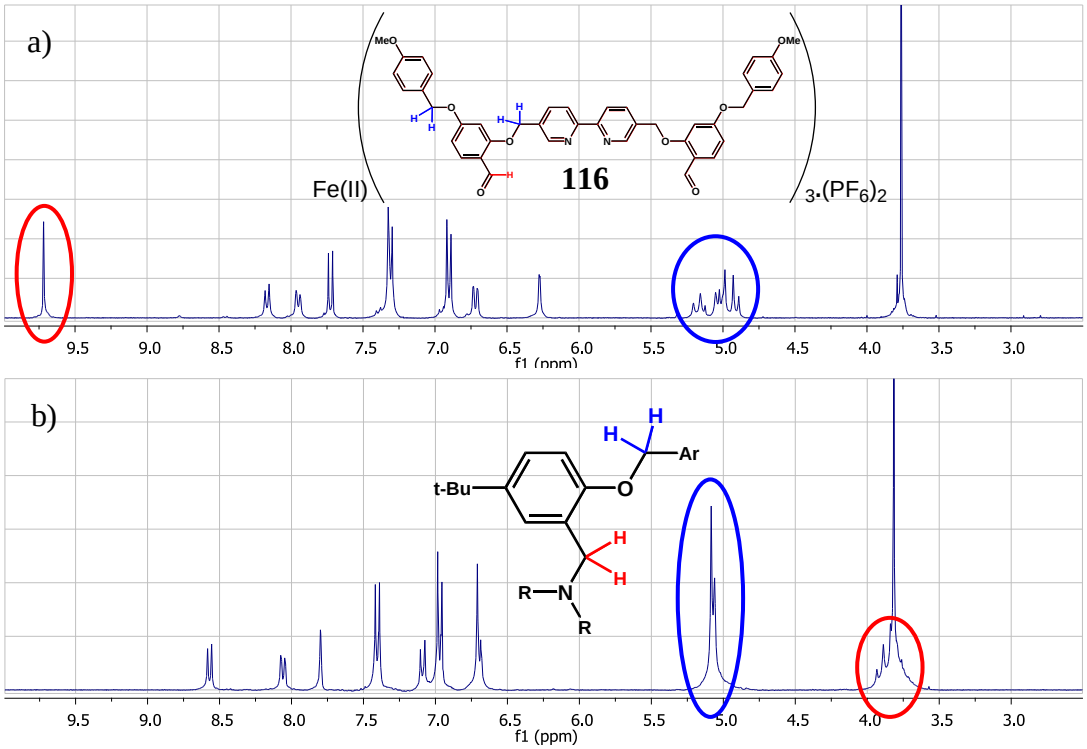

Figure 5.4 ^{1}H NMR spectra run in CD_3CN of a) metal-template precursor complex [Fe(**116**)]$(PF_6)_2$ and b) cryptate **182**.

Interestingly, the presence of non-equivalent methylene protons for the two different salicyloxymethylene groups, indicated a lack of rotational freedom around the Ar-O-CH_2 bonds of these appended groups. Reductive amination under analogous conditions to those used for the synthesis of cryptate **45** in the current study, resulted in the isolation of cryptate [Fe$\mathbf{L}^{\mathbf{1}}$]$(PF_6)_2$, **182**, in 87 % yield ($\mathbf{L}^{\mathbf{1}}$ = the corresponding demetallated cryptand). An indication of the success of this reaction was primarily obtained from the product's ^{1}H NMR spectrum in CD_3CN (***Figure 5.4*** b)). This spectrum revealed an absence of the aldehyde resonance, observed in the spectrum of the intermediate **181**, with the presence of an AB system corresponding to the non-equivalent methylene protons adjacent to the expected newly formed nitrogen bridgehead atoms. Interestingly, the AB signals observed for the non-equivalent methylene protons adjacent to the salicyloxymethylene groups in the tris-chelate intermediate, had become singlets (i.e. they were now equivalent). Finally, the mass spectrum confirmed the expected formula of this material by revealing a +2 species corresponding to the loss of two PF_6^- ions from the formula [Fe$\mathbf{L}^{\mathbf{1}}$]$(PF_6)_2$.

Unfortunately, limited time meant cryptate **182** has yet to be deprotected in order to investigate the possibility of further derivatisation of the resulting phenols via *O*-alkylation. The success of this latter reaction will determine the course of future work on this interesting system. In this regard, the hope is that the resolved enantiomers of this or analgous cryptates may be used as chiral induction subunits in larger more elaborate systems.

5.2.4 Dinuclear cryptates and tetranuclear polycycles

The isolation of a number of M_2L_3 and M_4L_6 complexes (outlined in Chapters 3 and 4) combined with the successful application of the metal-template procedure for the synthesis of the mononuclear pseudocryptands, **179** and **180**, and cryptates, **45** and **182** (discussed above) led to the investigation of a series of metal-template reductive amination experiments using dialdehydes **141**, **142** and **144**. Primarily this study aimed to assess the outcome of their metal-directed assembly with Fe(II) salts. This section briefly outlines the results from these studies and some preliminary results from subsequent reductive amination experiments.

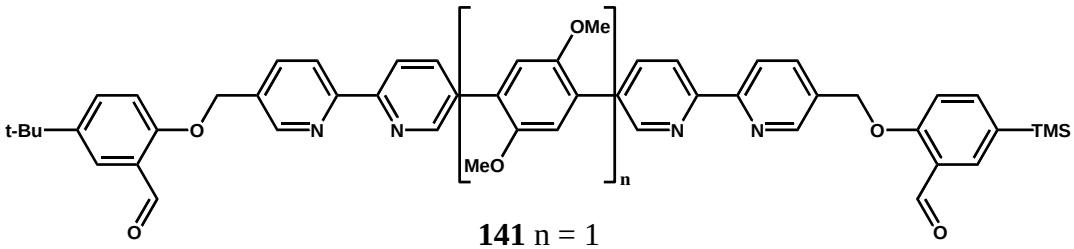

141 n = 1
142 n = 2
144 n = 0

The interaction of dialdehyde **141** (see ***Figure 5.5*** a)) for ^{1}H NMR spectrum) with Fe(II) under high dilution conditions and using short reaction times resulted in the predominance of a single product. This product was able to be partially purified by a challenging chromatographic procedure using C18 reverse phase silica gel, with a solution of NH_4PF_6 in acetonitrile and water as eluent. Whilst the ^{1}H NMR spectrum of this material indicated a slight impurity, observed proton resonances belonging to the product were consistent with the ligand retaining its two-fold symmetry within the complex with a single aldehyde proton resonance (***Figure 5.5*** b)). An AB system centered at 5.25 ppm was also

present corresponding to the non-equivalent salicyloxymethylene protons. Confirmation that the M_2L_3 precursor complex had formed was obtained from the ESI-HRMS of this material. This spectrum revealed +2 and +3 ions corresponding to successive losses of PF_6^- from the formula $[Fe_2(\mathbf{141})_3](PF_6)_4$, **183** (***Scheme 5.7***). The mass spectrum also revealed peaks corresponding to the M_4L_6 complex indicating that it was the impurity. With respect to the latter, the combination of more concentrated reaction mixtures and extended reaction duration for the interaction of dialdehyde **141** with Fe(II) resulted in the M_4L_6 complex being the sole product observed.

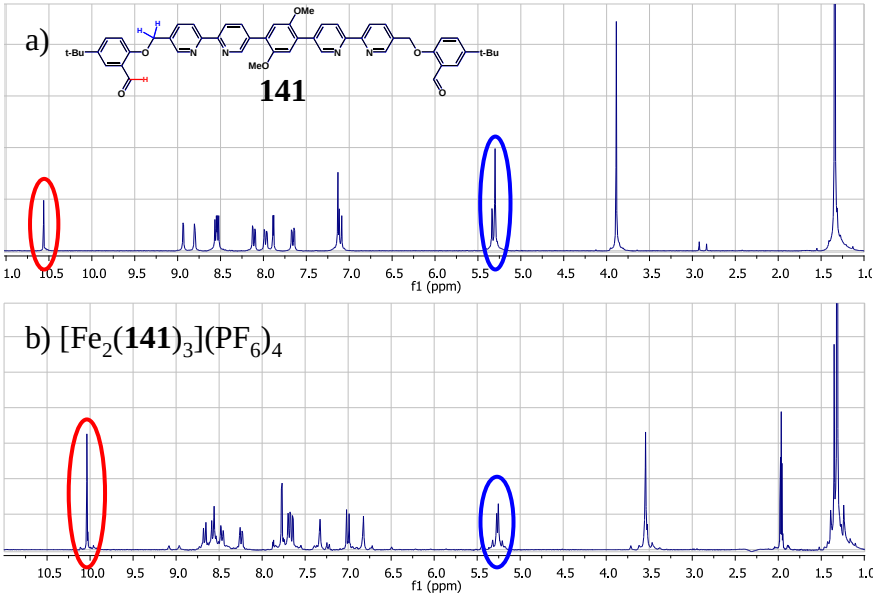

Figure 5.5 The ^{1}H NMR spectrum of a) dialdehyde **141** in CD_2Cl_2 and b) precursor $[Fe_2(\mathbf{141})_3](PF_6)_4$ in CD_3CN.

Isolation of the precursor complex $[Fe_2(\mathbf{141})_3](PF_6)_4$ represented a major step towards one of the initial targets of the current project. The first reductive amination attempt with $[Fe_2(\mathbf{141})_3](PF_6)_4$ employed the conditions developed for the synthesis of tertiary amines **176** and **177** (discussed above). In the first instance DMF was employed as the solvent. Unfortunately this solvent led to the slow degradation of the precursor complex, $[Fe_2(\mathbf{141})_3](PF_6)_4$, as evidenced by the slow change (over 1 – 2 hours at room temperature) of the intensely red coloured solution of this species to a straw yellow colour. As a result, acetonitrile was substituted for DMF in this reaction (***Scheme 5.7***). The ^{1}H NMR spectrum of the product isolated as its PF_6^- salt, was consistent with the ligand lying on a two-fold axis of

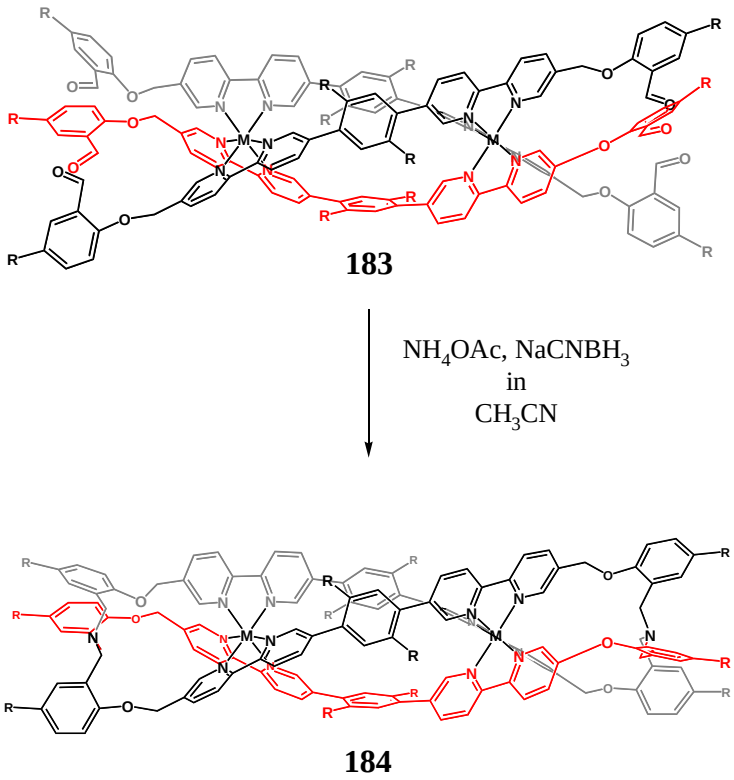

Scheme 5.7

symmetry (***Figure 5.6*** a)). Interestingly, the precursor aldehyde resonance at 10.58 ppm had disappeared and was replaced by an AB system centered at 4.34 ppm further downfield with respect to the signals observed for the analogous protons (approximately 4 ppm) in the related mononuclear cryptates **45** and **182**. Furthermore, the AB system was coupled to a proton with a resonance at 3.23 ppm (see partial ^{1}H COSY ***Figure 5.6*** b)). While the ^{1}H NMR spectrum of this material was broadly in agreement with that expected for **184**, the observation of the signal at 3.23 ppm appeared uncharacteristic.

Confirmation of the formula of the product described above was obtained by ESI-HRMS. The mass spectrum revealed +2 to +4 ions corresponding to successive losses of PF_6^- from the formula $[Fe_2(\mathbf{L}^2)_3](PF_6)_4$, **185** (where $\mathbf{L}^2$ is the diol product derived from the reduction of dialdehyde **141**) (see ***Figure 5.7*** a) for ChemDraw structure). Thus, the resonance observed at 3.23 ppm is that of the newly formed hydroxyl protons which are coupled to the adjacent methylene protons at 4.34 ppm. This coupling is indicative of slow exchange on the NMR time scale. The latter point combined with the well developed AB systems in the ^{1}H NMR spectrum of this product, indicates that the end groups form a quite

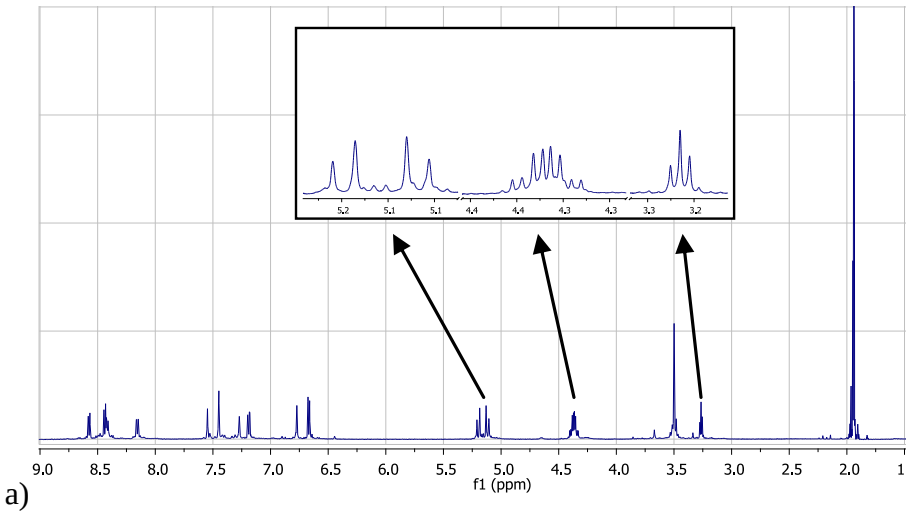

a)

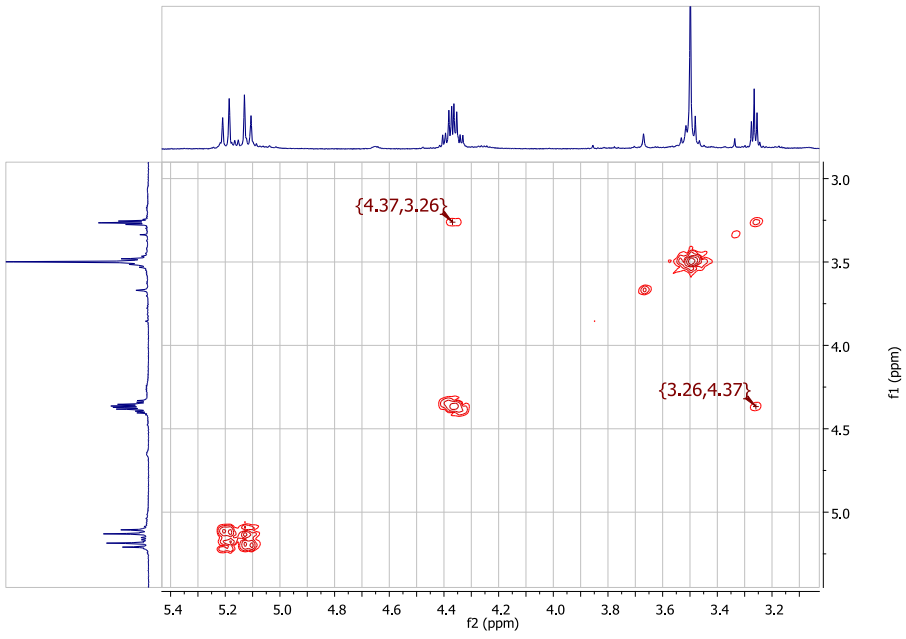

b)

Figure 5.6 a) The ^{1}H NMR spectrum of the product obtained from an attempted metal-template reductive amination sythesis of precursor $[Fe_2(\mathbf{141})_3](PF_6)_4$, and b) its ^{1}H-COSY illustrating the coupling between methylene and hydroxyl protons.

rigid structure. Thus, it is thought that due to the expected close proximity of the newly formed hydroxyl functionalities, an intramolecular hydrogen bonding network may have formed (for one possibility see ***Figure 5.7*** b)). Efforts are currently being made to recrystallise this material for X-ray and/or neutron diffraction studies. In any case, such secondary hydrogen bonding interactions may aid the further stabilization of related artificial metallohelicates.

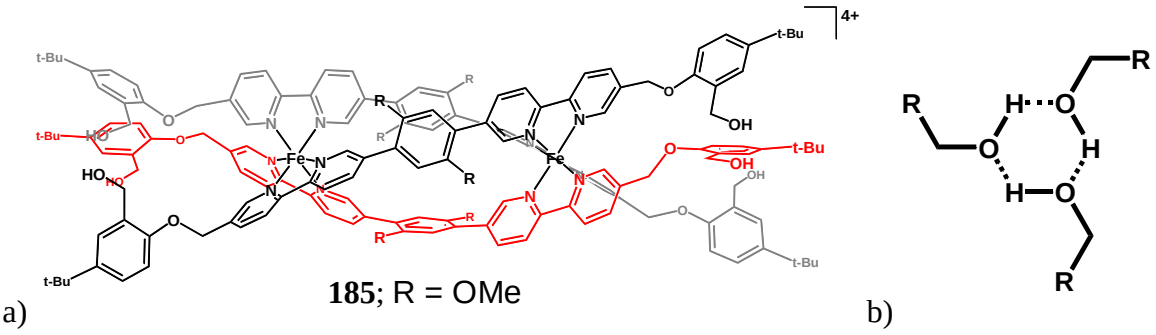

Figure 5.7 a) ChemDraw representation of $[Fe_2(\mathbf{L}^2)_3](PF_6)_4$, **185** and b) proposed trimeric hydrogen bonding network.

Ultimately, the simple lowering of the reaction temperature prior to the addition of the reducing agent proved to be beneficial, as it had for the synthesis of **45**, **179**, **180** and **182**. Thus, reacting precursor $[Fe_2(\mathbf{141})_3](PF_6)_4$ with NH_4OAc and $NaCNBH_3$ at 0 °C for several hours prior to allowing the reaction mixture to warm to room temperature, allowed the isolation of a different product. In this case, the ^1H NMR spectrum of the crude material so obtained, isolated as its PF_6^- salt, was quite complicated. However, the TLC of this material indicated predominance of a single product. Unfortunately, owing to the small sample available instructive NMR data has yet to be collected on this sample. The ESI-HRMS was collected to evaluate whether or not the intended dinuclear cryptate had formed in this reaction. The mass spectrum revealed +2 to +4 ions corresponding to successive losses of PF_6^- from the formula $[Fe_2(\mathbf{L}^3)](PF_6)_4$, **184** ($\mathbf{L}^3$ is the corresponding cryptand upon demetallation)(***Figure 5.8*** a)). ***Figure 5.8*** b) illustrates the good agreement between the theoretical and observed isotopic distributions expected for $[Fe_2(\mathbf{L}^3)]^{4+}$. Furthermore, based on peak intensities this spectrum suggested that $[Fe_2(\mathbf{L}^3)](PF_6)_4$ was the major product.

The above reaction was also attempted as a one-pot procedure starting from dialdehyde **141** and $Fe(BF_4)_2.6H_2O$. This experiment resulted in a very complex reaction mixture with the mass spectrum revealing peaks corresponding to the intended dinuclear cryptate **184** as well as a tetranuclear species. For comparison, a similar one-pot reaction was conducted using $Ni(NO_3)_2.6H_2O$ in the place of $Fe(BF_4)_2.6H_2O$. The product from this reaction, isolated as its PF_6^- salt, revealed a simpler mass spectrum with +2 to +4 ions corresponding to successive losses of PF_6^- from the formula $[Ni_2(\mathbf{L}^3)](PF_6)_4$, **186** (***Figure 5.9***

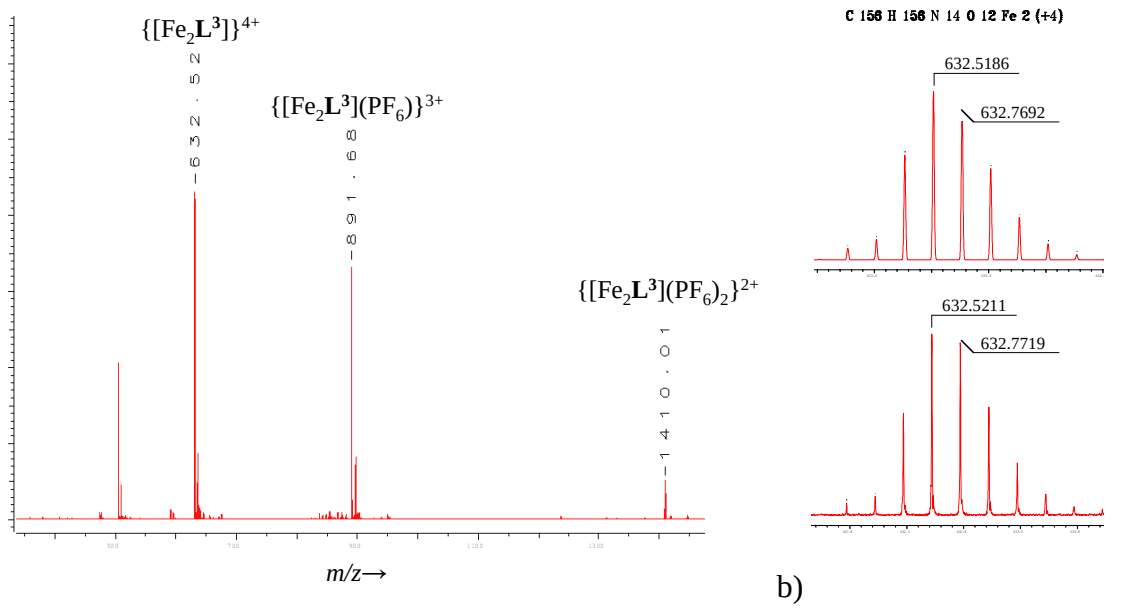

Figure 5.8 a) The mass spectrum of $[Fe_2(\mathbf{L^3})](PF_6)_4$, **184** and b) the theoretical (top) and observed (bottom) isotopic distribution of its +4 ion.

a)). ***Figure 5.9*** b) illustrates the good agreement between the theoretical and observed isotopic distributions expected for $[Ni_2(\mathbf{L^3})]^{4+}$. Although this work is incomplete, these results provide a proof of concept that will likely be reflected by the successful isolation in the near future of a dinuclear cryptate similar to that proposed at the beginning of the project.

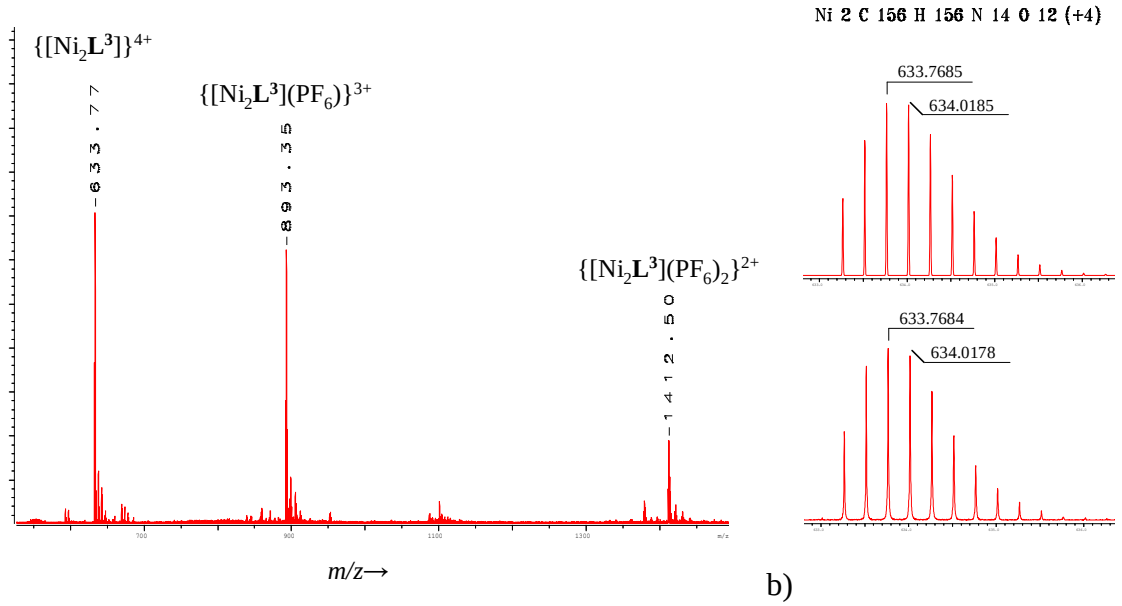

Figure 5.9 a) The ESI-HRMS mass spectrum of $[Ni_2(\mathbf{L^3})](PF_6)_4$, and b) the theoretical (top) and observed (bottom) isotopic distributions for $[Ni_2(\mathbf{L^3})]^{4+}$.

The isolation of the M_4L_6 complexes using quaterpyridine **50** with Fe(II), Co(II) and Ni(II) indicated that it may be possible to conduct the metal-template synthesis of an unprecedented tetranuclear tetracycle[38] via initially incorporating dialdehyde **144** in a related structure. In view of this, the outcome of the interaction of an octahedral metal ion with **144** in a 2:3 ratio, was assessed. TLC of the product isolated from the interaction of $Fe(BF_4)_2.6H_2O$ with **144** in acetonitrile revealed a single product. Furthermore, the ^{1}H NMR spectrum of this product was consistent with the ligand retaining its C_2-symmetry within the complex (i.e. a single aldehyde resonance and nine aromatic resonances were observed) (***Figure 5.10*** a)). The salicyloxymethylene protons are split into an AB system, similar to those previously observed. Confirmation of this product's formula was obtained by collecting its ESI-HRMS. The spectrum gave +3 and +4 ions corresponding to the loss of three and four PF_6^- ions from the formula $[Fe_4(\mathbf{144})_6](BF_4)_8$, **187**.

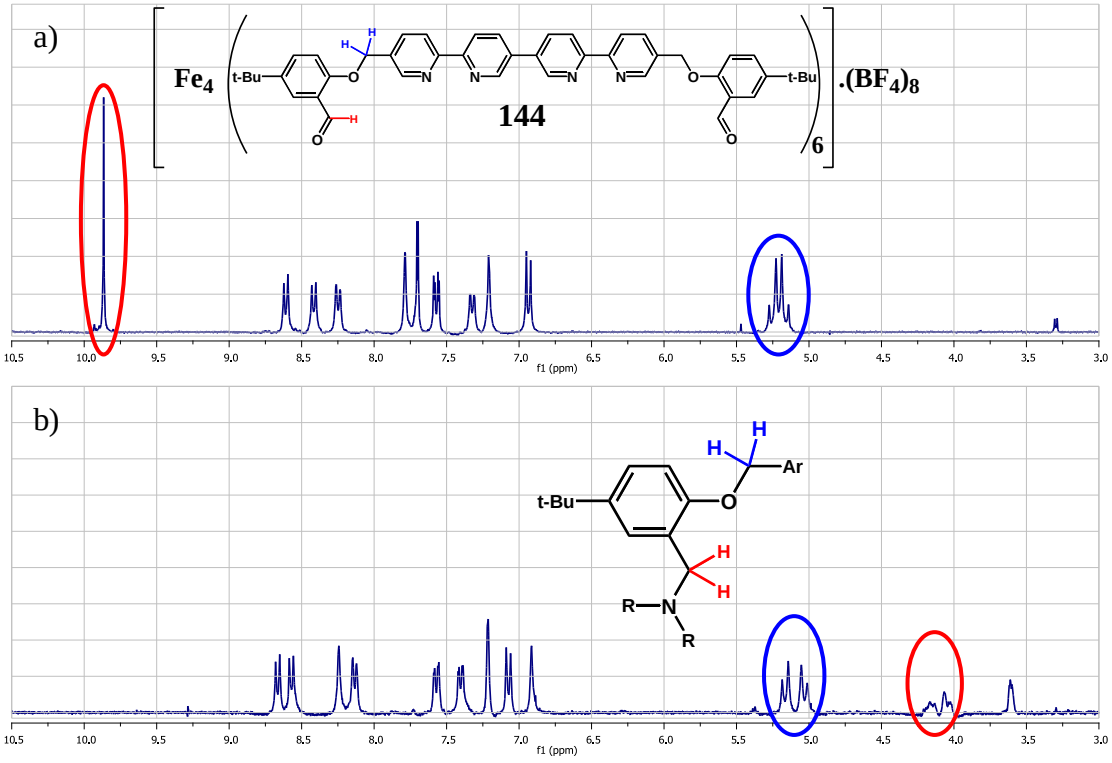

Figure 5.10 ^{1}H NMR spectrum of a) $[Fe_4(\mathbf{144})_6](BF_4)_8$, **187** and b) the reductive amination product $[Fe_4\mathbf{L}^4](PF_6)_8$, **188**, in CD_3CN.

The isolation of the precursor, $[Fe_4(\mathbf{144})_6](BF_4)_8$, led to the ambitious attempt to synthesise a corresponding unprecedented tetranuclear tetracyclic compound. For the successful synthesis of this species, a total of twelve successive imine condensation/reduction reactions would be required. The reductive amination of **187** was conducted under the same conditions as detailed above, and the resulting product isolated as its PF_6^- salt. This material was chromatographed on silica gel and the ^1H NMR spectrum of the purified product revealed nine aromatic resonances, consistent with the quaterpyridyl portions of the expected tetracyclic ligand existing on a two-fold axis of symmetry (***Figure 5.10*** b)). Again, the

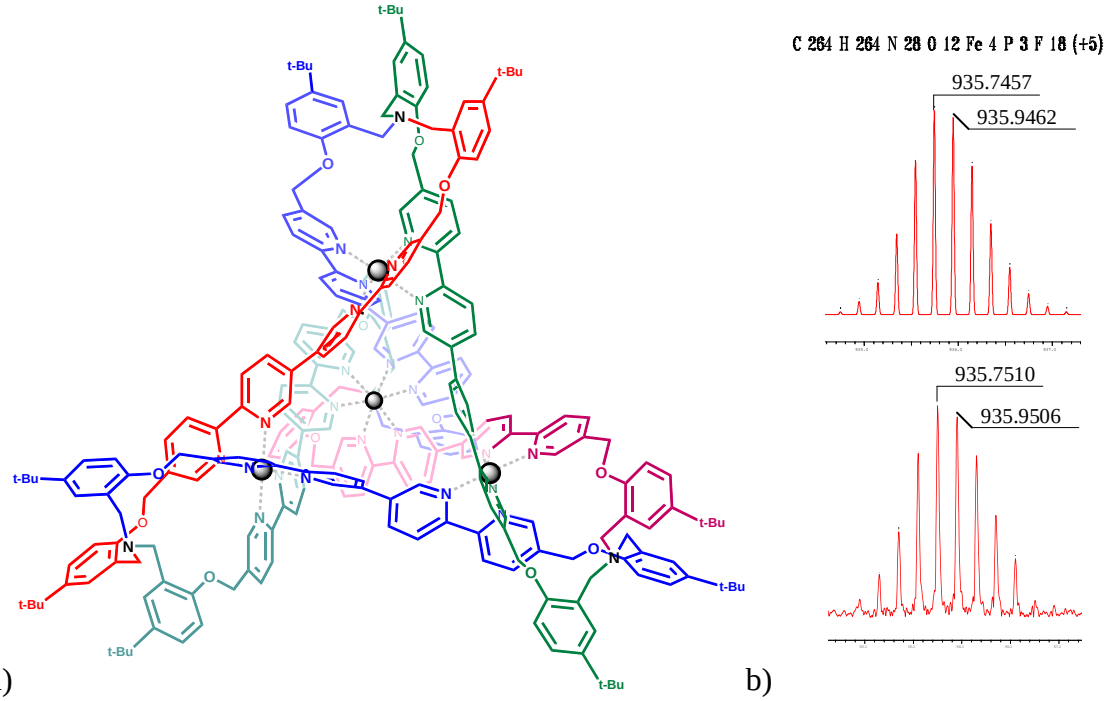

Figure 5.11 a) ChemDraw representation of $[Fe_4\mathbf{L}^4](PF_6)_8$, **188** and b) the theoretical (top) and observed (bottom) isotopic distributions of the +5 charged ion (within 6 ppm) observed in its mass spectrum.

salicyloxymethylene protons are split into an AB system. Most notably, the aldehyde resonance at 9.87 ppm is replaced by a signal corresponding to the methylene protons adjacent to the newly formed nitrogen bridgehead atoms. Although this resonance is partly obscured by an impurity, it appears also to be split into another AB system. The ultimate confirmation that the tetranuclear tetrahedral complex **188** had indeed formed came from its mass spectrum which revealed a series of +3 to +6 ions corresponding to the successive

losses of PF_6^- from the formula $[Fe_4\mathbf{L^4}](PF_6)_8$, **188** ($\mathbf{L^4}$ is the tetracyclic ligand resulting from the demetallation of **188**).

To demonstrate further the ability to synthesise such tetranuclear tetracyclic species, dialdehyde **142** was reacted with Fe(II) to afford the M_4L_6 complex **189**, $[Fe_4(\mathbf{142})_6](PF_6)_8$ (as evidenced by ESI-HRMS). Similar to the ^{1}H NMR spectrum of M_4L_6 **187**, the corresponding spectrum of this material revealed that the ligand existed on a two-fold axis of symmetry within the complex (***Figure 5.12*** a)).

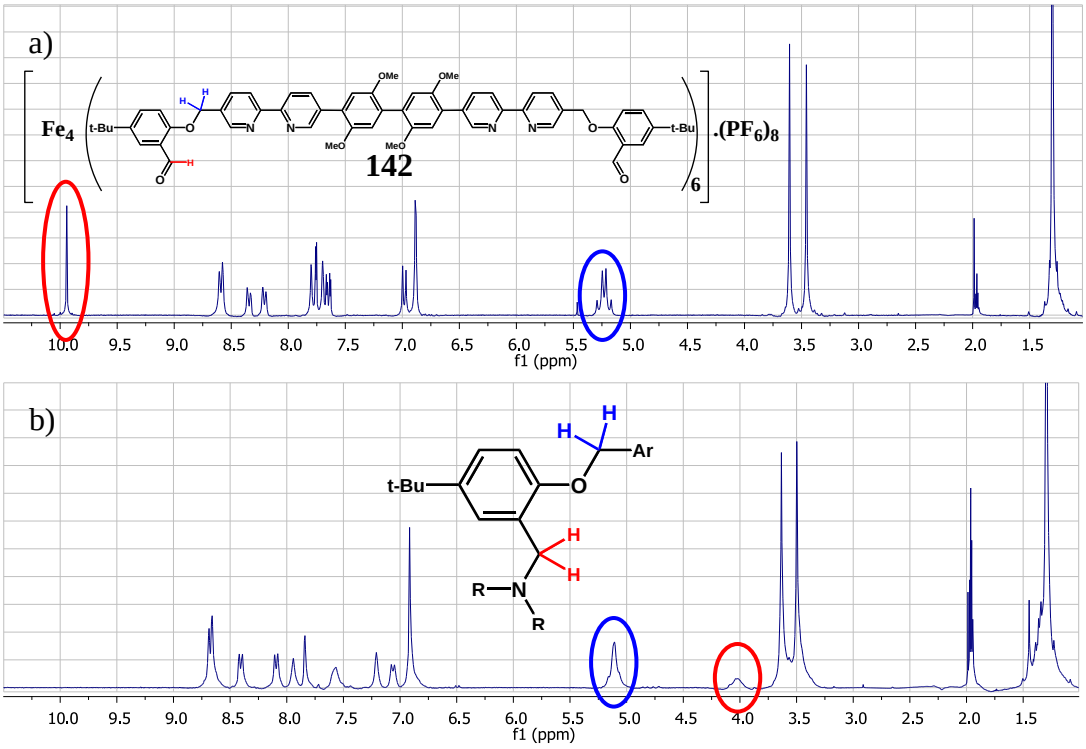

Figure 5.12 ^{1}H NMR spectrum of a) $[Fe_4(\mathbf{142})_6](PF_6)_8$, **189** and b) the reductive amination product $[Fe_4\mathbf{L^5}](PF_6)_8$, **190**, in CD_3CN.

This complex was subjected to the reductive amination procedure outlined above and afforded a product with a ^{1}H NMR spectrum that was broadly in agreement with the expected high symmetry of the intended product (***Figure 5.12*** b)). There is some hint of either a paramagnetic impurity or dynamic behaviour on the NMR timescale as indicated by broadened peaks in this spectrum. The mass spectrum of this material gave +5 to +8 ions corresponding to the successive losses of PF_6^- from the formula $[Fe_4\mathbf{L^5}](PF_6)_8$, **190** ($\mathbf{L^5}$ is the tetracyclic ligand resulting from the demetallation of **189** (***Figure 5.13*** a)). To stress the size

of this latter product, the molecular formula is $C_{360}H_{360}F_{48}Fe_4N_{28}O_{36}P_8$ with a molecular weight of 7034.1731. The expected structure of $[Fe_4\mathbf{L}^5](PF_6)_8$ is illustrated in ***Figure 5.13*** b). Indeed, this impressive structure provides a further example that illustrates the enhanced ability to synthesize larger more elaborate molecular systems by combining metallosupramollecular chemistry with traditional organic chemistry.[1]

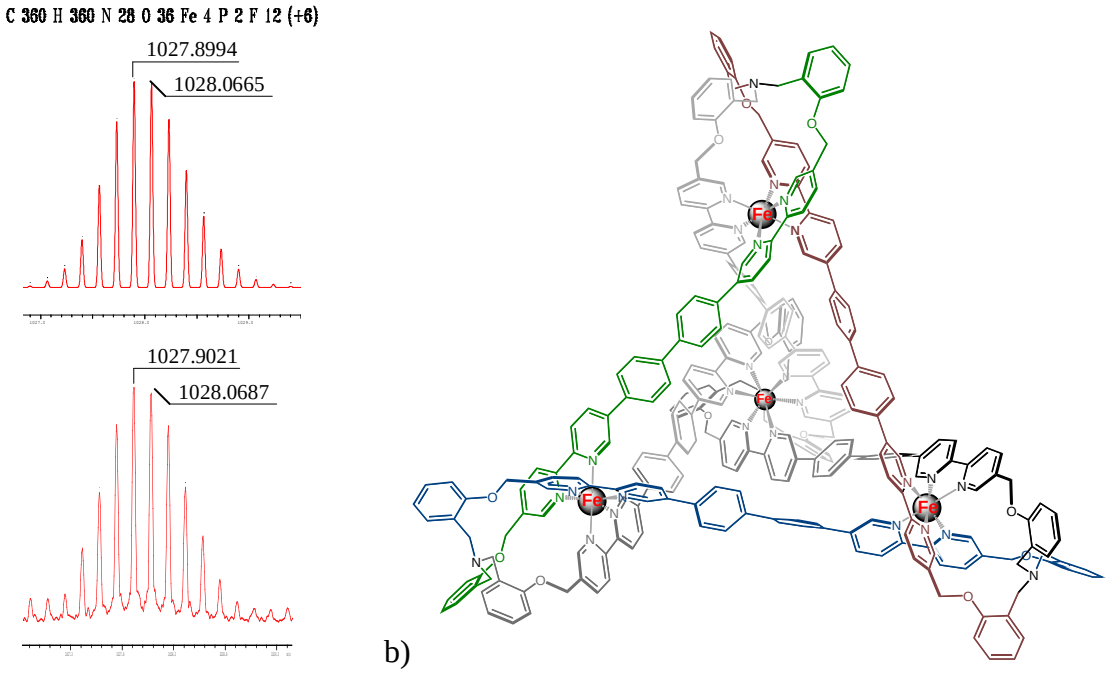

Figure 5.13 a) the theoretical (top) and observed experimental (bottom) isotopic distribution for $\{[Fe_4\mathbf{L}^5](PF_6)_2\}^{6+}$, and b) ChemDraw representation of $[Fe_4\mathbf{L}^5]^{8+}$ (*t*-Bu and methoxyl groups removed for clarity).

5.3 CONCLUSIONS

The non-template one pot reductive amination of tripodal species was investigated. These syntheses resulted in disappointing yields and led to an investigation of the adaption of a previously reported metal-template reductive amination procedure. This procedure proved quite successful using Fe(II) as the template, allowing the isolation of pseudocryptands **179** and **180** in good yields. It is expected that with further optimization (for example using a more labile metal ion) that upon demetallation related metal-template synthesis of tripodal

ligands will provide a high yielding alternative to the stepwise approach used to synthesize tripodal ligand **177**.

Mononuclear cryptate **182** was synthesized in high yield via an metal-template procedure analogous to that used to obtain cryptate **45**. Cryptate **182** is a molecule designed to allow further functionalisation by the removal of the PMB protecting groups followed by *O*-alkylation with desired alkyl halides.

Finally, a number of precursor complexes were synthesized of the dialdehyde derivatives **141**, **142** and **144**. The resulting dialdehyde precursor complexes were subsequently subject to reductive amination leading to the isolation of a number of unique macrocyclic metal complexes, including the dinuclear cryptates, **184** and **186**, and even more elaborate tetranuclear tetracyclic complexes, **188** and **190**. The successful syntheses of the latter species required a total of twelve successive *in situ* imine condensation/reduction reactions from a total of fourteen components. While this study is not yet complete it is anticipated that on scaling up the above-mentioned reactions, sufficient amounts of these unprecedented products will be available to allow their future full characterisation.

5.4 EXPERIMENTAL

See Chapter 2, section 2.3 Experimental for general descriptions of techniques and materials and Chapter 3, section 3.5 Experimental for X-ray structural data collection.

2-Benzyloxy-5-*tert*-butylbenzaldehyde (172): A DMF (25 cm^3) solution of 5-*tert*-butylsalicylaldehyde **96** (3.56 g, 20 mmol) and bromomethylbenzene (3.76 g, 22 mmol) in the presence of K_2CO_3 (6 g, 44 mmol) was stirred at room temperature over 10 h. H_2O (50 cm^3) was then added to the reaction mixture and the resulting mixture extracted with Et_2O (2 x 50 cm^3). The combined extracts were washed with saturated $NaHCO_3$ (30 cm^3) and H_2O (30 cm^3) followed by drying over Na_2SO_4. The crude product was purified by chromatography on silica gel with DCM:petrol (1:1) as eluent to afford **172** (5.1 g, 95 %) as a greasy white solid. ^{1}H NMR (300 MHz, $CDCl_3$): δ = 1.32 (s, 3 H, *t*-Bu), 5.18 (s, 2

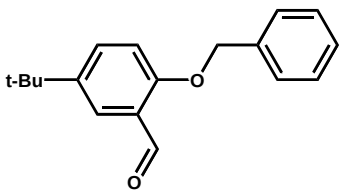

H, OCH_2Ph), 7.00 (d, J^3 = 8.8 Hz, 1 H, H-a), 7.33 – 7.48 (m, 5 H, Ph), 7.57 (dd, J^3 = 8.8 Hz, J^4 = 2.6 Hz, 1 H, H-b), 7.89 (d, J^4 = 2.6 Hz, 1 H, H-c), 10.57 (s, 1 H, CHO).

2-(4-Methoxybenzyloxy)benzaldehyde (173): Procedure as per the synthesis of **172** from 1-chloromethyl-4-methoxybenzene (7.52 g, 48 mmol), salicylaldehyde **95** (4.88 g, 40 mmol) using K_2CO_3 (20.7 g, 150 mmol) in DMF (30 cm^3). Addition of H_2O (100 cm^3) resulted in the precipitation of the crude product which was washed sequentially with 1 M NaOH, H_2O and a minimum volume of cold MeOH. This treatment yielded semipure (>98 %) **173** (9.6 g, 99 %) as a white solid. ^{1}H NMR (300 MHz, $CDCl_3$): δ = 3.82 (s, 3 H, OCH_3), 5.12 (s, 2 H, OCH_2Ar), 6.93 (d, J^3 = 8.8 Hz, 2 H, H-f), 7.04 (dd, J^3 = 7.7 Hz, J^3 = 7.5 Hz, 1 H, H-c), 7.06 (d, J^3 = 8.4 Hz, 1 H, H-a), 7.36 (d, J^3 = 8.8 Hz, 2 H, H-e), 7.53 (ddd, J^3 = 7.5 Hz, J^3 = 8.4 Hz, J^4 = 1.6 Hz, 1 H, H-b), 7.85 (dd, J^3 = 7.7 Hz, J^4 = 1.6 Hz, 1 H, H-d).

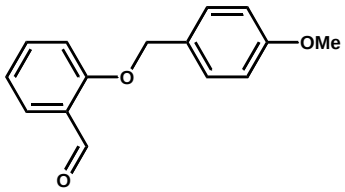

Tris-(2-benzyloxy-5-*tert*-butylbenzyl)-amine (174): A solution of protected benzaldehyde **172** (1.17 g, 4.37 mmol), NH_4OAc (130 mg, 1.7 mmol) and $NaBH(OAc)_3$ (1.39 g, 6.56 mmol) in dry THF (20 cm^3) was stirred at room temperature overnight. The reaction was quenched by the addition of H_2O (20 cm^3) and the resulting precipitate was isolated by filtration. The crude product was purified by chromatography on silica gel with DCM:petrol (1:1) as eluent to afford **174** (372 mg, 33 %) as a white crystalline solid. ^{1}H NMR (300 MHz, $CDCl_3$): δ = 1.27 (s, 9 H, t-Bu), 3.86 (s, 6 H, NCH_2Ar), 5.03 (s, 6 H, OCH_2Ar), 6.82 (d, J^3 = 8.6 Hz, 3 H, H-a), 7.16 (dd, J^3 = 8.6 Hz, J^4 = 2.6 Hz, 3 H, H-b), 7.25 – 7.45 (m, 15 H, Ph), 7.98 (d, J^4 = 2.6 Hz, 3 H, H-c); ^{13}C NMR (75 MHz, $CDCl_3$): δ = 31.86, 34.38, 52.55, 70.10, 110.94, 123.58, 125.76, 127.32, 127.78, 128.64, 137.81, 143.56, 154.59; X-ray quality crystals were obtained by slow evaporation of a DCM:petrol (1:1) solution of the product.

Tris-[2-(4-methoxybenzyloxy)benzyl]-amine (175): A solution of protected benzaldehyde **173** (500 mg, 2.06 mmol), NH_4OAc (130 mg, 1.7 mmol) and $NaBH(OAc)_3$ (1.39 g, 6.56 mmol) in dry DMF (15 cm^3) was stirred at room temperature overnight. TLC indicated a mixture of 1°, 2° and 3° amines. This reaction mixture was quenched by the addition of H_2O (30 cm^3) and the crude products were isolated by filtration. The crude products were then

sequentially washed with H_2O and a minimum volume of cold MeOH and dried on the freeze dryer. A solution of crude material, benzaldehyde **173** (250 mg, 1.03 mmol) and $NaBH(OAc)_3$ (0.5 g, 2.36 mmol) in DMF (15 cm^3) was stirred at room temperature overnight. Following workup, TLC of this material indicated the predominance of a single product. The crude product was purified by chromatography on silica gel with DCM:petrol (1:1) as eluent to afford **175** (296 mg, 62 %) as a fine white crystalline powder. ^{1}H NMR (300 MHz, $CDCl_3$): δ = 3.76 (s, 6 H, NCH_2Ar), 3.79 (s, 9 H, OCH_3), 4.95 (s, 6 H, OCH_2Ar), 6.85 (d, J^3 = 8.8 Hz, 6 H, H-f), 6.84 – 6.93 (m, 6 H, H-a & H-c), 7.14 (ddd, J^3 = 7.8 Hz, J^3 = 7.6 Hz, J^4 = 1.8 Hz, 3 H, H-b), 7.30 (d, J^3 = 8.8 Hz, 6 H, H-e), 7.70 (dd, J^3 = 7.5 Hz, J^4 = 1.8 Hz, 3 H, H-d); ^{13}C NMR (75 MHz, $CDCl_3$): δ = 52.66, 55.47, 69.89, 111.61, 114.13, 120.98, 127.33, 129.10, 129.32, 129.68, 156.97, 159.44; positive ion ESI-HRMS: m/z (*M* = $C_{45}H_{45}NO_6$ in CH_2Cl_2 / MeOH): calcd for $[M + H]^{1+}$: 696.3320, found 696.3264.

Tris-[2-(5'-methyl-[2,2']bipyridin-5-ylmethoxy)benzyl]-amine (176): A solution of aldehyde **99** (50 mg, 0.164 mmol), NH_4OAc (21 mg, 0.27 mmol) and $NaBH(OAc)_3$ (173 mg, 0.82 mmol) in dry DMF (5 cm^3) was stirred at room temperature for 24 h. The reaction was quenched by the addition of H_2O (10 cm^3) and the resulting precipitate was isolated by filtration. TLC of this crude material indicated a mixture of 3 products. A solution of the crude material, aldehyde **99** (20 mg, 0.066 mmol) and $NaBH(OAc)_3$ (70 mg, 0.33 mmol) in DMF (5 cm^3) was stirred at room temperature overnight. Following workup, TLC of this material indicated the predominance of a single product with two other minor products. This material was purified by chromatography on silica gel with DCM, MeOH and saturated NH_3 (99:0.75:0.25) as eluent to afford **176** (20 - 30 %) as a semipure white solid. ^{1}H NMR (300 MHz, $CDCl_3$): δ = 2.37 (s, 9 H, CH_3), 3.81 (s, 6 H, NCH_2Ar), 5.08 (s, 6 H, OCH_2Ar), 6.87 (d, J^3 = 8.4 Hz, 3 H, H-a), 6.94 (t, J^3 = 7.5 Hz, 3 H, H-c), 7.16 (t, J^3 = 7.5 Hz, 3 H, H-b), 7.57 (dd, J^3 = 8.4 Hz, J^4 = 2.4 Hz, 3 H, H-d), 7.70 (dd, J^3 = 8.1 Hz, J^4 = 1.5 Hz, 3 H), 7.79 (dd, J^3 = 8.4 Hz, J^4 = 1.8 Hz, 3 H), 8.23 (d, J^3 = 8.1 Hz, 3 H), 8.31 (d, J^3 = 8.4 Hz, 3 H), 8.47 (d, J^4 = 1.5 Hz, 3 H), 8.68 (b s, 3 H); ^{13}C NMR (75 MHz, $CDCl_3$): δ = 18.60, 52.74, 67.70, 111.51, 120.83, 121.39, 127.60, 128.87, 129.54, 132.72, 133.59, 136.26, 137.63, 148.33, 149.85, 153.59, 156.10, 156.57; positive ion ESI-HRMS: m/z (*M* = $C_{69}H_{75}N_7O_3$ in CH_2Cl_2 / MeOH): calcd for $[M + H]^{1+}$: 882.4126, found 882.4083.

Tris-[5-*tert*-butyl-2-(5'-methyl-[2,2']bipyridinyl-5-ylmethoxy) benzyl]-amine (177): A solution of aldehyde **100** (60 mg, 0.17 mmol), NH_4OAc (21 mg, 0.27 mmol) and $NaBH(OAc)_3$ (173 mg, 0.82 mmol) in dry DMF (4 cm^3) was stirred at room temperature for 24 h. The reaction was quenched by the addition of H_2O (4 cm^3) and the resulting precipitate isolated by filtration. TLC of this crude material indicated a mixture of three products. A solution of the crude material, aldehyde **100** (20 mg, 0.066 mmol) and $NaBH(OAc)_3$ (70 mg, 0.33 mmol) in DMF (4 cm^3) was stirred at room temperature overnight. Following workup, TLC of this material indicated the predominance of a single product with two other minor products. This material purified by chromatography on silica gel with DCM, MeOH and saturated NH_3 (99:0.75:0.25) as eluent to afford **177** (20 - 30 %) as a semipure white solid. ^{1}H NMR (300 MHz, CD_2Cl_2): δ = 1.27 (s, 27 H, t-Bu), 2.37 (s, 9 H, CH_3), 3.84 (s, 6 H, NCH_2Ar), 5.09 (s, 6 H, OCH_2Ar), 6.86 (d, J^3 = 8.5 Hz, 3 H, H-a), 7.20 (dd, J^3 = 8.5 Hz, J^4 = 2.5 Hz, 3 H, H-b), 7.58 (dd, J^3 = 8.2 Hz, J^4 = 1.8 Hz, 3 H, H-4′), 7.81 (br d, J^3 = 8.2 Hz, 3 H, H-4), 7.92 (d, J^4 = 2.5 Hz, 3 H, H-c), 8.25 (d, J^3 = 8.2 Hz, 3 H, H-3′), 8.33 (d, J^3 = 8.2 Hz, 3 H, H-3), 8.44 (br s, 3 H, H-6′), 8.66 (br s, 3 H, H-6); ^{13}C NMR (75 MHz, $CDCl_3$): δ = 18.27, 31.60, 34.30, 52.48, 67.85, 111.08, 120.41, 120.47, 123.87, 125.93, 128.22, 132.94, 133.68, 136.07, 137.40, 143.92, 148.25, 149.72, 153.44, 154.37, 155.92; positive ion ESI-HRMS: m/z (M = $C_{69}H_{75}N_7O_3$ in CH_2Cl_2 / MeOH): calcd for $[M + H]^{1+}$: 1050.6004, found 1050.5953.

[Fe(176)](PF$_6$)$_2$ (179): A stirred solution of aldehyde **99** (61 mg, 0.2 mmol), $Fe(BF_4)_2.6H_2O$ (23 mg, 0.067 mmol) in acetonitrile (10 cm^3) was refluxed for 40 min (for the ^{1}H NMR spectrum of [Fe(**99**)$_3$](PF$_6$)$_2$, **178**, see ***Figure 5.2*** b), page 219). The reaction mixture was cooled to room temperature and further acetonitrile (90 cm^3) added. To this, NH_4OAc (77 mg, 1.0 mmol) was added and the resulting mixture stirred for 0.5 h. The reaction mixture was then cooled to 0 °C in an ice bath followed by the addition of $NaCNBH_3$ (124 mg, 2.0 mmol). After 1 h the reaction mixture was allowed to warm to room temperature and stirred overnight. Following this, the solvent volume was reduced under vacuum to approximately 5 cm^3 and excess KPF_6 in H_2O (15 cm^3) was added. The resulting precipitate was isolated by filtration and washed with H_2O and a minimum volume of cold MeOH. The crude product was purified by chromatography on silica gel with CH_3CN, H_2O and saturated KNO_3

(7:1:0.5) as eluent to afford **179** (51 mg, 62 %) as a red solid. ^{1}H NMR (300 MHz, CD_3CN): δ = 2.24 (s, 9 H, CH_3), 3.94 (d, J^2 = 13.2 Hz, 3 H, NCH_2Ar), 4.01 (d, J^2 = 13.2 Hz, 3 H, NCH_2Ar), 5.04 (d, J^2 = 12.0 Hz, 3 H, OCH_2Ar), 5.09 (d, J^2 = 12.0 Hz, 3 H, OCH_2Ar), 7.05 – 7.20 (m, 12 H), 7.41 (br s, 3 H, H-6), 7.54 (ddd, J^3 = 7.5 Hz, J^3 = 7.5 Hz, J^4 = 1.8 Hz, 3 H, H-b), 7.80 (br s, 3 H, H-6′), 7.98 (d, J^3 = 8.3 Hz, H-4), 8.02 (d, J^3 = 8.3 Hz, H-4), 8.44 (d, J^3 = 8.3 Hz, H-3), 8.49 (d, J^3 = 8.3 Hz, H-3); ^{13}C NMR (75 MHz, CD_3CN): δ = 18.11, 51.64, 67.20, 112.37, 121.90, 123.74, 123.97, 132.70, 133.88, 136.52, 138.05, 138.88, 139.47, 152.29, 154.44, 156.45, 157.45, 157.42, 159.53; positive ion ESI-HRMS: m/z (M = $C_{57}H_{51}F_{12}FeN_7O_3P_2$ in CH_3CN / MeOH): calcd for $[M - PF_6]^{1+}$: 1082.3041, found 1082.3004; calcd for $[M - 2PF_6]^{2+}$: 468.6697, found 466.6699; X-ray quality crystals were obtained by diffusion of MeOH into a CH_3CN solution of the product.

$[Fe(L)](PF_6)_2$ (180): Procedure as per the synthesis of **179** from aldehyde **110** (52 mg, 0.1 mmol), $Fe(BF_4)_2.6H_2O$ (10 mg, 0.03 mmol), NH_4OAc (39 mg, 0.5 mmol) and $NaCNBH_3$ (62 mg, 1 mmol) in acetonitrile (80 cm^3 total). The crude product was purified by chromatography on silica gel with CH_3CN, H_2O and saturated KNO_3 (7:1:0.5) as eluent to afford **180** (44 mg, 77 %) as a red solid. ^{1}H NMR (300 MHz, CD_3CN): δ = 1.29 (s, 27 H, t-Bu), 1.5 – 2.0 (m, 18 H, CH_2), 3.54 (m, 6 H, OCH_2), 3.74 (m, 6 H, OCH_2), 3.95 (d, J^2 = 14.9 Hz, 3 H, NCH_2Ar), 4.05 (d, J^2 = 14.9 Hz, 3 H, NCH_2Ar), 5.08 (br s, 6 H, OCH_2Ar), 5.48 (br s, 3 H, OCHO), 7.04 (d, J^3 = 8.7 Hz, 12 H, H-e), 7.07 (d, J^3 = 8.7 Hz, 12 H, H-d), 7.35 (d, J^4 = 2.4 Hz, 3 H, H-c), 7.35 (d, J^3 = 8.7 Hz, 3 H, H-a), 7.57 (dd, J^3 = 8.7 Hz, J^4 = 2.4 Hz, 3 H, H-b), 7.61 (br s, 3 H), 7.94 (br s, 3 H), 8.04 (d, J^3 = 8.1 Hz, 3 H), 8.40 (dd, J^3 = 8.4 Hz, J^4 = 1.9 Hz, 3 H), 8.57 (d, J^3 = 8.1 Hz, 3 H), 8.61 (d, J^3 = 8.4 Hz, 3 H); positive ion ESI-HRMS: m/z (M = $C_{99}H_{105}F_{12}FeN_7O_9P_2$ in CH_3CN / MeOH): calcd for $[M - 2PF_6]^{2+}$: 796.3673, found 796.3642.

$[Fe(116)_3](PF_6)_2$ (181): A stirred solution of dialdehyde **116** (70 mg, 0.1 mmol), $Fe(BF_4)_2.6H_2O$ (11 mg, 0.033 mmol) in acetonitrile (10 cm^3) was refluxed for 40 min. The solvent was removed and the crude product purified by chromatography on silica gel eluting with, CH_3CN, H_2O and saturated KNO_3 (7:1:0.5). The purified material was precipitated by the addition of excess KPF_6 in H_2O (10 cm^3) and the product was isolated by filtration. This

precipitate was sequentially washed with H_2O, a minimum volume of cold MeOH and Et_2O to afford **181** (76 mg, 95 %) as a red solid. ^{1}H NMR (300 MHz, CD_3CN): δ = 3.76 (s, 18 H, OCH_3), 4.91 (d, J^3 = 11.3 Hz, 6 H, OCH_2Ar), 5.51 (d, J^3 = 11.3 Hz, 6 H, OCH_2Ar), 5.03 (d, J^3 = 14.3 Hz, 6 H, OCH_2Ar), 5.18 (d, J^3 = 14.3 Hz, 6 H, OCH_2Ar), 6.27 (s, 6 H, H-a), 6.72 (d, J^3 = 8.7 Hz, 6 H), 6.90 (d, J^3 = 8.7 Hz, 12 H, H-e), 7.31 (d, J^3 = 8.7 Hz, 12 H, H-d), 7.32 (overlapping, 6 H, H-6,6′), 7.73 (d, J^3 = 8.7 Hz, 6 H, H-c), 7.95 (d, J^3 = 8.3 Hz, 6 H, H-3,3′), 8.17 (d, J^3 = 8.3 Hz, 6 H, H-4,4′), 9.72 (s, 6 H, CHO); positive ion ESI-HRMS: m/z (M = $C_{126}H_{108}F_{12}FeN_6O_{24}P_2$ in CH_3CN / MeOH): calcd for $[M - 2PF_6]^{2+}$: 1072.8394, found 1072.8311.

$[Fe(L^1)](PF_6)_2$ (182): A solution of **181** (76 mg, 0.031 mmol) and NH_4OAc (154 mg, 2 mmol) in acetonitrile (80 cm^3) stirred for 0.5 h at room temperature. The reaction mixture was then cooled to 0 °C in an ice bath before the addition of $NaCNBH_3$ (124 mg, 2 mmol). After 1 h the reaction mixture was allowed to warm to room temperature and stirred overnight. Workup and purification were as described for **179** and afforded **182** (64 mg, 87 %) as a red solid. ^{1}H NMR (300 MHz, CD_3CN): δ = 3.81 (s, 18 H, OCH_3), 3.82 (d, J^2 = 15.4 Hz, 6 H, NCH_2Ar), 3.91 (d, J^2 = 15.4 Hz, 6 H, NCH_2Ar), 5.06 (s, 12 H, OCH_2Ar), 5.08 (s, 12 H, OCH_2Ar), 6.70 (br d, J^3 = 9.2 Hz, 6 H, H-b), 6.71 (s, 6 H, H-a), 6.97 (d, J^3 = 8.8 Hz, 6 H, H-e), 7.09 (d, J^3 = 9.2 Hz, 6 H, H-c), 7.40 (d, J^3 = 8.8 Hz, 6 H, H-d), 7.80 (s, 6 H, H-6,6′), 8.06 (br d, J^3 = 8.4 Hz, 6 H, H-4,4′), 8.57 (d, J^3 = 8.4 Hz, 6 H, H-3,3′); ^{13}C NMR (75 MHz, CD_3CN): δ = 55.19, 66.68, 70.27, 99.97, 108.16, 114.17, 118.86, 123.73, 128.25, 130.05, 131.10, 136.77, 137.17, 151.39, 157.89, 160.00, 161.71, 165.49, 187.11; positive ion ESI-HRMS: m/z (M = $C_{126}H_{114}F_{12}FeN_8O_{18}P_2$ in CH_3CN / MeOH): calcd for $[M - 2PF_6]^{2+}$: 1041.8812, found 1041.8712.

$[Fe_2(141)_3](PF_6)_4$ (183): A solution of $Fe(BF_4)_2.6H_2O$ (13.6 mg, 0.0403 mmol) and dialdehyde **141** (55 mg, 0.0665 mmol) in CH_3CN (50 cm^3) was heated with microwave energy in a sealed pressurised microwave vessel with temperature and pressure sensors and a magnetic stirrer bar (step 1 – ramped to 130 °C over 2 min using 100 % of 400 W; step 2 – held at 130 °C for 10 min using 25 % of 400 W). This crude material was purified by chromatography on silica gel with CH_3CN, H_2O and saturated KNO_3 (7:1:0.5) as eluent. The

purified product was isolated by precipitation with excess aqueous NH_3PF_6 in H_2O (20 cm^3) followed by filtration to afford **183** (25 mg, 41 %) as a red solid. ^1H NMR (300 MHz, CD_3CN): δ = 1.32 (s, 54 H, *t*-Bu), 3.54 (s, 18 H, OCH_3), 5.23 (d, J^2 = 13.9 Hz, 6 H, OCH_2Ar), 5.30 (d, J^2 = 13.9 Hz, 6 H, OCH_2Ar), 6.82 (s, 6 H, H-3,6), 7.00 (d, J^3 = 8.9 Hz, 6 H, H-a), 7.33 (br s, 6 H), 7.66 (dd, J^3 = 8.9 Hz, J^4 = 2.6 Hz, 6 H, H-b), 7.70 (br s, 6 H), 7.77 (d, J^4 = 2.6 Hz, 6 H, H-c), 8.24 (br d, J^3 = 8.4 Hz, 6 H), 8.47 (br d, J^3 = 8.5 Hz, 6 H), 8.57 (d, J^3 = 8.4 Hz, 6 H), 8.67 (d, J^3 = 8.5 Hz, 6 H), 10.04 (s, 6 H, CHO); positive ion ESI-HRMS: m/z (M = $C_{156}H_{150}F_{24}Fe_2N_{12}O_{18}P_4$ in CH_3CN / MeOH): calcd for $[M - 2PF_6]^{2+}$: 1440.9601, found 1440.9680; calcd for $[M - 3PF_6]^{3+}$: 912.3185, found 912.3218.

$[Fe_2(L)](PF_6)_4$ (184): Procedure as per the synthesis of **182** from precursor complex **183** (25 mg, 0.008 mmol), NH_4OAc (16 mg, 0.16 mmol) $NaCNBH_3$ (12 mg, 0.2 mmol) in acetonitrile (50 cm^3). The workup and purification was as for **179** and afforded **184** as a semipure red solid (yield not recorded due to the presence of an impurity). Positive ion ESI-HRMS: m/z (M = $C_{156}H_{156}F_{24}Fe_2N_{14}O_{12}P_4$ in CH_3CN / MeOH): calcd for $[M - 2PF_6]^{2+}$: 1410.0018, found 1410.0003; calcd for $[M - 3PF_6]^{3+}$: 891.6796, found 891.6838; calcd for $[M - 4PF_6]^{4+}$: 632.5186, found 632.5211.

$[Ni_2(L)](PF_6)_4$ (186): A stirred solution of dialdehyde **141** (20 mg, 0.024 mmol), $Ni(NO_3)_2.6H_2O$ (4.7 mg, 0.016 mmol) in acetonitrile (10 cm^3) was refluxed for 40 min. The reaction mixture was cooled to room temperature and further acetonitrile (50 cm^3) was added. To this solution NH_4OAc (37 mg, 0.48 mmol) was added and the resulting mixture stirred for 0.5 h. The reaction mixture was then cooled to 0 °C in an ice bath followed by the addition of $NaCNBH_3$ (124 mg, 2 mmol). After 1 h the reaction mixture was allowed to warm to room temperature and stirred overnight. Following this, the solvent was reduced under vacuum to a volume of approximately 5 cm^3 and excess KPF_6 in H_2O (15 cm^3) was added. The resulting precipitate was isolated by filtration and washed with H_2O and a minimum volume of cold MeOH. The crude product was purified by chromatography on silica gel with CH_3CN, H_2O and saturated KNO_3 (7:1:0.5) as eluent to afford **186** as a yellow solid (yield was not recorded due to the presence of an impurity). Positive ion ESI-HRMS: m/z (M = $C_{156}H_{156}F_{24}Ni_2N_{14}O_{12}P_4$ in CH_3CN / MeOH): calcd for $[M - 2PF_6]^{2+}$: 1411.5003, found

1411.4975; calcd for $[M - 3PF_6]^{3+}$: 892.6786, found 892.6802; calcd for $[M - 4PF_6]^{4+}$: 633.2678, found 633.2675.

$[Fe_4(144)_6](BF_4)_8$ (187): A stirred solution of dialdehyde **144** (160 mg, 0.231 mmol) and $Fe(BF_4)_2.6H_2O$ (52 mg, 0.154 mmol) in acetonitrile (15 cm^3) was refluxed for 48 h. The reaction mixture was filtered to remove excess ligand. The crude product was purified by chromatography on sephadex LH-20 with acetonitrile as eluent to afford **187** (173 mg, 89 %) as a red solid. ^{1}H NMR (300 MHz, CD_3CN): δ = 1.22 (s, 108 H, *t*-Bu), 5.17 (d, J^2 = 14.0 Hz, 12 H, OCH_2Ar), 5.25 (d, J^2 = 14.0 Hz, 12 H, OCH_2Ar), 6.93 (d, J^3 = 8.9 Hz, 12 H, H-a), 7.21 (d, J^4 = 1.8 Hz, 12 H, H-6′,6″), 7.33 (dd, J^3 = 8.4 Hz, J^4 = 1.8 Hz, 12 H, H-4′,4″), 7.57 (dd, J^3 = 8.9 Hz, J^4 = 2.7 Hz, 12 H, H-b), 7.70 (d, J^4 = 2.7 Hz, 12 H, H-c), 7.81 (s, 12 H, H-6,6‴), 8.25 (br d, J^3 = 8.4 Hz, 12 H, H-4,4‴), 8.42 (d, J^3 = 8.4 Hz, 12 H, H-3′,3″), 8.61 (d, J^3 = 8.4 Hz, 12 H, H-3,3‴), 9.87 (s, 12 H, CHO); ^{13}C NMR (75 MHz, CD_3CN): δ = 30.61, 34.09, 66.90, 113.13, 123.60, 124.21, 124.58, 125.08, 133.70, 136.25, 137.66, 139.91, 144.63, 151.80, 152.38, 157.79, 157.90, 158.90, 188.92; positive ion ESI-HRMS: m/z (M = $C_{264}H_{252}F_{32}Fe_4N_{24}O_{24}B_8$ in CH_3CN / MeOH): calcd for $[M - 3BF_4]^{3+}$: 1600.8966, found 1608.9083; calcd for $[M - 4BF_4]^{4+}$: 1178.9213, found 1178.9254.

$[Fe_4(L)](PF_6)_8$ (188): A solution of **187** (20 mg, 0.004 mmol) and NH_4OAc (32 mg, 0.42 mmol) in acetonitrile (50 cm^3) was stirred at room temperature for 0.5 h. The reaction mixture was cooled to 0 °C in an ice bath prior to the addition of $NaCNBH_3$ (60 mg, 0.96 mmol). This reaction mixture was held at 0 °C for 2 h prior to warming to room temperature and being stirred overnight. The solvent volume was reduced under vacuum to approximately 10 cm^3 and the product precipitated by the addition of an excess of NH_4PF_6 in H_2O (20 cm^3). The crude product was isolated by filtration and purified by chromatography on silica gel with CH_3CN, H_2O and saturated KNO_3 (7:1:0.5) as eluent to afford **188** (12 mg, 55 %) as a red semipure solid. ^{1}H NMR (300 MHz, CD_3CN): δ = 1.28 (s, 108 H, *t*-Bu), 4.05 (br d, 12 H, NCH_2Ar), 4.15 (br d, 12 H, NCH_2Ar), 5.03 (d, J^2 = 12.3 Hz, 12 H, OCH_2Ar), 5.16 (d, J^2 = 12.3 Hz, 12 H, OCH_2Ar), 6.91 (br s, 12 H) 7.07 (d, J^3 = 9.0 Hz, 12 H, H-a), 7.21 (d, J^4 = 1.8 Hz, 12 H, H-c), 7.40 (dd, J^3 = 9.0 Hz, J^4 = 1.8 Hz, H-b), 7.57 (br d, J^3 = 8.4 Hz, 12 H), 8.13 (br d, J^3 = 8.4 Hz, 12 H), 8.24 (br s, 12 H), 8.57 (d, J^3 = 8.4 Hz, 12 H), 8.67 (d, J^3 = 8.4 Hz,

12 H); positive ion ESI-HRMS: m/z (M = $C_{264}H_{264}F_{48}Fe_4N_{28}O_{12}P_8$ in CH_3CN / MeOH): calcd for $[M - 3PF_6]^{3+}$: 1656.2193, found 1656.2465; calcd for $[M - 4PF_6]^{4+}$: 1205.9233, found 1205.9367; calcd for $[M - 5PF_6]^{5+}$: 935.7457, found 935.7510; calcd for $[M - 6PF_6]^{6+}$: 755.6273, found 755.6303.

$[Fe_4(142)_6](PF_6)_8$ (189): A stirred solution of dialdehyde **142** (24 mg, 0.025 mmol) and $Fe(BF_4)2.6H_2O$ (5.6 mg, 0.0167 mmol) in acetonitrile (10 cm^3) was heated using microwave energy in a sealed pressurised microwave vessel with temperature and pressure sensors (step 1 – ramped to 120 °C over 2 min using 100 % of 400 W; step 2 – held at 120 °C for 40 min using 25 % of 400 W). The crude product was purified by chromatography on silica gel with CH_3CN, H_2O and saturated KNO_3 (7:1:0.5) as eluent to afford **188** (27 mg, 91 %) as a red solid. ^{1}H NMR (300 MHz, CD_3CN): δ = 1.30 (s, 108 H, t-Bu), 3.46 (s, 36 H, OCH_3), 3.60 (s, 36 H, OCH_3), 5.19 (d, J^2 = 14.0 Hz, 12 H, OCH_2Ar), 5.27 (d, J^2 = 14.0 Hz, 12 H, OCH_2Ar), 6.88 (s, 12 H, H-3,3′ or 6,6′), 6.89 (s, 12 H, H-3,3′ or 6,6′), 6.98 (d, J^3 = 8.9 Hz, 12 H, H-a), 7.65 (dd, J^3 = 8.9 Hz, J^4 = 2.6 Hz, 12 H, H-b), 7.70 (br s, 12 H), 7.75 (d, J^4 = 2.6 Hz, 12 H, H-c), 7.80 (br s, 12 H), 8.21 (br d, J^3 = 8.1 Hz, 12 H), 8.35 (br d, J^3 = 8.4 Hz, 12 H), 8.59 (br m, 24 H), 9.94 (s, 12 H, CHO); ^{13}C NMR (75 MHz, CD_3CN): δ = 30.65, 34.15, 56.22, 56.27, 67.04, 113.14, 113.66, 115.95, 123.65, 123.75, 124.21, 124.98, 128.82, 122.74,137.18, 137.64, 144.69, 149.99, 151.53, 151.90, 152.08, 156.97, 158.11, 158.67, 189.00; positive ion ESI-HRMS: m/z (M = $C_{360}H_{348}F_{48}Fe_4N_{24}O_{48}P_8$ in CH_3CN / MeOH): calcd for $[M - 4PF_6]^{4+}$: 1645.2897, found 1645.2743; calcd for $[M - 5PF_6]^{5+}$: 1287.2369, found 1287.2277; calcd for $[M - 6PF_6]^{6+}$: 1048.5383, found 1048.5332.

$[Fe_4(L)](PF_6)_4$ (190): A solution of **189** (27 mg, 0.0038 mmol) and NH_4OAc (39 mg, 0.5 mmol) in acetonitrile (50 cm^3) was stirred at room temperature for 0.5 h. The reaction mixture was cooled to 0 °C in an ice bath prior to the addition of $NaCNBH_3$ (31 mg, 0.5 mmol). This reaction mixture was held at 0 °C for 2 h before warming to room temperature and was stirred overnight. The volume was then reduced under vacuum to approximately 10 cm^3 and the product was precipitated by addition of an excess of NH_4PF_6 in H_2O (20 cm^3). The crude product was isolated by filtration and purified by chromatography on silica gel with CH_3CN, H_2O and saturated KNO_3 (7:1:0.5) as eluent to afford **190** (16 mg, 62 %) as a

semipure red solid. ^{1}H NMR (300 MHz, CD_3CN): δ = 1.30 (s, 108 H, *t*-Bu), 3.50 (s, 36 H, OCH_3), 3.63 (s, 36 H, OCH_3), 4.02 (br s, 24 H, NCH_2Ar), 5.11 (br s, 24 H, OCH_2Ar), 6.92 (s, 24 H), 7.06 (br d, 12 H), 7.21 (br s, 12 H), 7.57 (br s, 12 H), 7.84 (br s, 12 H), 7.94 (br s, 12 H), 8.09 (br d, 12 H), 8.38 (br d, 12 H), 8.68 (br d, 24 H); positive ion ESI-HRMS: m/z (*M* = $C_{360}H_{360}F_{48}Fe_4N_{28}O_{36}P_8$ in CH_3CN / MeOH): calcd for $[M - 5PF_6]^{5+}$: 1262.4722, found 1262.4823; calcd for $[M - 6PF_6]^{6+}$: 1027.8994, found 1027.9021; calcd for $[M - 7PF_6]^{7+}$: 860.3474, found 860.3631; calcd for $[M - 8PF_6]^{8+}$: 734.6834, found 734.6956.

5.5 REFERENCES

1. J. F. Stoddart and H.-R. Tseng, *Proc. Nat. Acad. Sci. U.S.A.*, 2002, **99**, 4797.
2. L. F. Lindoy, *The Chemistry of Macrocyclic Ligand Complexes*, Cambridge University Press, Cambridge, 1989.
3. D. F. Perkins, L. F. Lindoy, A. McAuley, G. V. Meehan and P. Turner, *Proc. Nat. Acad. Sci. U.S.A.*, 2006, **103**, 532.
4. D. F. Perkins, L. F. Lindoy, G. V. Meehan and P. Turner, *Chem. Commun.*, 2004, 152.
5. L. F. Lindoy and I. M. Atkinson, *Self-assembly in Supramolecular Chemistry*, Royal Society of Chemistry, Cambridge, UK., 2000.
6. B. Champin, P. Mobian and J.-P. Sauvage, *Chem. Soc. Rev.*, 2007, **36**, 358.
7. C. Dietrich-Buchecker, G. Rapenne and J.-P. Sauvage, *Coord. Chem. Rev.*, 1999, **185-186**, 167.
8. S. Saha and J. F. Stoddart, *Chem. Soc. Rev.*, 2007, **36**, 77.
9. C. Dietrich-Buchecker, J. Guilhem, C. Pascard and J. P. Sauvage, *Angew. Chem. Int. Ed.*, 1990, **29**, 1154.
10. C. Dietrich-Buchecker, G. Rapenne and J.-P. Sauvage, *Chem. Commun.*, 1997, 2053.
11. C. Dietrich-Buchecker and J. P. Sauvage, *Angew. Chem. Int. Ed.*, 1989, **28**, 189.
12. C. Dietrich-Buchecker, J. P. Sauvage, A. De Cian and J. Fischer, *Chem. Commun.*, 1994, 2231.
13. C. O. Dietrich-Buchecker, J. F. Nierengarten, J. P. Sauvage, N. Armaroli, V. Balzani and L. De Cola, *J. Am. Chem. Soc.*, 1993, **115**, 11237.
14. S. C. J. Meskers, H. P. J. M. Dekkers, G. Rapenne and J.-P. Sauvage, *Chem. Eur. J.*, 2000, **6**, 2129.
15. M. Meyer, A. M. Albrecht-Gary, C. O. Dietrich-Buchecker and J. P. Sauvage, *J. Am. Chem. Soc.*, 1997, **119**, 4599.
16. L.-E. Perret-Aebi, A. v. Zelewsky, C. Dietrich-Buchecker and J. P. Sauvage, *Angew. Chem. Int. Ed.*, 2004, **43**, 4482.
17. G. Rapenne, C. Dietrich-Buchecker and J. P. Sauvage, *J. Am. Chem. Soc.*, 1999, **121**, 994.

18. K. S. Chichak, S. J. Cantrill, A. R. Pease, S.-H. Chiu, G. W. V. Cave, J. L. Atwood and J. F. Stoddart, *Science*, 2004, **304**, 1308.
19. K. S. Chichak, S. J. Cantrill and J. F. Stoddart, *Chem. Commun.*, 2005, 3391.
20. K. S. Chichak, A. J. Peters, S. J. Cantrill and J. F. Stoddart, *J. Org. Chem.*, 2005, **70**, 7956.
21. C. D. Meyer, C. S. Joiner and J. F. Stoddart, *Chem. Soc. Rev.*, 2007, **36**, 1705.
22. K. R. Adam, I. M. Atkinson, J. Kim, L. F. Lindoy, O. A. Matthews, G. V. Meehan, F. Raciti, B. W. Skelton, N. Svenstrup and A. H. White, *Dalton Trans.*, 2001, 2388.
23. I. M. Atkinson, A. R. Carroll, R. J. Janssen, L. F. Lindoy, O. A. Mathews and G. V. Meehan, *J. Chem. Soc., Perkins Trans. 1*, 1997, **3**, 295.
24. R. J. Janssen, L. F. Lindoy, O. A. Mathews, G. V. Meehan, A. N. Sobolev and A. H. White, *Chem. Commun.*, 1995, 7.
25. A. Chandrasekaran, R. O. Day and R. R. Holmes, *J. Am. Chem. Soc.*, 2000, **122**, 1066.
26. J. Hwang, K. Govindaswamy and S. A. Kock, *Chem. Commun.*, 1998, 1667.
27. L. J. Prins, M. M. K. Blazquez, A. and G. Licini, *Tetrahedron Lett.*, 2006, **47**, 2735.
28. A. F. Abdel-Magid, K. G. Carson, B. D. Harris, C. A. Maryanoff and R. D. Shah, *J. Org. Chem.*, 1996, **61**, 3849.
29. C. D. Gutierrez, V. Bavetsias and E. McDonald, *Tetrahedron Lett.*, 2005, **46**, 3595.
30. N. Su, J. S. Bradshaw, X. X. Zhang, H. Song, P. B. Savage, G. Xue, K. E. Krakowiak and R. M. Izatt, *J. Org. Chem.*, 1999, **64**, 8855.
31. A. F. Abdel-Magid, C. A. Maryanoff and K. G. Carson, *Tetrahedron Lett.*, 1990, **31**, 5595.
32. S. P. Hajela, A. R. Johnson, J. Xu, C. J. Sunderland, S. M. Cohen, D. L. Caulder and K. N. Raymond, *Inorg. Chem.*, 2001, **40**, 3208.
33. D. C. Beshore and C. J. Dinsmore, *Org. Lett.*, 2002, **4**, 1201.
34. P. Forns, S. Sevilla, M. Erra, A. Ortega, J.-C. Fernandez, N. de la Figuera, D. Fernandez-Forner and F. Albericio, *Tetrahedron Lett.*, 2003, **44**, 6907.
35. D. S. Dalpathado, H. Jiang, M. A. Kater and H. Desaire, *Anal. Bioanal. Chem.*, 2005, **381**, 1130.

36. D. J. Bray, B. Antonioli, J. K. Clegg, K. Gloe, K. Gloe, K. A. Jolliffe, L. F. Lindoy, G. Wei and M. Wenzel, *Dalton Trans.*, 2008, 1683.

37. D. J. Bray, L.-L. Liao, B. Antonioli, K. Gloe, L. F. Lindoy, J. C. McMurtrie, G. Wei and X.-Y. Zhang, *Dalton Trans.*, 2005, 2082.

38. T. Castle, M. E. Evans and S. T. Hyde, *New. J. Chem.*, 2008, **32**, 1484.

Chapter 6

Summary and Future Work

6.1 OVERVIEW OF THE PRESENT STUDY

A series of dimethylquaterpyridyl ligands has been synthesized in order to investigate the metallosupramolecular products derived from their interaction with octahedral metal ions. In this regard, the metal-directed assembly of the linear 5,5‴-dimethylquaterpyridine **50** with Fe(II), Co(II) and Ni(II) salts, in a 3:2 ratio, leads to tetrahedral M_4L_6 cationic hosts. Further, anion binding studies revealed that $[Fe_4(\mathbf{50})_6]^{8+}$ selectively binds PF_6^- over BF_4^-.

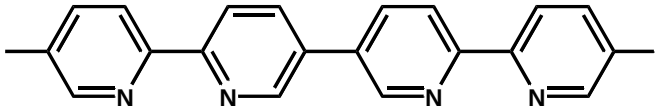

50

In contrast, reaction of **50** with $RuCl_3$ in a 3:2 ratio in ethylene glycol using microwave heating at 230° C afforded triple helicate **160** in moderate yield (40%). This species interacts selectively with DNA, with the *M*-helicate binding selectively to calf thymus and various other B-DNA strands.

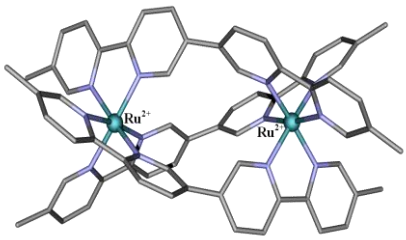

160

To extend these studies, the dimethoxyphenylene- and tetramethoxybiphenylene-bridged quaterpyridines **128** and **129** were prepared by a combination of Stille and Suzuki coupling methodologies and the corresponding metal-directed self assembly reactions examined. Interaction of these ligands with Fe(II) and Ni(II) afforded *mixtures* of the M_2L_3 and M_4L_6 species. Control over the ratio of M_2L_3 and M_4L_6 species is possible by variation of reaction times and dilution factor; short reaction times and high dilution

favour the production of M_2L_3 species, while long reaction times and concentrated reaction mixtures favour production of the M_4L_6 species. Indeed, these observations are indicative of the M_2L_3 species being kinetic products while the M_4L_6 species appear to be the thermodynamically preferred products. Interestingly, the M_2L_3 and M_4L_6 species incorporating quaterpyridines **128** and **129** fluoresce when irradiated at the wavelength of the CT-bands associated with the presence of the dimethoxyphenylene- and tetramethoxybiphenylene-spacer. In this regard, a change in emission intensity was observed when $[Fe_4(\mathbf{129})_6]^{8+}$ was exposed to BPh_4^-, thus indicating that the M_4L_6 species derived from **128** and **129** may find application in size selective host-guest signaling devices.

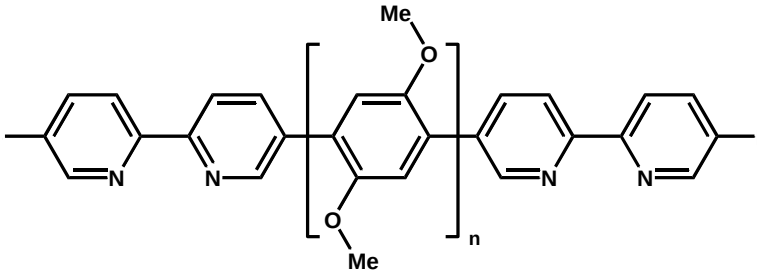

128; n = 1
129; n = 2

A series of bipyridyl and quaterpyridyl derivatives incorporating salicyloxy moieties were synthesized for incorporation into tripodal ligands, cryptates and larger tetranuclear polycyclic species via a one pot metal-template reductive amination procedure. Two pseudocryptands were synthesized in good yields and it is expected that, following optimization and demetallation, this synthetic approach will provide a high yielding alternative relative to other stepwise approaches. As a highlight, the successful syntheses of two dinuclear cryptates and two tetranuclear polycycles have been achieved. The syntheses of these latter products are the result of the application of preliminary observations made from the metal-directed assembly of simpler model quaterpyridines **50**, **128** and **129** combined with the efficient metal-template reductive amination procedure developed previously by Perkins *et al.*[1,2] There is no doubt that these exciting molecules highlight the exceptional influence that metal-template processes continue to have over metallosupramolecular design and outcomes.[3-19]

6.2 FUTURE STUDIES

6.2.1 Investigation of the above-mentioned series of M_4L_6 tetrahedra.

The selectivity for PF_6^- over BF_4^- of $[Fe_4(\mathbf{50})_6]^{8+}$ indicates that related selectivity can be expected for larger tetrahedra derived from the extended quaterpyridine ligands **128** and **129** and appropriate anions. Such studies might well include the environmentally problematic but radiopharmaceutically important pertechnetate anion.[20] The chiral nature of these tetrahedra also raises the possibility of enantioselective anion recognition.[21] In this regard, the separated enantiomers of the racemate of $[Fe_4(\mathbf{50})_6](PF_6)_8$ show a retarded rate of racemisation similar to that of related M_4L_6 tetrahedra.[22,23] Future work will initially focus on a systematic study of potential anionic guest species of appropriate size relative to the cavity volumes of each of the tetrahedra isolated during the project. With respect to this, further investigation into the potential application of the M_4L_6 incorporating **128** and **129** as signaling devices also appears quite promising.

Crystal structures of several M_4L_6 tetrahedra derived from the self-assembly of quaterpyridines **50**, **128** and **129** revealed metal to metal distances of approximately 9.4 Å, 13.2 Å and 17.2 Å, respectively. These distances translate into approximate enclosed volumes of 100 $Å^3$, 270 $Å^3$ and 600 $Å^3$. Thus, in theory this selection of tetrahedral cages provides a size-graded series of self-assembled "nanoreactors" in which to examine selective chemistry. In this regard, the above-mentioned series of M_4L_6 cages should exhibit properties in common with other reported[24-32] nanoreactor examples, such as substrate size and shape selectivities, and potentially, product chemo-, regio- and stereoselectivities. Being poly*cationic*, they are complementary to the poly*anionic* bis-catechol derived tetrahedra so successfully exploited for this purpose by Raymond's group.[25-27,33] Like the latter systems (and the related tetrahedra studied by Ward's group)[34] they exist in chiral forms, so enantioselectivity in the chemistry of the resolved species may be anticipated. Moreover, the synthetic approach used to synthesize bridged quaterpyridines **128** and **129** is amenable to the addition of further functionality to their respective bridging units in order to influence these systems' host-guest chemistry.

6.2.2 DNA binding of Ru(II) triple helicates

As indicated above, self-assembly of quaterpyridine **50** with various Ru(II) precursors in a 3:2 ratio afforded the racemic triple helicate **160**. This self-assembly-derived Ru(II) M_2L_3 helicate is a rare example of such a product, being only one of two reported[35] examples to date. Furthermore, Hannon's group reported[35] that helicate **191** (incorporating Fe(II)) binds to DNA non-covalently with binding constants of the same order of magnitude as cisplatin. Interestingly, helicate **191** is also active against some important cancer lines. Indeed much interest in these chiral helicates[35-47] and positively charged metal complexes[48-57] (often exhibiting stereoselective DNA binding) derives from their novel (non-covalent) modes of interaction with DNA and the resulting potential to provide new classes of DNA-directed probes and drugs.[48,51,58]

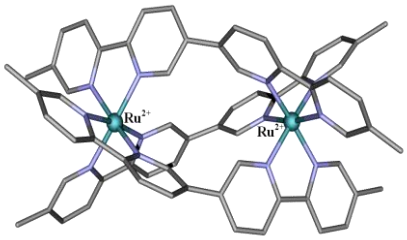

160

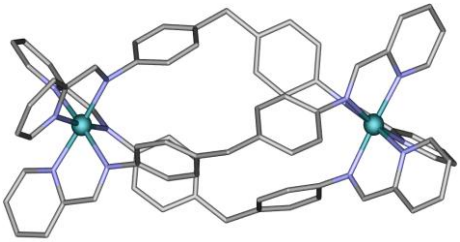

191

The enantiomers of triple helicate **160** were shown to exhibit differential binding with duplex DNA. In relation to this, the *P*- and *M*-helicates were separated very efficiently by a reported DNA affinity chromatography procedure.[59] The precise modes of binding of the *P*- and *M*-helicates to duplex DNA has not yet been determined and will be the subject of a range of qualitative and quantitative binding experiments.[†] On size and steric grounds it is likely that the *M*-enantiomers of **160** will bind in the major groove of DNA as shown in ***Figure 6.1***. Importantly, the Ru(II) helicates derived from quaterpyridines **50**, and the extended systems **128** and **129** (and analogues) will provide a valuable series for probing the subtleties of the binding modes of these systems to DNA. Furthermore, the synthetic approach to quaterpyridines **128** and **129** is highly amenable to

[†] Work in this area is currently underway in collaboration with A/Prof. Grant Collins of the Australian Defence Force Academy.

derivatisation of the respective phenylene and biphenylene bridges for the possible enhancement of DNA binding site selectivity.

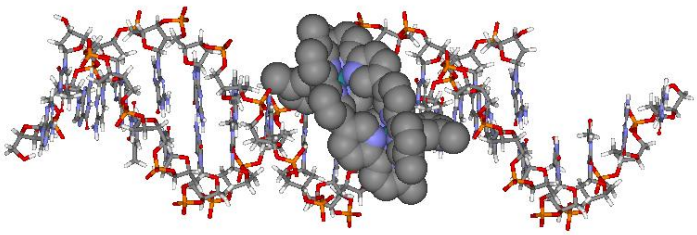

Figure 6.1 An illustration representing the size compatability of helicate **160** for the major groove of a sequence of DNA.

6.2.3 Metal-template synthesis of dinuclear cryptates and tetranuclear polycycles.

Finally, preliminary results have indicated that both dinuclear cryptates and tetranuclear tetracycles can be synthesized. Hence, one major thrust in terms of future work will be to optimize the synthesis of these species. The expectation is that these systems will exhibit interesting properties. In this regard, the combination of the expected stability of the polycyclic metal complexes with the interesting photophysical properties presented by the related tetrahedra derived from quaterpyridines **128** and **129**, are likely to provide noteworthy results. Indeed, with respect to the tetranuclear polycyclic complexes, the potential for interesting host-guest chemistry can be anticipated.

6.3 REFERENCES

1. D. F. Perkins, L. F. Lindoy, A. McAuley, G. V. Meehan and P. Turner, *Proc. Nat. Acad. Sci. U.S.A.*, 2006, **103**, 532.
2. D. F. Perkins, L. F. Lindoy, G. V. Meehan and P. Turner, *Chem. Commun.*, 2004, 152.
3. C. Dietrich-Buchecker, G. Rapenne and J.-P. Sauvage, *Coord. Chem. Rev.*, 1999, **185-186**, 167.
4. C. Dietrich-Buchecker, J. Guilhem, C. Pascard and J. P. Sauvage, *Angew. Chem. Int. Ed.*, 1990, **29**, 1154.
5. C. Dietrich-Buchecker, G. Rapenne and J.-P. Sauvage, *Chem. Commun.*, 1997, 2053.
6. C. Dietrich-Buchecker and J. P. Sauvage, *Angew. Chem. Int. Ed.*, 1989, **28**, 189.
7. C. Dietrich-Buchecker, J. P. Sauvage, A. De Cian and J. Fischer, *Chem. Commun.*, 1994, 2231.
8. C. O. Dietrich-Buchecker, J. F. Nierengarten, J. P. Sauvage, N. Armaroli, V. Balzani and L. De Cola, *J. Am. Chem. Soc.*, 1993, **115**, 11237.
9. S. C. J. Meskers, H. P. J. M. Dekkers, G. Rapenne and J.-P. Sauvage, *Chem. Eur. J.*, 2000, **6**, 2129.
10. M. Meyer, A. M. Albrecht-Gary, C. O. Dietrich-Buchecker and J. P. Sauvage, *J. Am. Chem. Soc.*, 1997, **119**, 4599.
11. L.-E. Perret-Aebi, A. v. Zelewsky, C. Dietrich-Buchecker and J. P. Sauvage, *Angew. Chem. Int. Ed.*, 2004, **43**, 4482.
12. G. Rapenne, C. Dietrich-Buchecker and J. P. Sauvage, *J. Am. Chem. Soc.*, 1999, **121**, 994.
13. K. S. Chichak, S. J. Cantrill, A. R. Pease, S.-H. Chiu, G. W. V. Cave, J. L. Atwood and J. F. Stoddart, *Science*, 2004, **304**, 1308.
14. K. S. Chichak, S. J. Cantrill and J. F. Stoddart, *Chem. Commun.*, 2005, 3391.
15. K. S. Chichak, A. J. Peters, S. J. Cantrill and J. F. Stoddart, *J. Org. Chem.*, 2005, **70**, 7956.
16. A. J. Peters, K. S. Chichak, S. J. Cantrill and J. F. Stoddart, *Chem. Commun.*, 2005, 3394.

17. B. Champin, P. Mobian and J.-P. Sauvage, *Chem. Soc. Rev.*, 2007, **36**, 358.
18. C. D. Meyer, C. S. Joiner and J. F. Stoddart, *Chem. Soc. Rev.*, 2007, **36**, 1705.
19. S. Saha and J. F. Stoddart, *Chem. Soc. Rev.*, 2007, **36**, 77.
20. P. Misra, V. Humblet, N. Pannier, W. Maison and J. V. Frangionic, *J. Nucl. Med.*, 2007, **48**, 1379.
21. H. Miyaji, S.-J. Hong, S.-D. Jeong, D.-W. Yoon, H.-K. Na, J. Hong, S. Ham, J. L. Sessler and C.-H. Lee, *Angew. Chem. Int. Ed.*, 2007, **46**, 2508.
22. A. V. Davis, D. Fiedler, M. Ziegler, A. Terpin and K. N. Raymond, *J. Am. Chem. Soc.*, 2007, **129**, 15354.
23. A. J. Terpin, M. Ziegler, D. W. Johnson and K. N. Raymond, *Angew. Chem. Int. Ed.*, 2001, **40**, 157.
24. T. S. Koblenz, J. Wassenaar and J. N. H. Reek, *Chem. Soc. Rev.*, 2008, **37**, 247.
25. D. Fiedler, R. G. Bergman and K. N. Raymond, *Angew. Chem. Int. Ed.*, 2004, **43**, 6565.
26. D. Fiedler, D. H. Leung, R. G. Bergman and K. N. Raymond, *Acc. Chem. Res.*, 2005, **38**, 349.
27. D. Fiedler, H. van Halbeek, R. G. Bergman and K. N. Raymond, *J. Am. Chem. Soc.*, 2006, **128**, 10240.
28. T. S. Koblenz, J. Wassenaar and J. N. H. Reek, *Chem. Soc. Rev.*, 2008, **37**, 247.
29. J.-P. Bourgeois and M. Fujita, *Aust. J. Chem.*, 2002, **55**, 619.
30. J. Kang and J. Rebek, *Nature*, 1997, **385**, 50.
31. J. Kang, J. Santamaria, G. Hilmersson and J. Rebek, *J. Am. Chem. Soc.*, 1998, **120**, 7389.
32. M. Yoshizawa, Y. Takeyama, T. Kusukawa and M. Fujita, *Angew. Chem. Int. Ed.*, 2002, **41**, 1347.
33. M. D. Pluth, R. G. Bergman and K. N. Raymond, *Angew. Chem. Int. Ed.*, 2007, **46**, 8587.
34. R. Frantz, S. Grange, N. K. Al-Rasbi, M. D. Ward and J. Lacour, *Chem. Commun.*, 2007, 1459.
35. G. I. Pascu, A. C. G. Hotze, C. Sanchez-Cano, B. M. Kariuki and M. J. Hannon, *Angew. Chem. Int. Ed.*, 2007, **46**, 4374.

36. B. Schoentjes and J.-M. Lehn, *Helv. Chim. Acta*, 1995, **78**, 1.
37. M. J. Hannon, V. Moreno, M. J. Prieto, E. Moldrheim, E. Sletten, I. Meistermann, C. J. Isaac, K. J. Sanders and A. Rodger, *Angew. Chem. Int. Ed.*, 2001, **40**, 879.
38. J. Malina, M. J. Hannon and V. Brabec, *Chem. Eur. J.*, 2007, **13**, 3871.
39. S. Khalid, M. J. Hannon, A. Rodger and P. M. Rodger, *J. Mol. Graphics Modell.*, 2007, **25**, 794.
40. J. Malina, M. J. Hannon and V. Brabec, *Nucl. Acids Res.*, 2008, **36**, 3630.
41. J. Malina, M. J. Hannon and V. Brabec, *Chem. Eur. J.*, 2008, **14**, 10408.
42. I. Meistermann, V. Moreno, M. J. Prieto, E. Moldrheim, E. Sletten, S. Khalid, P. M. Rodger, J. C. Peberdy, C. J. Isaac, A. Rodger and M. J. Hannon, *Proc. Nat. Acad. Sci. U.S.A.*, 2002, **99**, 5069.
43. A. Oleksi, A. G. Blanco, R. Boer, I. Usón, J. Aymamí, A. Rodger, M. J. Hannon and M. Coll, *Angew. Chem. Int. Ed.*, 2006, **45**, 1227.
44. G. I. Pascu, A. C. G. Hotze, C. Sanchez-Cano, B. M. Kariuki and M. J. Hannon, *Angew. Chem. Int. Ed.*, 2007, **46**, 4374.
45. J. C. Peberdy, J. Malina, S. Khalid, M. J. Hannon and A. Rodger, *J. Inorg. Biochem.*, 2007, **101**, 1937.
46. S. Khalid, M. J. Hannon, A. Rodger and P. M. Rodger, *Chem. Eur. J.*, 2006, **12**, 3493.
47. C. Uerpmann, J. Malina, M. Pascu, G. J. Clarkson, V. Moreno, A. Rodger, A. Grandas and M. J. Hannon, *Chem. Eur. J.*, 2005, **11**, 1750.
48. B. M. Zeglis, V. C. Pierre and J. K. Barton, *Chem. Commun.*, 2007, 4565 (and references therein).
49. V. Brabec and O. Nováková, *Drug Resistance Updates*, 2006, **9**, 111.
50. F. Pierard and A. Kirsch-De Mesmaeker, *Inorg. Chem. Commun.*, 2006, **9**, 111.
51. C. B. Spillane, M. N. V. Dabo, N. C. Fletcher, J. L. Morgan, F. R. Keene, I. Haq and N. J. Buurma, *J. Biol. Inorg. Chem.*, 2008, **102**, 673 (and references therein).
52. J. L. Morgan, C. B. Spillane, J. A. Smith, D. P. Buck, J. G. Collins and F. R. Keene, *Dalton Trans.*, 2007, 4333.
53. T. Biver, F. Secco and M. Venturini, *Coord. Chem. Rev.*, 2008, **252**, 1163.
54. L. J. K. Boerner and J. M. Zaleski, *Curr. Opin. Chem. Biol.*, 2005, **9**, 135.

55. M. J. Hannon, *Chem. Soc. Rev.*, 2007, **36**, 280.

56. C. Metcalfe and J. A. Thomas, *Chem. Soc. Rev.*, 2003, **32**, 215.

57. V. Rajendiran, M. Murali, E. Suresh, S. Sinha, K. Somasundaram and M. Palaniandavar, *Dalton Trans.*, 2008, 148.

58. M. J. Hannon, *Chem. Soc. Rev.*, 2007, **36**, 280 (and references therein).

59. J. A. Smith and F. R. Keene, *Chem. Commun.*, 2006, 2583.

Appendix A

Example NMR Spectra

Assignment of the ^{1}H NMR spectra of the compounds reported in this thesis were, for the most part, straightforward due to the obvious nature of the couplings of the 2,5-disubstituted pyridines involved. NOESY experiments were used to identify aromatic protons *ortho* to saturated substituents and ^{1}H-^{1}H COSY experiments were used to elucidate correlations where needed. A representative selection of the NMR spectrum from those reported in experimental sections of this thesis is presented below. All NMR spectra are stored electronically and are available on request.

Appendix A.1 - *5-Bromo-5′-methyl-2,2′-bipyridine (84):* There are a total of six aromatic proton resonances and one methyl proton resonance in the ^{1}H NMR spectrum of bromobipyridine **84** (***Figure A.1***). Irradiation of the 4′-proton resonance at 7.63 ppm resulted in the observation of NOEs between it and the 3′-proton (8.31 ppm) and methyl-protons (2.39 ppm) (***Figure A.2***).

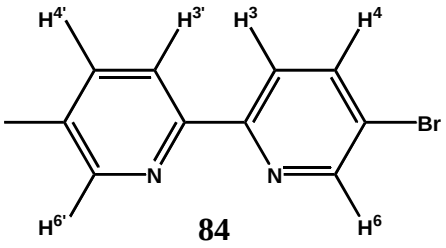

84

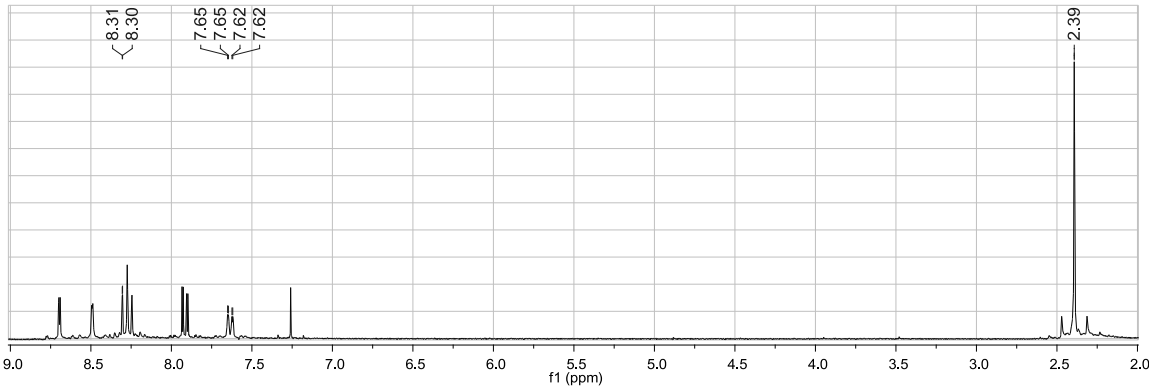

Figure A.1 The ^{1}H NMR spectrum of **84** in $CDCl_3$.

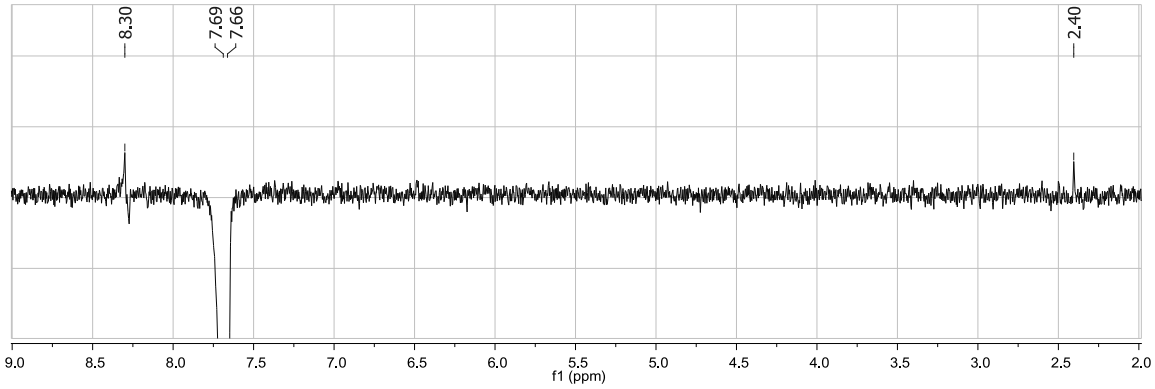

Figure A.2 The 1D NOESY spectrum of **84** in $CDCl_3$.

The NOEs combined with the "ortho" and "meta" couplings enabled the full assignment of the ^{1}H NMR spectrum of **84** (see ***Figure A.3*** for the aromatic assignments).

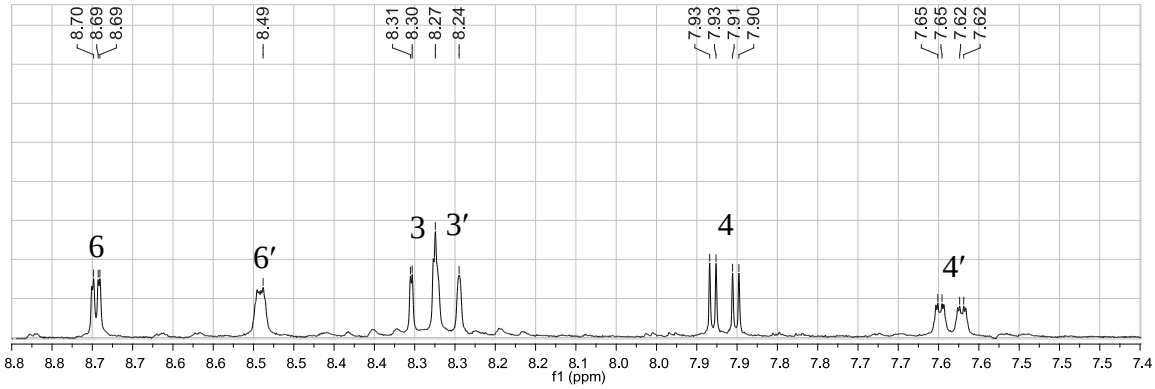

Figure A.3 The ^{1}H NMR spectrum assignments of the aromatic region of **84**.

Appendix A.2 - *1,4-Bis[5′-(5″-(2-formyl-4-tert-butylphenoxymethyl)-2′,2″-bipyridinyl)]-2,5-dimethoxybenzene (141):* There are a total of ten aromatic proton resonances, a salicyloxymethylene proton resonance, a methoxyl proton resonance and a *t*-butyl-proton resonance in the ^{1}H NMR spectrum of **141** (***Figure A.4***).

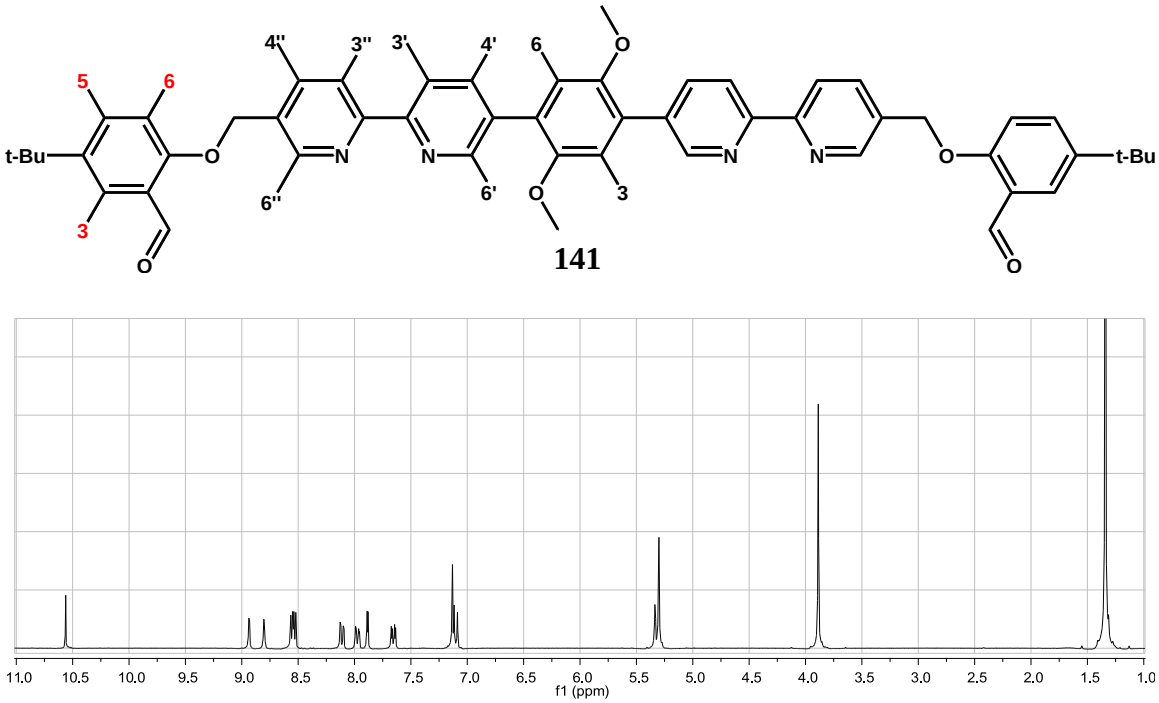

Figure A.4 The ^{1}H NMR spectrum of dialdehyde **141** in CD_2Cl_2.

Irradiation of the salicyloxymethylene proton resonance at 5.32 ppm resulted in the observation of NOEs between it and protons in the 6-position on the salicyloxy-moiety and 6′′-protons of the outer pyridyl rings (***Figure A.5***).

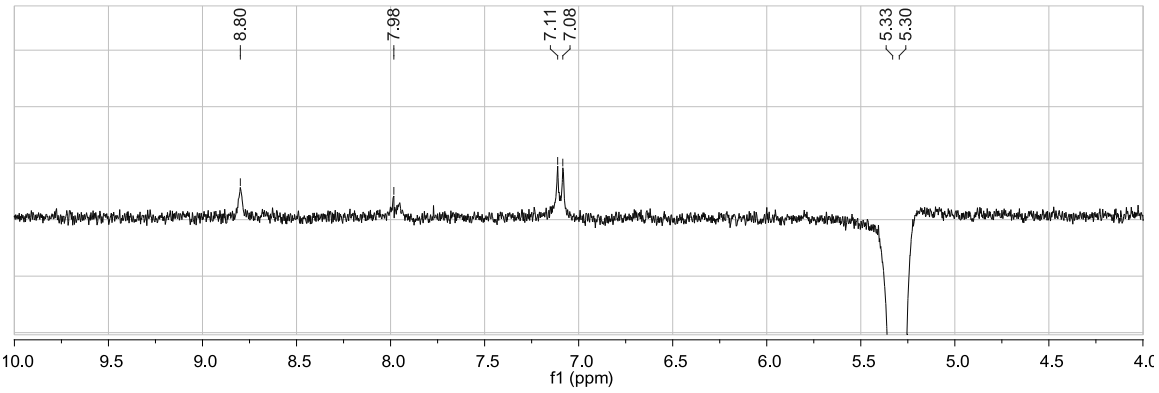

Figure A.5 The 1D NOESY spectrum of **141** in CD_2Cl_2.

The ^{1}H-^{1}H-COSY spectrum of **141** allowed the observation of correlations between the 3′- and 4′-protons and between the 3′′- and 4′′-protons (***Figure A.6***).

Correlations between the 5- and 6-position protons on the salicyloxy moiety were also observed.

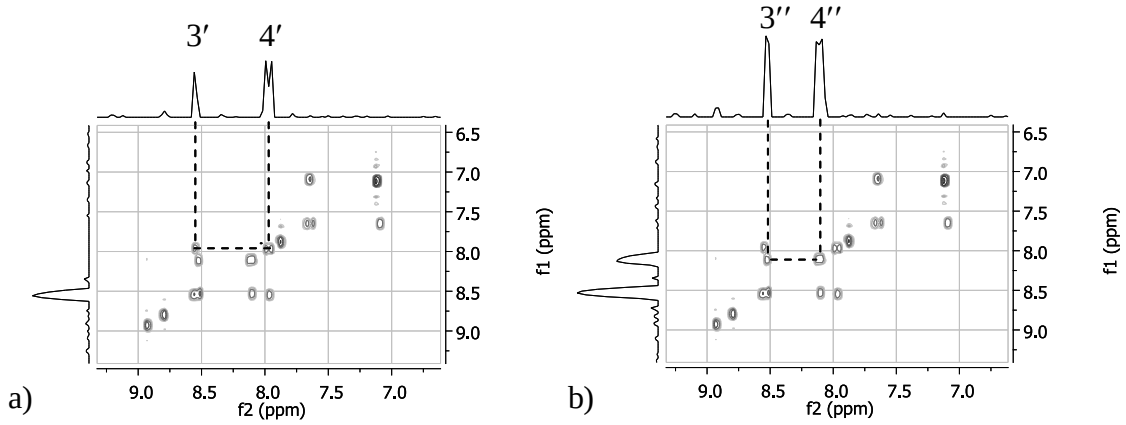

Figure A.6 The aromatic region of the ^{1}H-^{1}H COSY spectra of **141**, a) highlights the correlation between the 3′- and 4′-protons, while image b) highlights the correlation between the 3′′- and 4′′-protons.

The assignments for the aromatic region of the ^{1}H NMR spectrum of quaterpyridine **141** are illustrated in ***Figure A.7***. Coupling constants are as reported in the experimental section in Chapter 2.

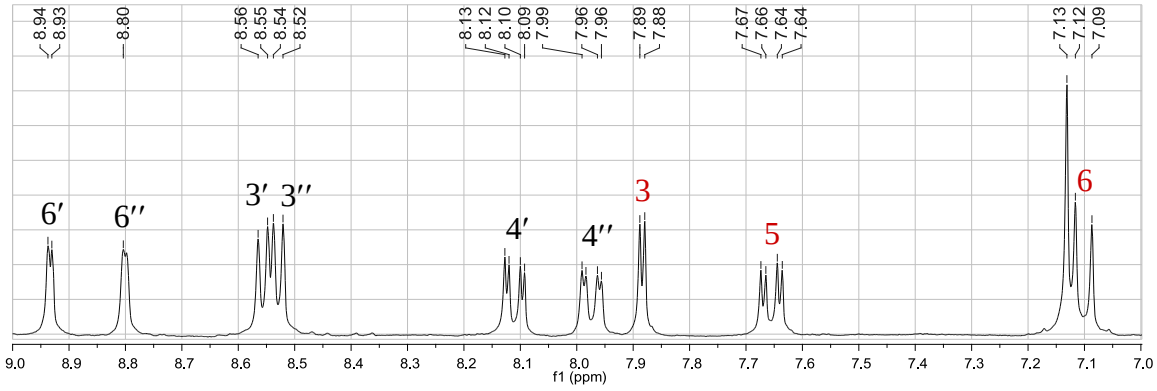

Figure A.7 The ^{1}H NMR spectrum assignments of the aromatic region of **141**.

Appendix A.3 - *5,5‴-Dimethyl-2,2′:5′,5″:2″,2‴-quaterpyridine (50):* The ^{1}H NMR spectrum of quaterpyridine **50** is indicative of its *C2*-symmetry with a single proton resonance for the methyl groups and six aromatic resonances (***Figure A.8***)

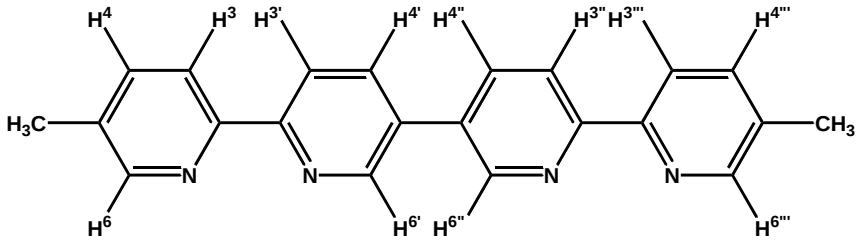

50

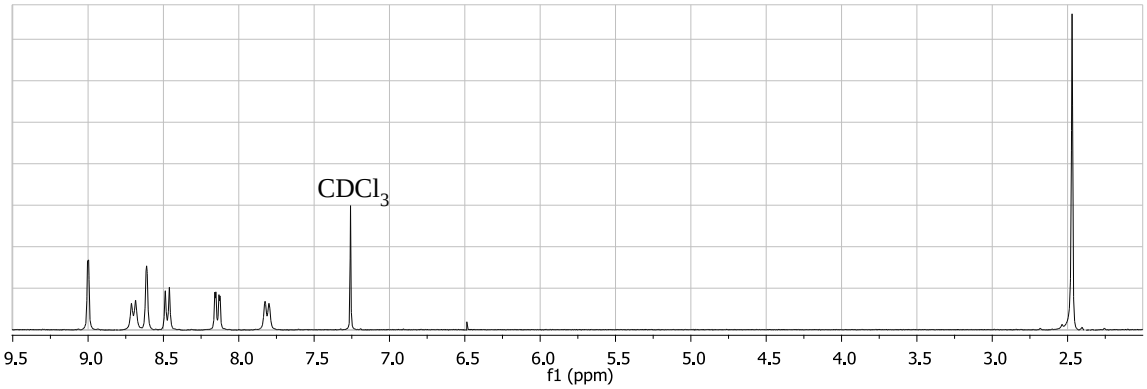

Figure A.8 The ^{1}H NMR spectrum of quaterpyridine **50** in $CDCl_3$.

1D slices of the NOESY spectrum of quaterpyridine **50** revealed correlations between protons in the 6,6‴-positions with the methyl-protons and between protons in the 4,4‴-positions with the methyl protons (***Figure A.9***).

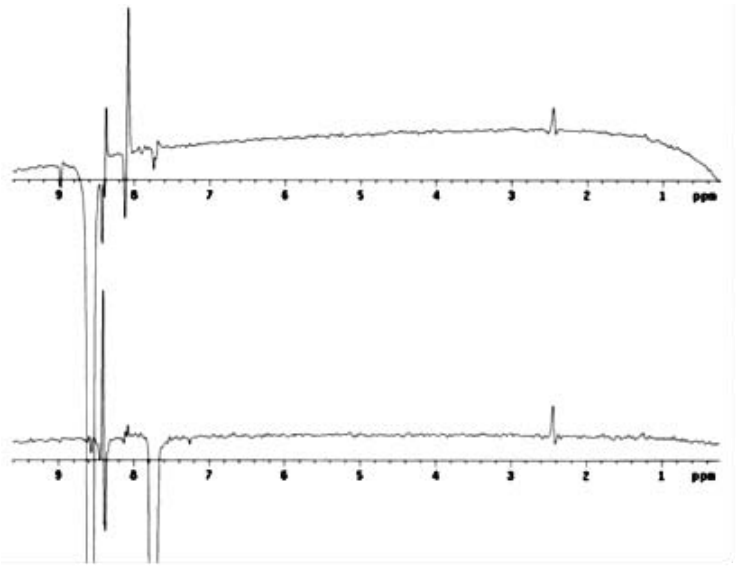

Figure A.9 1D slices through a NOESY spectrum of quaterpyridine **50**; correlation between protons in the 6,6′′′-positions with the methyl protons (above) and correlation observed between protons in the 4,4′′′-positions with the methyl protons (below).

The aromatic region of the ^{1}H-^{1}H COSY spectrum of **50** reveals correlations between the 3,3′′′-protons and the 4,4′′′-protons, and between the 4,4′′′-protons and the 6,6′′′-protons. Correlations between the 3′,3′′-protons and the 4′,4′′-protons, and between the 4′,4′′-protons and the 6′,6′′-protons were also observed.

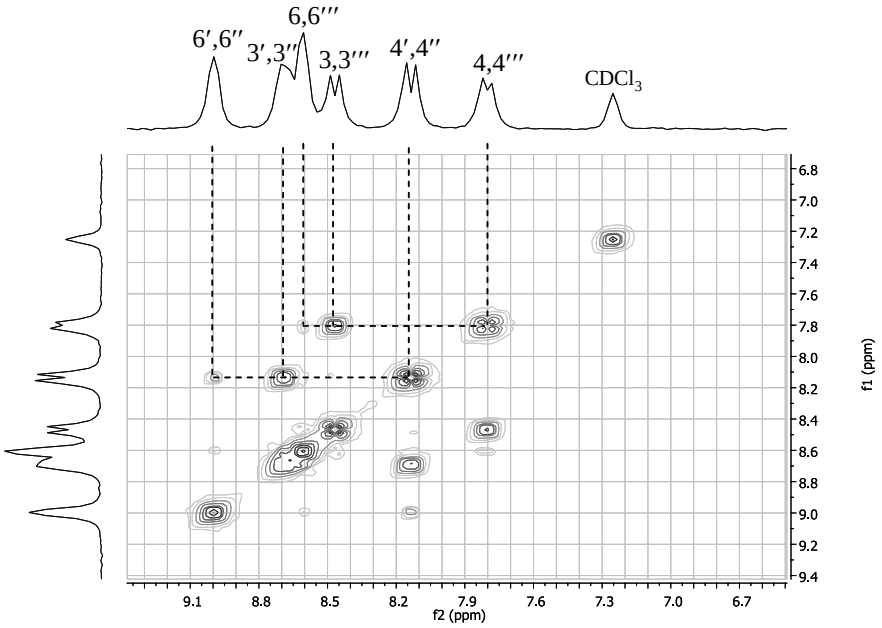

Figure A.10 The aromatic region of the ^{1}H-^{1}H COSY spectrum of **50** highlighting proton correlations between the inner and outer pyridyl rings.

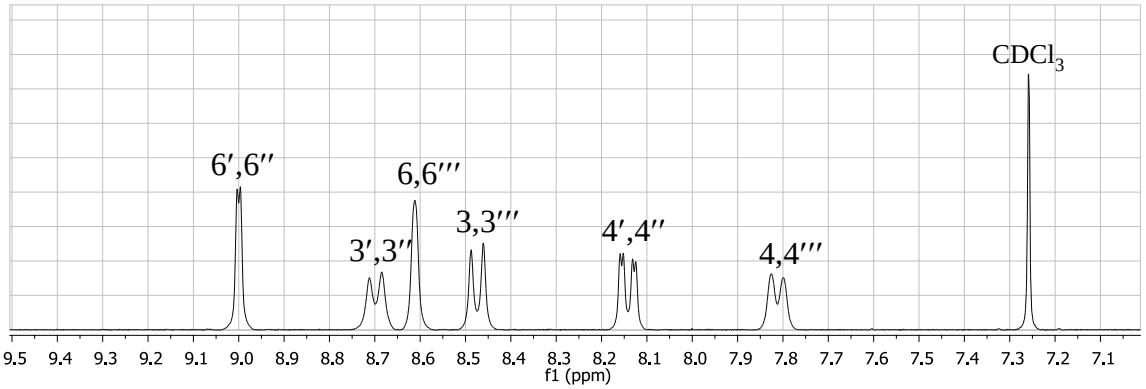

Figure A.11 The ^{1}H NMR spectrum assignments of the aromatic region of **50** in $CDCl_3$.

Appendix A.4 ***[Ru$_2$(50)$_3$](Cl)$_4$ (160):*** The ^{1}H NMR spectrum of **160** as its chloro salt run in D_2O is presented in ***Figure A.12***. Assignment of the ^{1}H NMR spectrum of the chloro salt was required for the DNA binding studies currently underway.[†] The spectrum in ***Figure A.12*** indicates that quaterpyridine exists in the complex such that it retains its C2-symmetry (i.e. there are six aromatic-proton resonances and one methyl-proton resonance).

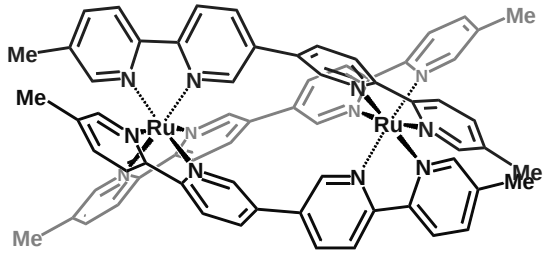

$[Ru_2(\mathbf{50})_3]^{4+}$

[†] Work in this area is currently underway in collaboration with A/Prof. Grant Collins of the Australian Defence Force Academy.

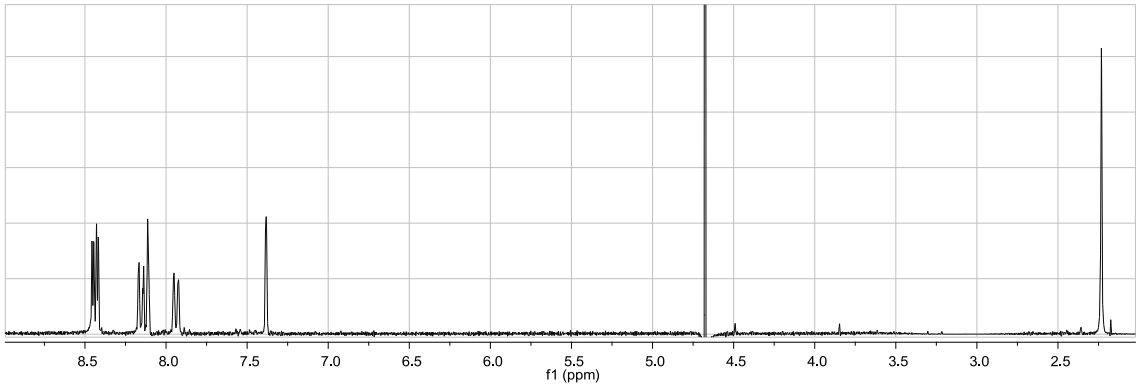

Figure A.12 The ^{1}H NMR spectrum of $[Ru_2(\mathbf{50})_3](Cl)_4$ in D_2O.

Irradiation at the methyl-proton resonance at 2.23 ppm resulted in the observation of NOEs between it and the 4,4′′′-protons and the 6,6′′′-protons of the outer pyridyl rings (***Figure A.13***).

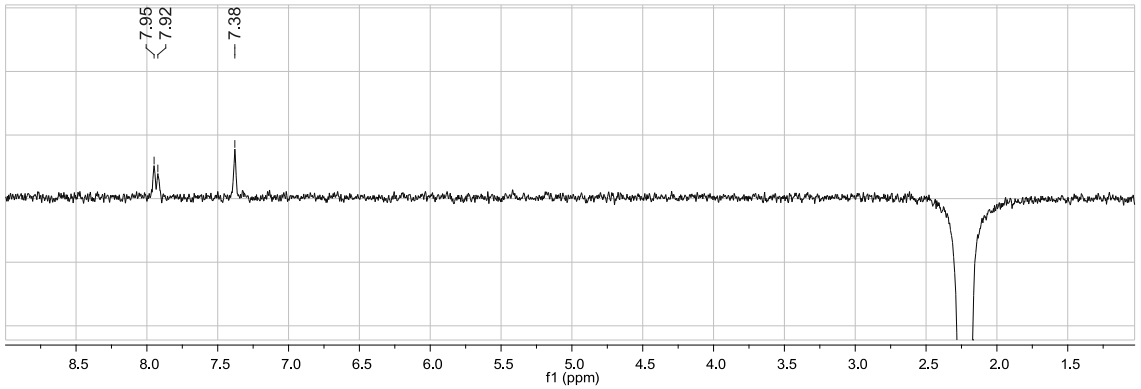

Figure A.13 The 1D NOESY spectrum $[Ru_2(\mathbf{50})_3](Cl)_4$ in D_2O.

A ^{1}H-^{1}H COSY spectrum allowed the overlapping 3,3′′′-protons and 3′,3′′-protons resonances to be distinguished (***Figure A.14***). Clear correlations were observed between the 3,3′′′-protons and the 4,4′′′-protons, as well as between the 3′,3′′-protons and the 4′,4′′-protons. Another correlation between the 6,6′′′-protons and the 4,4′′′-protons was also observed.

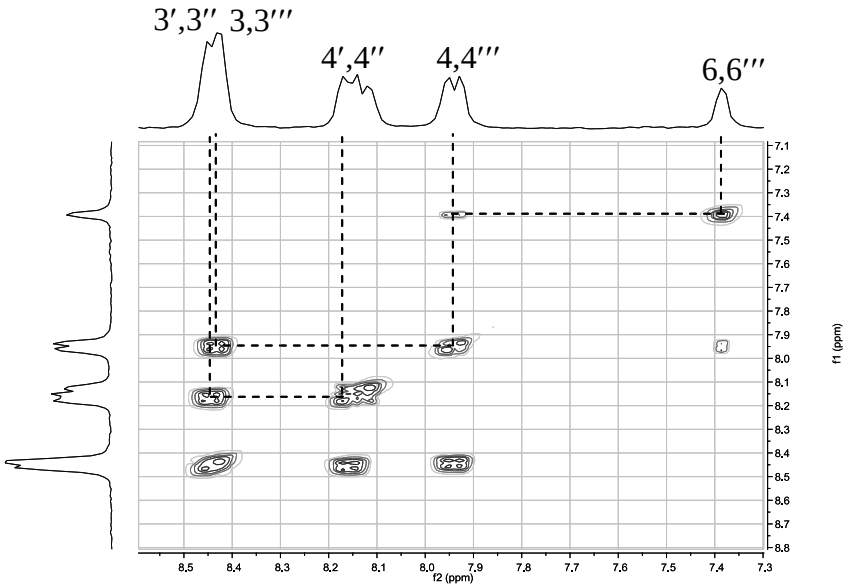

Figure A.14 The aromatic region of the ^{1}H-^{1}H COSY spectra of $[Ru_2(\mathbf{50})_3](Cl)_4$ highlighting couplings between the 3,3‴-protons and the 4,4‴-protons as well as the 3′,3″-protons and the 4′,4″-protons.

The assignments for the aromatic region of the ^{1}H NMR spectrum of $[Ru_2(\mathbf{50})_3](Cl)_4$ are illustrated in ***Figure A.15***. Coupling constants reported in the experimental section in Chapter 3 are for the PF_6^- salt.

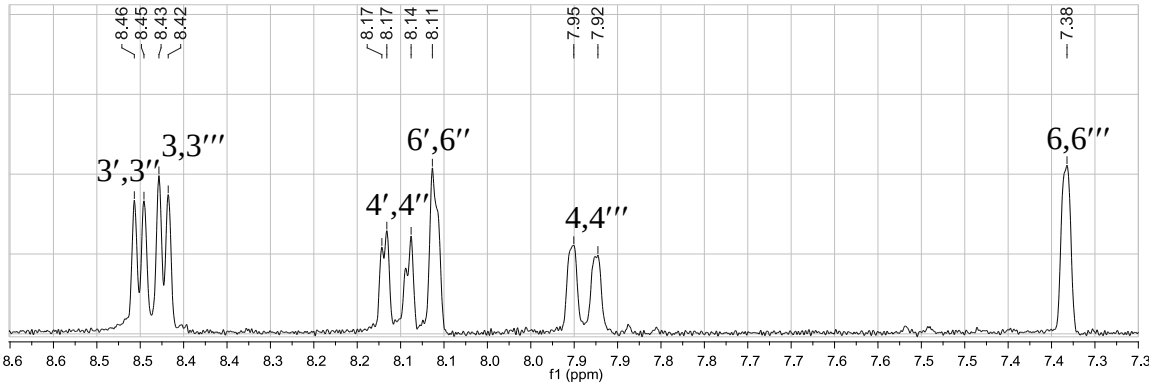

Figure A.15 The ^{1}H NMR spectrum assignments of the aromatic region of $[Ru_2(\mathbf{50})_3](Cl)_4$.

Appendix A.5 ***[Fe$_4$(50)$_6$(BF$_4$)](BF$_4$)$_7$ (155):*** The seven observed ^{1}H NMR resonances in the ^{1}H NMR spectrum of [Fe$_4$(**50**)$_6$⊃BF$_4$](BF$_4$)$_7$, **155**, are consistent with quaterpyridine **50** possessing *C2*-symmetry within the complex (***Figure A.12***).

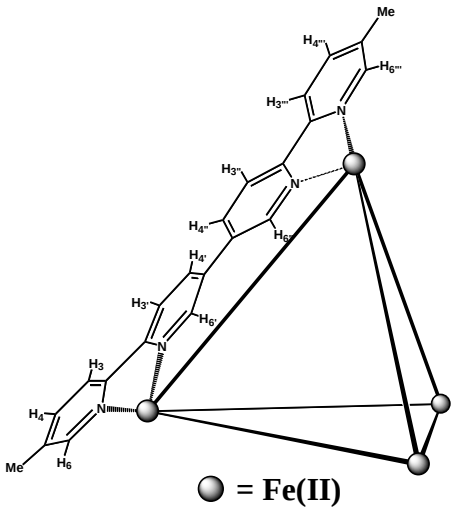

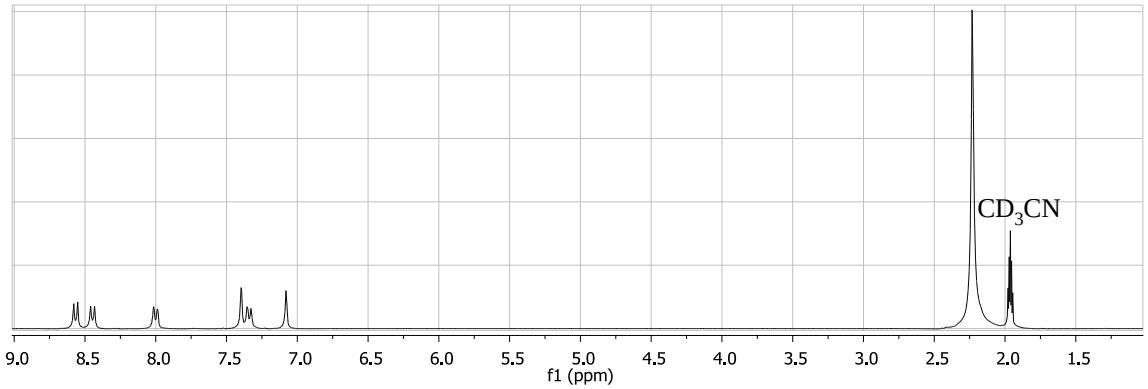

Figure A.16 The ^{1}H NMR spectrum of [Fe$_4$(**50**)$_6$⊃BF$_4$](BF$_4$)$_7$ in CD$_3$CN.

1D slices of the NOESY spectrum of [Fe$_4$(**50**)$_6$(BF$_4$)](BF$_4$)$_7$ revealed correlations between 4,4′′′;6,6′′′-protons and the methyl-protons (***Figure A.13***).

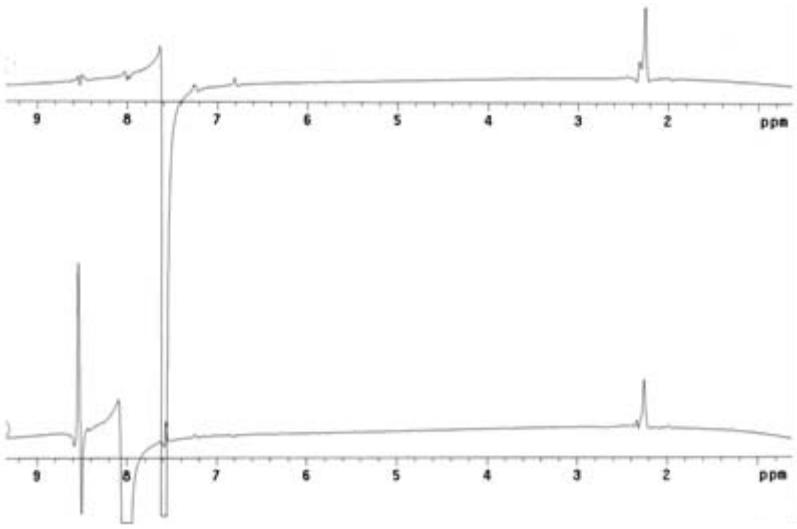

Figure A.17 1D slices through NOSEY spectrum of $[Fe_4(\mathbf{50})_6 \supset BF_4](BF_4)_7$ revealed correlations between the 6,6′′′-protons and the methyl protons (top), and between the 4,4′′′-protons and the methyl protons (bottom).

A ^{1}H-^{1}H COSY spectrum of $[Fe_4(\mathbf{50})_6 \supset BF_4](BF_4)_7$ allowed clear correlations to be observed between the 3,3′′′-protons and the 4,4′′′-protons, as well as between the 3′,3′′-protons and the 4′,4′′-protons (***Figure A.18***). Another correlation between the 6′,6′′-protons and the 4′,4′′-protons was also observed.

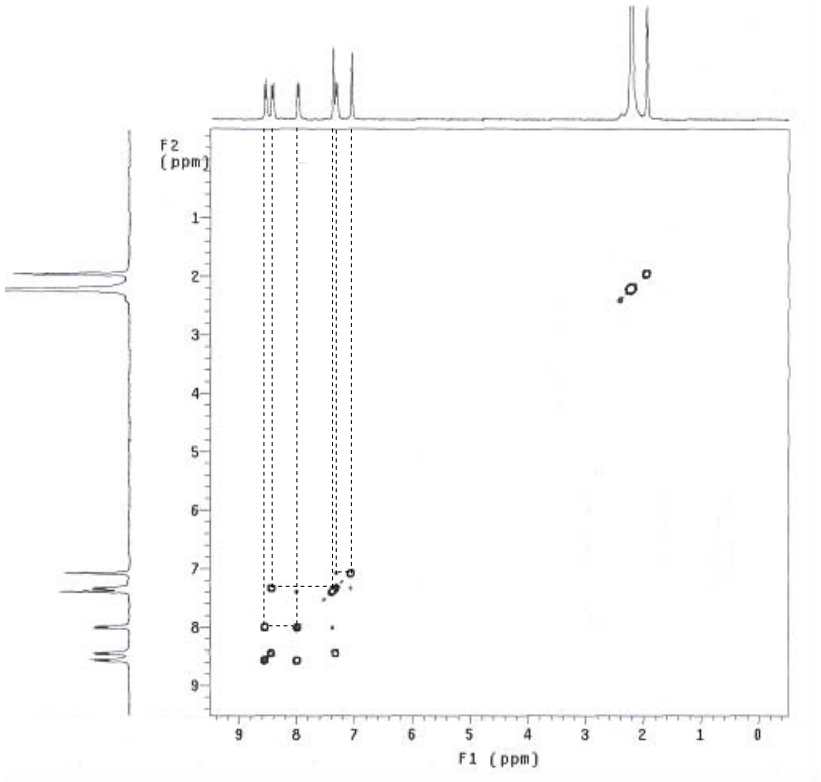

Figure A.19 The ^{1}H-^{1}H COSY spectrum of $[Fe_4(\mathbf{50})_6 \supset BF_4](BF_4)_7$ illustrating the correlations between the protons.

The assignments for the aromatic region of the ^{1}H NMR spectrum of $[Fe_4(\mathbf{50})_6 \supset BF_4](BF_4)_7$ are illustrated in ***Figure A.20***. The coupling constants are reported in the experimental section in Chapter 3.

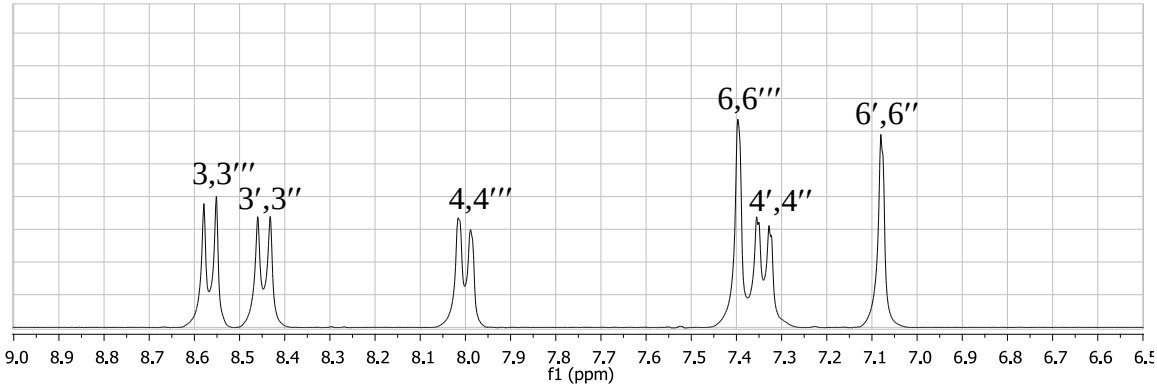

Figure A.20 The ^{1}H NMR spectrum assignments of the aromatic region of $[Fe_4(\mathbf{50})_6 \supset BF_4](BF_4)_7$.

Appendix B

X-Ray Crystallography

B.1 General Crystallographic Descriptions

The crystallographic cif files for structures reported in this thesis are included on a disc at the end of this thesis. These cif files are identified by the product number used in the main text of this thesis (***Table B.1***).

Product Name	Product Number
5,5′-Bis(trimethylsilylmethyl)-2,2′-bipyridine	92
$[Fe_4(\mathbf{50})_6 \supset FeCl_4](PF_6)_7$	153
$[Fe_4(\mathbf{50})_6 \supset FeCl_4](BPh_4)_6$	154
$[Fe_4(\mathbf{50})_6 \supset BF_4)](BF_4)_7$	155
$[Fe_4(\mathbf{50})_6 \supset PF_6](PF_6)_7$	156
$[Fe_4(\mathbf{50})_6][ZnCl_4]_4$	157
$[Ru_2(\mathbf{50})_3](PF_6)_4$	160
$[Fe_4(\mathbf{128})_6](PF_6)_8$	162
$[Ni_2(\mathbf{128})_3](PF_6)_4$	163
$[Fe_4(\mathbf{129})_6](PF_6)_8$	165
$[Ni_4(\mathbf{129})_6](PF_6)_8$	166
$[Ni_2(\mathbf{149})_3](PF_6)_4$	170
$[Ni_2(\mathbf{150})_3](PF_6)_4$	171
$[Ni_2(\mathbf{151})_3](PF_6)_4$	172
Tris-(2-benzyloxy-5-*tert*-butylbenzyl)-amine	174
$[Fe(\mathbf{176})](PF_6)_2$	179

Table B.1 Lists product formulae/names with the cif file numbers used to identify compounds in the main text of this thesis and on the supplementary disc inside the back cover.

Data for **92** and **174** were collected and refined by Dr Murray Davies (James Cook University) using a Bruker SMART 1000 CCD area detector diffractometer employing graphite-monochromated Mo-K*a* radiation generated from a sealed tube (0.71069 Å) at 293(2) K. Data for **153** were collected with ω scans to approximately 56° 2θ using a Bruker SMART 1000 diffractometer employing graphite-monochromated Mo-K*a* radiation generated from a sealed tube (0.71073 Å) at 150(2) K. Data for **154**, **155**, **157**, **160**, **162**, **163**, **166**, **170**, **172** and **179** were collected on a Bruker-Nonius APEX2-X8-FR591 diffractometer employing graphite-monochromated Mo-Kα radiation generated from a rotating anode (0.71073 Å) with ω and ψ scans to approximately 56° 2θ at 150(2) K.[1] Data for **156, 165** and **171** were collected at approximately 100 K using double diamond monochromated synchrotron radiation (0.48595 Å) and ω and ψ scans at the ChemMatCARS beamline at the Advanced Photon Source. Data integration and reduction were undertaken with SAINT and XPREP**.**[2] Subsequent computations were carried out using the WinGX-32 graphical user interface.[3] Structures were solved by direct methods using SIR97.[4] Multi-scan empirical absorption corrections, when applied, were applied to the data set using the program SADABS.[5] Data were refined and extended with SHELXL-97.[6] In general, non-hydrogen atoms with occupancies greater than 0.5 were refined anisotropically. Carbon-bound hydrogen atoms were included in idealised positions and refined using a riding model. Oxygen and bound hydrogen atoms were first located in the difference Fourier map before refinement. Where these hydrogen atoms could not be located, they were not modeled. Disorder was modeled using standard crystallographic methods including constraints, restraints and rigid bodies where necessary. Queries regarding crystallography can be directed to Dr Jack Clegg, School of Chemistry, F11, The University of Sydney, NSW, 2006, Australia (clegg_j@chem.usyd.edu.au). Structural data are summarised below and crystallographic information files are presented on the accompanying compact disc.

5,5′-Bis(trimethylsilylmethyl)-2,2′-bipyridine (92): This structure was collected by Dr Murray Davies (James Cook University) and published in *Acta Crystallographica Section E.* See the paper entitled **5,5′-Bis(trimethylsilylmethyl)-2,2′-bipyridine** in Appendix D

for details of the collection of crystallographic data for **92** as well as its crystallographic description.

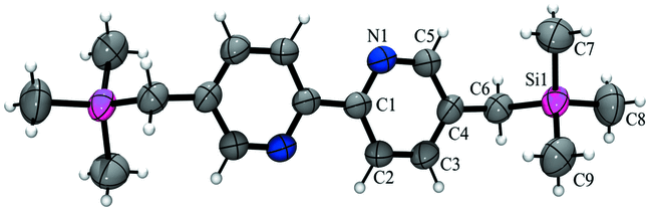

92

[Fe$_4$(50)$_6$⊃FeCl$_4$](PF$_6$)$_7$, (153): Formula $C_{132}H_{132}Cl_4F_{42}Fe_5N_{24}O_{12}P_7$, *M* 3682.46, cubic, space group *P* $\bar{4}_3$n(#218), *a* 21.7946(6), *b* 21.7946(6), *c* 21.7946(6) Å, *V* 10352.5(5) Å^3, D_c 1.181 g cm^{-3}, *Z* 2, crystal size 0.15 by 0.14 by 0.13 mm, colour red, habit tetrahedron, temperature 150(2) Kelvin, λ(MoKα) 0.71073 Å, μ(MoKα) 0.534 mm^{-1}, *T*(SADABS)$_{min,max}$ 0.825404, 1.0000, 2θ_{max} 56.62, *hkl* range -28 28, -28 29, -28 27, *N* 95183, N_{ind} 4262(R_{merge} 0.0980), N_{obs} 2740(I > 2σ(I)), N_{var} 171, residuals* *R*1(*F*) 0.0596, *wR*2(F^2) 0.1827, GoF(all) 0.968, $\Delta\rho_{min,max}$ -0.792, 0.756 e$^-$ Å^{-3}.

*$R1 = \Sigma||F_o| - |F_c||/\Sigma|F_o|$ for $F_o > 2\sigma(F_o)$; $wR2 = (\Sigma w(F_o^2 - F_c^2)^2/\Sigma(wF_c^2)^2)^{1/2}$ all reflections

$w=1/[\sigma^2(F_o^2)+(0.1243P)^2+0.0000P]$ where $P=(F_o^2+2F_c^2)/3$

[Fe$_4$(50)$_6$⊃FeCl$_4$](BPh$_4$)$_6$, (154): Formula $C_{552}H_{454}B_{12}Cl_8Fe_{10}N_{48}O_{0.50}$, *M* 8739.45, monoclinic, space group $P2_1$(#4), *a* 26.9590(6), *b* 37.7214(9), *c* 30.7607(7) Å, β 108.8010(10), *V* 29612.4(12) Å^3, D_c 0.980 g cm^{-3}, *Z* 2, crystal size 0.300 by 0.250 by 0.200 mm, colour red, habit block, temperature 150(2) Kelvin, λ(MoKα) 0.71073 Å, μ(MoKα) 0.324 mm^{-1}, *T*(SADABS)$_{min,max}$ 0.6640, 0.7454, 2θ_{max} 50.00, *hkl* range -32 32, -44 44, -36 36, *N* 474451, N_{ind} 103962(R_{merge} 0.1190), N_{obs} 47025(I > 2σ(I)), N_{var} 4609, residuals* *R*1(*F*) 0.1231, *wR*2(F^2) 0.3286, GoF(all) 1.102, $\Delta\rho_{min,max}$ -0.576, 1.536 e$^-$ Å^{-3}.

*$R1 = \Sigma||F_o| - |F_c||/\Sigma|F_o|$ for $F_o > 2\sigma(F_o)$; $wR2 = (\Sigma w(F_o^2 - F_c^2)^2/\Sigma(wF_c^2)^2)^{1/2}$ all reflections
$w=1/[\sigma^2(F_o^2)+(0.1000P)^2+100.0000P]$ where $P=(F_o^2+2F_c^2)/3$

$[Fe_4(50)_6\supset BF_4)](BF_4)_7$, (155): Formula $C_{162}H_{172.2}B_8F_{32}Fe_4N_{27}O_{9.60}$, *M* 3569.47, cubic, space group $P\ \bar{4}_3n$(#218), *a* 22.0042(2), *b* 22.0042(2), *c* 22.0042(2) Å, *V* 10654.10(17) $Å^3$, D_c 1.113 g cm^{-3}, *Z* 2, crystal size 0.500 by 0.200 by 0.150 mm, colour red, habit prism, temperature 150(2) Kelvin, λ(MoKα) 0.71073 Å, μ(MoKα) 0.347 mm^{-1}, $T(\text{SADABS})_{min,max}$ 0.800, 0.949, $2\theta_{max}$ 56.00, *hkl* range -29 28, -29 26, -29 26, *N* 81593, N_{ind} 4294(R_{merge} 0.0478), N_{obs} 3251(I > 2σ(I)), N_{var} 196, residuals* *R*1(*F*) 0.0616, *wR*2(F^2) 0.2026, GoF(all) 1.106, $\Delta\rho_{min,max}$ -0.610, 0.469 e^- $Å^{-3}$.

*$R1 = \Sigma||F_o| - |F_c||/\Sigma|F_o|$ for $F_o > 2\sigma(F_o)$; $wR2 = (\Sigma w(F_o^2 - F_c^2)^2/\Sigma(wF_c^2)^2)^{1/2}$ all reflections
$w=1/[\sigma^2(F_o^2)+(0.1387P)^2+1.7003P]$ where $P=(F_o^2+2F_c^2)/3$

$[Fe_4(50)_6\supset PF_6](PF_6)_7$, (156): Formula $C_{141}H_{156}F_{48}Fe_4N_{24}O_{15}P_8$, *M* 3810.06, cubic, space group $P\ \bar{4}_3n$(#218), *a* 21.8735(2), *b* 21.8735(2), *c* 21.8735(2) Å, *V* 10465.38(17) $Å^3$, D_c 1.209 g cm^{-3}, *Z* 2, crystal size 0.080 by 0.070 by 0.060 mm, colour red, habit prism, temperature 100(2) Kelvin, λ(synchrotron) 0.48595 Å, μ(synchrotron) 0.227 mm^{-1}, $T(\text{SADABS})_{min,max}$ 0.872, 0.986, $2\theta_{max}$ 34.96, *hkl* range -26 27, -27 26, -26 27, *N* 64646, N_{ind} 3459(R_{merge} 0.0541), N_{obs} 3095(I > 2σ(I)), N_{var} 201, residuals* *R*1(*F*) 0.0596, *wR*2(F^2) 0.1721, GoF(all) 1.131, $\Delta\rho_{min,max}$ -0.621, 0.599 e^- $Å^{-3}$.

*$R1 = \Sigma||F_o| - |F_c||/\Sigma|F_o|$ for $F_o > 2\sigma(F_o)$; $wR2 = (\Sigma w(F_o^2 - F_c^2)^2/\Sigma(wF_c^2)^2)^{1/2}$ all reflections
$w=1/[\sigma^2(F_o^2)+(0.1107P)^2+4.6683P]$ where $P=(F_o^2+2F_c^2)/3$

$[Fe_4(50)_6][ZnCl_4]_4$, (157): Formula $C_{156}H_{160}Cl_{16}Fe_4N_{25}O_8Zn_4$, *M* 3565.17, monoclinic, space group *P*2/n(#13), *a* 17.7800(10), *b* 17.8806(10), *c* 31.0654(17) Å,

β 94.113(4), *V* 9850.8(9) Å^3, D_c 1.202 g cm^{-3}, *Z* 2, crystal size 0.400 by 0.350 by 0.300 mm, colour red, habit prism, temperature 150(2) Kelvin, λ(MoKα) 0.71073 Å, μ(MoKα) 1.033 mm^{-1}, T(SADABS)$_{min,max}$ 0.623, 0.734, 2θ_{max} 56.00, *hkl* range -23 23, -22 23, -41 41, *N* 152138, N_{ind} 23743(R_{merge} 0.0382), N_{obs} 15418(I > 2σ(I)), N_{var} 971, residuals* *R*1(*F*) 0.0799, *wR*2(F^2) 0.2685, GoF(all) 1.091, $\Delta\rho_{min,max}$ -1.462, 1.185 e$^-$ Å^{-3}.

*$R1 = \Sigma||F_o| - |F_c||/\Sigma|F_o|$ for $F_o > 2\sigma(F_o)$; $wR2 = (\Sigma w(F_o^2 - F_c^2)^2/\Sigma(wF_c^2)^2)^{1/2}$ all reflections

$w=1/[\sigma^2(F_o^2)+(0.1787P)^2+0.0000P]$ where $P=(F_o^2+2F_c^2)/3$

[Ru$_2$(50)$_3$](PF$_6$)$_4$, (160): Formula $C_{70.50}H_{63}F_{24}N_{14.25}O_{1.125}P_4Ru_2$, *M* 1909.87, trigonal, space group $P6_3$(#173), *a* 13.6600(7), *b* 13.660, *c* 57.016(3) Å, γ 120.00º, *V* 9213.6(7) Å^3, D_c 1.377 g cm^{-3}, *Z* 4, crystal size 0.20 by 0.18 by 0.02 mm, colour orange, habit plate, temperature 150(2) Kelvin, λ(MoKα) 0.71073 Å, μ(MoKα) 0.492 mm^{-1}, T(SADABS)$_{min,max}$ 0.863, 0.990, 2θ_{max} 56.48, *hkl* range -14 14, -17 17, -75 75, *N* 47169, N_{ind} 14750(R_{merge} 0.0322), N_{obs} 12114(I > 2σ(I)), N_{var} 799, residuals* *R*1(*F*) 0.0984, *wR*2(F^2) 0.2675, GoF(all) 1.116, $\Delta\rho_{min,max}$ -3.936, 3.324 e$^-$ Å^{-3}.

*$R1 = \Sigma||F_o| - |F_c||/\Sigma|F_o|$ for $F_o > 2\sigma(F_o)$; $wR2 = (\Sigma w(F_o^2 - F_c^2)^2/\Sigma(wF_c^2)^2)^{1/2}$ all reflections

$w=1/[\sigma^2(F_o^2)+(0.1201P)^2+63.1133P]$ where $P=(F_o^2+2F_c^2)/3$

The crystal used in the present study proved to be a 15% racemic twin as evidenced by a refined Flack parameter of 0.15.[7]

[Fe$_4$(128)$_6$](PF$_6$)$_8$, (162): Formula $C_{186}H_{146.30}F_{48}Fe_4N_{27}O_{21.35}P_8$, *M* 4484.36, triclinic, space group $P\bar{1}$(#2), *a* 20.2470(12), *b* 20.7900(12), *c* 30.5460(17) Å, α 82.126(3), β 76.935(3), γ 73.436(3)º, *V* 11969.0(12) Å^3, D_c 1.244 g cm^{-3}, *Z* 2, crystal size 0.250 by 0.150 by 0.100 mm, colour red, habit prism, temperature 150(2) Kelvin, λ(MoKα) 0.71073 Å, μ(MoKα) 0.387 mm^{-1}, T(SADABS)$_{min,max}$ 0.744008, 1.00000, 2θ_{max} 58.90, *hkl* range -27 27, -28 28, -42 41, *N* 345768, N_{ind} 65517(R_{merge} 0.0463),

N_{obs} 43109(I > 2σ(I)), N_{var} 2751, residuals* *R*1(*F*) 0.1275, *wR*2(F^2) 0.3964, GoF(all) 1.080, $\Delta\rho_{min,max}$ -1.543, 1.756 e^- $Å^{-3}$.

*$R1 = \Sigma||F_o| - |F_c||/\Sigma|F_o|$ for $F_o > 2\sigma(F_o)$; $wR2 = (\Sigma w(F_o^2 - F_c^2)^2/\Sigma(wF_c^2)^2)^{1/2}$ all reflections

$w=1/[\sigma^2(F_o^2)+(0.2000P)^2+50.5000P]$ where $P=(F_o^2+2F_c^2)/3$

[Ni_2(128)$_3$](PF_6)$_4$, (163): Formula $C_{45}H_{39}F_{12}N_6NiO_3P_2$, *M* 1060.47, hexagonal, space group $P6_3$(#173), *a* 13.460(2), *b* 13.460(2), *c* 30.805(5) Å, γ 120.00º, *V* 4833.5(12) $Å^3$, D_c 1.457 g cm^{-3}, *Z* 4, crystal size 0.150 by 0.10 by 0.05 mm, colour yellow, habit plate, temperature 150(2) Kelvin, λ(MoKα) 0.71073 Å, μ(MoKα) 0.560 mm^{-1}, $T(SADABS)_{min,max}$ 0.831645, 1.00000, $2\theta_{max}$ 45.00, *hkl* range -14 14, -14 14, -33 33, *N* 50725, N_{ind} 4231(R_{merge} 0.0417), N_{obs} 4004(I > 2σ(I)), N_{var} 438, residuals* *R*1(*F*) 0.0841, *wR*2(F^2) 0.2315, GoF(all) 1.085, $\Delta\rho_{min,max}$ -1.463, 0.665 e^- $Å^{-3}$.

*$R1 = \Sigma||F_o| - |F_c||/\Sigma|F_o|$ for $F_o > 2\sigma(F_o)$; $wR2 = (\Sigma w(F_o^2 - F_c^2)^2/\Sigma(wF_c^2)^2)^{1/2}$ all reflections

$w=1/[\sigma^2(F_o^2)+(0.1276P)^2+16.3939P]$ where $P=(F_o^2+2F_c^2)/3$

[Fe_4(129)$_6$](PF_6)$_8$, (165): Formula $C_{18}H_{18}F_6Fe_0N_{18}O_{36}P_3$, *M* 1269.41, tetragonal, space group $I4_1/a$(#88), *a* 42.764(2), *b* 42.764(2), *c* 17.3170(16) Å, *V* 31669(4) $Å^3$, D_c 0.532 g cm^{-3}, *Z* 8, crystal size 0.10 by 0.070 by 0.05 mm, colour red, habit prism, temperature 100(2) Kelvin, λ(synchrotron) 0.49594 Å, μ(synchrotron) 0.045 mm^{-1}, $T(?)_{min,max}$?, ?, $2\theta_{max}$ 29.96, *hkl* range -44 44, -38 44, -18 18, *N* 34465, N_{ind} 7453(R_{merge} 0.0609), N_{obs} 6168(I > 2σ(I)), N_{var} 667, residuals* *R*1(*F*) 0.1694, *wR*2(F^2) 0.4145, GoF(all) 1.797, $\Delta\rho_{min,max}$ -1.191, 1.310 e^- $Å^{-3}$.

*$R1 = \Sigma||F_o| - |F_c||/\Sigma|F_o|$ for $F_o > 2\sigma(F_o)$; $wR2 = (\Sigma w(F_o^2 - F_c^2)^2/\Sigma(wF_c^2)^2)^{1/2}$ all reflections

$w=1/[\sigma^2(F_o^2)+(0.2000P)^2+0.0000P]$ where $P=(F_o^2+2F_c^2)/3$

$[Ni_4(129)_6](PF_6)_8$, (166): Formula $C_{264}H_{280}F_{45}N_{30}Ni_4O_{35.57}P_8$, *M* 5779.90, triclinic, space group *P* $\bar{1}$(#2), *a* 21.159, *b* 24.202, *c* 37.734 Å, α 78.50, β 79.57, γ 76.78°, *V* 18246.8 $Å^3$, D_c 1.052 g cm^{-3}, *Z* 2, crystal size 0.250 by 0.180 by 0.100 mm, colour yellow, habit block, temperature 150(2) Kelvin, λ(MoKα) 0.71073 Å, μ(MoKα) 0.316 mm^{-1}, $T(SADABS)_{min,max}$ 0.6737, 0.7457, $2\theta_{max}$ 50.00, *hkl* range -25 24, -28 28, -44 44, *N* 443414, N_{ind} 63079(R_{merge} 0.0693), N_{obs} 39106(I > 2σ(I)), N_{var} 3797, residuals* *R*1(*F*) 0.1014, *wR*2(F^2) 0.2752, GoF(all) 1.066, $\Delta\rho_{min,max}$ -0.873, 1.071 e^- $Å^{-3}$.

*$R1 = \Sigma||F_o| - |F_c||/\Sigma|F_o|$ for $F_o > 2\sigma(F_o)$; $wR2 = (\Sigma w(F_o^2 - F_c^2)^2/\Sigma(wF_c^2)^2)^{1/2}$ all reflections
$w=1/[\sigma^2(F_o^2)+(0.1000P)^2+68.0000P]$ where $P=(F_o^2+2F_c^2)/3$

$[Ni_2(149)_3](PF_6)_4$, (170): Formula $C_{94}H_{86.4}F_{24}N_{12}Ni_2O_{10.20}P_4$, *M* 2244.61, Monoclinic, space group *C*2/c(#15), *a* 23.0800(16), *b* 15.0530(11), *c* 32.656(3) Å, β 105.778(4), *V* 10918.0(15) $Å^3$, D_c 1.362 g cm^{-3}, *Z* 4, crystal size 0.300 by 0.250 by 0.100 mm, colour yellow, habit needle, temperature 150(2) Kelvin, λ(MoKα) 0.71073 Å, μ(MoKα) 0.502 mm^{-1}, $T(SADABS)_{min,max}$ 0.813, 0.951, $2\theta_{max}$ 50.00, *hkl* range -21 27, -17 17, -38 38, *N* 111989, N_{ind} 9594(R_{merge} 0.0267), N_{obs} 8211(I > 2σ(I)), N_{var} 798, residuals* *R*1(*F*) 0.0735, *wR*2(F^2) 0.2345, GoF(all) 1.094, $\Delta\rho_{min,max}$ -0.568, 1.084 e^- $Å^{-3}$.

*$R1 = \Sigma||F_o| - |F_c||/\Sigma|F_o|$ for $F_o > 2\sigma(F_o)$; $wR2 = (\Sigma w(F_o^2 - F_c^2)^2/\Sigma(wF_c^2)^2)^{1/2}$ all reflections
$w=1/[\sigma^2(F_o^2)+(0.1529P)^2+26.7618P]$ where $P=(F_o^2+2F_c^2)/3$

$[Ni_2(150)_3](PF_6)_4$, (171): Formula $C_{114.50}H_{125.75}F_{24}N_{13.75}Ni_2O_{11.50}P_4$, *M* 2575.83, monoclinic, space group $P2_1$/c(#14), *a* 26.028(2), *b* 22.7450(17), *c* 21.4660(16) Å, β 113.663(2), *V* 11639.6(16) $Å^3$, D_c 1.470 g cm^{-3}, *Z* 4, crystal size 0.100 by 0.050 by 0.050 mm, colour yellow, habit needle, temperature 100(2) Kelvin, λ(??) 0.49594 Å, μ(??) 0.259 mm^{-1}, $T(SADABS)_{min,max}$ 0.5994, 0.7444, $2\theta_{max}$ 38.62, *hkl* range -33 33, -30 26, -27 28, *N* 99393, N_{ind} 27767(R_{merge} 0.0847), N_{obs} 16878(I > 2σ(I)), N_{var} 1577,

residuals* $R1(F)$ 0.0624, $wR2(F^2)$ 0.1880, GoF(all) 1.010, $\Delta\rho_{min,max}$ -0.858, 1.628 e^- $Å^{-3}$.

*$R1 = \Sigma||F_o| - |F_c||/\Sigma|F_o|$ for $F_o > 2\sigma(F_o)$; $wR2 = (\Sigma w(F_o^2 - F_c^2)^2/\Sigma(wF_c^2)^2)^{1/2}$ all reflections
$w=1/[\sigma^2(F_o^2)+(0.1010P)^2+7.1972P]$ where $P=(F_o^2+2F_c^2)/3$

$[Ni_2(151)_3](PF_6)_4$ (172): Formula $C_{98.70}H_{97.05}F_{24}N_{13.95}Ni_2O_9P_4$, *M* 2317.49, triclinic, space group $P\bar{1}$(#2), *a* 14.9978(6), *b* 15.0666(6), *c* 25.7786(11) Å, α 91.398(2), β 104.152(2), γ 99.563(2)º, *V* 5556.9(4) $Å^3$, D_c 1.385 g cm^{-3}, *Z* 2, crystal size 0.300 by 0.100 by 0.100 mm, colour yellow, habit needle, temperature 150(2) Kelvin, λ(MoKα) 0.71073 Å, μ(MoKα) 0.496 mm^{-1}, $T(SADABS)_{min,max}$ 0.799, 0.952, $2\theta_{max}$ 50.00, *hkl* range -17 17, -17 17, -30 30, *N* 107006, N_{ind} 19484(R_{merge} 0.0534), N_{obs} 13655(I > 2σ(I)), N_{var} 1534, residuals* R(F^2) 0.0734, $R_w(F^2)$ 0.2194, GoF(all) 1.072, $\Delta\rho_{min,max}$ -0.552, 0.993 e^- $Å^{-3}$.

*$R = \Sigma|F_o^2 - F_c^2|/\Sigma F_o^2$; $R_w = (\Sigma w(F_o^2 - F_c^2)^2/\Sigma(wF_c^2)^2)^{1/2}$
$w=1/[\sigma^2(F_o^2)+(0.1364P)^2+8.2419P]$ where $P=(F_o^2+2F_c^2)/3$

Tris-(2-benzyloxy-5-*tert*-butylbenzyl)-amine (174): Formula $C_{54}H_{63}NO_{3.50}$, *M* 782.05, trigonal, space group $R\bar{3}$(#148), *a* 19.4736(13), *b* 19.4736(13), *c* 21.2569(14) Å, α 90.00 º, β 90.00 º, γ 120.00 º, *V* 6981(1) $Å^3$, D_c 1.116 g cm^{-3}, *Z* 6, crystal size 0.250 by 0.250 by 0.250 mm, colour colourless, habit prism, temperature 293(2) Kelvin, μ(MoKα) 0.17 mm^{-1}, $T(SADABS)_{min}$ = 0.983, $T(SADABS)_{max}$ = 0993, θ_{max} 28.4 º.

*$R[F^2 > 2\sigma(F^2)] = 0.059$, $wR(F^2)$ 0.242, *S* = 0.95, 3799 reflections, 227 parameters, $\Delta\rho_{min,max}$ -0.29, 0.18 e $Å^{-3}$, H atoms treated by a mixture of independent and constrained refinement.

$w = 1/[\sigma^2(F_o^2)+(0.1339P)^2]$ where $P = (F_o^2+2F_c^2)/3$

$[Fe(176)](PF_6)_2$ (179): Formula $C_{57}H_{51}F_{18}FeN_7O_3P_3$, *M* 1372.81, trigonal, space group $R\bar{3}$(#148), *a* 14.7878(9), *b* 14.7878(9), *c* 45.461(6) Å, γ 120.00º, *V* 8609.5(14) $Å^3$,

D_c 1.589 g cm^{-3}, Z 6, crystal size 0.250 by 0.150 by 0.100 mm, colour purple, habit prism, temperature 150(2) Kelvin, λ(MoKα) 0.71073 Å, μ(MoKα) 0.458 mm^{-1}, T(SADABS)$_{min,max}$ 0.6494, 0.7457, 2θ_{max} 50.00, *hkl* range -17 17, -16 17, -52 54, N 20775, N_{ind} 3381(R_{merge} 0.0652), N_{obs} 2481(I > 2σ(I)), N_{var} 266, residuals* $R1(F)$ 0.0794, $wR2(F^2)$ 0.2285, GoF(all) 1.097, $\Delta\rho_{min,max}$ -1.104, 1.603 e$^-$ Å^{-3}.

*$R1 = \Sigma||F_o| - |F_c||/\Sigma|F_o|$ for $F_o > 2\sigma(F_o)$; $wR2 = (\Sigma w(F_o^2 - F_c^2)^2/\Sigma(wF_c^2)^2)^{1/2}$ all reflections

$w=1/[\sigma^2(F_o^2)+(0.1065P)^2+87.6952P]$ where $P=(F_o^2+2F_c^2)/3$

B.2 References

1. Bruker-Nonius (2003). APEX v2.1, SAINT v.7 and XPREP v.6.14. Bruker AXS Inc. Madison, Wisconsin, USA.
2. Bruker (1995), SMART, SAINT and XPREP. Bruker Analytical X-ray Instruments Inc., Madison, Wisconsin, USA.
3. *WinGX-32: System of programs for solving, refining and analysing single crystal X-ray diffraction data for small molecules*, L. J. Farrugia, *J. Appl. Cryst.* **1999**, *32*, 837.
4. A. Altomare, M. C. Burla, M. Camalli, G. L. Cascarano, C. Giocavazzo, A. Guagliardi, A. G. C. Moliterni, G. Polidori, S. Spagna, *J. Appl. Cryst.*, **1999**, *32*, 115.
5. G. M. Sheldrick, *SADABS: Empirical Absorption and Correction Software*, University of Göttingen, Germany, 1999-2003.
6. G. M. Sheldrick, *SHELXL-97: Programs for Crystal Structure Analysis*, University of Göttingen, Germany, 1997.
7. Flack H D (1983), *Acta Cryst*. A39, 876-881.

Appendix C

Electrochemistry

Appendix C.1 Cyclic Voltammetry and Oxidative Bulk Electrolysis of $[Fe_4(50)_6]^{8+}$ samples

The complete oxidation of $[Fe_4(\mathbf{50})_6 \supset FeCl_4](PF_6)_n$ (n = 6 or 7) such that all iron centres are converted to Fe(III) using bulk electrolysis would in theory allow its absolute stoichiometry to be confirmed. For example, if the complex consists of four Fe(II) centres and one Fe(III) centre then a four electron oxidative process should be observed, or conversely if the complex has five Fe(II) centres a five electron oxidative process should be observed. Thus by using Faraday's law, $\boldsymbol{N = Q/nF}$ (*N* = the number of moles of analyte, Q = the charge, n = the number of electrons in the redox process and F = the Faraday constant), Q can be measured experimentally by bulk electrolysis allowing n to be estimated. In order to carry out the bulk electrolysis the required applied potential needs to be determined. To do this a differential pulse or cyclic voltammogram may be collected. The oxidative potential may then be selected to ensure the redox active species will be oxidised.

In the first instance ferrocene (sublimed material) was used as a model to assess the intended experimental conditions. The CV of ferrocene was conducted on an approximately 1 mM CH_3CN solution with 0.1 M tetrabutylammonium hexafluorophosphate ($TBAPF_6$) as electrolyte using a glassy carbon working electrode and a silver wire reference electrode. The scan rate was varied from 50 to 100 mV s^{-1} with no significant change in voltammograms. As expected the CV results show a single wave ($E_{1/2}$= 0.454 V; ΔE_p=111 mV; 1 e^-) under the conditions employed (***Figure C.1***). The oxidative potential of 0.8 V was selected for the oxidative bulk electrolysis experiment.

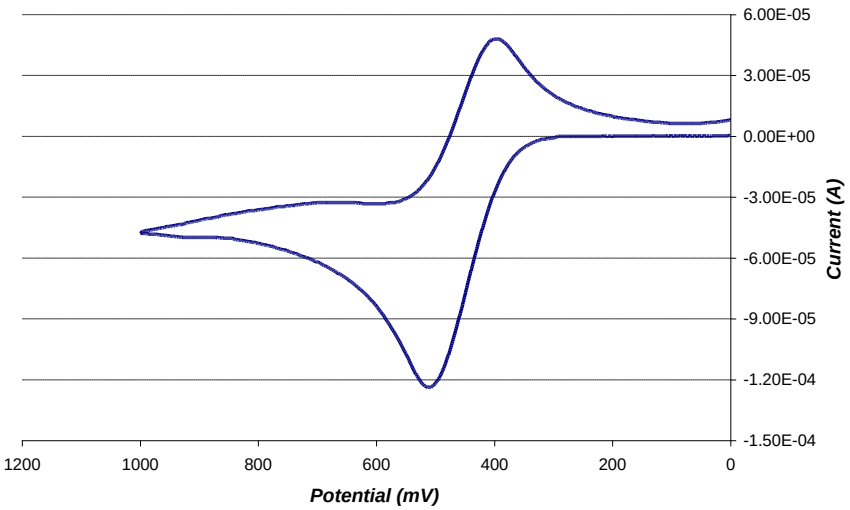

Figure C.1 The CV of ferrocene with a scan rate of 100 mV s^{-1}.

The oxidative bulk electrolysis of a sample of ferrocene (14.662 mg, 78.809 μmole) was conducted using a Pt mesh working electrode, Ag wire reference electrode and a Pt wire counter electrode, in 0.1 M tetrabutylammonoium hexafluorophosphate (TBAF). The electrodes were kept separated by glass frits in a specially designed electrochemical cell. The oxidative potential was set to 0.8 V with the oxidative bulk electrolysis being discontinued when the current reached 1 % of the initial current (***Figure C.2***). The experimentally determined measure of Q for the $1e^-$ oxidation of ferrocene was 6.974 C versus that of the theoretically determined value of Q, which was 7.605 C. This equates to 92 % of the expected charge, which is a substantial underestimate most probably due to the solvent of crystallisation of the ferrocene sample not being included in the molecular weight of the sample, thus resulting in an overestimate of the theoretical Q value.

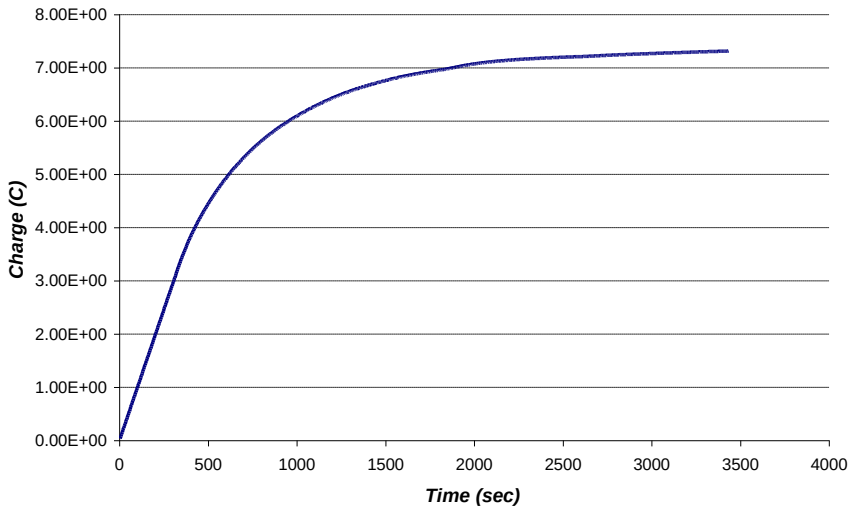

Figure C.2 The bulk electrolysis of ferrocene using a oxidative potential of 0.8 V.

The CV of $[Fe_4(\mathbf{50})_6 \supset FeCl_4](PF_6)_7$ was collected under the same conditions as those used for the collection of the ferrocene CV (described above). The CV results show a single wave ($E_{1/2}$= 1.08 V; ΔE_p=111 mV; 4 e^-) under the conditions employed (***Figure C.3***). Hence, an oxidative potential of 1.4 V was considered appropriate for the oxidative bulk electrolysis experiment.

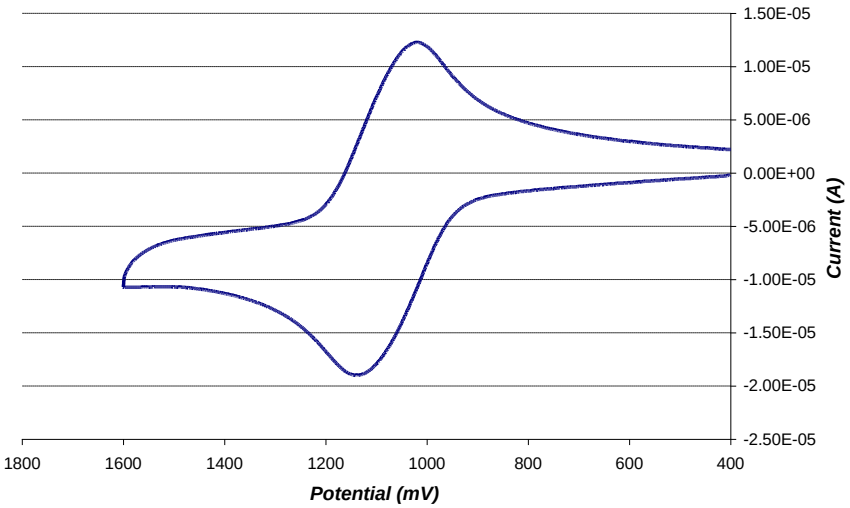

Figure C.3 The CV of $[Fe_4(\mathbf{50})_6 \supset FeCl_4](PF_6)_7$ with a scan rate of 100 mV s^{-1}.

The oxidative bulk electrolysis of $[Fe_4(\mathbf{50})_6 \supset FeCl_4](PF_6)_7$ (15.147 mg, 4.33 μmole) was conducted as for ferrocene (outlined above) using an oxidative potential of 1.4 V (***Figure C 4***). Interestingly, the deep red coloured solution of the complex goes to a light green colour on oxidation of the Fe(II) tris-bipyridyl moieties. The experimentally determined measure of Q for the $4e^-$ oxidation of $[Fe_4(\mathbf{50})_6 \supset FeCl_4](PF_6)_7$ was 1.692 C versus that of the theoretically determined value of Q, which was 1.673 C. The former result equates to 101 % of the expected charge. This is an unexpected result as underestimates using this technique are more common. However, there is no doubt that the bulk electrolysis indicates $[Fe_4(\mathbf{50})_6 \supset FeCl_4](PF_6)_7$ is the correct formula; $[Fe_4(\mathbf{50})_6 \supset FeCl_4](PF_6)_6$ would require a five e^- reduction with a theoretically determined value of Q of 2.18 C and at best the agreement with the predicted Q is 78 %.

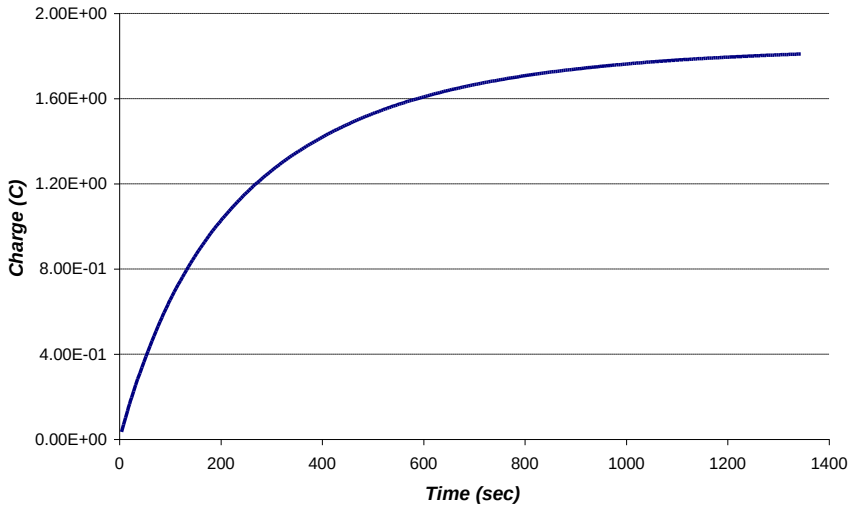

Figure C.4 The bulk electrolysis of $[Fe_4(\mathbf{50})_6 \supset FeCl_4](PF_6)_7$ using a oxidative potential of 1.4 V.

Further validation of the conditions employed for the oxidative bulk electrolysis experiments outlined above was obtained by investigating the oxidation of $[Fe_4(\mathbf{50})_6 \supset BF_4](BF_4)_7$. Initially, the CV of $[Fe_4(\mathbf{50})_6 \supset BF_4](BF_4)_7$ was collected to determine the oxidation potential needed for its oxidation (***Figure C 5***). As expected, the CV results show a single wave ($E_{1/2}$= 1.14 V; ΔE_p= 99 mV; 4 e^-) under the conditions

employed. The oxidative potential of 1.4 V was selected for the oxidative bulk electrolysis experiment.

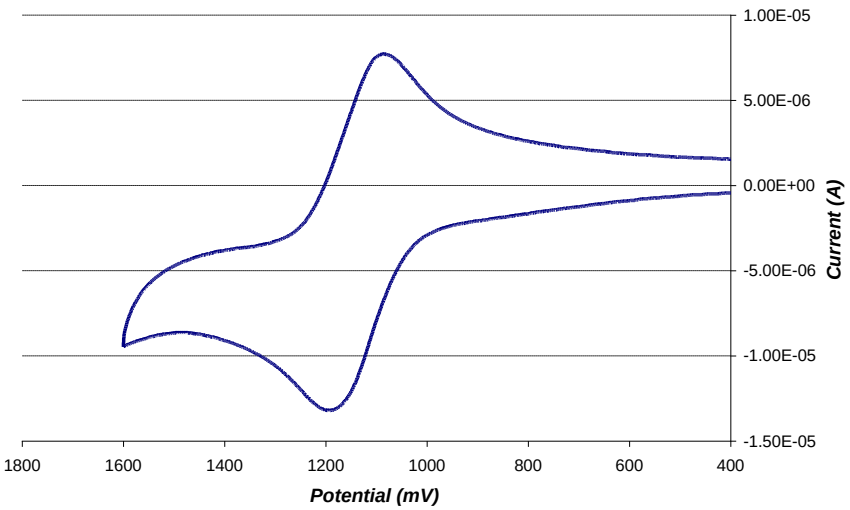

Figure C.5 The CV of $[Fe_4(\mathbf{50})_6\supset BF_4](BF_4)_7$ with a scan rate of 100 mV s^{-1}.

The oxidative bulk electrolysis of $[Fe_4(\mathbf{50})_6\supset BF_4](BF_4)_7$ (12.603 mg, 4.172 μmole) was conducted as for ferrocene (outlined above) using an oxidative potential of 1.4 V. Again, the deep red colour of the solution of the complex goes to a light green on oxidation of the Fe(II) tris-bipyridyl moieties. The experimentally determined measure of Q for the $4e^-$ oxidation of $[Fe_4(\mathbf{50})_6\supset BF_4](BF_4)_7$ was 1.547 C versus that of the theoretically determined value of Q, which was 1.611 C. This equates to 96 % of the expected result for the four e^- oxidation of $[Fe_4(\mathbf{50})_6\supset BF_4](BF_4)_7$.

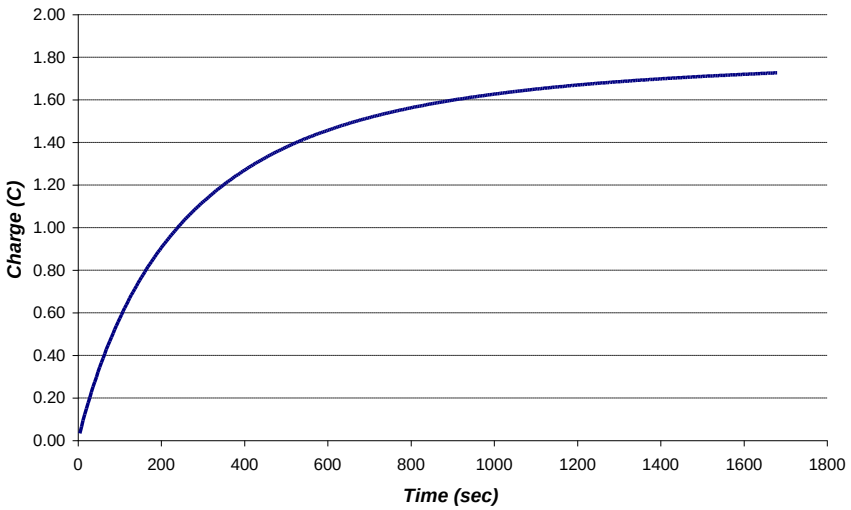

Figure C.6 The bulk electrolysis of $[Fe_4(\mathbf{50})_6\supset BF_4](BF_4)_7$ using a oxidative potential of 1.4 V.

It is known that the Fe(II)/Fe(III) redox couple of $[Fe(bpy)_3]^{2+}$ is reversible, thus indicating the integrity of this complex in both its reduced and oxidised forms. In this regard, a further experiment designed to assess the integrity of the oxidised M_4L_6 species was conducted. To do this the solution from the oxidative bulk electrolysis of $[Fe_4(\mathbf{50})_6\supset BF_4](BF_4)_7$ was subsequently reduced by applying a potential of 0.8 V. Again the reduction was continued until the current reach 1% of the initial current. The green colour of the oxidised complex solution returned to a deep red colour reminiscent of $[Fe_4(\mathbf{50})_6\supset BF_4](BF_4)_7$. However, the CV collected on this reduced complex solution revealed that the redox couple had shifted to a less positive potential (***Figure C.7***). This observation is consistent with the decomposition of $[Fe_4(\mathbf{50})_6\supset BF_4](BF_4)_7$. Clearly further investigation of the resulting product(s) from this process is needed.

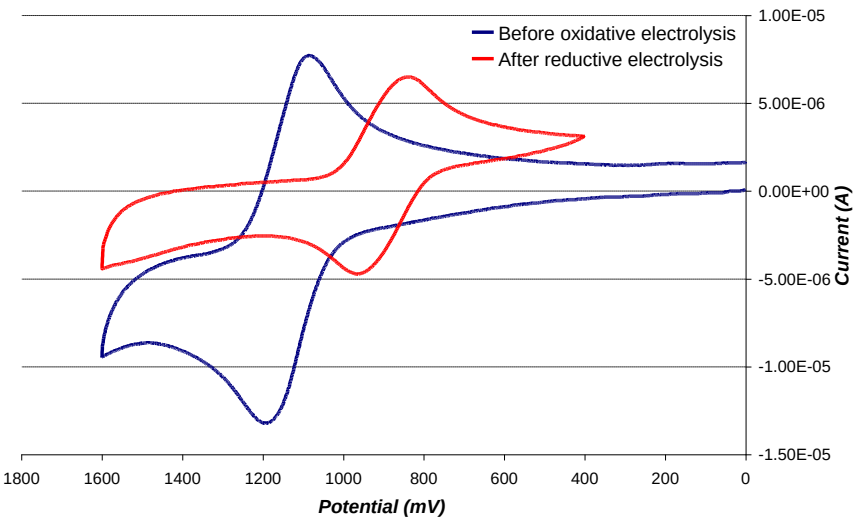

Figure C.7 CV of a solution of $[Fe_4(\mathbf{50})_6\supset BF_4](BF_4)_7$ before and after bulk electrolysis experiments.

The CV of $[Fe_4(\mathbf{50})_6\supset BF_4](BF_4)_7$ over a potential range of 2000 to -2000 mV was also collected (***Figure C.8***). There is a single wave corresponding to the Fe(II) / Fe(III) redox couple ($E_{1/2}$ = 1.14 V; ΔE_p = 99 mV; 4 e^-) and another more complex wave observed at more negative potential ($E_{1/2}$ = -1.6 mV) most probably corresponding to the reduction of the quaterpyridine. Again further investigation of the electrochemistry of this system is required.

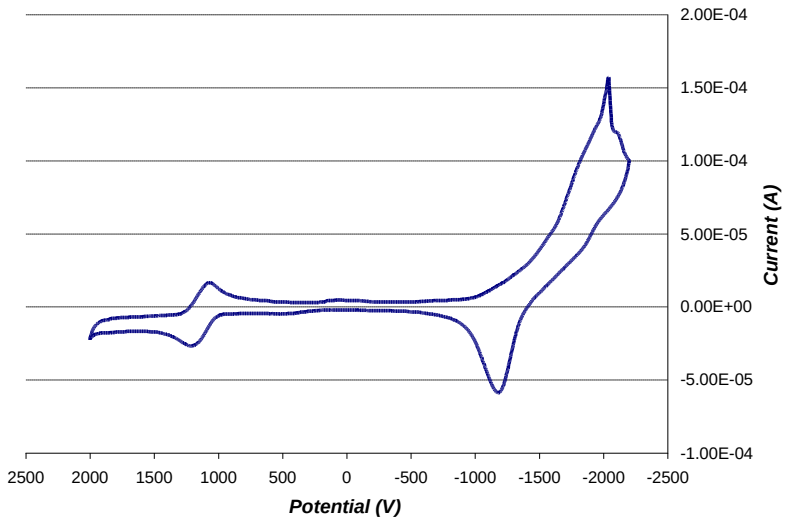

Figure C.8 CV of a solution of $[Fe_4(\mathbf{50})_6\supset BF_4](BF_4)_7$ with a scan rate of 100 mV s^{-1}.

Appendix C.2 Cyclic Voltammetry of $[Ru_2(50)_3](PF_6)_4$

The CV was conducted on an approximately 1 mM CH_3CN solution of $[Ru_2(\mathbf{50})_3](PF_6)_4$ with 0.1 M $TBAPF_6$ as electrolyte using a Pt-disc working electrode and a silver wire reference electrode. The scan rate was varied from 50 to 200 mV s^{-1} with no visible change in voltamograms. The CV illustrated in ***Figure C.9*** was collected by scanning at a rate of 100 mV s^{-1} over a potential range of -2.0 V to 2.0 V; a total of 10 cycles revealed no change in the CV. The CV results show a *pseudo*-reversible redox wave corresponding to the Ru(II) / Ru (III) redox couple ($E_{1/2}$ = 1.43V; ΔEp = 101 mV; 2 e^-) under the conditions employed and a much more complex set of redox processes in the potential range of approximately -0.5 V to -2.0 V. Again these latter redox processes are most probably due to the reduction / oxidation of the quaterpyridyl ligand.

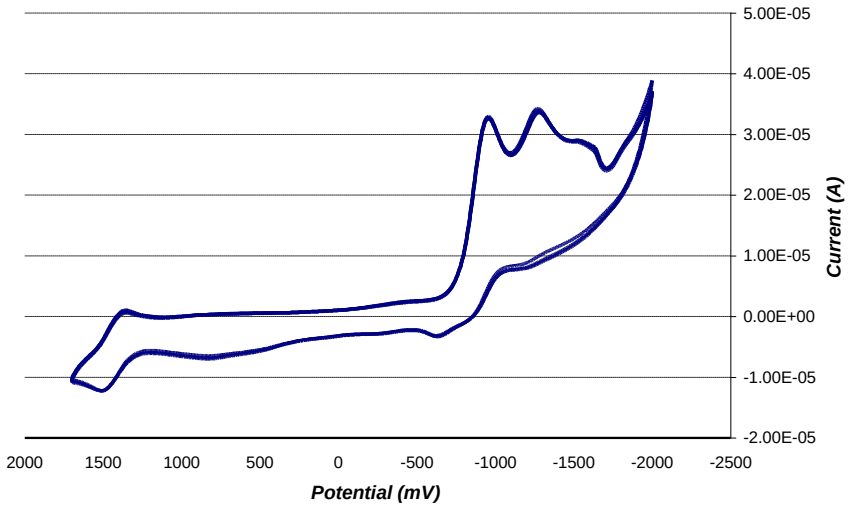

Figure C.8 CV of a solution of $[Ru_2(\mathbf{50})_3](PF_6)_4$ with a scan rate of 100 mV s^{-1}.

Appendix D

DNA Binding Studies

Appendix C.1 DNA binding affinity chromatography:

A 20 mM sodium phosphate/0.15 M sodium chloride/pH 7.5 buffer solution was used as eluent for all chromatographic separations. The DNA sequences employed included an immobilised AT duplex DNA 12-mer, a tridecanucleotide possessing an unpaired adenine base (or ″bulge″) d(CCGAGAATTCCGG)$_2$, an icosamer featuring a 6-base CT hairpin loop, d(CACTGGTCTCTCTACCAGTG), and a GC duplex DNA 12-mer. Enantiomeric purity of the separated *M* and *P* $[Ru_2(\mathbf{2})_3]^{4+}$ enantiomers resulting from the various chromatography experiments were assessed by CD spectroscopy. See Smith *et al.*[1] for general chromatography details.

Appendix C.2 Calf-thymus DNA titrations

UV/visible spectrophotometric measurements were made on a Cary 50 Bio UV/visible spectrophotometer. The *P*- and *M*-enatiomers of $[Ru_2(\mathbf{50})_3](PF_6)_4$ were anion exchanged using Amberlite resin IRA-400 (Cl) to the $[Ru_2(\mathbf{50})_3]Cl_4$ form to facilitate water solubility. All solutions were made up in Tris buffer (5 mM Tris-HCl, 50 mM NaCl, 7.2 pH). Calf thymus DNA (ct-DNA) was purchased from Sigma Aldrich. The concentrations of ct-DNA solutions were determined spectrophotometrically using the molar extinction coefficient ε_{260} = 6600 M^{-1} cm^{-1} (all ct-DNA concentrations with respect to base pairs). Titrations were conducted by keeping the metal complex concentration constant at 10 μM and sequentially titrating in a solution with 10 μM complex (*P* or *M* helicate) : 600 μM ct-DNA. The first spectrum was collected on the ct-DNA free 10 μM complex solution followed by the addition of successive 50 μl aliquots of the complex/ct-DNA solution until an approximate 20 : 1 ratio of DNA to complex was reached. ***Figure D.1*** is representative of titration data for *P*-$[Ru_2(\mathbf{50})_3]Cl_4$ and *M*-$[Ru_2(\mathbf{50})_3]Cl_4$.

In the presence of ct-DNA, hypochromicity was observed for both the *P* and *M* helicates in both the π-π* and MLCT bands (***Figure D.1***). An apparent binding constant (K_b) value of 2.0 x 10^5 M^{-1} for *M*-$[Ru_2\mathbf{L}_3]Cl_4$ was determined from this titration data (see inset, ***Figure D.1***). The same spectrophotometric titration conducted with *P*-$[Ru_2L_3]^{4+}$ consistently gave K_b values in the range 4.0 x 10^5 to 2.6 x 10^6 M^{-1} in an apparent conflict with the chromatography data. Note that the ε value for the Cl^- salt in Tris buffer was

16000 $M^{-1}cm^{-1}$ which is significantly less than that recorded for the PF_6^- salt in acetonitrile, however the general form of the absorption spectrum remains the same.

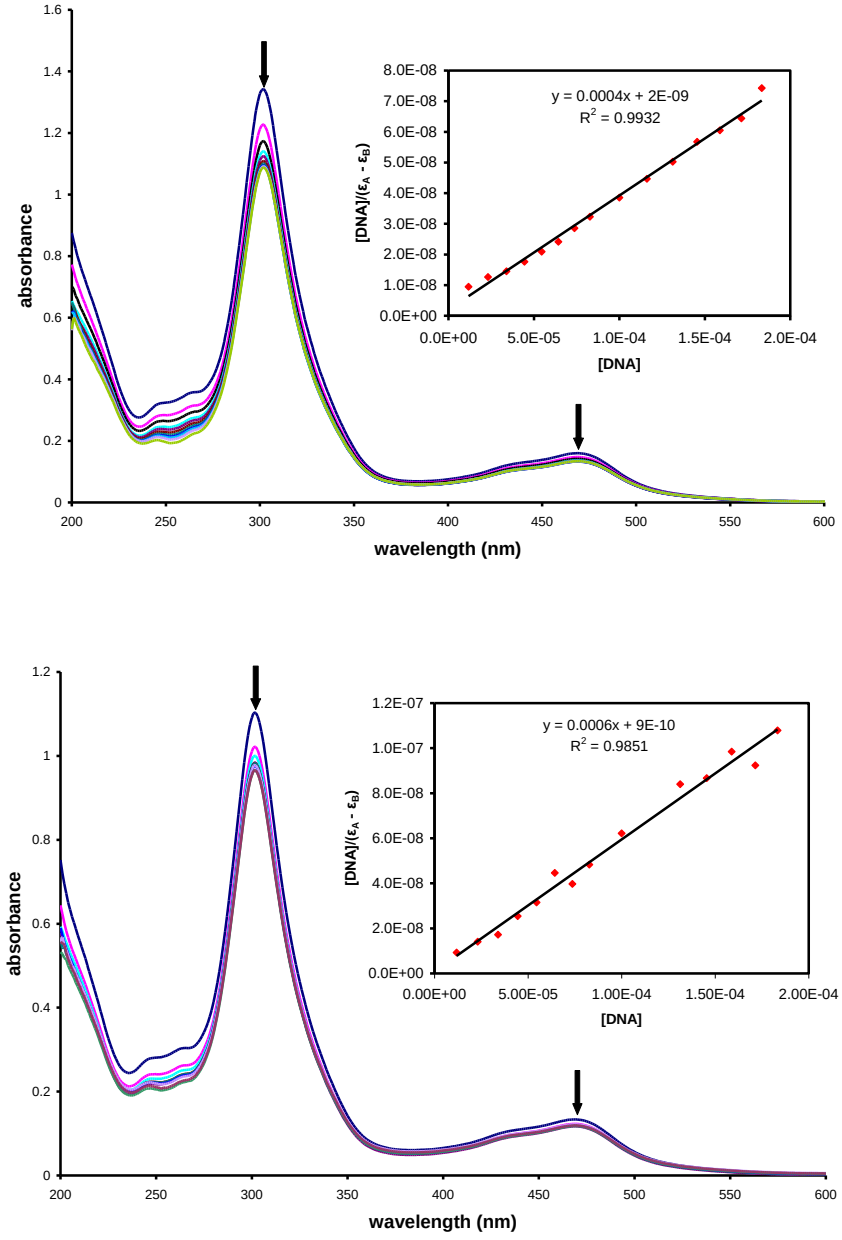

Figure D.1 Spectrophometric titration data from titrations of *M*-$[Ru_2L_3]Cl_4$ (top) and *P* $[Ru_2L_3]Cl_4$ (below) with ct-DNA at 293 K.

Appendix D.3 Dialysis experimental method

A 300 uM ct-DNA solution was made up in Tris buffer and placed on the inside of a 1 ml cellulose ester membrane Spectra/Por® DispoDialyzer®. This ct-DNA loaded dialysis tube was then submerged in a 20 uM racemic mixture of $[Ru_2(\mathbf{50})_3]Cl_4$ made up in Tris buffer. The dialysis was left for 18 h and the complex solution was inspected using CD spectroscopy to determine if enrichment of an enantiomer was evident. The *P*-helicate was observed to be enriched, thus indicating that the *M*-helicate is preferentially bound to the ct-DNA (***Figure D.2***).

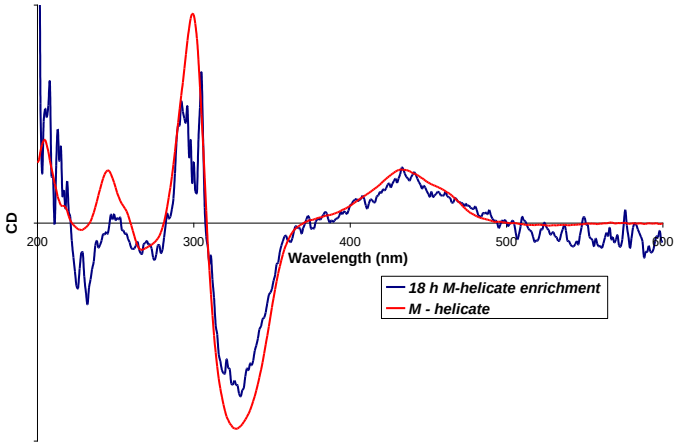

Figure D.2 CD of the $[Ru_2(\mathbf{50})_3]Cl_4$ solution after 18 hours of dialysis indicating an enrichment in the *M*-helicate.

D.4 References

1. J. A. Smith and F. R. Keene, *Chem. Commun.*, 2006, 2583-2585.

Appendix E

Publications and Presentations

Refereed Papers

1. *A new FeII quaterpyridyl M_4L_6 tetrahedron exhibiting selective anion binding.* C. R. K. Glasson, G. V. Meehan, J. K. Clegg, L. F. Lindoy, P. Turner, M. B. Duriska and R. Willis, *Chem. Commun.*, 2008, 1190-1192. DOI: 10.1039/b717740b

2. *Recent developments in the d-block metallo-supramolecular chemistry of polypyridyls.* C. R. K. Glasson, L. F. Lindoy and G. V. Meehan, *Coord. Chem. Rev.*, 2008, **252**, 940-963. DOI: 10.1016/j.ccr.2007.10.013

3. *5,5'-Bis[(trimethylsilyl)methyl]-2,2'-bipyridine.* Murray S. Davies, Christopher R. K. Glasson, George V. Meehan, *Acta Crystallographica*, Section E: Structure Reports Online (2008), E64(2), o364. doi:10.1107/S1600536807052154

4. *Microwave synthesis of a rare $[Ru_2L_3]^{4+}$ triple helicate and its interaction with DNA.* C. R. K. Glasson, J. K. Clegg, L. F. Lindoy, G. V. Meehan, J. Smith, R. F. Keene and C. Motti, *Chem. Eur. J.* 2008, **14**, 10535 – 10538. DOI: 10.1002/chem.200801790

Contributed Papers at National and International Meetings

1. Connect 2005 The 12th RACI convention 3 – 7th of July 2005 (Sydney)
   Poster: - ***Metal Directed Self-assembly of 5,5'''-Dimethyl-2,2':5',5'':2'',2'''-Quaterpyridine Using Ferrous Salts***. Jack K. Clegg, Christopher R. Glasson, Leonard F. Lindoy, John C. McMurtrie, George V. Meehan, Rick Willis.

2. ICO7 Conference of the Inorganic Chemistry Division – RACI 4 – 8th of February 2007 (Hobart).
   Poster: - ***New M_2L_3 Helicates and M_4L_6 Tetrahedra Incorporating 5,5'''-Dimethyl-2,2':5',5'':2'',2'''-Quaterpyridine and Extended Analogues***.
   Jack K. Clegg, Christopher R. Glasson, Leonard F. Lindoy, John C. McMurtrie, George V. Meehan, Rick Willis.

3. RACI Inorganic Symposium, Queensland Division 2006 (Towoomba)
   Seminar: - ***Metal Directed Synthesis of Supra and Supermolecular Cages.***
   Jack K. Clegg, Christopher R. Glasson, Leonard F. Lindoy, John C. McMurtrie, George V. Meehan, Rick Willis.

4. RACI Inorganic Symposium, Queensland Division 2008 (Brisbane)
   Seminar: - ***Metallosupramolecular Templates in Synthesis.*** Jack K. Clegg, Christopher R. Glasson, Leonard F. Lindoy, John C. McMurtrie, George V. Meehan, Rick Willis.

5. ICO8 Conference of the Inorganic Chemistry Division – RACI 14 – 18th of December 2008 (Christchurch).

Poster: - ***Metallosupramolecular Templates in Synthesis.*** Jack K. Clegg, Christopher R. Glasson, Leonard F. Lindoy, John C. McMurtrie, George V. Meehan, Rick Willis.